PG-002

Design of Buildings and Structures in Low to Moderate Seismicity Regions

Lam & Chan

Design of Buildings and Structures in Low to Moderate Seismicity Regions

This Professional Guide represents CNERC's continued contribution towards the building of a resilient world community. The underlying objective is to maintain living standards and improve safety in the face of natural disasters such as earthquakes. The scope of the undertaking in its entirety is broad, drawing expertise from many allied disciplines. Managing natural disasters entails developing adequate mitigation measures and preparedness levels. This Professional Guide is concerned specifically with mitigating the impact of future disasters by improving the robustness of newly constructed buildings in regions of low to moderate seismicity through a better understanding of hazard assessment and design methodology. The targeted readers are designers of building structures and policy makers in these regions.

The Chinese National Engineering Research Centre for Steel Construction (Hong Kong Branch)
The Hong Kong Polytechnic University

ISBN 978-962-367-818-6

www.polyu.edu.hk/cnerc-steel/

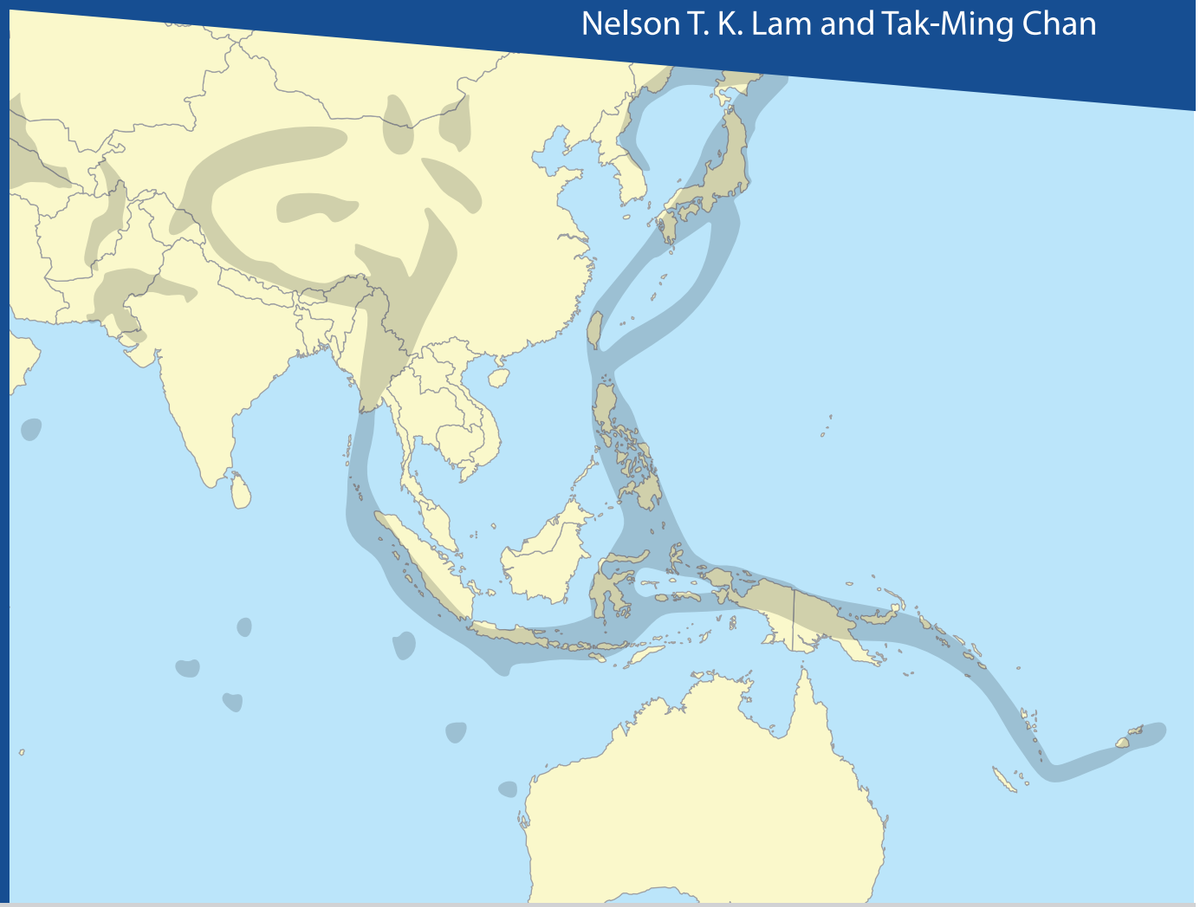
THE HONG KONG POLYTECHNIC UNIVERSITY
香港理工大學

國家鋼結構工程技術研究中心香港分中心
Chinese National Engineering Research Centre
For Steel Construction (Hong Kong Branch)

Design of Buildings and Structures in Low to Moderate Seismicity Regions

Professional Guide: PG-002

Nelson T. K. Lam and Tak-Ming Chan



The Institution of Structural Engineers
This publication has been supported by
The Institution of Structural Engineers' Research Panel

THE UNIVERSITY OF MELBOURNE
CDMPS
CENTRE FOR DISASTER MANAGEMENT AND PUBLIC SAFETY

Design of Buildings and Structures in Low to Moderate Seismicity Regions

Nelson T. K. Lam and Tak-Ming Chan

Copyright © 2018 by The Chinese National Engineering Research Centre for Steel Construction (Hong Kong Branch), The Hong Kong Polytechnic University

The moral right of the authors has been asserted.

All rights reserved.

Without limiting the rights under copyright reserved above, no part of this publication may be reproduced, stored in a retrieval system or transmitted in any form or by means (electronic, mechanical, photocopying, recording or otherwise) without the prior permission of both the copyright owner and the publisher of the book.

Although care has been taken to ensure, to the best of our knowledge, that all data and information contained herein are accurate to the extent that they relate to either matters of fact or accepted practice or matters of opinion at the time of publication. The Chinese National Engineering Research Centre for Steel Construction (Hong Kong Branch) at The Hong Kong Polytechnic University assumes no responsibility for any errors in or misinterpretations of such data and or information or any loss or damage arising from or related to their use.

Printed in Hong Kong Special Administrative Region, China.

ISBN-13: 978-962-367-818-6 Paperback





https://www.polyu.edu.hk/cnerc-steel/

The Chinese National Engineering Research Centre for Steel Construction (Hong Kong Branch) (CNERC) was established under support of the Innovation and Technology Funds of the Government of Hong Kong SAR in October 2015. The CNERC is dedicated to promote technological developments of the Hong Kong Construction Industry, to enhance its sustainable infrastructure developments, and to promote internationalization of its professional services. The primary objectives of the CNERC are:

- To establish a high level technological platform to promote effective design and construction of modern building and civil engineering structures as well as sustainable infrastructure development in Hong Kong.
- To advance technological capabilities of the Hong Kong Construction Industry in design and construction of super high-rise buildings, long-span bridges and buildings of large enclosure using high performance materials in Hong Kong as well as in overseas.

The CNERC is keen to promote engineering research and application of modern construction technology, and it is actively engaged with international as well as national exchanges in innovative technology, design and construction of steel structures.

Supporting Organisations



https://unimelb.edu.au/cdmps/

The Centre for Disaster Management and Public Safety (CDMPS) was established in 2014 at the University of Melbourne to promote disaster management research. It fosters interdisciplinary research collaborations, provides training and skills development for researchers, and promotes knowledge exchange and impact with regional, national and international stakeholders. It undertakes world-class research and translates them into innovative solutions and tools that address real challenges facing governments and professionals in the disaster management and public safety environment.



https://www.istructe.org/

The Institution of Structural Engineers is the world's largest membership organisation dedicated to the art and science of structural engineering. The Institution has over 28,000 members working in 105 countries around the world. The Institution is an internationally recognised source of expertise and information concerning all issues that involve structural engineering and public safety within the built environment. The core work of the Institution is supporting and protecting the profession of structural engineering by upholding professional standards and acting as an international voice on behalf of structural engineers.

This publication has been supported by the Institution of Structural Engineers' Research Panel.

Foreword

As a seismic engineer from an area of markedly low seismicity (United Kingdom), I have long been acutely aware of the particular difficulties that designers need to face in areas of low to moderate seismicity. Many lay people in the U.K. are surprised to hear that British earthquakes ever happen (they do!), but as responsible professionals, British engineers cannot ignore the issue even here. As a result, for the last 50 years, very considerable amounts of time and money have been spent (rightly in my opinion) on ensuring that U.K. nuclear power stations are designed to withstand a rare – but still credible – earthquake.

Whether more needs to be done in an area of 'very low' seismicity like the British Isles is another difficult question, which is not at all easy to answer. The official position – again, correct in my opinion – is that seismic measures are needed in a limited number of special cases, but standard structures, such as apartment blocks, commercial offices and minor bridges, do not need specific seismic protection. The main subject of this volume – low to moderate seismicity – represents a significantly increased level of seismic hazard, and the contributing authors seem to agree, emphatically, that for these areas, seismic design measures should be much more widespread than that. The seismic Eurocode, EN1998 (Eurocode 8), agrees.

The latest draft of the revised edition of Eurocode 8, dated 2017, defines low seismicity as, broadly speaking, corresponding to a 475 year return PGA (peak ground acceleration) on rock of 4% to 10%g and moderate seismicity as 10% to 20%g. The Eurocode is likely to recommend that the lateral strength of all structures in areas of low seismicity is sufficient to limit ductility demand to low levels under the design earthquake. For moderate seismicity, some degree of seismic detailing is likely to be required as well. These provisions are yet to be finalised, but I doubt whether the final version of EN1998, expected to be ratified in 2021, will be significantly different.

In my experience, the 'particular difficulties' applying to areas of low to moderate seismicity are of two distinct types. Firstly, there is the problem of getting reliable estimates of seismic hazard for structural engineers to use as the basis for their designs. Let me illustrate this by an example. The Pacific seaboard of Chile – one of the most seismic places on earth - suffers great earthquakes once or twice a generation, and damaging ones much more often. As a result, the country has many years of both instrumental and historical data on which to base its catalogues of earthquakes, captured both in Chile, and (for the larger events) worldwide. Usually, it is not too hard to associate at least the larger events with their causative faults. Moreover, Chile has for many years invested in its network of strong ground motion instruments, and consequently has plentiful data for establishing the 'ground motion prediction equations' (GMPEs) that describe the level of shaking due to a given earthquake magnitude and distance. GMPEs and earthquake catalogues together provide the fundamental data which seismic hazard analysts use to create their hazard maps.

With low to moderate seismicity, none of this applies; unlike magnitude 7+ events, earthquakes with low magnitudes are not picked up and recorded instrumentally around the world and the instrumental data, only dating to the early 20th century, is harder to supplement with historical records before 1900, which are usually unreliable and often non-existent. Reliable and

appropriate GMPEs are also difficult to establish, because there are likely to be few, if any, local strong motion recordings. In addition to this, there is another, fundamental problem that seismic hazard analysts face. In Chile, the worst that could happen seismically occurs every generation or so, but with low seismicity, it is the extreme events that are the main concern, and they may have return periods of thousands of years. So the seismic hazard specialist has a double problem – scant data which must then be extrapolated to extreme limits. This poses enormous geological, engineering and statistical problems.

But there is a second problem, which comes back to my field – that of structural engineering. Suppose we did have confidence in our predictions of seismic hazard, extending to very long return periods. What level of seismic protection would then be sensible to provide, given that it will require extra resources and compete with other objectives, such as providing energy efficiency or flood protection, and also compete with other needs, such as achieving the greatest number of hospital beds or dwellings that can be built with the resources available. The fact that the concern lies largely with 'extreme events', referred to above, makes this particularly difficult. How do we set off the need to avert a catastrophe that might not occur for several generations with the need to provide hospital beds for our ageing population, required now? In the U.K., the general public would rightly reject the advice of an 'expert' like myself that more money should be spent to provide seismic resilience for the places where they live and work. After all, only about a dozen people have been killed by British earthquakes in the last 400 years. The U.K. 'expert' can justify his or her neglect of seismic loading by pointing out that the Eurocodes specify robustness measures for all structures, whether seismically designed or not. These measures include detailing provisions, horizontal and vertical ties, minimum material standards including ductility, and so on. The measures are primarily intended to cope with rare events like gas explosions or vehicle strikes, but they would help a lot in a small earthquake too, and serve to mitigate the low seismic risk. For low to moderate seismicity regions, as Eurocode 8 recognises, these measures are not by themselves sufficient, and the need is to find structural ways of enhancing seismic resilience, while having a low impact on resources.

The contributors to this Professional Guide are well aware of all these issues and provide their own solutions. The authors come from a wide range of countries in Asia, as well as Australia, and it provides a fascinating and valuable insight into how engineers from the Region are developing their own distinct approach to what remains an under-researched topic.

Edmund Booth
Consulting Engineer
United Kingdom

Foreword

Hong Kong lies within the Eurasian Plate and is remote from the earth's more seismic active belts. Although the seismicity of Hong Kong is regarded as low to moderate, as a densely populated area in the region, Hong Kong has been preparing itself against the consequence of earthquake hazard through a series of coordinated investigations. Those investigations include studies of seismic hazard in Hong Kong, review of earthquake data for the Hong Kong region and consultations on the introduction of seismic-resistant building design standards for Hong Kong conducted by relevant departments and offices of the Hong Kong SAR Government with the strong support of academics and practitioners.

The Faculty of Construction and Environment at The Hong Kong Polytechnic University is a leading internationally recognised academic body in the construction, environment, and sustainable urban development fields. Our mission is to meet the needs of infrastructure development and environmental conservation in Hong Kong, the Chinese Mainland and beyond by

(1) offering a broad range of internationally competitive academic programmes relevant to the needs of industry and society;
(2) conducting world-class high-impact research that leads to innovations in construction, environment, urban management and spatial information; and
(3) supporting industry and society through technology transfer and other forms of professional services.

We are committed to bridging between innovation and application to enhance the socio-economic development of the region.

I congratulate Prof. Kwok-Fai Chung, Director of the Chinese National Engineering Research Centre for Steel Construction (Hong Kong Branch) at The Hong Kong Polytechnic University, for his leadership and visionary blueprint in developing a series of "Professional Guides" to promote technological advancement in sustainable infrastructure development in Hong Kong and beyond.

Prof. Nelson T. K. Lam and Dr. Tak-Ming Chan are applauded for the initiative they have taken in developing this Professional Guide on the "Design of Buildings and Structures in Low to Moderate Seismicity Regions", an initiative which received enormous support from a group of experienced researchers and practitioners in order to address this topical issue facing Hong Kong and the region.

I wish this Guide every success. Readers will benefit from the experiences shared by contributors from belt-and-road countries and beyond.

Professor You-Lin Xu
Dean, Faculty of Construction and Environment
Yim, Mak, Kwok & Chung Professor in Smart Structures
The Hong Kong Polytechnic University
Hong Kong SAR, China

Foreword

Engineers around the world have long been developing resilient infrastructure to safeguard the well-beings of their citizens against different levels of seismic hazards. Striving for economic growth and sustainable infrastructure development, comprehensive design provisions against various levels of earthquake have been developed for buildings and structures.

Although many strong earthquakes have struck China during the past years, many small to moderate earthquakes have been recorded in different parts of China from time to time. Though these earthquakes may strike with various levels of seismicity loadings, they would have devastating consequences on buildings and structures where no appropriate precaution was taken during their construction. As recorded in the ancient history, many buildings and structures in several prosperous cities, situated in regions of no apparent seismic hazards, turned into ruins overnight when struck by sudden earthquakes. Only in recent decades, have these incidents been fully explained by what is now commonly known as "unforeseen hazards owing to low to moderate seismicity".

Published by the Chinese National Engineering Research Centre for Steel Construction (Hong Kong Branch) at The Hong Kong Polytechnic University, this Professional Guide on the "Design of Buildings and Structures in Low to Moderate Seismicity Regions" provides a lot of information enabling engineers to examine the fundamental concepts and methods in assessing various levels of seismicity as well as those provisions necessary to protect against seismic hazards in the Asian Pacific Region. It also provides a platform for engineers to share experiences on the structural design of buildings and structures. Hopefully, from now on, new cities to be built in regions of low to moderate seismicity will be well prepared against seismic hazards, and the public will be protected adequately through well-informed structural engineering design.

All authors contributing to this Professional Guide and both Editors, Prof. Nelson T. K. Lam and Dr. Tak-Ming Chan are to be congratulated for compiling this remarkable document. Prof. Kwok-Fai Chung, Director of the Chinese National Engineering Research Centre For Steel Construction (Hong Kong Branch) should also be congratulated because of his admirable foresight in conceiving the creation of this document.

Professor Xu-Hong Zhou
Academician
Chinese Academy of Engineering
Chongqing University
China

Foreword

In recent years, there has been growing interest worldwide on the adoption of seismic design as an integral part of the design requirements towards disaster mitigation. Many regions have since developed their own seismic codes, while others are adapting from codes like Eurocode 8. Formulation of codes as well as associated design guidelines is a major undertaking demanding a knowledge of seismology, site and ground conditions, and engineering practice of the regions. This process often involves seeking consensus amongst stakeholders.

In the U.S., national model building codes now include seismic design requirements that directly impact regions where seismicity is low or moderate. The core requirements can be found in Minimum Design Loads for Buildings and Other Structures (ASCE/SEI 7-16, 2016), which have been largely inspired by the 2015 National Earthquake Hazard Reduction Program (NEHRP) recommendations. Through adoption of these codes, many state and local jurisdictions in areas of 'low to moderate seismicity' now have reasonably comprehensive seismic design provisions, requiring structural engineers to understand and apply code requirements, and additionally, explain them to architects, building owners, and contractors. Seismic design provisions are, however, not straightforward. The consequence of not applying these provisions correctly could be serious, resulting in buildings with inadequate strength and ductility, or that are unnecessarily costly and inefficient.

Nearer to home, based on seismic hazard studies and research, the seismicity of Hong Kong is classified as 'low to moderate'. While it may be correct to predict that potentially destructive earthquakes do not occur in regions of 'low to moderate seismicity', which are far away from tectonic plate boundaries, 'low probability, high consequence' events could be equally disastrous given their unpredictability and frequency, and inadequate robustness and redundancy in some of our building structures. As an international financial centre and a densely populated metropolis, Hong Kong cannot afford the consequence of earthquake attacks. There is a compelling case for seismic preparedness, and suitable protection measures are overdue.

I have in the last 20 years closely followed the earthquake engineering activities at the University of Melbourne with interest and admiration. Prompted by the 1989 Newcastle earthquake, the Melbourne team spearheaded by Prof. Nelson T. K. Lam and Prof. John L. Wilson were instrumental in modelling the regional and site seismic hazard of Australia and studying the vulnerability of buildings of different structural forms subjected to these hazards. Methodologies and design procedures developed from their research were then extended to 'low to moderate seismicity' regions like Hong Kong, Malaysia, Singapore, India, Vietnam and Sri Lanka, culminating in a huge body of knowledge readily and suitably applicable for formulation of national codes and improvement of engineering practice. I note that their work has been very well received by engineering communities in this part of the world.

I warmly welcome the publication of "Design of Buildings and Structures in Low to Moderate Seismicity Regions". The authors are wise in keeping the regions to Asia Pacific! It will be a valuable resource to those engaged in day to day practical design work, and those getting themselves ready to embrace new seismic codes. It is the first publication dedicated exclusively to 'low to moderate seismicity' seismic design and will fill a vacuum amongst the popular seismic

design textbooks. This publication is organised into two sections. The first section covers design considerations which will be useful background materials on seismic design concepts and fundamentals, and the second, seismology and case studies reflecting various practice in the Region.

Seismic design is in essence good structural and foundation design. It aims to achieve robustness, promotes simplicity and symmetry in structural arrangement, advocates a healthy dosage of redundancy, and champions regularity in vertical profiling to minimize the need for transfer structures, while paying close attention to ground condition considerations like amplification effects and liquefaction potentials. These will then be complemented by enhanced ductility detailing.

I commend the Institution of Structural Engineers, Chinese National Engineering Research Centre for Steel Construction (Hong Kong Branch) of The Hong Kong Polytechnic University, and the Centre for Disaster Management and Public Safety of the University of Melbourne for lending their support in enabling this publication to be realised. It is a worthwhile effort that will surely benefit the engineering profession.

The Asian Pacific Region, with its vast coastlines, high population concentration, varied geology and fragile infrastructure in many places, is particularly vulnerable to earthquake attacks. Our cities and communities are not totally resilient, and there remains considerable work to be done. While structural and geotechnical engineers may not be able to tame mother nature, we have a duty to create awareness and prepare for the unforeseen. This publicaiton will lead the way.

Y. K. Cheng
Past President
The Institution of Structural Engineers
United Kingdom

Foreword

Although Australia is not in the proximity of any tectonic plate boundaries, significant hazards owing to low to moderate seismicity do exist, and hence, need be factored into day-to-day structural engineering practice. The same is said of many other countries in the Asian Pacific Region. Technology to counter natural disasters and to foster public safety is fast developing to fulfil the needs of the community in general. However, tertiary institutions in the Region providing undergraduate education of civil and structural engineers are typically not able to provide adequate coverage by their curriculum of certain advanced topics.

Structural design against seismic hazards has always been an important subject of interest at the University of Melbourne, which has some 30 years of track record in research, graduate teaching and continual professional development training, code drafting and industry engagement activities surrounding this specialised area of expertise. The writing of this Professional Guide on the "Design of Buildings and Structures in Low to Moderate Seismicity Regions" was in response to a growing demand by practising structural engineers of a guideline to facilitate learning of fundamentals and up-to-date analytical techniques in support of the earthquake resistant design of buildings and structures.

Both Prof. Nelson T. K. Lam and Dr. Tak-Ming Chan drew upon the critical mass of experts, both experienced academics and professional engineers, from a number of countries in the Region to put together a well-structured volume of technical materials for free access by practising engineers and researchers from around the world. Much of the contents presented herein are beyond the scope of textbooks published on this subject. It can be used for self-learning as a stand-alone reference material, or for supporting coursework programs at the graduate level.

I am very delighted to have the opportunity to support this very valuable Professional Guide. I wish you best and have a good read, and I hope by working together we help deliver a more resilience world.

Professor Abbas Rajabifard
Head, Department of Infrastructures Engineering
Director, Centre for Disaster Management and Public Safety
The University of Melbourne
Australia

Foreword

Owing to tremendous socio-economic developments occurring in many parts of the world, a change in attitude towards hazards, both natural and man-made, is taking place. Resulting from a general increase of knowledge about hazards, and hence, an increased concern for potential losses, engineers, property owners and even policy-makers pay serious attention towards urban hazard mitigation. To protect the public, it has long been considered necessary to devote resources to minimizing or even eliminating hazards during infrastructure development. Seismic hazards, however, are treated differently, and this is particularly true in low to moderate seismicity regions.

It should be noted that for highly developed cities located in regions of high seismicity, seismic hazard threats are considered to be real and probable, and construction design and practice in these cities is heavily affected accordingly. However, for cities located in regions of low to moderate seismicity, no systematic earthquake mitigation measures may be considered worthwhile. Hence, many buildings and structures in these cities are provided with little or even no seismic resistance. If a moderate, or even a small, earthquake strikes, these cities will suffer from highly disproportionate amounts of damage, compared with cities located in regions of high seismicity.

This Professional Guide on the "Design of Buildings and Structures in Low to Moderate Seismicity Regions" is published to assist practitioners to broaden their depth of understanding of seismic loading probabilities and appropriate resistance measures in buildings and structures. It is dedicated to experience sharing by experts from some Asian Pacific countries and cities situated in regions of low to moderate seismicity. It allows readers in these regions, Hong Kong to appreciate the various levels of seismic provision from a holistic perspective.

I would like to express my sincere gratitude to Prof. Nelson T. K. Lam and Dr. Tak-Ming Chan, both Editors of the Professional Guide, and to all contributing authors for sharing their experience for the benefit of practitioners in the region. The Chinese National Engineering Research Centre for Steel Construction (Hong Kong Branch) is delighted to publish this document as part of its mission to promote development of sustainable infrastructure in Hong Kong as well as in the Asian Pacific Region.

Professor Kwok-Fai Chung
Director
Chinese National Engineering Research Centre for Steel Construction (Hong Kong Branch)
The Hong Kong Polytechnic University
Hong Kong SAR, China

Preface

The production of this Professional Guide stemmed from a sharing platform established at the International Conference on Earthquakes and Structures in August 2017. Experts in this field had congregated in Seoul, Korea to make technical presentations on the two special themes "Code developments in regions of low to moderate seismicity: I) Seismic hazard studies, and II) Structural design of buildings". Communications in the following months between the key contributors concluded that a technical publication was urgently needed, which would guide in the design of buildings in areas of low to moderate seismicity, and assist practitioners and researchers to deal with the challenges associated with:

i) the determination of the appropriate seismic action model for use in design, and

ii) the structural design of buildings to address the identified risks.

With the support of contributors from reputable institutions in the region, the excellent progress made in the past six months has led to the publication of this Professional Guide.

This Professional Guide comprises two sections with fourteen Chapters in total. Section A focuses on Design Considerations and Methodology: Introduction (Chapter 1), General Design Considerations (Chapter 2), Earthquake Loading (Chapter 3), Structural Analysis (Chapter 4), Concrete Design (Chapter 5), Steel Design (Chapter 6), Case Studies (Chapter 7) and Transfer Structures (Chapter 8). Section B presents Reports from: China (Chapter 9), India (Chapter 10), Korea (Chapter 11), Malaysia and Singapore (Chapter 12), Sri Lanka (Chapter 13) and Vietnam (Chapter 14).

We would like to take this opportunity to thank all the contributing authors for sharing their up-to-date technical knowledge. We also thank members of the International Scientific Committee for providing valuable feedbacks to the manuscripts. Special thanks go to Prof. Mike Anson for his editorial work on the drafts, and also to Mr. Y. K. Cheng, Mr. E. P. Lim and Dr. Daniel T. W. Looi for providing detailed feedback on the technical contents of all chapters.

Publication of this Professional Guide was only possible because of the support of the Chinese National Engineering Research Centre for Steel Construction (Hong Kong Branch) at The Hong Kong Polytechnic University. The support of Prof. Kwok-Fai Chung is acknowledged specifically in this regard. We would also like to express gratitude to Dr. Ivan W. H. Lau and Miss Paola Pannuzzo for their input to the publication production process.

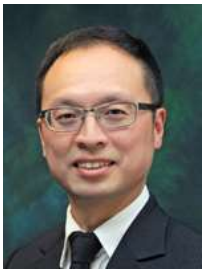
We sincerely hope that readers find this Professional Guide instructive and stimulating.

Nelson T. K. Lam and Tak-Ming Chan
Editors

Editors



Nelson T. K. Lam is Professor in the Department of Infrastructure Engineering at the University of Melbourne. He has 35 years of experience in structural engineering, and has been working in the specialized field of earthquake engineering, impact dynamics and structural dynamics. He is member of the Seismic and Dynamic Events Panel commissioned by the London Headquarter of The Institution of Structural Engineers, and also a member of the standing committee for future revisions to the Australian standard for seismic actions. His research achievement was recognized by the awards of the Chapman Medal (1999, 2010) and Warren Medal (2006) by Engineers Australia. He is also recipient of Award for Teaching Excellence given out by Engineers Australia in 2012, and Academic Staff Teaching Award by Melbourne School of Engineering in 2013.



Tak-Ming Chan is currently an Assistant Professor at The Hong Kong Polytechnic University, and an honorary academic staff at the University of Warwick in the U.K. He is Deputy Secretary-General of the Chinese National Engineering Research Centre for Steel Construction (Hong Kong Branch). He is also a Council Member of the Institution of Structural Engineers. He has 17 years of experience in structural engineering specialized in steel structures and has been leading research projects on stability of steel structures and earthquake engineering. His research achievement has been recognized by the Commendation Merit Awards by the Hong Kong Institution of Engineers (2016, 2017 and 2018). He is also the recipient of the Teaching Excellence Award from Department of Civil and Environmental Engineering at The Hong Kong Polytechnic University in 2017.

Contributors

S. Banerjee	IIT – Madras, India
A. Boominathan	IIT – Madras, India
José M. Castro	University of Porto, Portugal
Tak-Ming Chan	The Hong Kong Polytechnic University, Hong Kong
Hyung-lk Cho	Korea Institute of Geoscience and Mineral Resources, Korea
Saman De Silva	RMIT University, Australia
J. Dhanya	IIT – Madras, India
Janaka Gamage	RMIT University, Australia
M. C. Hee	The Institution of Engineers Malaysia, Malaysia
Goman W. M. Ho	ARUP Group, Hong Kong
Dong-Soo Kim	Korea Advanced Institute of Science and Technology, Korea
Nelson T. K. Lam	The University of Melbourne, Australia
Ek P. Lim	The Institution of Engineers Malaysia, Malaysia
Daniel T. W. Looi	The University of Hong Kong, Hong Kong
Elisa Lumantarna	The University of Melbourne, Australia
Luís Macedo	University of Porto, Portugal
S. Manandhar	KEPCO Research Institute, Korea
Alireza Mehdipanah	The University of Melbourne, Australia
Scott J. Menegon	Swinburne University of Technology, Australia
P. Muthuganeisan	IIT – Madras, India
Tuan D. Ngo	The University of Melbourne, Australia
Hai H. Nguyen	Institute of Building Science and Technology, Vietnam
Minh D. Nguyen	Institute of Building Science and Technology, Vietnam
Nam H. Nguyen	The University of Melbourne, Australia
S. T. G. Raghukanth	IIT – Madras, India
Hing-Ho Tsang	Swinburne University of Technology, Australia
Srikanth Venkatesan	RMIT University, Australia
Aaron J. Wang	CapitaLand China Corporate, China
John L. Wilson	Swinburne University of Technology, Australia
Mehair Yacoubian	The University of Melbourne, Australia

International Scientific Committee

Chairmen:	Kwok-Fai Chung	The Hong Kong Polytechnic University, Hong Kong
	Leroy Gardner	Imperial College London, U.K.
Advisor:	Xu-Hong Zhou	Chongqing University, China
Members:	S. Banerjee	IIT – Madras, India
	Edmund Booth	The Institution of Structural Engineers, U.K.
	José M. Castro	University of Porto, Portugal
	Ahmed Elghazouli	Imperial College London, U.K.
	Hyung-lk Cho	Korea Institute of Geoscience and Mineral Resources, Korea
	Ek P. Lim	The Institution of Engineers Malaysia, Malaysia
	Abbas Rajabifard	The University of Melbourne, Australia
	S. T. G. Raghukanth	IIT – Madras, India
	John L. Wilson	Swinburne University of Technology, Australia

Technical Publications Committee

Chairman:	Kwok-Fai Chung	The Hong Kong Polytechnic University, Hong Kong
Advisor:	Mike Anson	The Hong Kong Polytechnic University, Hong Kong
Secretary:	Ivan W. H. Lau	The Hong Kong Polytechnic University, Hong Kong
Members:	Tak-Ming Chan	The Hong Kong Polytechnic University, Hong Kong
	Gary S. K. Chou	Chun Wo Construction Holdings Company Ltd., Hong Kong
	H. C. Ho	The Hong Kong Polytechnic University, Hong Kong
	K. K. Kwan	ARUP Group, Hong Kong
	K. S. Kwan	Housing Department, HKSAR Government
	Paul H. F. Lam	The City University of Hong Kong, Hong Kong
	Daniel T. W. Looi	The University of Hong Kong, Hong Kong
	Joseph Y. W. Mak	The Hong Kong Polytechnic University, Hong Kong
	Ray K. L. Su	The University of Hong Kong, Hong Kong
	Michael C. H. Yam	The Hong Kong Polytechnic University, Hong Kong
	Alan H. N. Yau	AECOM Asia Company Limited, Hong Kong
	Ben Young	The University of Hong Kong, Hong Kong

Contents

Forewords iii
Preface xi
Editors xii
Contributors xiii
Committees xiv

Part A Design Considerations and Methodology

Chapter 1 **Introduction**
Nelson T. K. Lam and Tak-Ming Chan 1

Chapter 2 **General Design Considerations**
Performance Objectives, Design Methodology and Procedures for Regions of Low Seismicity 5
Scott J. Menegon, John L. Wilson and Nelson T. K. Lam

Chapter 3 **Earthquake Loading**
Earthquake Loading Characterisation for Regions of Low to Moderate Seismicity 15
Hing-Ho Tsang and Nelson T. K. Lam

Chapter 4 **Structural Analysis**
Methods of Structural Analysis for Buildings in Regions of Low to Moderate Seismicity 45
Elisa Lumantarna, Alireza Mehdipanah, Nelson T. K. Lam and John L. Wilson

Chapter 5 **Concrete Design**
Design of Reinforced Concrete Walls for Regions of Low Seismicity 69
Scott J. Menegon, John L. Wilson and Nelson T. K. Lam

Chapter 6 Steel Design

Design and Performance of Steel Buildings in Regions of Low to Moderate Seismicity 83

Luís Macedo, José M. Castro, Tak-Ming Chan and Goman W. M. Ho

Chapter 7 Case Studies

A Case Study of Code Compliant Design of Buildings in Regions of Low to Moderate Seismicity 99

Daniel T. W. Looi, Ek P. Lim and M. C. Hee

Chapter 8 Transfer Structures

Simplified Design Checks for Buildings with a Transfer Structure in Regions of Low Seismicity 113

Mehair Yacoubian, Nelson T. K. Lam and Elisa Lumantarna

Part B Country Reports (listed in alphabetical order)

Chapter 9 China

9.1 Recommended Earthquake Loading Model for Performance-Based Design of Building Structures in Hong Kong 141

Hing-Ho Tsang and Nelson T. K. Lam

9.2 Should We Use the Chinese Seismic Code for Hong Kong? 157

Goman W. M. Ho

9.3 Seismic Design and Engineering Practice in China 167

Aaron J. Wang

Chapter 10 India

10.1 A Probabilistic Seismic Hazard Map of India 183

S. T. G. Raghukanth, J. Dhanya and P. Muthuganeisan

10.2 Seismic Hazard Assessment of the City of Chennai, India 215

S. Banerjee and A. Boominathan

Chapter 11 Korea

New Site Classification Scheme and Design Response Spectra for Korea 233

Dong-Soo Kim, Satish Manandhar and Hyung-Ik Cho

Chapter 12 Malaysia and Singapore

12.1 Seismic Hazard Modelling for Peninsular Malaysia and Singapore 241

Daniel T. W. Looi, Hing-Ho Tsang and M. C. Hee

12.2 Site Classification Scheme and Response Spectrum Models for Malaysia 255

Daniel T. W. Looi, Hing-Ho Tsang, Nelson T. K. Lam and M. C. Hee

Chapter 13 Sri Lanka

Seismic Hazard Maps and Design Response Spectra for Sri Lanka – A Generic Approach 263

Srikanth Venkatesan, Janaka Gamage, Saman De Silva

Chapter 14 Vietnam

A Review of the Vietnamese Seismic Design Code 283

Tuan D. Ngo, Nam H. Nguyen, Minh D. Nguyen, and Hai H. Nguyen

Introduction

Nelson T. K. Lam[a] and Tak-Ming Chan[b]

[a] Department of Infrastructure Engineering
The University of Melbourne, Australia

[b] Department of Civil and Environmental Engineering
The Hong Kong Polytechnic University, Hong Kong

Keywords: seismic design, low seismicity, moderate seismicity, professional guide

This Professional Guide represents a small contribution towards the building of world community resilience to natural disasters. The underlying objective is to maintain living standards, and improve security, in the face of regular natural disasters such as earthquakes. The scope of the undertaking in its entirety is very broad. Expertise from many disciplines has been drawn upon. Managing natural disasters entails developing adequate mitigation measures and adequate levels of preparedness, and putting in place the capacity to respond effectively as the disaster arises and to engineer a smooth recovery back to the norm. Many disaster mitigation measures exist involving both existing and newly constructed built facilities. This Professional Guide is concerned specifically with mitigating the impact of future disasters by improving the robustness of newly constructed buildings in regions of low to moderate seismicity. The targeted readers are designers and regulators of building structures situated in these regions.

Some 98% of earthquakes occur in high, or very high, seismically active regions that are close to the tectonic plate margins. Potentially, destructive earthquakes do occur in regions of low to moderate seismicity that are remote from any tectonic plate boundaries. The latter type is intra-plate earthquakes. Land areas affected by intra-plate earthquakes constitute some 90 percent of the landmass, the focus of attention of this Professional Guide. Although the strongest recorded ground shakings have been generated by large magnitude earthquakes occurring in highly or very highly seismic regions, intra-plate earthquakes can be of low probability and yet of high consequence, because of the unpredictable nature of this type of earthquake coupled with the lack of robustness of building structures that are typically found in regions of low seismicity.

The writing of the book was motivated by the lack of knowledge and experience of current building design engineers on the design of buildings appropriate for regions where seismic events are rare. A few well known highly recommended textbooks include : (i) Naeim (2001), a compilation of articles introducing many different facets of earthquake engineering, co-authored by different discipline experts from engineering seismology to structural design; (ii) Booth (2014) gives a clear perspective on seismically induced damage to buildings, and structural collapse, followed by a systematic and comprehensive treatment of earthquake resistance for many different forms of building; (iii) Chopra (2011) is analytically intensive relating to the dynamic analysis of structures; (iv) Dowrick (2000) gives detailed treatment on the Earthquake Resistant design of buildings, engineering seismology and seismic hazards ; and (v) Fardis (2009) provides guidance specifically on the seismic design of concrete buildings as conforming to Eurocode 8. These are mainstream earthquake engineering textbooks authored by world renowned

experts working in this field.

This Professional Guide, has a different emphasis, containing a compilation of articles concerned with the skills and knowledge required of the designer of a building structure located in regions of low to moderate seismicity. The earthquake processes and the modelling of earthquake ground motions in regions of low to high seismicity are governed by the common principles of physics, as is also the case for the dynamics of structures. However, the approach to seismic hazard engineering design differs significantly between these two types of environment. Differences in emphasis are reflected in the chapter by chapter summary below.

This Professional Guide consists of two parts. Part A (Chapters 2 - 8), covering design considerations and methodology, is intended for front-line structural designers. The remaining chapters, in Part B, are contributions by authors from different countries all over Asia, which provide details of seismic hazard analysis and response spectrum modelling applying in those countries.

Many aspects of seismic hazard analysis, ranging from modelling the source of earthquakes to soil site classification considerations are covered, to demonstrate the different modelling approaches adopted by different countries. It is worth noting that the natural period of vibration of subsoil has been recently adopted by Malaysia and Korea as a site classification criterion, and is recommended for use in Hong Kong. This is an important advance over the traditional approach to the classification of soil sites, which are based on the stiffness properties of soil layers in the upper 30 m, or so. Part B, is primarily intended for use as a reference by "advanced" readers, including code drafters and personnel engaged in recommending seismic loading requirements. Designers eager to gain an insight into the underlying earthquake action processes are also encouraged to study this part of the Professional Guide.

The rest of this chapter, below, gives brief introductions to the chapters of Part A.

Chapter 2 compares regions of low to high seismicity and their associated return periods in relation to design performance objectives. In a region of low seismicity, emphasis is placed on ensuring satisfactory ultimate performance of the building following a very rare, high return period, seismic event. There are justifications, for low seismicity regions, for design to be based on return periods much longer than the current norm of 500 years. Australia, a country of low to moderate seismicity, plans accordingly to revise its seismic action standard in the next 3 - 5 years. At present, the design earthquake return period is set at 500 years but a minimum threshold PGA level of 0.08g has been imposed to override values derived from probabilistic seismic hazard analysis. Eurocode 8 is based on design return periods of up to 500 years although high return periods have been stipulated in the National Annexes of some countries. In summary, many improvements are in hand, relating to the definitions of design objectives and the setting of design return periods.

Chapter 3 introduces alternative seismic loading representative formats incorporating the concepts of acceleration, velocity and displacement demands so that the nature of the dynamic action and the response behaviour of the structure are more transparent to the designer (noting that designers who lack understanding of the fundamentals tend to be reluctant to take on a new design approach). The concept of a minimum design PGA value, an important consideration in a region of low seismicity is introduced along with an outline outcome of a study undertaken recently by the authors, to quantify the minimum design requirements based on the use of a global uniform intra-plate seismic hazard model.

The purpose of recommending a minimum ground motion intensity threshold is to ensure that all areas in regions of low seismicity are provided with at least a minimum amount of protection against intra-plate earthquake hazards which very often occur in "unexpected" locations. The concept of the site natural period and its use in classifying soil sites (as opposed to the use of the V(30m) parameter) is introduced at the end of the chapter as a means of addressing the adverse effects of resonance between structure and soil. This factor is particularly important with construction of limited ductility which is typical in areas of low seismicity.

Chapter 4 introduces a static analysis procedure, a modification of the lateral force code method of analysis, making the method more powerful and versatile in the following two respects: (i) the method gives results consistent with those derived from dynamic analysis and (ii) is more versatile, being suitable for buildings with irregular features. Although contemporary commercial software packages do possess dynamic analysis capabilities, engineers usually find it easier to make independent static analysis- 'deemed to satisfy'-checks rather than to perform full dynamic analyses. This particularly applies in regions of low seismicity where most design engineers are not at all experienced in dynamic analysis.

Chapter 5 gives recommendations on the design and detailing of reinforced concrete, aimed at achieving a limited amount of ductility, applicable to regions of low seismicity, without imposing those very onerous confinement and strength hierarchy requirements which provide full ductility. Emphasis is placed, instead, on those less intrusive measures that are readily implementable in regions of low seismicity. Such measures include the introduction of code provisions which ensure that the reinforcement content is above the minimum threshold to facilitate an even crack distribution, that structural walls are reinforced with two layers of reinforcement and not only one and that high axial load ratios on columns and the use of non-ductile reinforcement are prohibited.

Chapter 6 assesses steel buildings in regions of low to moderate seismicity such as Hong Kong and Portugal. Based on assessments of 30 archetypal moment resisting steel framed buildings, designed in accordance with Eurocode 8, the consequences of adopting the code recommended behaviour factors are evaluated in terms of expected direct economic losses. Results highlight the importance of a critical selection of behaviour factors during the design process and consideration of those site-specific hazards which might reduce expected seismic losses

Chapter 7 illustrates methodologies introduced in the earlier chapters, through computer models of real buildings, as examples. This is intended to assist designers to implement design procedures in practice. The calculation of site natural period, based on borehole log information, is illustrated with worked examples at the beginning of the chapter, followed by a demonstration of the analysis method introduced in chapter 4, based on the computer models of real buildings.

Chapter 8 is concerned with buildings featuring either a transfer plate or girders at podium level. Whilst this type of building is very common in regions of low seismicity their likely behaviour when subject to a potential earthquake is not well understood. This chapter introduces a simplified method, based on displacement principles, for estimating the adverse effects of the 'transfer' structure on the shear forces in the tower walls. Research findings reported in this chapter, are not definitive at this stage. Nonetheless this chapter shows how displacement based solutions can be developed to provide realistic estimates of the complex adverse effects of a transfer structure.

References

Naeim F. (2001) The Seismic Design Handbook, Springer
Booth E. (2014) Earthquake Design Practice for Buildings 3rd edition, ICE publishing.
Dowrick D. (2000) Earthquake Resistant Design and Risk Reduction, John Wiley & Sons.
Chopra A.K. (2011) The Dynamics of Structures, John Wiley & Sons.
Fardis M. N. (2009) Seismic Design, Assessment and Retrofitting of Concrete Buildings: based on EN Eurocode 8, Springer.

Performance Objectives, Design Methodology and Procedures for Regions of Low Seismicity

Scott J. Menegon[a], John L. Wilson[a] and Nelson T. K. Lam[b]

[a] Centre for Sustainable Infrastructure
Swinburne University of Technology, Australia

[b] Department of Infrastructure Engineering
The University of Melbourne, Australia

In this opening chapter the concept of performance based seismic design is introduced followed by a discussion into design return period, return period selection and performance objectives considerations for both low and high seismic regions. This Professional Guide is intended for use internationally, with particular reference to regions of low seismicity in Asia and Australia. There are frequent references to the regulatory structure in Australia, which has a long history of seismic codification, relative to other low seismic regions, and is wholly within an intraplate (low seismicity) environment. There are also references to Eurocode 8, New Zealand standards and documented design guidelines developed in North America.

Keywords: seismic design, performance objectives, design criteria, return period

1. Introduction

In regions of 'low seismicity' the seismic design and analysis of structures was typically not required, or where required, was often be ignored by designers. This is in stark contrast to regions of 'high seismicity', e.g. New Zealand, Japan or the west coast of the U.S., where seismic design procedures can be traced back to the 1920s or 30s (Paulay and Priestley, 1992). Taking Australia as an example, prior to 1979, no earthquake code or document had been published, nor mandated by building authorities. Australia's first earthquake loading code, AS 2121 (Standards Association of Australia, 1979) was published in 1979, partially in response to the 1968 magnitude 6.8 earthquake in Meckering, Western Australia. Some developed economies in regions of low seismicity, including a few in the economically vibrant regions of south-east Asia, are still without comprehensive building design codes concerned with seismic actions.

This lack of historical perspective on seismic design has resulted in a building stock legacy that has largely not been designed, nor assessed, for earthquake resistance in many regions of low seismicity around the world. This has also contributed to many misconceptions in the design community regarding seismic design, particularly the commonly held belief that if the base shear resulting from wind actions exceeds the base shear from an equivalent static seismic analysis, seismic actions can simply be ignored. This assumption is generally false, as most force-based seismic design procedures inexplicitly allow the inelastic response of the structure to be represented by a force reduction factor. Seismic actions comprise a separate load case and the structure needs to be designed and detailed accordingly.

2. Performance based seismic design

Vision 2000, a document prepared by the Structural Engineers Association of California (SEAOC) in 1995, defined performance objectives as the "coupling of expected performance levels with expected levels of seismic ground motions". This notion of associating an expected building performance level with an expected level of seismic ground shaking is referred to as performance based seismic design.

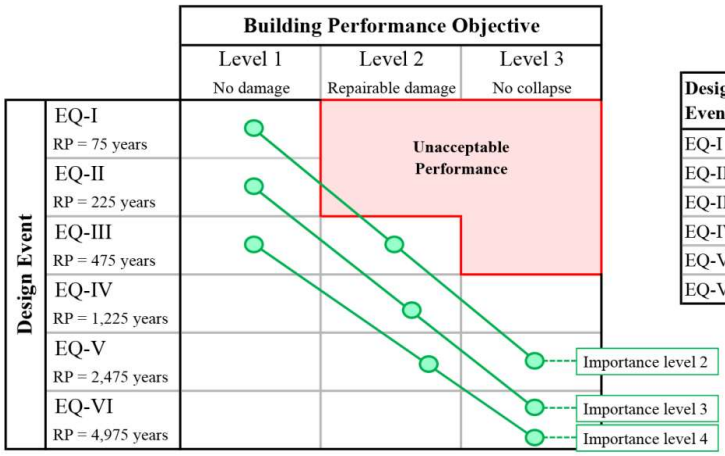
The building performance levels are usually expressed by easy to understand terms such as: level 1, no damage or no effect on the ability of the building to function as intended; level 2, reparable damage; and level 3, near collapse (or collapse prevention) during a maximum considered earthquake (MCE) event. Many other terminologies have been used varying between the different regulatory frameworks. The level of seismic ground shaking is usually expressed as a return period event, calculated as a probability of exceedance over the design life of the building.

In Eurocode 8 part 1 (CEN, 2004), which was first implemented in the past decade, seismic design is based on fulfilling the dual criteria of ensuring "no collapse" and "damage limitation" to the building. These two criteria correspond to the "ultimate" and "serviceability" limit state design objectives respectively. The state of "no collapse" is essentially concerned with protection of life in a rare earthquake event by ensuring that no part of the structure collapses and that adequate residual resistance of the building is maintained to withstand aftershocks and other environmental actions. Although building safety has been addressed, whether repairs are required for the purpose of resuming usual building functionality, can be uncertain. The "no collapse", or "no local collapse " design objective as stipulated in Eurocode 8, is comparable to the "life safety" performance objective as defined in the SEAOC Vision 2000 document (SEAOC, 1995) and the "significant damage" (SD) performance objective stipulated in EC8-part 3, which is concerned with seismic assessment and retrofitting.

In low seismic regions the "no collapse" performance objective is the dominating objective except for Class IV (lifeline) facilities where damage limitations are just as important. It is noted that the "no collapse" objective in Eurocode 8 is not to be confused with the "near collapse" or "collapse prevention" objective, in the North American terminology described above (Booth, 2014). "Near collapse", or "collapse prevention" is concerned with wholesale collapse of the building in a "very rare" event which can be equated to the defined Maximum Considered Earthquake (MCE).

Priestley, Calvi and Kowalsky (2007) and Sullivan, Priestley and Calvi (2012) recently proposed a matrix of seismic performance objectives for buildings, presented in Figure 1.

Sullivan et al. (2012) proposes that two zones be established: Zone A, moderate to high seismicity, where Levels 1, 2 and 3 performance objectives shall be met; and Zone B, low seismicity, where only Level 3 performance objective shall be met. In regions of high seismicity, it is likely that Levels 1 or 2 will govern the design. In regions of low seismicity where earthquakes are rare and the difference between low and high return period events can be significant, Sullivan et al. (2012) recommend the focus be placed on solely meeting the Level 3 objective, which ensures that loss of life is prevented under long return period events.



Design Event	Return Period	Probability of Exceedance
EQ-I	75 years	50% in 50 years
EQ-II	225 years	20% in 50 years
EQ-III	475 years	10% in 50 years
EQ-IV	1,225 years	4.0% in 50 years
EQ-V	2,475 years	2.0% in 50 years
EQ-VI	4,975 years	1.0% in 50 years

Figure 1. Sullivan et al. (2012) proposed seismic performance objectives (Menegon et al. 2017).

3. Design objectives and return period

In Eurocode 8, the no collapse performance objective is based upon a design return period of 500 years which corresponds to a probability of exceedance of 10% in a 50 years design lifespan of a building. Thus, the concept of Maximum Considered Earthquake (MCE) has not been incorporated into its underlying design philosophy given that the code was drafted in the mid 1990s, at which time it was still the norm to not consider designing to a return period exceeding 500 years. Seismic design provisions around the world have evolved since that time.

At present, there is a general consensus amongst earthquake engineers that a MCE event for normal buildings should have a 2500-year return period (RP) (rounded up from 2475 years), which is strictly consistent with a probability of exceedance (PE) of 2% in 50 years (i.e. there is a 2% chance a building with a design life of 50 years would undergo MCE level ground accelerations during its life span). The old version of ASCE/SEI 7-05 (American Society of Civil Engineers, 2005), which outlines the minimum design loads for buildings (including seismic provisions) and is referenced by the International Building Code (IBC) for use in California and many other states in the US, specifies that a probabilistic MCE event shall have a PE of 2% in 50 years (i.e. a RP of 2500 years). It is noted that since the 2012 edition of the IBC (International Code Council (ICC), 2012) and the release of ASCE/SEI 7-10 (American Society of Civil Engineers, 2010), the hazard definition has changed from a PE of 2% in 50 years to a risk-targeted performance requirement where there is a 1% chance of collapse in 50 years. However despite this change in hazard definition, the primary intended performance of the former has been retained (Building Seismic Safety Council, 2009).

It is important to draw the link between "collapse prevention" and “no collapse" (or "life safety") design criteria in order that both criteria are fulfilled in the structural design of the building. In a high seismicity environment dominated by identified active faults the intensity of ground shaking can be increased by a factor of 1.5 from 475 years to 2475 years (Tsang, 2014). Code compliant construction that has been designed to fulfil the no collapse performance objective is expected to have also fulfilled the collapse prevention

objective because of the usually adequate additional reserve capacity of the building to resist collapse beyond the no collapse limit.

Structural designers operating in low seismicity regions are cautioned, herein, that the factor of increase of the ground motion intensity (corresponding to the increase of RP from 475 to 2475 years) can exceed 1.5 by a wide margin. A factor varying between 2.4 and 5 is predicted for intraplate earthquakes, as shown in Figure 2 and other sources (Tsang, 2014; Geoscience Australia, 2012). Therefore, designing a building to the no collapse performance limit state for a RP of 500 years would not in itself be able to offer the building adequate protection from the near collapse limit state in a Maximum Considered Earthquake (MCE). The trend of moving away from the conventional practice of designing to a return period of 475 years was initiated by the influential FEMA450 document (BCCS, 2003), which was to guide the design of new buildings in the United States. The design seismic action was recommended based on an MCE of 2475 years scaled down by a factor of 2/3 (reciprocal of 1.5). This scaling factor can be interpreted as the margin between the state of no collapse and collapse prevention of the structure in order that code compliant buildings can always be assured of their ability not to collapse in a very rare earthquake event (Fardis, 2009).

The 2005 edition of the *National Building Code of Canada* (NRCC, 2005) increased the return period from 475 years to 2475 years without applying a scaled down factor of 2/3 (Mitchell et al., 2010) but a generous 2.5% drift limit, which is consistent with the *Collapse Prevention* performance objective, has been specified. The national annex to EC8 for the United Kingdom (BSI, 2008) also specifies a return period of 2475 years, to override the recommendation of 475 years in EC8 – Part 1 (CEN, 2004) to design for the *No Collapse* (*Life Safe*) performance objective. The UK requirement is more stringent than requirements in Canada.

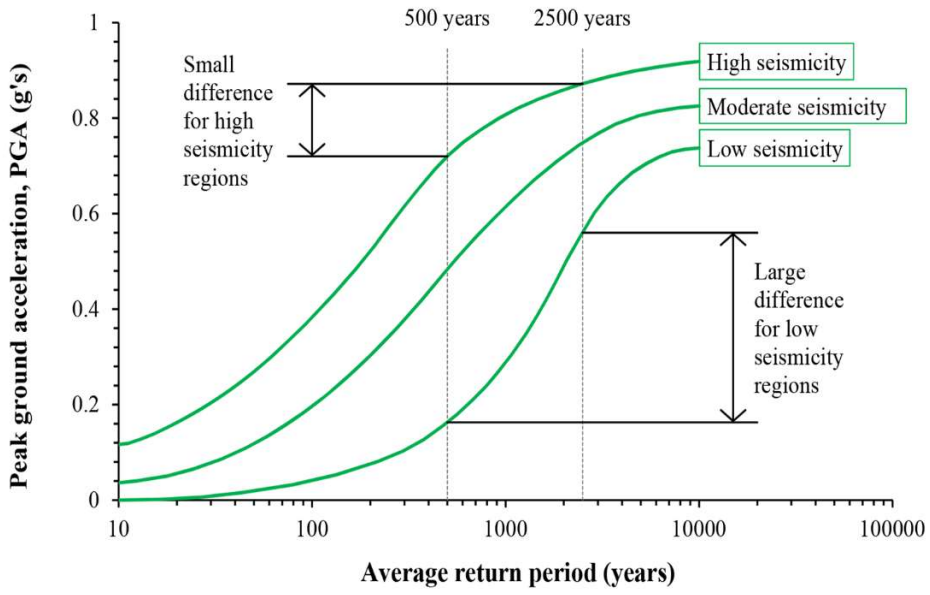


Figure 2. Return period factor in low and high seismicity regions (Paulay and Priestley, 1992)

Tsang (2014) presents a concise argument for adopting a 2500-year RP MCE event for the seismic design of buildings in Hong Kong and other regions of low seismicity, which would include Australia. It is argued, that a maximum allowable annual fatality risk (i.e. reliability level) of a building occupant during an earthquake should be of the order of 10-6 and that to achieve such a reliability level, a collapse prevention performance objective must be met allowing for a 2500-year RP (MCE) event.

4. Seismic performance objectives in a low and a high seismicity country

The seismic performance objectives for Australia will be discussed alongside the seismic performance objectives for New Zealand. Many Australian standards are published as joint Australian and New Zealand Standards and as such, the two countries share many similarities in terms of design procedures, methodologies, general terminology and compliance procedures. The common terminology and shared design codes, albeit only some, make New Zealand an ideal example for contrasting Australia, a region of low seismicity, against a region of high seismicity.

The Building Code of Australia (BCA) does not provide clear seismic performance objectives for Australian buildings. Instead it provides vague performance metrics that could easily be subject to extremely varying interpretations within the engineering community. The performance requirements from the BCA (Section BP1.1(a)) are summarized below:

a building during construction and use, with appropriate degrees of reliability, must

i. perform adequately under all reasonably expected design actions; and
ii. withstand extreme or frequently repeated design actions; and
iii. be designed to sustain local damage, with the structural system as a whole remaining stable and not being damaged to an extent disproportionate to the original local damage; and
iv. avoid causing damage to other properties

The vague performance metrics in the BCA – whether intentional or not – impel designers to adopt the prescriptive deemed-to-satisfy approach, in which designers are instructed to use the joint Australian and New Zealand standard for Structural design actions, Part 0: General principles, AS/NZS 1170.0 (Standards Australia and Standards New Zealand, 2002). AS/NZS 1170.0 is written as a "means for demonstrating compliance with the requirements of Part B1 of the Building Code of Australia" and establishing "compliance with Clause B1 'Structure' of the New Zealand Building Code (NZBC)".

Taking New Zealand as an example of a country with high seismicity. The Joint Australian-New Zealand standard for general principles of structural design actions (AS/NZS 1170.0) generally requires buildings in New Zealand to be designed for two performance objectives: ultimate limit state (ULS) and serviceability limit state (SLS). Importance Level 2 and 3 structures require two limit state objectives (i.e. ULS and SLS-1), whilst Importance Level 4 structures require an additional serviceability limit state (i.e. SLS-2) objective. AS/NZS 1170.0 defines the SLS-1 and SLS-2 limit states as follows:

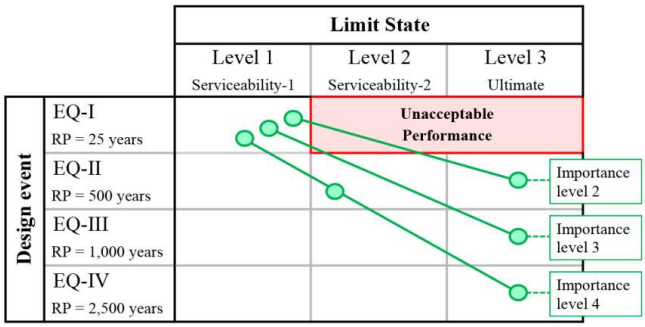
- SLS-1 – the structure and the non-structural components do not require repair after the SLS-1 earthquake.

- SLS-2 – the structure maintains operational continuity after the SLS-2 earthquake

In New Zealand it appears that for normal buildings, an MCE event with a 500-year RP is significantly low than it should be. It was seen, however, following the Christchurch earthquake, which was considered to be in excess of a 2500-year RP event (Goldsworthy, 2012; Kam and Pampanin, 2011; Tsang, 2011), that the majority of the building stock did, in fact, achieve collapse prevention performance objective. This is due in part to the conservative nature of using force-based (or strength-based) design methods for ensuring the collapse of a building does not occur. This is discussed in Volume 3 of the Canterbury Earthquakes Royal Commission (Canterbury Earthquakes Royal Commission, 2012) where it is argued that the conservative nature of ultimate limit state design provides the building with adequate reserve strength, which allows adequate performance during a larger event. More specifically, "the conservative aspects of designing for ULS (that is using the low characteristic material strengths, strength reduction factors, etc.) gives a structure protection against collapse in an earthquake above the ULS design level of shaking". These conservative aspects of force-based ULS design and the deeply engrained design philosophy in New Zealand material codes, which strive for a fully ductile structural system by adopting strict capacity design principles, led to adequate performance under what would be considered a 'real' MCE event (i.e. an event with a PE of 2% in 50 years). The building performance requirements and associated return periods for buildings in New Zealand are outlined in AS/NZS 1170.0 and are summarised in Figure 3.

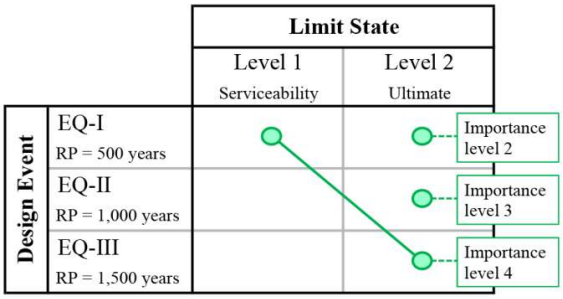
AS/NZS 1170.0 requires all buildings in Australia to be designed for ULS earthquake actions based on a given return period for the Importance Level associated with that building. The Importance Level and return period for earthquake actions are both specified in the BCA. The respective seismic hazard for a given return period can then be determined using AS 1170.4, which also requires designers to perform a 'special study' to ensure that Importance Level 4 buildings remain serviceable (i.e. operational) after the equivalent design event for an Importance Level 2 building. The seismic performance objectives for Australian buildings are summarised in Figure 4.

AS/NZS 1170.0 defines ULS as "states associated with collapse, or with similar forms of structural failure", implying that ultimate limit state in the Australian and New Zealand design context relates to a collapse prevention performance objective. This suggests that the Australian seismic design approach is somewhat in line with that recommended by Sullivan et al. (2012) for a Zone B (i.e. region of low seismicity) country. However, this statement is not entirely accurate, given that the RP event that is being stipulated in the BCA is significantly lower than that recommended by Sullivan et al. (2012) or that discussed in other literature. This means the current code stipulations in Australia on design return periods (for seismic actions) are at odds with much of the literature and other design codes around the world.



Design Event	Return Period	Probability of Exceedance
EQ-I	25 years	87% in 50 years
EQ-II	500 years	9.5% in 50 years
EQ-III	1,000 years	4.9% in 50 years
EQ-IV	2,500 years	2.0% in 50 years

Figure 3. New Zealand seismic performance objectives (Menegon et al. 2017)



Design Event	Return Period	Probability of Exceedance
EQ-I	500 years	9.5% in 50 years
EQ-II	1,000 years	4.9% in 50 years
EQ-III	1,500 years	3.3% in 50 years

Figure 4. Australian seismic performance objectives (Menegon et al. 2017)

5. Analysis and design procedure

The seismic design approach stipulated in Eurocode 8 and in the Australian standard for seismic actions AS1170.4 have both been translated from the conventional force based approach used originally in the high seismicity region of western North America. This approach involves analysing the structure as a linear-elastic system subject to a set of equivalent earthquake design forces, which are taken as the elastic forces divided by a force reduction factor. The elastic forces are the maximum forces the building would be subjected to if the structure were to maintain a linear-elastic response under the associated level of seismic hazard being considered. The force-based approach is based on the 'equal displacement phenomenon' that assumes the inelastic displacement of the structure approximately equals the linear elastic displacement of an equivalent building system. The underlying assumption is that strength is being traded for ductility, i.e. the structure is resisting the applied kinetic energy from the earthquake ground accelerations by a combination of both elastic strain energy and the energy associated with inelastic plastic deformation of the structure – as opposed to purely elastic strain energy in the case of a linear-elastic responding system.

The force-based approach involves the use of what is known as the "force reduction factor", which is used to inexplicitly account for inelastic behaviour in the design process. This means that the performance of the building during the design earthquake event is not equal to the displacement corresponding to that of the elastic design model of the building, but rather to a point equal to the force reduction factor multiplied by the response of the elastic design model. This is one of the primary differences between wind actions and seismic actions and in part why the commonly held belief that if the base

shear resulting from wind actions exceeds the base shear from an equivalent static seismic analysis, seismic actions can simply be ignored, is inappropriate and false. It is imperative that the designer details the structure to ensure it has the level of ductility assumed in the seismic design calculations, irrespective of how large the wind actions are.

In Eurocode 8 the force reduction factor, which is called the behaviour factor (q), takes into account the capacity of the structure at the member level to withstand seismic actions beyond its notional capacity limits. Design actions (such as bending moments and shear forces) are to be scaled down by the factor of 1/q and no scaling factor is to be applied in the calculation of drifts, or deformations, in the structure. In regions of low seismicity, "Design Category Low" (DCL) design and detailing rules may be applied and the respective q value can be adopted. It is imperative, though, that the required detailing rules associated with DCL be specified within the design documentation to ensure the amount of inelastic behaviour assumed in the design can actually be developed in the structure. Adopting a q value of 1.5 is conservative, except for non-ductile construction such as unreinforced masonry structures. When there are "hot spots" in a low seismicity environment, a higher tier of rules for design and detailing (such as DCM) may be applied. Alternatively, higher seismic actions in the designated areas may be countered by increasing the strength demand whilst uniformly adopting DCL design and detailing rules.

In the Australian Standard (AS1170.4, 2007) the force reduction factor is a combination of (i) the structural performance factor (S_p), which takes into account contributions from the over-strength of materials and the structural system as a whole and (ii) the ductility factor (μ), which takes into account contributions from the ability of the structure to deform in a ductile manner (AEES, 2009). The value of S_p is taken by default as 0.77 and the value of μ is taken as 2.0, by default, for limited ductile reinforced concrete, structural steel or composite structures which employ concrete and steel as construction materials. The composite factor of 2.6 (being μ/Sp or 2/0.77) that is used as the default design value in Australia can be compared to the slightly lower, more conservative, q value of 2.0 recommended in the *National Building Code of Canada* (NBCC) 2005 edition. Recommendations on structural response factors for the design of reinforced concrete can be found in Chapter 5 which is concerned with the design of reinforced concrete.

6. Conclusions

This chapter introduces the concept of performance based design objectives and outlines the seismic design criteria and return period considerations for both low and high seismicity countries using Australia and New Zealand as key examples. References have also been made to Eurocode 8 and documented design guidelines developed in North America. Discrepancies in the design return period requirements stipulated by the BCA and AS/NZS 1170.0 and those recommended in the literature are highlighted. At the end of the chapter, the principles of force-based design and the current force reduction factors stipulated in various codes of practices are discussed.

Acknowledgements

Much of the material in this chapter consists of excerpts from the journal article by Menegon et al. (2017). Those parts of the text related to Eurocode 8 were developed as a team, by the third author, Dr. Hing-Ho Tsang, Dr. Daniel Looi and Ir. M. C. Hee when drafting the National Annex to Eurocode 8 for Malaysia.

References

American Society of Civil Engineers (2005) "ASCE/SEI 7-05 Minimum Design Loads for Buildings and Other Structures", American Society of Civil Engineers, Reston, VA.

American Society of Civil Engineers (2010) "ASCE/SEI 7-10 Minimum Design Loads for Buildings and Other Structures", American Society of Civil Engineers, Reston, VA.

Australian Earthquake Engineering Society (AEES) (2009) "AS 1170.4 Commentary: Structural Design Actions – Part 4 Earthquake Actions", Victoria: Australian Earthquake Engineering Society.

Booth, E. (2014) "Personal communication with the third author in December 2014".

British Standards Institute (2008) "UK National Annex to Eurocode 8: Design of structures for earthquake resistance - Part 1: General rules, seismic actions and rules for buildings", British Standards Institute, London.

Building Seismic Safety Council (2009) "NEHRP Recommended Seismic Provisions for New Buildings and Other Structures (FEMA P-750)", Building Seismic Safety Council, Washington, DC.

Structural Engineers Association of California (SEAOC) (1995) "Vision 2000: Performance Based Seismic Engineering of Buildings", Californian Office of Emergency Services, Sacramento, CA.

Canterbury Earthquakes Royal Commission (2012) "Volume 3 Low-Damage Building Technologies", Christchurch.

European Committee for Standardization (CEN) (2004) "Eurocode 2: Design of Concrete Structures - Part 1-1: General rules and rules for buildings, European Committee for Standardization (CEN)", Brussels, Belgium.

Fardis, M.N. (2009) "Seismic Design Assessment and Retrofitting of Concrete Buildings based on EN – Eurocode 8", Springer.

Goldsworthy, H.M. (2012) "Lessons on building design from the 22 February 2011 Christchurch earthquake", Australian Journal of Structural Engineering, Vol. 13(2), pp. 159-173.

International Code Council (Icc) (2012) "2012 International Building Code, International Code Council (ICC)", Country Club Hills, IL.

Kam, W.Y. and Pampanin, S. (2011) "The seismic performance of RC buildings in the 22 February 2011 Christchurch Earthquake", in Structural Concrete, Vol. 12(4), pp. 223-233.

Menegon, S.J., Wilson, J.L., Lam, N.T.K. and McBean, P., 2017, "RC Walls in Australia: Seismic Design and Detailing to AS 1170.4 and AS 3600", Australian Journal of Structural Engineering (in press).

National Construction Code(2016) "National Construction Code 2016, Volume One, Building Code of Australia, Class 2 to Class 9 Buildings", The Australian Building Codes Board, Canberra, ACT.

National Research Council of Canada (NRCC) (2015) "National Building Code of Canada" (NBCC), Ottawa, Canada.

Priestley, M.J.N., Calvi, G.M. and Kowalsky, M.J. (2007) "Displacement-Based Seismic Design of Structures", IUSS Press, Pavia, Italy.

Standards Association of Australia(1979) "AS 2121-1979 The Design of Earthquake-Resistant Buildings", Standards Association of Australia, North Sydney, NSW.

Standards Australia (1993a) AS 1170.4-1993 "Minimum design loads on structures, Part 4: Earthquake loads", Standards Australia, Homebush, NSW.

Standards Australia (1993) "AS 1170.4 Supplement 1-1993 Minimum designs on structures, Part 4: Earthquake loads-commentary", Standards Australia, Homebush, NSW.

Standards Australia, 2007, "AS 1170.4-2007 Structural design actions, Part 4: Earthquake actions in Australia", Standards Australia, Sydney.

Standards Australia (2009) "AS 3600-2009 Concrete structures, SAI Global Limited, Sydney.

Standards Australia and Standards New Zealand, 2001, AS/NZS 4671:2001 Steel reinforcing materials", Standards Australia International Ltd and Standards New Zealand, Sydney and Wellington.

Standards Australia and Standards New Zealand (2002) "AS/NZS 1170.0:2002 Structural design actions, Part 0: General principles", SAI Global Limited and Standards New Zealand, Sydney and Wellington.

Standards New Zealand (2004) "NZS 1170.5:2004 Structural Design Actions Part 5: Earthquake actions - New Zealand", Standards New Zealand, Wellington.

Standards New Zealand (2006) "NZS 3101:Part 1:2006 Concrete Structures Standard Part 1 - The Design of Concrete Structures", Standards New Zealand, Wellington.

Sullivan, T.J., Priestley, M.J.N. and Calvi, G.M. (Editors) (2012) "A Model Code for the Displacement-Based Seismic Design of Structures", IUSS Press, Pavia, Italy.

Tsang, H.-H. (2011) "Should we design buildings for lower-probability earthquake motion?", Natural Hazards, Vol. 58(3), pp. 853-857.

Tsang, H.-H. (2014) "Seismic performance requirements and collapse risk of structures", Proceedings of the Advances in Seismic Engineering - Annual Seminar 2014, Hong Kong.

Earthquake Loading Characterisation for Regions of Low to Moderate Seismicity

Hing-Ho Tsang[a] and Nelson T. K. Lam[b]

[a] Department of Civil and Construction Engineering
Swinburne University of Technology, Australia

[b] Department of Infrastructure Engineering
The University of Melbourne, Australia

The earthquake loading model, the subject matter of this chapter, is to be decided first in the design process. No prior knowledge of earthquake engineering and structural dynamics is assumed of the reader. Basic principles and generic modelling techniques are explained early in the chapter for the benefit of those who are not already familiar with the fundamentals. Later sections are fully devoted to the modelling of earthquake actions on rock and flexible soil sites in regions of low to moderate seismicity. These are important key features which should be of interest to both regulators (code drafters) and designers.

Keywords: seismic design, loading characterization, low to moderate seismicity

1. Introduction

This chapter is primarily concerned with the presentation and interpretation of earthquake loads (seismic actions) and how challenges in the modelling of seismic hazards are tackled in a tectonically stable region where locally recorded data is typically lacking. Engineers who are not already familiar with the topic of seismic design are usually directed to world acclaimed textbooks including that of Chopra (2017) which places emphasis on the analytical aspects of the seismic design of the structure providing an in-depth treatment of structural dynamics phenomena and their mathematical modelling. Another highly recommended text is that of Fardis (2009) which places emphasis on the philosophies and considerations of seismic design and the assessment and retrofitting of RC buildings. Much of the contents in both textbooks concerns the application of a predefined earthquake loading model in analysis but neither explain how the loading model should be determined in the first place.

This chapter includes a range of basic topics including structural idealisation, dynamic equilibrium in natural vibration and base excited conditions and the presentation of their solutions as response spectra in different formats. This is followed by an introduction to probabilistic seismic hazard analysis and the uniform hazard spectrum (Section 2). A rundown of the earthquake loading models stipulated in major building codes of practice is then presented (Section 3). Textbooks by Naeim (2001) and Dowrick (2009) cover these topics. However, no detailed coverage exists for low to moderate seismicity conditions. In this chapter, a section is fully devoted to modelling considerations in regions of low to moderate seismicity (Section 4). Finally, a soil amplification model, recommended as a replacement for current code models for such regions, is introduced Section 5.

2. Basic principles

A thorough understanding of the derivation of a response spectrum model is essential for their correct, and effective, application in structural design practice. This section introduces the modelling of earthquake loads, step-by-step, starting from structural idealisation, followed by dynamic equilibrium analysis, the procedure for constructing a design spectrum, ground motion modelling, probabilistic seismic hazard analysis and the concept of the uniform hazard spectrum.

2.1 Structural idealisation

Analysis of the lateral resisting behaviour of a multi-storey building structure subject to seismic conditions can be simplified using a "stick model" (as depicted in Fig.1). Lumped masses are shown attached to the "stick" at regular intervals up the height of the building to emulate the masses of the building floors. The stick model is a reasonable, and commonly adopted, form of structural idealisation of the building, provided that the floor diaphragms can be assumed perfectly rigid in their own planes so that all masses at the same level in the building are subject to identical motion time-histories during an earthquake. This stick model can also be described as a multi-degree-of-freedom (MDOF) lumped mass system.

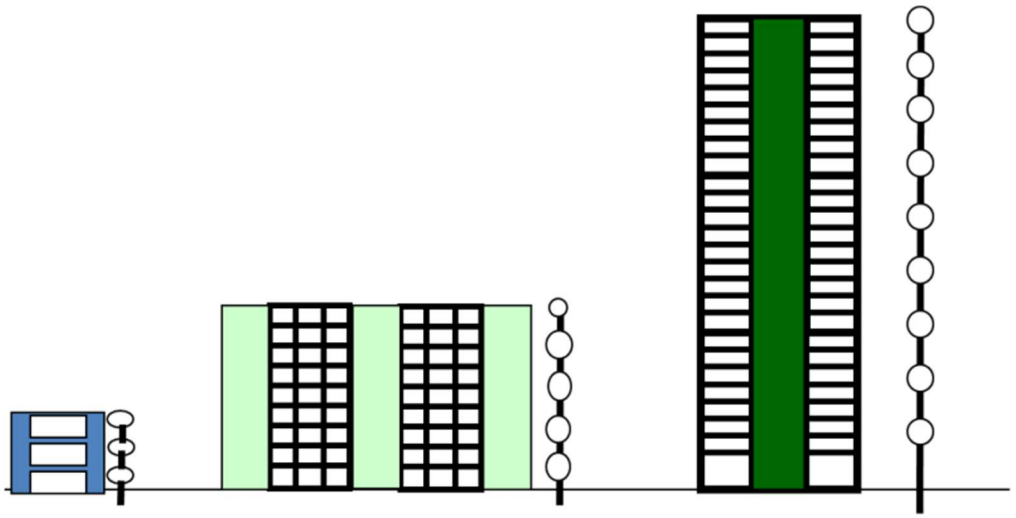


Figure 1. Idealisation of multi-storey buildings into stick models

The dynamic response behaviour of the MDOF lumped mass systems as depicted in Fig.1 can be resolved into a number of vibration modes each of which can be represented by an equivalent SDOF lumped mass system based on principles of modal superposition, forming part of the modal analysis methodology (Figure 2). Detailed descriptions of modal analysis can be found in most textbooks in the field of structural dynamics (e.g. Chopra 2017). The behaviour of a SDOF system in response to externally applied excitations is central to the response analysis of a building structure subject to seismic actions and other forms of dynamic actions.

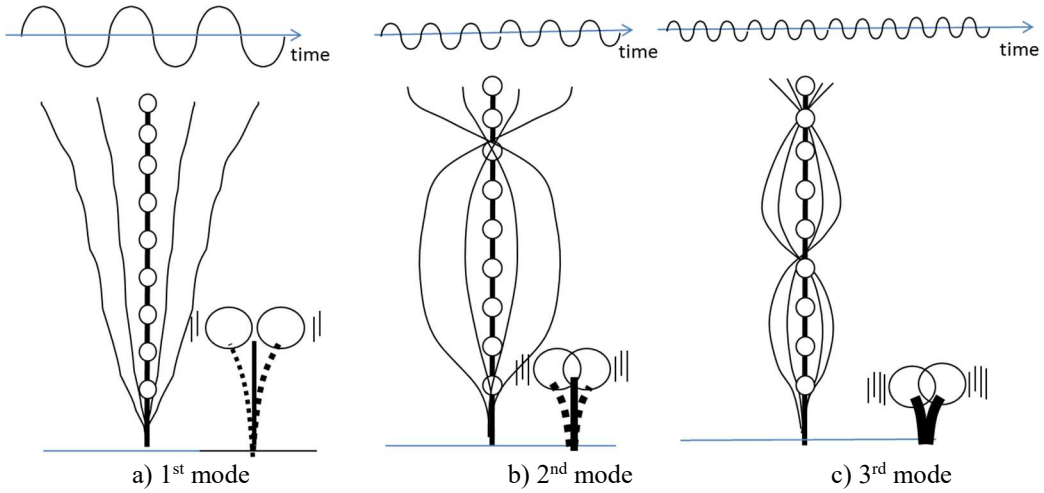


Figure 2. Use of single-degree-of-freedom lumped mass models in a modal analysis

The SDOF lumped mass model is depicted in different forms in the literature to illustrate the same principles. The "table" model of Figure 3(a), which can also be described as an idealized single-storey frame, is used below in this section to illustrate the motion behaviour of the building floor and the associated equilibrium of forces. The single lumped mass stick model of Figure 3(b) is commonly used in illustrations, as is the "trolley model" of Figure 3(c).

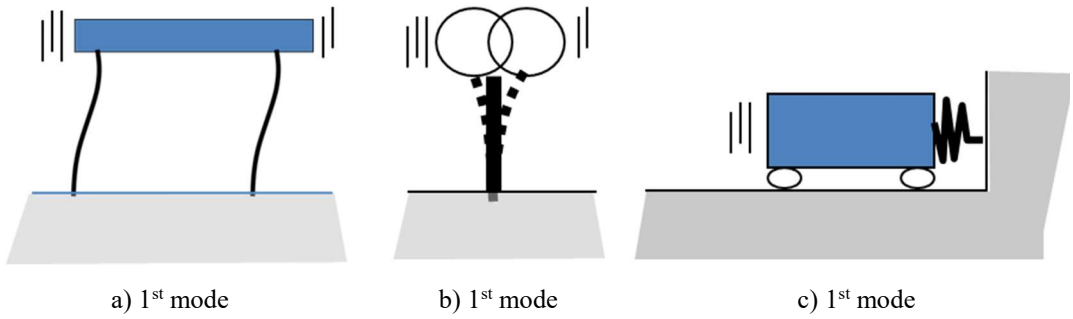
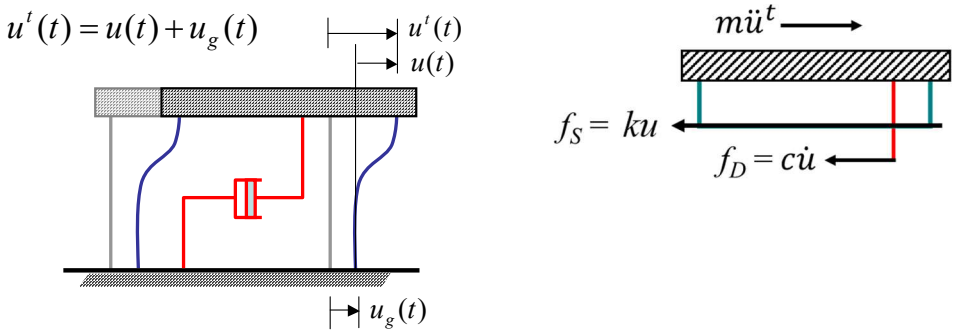


Figure 3. Different forms of single-degree-of-freedom lumped mass models

2.2 Horizontal dynamic equilibrium of forces

The dynamic equilibrium of an idealised single-storey frame induced into vibration by a horizontal ground displacement (Figure 4) is illustrated. For the sake of simplicity, all masses of the building frame are lumped at roof level as illustrated in Figure 4(a). The total (or absolute) displacement $u^t(t)$ of the mass has two components: (1) ground displacement induced by the earthquake $u_g(t)$; and (2) relative displacement between the mass and the ground $u(t)$ (i.e. equal to the deflection of the columns) resulting from the vibration of the structure.

$$u^t(t) = u(t) + u_g(t) \tag{1}$$



a) Motion Diagram b) Free Body Diagram of Force

Figure 4. Dynamic behaviour of a single-degree-of-freedom lumped mass model

Consider the free body diagram of the "table top" of the frame (the lumped mass m) as shown in Figure 4(b). The internal force f_S and damping force f_D are in equilibrium with the inertial force. By Newton's Second Law of Motion, the following equation represents the equilibrium of forces at any snapshot of time.

$$-ku - c\dot{u} = m\ddot{u}^t \tag{2}$$

Rearranging Eq. (2), in combination with Eq. (1), leads to Eq. (3) which is the governing equation of dynamic equilibrium of the SDOF system depicted in Figure 4.

$$m\left(\ddot{u} + \ddot{u}_g\right) + c\dot{u} + ku = 0 \quad \text{or} \quad m\ddot{u} + c\dot{u} + ku = -m\ddot{u}_g \tag{3}$$

The idealised structure can be subject to an externally applied dynamic (e.g. wind) force *p(t)* as shown by the diagram on the left of Figure 5, to applied base excitations (e.g. earthquake) as shown by the diagram on the right of the same figure. Comparing the two diagrams in the same figure reveals their equivalence. It is shown that an earthquake by itself does not impose any externally applied pressure (forces) on the structure, unlike a windstorm. The building is simply made to move (or displace) in an earthquake. Inertial forces are then resulted from accelerations that are associated with the ground motion.

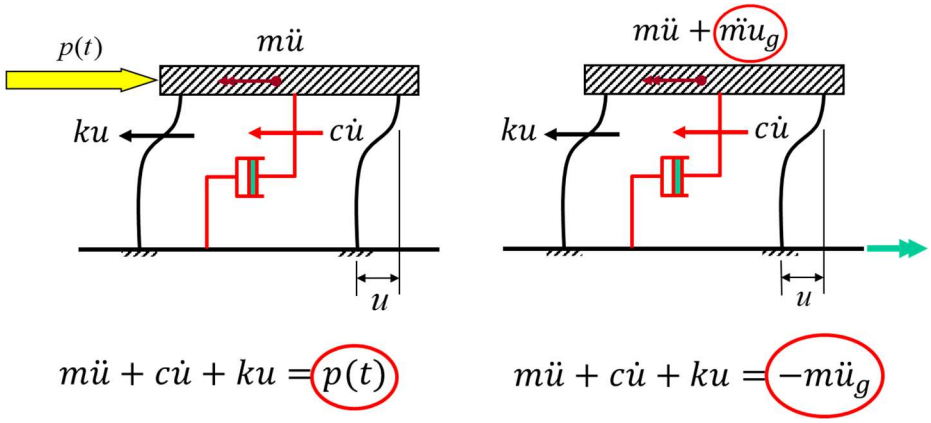


Figure 5. An analogy between external loads and earthquake-induced loads.

Dividing Eq. (3) by mass m gives Eq. (4).

$$\ddot{u} + 2\zeta\omega_n\dot{u} + \omega_n^2 u = -\ddot{u}_g \quad \text{where} \quad \omega_n = \sqrt{\frac{k}{m}} \quad \text{and} \quad \zeta = \frac{c}{2\sqrt{km}} \tag{4}$$

For a given ground acceleration time-history $\ddot{u}_g(t)$, the displacement time-history $u(t)$ of the responding structure depends only on the two parameters, the natural frequency ω_n, or natural period of vibration $T(=2\pi/\omega_n)$ of the system and its damping ratio ζ. Once the displacement time-history of the floor is known, its acceleration time-history response can be found by calculus. An example of the acceleration response of a SDOF system, defined by T = 0.5s and ζ = 0.05, when subject to an idealised ground acceleration pulse is shown in Figure 6. Any two systems having the same values of T and ζ would respond in exactly the same way (i.e. the same $u(t)$) even though one system may be more massive than (or stiffer than) the other system.

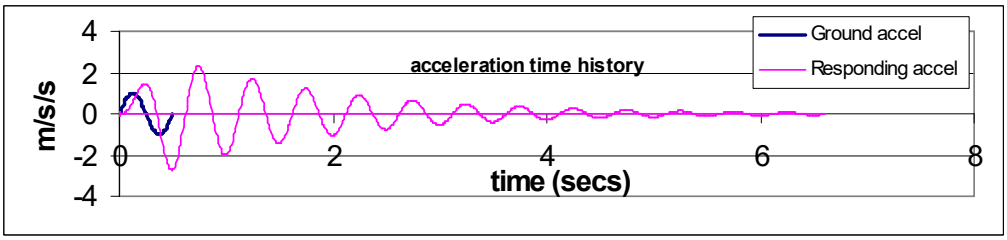


Figure 6. Example SDOF system (T = 0.5s, ζ = 0.05) responding to a ground pulse

Ground motions generated by an earthquake are non-stationary and random in nature, and so irregular that a closed-form analytical solution to the equation of motion is not feasible. Numerical methods, therefore, are used to model response behaviour. Once the deflection time-history has been evaluated using dynamic analysis, internal forces can be found by a quasi-static analysis of the structure at any snapshot of time.

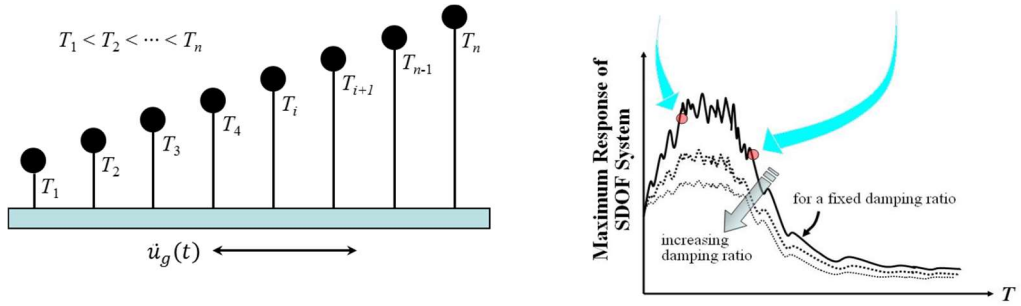
2.3 Response Spectral Acceleration (RSA) and Response Spectrum (RS)

In the design process, structural engineers are concerned mainly with peak values of the structural response, expressed in terms of displacements, forces and moments. The concept of an earthquake response spectrum (RS) serves this purpose well. The RS is a convenient means of presenting the estimated peak values for the whole range of linear elastic SDOF systems in response to earthquake ground motion, as shown in Figure 7(a). RS is a plot of the maximum absolute response values, expressed as a function of the system's natural vibration period T, (or a related parameter such as angular frequency ω_n, or cyclic frequency f_n). Each plot is based on a particular damping ratio ζ. Multiple plots can be shown in the same diagram to represent behaviour associated with the range of values of ζ typically encountered in real conditions, as shown in Figure 7(b).

In structural design, the quantity of interest is the maximum (absolute) acceleration response of the lumped mass, $max|\ddot{u}^t(t)|$, to the earthquake load. This quantity is commonly referred to as the response spectral acceleration (RSA). A series of acceleration RS (for different structure damping ratios) is presented in Figure 8, based on the base excitations defined by the well known ground motion accelerogram recorded at El Centro in southern California in 1940.

2.4 Idealised Elastic Response Spectrum (ES)

Idealised elastic response spectrum, which can be abbreviated as "Elastic Spectrum" (ES), allows the analysis and design of a structure, as prescribed in a typical code of practice for seismic design of building structures. An ES should ideally be representative of earthquake ground motions that are likely to occur at the site of interest. The direct use of an RS calculated from actual accelerograms recorded from earthquakes is, however, inconvenient for such a purpose, because the spectral shape is highly irregular, featuring sharp fluctuations in spectral values over small changes in the structural period *T*. Thus, for practical design purposes, the ES should consist of a set of smooth curves and/or straight lines containing one curve for each level of damping. The idealisation of the response spectrum is therefore essential for practical application.



(a) Family of SDOF Damped Oscillators (b) Response Spectrum (RS)

Figure 7. Concept of Response Spectrum (RS)

The mean RS obtained from an ensemble of earthquake ground motions is much smoother than the RS of an individual accelerogram, as shown by the solid line example in the schematic diagram of Figure 8. The mean RS is accordingly idealised as a "plateau" at low natural periods and as a "hyperbolic curve" at higher periods. At the zero natural period (representing an infinitely rigid structure), the acceleration of the structure, in theory, is identical to that of the ground. The peak acceleration at the centre of mass of the structure is accordingly equal to the peak ground acceleration (*PGA*) in which case the spectral ratio equals unity. As the natural period of the structure (*T*) increases slightly, the spectral value increases rapidly until the "plateau" is reached. The ratio of the spectral value at the plateau to the PGA value is typically of the order of 2.5. In practice, a conservative approach is recommended and the "plateau" is extended to the natural period zero axis. This is because of the unpredictable nature of the response spectrum at very low periods, coupled with the uncertainties associated with estimating building natural periods.

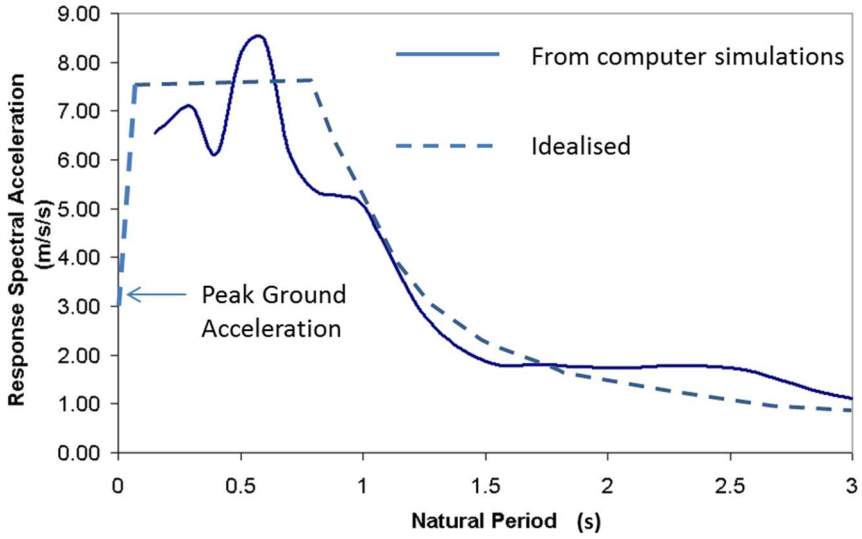


Figure 8. Example response spectrum of accelerogram recorded at 1940 El Centro, southern California, United States

Deriving an ES can be more complicated for sites subject to a variety of seismic sources, e.g. low-period (high-frequency) motions from nearby small earthquakes and high-period (low-frequency) motions from distant moderate to large earthquakes (Tsang 2015). An alternative way of determining an ES is to compute a uniform hazard spectrum (UHS), whereby each spectral ordinate is based on a probabilistic seismic hazard assessment (PSHA) procedure which takes account of contributions from all potential earthquake sources. Such a UHS has a uniform (or constant) probability of exceedance at all values of T. A UHS is effectively the ES enabling the production of structural designs all with the same probability of failure irrespective of the assumed value of T for the structure.

Using the method described above, parameterisation is required, if a consistent ES format is to be applied to a country or a region. In the following sections, parameterisation schemes incorporated in various major codes of practice around the globe are introduced.

From static analysis, RSA is related to peak base shear values $(V_b)_{max,}$ i.e. the equivalent static force $F_{max,}$ by:

$$(V_b)_{\max} = F_{\max} = mRSA = w\frac{RSA}{g} \tag{5}$$

where w is the seismic weight of the structure and g is the gravitational acceleration (9.81 m/s^2).

When written in this form, RSA/g may be interpreted as the base shear coefficient or lateral force coefficient (in units of g). The RSA (or RSA/g) parameter is used in building codes as the coefficient by which the structural weight is multiplied to obtain the design base shear force. A RS is therefore very useful in design because the manner in which structures of different natural periods of vibration will respond to a specific earthquake ground motion model can be found readily.

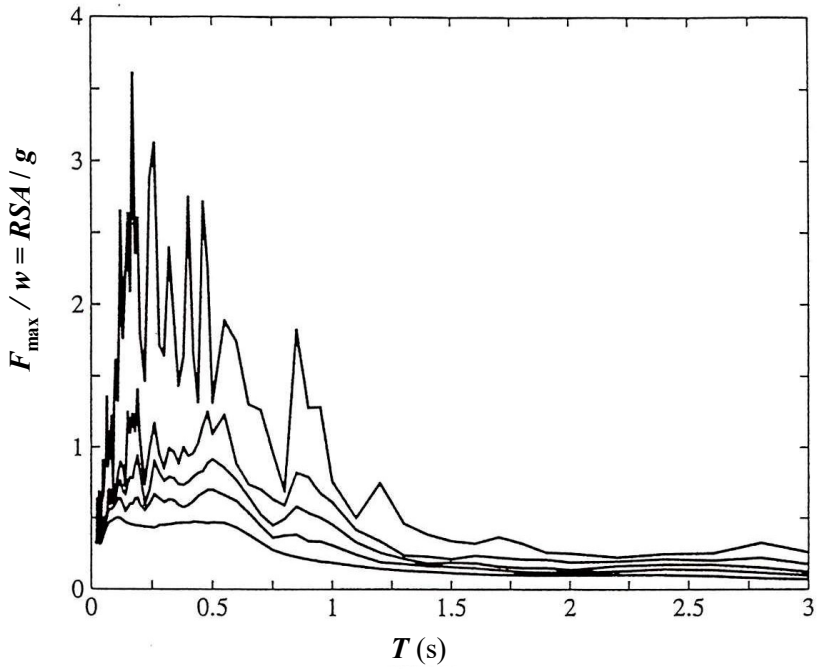


Figure 9. Normalised acceleration, or base shear coefficient, response spectrum for El Centro ground motion; ζ = 0, 2, 5, 10, and 20%. (reproduced from Chopra 2017)

2.5 Peak Ground Acceleration (PGA)

The ES specifies the design ground motions or equivalent static loadings for structural analysis and design. Thus, the seismic hazard level of the site should be reflected in the spectral parameters characterising the ground motion. In an acceleration RS, either the peak ground motion measurements (PGA or PGV) or spectral acceleration values at certain natural period(s) of vibration, *RSA(T)*, can be used as scaling parameter(s). The literal meaning of the term peak ground acceleration (PGA) refers to the highest (or lowest) point on one of the peaks (or troughs) in a recorded ground acceleration time-history, which can be ultra sensitive to high frequency signals (noise) in the record even though such noise only has a very minor influence on structural response behaviour. The implication is that the *PGA* value can be lowered considerably by artificially removing all the (tall and sharp) "spikes" from the record, knowing there can be little effect on the potential response behaviour of the structure. It is widely recognised that the maximum response spectral value (RSA_{max}), the highest point on the acceleration response spectrum, is much better correlated with the potential earthquake hazard than the *PGA* value. The term "effective PGA" (EPGA) which is defined herein as RSA_{max} divided by a dynamic amplification factor (typically 2.5 or 2.75) has been used by codes of practice to characterise the intensity of ground shaking. Similar terminology such as hazard factor (Z), or acceleration coefficient (a_g), which are similar in meaning to *EPGA*, have also been used to characterise city seismic hazard levels.

Each region, typically the size of a city, is assigned a set of parameters for ES construction purposes, stipulated in the relevant codes of practice. Each of the key parameters, e.g. PGA, is presented as a zonation map, or a table in which the parameter values are listed for the individual towns/cities concerned.

PGA has been used as the scaling parameter for constructing ES in the following major codes of practice:

- Chinese Code for Seismic Design of Buildings, GB 50011 (2010)
- Eurocode 8, EN 1998-1(2004) or CEN (2004),
- Australian Standard, AS 1170.4 (2007) or SA (2007) and
- New Zealand Standard, NZS 1170.5 (2004) or SNZ (2004).

2.6 Ground Motion Models (GMMs)

A RS based on averaging RSA accelerogram values can be used to represent the potential hazard of a particular earthquake scenario, defined in terms of a magnitude-distance (*M*-*R*) combination along with the site class. For example, a RS can represent the effects of ground shaking by a magnitude 6 earthquake at a distance of 20 km on stiff soil sites (i.e. M6 at R = 20 km for stiff soil sites). The RS changes with the magnitude and/or distance. Mathematical expressions providing predictions of the RS as a function of *M*, *R* and site class (and faulting mechanism with certain GMMs) are called *Ground Motion Prediction Equations* (GMPEs). To develop a GMM, or GMPE, statistical analysis of the RS values based on an ensemble of earthquake ground motions are commonly used to develop the earthquake loading model. Earthquake records are then sorted in accordance with the design parameters: earthquake magnitude, site-source distance, faulting mechanism and site soil conditions. This approach to the development of a ground motion model is only feasible for heavily instrumented, tectonically active, regions where strong motion records of shallow earthquakes are in abundance. Thus, conventional GMMs have been developed mainly from strong motion accelerogram data collected in tectonically active regions in western North America. For a reference site class, an ES can be based on a range of possible earthquake scenarios (i.e. possible *M*-*R* combinations) related to the various identified fault sources surrounding the city. A reference site class is the most common class of site existing in a city, enabling the maximum number of common site condition accelerograms to be included in the database for statistical analyses. Empirical GMPE models developed in western North America typically relate to "stiff soil sites" as most data collected applies to such site conditions (Boore et al. 2014; Abrahamson et al. 2014; Campbell and Bozorgnia 2014; Idriss 2014; Chiou and Youngs 2014). The most reliable model predictions relate to this reference site class.

In other regions, such as tectonically stable regions of low to moderate seismicity, the process of developing a GMM is hampered by the lack of local earthquake records. An alternative approach, that of stochastic simulations of the seismological model, which includes the generation of artificial earthquake accelerograms has become the commonly-adopted approach in stable continental regions such as Central and Eastern North America. The seismological model itself is partly based on theoretical principles and partly on the analysis of seismogram data recorded during small magnitude earthquakes and tremors originating at long distances. (see literature review of articles on stochastic simulations of the seismological model (e.g. Lam et al. 2000)). Rock site seismological models, for areas of low to moderate seismicity, are more reliable than soil site models. The program GENQKE implements rock site stochastic simulations (Lam 2002). More detailed descriptions of ground motion modelling in tectonically stable regions of low-to-moderate seismicity are given in Section 4, below.

2.7 Probabilistic Seismic Hazard Analysis (PSHA)

To develop an ES, it is necessary to integrate an RS associated with a range of earthquake scenarios, for the reference site class concerned, as predicted by a GMPE. The integration procedure involves numerical simulations based on the established principles of conditional probability and is known as probabilistic seismic hazard analysis (PSHA). Most PGA or hazard factor values stipulated as standards for seismic actions are based on PSHA results. Thus, an ES cannot be associated with a particular earthquake scenario nor with any particular accelerogram. Consequently, it is inappropriate to simulate earthquake ground motions based on an ES. The PSHA procedure which is typically undertaken by seismologists and risks analysts, using specialist software, comprises the following calculation steps in deriving the Design PGA and ES for a city:

1) Identifying potential fault sources around the city
2) Modelling the recurrence behaviour of earthquakes relating to each identified fault source
3) Modelling the GMPE for different ranges of M-R combinations
4) Integrating contributions from one or more sources having influence on the hazard of the city

PSHA results based on the use of GMMs derived for tectonically active regions cannot automatically be taken as representative of places in tectonically stable regions such as Central North America, Australia, and Southern India. Thus, alternative GMMs developed for intra-plate seismo-tectonic environment need to be sought for realistic hazard predictions in areas of low to moderate seismicity.

2.8 Uniform Hazard Spectrum (UHS)

ES is normally constructed based on one to two spectral values (RSA(T) or PGA) according to the standard spectral shape as specified in codes of practice. The single-parameter or dual-parameter scaling approach has been adopted because PSHA was typically conducted for PGA (and sometimes PGV) only, partly because GMPEs were only available for PGA (and PGV) in the 1960's and 1970's. The resulting ES, adopted in many current codes of practice, does not have a uniform probability of exceedance (PE) at all natural periods of vibration.

Importantly, UHS takes account of seismic hazards from all potential seismic sources surrounding the site. Normally, low-period spectral values of the UHS are attributable to near-source (moderate) earthquakes, whereas the high-period end reflects the potential hazard from more distant (larger) earthquakes. The spectral shape of the UHS is therefore usually not consistent with that of an RS from any recorded accelerogram. Since the 1990's, the concept of the uniform hazard spectrum (UHS) has become commonly accepted, for the construction of site-specific ES when GMPEs are normally used for predicting RSA values across the entire range of natural periods of the building. The response spectral ordinates for a range of periods of oscillation are computed using the same PSHA procedure. The advantage over the scaled-spectrum approach is the uniform (and constant) PE at all structural periods, hence representing region-specific, and site-specific, frequency content more accurately.

The International Building Code (2015) (B 2015) adopted in the United States (abbreviated herein as IBC), gives RSA values at natural periods of 0.2 s and 1.0 s as scaling parameters for constructing the ES. Such a dual-parameter approach represents an

attempt to mimic the shape of the UHS. In the 2015 version of the National Building Code of Canada (NRC 2015) abbreviated herein as NBCC, PGA and RSA values, at natural periods of 0.2, 0.5, 1.0 and 2.0 s which make up a total of five parameters for constructing an ES closely matching the shape of the UHS. Contour maps for Canada, for each of the five parameters, have been published.

3. Elastic response spectrum (ES) models in codes of practice

3.1 International building codes of the united states (IBC 2015)

In IBC (2015), the ES is specified as in Figure 10. Apart from the RSA values at natural periods 0.2 s (S_s) and 1.0 s (S_1), the site coefficients F_a and F_v, are two other scaling parameters which take site effects into account for the low period and high period ranges respectively. Further information on site coefficients is provided in the next section. The 'corner' period T_1 is determined on the basis of the four scaling parameters.

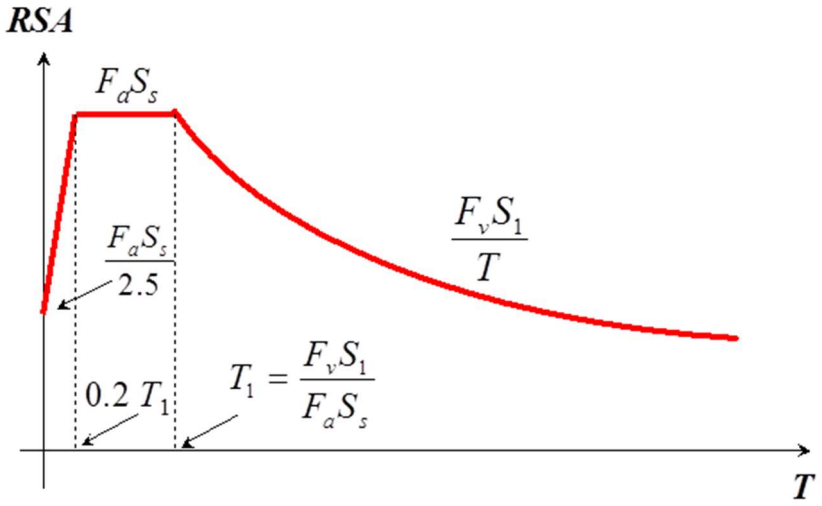


Figure 10. The format of ES adopted in IBC

The ES in the IBC comprises three parts which closely follow the spectral shape of the idealised RS as shown in Figure 8:

1) A linearly increasing line from PGA at $T = 0$ to RSA_{max} at $0.2T_1$.
2) A flat part at RSA_{max} from $T = 0.2\ T_1$ to $T = T_1$.
3) A decreasing curve, as a function of $1/T$.

As stated in the ASCE/SEI Standard 7-16 Minimum Design Loads for Buildings and Other Structures (ASCE/SEI 2016), another corner period T_2 ($\geq$ 4.0 s) is specified in the ES, beyond which, the values of RSA follow a curve which features the rate of decrease of $1/T^2$ in response spectral values.

3.2 The Chinese code (GB 50011-2010)

In Chapter 5: Earthquake Action and Seismic Checking for Structures – Section 5.1 of the Chinese Code (which is abbreviated herein as "GB"), the ES is specified with a detailed description and the required equations. Unless otherwise specified, the structural damping ratio is set at 5% of critical damping.

The ES in GB comprises four parts as follows:

1) A linearly increasing line from PGA at $T = 0$ to RSA_{max} at 0.1 s.
2) A flat part at RSA_{max} from $T = 0.1$s to $T = T_1$. The characteristic period T_1 is discussed below.
3) A decreasing curve as a function of $1/T^{0.9}$ is adopted between $T = T_1$ and $T = 5\ T_1$.
4) A decreasing linear function is adopted between $T = 5\ T_1$ and $T = 6.0$ s.

The spectral shape of the ES in GB is broadly consistent with the idealised ES shown in Figure 8. There are two major differences:

a) the hyperbolic curve of decay between $T_1 < T < 5\ T_1$ has a smaller exponent (=0.9) than the unity (=1.0) of the idealised ES;
b) for $T > 5\ T_1$, the linear rate of decrease of spectral values is more gradual than the rate of decay defined by $1/T^{0.9}$.

Both modifications result in higher spectral values in the long-period range, mainly taking account of the more conservative estimates of design loadings, as well as the larger uncertainties relating to ground motion characteristics at high natural periods of vibration exceeding 1.0 s.

The characteristic (corner) period T_1 is another scaling parameter used in constructing the ES based on GB. The ES in GB is regionally dependent as well as site class dependent. The characteristic (corner) period T_1 is primarily based on the design earthquake group (reference site class II). Based on this classification scheme, each grid is specified by the value of T_1 shown on the zonation map.

3.3 Other major codes of practice

In the Australian Standard (AS1170.4 2007) and in Eurocode (EN1998-1 2004), abbreviated herein as "AS" and "EC" respectively, the spectral shape of the ES follows the ASCE/SEI Standard exactly. The second corner period T_2 is set at 1.5 s and 2.0 s (Type 1) respectively.

In the New Zealand Standard (NZS1170.5 2004), the ES hyperbolic curve of decay is divided into three parts. The function of $1/T^{0.75}$ up to 1.5s is followed by a function of $1/T$ up to 3.0s and a function of $1/T^2$ beyond 3.0s. That is, the second corner period T_2 is set at 3s.

In NBCC (2015), the exact UHS spectral values have been adopted in constructing the reference site ES (firm soil) condition, with all spectral ordinates having a uniform (or constant) probability of exceedance. As the spectral ordinates are determined directly for each geographical location, the spectral shape is controlled by the seismicity pattern at the specific location. There is no spectral shape consistent across the whole of Canada.

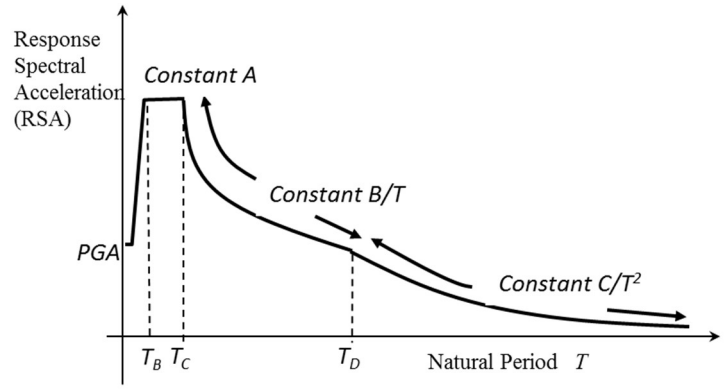
4. Concepts of particular relevance to low to moderate seismicity regions

4.1 Classical response spectrum model

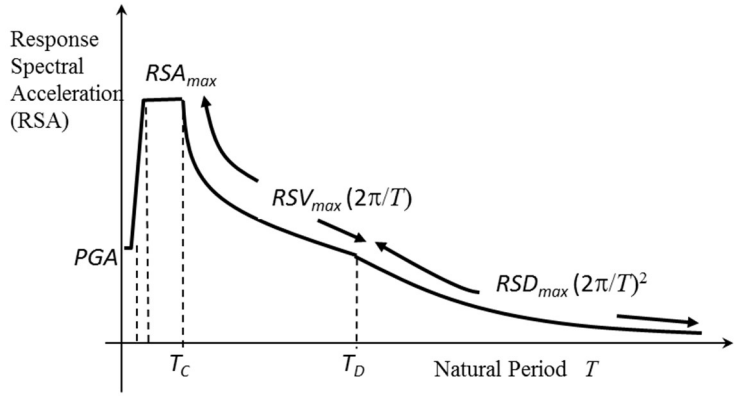
The classical response spectrum model developed originally by Newmark and Hall (1982) was intended to be generic in nature but most codes of practice have not adopted the classical model in which the ES is divided into the three zones of acceleration, velocity and displacement control (Figure 11a). Displacement controlled behaviour is typically not

featured in code models. But in regions of low to moderate seismicity, characterised by moderate intensity ground shaking, it is particularly important to feature displacement controlled behaviour in the ES. This is because of the limited displacement of the ground that is generated by small and medium-sized earthquakes. The drift demand of a high period structure can be predicted directly by reference to the peak response spectral displacement (RSD_{max}) and the step of estimating seismic forces as is done conventionally can be bypassed. By similar reasoning, the drift demand of a low period structure can be predicted directly by reference to the peak response spectral acceleration (RSD_{max}) and peak response spectral velocity (RSD_{max}) (Figure 11b).

The physical meaning of the classical model can be easily understood if the ES is presented in multiple formats namely the acceleration, velocity and displacement format. Standards and Codes of practice for structural design typically present an ES in the acceleration format only in which the RSA value (variable on the vertical axis) is presented as a function of the natural period (T) of the structural system (variable on the horizontal axis). In a similar manner, the velocity format has the response spectral velocity (RSV) presented as a function of T where RSV is indicative of the maximum relative velocity developed in the system during the course of ground shaking. Similarly, the displacement ES format features the use of the response spectral displacement (RSD), presented as a function of T. Eqs. (6a) – (6c), defining the relationships between RSA, RSV and RSD, can be approximated by applying the basic principles of mechanics.



(a) Typical code format



(b) Response spectral maxima parameterisation

Figure 11. The three zones of an elastic response spectrum (ES)

$$RSV = RSA \times \frac{T}{2\pi} \tag{6a}$$

$$RSD = RSV \times \frac{T}{2\pi} \tag{6b}$$

$$RSD = RSA \times \left(\frac{T}{2\pi}\right)^2 \tag{6c}$$

Eqs. (6a) & (6b) can be derived by equating kinetic energy with the energy of absorption of a linear elastic system (Eq. 7a & 7b). The derivation of these equations makes use of the well-known relationship, Eq. 7c, from which the natural period of vibration (T) can be found when the mass (m) and stiffness (k) of the system are known.

$$\frac{1}{2} mRSV^2 = \frac{1}{2} \frac{F^2}{k} \tag{7a}$$

$$\frac{1}{2} mRSV^2 = \frac{1}{2} kRSD^2 \tag{7b}$$

$$T = 2\pi \sqrt{\frac{m}{k}} \tag{7c}$$

where the term on the RHS of Eqs. (7a) and (7b) represents the area enclosed by the triangular force-displacement diagram.

It is shown in Figure 12(a) that the hyperbola in the acceleration (RSA) format is a flat line in the velocity (RSV) format of Figure 12(b). The constant velocity demand shown in the figure correlates directly with the peak ground velocity (PGV). Similarly, the hyperbola in the RSV format is a flat line in the displacement (RSD) format of Figure 12(c). The constant displacement demand shown in the figure relates directly to the peak ground displacement (PGD). Thus, any part of the ES has the response spectral behaviour characterised by some form of period insensitivity, which is a very useful observation from the design practice perspective, given the difficulties in predicting the natural period of vibration of real buildings. In other words, the constant (and maximum) values of RSA, RSV and RSD are functions of the PGA, PGV, and PGD of the ground shaking as shown by Eqs. 8(a) – 8(c).

$$RSA_{\max} = \alpha_A \cdot PGA \tag{8a}$$

$$RSV_{\max} = \alpha_V \cdot PGV \tag{8b}$$

$$RSD_{\max} = \alpha_D \cdot PGD \tag{8c}$$

where the value of α_A and α_V is typically in the range: 2.5 – 3.0 and 1.8 – 2.0 respectively; and α_D has been recommended a value of 1.4 by Newmark & Hall (1982).

The fourth format correlating *RSD* (in the horizontal axis) with the RSA (in the vertical axis) is called the acceleration-displacement response spectrum (ADRS) diagram. The construction of this diagram is illustrated in Figure 13.

Ideally, the three ground motion parameters: PGA, PGV and PGD would be better

obtained independently in order to provide an accurate estimate of the ES, which is characterised by values of RSA_{max}, RSV_{max} and RSD_{max}. When sufficient information is not available the following rules of the thumb (Eqs. 9(a) – 9(c)) may be employed to help construct the ES on rock sites, say, to model the effects of a local earthquake not more than 50 km from the epicentre.

$$RSA_{\max} = RSV_{\max} \times \frac{2\pi}{T_1} \quad \text{where} \quad T_1 = 0.3s \tag{9a}$$

$$RSD_{\max} = RSV_{\max} \times \frac{T_2}{2\pi} \quad \text{where} \quad T_2 = 0.5 + \frac{M-5}{2} \tag{9b}$$

M is the moment magnitude of the earthquake

A T_2 value of 2.0 s is a reasonable, and conservative, assumption to make for local earthquakes occurring in intra-plate regions of low to moderate seismicity. The listed rules-of-thumb infer RSA_{max} (g's) as 4 times PGV (mm/s) divided by 1000; RSV_{max} (mm/s) as 1.8 times PGV (mm/s); and RSD_{max} (mm) as 0.6 times PGV (mm/s). Thus, the RS can be constructed in the different formats described above once the value of PGV is known. If only the PGA value is known, the rule-of-thumb conversion of PGV (mm/s) = 750 times PGA (g's) may be applied.

In the following example, a classical ES model is to be constructed for a city with a PGA value of 0.08g, say. The following inferences can be drawn: PGV = 60 mm/s, RSA_{max} = 0.24g, RSV_{max} = 108 mm/s and RSD_{max} = 36 mm based on T_2 = 2s (only 25 mm approximately in the case of Australia as T_2 = 1.5s is assumed).

Intuitively, the *RSA* format is convenient to use when designing low rise (low period) buildings whereas the RSV, and RSD formats, are convenient when designing medium rise, and high rise, buildings respectively, Period insensitivity in the ES is a useful phenomenon that can be utilised for circumventing challenges associated with uncertainties over the predicted natural period of vibration of a building structure.

Although structural engineers would typically ignore contributions by non-structural components (NSC) such as facades and partitions to the potential response behaviour of the building, there are concerns that NSC can result in a lowering of the natural period of the building thereby increasing the seismic forces applied. But to include the effects of NSC in the analysis can be time-consuming and would also introduce many uncertainties in the analysis of building behaviour. If the building is acceleration (force) controlled, the influence of the NSC needs not be considered when estimating the seismic forces given the insensitivity of seismic force applied to changes in the value of *T*.

By the same argument, if the building is sufficiently slender and tall (in order that its behaviour in seismic conditions is displacement controlled) the influence of the NSC need not be considered when modelling the building drift demand. If the building is velocity (energy) controlled the influence of the NSC on the kinetic energy demand also need not be considered, where estimates of energy demand can be made using the left-hand side of Eqs. (7a) and (7b) along with a constant *RSV* value. Given that the kinetic energy is known, the seismic force demand, and drift demand, of the building can be estimated accordingly, for the given mass and stiffness properties of the building in the structural model when contributions by NSC are ignored. In conclusion, the notion that the NSC increases the force, and drift, demand of the building in seismic conditions is a myth. Engineers with the skills to employ displacement, or energy, principles in the seismic analysis of a building

should be able to circumvent this issue. However, the influence of NSC on the potential failure mechanism of the adjoining structural element can be real.

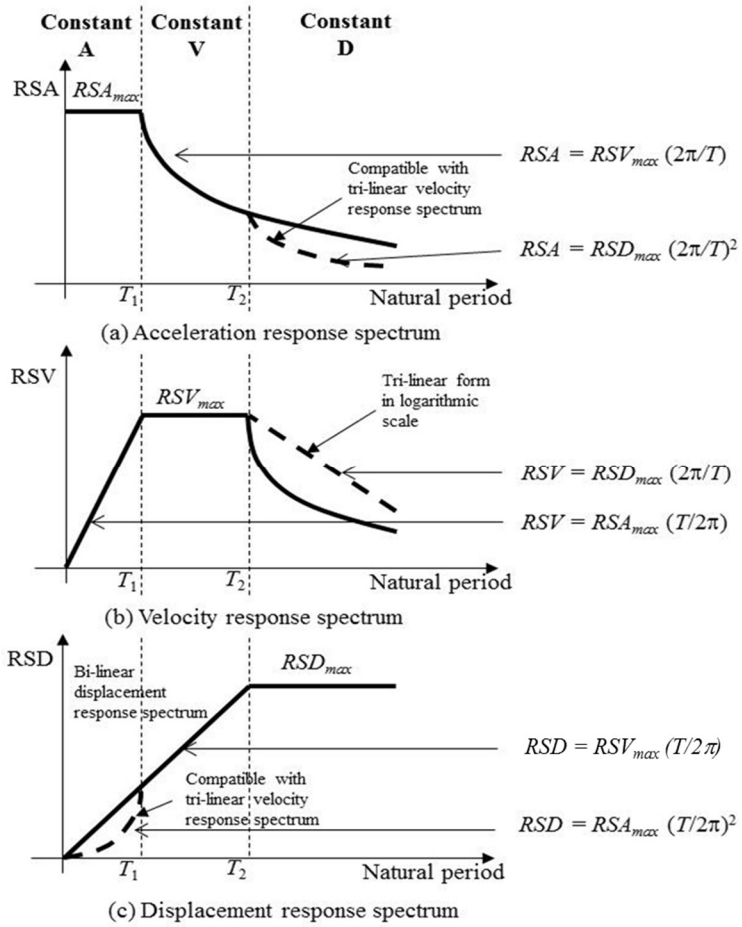


Figure 12. Elastic response spectrum (ES) model in acceleration, velocity and displacement formats

4.2 Minimum design seismic hazard

In regions of low to moderate seismicity, the number of historical earthquake events with a magnitude, M > 4, exceeding the structural damage threshold, are few in number. The main concern with probabilistic seismic hazard modelling analysis is an underestimation of seismic hazard in areas where no local seismic activity appears in the historical record and no fault structure has been found. Consequently, such areas can be assigned a nominal level of seismic hazard. Examples of such areas can be found in many parts of Australia, Peninsular Malaysia and the island of Sri Lanka. Intra-plate seismicity, by definition, exists in all areas distant from tectonic plate margins. Thus, earthquake events are assumed to be possible at virtually any place on earth (Bird 2010; Okal & Sweet 2007). Some of these areas may show little sign of activity because the period of observation is not sufficiently long or because the catchment area is too small. To define areas in an intra-plate region where earthquake tremors have never been recorded as "earthquake free", significantly discounts the actual underlying hazard, and risk. For example, for Peninsular Malaysia, where no $M > 5$ event has been recorded in the past 50 years the level of seismicity cannot be discounted to zero. The same argument applies to

the island states of Singapore and Sri Lanka. Unfortunately, there is no general consensus over the minimum threshold (baseline) hazard to adopt for structural design purposes in these areas, to allow for intra-plate seismicity.

A new form of investigation involving a global survey of the frequency of local earthquakes in intra-plate regions found that 5 - 10 earthquakes exceeding magnitude 5 occur in a normalised land area of one million square kilometres in a 50 year period. In view of the uncertainties it is considered prudent to use the larger count of 10 for calculation of background seismic hazard. The normalised count of events exceeding M5.5 was accordingly taken as 3-4. Going by this trend, only one event exceeding M6 is predicted. Clearly, the background hazard is mostly contributed to by small events of up to M5.5. Earthquakes of this order of magnitude can be generated by the rupturing of faults over a length not exceeding 5km. Thus, a geological survey of known faults, as a means of modelling background seismic hazard is not viable, given the difficulties of detecting potential fault sources which are small. The relevant period for this counting scheme could not have been longer than 50 years because of the paucity of historical data in regions which are not active. Thus, a large normalised area (of 1 million square kilometer) was used to compensate for the short time span of the survey (Lam 2016).

The rate of occurrence has been found to translate to an *EPGA* value of 0.1g for a RP of 2500 years, or 0.07g for a notional RP of 500 years which is taken typically as the hazard factor in earthquake loading standards. The design ground motion intensity of ordinary buildings is based on this hazard factor. The associated ES is then modified in accordance with the site classification to take account of soil amplification effects. Recommendations from the literature around the globe supporting this level of minimum hazard are summarised in Table 1.

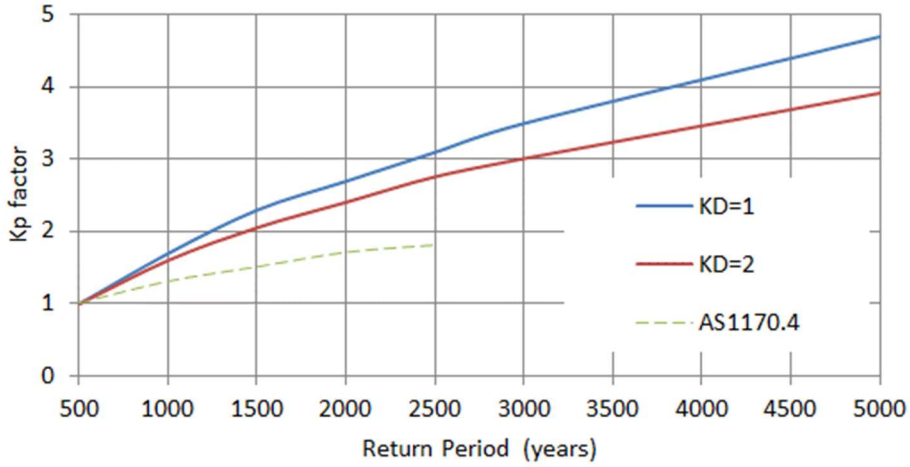
4.3 Behaviour of ground motion intensity with increasing return period

Calculations for the EPGA values were then repeated for return periods up to 5000 years. *RSA* values that have been normalised with respect to the 500 year reference RP value are presented in Figures 14a and 14b in the form of return period (K_p) factors for comparison with recommendations in codes of practice (e.g., AS1170.4 2007). It is shown that the value of K_p for a return period of 2500 years is of the order of 3.0, to be compared with the code specified value of 1.8. K_p values calculated for 0.3s and 1.0s periods show similar comparisons.

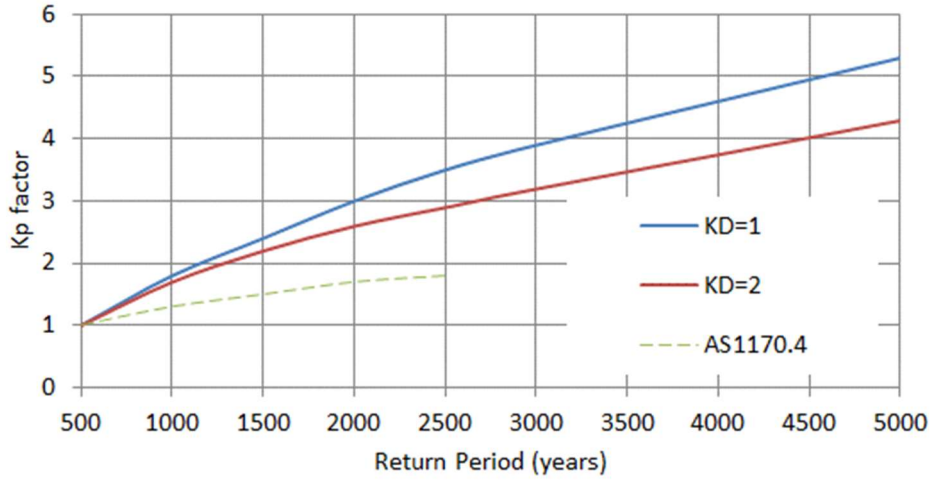
It is stated in the footnote attached to Clause 2.1 in Eurocode 8 – Part 1 that ground motion intensity in a rare earthquake event, consistent with a 10% chance of exceedance for a design life of 50 years (i.e. return period of 475 years) is recommended for the design seismic action. It is noted that this recommendation was drafted in the late 1990's at a time when it was still the norm not to consider return periods exceeding 500 years in the design of structures supporting ordinary buildings. Implicit in the no collapse (NC) performance criterion is that the building is expected to have sufficient additional reserve capacity to sustain a very rare, and extreme, earthquake event without experiencing wholesale collapse (Fardis 2009).

Seismic actions to be considered for design purposes are based on a return period of 2500 years when fulfilling the performance criterion of collapse prevention, and then scaled down by a factor of 2/3 (reciprocal of 1.5) for fulfilling the NC, or life safe, performance criterion (Fardis 2009). In a high seismicity region, the scaled-down intensity of ground shaking would be close to the intensity corresponding to a RP of 475 years. It is shown in Figures 14a and 14b that the scaled-down intensity could be a great deal higher

than the intensity corresponding to a RP of 475 years. Thus, the term "notional return period" is introduced herein to refer to the scaled down intensity which may or may not be consistent with the intensity corresponding to a RP of 475 years.



(a) 0.3s period



(b) 1.0s period

Figure 14. Return Period Factor M_{min} = 4 and M_{max} = 7 (response spectral values are based on 5% viscous damping)

Table 1. Recommendations derived from the literature on minimum seismic hazard

Ref.	Literature References	Comments / Recommendations
1	Mulargia, Stark & Geller (2017)	"The insufficiency of the available seismicity data means that it is highly questionable that PSHA can provide reliable and accurate hazard analyses".
2	Lam, Tsang, Lumantarna & Wilson (2016)	Minimum design PGA value of 0.07g is recommended for stable regions.
3	Wilson (2015)	Minimum design PGA value of 0.08g is recommended for the stable region of Australia.
4	Tongkul (2016)	Design PGA value of 0.05g – 0.1g is recommended for Peninsular Malaysia and Sarawak.
5	Pinto (2000)	Minimum design PGA value of 0.07g – 0.1g.

4.4 Ground motion models for different tectonic and crustal classifications

The Next Generation Attenuation of eastern North American (NGA-East) database comprises 29000 records from 81 intra-plate earthquake events recorded at 1379 stations (PEER 2015). Ground Motion Models (GMMs) derived from this database, which is currently the most elaborate intra-plate earthquake database, should be taken as indicative of the intrinsic source characteristics of earthquakes generated in an intra-plate environment. A literature review of seismological ground motion model studies in *Eastern North America* (ENA) identified some 40 models developed in the period 1983-2014 (PEER 2015). Many of these models are seismological models requiring stochastic simulations to transform them into GMMs for engineering applications. A subset of 22 models was selected based on the quality and age of the data. Further screening managed to reduce the 22 models to 6 representative models (PEER 2015). The point source simulation models of Atkinson and Boore (1995), Boatwright and Seekins (2011) and Boore (2010), abbreviated herein as AB95, BS11 and BCA10d respectively have been found to generate ground motions that are the most consistent with recorded data.

An independently developed GMM by Darragh et al. (2015), abbreviated herein as *DASG15*, as introduced in PEER (2015), has also been constructed from a seismological model, derived more recently from the broadband inversion of the *NGA-East* database. Good consistencies have been observed with predictions by DASG15 and AB95 whereas other GMMs such as those developed by Shajouei and Pezeshk (2015) and Pezeshk et al. (2015), abbreviated as *SP15* and *PZCT15* respectively, are not as consistent.

The crustal conditions of tectonically stable regions can either be shield (or cratonic) or non-cratonic for a range of regions around the world. It is shown that two tectonically stable regions can have different crustal classifications. For example, the crustal conditions in Southeastern Australia and Peninsular Malaysia are much closer to those of California than of Central North America. Most ground motion data used to develop ground motion models of NGA-East were collected from the shield crustal region of Central North America (i.e., region 2 as defined in chapter 1 of PEER2015/04). However, it is a mistake to consider NGA-East models to be automatically suited for application across all intra-plate regions. Adapting GMMs for use in low-to-moderate seismicity

countries must take into account factors controlling (a) the wave generation behaviour at the source of the earthquake in a given tectonic setting and (b) the wave modification behaviour of the earth's (basement rock) crust. These are not to be confused with the modification behaviour due to near-surface sediments. Most of the GMMs of NGA-East are implicitly representative of shield, or cratonic, conditions, which are identified with negligible modifications to seismic waves as they propagate up the crustal layers. In contrast, a GMM model adopted for use in non-cratonic regions requires substantial modification to take account of the wave amplification and attenuation within the upper 3 – 4 km of the earth's crust.

The authors have experience of combining the source model of AB95 with the (non-cratonic) crustal model of generic rock (Boore and Joyner, 1997, abbreviated herein as BJ97) for predicting ground motions generated by intra-plate earthquakes in what has been described as the Component Attenuation Model framework (Lam et al. 2000; 2010). The crustal model of BJ97 has since been made more versatile by parameterising the V_s (30 m) value as an input parameter (Chandler et al. 2005; Boore 2016) in order that any crustal velocity profiles that are intermediate between the classical generic rock and generic hard rock limits can be incorporated into an existing ground motion simulation framework. An alternative crustal velocity profile modelling approach has also been developed for various crustal conditions (Chandler et al. 2005; 2006a). Simulated RSA values for the non-cratonic version of AB95 based on the classical generic rock class of Boore and Joyner (1997) are representative of non-cratonic regions. The credibility of those simulations under the framework of the Component Attenuation Model has been established by demonstrating agreement with field observations from different countries (expressed in the form of Intensity data) as shown in some earlier journal publications by the authors and their co-workers over the years (e.g., Chandler and Lam 2002; Chandler et al. 2006b; Lam et al. 2003 & 2006; Tsang and Lam 2010; Yaghmaei-Sabegh and Lam 2010). Predictions by the (non-cratonic) model can be significantly higher than the upper limit of predictions by the NGA-West2 models. Thus, the use of NGA-West2 models or NGA-East models in PSHA could result in the seismic hazard being understated in tectonically stable, and non-cratonic regions, such as Southeastern Australia, Malaysia and a large part of China.

5. Site classification and soil response spectra

Zoning maps of certain parameters, as shown in the previous section, specify only one value for each region of the grid. Such a value represents the hazard level of an average (or reference) site in the region. The site-to-site variability of design ground motions has to be taken into account by scaling parameter(s). In codes of practice, a site can be classified into a number of pre-defined site classes, and site effects are commonly related to a reference site class.

Generally, site effects characterise the filtering mechanisms and superposition of reflected waves within the soil sedimentary layers overlying the bedrock. Ground motions can be significantly modified, in terms of amplitude and frequency content, as seismic waves propagate through the near-surface sedimentary layer. The degree of site effects mainly depends on the level of shaking, the thickness of the soil layer, and the properties of the soil (e.g. shear modulus and plasticity) as well as the bedrock materials underneath (shear modulus mainly).

Site effects can be conveniently observed on response spectra. Figure 15 shows the

acceleration RS recorded on rock and soil sites, respectively, at Oakland Outer Harbour in the 1989 earthquake at Loma Prieta, California, United States (Dickenson et al. 1991). It is clear that the spectral acceleration values are a few times larger on a soil site than on a rock site. The amplification ratio is of the order of four times for the peaks at 0.7 s. Such significant effects have to be properly taken into account in constructing ESs based on codes of practice.

In situations where a distinct soil-rock interface exists, the amplification ratio usually has its maximum value at the site natural period of the soil layer (T_S), which can be estimated using Eq. (10) if the thickness (d_i) and shear wave velocity (SWV) ($V_{s,i}$) of the individual soil layers are known. Alternatively, the value of T_S can be expressed in terms of the total thickness of the soil layers (H_S) and their weighted average SWV (V_S) as shown in Eq. (10).

$$T_S = \sum_{i=1}^{n} \frac{d_i}{V_{s,i}} \times 4 = \frac{4H_S}{V_S} \tag{10}$$

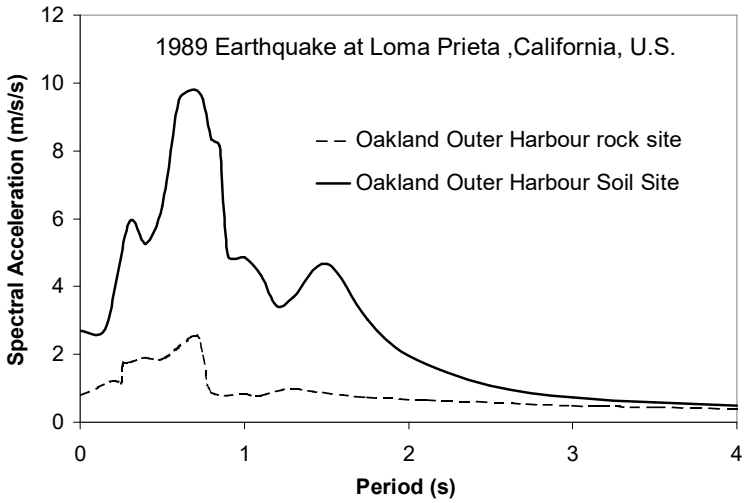


Figure 15. Acceleration RS recorded on rock and soil sites, respectively, at Oakland Outer Harbour in the 1989 earthquake at Loma Prieta, California, United States (Tsang *et al.* 2017a)

5.1 IBC (2015), EC (2004) and NBCC (2015)

Although the importance of the total soil layer thickness has been well recognised, site classification nowadays is based solely on the properties, to a certain depth, of the near-surface materials, since incorporated into the 1994 NEHRP Provisions (BSSC 1995). This definition permits sites to be classified unambiguously, as pointed out in Dobry et al. (2000).

In IBC, EC and NBCC, a site is classified according to the value of the average SWV ($V_{s,30}$), or the value of Standard Penetration Resistance Test (SPT-N) (for cohesionless soil), or the value of undrained shear strength (for cohesive soil), over the upper 30 m (or 100 feet). The IBC classification scheme is described in more detail in this sub-section. NBCC essentially adopted the same classification scheme as in IBC, whilst that in EC is slightly different. In IBC, a site is classified as either Site Class A, B, C, D, E or F based on the site soil properties. Profiles containing distinctly different soil and/or rock layers are subdivided into layers designated by a number from 1 to *n* at the bottom for the total of *n*

distinct layers in the upper 30 m. The symbol i refers to any one of the layers between 1 and n. The average shear wave velocity $V_{s,30}$ can be calculated by applying Eq. (11).

$$V_{s,30} = \frac{\sum_{i=1}^{n} d_i}{\sum_{i=1}^{n} \frac{d_i}{V_{s,i}}} \tag{11}$$

where $V_{s,i}$ = The shear wave velocity in m/s;

d_i = The thickness of any layer between 0 and 30 m.

Eq. (11) also applies to the computation of the values of SPT–N and undrained shear strength. The classification scheme is shown in Table 2. Note that IBC contains more detailed descriptive criteria (e.g. based on plasticity index, PI) and steps for classifying a site into Site Classes E and F. Refer to the code for details.

As mentioned in Section 5.1, the site-dependent ES as shown in Figure 9 is scaled by the site coefficients F_a and F_v, to take into account the site effects for short-period and long-period ranges respectively. The derived short-period site coefficients are based on recorded motions over the period range 0.1s to 0.5s, whilst the long-period site coefficients are based on recorded motions over the period range of 0.4s to 2.0s.

Table 2. Site classification scheme adopted in IBC

Site Class	Soil Profile Name	$V_{s,30}$ (m/s)	SPT–N	Undrained Shear Strength (kPa)
A	Hard rock	> 1500	N.A.*	N.A.*
B	Rock	760 – 1500	N.A.*	N.A.*
C	Very dense soil and soft rock	360 – 760	> 50	> 100
D	Stiff soil	180 – 360	15 – 50	50 – 100
E	Soft soil	< 180	< 15	< 50
F	Special soils requiring site-specific evaluation			

* N.A. = Not applicable

The site-dependent ES in NBCC is also scaled by the site coefficients F_a and F_v, as modified based on a reference Site Class C. EC applies a uniform soil factor S across the whole ES for each site class (ground type), whilst varying the corner period T_1 between 0.4s to 0.8s (for Type 1 spectrum model). Larger values of T_1 essentially translate to a higher demand at the long-period range.

5.2 AS (2007) and NZS (2004)

In AS and NZS, the site classification schemes are very similar. Sites are classified into five classes using methods recommended in the standard. For rock sites, compressive strength or average SWV over the top 30 m is used. For soil sites, the site natural period T_S (refer to Eq. (10)), depths of soils H_S, undrained shear strength and SPT–N values are used.

As stated in the Commentary to AS (AEES, 2007) and NZS (SNZ, 2004), the basic parameter for site classification in the standard is the site natural period. The site-period approach recognises that deep deposits of stiff or dense soils exhibit long-period site response characteristics not shown by deposits of only a few tens of metres of the same

material. The approach adopted in IBC of placing deep stiff soil sites in Site Class D – stiff soil, with relatively short-period spectral characteristics may be non-conservative in the medium to long period spectral range.

A hierarchy of measurement methods, listed in order of preference, is provided. The most preferred method to determine site periods is based on four times the shear-wave travel-time from the surface to the underlying rock. Using bore logs, and measurement of geotechnical properties is the second preferred method.

Upon classifying a site, an ES can be drawn up according to the *spectral shape factor* C_h (as a function of T) corresponding to the site class specified in the standard.

5.3 GB (2010)

In GB, a site is initially classified according to the value of equivalent SWV (V_s) which can be calculated from Eq. (12).

$$V_S = \frac{H_S}{\sum_{i=1}^{n} \frac{d_i}{V_{s,i}}} \tag{12}$$

where H_S is the total thickness of soil sediment, or 20 m, whichever is the smaller, d_i is the thickness of any layer within H_S.

Based on the equivalent SWV (V_S), the site is classified into a specific soil type. A site is then assigned to one of the classes I_0, I_1, II, III, IV, according to both the equivalent SWV (soil type) and the total thickness (in units of m) of the overlying soil.

Upon assigning the site to a class, together with the design earthquake group as determined in Section 6.2, the characteristic (corner) period T_1 can be obtained. Larger values of T_1 essentially translate to a higher demand at the long-period range for softer or deeper soil sites. It is noted that the value of T_1 has to be increased by 0.05 s when constructing an ES for a low-probability of exceedance design level.

5.4 Elastic response spectrum (ES) for flexible soil sites

A heuristic site-specific elastic response spectrum (ES) model for flexible soil sites (T_i > 0.5 s) which takes into account resonant-like amplification behaviour of soil sediments has been developed. The construction of the idealised soil ES model, with parameters of site natural period (T_s) and soil amplification factor (S), as depicted in Figure 16, was first proposed by Lam et al. (2001). Analytical investigations undertaken by Tsang et al. (2006a; 2006b; 2012) employing fundamental principles in relation to the reflection and propagation of shear waves in a homogenous soil medium, elaborated the idea much further, resulting in the development of an algorithm for determining the values of these two parameters, as an alternative approach to that of the classical 1D site response analysis using program SHAKE (Schnabel et al. 1972). Predictions by the alternative calculation methodology, which is much simpler and transparent to the user, has been well validated against results obtained from dynamic analyses of soil column models derived from real borehole records, as well as from strong motion data recorded during the 1994 Northridge earthquake.

This alternative soil response modelling methodology has been refined and simplified further into a model of potential utility in structural design practice (Tsang et al, 2017a; 2017b). In the proposed procedure, the initial small-strain site natural period (T_i) is first calculated from information on the shear wave velocity (SWV) values (inferred from

SPT-N values) and the thicknesses of the individual soil layers. The effects of period-shift resulting from shear straining (non-linearity) of the soil materials are taken into account in the estimation of the (shifted/final) large-strain site natural period (T_S). Design charts have also been developed for T_S and S as functions of the SWV of the soil, the intensity of ground shaking and the rigidity of the bedrock medium. These factors are represented by parameters $V_{s,i}$, RSV_{Ti} and V_R respectively. See Figs.17, 18a & 18b for example design charts used to construct the ES model for a flexible soil site. The proposed ES model, presented in the displacement format and the acceleration-displacement response spectrum (ADRS) format (Figure 13) can be compared with results from higher-tier site response analysis (using program STRATA) and code specified ES models to see the significant differences. Some example comparisons are in Tsang et al. (2017a), and an example for a flexible soil site is reproduced in Figure 19.

The approach to site classification and modelling of an ES for a flexible soil site as described in this section, featuring the site natural period as the controlling parameter, is consistent with recommendations by Pitilakis et al. (2012 & 2013).

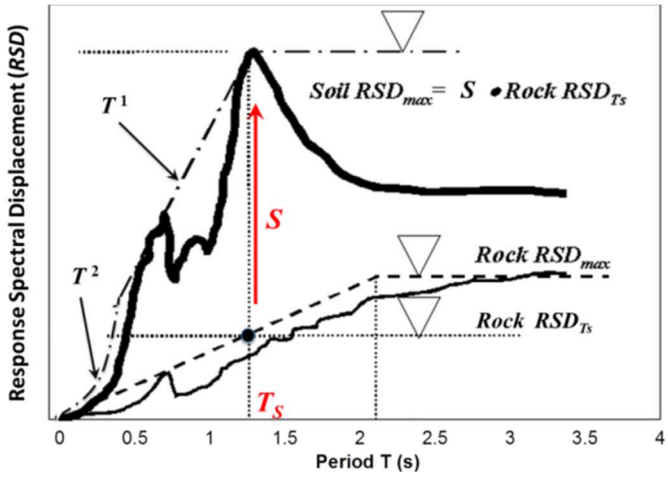


Figure 16. Schematic diagram of the proposed site-specific ES model (in RSD format) (Tsang et al. 2017a)

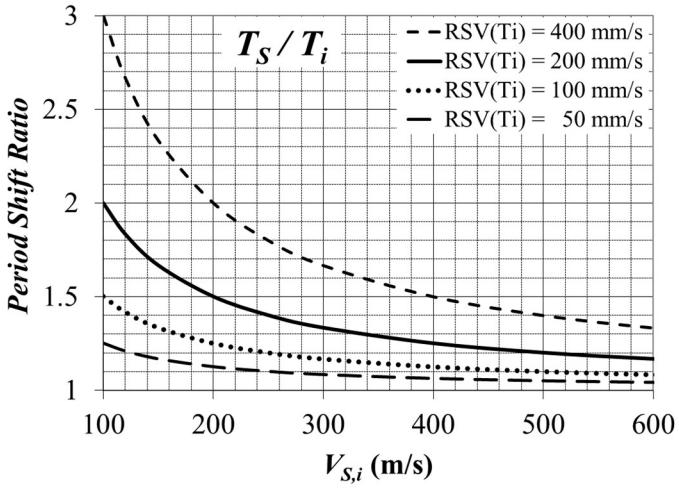
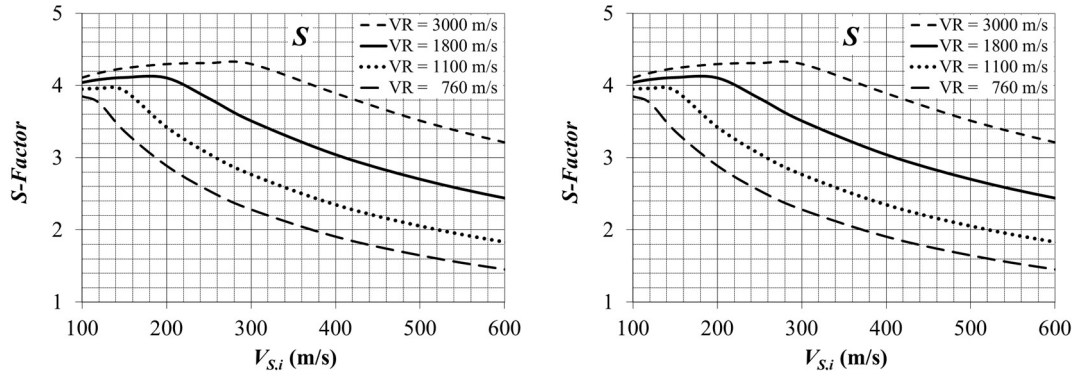


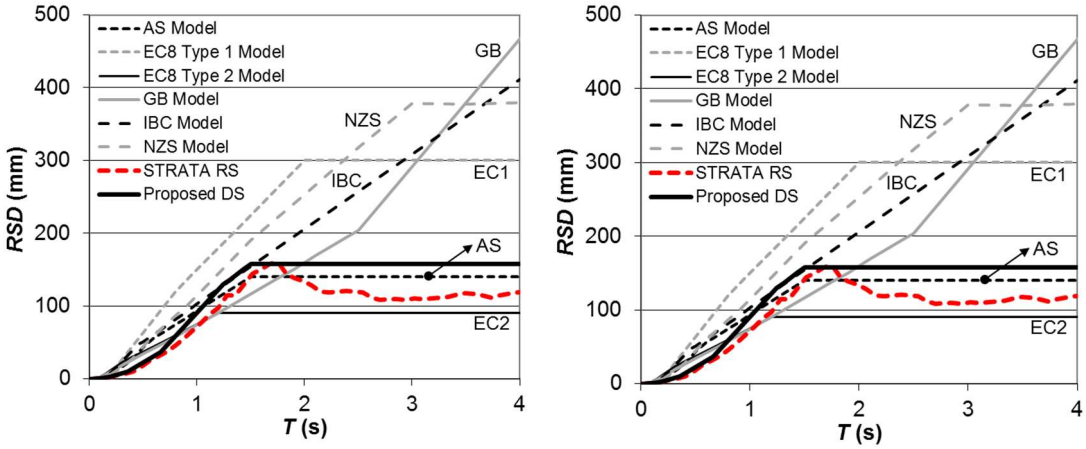
Figure 17. Design chart for the period-shift ratio TS/Ti as functions of intensity of shaking (RSVTi) and initial soil SWV (VS,i) (Tsang et al. 2017a)



(a) function of initial SWV on soil and rock ($V_{S,i}$,V_R) fixed at RSV_{Ti}= 200 mm/s

(b) function of intensity and initial SWV on soil (RSV_{Ti},$V_{S,i}$) fixed at V_R = 3000 m/s

Figure 18. Design charts for site amplification factor (*S-Factor*) (Tsang et al. 2017a)



(a) RSD format

(b) ADRS format

Figure 19. Example comparison of the proposed ES model with results from higher-tier site response analysis (using program STRATA) and code models (Tsang et al. 2017a)

6. Conclusions

This chapter introduces contemporary methodologies concerned with the modelling of seismic actions and the multitude of formats used to present key information. There is no intention of using the chapter to waive away the need for the reader to systematically plough through the literature to gain the requisite working knowledge across so many topics. The earlier sections of the chapter, however, may well help to speed up this learning process. Seismic hazard modelling in regions of low to moderate seismicity is a controversial topic presenting many factors for code drafters and users to consider. It is hoped that readers of this chapter will gain a clear perspective on the factors concerned. Code drafters, in the future, may also apply the guiding principles, when developing realistic earthquake loading models, as appropriate, for the range of site classes.

References

Abrahamson, N., Silva, W.J. and Kamai, R. (2014)"Summary of the ASK14 ground motion relation for active Crustal regions, Earthq. Spectra, 30(3), 1025-1055.

ASCE/SEI 7-16 (2016) "Minimum Design Loads for Buildings and Other Structures". USA: Structural Engineering Institute (SEI), American Society of Civil Engineers (ASCE).

Atkinson, G.M. and Boore, D.M. (1995)"Ground Motion Relations for Eastern North America", Bull. Seismol. Soc. Am., 85, 17-30.

Australian Standard: AS 1170.4 (2007) "Structural Design Actions – Part 4 Earthquake Actions", Standards Australia.

Bird, P., Kreemer, C. and Holt, W.E. (2010)"A Long-term Forecast of Shallow Seismicity based on the global strain rate map, Seismol. Res. Lett., 81(2), 184-194.

Boatwright, J. and Seekins, L. (2011)"Regional spectral analysis of three moderate earthquakes in northeastern North America", Bull. Seismol. Soc. Am., 101, 1769–1782.

Boore, D.M. (2016)"Determining generic velocity and density models for crustal amplification calculations, with an update of the Boore and Joyner (1997) generic site amplification for Vs(Z) = 760 m/s, Bull. Seismol. Soc. Am., 106(1), 316-320.

Boore, D.M. and Joyner, W.B. (1997) Site amplifications for generic rock sites, Bull. Seismol. Soc. Am., 87, 327–341.

Boore, D.M., Campbell, K.W. and Atkinson, G.M. (2010)"Determination of stress parameters for eight well-recorded earthquakes in eastern North America", Bull. Seismol. Soc. Am., 100, 1632–1645.

Boore, D.M., Stewart, J.P., Seyhan, E. and Atkinson, G.M (2014)"NGA-West2 equations for predicting PGA, PGV, and 5% damped PSA for shallow crustal earthquakes", Earthq. Spectra, 30(3), 1057-1085.

Building Seismic Safety Council (2015) "NEHRP Recommended Seismic Provisions for New Buildings and Other Structures, Part 1 Provisions, Part 2 Commentary", FEMA Report No. P-1050-1, Vol. 1, National Institute of Building Sciences, Washington, D.C.

Campbell, K.W. and Bozorgnia, Y. (2014) "NGA-West2 Ground Motion Model for the average horizontal components of PGA, PGV, and 5% damped linear acceleration response spectra", Earthq. Spectra 30(3), 1087-1115.

Chandler A.M. and Lam N.T.K. (2002)"Intensity Attenuation Relationship for the South China Region and Comparison with the Component Attenuation Model", Journal of Asian Earth Sciences. 20, 775-790.

Chandler, A.M., Lam, N.T.K. and Tsang, H.H. (2005) "Shear Wave Velocity Modelling in Bedrock for Analysis of Intraplate Seismic Hazard", Soil Dynamics & Earthquake Engineering 25: 167-185.

Chandler, A.M., Lam, N.T.K., Tsang, H.H. (2006a) "Near-surface Attenuation Modelling based on Rock Shear-Wave Velocity Profile", Soil Dynamics and Earthquake Engineering, 26(11):1004-1014.

Chandler, A.M., Lam, N.T.K. and Tsang, H.H. (2006b) "Regional and Local Factors in Attenuation Modelling", Journal of Asian Earth Sciences. 27: 892 - 906.

Chiou, B.S.J. and Youngs, R.R. (2014) "Update of the Chiou and Youngs NGA model for the average horizontal component of peak ground motion and response spectra", Earthq. Spectra, 30(3), 1117-1153.

Chopra, A.K. (2017) "Dynamics of Structures: Theory and Applications to Earthquake Engineering" (5th Edition), Pearson.

Darragh, B., Abrahamson, N.A., Silva, W.J. and Gregor, N. (2015)"Development of hard rock ground motion models for Region 2 of Central and Eastern North America", PEER Report No. 2015/04, Pacific Earthquake Engineering Research Center, University of California, Berkeley, 51-84.

Dickenson, S.E., Seed, R.B., Lysmer, J., Mok, C.M. (1991)"Response of soft soils during the 1989 Loma Prieta earthquake and implications for seismic design criteria", Proceedings of the 4th Pacific Conference on Earthquake Engineering, 3, 191-204, Auckland, New Zealand.

Dowrick, D. (2009) "Earthquake Resistant Design and Risk Reduction", 2nd Edition, Wiley, New York.

EN 1998-1 (2004) "Eurocode 8: Design of Structures for Earthquake Resistance – Part 1: General Rules, Seismic Actions and Rules for Buildings." United Kingdom: European Committee for Standardisation.

Fardis, M.N., (2009) "Seismic design, assessment and retrofitting of concrete buildings: based on EN-Eurocode 8", Springer.

GB 50011 (2010) "Code for Seismic Design of Buildings. Beijing, China: The Ministry of Housing and Urban-Rural Development of the People's Republic of China", China Architecture & Building Press.

Idriss, I.M. (2014) "An NGA-West2 empirical model for estimating the horizontal spectral values generated by shallow crustal earthquakes." Earthq. Spectra, 30(3), 1155-1177.

International Building Code (IBC 2015) "Country Club Hill, Illinois, USA: International Code Council.

Lam N.T.K. (2002) "Program "GENQKE" User's Manual, Infrastructure Engineering", Melbourne School of Engineering, The University of Melbourne.

Lam, N.T.K., Asten, M., Roberts, J., Srikanth, V., Wilson, J.L.W., Chandler, A.M. and Tsang H.H. (2006) "Generic Approach for Modelling Earthquake Hazard", Invited paper, Journal of Advances in Structural Engineering. 9(1): 67-82.

Lam, N.T.K., Sinadinovski, C., Koo, RCH and Wilson, J.L. (2003) "Peak Ground Velocity modelling for Australian intraplate earthquakes", Journal of Seismology and Earthquake Engineering, 5(2), 11-22.

Lam, N.T.K., Tsang, H.H., Lumantarna, E. & Wilson, J.L. (2016) "Minimum loading requirements for areas of low seismicity, Earthquakes and Structures, 11(4): 539-561.

Lam, N.T.K., Wilson, J.L. and Chandler, A.M. (2001)"Seismic Displacement Response Spectrum Estimated from the Frame Analogy Soil Amplification Model, Engineering Structures, 23, 1437-1452.

Lam, N.T.K., Wilson, J.L. and Hutchinson, G.L. (2000)"Generation of Synthetic Earthquake Accelerograms Using Seismological Modelling: A Review", Journal of Earthquake Engineering, 4(3), 321-354.

Lam, N.T.K., Wilson, J.L. and Tsang, H.H. (2010) "Modelling earthquake ground motions by stochastic method", In: Stochastic Control, Chris Myers (Ed.), ISBN: 978-953-307-121-3, InTech; 475-492.

Mulargia, F., Stark P.B., Geller R.J. (2017)"Why is Probabilistic Seismic Hazard Analysis (PSHA) still used?", Physics of the Earth and Planetary Interiors, 264, 63–75. http://dx.doi.org/10.1016/j.pepi.2016.12.002.

Naeim, F. (Ed.) (2001) "The Seismic Design Handbook, Springer. National Building Code of Canada (NBCC 2015) Part 4: Structural design. Ottawa, Canada", Canadian Commission on Building and Fire Codes, National Research Council of Canada.

New Zealand Standard: NZS 1170.5 (2004), Structural Design Actions Part 5: Earthquake Actions – New Zealand. Wellington, New Zealand: Standards New Zealand; 2004.

Newmark, N.M. and Hall, WJ. (1982), Earthquake Spectra and Design. Berkeley, California, USA: Earthquake Engineering Research Institute.

Ogweno, L.P. and Cramer, C.H. (2014) "Comparing the CENA GMPEs Using NGA-East Ground Motion Database", Seismol. Res. Lett., 85 (6), 1377-1393.

Okal, E.A. and Sweet, J.R. (2007), "Frequency-size distributions for intraplate earthquakes", Geolog. Soc. Am. Special Papers, 425, 59-71.

Pacific Earthquake Engineering Center (2015), NGA-East: median ground-motion models for the Central and Eastern North America Region, PEER Report No. 2015/04, Pacific Earthquake Engineering Research Center, University of California, Berkeley.

Pezeshk, S., Zandieh, A., Campbell, K.W. and Tavakoli, B. (2015), " Ground motion prediction equations for CENA using the Hybrid Empirical Method in conjunction with NGA-West2 Empirical Ground Motion Models", PEER Report No. 2015/04, Pacific Earthquake Engineering Research Center, University of California, Berkeley, 119-130.

Pinto, P., (2000) "Design for low/moderate seismic risk", Proceedings of the 12th World Conference of Earthquake Engineering 12WCEE, 30th January – 4th February, Auckland, New Zealand.

Pitilakis, K., Riga, E. and Anastasiadis, A. (2012) "Design spectra and amplification factors for Eurocode 8", Bulletin of Earthquake Engineering 2012;10(5):1377-1400.

Pitilakis, K., Riga, E. and Anastasiadis, A. (2013) "New code site classification, amplification factors and normalized response spectra based on a worldwide ground-motion database", Bulletin of Earthquake Engineering,11(4):925-966.

Schnabel, P.B., Lysmer, J. and Seed, H.B. (1972) SHAKE: a computer program for earthquake response analysis of horizontally layered sites. Earthquake Engineering Research Center Report: EERC 72-12, USA: University of California at Berkeley.

Shahjouei, A. and Pezeshk, S. (2015) "Hybrid Empirical Ground Motion Model for Central and Eastern North America using Hybrid Broadband Simulations and NGA-West2 GMPEs", PEER Report No. 2015/04, Pacific Earthquake Engineering Research Center, University of California, Berkeley, 165-168.

Tongkul, F., 2016, feedbacks process within the NA public consultation period.

Tsang H.H. (2015). Evaluation of Codified Elastic Design Spectrum Models for Regions of Low-to-Moderate Seismicity. Soil Dynamics and Earthquake Engineering, 70:148-152.

Tsang, H.H., Chandler, A.M., Lam, N.T.K. (2006) "Estimating non-linear site response by single period approximation", Earthquake Engineering and Structural Dynamics", 35(9),1053-1076.

Tsang, H.H., Chandler, A.M., Lam, N.T.K. (2006) "Simple models for estimating period-shift and damping in soil", Earthquake Engineering and Structural Dynamics, 35(15),1925-1947.

Tsang, H.H., Sheikh, M.N., Lam, N.T.K., Chandler, A.M., Lo, S.H. (2010) "Regional Differences in Attenuation Modelling for Eastern China", Journal of Asian Earth Sciences, 39(5):441-459.

Tsang, H.H., Sheikh, M.N., Lam, N.T.K. (2012) "Modeling Shear Rigidity of Stratified Bedrock in Site Response Analysis", Soil Dynamics and Earthquake Engineering, 34(1):89-98.

Tsang, H.H., Wilson, J.L., Lam, N.T.K. & Su, R.K.L. (2017a) "A design spectrum model for flexible soil sites in regions of low-to-moderate seismicity", Soil Dynamics & Earthquake Engineering, 92, 36-45.

Tsang, H.H., Wilson, J.L., Lam. N.T.K. (2017b). "A Refined Design Spectrum Model for Regions of Lower Seismicity". Australia Journal of Structural Engineering, 18:3-10.

Wilson J.L., Lam N.T.K. & Gad E.F., (2015) "Hazard Identification and Behaviour of Reinforced Concrete Framed Buildings in Regions of Lower Seismicity", Proceedings of the 10th Pacific Conference on Earthquake Engineering, 6th to 8th November, Sydney, Australia.

Yaghmaei-Sabegh, S and Lam, N.T.K. (2010)"Ground motion modelling in Tehran based on the stochastic method", Soil Dynamics and Earthquake Engineering. 30: 525-535.

Methods of Structural Analysis for Buildings in Regions of Low to Moderate Seismicity

Elisa Lumantarna[a,c], Alireza Mehdipanah[a,c], Nelson T. K. Lam[a,c] and John L. Wilson[b,c]

[a] Department of Infrastructure Engineering
The University of Melbourne, Australia

[b] Centre for Sustainable Infrastructure
Swinburne University of Technology, Australia

[c] Bushfire and Natural Hazards Cooperative Centre, Australia

This chapter is concerned with the seismic load structural analysis of multi-storey buildings sited in regions of low to moderate seismicity. Due to functional and other architectural requirements most buildings contain vertical irregularities (causing load path discontinuities) or plan irregularities (core walls placed eccentrically), or both. The code lateral force method of analysis is therefore not allowable. Contemporary earthquake design standards and assessment procedures require dynamic analyses to be performed on such structures. This chapter introduces the Generalised Force Method of analysis, which is essentially an enhanced static method, shown to provide accurate estimates of deflections and internal forces within the building comparable to those derived using dynamic analyses. The method incorporates allowances for higher mode effects based on parametric studies involving multi-storey buildings featuring vertical irregularities. The methods developed are illustrated by two multi-storey building examples.

Keywords: generalised force method, static analysis method, irregularity

1. Introduction

Most of the multi-storey building stock in Australia, and worldwide, features irregularities. These can be in the form of plan irregularities caused by shear walls and cores placed eccentrically, and vertical irregularities due to setbacks and load path discontinuities.

Seismic building design standards commonly provide for a 'code lateral force method', the terminology used in Eurocode 8 (EN 1998-1, 2004) or the 'equivalent static analysis method', the terminology used in AS1170.4 (Standards Australia, 2007). These are analysis methods which emulate seismic behaviour by applying equivalent static forces to the building. For analysis by static methods alone to be permissible, stringent requirements exist on vertical and plan regularity.

Only a few seismic building design standards (e.g., Eurocode 8 (EN 1998-1 2004); FEMA 450-1 (Building Seismic Safety Council 2003); FEMA 356 (ASCE 2000) currently include provisions for the design and analysis of irregular buildings. These design guidelines generally require a three-dimensional (3D) dynamic analysis to be performed. The modelling of buildings for dynamic analyses in 3D is complex, and interpretation of the results requires expert judgement. This is why it is important to exercise a controlled

use of complex analyses involving finite element (FE) packages. The simple, and yet accurate, analysis method (referred to herein as the Generalised Force Method) introduced in this chapter can be applied to multi-storey buildings featuring vertical irregularities. The method is shown to provide reliable predictions on deflection behaviour and internal forces (including base shear) within the building incorporating higher mode effects. The demand on memory for computation is low. The Generalised Force Method, therefore, can be employed as a tool for benchmarking computer produced estimates of dynamic response behaviour, thereby exercising control over the use of complex analyses, and providing better understanding, guiding design, by study of the trends in calculated results.

Section 2, below, presents the method developed for the analysis of low rise (6-storey) multi-storey buildings. The method is extended in Section 3 to account for the effects of the higher response modes of much taller (20-storey) multi storey buildings. Examples based on two multi-storey buildings, featuring vertical irregularities, illustrate the method. The focus of the chapter is on illustrating the method of analysis for a torsionally balanced (TB) multi-storey building. Details of an extended GFM, enabling analysis of torsionally unbalanced (TUB) buildings are in Lam et al. (2016).

2. Generalised force method (GFM) for low rise buildings

The Generalised Force Method (GFM) for the analysis of low-rise TB multi-storey buildings, introduced in this section, can be used to obtain displacements and inter-storey drift without the need for dynamic analyses.

First, an equivalent static analysis is performed in accordance with a code specified standard seismic design procedure (e.g., AS 1170.4:2007 (Standards Australia 2007), Eurocode 8 (EN 1998-1 2004)). The deflection obtained at each floor is shown schematically in Figure 1.

The multi-storey building response can be idealised into a single-degree-of-freedom (SDOF) system and this involves calculation of the effective displacement of the building (δ_{eff}) using Eq. (1):

$$\delta_{eff} = \frac{\sum m_i \delta_i^2}{\sum m_i \delta_i} \tag{1}$$

and the effective mass (m_{eff}), using Eq.(2):

$$m_{eff} = \frac{(\sum m_i \delta_i)^2}{\sum m_i \delta_i^2} \tag{2}$$

where m_i and δ_i are the mass and displacement of floor i, respectively.

The effective stiffness (k_{eff}) of the building is then calculated using Eq. (3):

$$k_{eff} = \frac{V}{\delta_{eff}} \tag{3}$$

where V is the horizontal equivalent static shear force.

The effective natural period (T_{eff}) is then found using Eq. (4).

$$T_{eff} = 2\pi \sqrt{\frac{m_{eff}}{k_{eff}}} \tag{4}$$

The capacity diagram can be plotted as an acceleration vs displacement format (Figure 2a), where the effective acceleration (a_{eff}) is defined by Eq. (5)

$$a_{eff} = \frac{V}{m_{eff}} \tag{5}$$

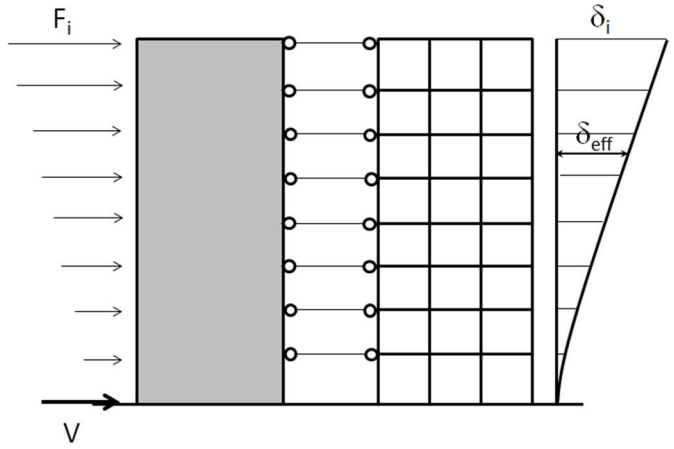
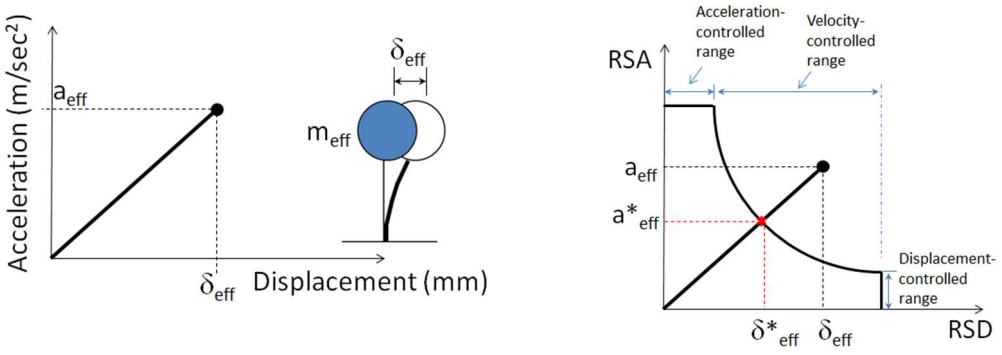


Figure 1. Displacement behaviour derived from equivalent static analysis



(a) (b)

Figure 2. (a) Capacity diagram in the acceleration vs displacement format, (b) Superposition of the capacity and predicted demand diagrams

The capacity diagram (a straight line) is then constructed from estimates of the value of δ_{eff} and a_{eff} as obtained from Eqs. (1) and (5) respectively (Figure 2a). The capacity diagram is then superimposed on the demand diagram in the acceleration-displacement response spectrum format (the ADRS diagram) as shown schematically in Figure 2b to identify the 'performance point', the intercept between the two diagrams. The displacement demand of the building (δ^*_{eff}) is then read off from the diagram. The construction of the ADRS

diagram is introduced in Wilson and Lam (2006). The displacement profiles and seismic inertia forces at each floor level can then be adjusted by scaling based on Eqs. (6a) and (6b):

$$\delta_i^* = \frac{\delta_{eff}^*}{\delta_{eff}} \delta_i \tag{6a}$$

$$F_i^* = \frac{\delta_{eff}^*}{\delta_{eff}} F_i \tag{6b}$$

where δ_i and F_i are displacement and inertia force values at floor level i from equivalent static analysis; δ_{eff} is the corresponding effective displacement; and δ_i* and F_i* are the revised displacements and inertia forces at level i.

The inter-storey drift (θ_i*) can be determined using Eq. (6c).

$$\theta_i^* = \frac{\delta_i^* - \delta_{i-1}^*}{h_i} \tag{6c}$$

where h_i is height at level i.

The storey shear (V_i) can then be found using Eq. (6d).

$$V_i = \sum_i^n F_i^* \tag{6d}$$

where n is the number of floor levels in the building.

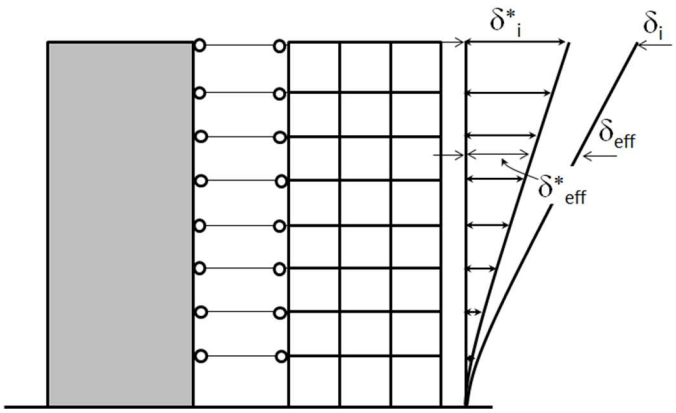


Figure 3. Displacement demand behaviour of building

Individual steps in the Generalised Force Method (GFM) are listed in Table 1. The procedure is illustrated by working through a six-storey building example which features vertical irregularities. The building is laterally supported jointly, by moment resisting frames and reinforced concrete shear walls. The lateral load resisting elements are located in such a way that the building is symmetrical on plan. Some of the columns in the moment resisting frames on the 2nd floor feature a discontinuity which is a form of vertical irregularity. The plan view of the typical floor, alongside the 2nd floor, are presented in Figures 4a and 4b, respectively. A three-dimensional view of the building model is

presented in Figure 5. The height of the building is 21.2 m. The geometric and material properties of the elements of the buildings are listed in Table 2. The equivalent static analysis can be performed in accordance with provisions in the Australian Standards for Earthquake Actions AS1170.4-2007.

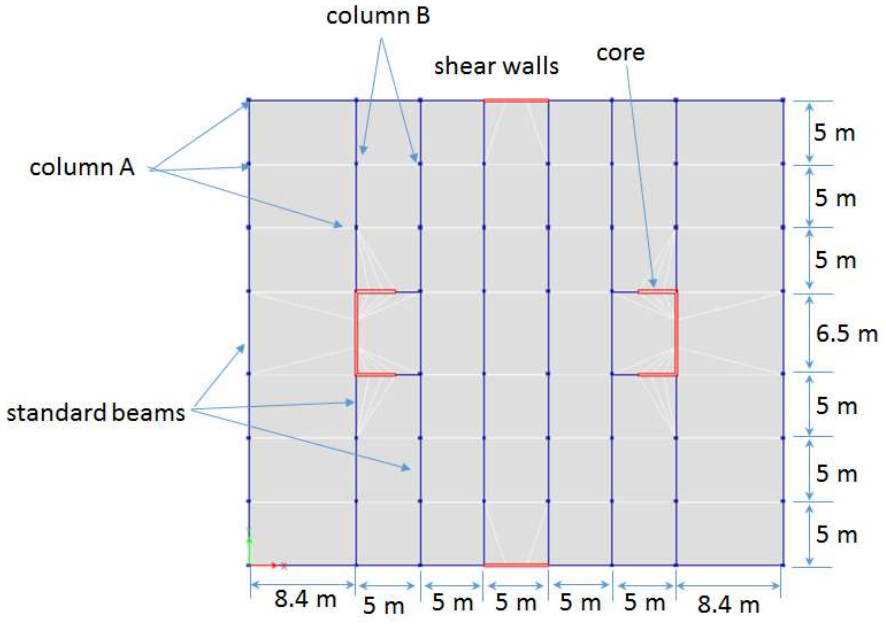
Table 1. Summary of GFM procedure (without higher mode effects)

Step	Descriptions	Equations/Figures
1	Use code equation to estimate natural period of the building (as function of height of the building).	Code equation
2	Use code equation to determine the amount of seismically induced base shear on the building.	Code equation
3	Distribute the base shear up the height of the building as design seismic inertia forces.	Figure 1
4	Determine the deflection of the building when subject to the design seismic inertia forces obtained from step 3.	Figure 1
5	Determine the value of the effective displacement (δ_{eff}) based on the calculated deflection profile of the building from step 4.	Equation (1)
6	Determine the value of the effective mass (m_{eff}).	Equation (2)
7	Determine the value of the effective stiffness (k_{eff}).	Equation (3)
8	Determine the value of the effective natural period of the building (T_{eff}).	Equation (4)
9	Determine the value of the effective acceleration (a_{eff})	Equation (5)
10	Determine the seismic demand based on intercepting the demand diagram with the capacity curve at the "performance point" (a^*_{eff}, δ^*_{eff})	Figure 2
11	Revise the displacement profiles and seismic inertia forces of the individual floors (obtained initially in steps 3 and 4) based on the performance point identified in step 10.	Equation (6), Figure 3

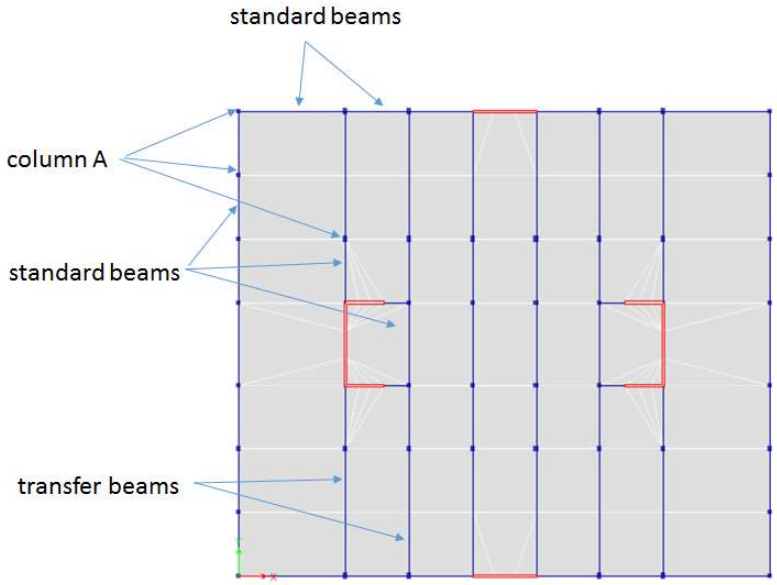
Table 2. Dimensions of principal structural elements and material properties (mm)

Element	Slab	Walls		Beams		Columns	
Type		core	shear	standard	transfer	A	B
Material	RC	RC	RC	RC	RC	RC	RC
Width (mm)	-	200	200	280	300	350	300
Depth (mm)	250	-	-	450	1600	350	300
Length (mm)	-			-	-		

RC – reinforced concrete with modulus of elasticity of 24.5 GPa and density of 2500 kg/m^3



(a) typical floor



(b) 2nd floor

Figure 4. Plan views of example 6-storey building

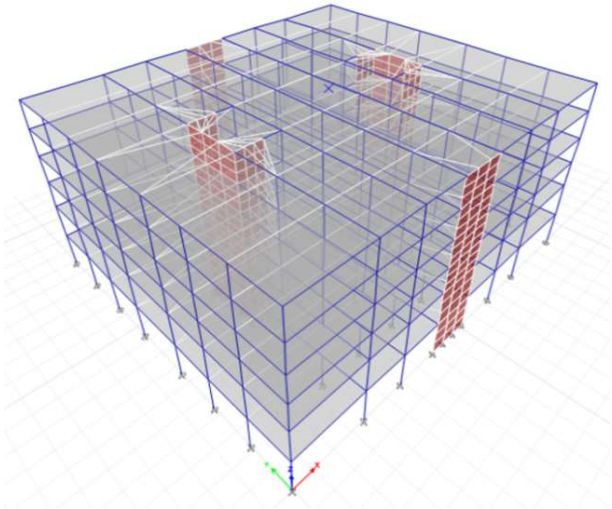


Figure 5. 3D view of example 6-storey building

Step 1

Apply lateral loads to the building according to the equivalent static analysis method of AS1170.4-2007. The fundamental natural period of the building was estimated using Eq. (7) in accordance with the Standard:

$$T_1 = 1.25 k_t h_n^{0.75} \tag{7}$$

where k_t is 0.05 for buildings that are laterally supported by concrete walls and h_n is the distance from the base of the structure to the uppermost seismic weight or mass (= 21.2 m). The fundamental natural period of the building is 0.6 sec based on Eq. (7).

Step 2

Estimate base shear using the following expression specified by the Standard:

$$V = \left[k_p Z C_h(T_1) {}^{S_p}/_{\mu} \right] W_t \tag{8}$$

where k_p is the probability factor; Z the hazard factor; $C_h(T_1)$ the spectral shape factor for the fundamental natural period of the building; W_t the seismic weight of the building; S_p the structural performance factor; and μ the structural ductility factor.

The building was assumed to be constructed on a class B site in Melbourne (Z = 0.08) and was designed for the 1/500 annual probability of exceedance. The spectral shape for a class B site is shown in Figure 6. The S_p and μ values were assumed equal to 1.0. The base shear for the building was found to be 8162 kN, applying Eq. (8).

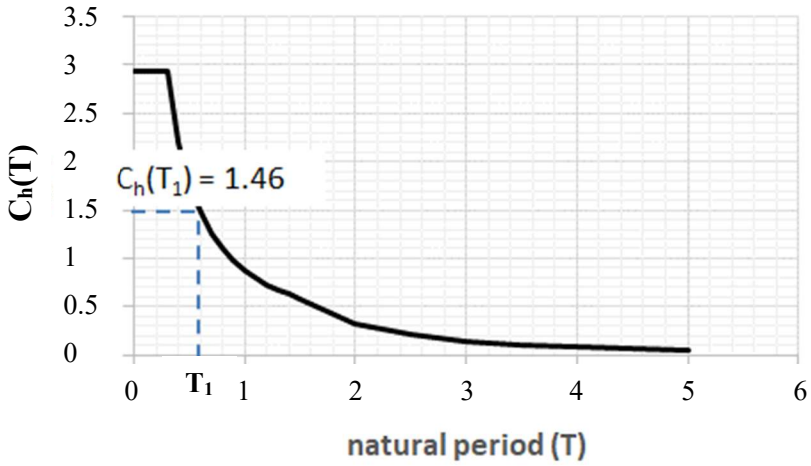


Figure 6. Comparison between GFM results and a dynamic analysis of a 6-storey building

Step 3

The estimated amount of base shear is distributed up the height of the building based on the following expression in accordance with the Standard:

$$F_i = \frac{W_i h_i^k}{\sum_{j=1}^{n}(W_j h_j^k)} V \tag{9}$$

where W_i is the seismic weight of the building at the i^{th} level; h_i the height of level i, n the number of levels in the building; k is an exponent dependent on the fundamental natural period of the building. This was taken as 1 for $T_1 \leq 0.5$ sec, 2 for $T_1 \geq 2.5$ sec and an interpolated value between 1 and 2 for 0.5 sec < T_1 < 2.5 sec. The distribution of inertia force between individual floors is shown in Table 3.

Step 4

The deflection of the building when subject to the design seismic forces, step 3 above, can be determined by a linear static analysis of a 2D, or a 3D, finite element model of the building. Alternatively, an analysis method introduced by the authors (Lam et al., 2010) can be used to provide estimates of the deflection of the building using simple, Excel spreadsheet manual calculations. The method can provide deflection estimates for multi-storey buildings laterally supported by walls, moment resisting frames and combined walls and moment resisting frames.

Linear static analysis was conducted on a two-dimensional finite element model of the building using ETABS (2015). The deflections are given in Table 4.

Table 3. Lateral inertia forces applied to individual floors

Level	Mass (m_i) tonnes	Height (z_i) m	Lateral force ($F_i = \frac{m_i z_i^{1.05}}{\sum m_i z_i^{1.05}} V$) kN
6	1243	21.2	2267.2
5	1322	18	2031.1
4	1201	14.8	1502.6
3	1193	11.6	1155.6
2	1193	8.4	823.4
1	1147	4.2	382.3
0	0	0	0

Table 4. Displacements of the building due to design seismic forces

Level	Mass (m_i) tonnes	Height (z_i) m	Lateral force (from step 3) kN	Displacement (δ_i) mm
6	1243	21.2	2267.2	12.9
5	1322	18	2031.1	10.8
4	1201	14.8	1502.6	8.6
3	1193	11.6	1155.6	6.3
2	1193	8.4	823.4	4.1
1	1147	4.2	382.3	1.6
0	0	0	0	0

Step 5

Given the displacements of Table 4 and Eq. (1), δ_{eff} = 9.5 mm.

Step 6

Given the mass and displacement values from Table 4 and Eq. (2), m_{eff} = 5789 tonnes.

Step 7

Given the base shear of 8162 kN (step 2) and effective displacement of 9.5 mm (step 5) and Eq. (3), k_{eff} = 861128 kN/m.

Step 8

Given the effective mass of 5789 tonne (step 6) and effective stiffness of 871128 kN/m (step 7) and Eq. (4), T_{eff} = 0.5 sec.

Step 9

Given the base shear of 8162 kN and effective mass of 5789 tonnes and Eq. (5), a_{eff} = 1.41 m/sec^2.

Step 10

The capacity line, based on the calculated values of δ_{eff} and a_{eff}, was then plotted and superimposed on the demand diagram in the acceleration-displacement response spectrum format (the ADRS diagram) as shown in Figure 7. The performance point representing the displacement demand of the building, δ^*_{eff}, was found to be 9.0 mm approximately.

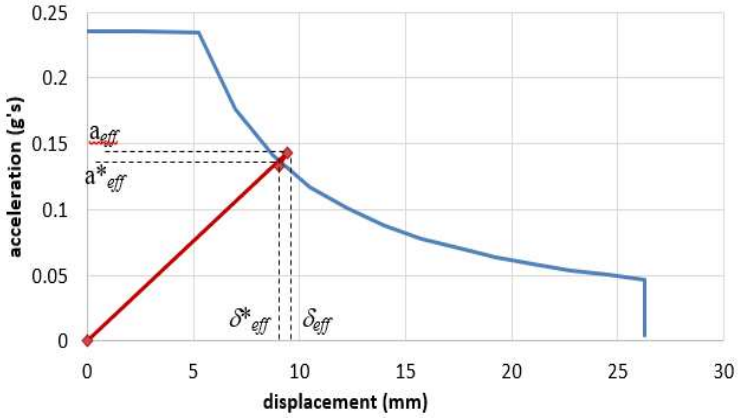


Figure 7. Superimposing the capacity curve onto the ADRS diagram

Step 11

Given the value of δ^*_{eff} and Eqs. (6a) and (6b), the floor displacement and inertia force profiles were then adjusted by applying a scaling factor. The scaled displacement and inertia forces along with inter-storey drift values (Eq.6c) and storey shear forces (Eq. 6d) are given in Table 5.

The floor displacements based on the GFM as described, were then compared with the dynamic modal analysis results, in Figure 8. The dynamic analysis used the program based on the design response spectrum given in AS1170.4-2007 for a class B site. A $k_p Z$ value of 0.08g was adopted for the analysis. The comparison shows that GFM is able to provide reasonable estimates of the displacements and shear forces applying to the 6-storey building.

Table 5a. Displacement and inter-storey drift values based on the performance point

Level	δi (Step 4) mm	$\delta_i^* = \delta^*_{eff}/\delta_{eff}\delta_i$ mm	$\theta_i^* = (\delta_i^* - \delta_{i-1}^*)/h_i$ %
6	12.9	12.3	0.062%
5	10.8	10.3	0.065%
4	8.6	8.2	0.068%
3	6.3	6.0	0.065%
2	4.1	3.9	0.057%
1	1.6	1.5	0.036%
0	0	0	0

Table 5b. Displacement and inter-storey drift values based on the performance point

Level	F_i (Step 3) kN	$F_i^* = \delta_{eff}{}^* / \delta_{eff} F_i$ mm	$V_i = \sum_{j=i}^{n} F_j^*$ kN
6	2267.2	2155.8	
5	2031.1	1931.2	2155.8
4	1502.6	1428.7	4087.1
3	1155.6	1098.8	5515.8
2	823.4	782.9	6614.5
1	382.3	363.5	7397.5
0	0	0	7760.9

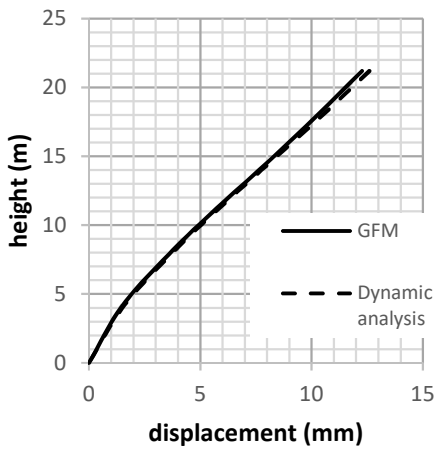
3. GFM for TB buildings incorporating higher mode effects

Higher mode effects were ignored in the analysis of Section 2, since the building was only 6-storeys high. Higher mode effects on taller buildings become significant when those responses become large enough to contribute to the overall response. This is illustrated schematically in Figure 9 on a displacement response spectrum diagram. When the spectral displacement at the fundamental period (RSD(T_1)) is much higher than that at the second modal period of the building (RSD(T_2)) as presented schematically in Figure 9a, the higher mode effects on displacement behaviour are insignificant. The effects of higher modes can become significant, however, when the response spectral displacement at the second modal natural period of the building is similar in scale to the spectral displacement at the fundamental natural period (Figure 9b).

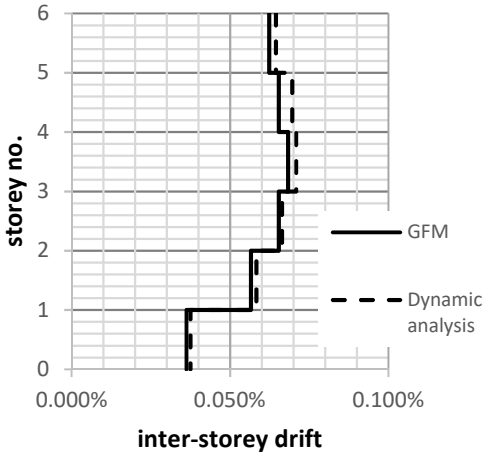
To illustrate the effects of higher modes, a dynamic modal analysis was conducted on a TB 20-storey building with the plans shown in Figure 4 and geometries in Table 2. The building was subject to the design response spectrum appropriate for a class C site (stiff soil) as proposed by Tsang et al. (2017) for regions of low seismicity. The design response spectrum in the displacement and ADRS format is illustrated in Figure 10. The k_p Z value of 0.08g was adopted for the analysis. The number of storeys and the design response spectrum were selected to illustrate higher mode effects. Results from the dynamic analysis are compared to those using the method of Section 2, above (refer to Figure 11). Higher mode effects on displacement demand are, this time, shown to be significant.

Higher modes effects on a building can be taken into account by an analysis method incorporating the generalised modal values shown in Figure 12 and by assuming that the second mode natural period (T_2) is 0.25 times the building's fundamental natural period (T_1). The modal factors presented in Figure 12 are products of the 'participation' factor and the modal deflection shape factor ($\Gamma.\phi$). Results shown in Figure 12 are mean values of dynamic analysis results obtained by the authors on multi-storey buildings of various heights. The buildings were supported by reinforced concrete walls and moment resisting frames featuring vertical irregularities in the form of discontinuities in some of the

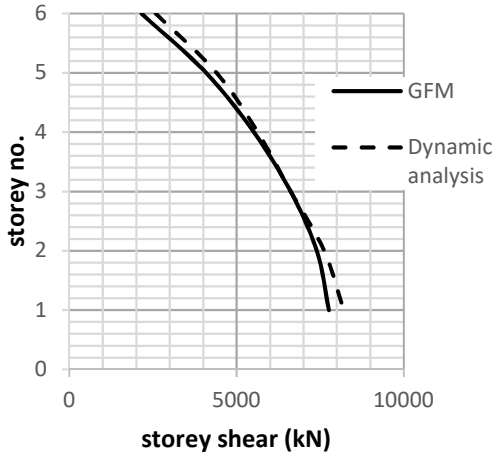
columns. Several building configurations with differing moment resisting frame contributions to the lateral stiffness of the building were analysed. Details can be found in Mehdipanah et al. (2016). The study results are given in Figure 13 as modal values versus normalised building height, for the first and second modes.



(a) Deflection

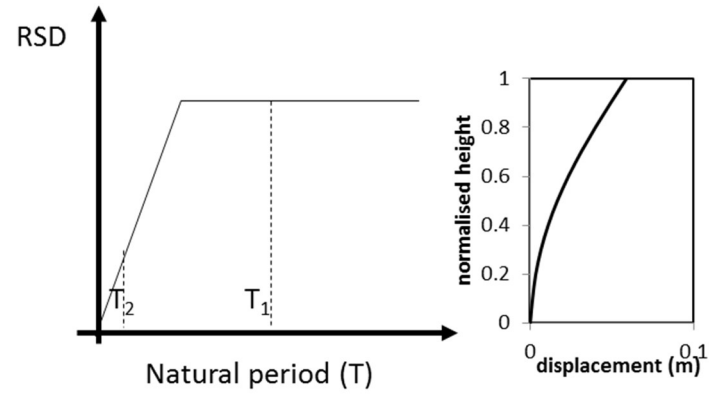


(b) Inter-storey drift

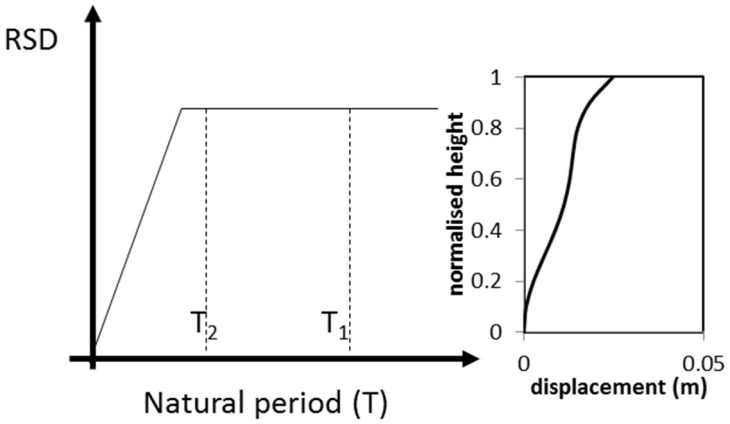


(c) Storey shear

Figure 8. Comparison between GFM results and a dynamic analysis of a 6-storey building

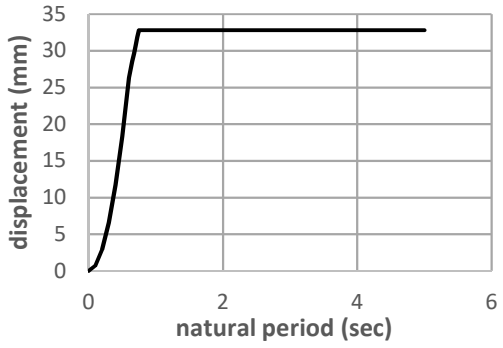


(a) Insignificant higher mode effects

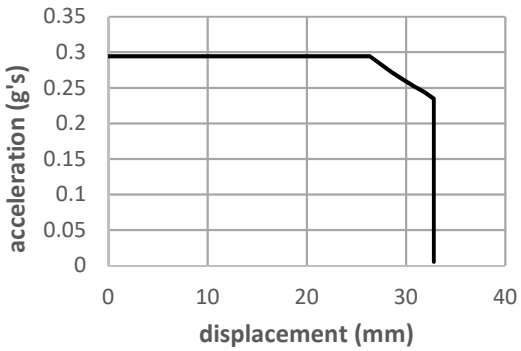


(b) Significant higher mode effects

Figure 9. Higher mode effects on displacement demand behaviour



(a) displacement format



(b) ADRS format

Figure 10. Design response spectrum for class C site and k_p Z of 0.08 (Tsang et al. 2017)

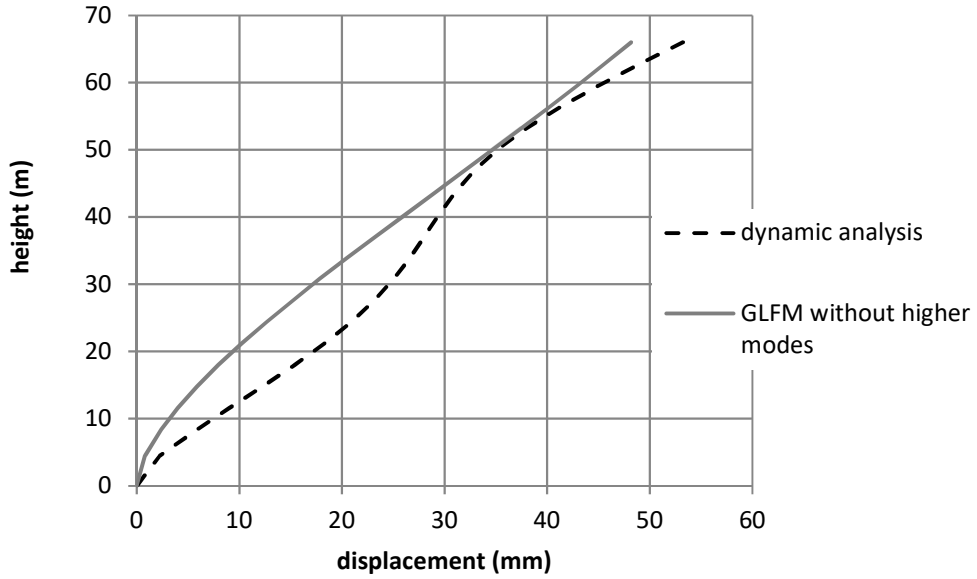


Figure 11. Comparison of GFM and dynamic analysis results for the example 20 storey building

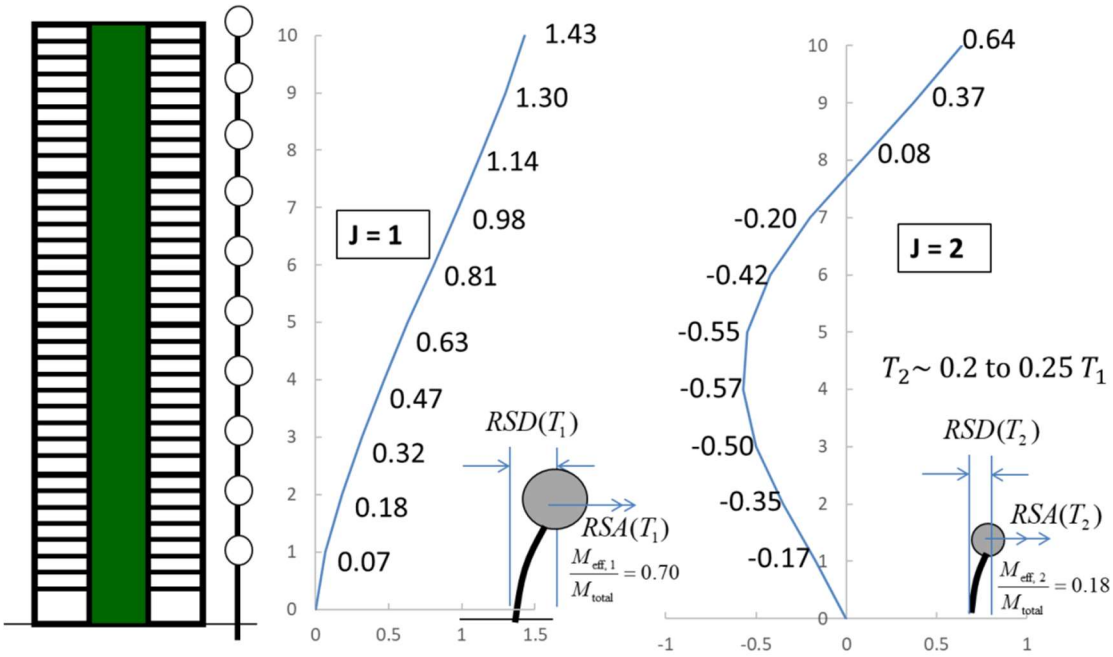


Figure 12. Generalised modal factors ($\Gamma_j . \phi_j$)

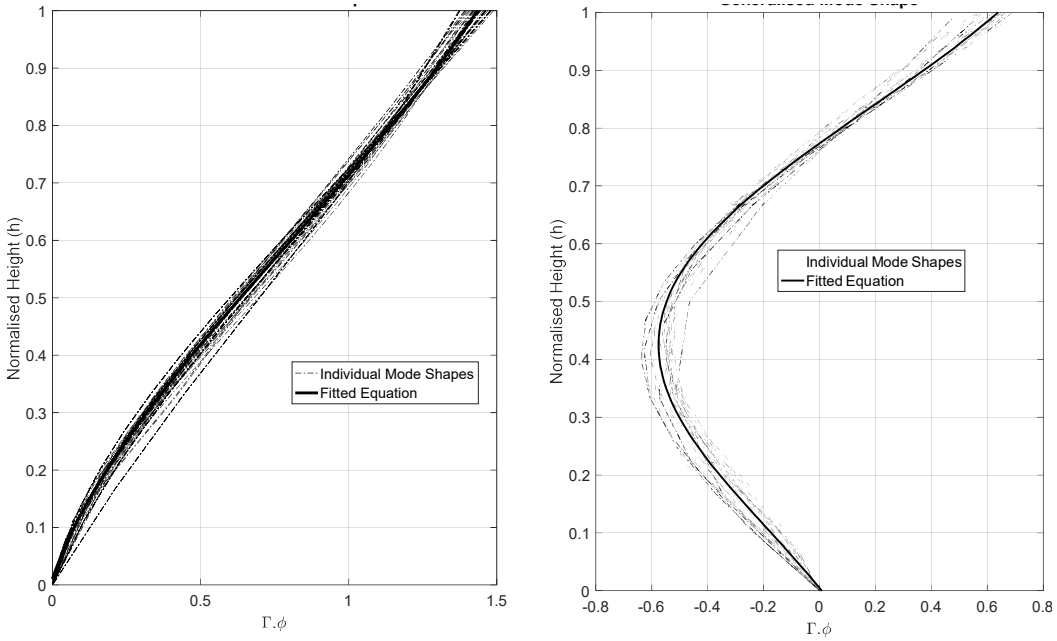


Figure 13. Modal displacements derived from parametric studies (Mehdipanah et al. 2016)

Given the mean value of T_2/T_1 of 0.25 and the generalised modal values presented in Figure 13, contributions from the second mode of vibration to the overall displacement response behaviour of the building ($\delta^*_{i,2}$) can be defined by:

$$\delta_{i,2} = \Gamma_2.\phi_{i,2}.RSD(0.25T_1) \tag{10a}$$

where $\Gamma_2.\phi_{i,2}$ is the modal displacement at the i^{th} level of the building; $RSD(0.25T_1)$ the spectral displacement at the second modal natural period (taken as 0.25 of T_1); and T_1 the fundamental natural period of vibration as defined by Eq. (4). Contributions from the second mode of vibration to the inter-storey drift can be defined by:

$$\theta_{i,2} = \frac{\left(\Gamma_2.\left(\phi_{i,2}-\phi_{i-1,2}\right).RSD(0.25T_1)\right)}{h_i} \tag{10b}$$

where h_i is the height of level i.

The contribution from the second mode of vibration, defined by Eq. (10), can be incorporated using the *square-root-of-the-sum-of-the-squares* (SRSS) combination rule:

$$\delta^*_{i,higher\ modes} = \sqrt{\delta_i^{*2} + \left(\Gamma_2.\phi_{i,2}.RSD(0.25T_1)\right)^2} \tag{11a}$$

$$\theta^*_{i,higher\ modes} = \sqrt{\theta_i^{*2} + \left(\frac{\left(\Gamma_2.\left(\phi_{i,2}-\phi_{i-1,2}\right).RSD(0.25T_1)\right)}{h_i}\right)^2} \tag{11b}$$

where δ_i^* and θ_i^* are the displacement and inter-storey drift based on the method of Section 2, above.

Similarly, the contribution of the second mode of vibration to the inertia force ($F_{i,2}$) at each level can be defined by:

$$F_{i,2} = m_i.\Gamma_2.\phi_{i,2}.RSA(0.25T_1) \tag{12a}$$

and its contribution to the storey shear:

$$V_{i,2} = \sum_{i}^{n} F_{i,2} \tag{12b}$$

where m_i is the mass of floor level i and $RSA(0.25T_1)$ is the spectral acceleration at the second modal period (taken as 0.25 of T_1) of the building.

By combining the second mode of vibration combination with the storey shear values obtained using the GFM method of Section 2, the storey shears can be defined by:

$$V^*_{i,higher\ modes} = \sqrt{V_i^{*2} + \left(\sum_{i}^{n}\left(m_i.\Gamma_2.\phi_{i,2}.RSA(0.25T_1)\right)\right)^2} \tag{13a}$$

where V_i^* is the storey shear obtained from the method of Section 2.

The procedure for the Generalised Force Method of analysis (GFM) incorporating higher modes is summarised in Table 6. The inertia forces can be determined from the difference between the storey shears acting at successive floor levels:

$$F^*_{i,higher\ modes} = V^*_{i-1,higher\ modes} - V^*_{i,higher\ modes} \tag{13b}$$

The method is illustrated with a 20-storey building example. The building plan is presented in Figure 4 and the geometries, in Table 2. The three-dimensional model is shown in Figure 14.

Table 6. GFM procedure incorporating higher mode effects

Step	Descriptions	Equations/Figures
1	Apply steps 1-11 listed in Table 1 for finding the displacement profile, inter-storey drifts, seismic inertia forces and storey shears δ_i^*, θ_i^*, F_i^* and V_i^*, the effective displacement δ_{eff}^*, and the fundamental natural period of vibration (T_1) of the building	Figures 1-3 Equations (1) - (6)
2	Modify the displacement profile from δ_i^* to $\delta_{i,higher\ modes}^*$ to incorporate the higher mode effects	Equations (10a) and (11a)
3	Modify the inter-storey drifts from θ_i^* to $\theta_{i,higher\ modes}^*$ to incorporate the higher mode effects	Equations (10b) and (11b)
4	Determine the higher mode contribution to the seismic inertia force of the individual floors from $F_{i,2}$ and determine the storey shear $V_{i,highe\ \ modes}^*$ incorporating the higher mode effects. Determine the inertia forces $F_{i,higher\ modes}^*$ acting on the floor levels based on the storey shears.	Equations (12a), (12b), (13a) and (13b)

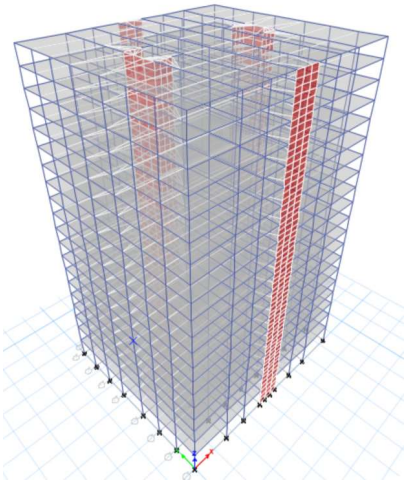


Figure 14. 3D building model of the example 20-storey building

Step 1

The GFM introduced in Section 2, was applied to obtain the displacement profile, inter-storey drifts, seismic inertia forces and storey shears. The capacity curve is superimposed on the ADRS diagram demand curve in Figure 15. The effective displacement δ_{eff}^*, at the intersection point between the capacity and demand curves in Figure 15, is 33 mm and the fundamental natural period of vibration (T_1) of the building is 2.4 sec. The displacement profile, storey drifts and storey shears for the building are shown in Figure 16, representing the dynamic behaviour of the building, ignoring higher mode effects.

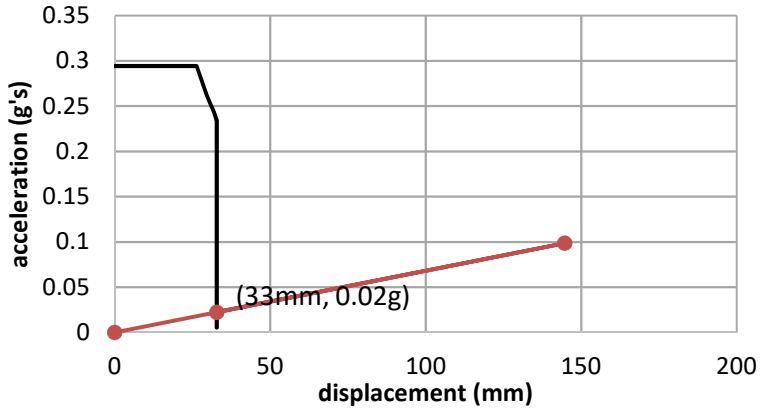
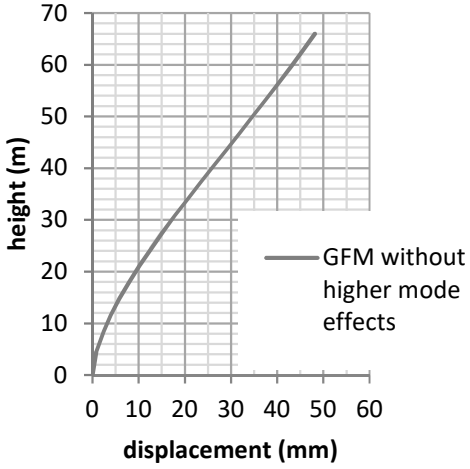
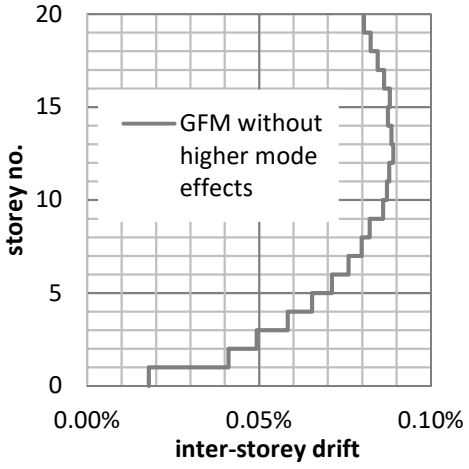


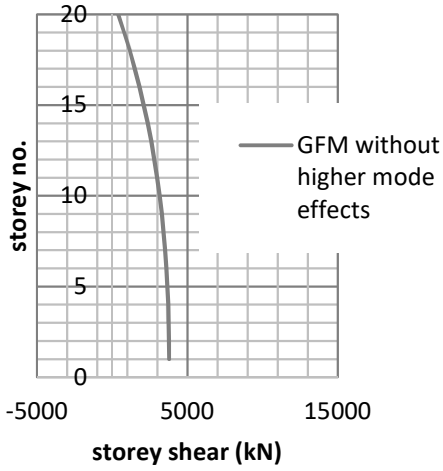
Figure 15. Superimposing the capacity curve onto the ADRS diagram



(a) deflection



(b) inter-storey drift



(c) Storey shear

Figure 16. Results from GFM without allowance for higher mode effects of a 20-storey building

Step 2

The displacement profile of the building obtained from step 1 was then adjusted with a scaling factor defined by Eq. (11a) to incorporate higher mode effects. The values for second mode of vibration ($\Gamma_2.\phi_{i,2}$) were based on the information shown in Figure 12. The response spectral displacement was obtained from the displacement response spectrum of Figure 17 and a 0.25 T_1 value of 0.6 sec. The revised displacement values are listed in Table 7.

Step 3

The inter-storey drift values obtained from step 1 were revised using Eq. (11b) to incorporate higher mode effects. The revised inter-storey drift values are listed in Table 8.

Step 4

The storey shear forces obtained from step 1 were also revised using Eq. (13) to incorporate higher mode effects. The revised storey shears are listed in Table 9.

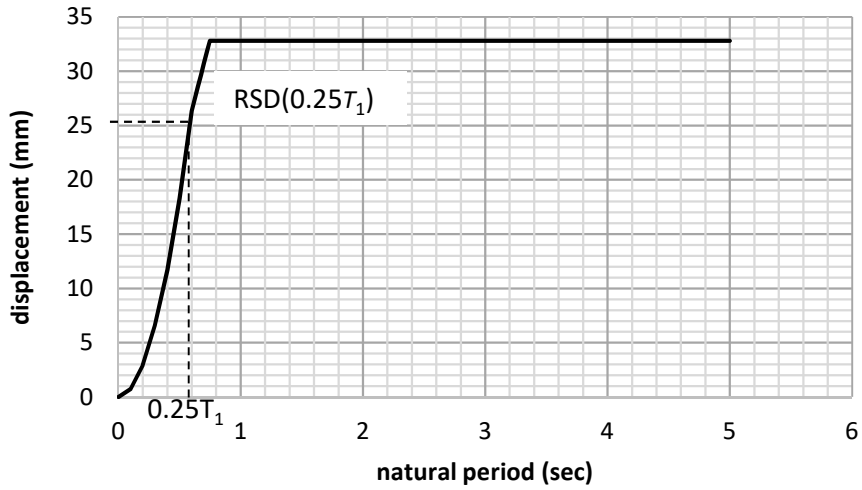


Figure 17. Displacement response spectrum and RSD(0.25T_1) value, for class C site and k_p Z of 0.08 (Tsang et al. 2017)

Table 7. Revised displacement profile incorporating higher mode effects

Level	height m	normalised height	δ_i^* (Step 1) mm	$\Gamma_2.\phi_{i,2}$	$\Gamma_2.\phi_{i,2}.RSD(0.25T_1)$ mm	$\delta^*_{i,higher\ modes}$ (Eq. 11a) mm
20	66	10.0	48.2	0.64	17.0	51.1
19	62.8	9.5	45.6	0.52	13.8	47.6
18	59.6	9.0	43.0	0.38	10.2	44.1
17	56.4	8.5	40.2	0.24	6.4	40.8
16	53.2	8.1	37.5	0.09	2.5	37.6
15	50	7.6	34.7	-0.05	-1.2	34.7
14	46.8	7.1	31.9	-0.18	-4.7	32.2
13	43.6	6.6	29.0	-0.30	-7.9	30.1
12	40.4	6.1	26.2	-0.40	-10.6	28.3
11	37.2	5.6	23.4	-0.48	-12.7	26.6
10	34	5.2	20.6	-0.53	-14.3	25.0
9	30.8	4.7	17.8	-0.57	-15.1	23.4
8	27.6	4.2	15.2	-0.58	-15.4	21.6
7	24.4	3.7	12.7	-0.56	-15.0	19.6
6	21.2	3.2	10.2	-0.52	-14.0	17.3
5	18	2.7	7.9	-0.47	-12.5	14.8
4	14.8	2.2	5.9	-0.40	-10.6	12.1
3	11.6	1.8	4.0	-0.31	-8.4	9.3
2	8.4	1.3	2.4	-0.22	-6.0	6.5
1	4.5	0.7	0.8	-0.11	-3.0	3.1
0	0	0.0	0.0	0.00	0.0	0.0

Table 8. Inter-storey drifts incorporating higher mode effects

Level	height m	normalised height	θ_i^* (Step 1) %	$\Gamma_2.\phi_{i,2}$	$\frac{\left(\Gamma_2.(\phi_{i,2}-\phi_{i-1,2}).RSD(0.25T_1)\right)}{h_i}$ %	$\theta^*_{i,higher\ modes}$ (Eq. 11b) %
20	66	10.0	0.080%	0.64	0.10%	0.13%
19	62.8	9.5	0.082%	0.52	0.11%	0.14%
18	59.6	9.0	0.084%	0.38	0.12%	0.15%
17	56.4	8.5	0.086%	0.24	0.12%	0.15%
16	53.2	8.1	0.088%	0.09	0.12%	0.15%
15	50	7.6	0.087%	-0.05	0.11%	0.14%
14	46.8	7.1	0.088%	-0.18	0.10%	0.13%
13	43.6	6.6	0.089%	-0.30	0.09%	0.12%
12	40.4	6.1	0.088%	-0.40	0.07%	0.11%
11	37.2	5.6	0.087%	-0.48	0.05%	0.10%
10	34	5.2	0.086%	-0.53	0.03%	0.09%
9	30.8	4.7	0.082%	-0.57	0.01%	0.08%
8	27.6	4.2	0.080%	-0.58	-0.01%	0.08%
7	24.4	3.7	0.076%	-0.56	-0.03%	0.08%
6	21.2	3.2	0.071%	-0.52	-0.05%	0.09%
5	18	2.7	0.065%	-0.47	-0.06%	0.09%
4	14.8	2.2	0.058%	-0.40	-0.07%	0.09%
3	11.6	1.8	0.049%	-0.31	-0.08%	0.09%
2	8.4	1.3	0.041%	-0.22	-0.08%	0.09%
1	4.5	0.7	0.018%	-0.11	-0.07%	0.07%
0	0	0.0	0.080%	0.00	0.10%	0.13%

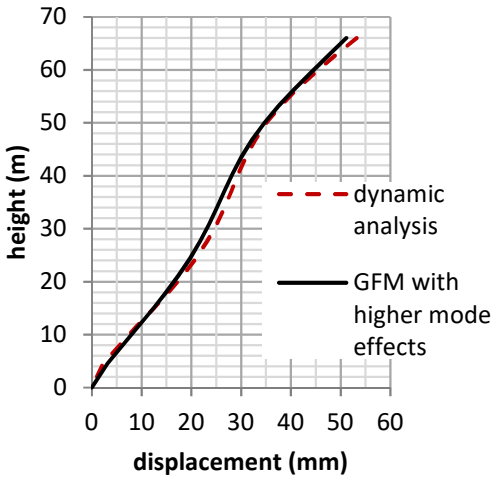
The displacement profile, inter-storey drifts and storey shears for the 20-storey buildings, as derived from the modified GFM and presented in this chapter are plotted in Figure 18 alongside dynamic analysis results. It is shown that the modified GFM provided reasonably accurate estimates of the seismically induced displacement and shear demands for the 20-storey building.

4. Conclusions

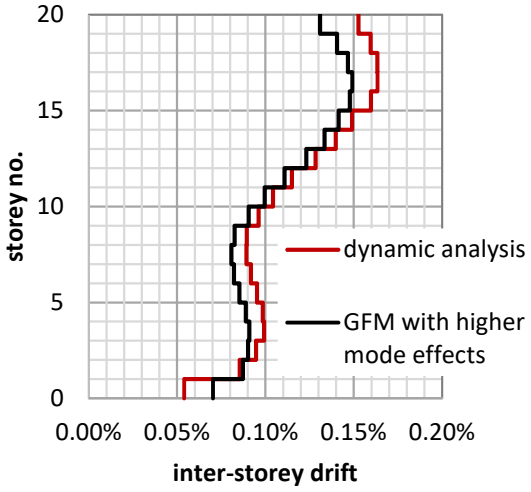
Many reinforced concrete buildings feature vertical irregularities. Contemporary seismic design guidelines generally require dynamic analyses to be conducted on such buildings. This chapter introduces a simple and accurate method of analysis, referred to, herein, as the Generalised Force Method (GFM), which provides estimates of displacements and storey shears for a multi-storey building featuring vertical irregularities. The method is first illustrated with an analysis of an example 6-storey building. A second, 20-storey building example, incorporating contributions by higher modes of vibration, is then analysed. For both examples GFM method results were compared with reported dynamic analysis results and found to be in good agreement.

Table 9. Storey shear forces and inertia forces incorporating higher mode effects

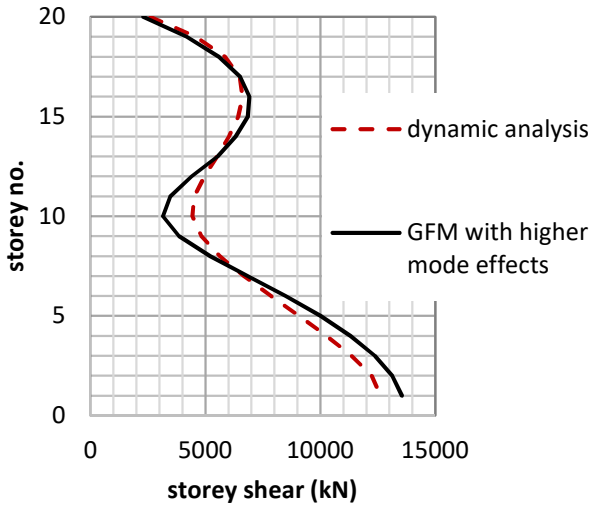
Level	mass (tonnes)	V_i^* (Step 1) (kN)	$\Gamma_2.\phi_{i,2}$	$\sum_i^n \left(m_i.\Gamma_2.\phi_{i,2}.RSA(0.25T_1) \right)$ (kN)	$V^*_{i,higher\ modes}$ (Eq. 13a) (kN)	$F^*_{i,higher\ modes}$ (Eq. 13b) (kN)
20	1240		0.64			2297
19	1252	408	0.52	2260	2297	1887
18	1252	802	0.38	4106	4184	1409
17	1259	1167	0.24	5470	5593	912
16	1265	1504	0.09	6329	6505	408
15	1265	1812	-0.05	6671	6913	-78
14	1276	2096	-0.18	6506	6835	-521
13	1147	2356	-0.30	5859	6315	-781
12	1319	2590	-0.40	4890	5533	-1132
11	1193	2801	-0.48	3395	4401	-928
10	1193	2988	-0.53	1771	3473	-320
9	1193	3153	-0.57	-49	3153	692
8	1193	3296	-0.58	-1980	3845	1372
7	1202	3419	-0.56	-3941	5217	1623
6	1213	3522	-0.52	-5864	6840	1641
5	1213	3605	-0.47	-7677	8482	1514
4	1220	3672	-0.40	-9297	9996	1313
3	1229	3721	-0.31	-10679	11309	1056
2	1229	3756	-0.22	-11781	12366	760
1	1350	3779	-0.11	-12570	13125	421
0	0	3787	0.00	-13006	13546	0



(a) Displacement



(b) Inter-storey drift



(c) Storey shear

Figure 18. Results from GFM with higher mode effects, 20-storey building

Acknowledgements

The support of the Commonwealth Australia through the Cooperative Research Centre program and the University of Melbourne Early Career Researcher Grants Scheme is acknowledged.

References

ASCE (2000) Prestandard and commentary for the seismic rehabilitation of buildings FEMA 356. Washington, D.C.: Federal Emergency Management Agency.

Building Seismic Safety Council (2003) NEHRP Recommended Provisions for Seismic Regulations for New Buildings and Other Structures Part I : Provisions (FEMA 450-1). Washington, D.C.: Federal Emergency Management Agency.

EN 1998-1 (2004) Eurocode 8: Design of structures for earthquake resistance – Part 1: General rules, seismic actions and rules for buildings. BSI.

ETABS, C. (2015) 15.0. Berkeley. CA: Computers and Structures Inc.

Lam, N.T.K., Wilson, J.L. and Lumantarna, E. (2016) "Simplified elastic design checks for torsionally balanced and unbalanced low-medium rise buildings in lower seismicity regions." Earthquakes and Structures 11(50): DOI 10.12989/eas.2016.11.5.741.

Lam, N.T.K., Wilson, J.L. and Lumantarna, E. (2010) "Modelling of seismically induced storey-drift in buildings." Structural Engineering and Mechanics 35(4): 459-478.

Mehdipanah, A., Lam, N.T.K., Lumantarna, E. (2016) "Behaviour of buildings featuring transfer beams in the regions of low to moderate seismicity." 2016 Australasian Structural Engineers Conference (ASEC), 23-25 Nov 2016, Brisbane, Australia.

Standards Australia (2007) AS 1170.4-2007 Structural Design Actions – Part 4 Earthquake Actions. Sydney: Standards Australia.

Tsang, H.H., Wilson, J.L., Lam, N.T.K. (2017) "A refined design spectrum model for regions of lower seismicity." Australian Journal of Structural Engineering, in press.

Wilson, J.L., Lam, N.T.K. (2006) Earthquake design of buildings in Australia by velocity and displacement principles." Australian Journal of Structural Engineering 6(2): 103-118.

Design of Reinforced Concrete Walls for Regions of Low Seismicity

Scott J. Menegon[a], John L. Wilson[a] and Nelson T. K. Lam[b]

[a] Centre for Sustainable Infrastructure
Swinburne University of Technology, Australia

[b] Department of Infrastructure Engineering
The University of Melbourne, Australia

The design and detailing of reinforced concrete (RC) buildings in regions of low seismicity, such as Australia, has historically differed significantly from typical design procedures in regions of high seismicity, such as New Zealand or the west coast of the US. This is due, in part, to the fact that seismic design has not been traditionally practised in low seismicity regions, resulting in ingrained design methodologies that commonly lead to structures which are code-compliant, but brittle and vulnerable during earthquakes. This chapter serves as a primer to a comprehensive research study, which the authors are currently conducting into the seismic performance of RC wall buildings in regions of low seismicity. The chapter discusses the already completed large scale experimental testing programme and provides recommendations for good RC wall detailing in regions of low seismicity.

Keywords: reinforced concrete walls, RC walls, RC wall design, RC wall detailing

1. Introduction

Seismic design codes in regions of low seismicity have historically copied or been heavily influenced by codes of practice in regions of high seismicity. However low seismic regions differ from high seismic regions in two key ways; the first being that the intensity of ground shaking between long and short return period events is much more severe and the second being that the displacement demands are more modest due to the upper magnitude limit of intraplate earthquakes characteristic of low seismic regions. For these reasons, copying design codes and practices from high seismic regions can simultaneously be overly conservative in some aspects yet inappropriate in others.

The authors have been undertaking a long term Australian Research Council (ARC) funded research program to assess and reduce the seismic risk and rationalise the seismic design procedures and practices in Australia. While the primary focus is Australia, the research outcomes and findings are relevant to most regions of low seismicity around the world. This has included research studies that have: resulted in the development of the Component Attenuation Model (CAM) (Lam et al., 2000a; Lam et al., 2000b), which lead to the development and implementation of a new response spectrum for Australia (Wilson and Lam, 2003); assessed the seismic performance of unreinforced masonry structures (Griffith et al., 2004; Griffith, Lam and Wilson, 2006); and assessed the seismic performance and drift capacity of soft-storey RC buildings with non-ductile RC columns (Wibowo et al., 2011; Wibowo et al., 2014; Wilson et al., 2015). The most recent phase of this research program concerns the assessment of the seismic performance of RC wall buildings in regions of low seismicity.

Limited ductile RC walls are utilised as the primary lateral load resisting system in most low, mid and high-rise multi-storey buildings in Australia (Menegon et al., 2017c). Yet, in many respects their behaviour has been largely un-researched, particularly the post-peak lateral displacement behaviour. Wall construction methods, similar to those seen in Australia, are widely used in buildings in other regions of low seismicity around the world. This current phase of research was initiated to firstly better understand the lateral displacement behaviour of limited ductile RC walls and secondly, to develop guidelines and procedures for accurately assessing the seismic performance of these walls when they are part of the whole building system.

This chapter serves as an interim primer, while a more comprehensive and complete design guide is being produced that will focus more specifically on the displacement-based design of RC walls, that will discuss the initial findings of this recent research initiative into the seismic performance of RC wall buildings in regions of low seismicity. This chapter includes a brief summary of the large scale experimental testing program that has been performed into RC walls and provides some preliminary recommendations for the design and detailing of RC walls in regions of low seismicity

2. Low seismic regions versus high seismic regions

Earthquake design of buildings in regions of high seismicity is typically governed by high magnitude events occurring on tectonic plate boundaries (i.e. interplate earthquakes). This is in contrast to regions of low seismicity where more moderate magnitude earthquakes, occurring away from the plate boundaries (i.e. intraplate earthquakes), govern the design. The frequency content and duration of strong ground motions generated by smaller magnitude intraplate events result in a design response spectrum with significantly lower maximum displacement demands. This maximum displacement demand can be quite modest and comparable to the ultimate displacement capacity of many structures, whereas in regions of high seismicity, the displacements that are generated by strong ground shaking of a large magnitude earthquake are usually capped at a very high level thereby giving no incentives to the designer to make use of displacement-controlled principles to check for stability

Figure 1 compares the acceleration-displacement response spectrum (ADRS) of a typical rock site in Australia and New Zealand with a hazard factor of 0.08g and 0.30g respectively. The ADRS curve for the Australian and New Zealand site are constructed using the AS 1170.4 (Standards Australia, 2007) and NZS 1170.5 (Standards New Zealand, 2004) response spectrums respectively. Figure 1 shows that the site in New Zealand, where the hazard is nearly 4 times greater, has a maximum acceleration demand that is only approximately 2.4 times greater than the Australian site, whereas the maximum displacement demand increases by a factor closer to 9. The larger relative difference between the maximum displacement demands is due to the different second corner period (i.e. T_2) of the Australian and New Zealand response spectrum, which is equal to 1.5 and 3.0 seconds respectively. The second corner period typically dictates the displacement-controlled region of the response spectrum and is relative to the maximum magnitude event considered in the respective region. The maximum magnitude event for Australia has been taken as 7 (Lam et al., 2000a; Lam et al., 2000b) and hence results in a much small second corner period than that of New Zealand where much larger magnitude earthquake events can occur.

The displacement-controlled behaviour in regions of low seismicity can be used to

great effect when checking the seismic compliance of a large quantity of existing building stock. A designer can simply calculate the ultimate displacement of the structure and check it against the corresponding maximum displacement demand for the site. If the ultimate displacement exceeds the associated maximum demand then the building automatically achieves satisfactory seismic compliance. This can be a powerful 'first tier' level of analysis in regions of low seismicity due to its inherent speed and the avoidance of complex calculations.

The second corner displacement-controlled behaviour of the Australia response spectrum also extends to torsional raking effects in Buildings. Torsional effects can be detrimental to a building, potentially causing catastrophic failures. Torsional effects can also greatly increase storey drift at the corners of buildings, potentially causing failure of poorly detailed cladding systems and gravity frames which are not commonly detailed to sustain large amounts of inter-storey drift, i.e. not designed to be ductile.

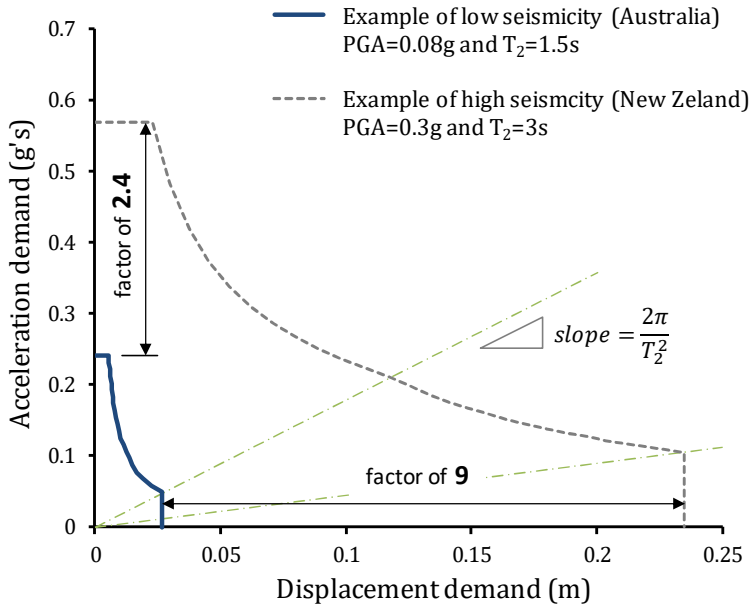


Figure 1. Difference between regions of low seismicity and high seismicity

Lumantarna et al. (2013) recently conducted a study into the effects of torsion on SDOF structures exhibiting both elastic and inelastic behaviour. The findings of the research indicated a similar concept to the displacement-controlled phenomena; where continually increasing the buildings eccentricity does not indefinitely increase the torsional actions on the structure. It was found that the peak displacement demand, amplified by torsion, on an element consistently never exceeded 1.6 times the RSd_{max} value. This implies that if the displacement capacity of a structure is greater than $1.6 \times 1.5 \times RSd_{max}$ for the site, the building is compliant for seismic actions regardless of the eccentricity. This study is ongoing and is currently being extended to research this behaviour in multi-storey buildings, i.e. MDOF structures.

3. RC wall construction in low seismic regions

RC wall construction in regions of low seismicity differs somewhat significantly from regions of high seismicity. In the latter, walls are typically detailed with high levels of confinement in the end regions of the wall with concentrated vertical reinforcement. The confinement allows for large compressive strains to be developed while also preventing buckling of the vertical reinforcement under reversed cyclic loading. In regions of low seismicity, such as Australia, walls are typically detailed with a constantly spaced grid of vertical and horizontal reinforcement in four layers, two per face. No confinement is typically provided in the end regions, however 'U' bars are usually provided at the ends of walls and at wall intersections. Lap splicing of the vertical reinforcement at the base of the wall, typically in the plastic hinge zone, is standard practice. The most common types of wall cross section used are rectangular walls and box shaped building cores. The reader is directed to Menegon et al. (2017c) for further details on RC wall construction in Australia.

Wall construction of this nature usually results in a 'limited ductile' classification to the Australian earthquake code, AS 1170.4 (Standards Australia, 2007) and allows a displacement ductility value of 2.0 and an overstrength factor of 1.3 to be adopted. This results in a force reduction factor of 2.6 when using force-based seismic design procedures, e.g. the equivalent static analysis to AS 1170.4.

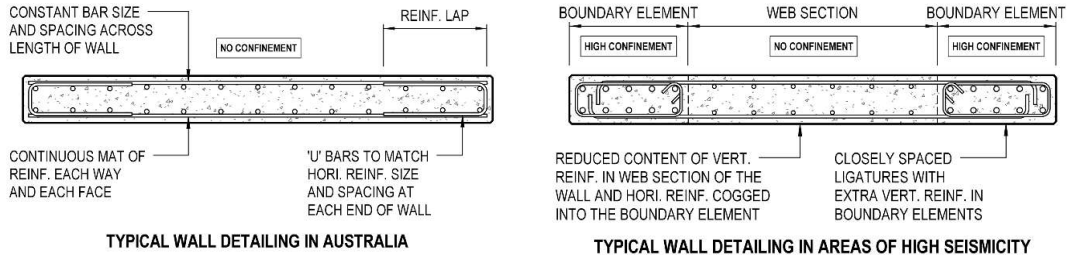


Figure 2. Right: typical wall detailing in a region of low seismicity, such as Australia. Left: typical wall detailing in a region of high seismicity. (Menegon et al., 2017c)

4. Limited ductile RC wall

The authors have recently completed a large-scale experimental testing program into the in-plane lateral displacement behaviour of limited ductile RC walls. The experimental program included 17 boundary element prism tests (e.g. Menegon et al. (2015b) and Menegon, Wilson and Lam (2015a)) and 5 large scale RC wall tests (e.g. Menegon et al. (2017a) and Menegon et al. (2017b)). Both traditional monolithic cast in-situ RC walls and the more recent jointed precast walls were considered in this study. Pre-cast walls have become increasingly popular in Australia, particularly for low and mid-rise buildings.

The large-scale wall tests were designed and detailed to best match standard industry practice as identified by Menegon et al. (2017c). The walls were tested under a quasi-static reversed cyclic loading regime with a shear-span ratio of 6.5 (i.e.. $M^*/(V^*L_w) = 6.5$). The testing was performed using the Multi-Axis Substructure Testing (MAST) system in the Smart Structures Laboratory (SSL) at Swinburne University of Technology. The MAST system is a state-of-the-art test machine capable of applying full six degree-of-freedom (DOF) loading in mixed-mode, switched-mode, hybrid or a combination therein (Hashemi et al., 2015). The 5 large-scale RC wall tests consisted of 1 rectangular wall and 4 building

core specimens. Of the 4 building cores,1 was a monolithic cast in-situ specimen and 3 were jointed precast sections. The rectangular wall was a monolithic cast in-situ element. The cross sections of each specimen are shown in Figures 3 and 4.

The test setup, loading protocols and results of the cast in-situ rectangular wall and building core specimens are presented in Menegon et al. (2017b). The test results of the precast building core tests and the boundary element prisms tests are largely unpublished at the time of writing this chapter.

.

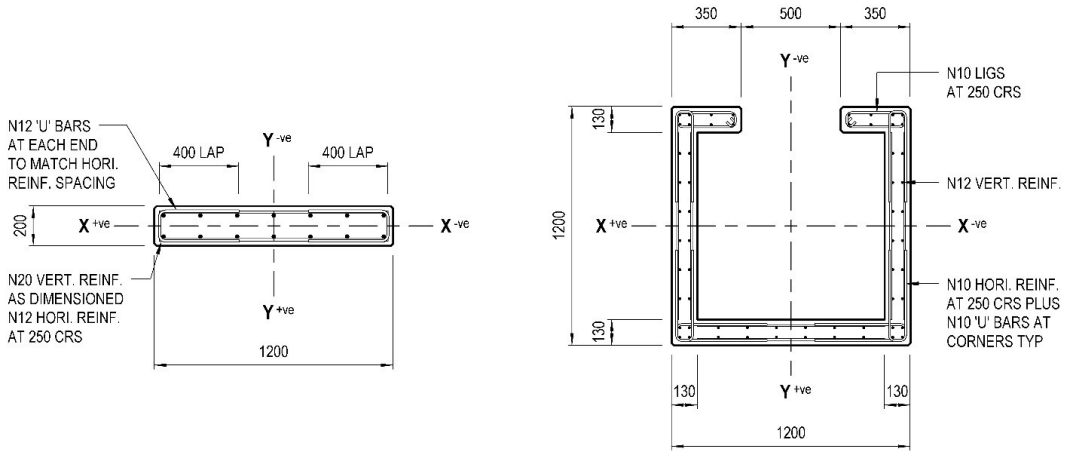
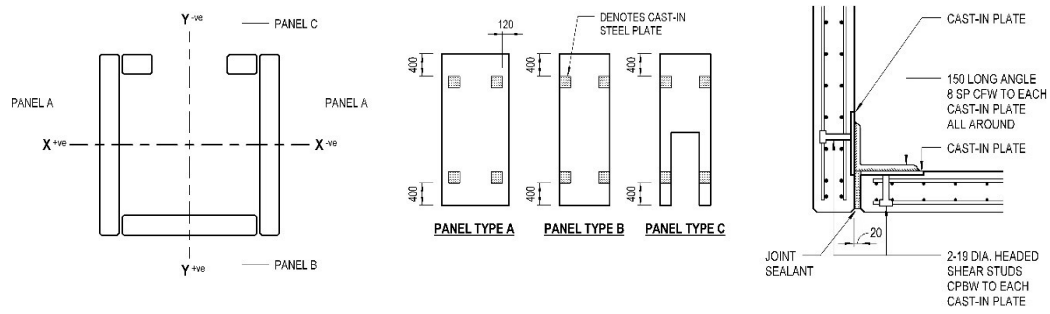


Figure 3. Cast in-situ rectangular wall and building cores specimens



(a) cross section (b) panel elevations (c) connection detail

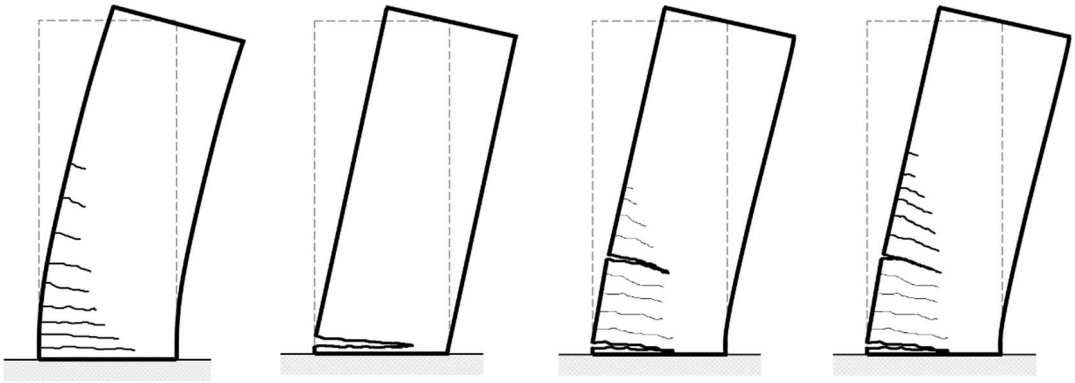
Figure 4. Typical cross section and connection detail of a jointed building core specimen

Two of the key findings of the large-scale experimental program were the atypical plastic hinge development that was observed and the large in-plane lateral drifts the specimens could resist prior to complete structural collapse, i.e. axial load failure of the specimens. The walls were tested using axial load ratios, i.e. $N^*/(f_c'A_c)$) where N* is the design axial force and Ac is the gross cross-sectional area of the wall, typical to what is commonly seen in industry, which was identified to be between about 5 and 10 per cent (Menegon et al., 2017c). The cast in-situ rectangular wall and building core specimens were

tested with axial load ratios of 6.5 and 7.7 per cent respectively. These relatively low axial load ratios allowed the specimens to reach 4.4 and 4.6 per cent drift respectively prior to axial load failure occurring.

The atypical plastic hinge behaviour was a result of the lap splice at the base of the wall. Typically in RC wall testing – when no lap splice is at the base of the wall – the wall develops one of two plastic hinge models. The first being the typical plastic hinge model which has distributed cracking extending some length up the height of the wall with the inelastic tension strain distributed somewhat evenly across these cracks. The second being a single crack plastic hinge, where the wall is detailed such that only a single crack develops at the base of the wall with all the inelastic tension strain being concentrated in this one location, resulting in a significantly reduced lateral displacement capacity compared to the former. This behaviour usual occurs in under reinforced cross sections where the cracking moment of the wall is greater than the ultimate moment capacity of the wall. These models are depicted in Figure 5(a) and 5(b) respectively.

The walls in this experimental program were detailed with a lap splice at the base of the wall in the plastic hinge region, which is standard practice in Australia, and as such developed a different plastic hinge mechanism. The lap splice resulted in a region of wall with effectively double the amount of vertical reinforcement, creating a localised region of overstrength where the moment capacity was significantly higher than the section of immediately above and below. This region of overstrength allowed only hairline cracks to develop across the lap splice and forcing the development of two major cracks, one above and one below the lap splice. The majority of the inelastic tension strain was concentrated at these two cracks resulting in a two-crack plastic hinge model (Figure 5(c)). A variation of the two-crack plastic hinge model was observed in some specimens, where instead of one major crack being developed above the lap splice, multiple cracks developed (Figure 5(d)). The type c and type d plastic hinge response is dictated by the ratio of the applied moment at the base of the wall to the applied moment at the top of the lap splice. This ratio is dependent on the length of the lap splice and the shear-span ratio of the wall (i.e. slenderness). This behaviour is further discussed in Menegon et al. (2017b).



(a) traditional plastic hinge model with distributed cracking

(b) single crack plastic hinge model (under-reinforced section)

c) two-crack plastic hinge model (lap splice at the base of the wall)

(d) shift plastic hinge model (lap splice at the base of the wall)

Figure 5. Plastic hinge development in RC walls (Menegon et al., 2017b)

5. Detailing of RC walls in low seismic regions

In regions of low seismicity, such as Australia, for many years the seismic design of buildings was not performed nor required by building codes. It has only been in more recent times that designers in these regions have had to undertake seismic design and analysis of structures. This lack of attention to seismic design over many years has resulted in many misconceptions and a low level of education surrounding seismic design and its inherent assumptions, particularly with regards to the concept of trading strength for ductility. Force-based seismic design allows the structure to absorb part of the energy imparted by the earthquake via inelastic plastic deformation of its elements. This is accounted for in design by the force reduction factor (e.g. R_f), which is used to reduce the equivalent elastic design earthquake loads on the structure. The force reduction factor consists of two components, the first being overstrength (Ω) and the second being displacement ductility (μ), and is equal to the product of these two components, i.e. $R_f=\Omega\mu$. It should be noted that in AS 1170.4 the overstrength factor is represented by the structural performance factor (S_p), which is equal to the reciprocal of the overstrength factor, i.e. $S_p=1/\Omega$. Meaning the force reduction factor can equally be represented as ductility divided by the structural performance factor, i.e. $R_f= \mu/S_p$.

There are essentially three ductility classes that can be adopted when performing force-based seismic analysis in accordance with the Australian earthquake code, AS 1170.4 (Standards Australia, 2007) for buildings or structures designed and detailed in accordance with the Australian concrete code, AS 3600 (Standards Australia, 2009). These three classifications are: 'limited ductile', where $\mu=2$ and $\Omega=1.3$; 'moderately ductile', $\mu=3$ and $\Omega=1.5$; and 'fully ductile', where $\mu=4$ and $\Omega=1.5$. The limited ductile classification can be adopted if the building is detailed in accordance with the main body of AS 3600, whereas the moderately ductile classification can be adopted if the building is detailed in accordance with the main body and the earthquake section (i.e. Appendix C) of AS 3600. The fully ductile classification is rarely adopted in Australia as it requires the building to be design in detailed in accordance with the New Zealand earthquake code, NZS 1170.5 (Standards New Zealand, 2004) and the New Zealand concrete code, NZS 3101 (Standards New Zealand, 2006). The three ductility classes are summarised in Table 1.

Within the design community in Australia there is currently a widespread lack of appreciation and understanding of the fundamental assumption of force-based seismic design, which is that strength is being traded for ductility. As a result, poor detailing practices are often adopted when designing and detailing RC walls, which in turn greatly reduce the displacement ductility capacity of the system. To many, these detailing practices have been accepted as pseudo industry standards. To assume some level of ductility when determining the earthquake actions on the building (e.g. $\mu=2$), but then, to detail the structure in a manner that results in little or no ductility, is obviously contradictory.

The limited ductile classification is recommended for the majority of buildings in Australia and caution is suggested in adopted the more ductile classifications. Blindly assuming high amounts of ductility in the design without providing the associated level of detailing could result in a brittle building that has the potential to fail suddenly in a catastrophic manner during a major earthquake.

The following detailing practices, which are widely observed in Australia, particularly in jointed precast structures, significantly reduce the displacement ductility capacity of a system and their use is cautioned against:

1. Detailing RC walls with a single central layer of vertical and horizontal reinforcement.
2. Detailing RC walls using low ductility reinforcement, usually in the form of welded wire mesh.
3. Detailing RC walls using low percentages of vertical reinforcement, which inhibits the wall's ability to develop desirable distributed cracking, i.e. Figure 5(a) versus 5(b).
4. Detailing dowel connections in precast wall panels such that the area of the dowel reinforcement is less than the area of the main vertical reinforcement in the wall panel.

The reader is directed to Menegon et al. (2017d) for detailed discussions regarding each of these detailing practices and how they can adversely affect the displacement ductility of RC walls.

Table 1. AS 1170.4 ductility and overstrength factors for RC walls.

Classification	μ	**Ω**	R_f	**Notes**
Limited ductile	2	1.3	2.6	Building must be detailing in accordance with the main body of AS 3600.
Moderately ductile	3	1.5	4.5	Building must be detailing in accordance with the main body and earthquake section (Appendix C) of AS 3600.
Fully ductile	4	1.5	6.0	Building must be designed and detailing in accordance with New Zealand codes NZS 1170.5 and NZS 3101.

While the authors are not advocates of any of these practices, it is appreciated that due to various project constraints it may be desired that they be adopted. If this is the case, it is recommended that a new ductility classification called 'non-ductile' be adopted. This classification would allow these detailing practices to be used, however a displacement ductility factor of 1.0 (i.e. μ=1.0) would need to be used when calculating the seismic actions. This new ductility classification would still have an overstrength factor of 1.3 (i.e. Ω=1.3) because despite no ductile lateral load path being explicitly provided in the structure, it would likely still have the same amount of inherent overstrength as the limited ductile classification.

This would result in designers having effectively three ductility classes to select from when designing RC wall buildings, i.e. non-, limited and moderately ductile. Menegon et al. (2017d) provided detailing recommendations for each ductility class, which have been presented in Table 2. The detailing requirements in Table 2 are generally more stringent than the requirements in the current version of AS 3600, which is largely out-dated or incomplete with respect to earthquake and ductility requirements. However, it should be

noted that at the time of producing this chapter, a revised draft version of AS 3600 has been released for public comment, which includes many of the items presented in Table 2.

A common argument for allowing the use of these poor detailing practices, while still assuming some level of ductility when determining the earthquake forces, is that the central core is taking all the lateral load and the exterior or peripheral RC walls (often precast) are 'load bearing only elements' and as such, it only matters how the central core is detailed. It would be a false assumption to assume these walls are load bearing only elements as an earthquake will distribute load based on the strength, stiffness and ductility of the elements in the system regardless of how one describes them.

When performing lateral analysis, it may appear that the central core takes all the lateral load (when the forces are distributed using initial or effective stiffnesses), however the real force distribution that would occur if the overall systems inelastic displacements were taken into consideration would likely be very different. The ductility class assumed for the building should be that of the least ductile element within the lateral load resisting system of the building.

Attention also needs to be given to the slenderness ratios of walls, i.e. height-to-thickness ratios, to prevent out-of-plane instabilities under reversed lateral load, as discussed and shown in various experimental programs by Menegon et al. (2015b), Rosso et al. (2016) and Dashti et al. (2017). These studies are ongoing research efforts and do not currently provide firm guidance or design rules for designers. In the meantime, Wallace (2012) has recommended limiting the h/t_w ratio to 16 or less, where h is the inter-storey unrestrained height of the wall. Wallace (2012) also precautions that a value of 16 may still be insufficient to prevent out-of- plane instabilities in some wall configurations, however, until more comprehensive studies are completed, a h/t_w limit of 16 (as proposed in Table 2) is being recommended for plastic hinge regions or elsewhere in RC walls where significant inelastic plastic tension strains can be developed.

Consideration must also be given to ensure a desirable flexure failure occurs and not an undesirable brittle shear failure. This could be achieved by designing for a minimum shear force value that corresponds to the actual in-situ flexural moment capacity of the wall, i.e. a value equal to the design shear force multiplied by the actual moment capacity of the wall divided by the design moment acting on the wall. Priestley et al. (2007) proposes that the overstrength for an RC element, where the capacity has been calculated using characteristic material properties and no allowance for strain-hardening in the reinforcement, can be taken as 1.6. Therefore, $\phi V_u \geq (1.6M_u/M^*)V^*$

Finally, some building configurations can result in walls having very low aspect ratios or similarly, low shear-span ratios. It should be noted that the latter can be the result of coupling between adjacent elements rather than the physical properties of the individual element. In these scenarios, it is recommended to design the wall as a non-ductile element using strut and tie methods, as proposed in Table 2.

Table 2. Recommended detailing practices for RC walls (Menegon et al., 2017d)

	Non-Ductile	**Limited Ductile**	**Moderately Ductile**
Ductility factor, $\boldsymbol{\mu}$	1	2	3
Overstrength factor, $\boldsymbol{\Omega}$	1.3	1.3	1.5
Structural performance factor, $\boldsymbol{S_p}$	0.77	0.77	0.67
Force reduction factor, $\boldsymbol{R_f}$	1.3	2.6	4.5
Low ductility reinforcement	Permitted	Not permitted	Not permitted
Centrally reinforced walls	Permitted	Not permitted	Not permitted
Vertical reinforcement ratio in plastic hinge regions of the wall[1]	Current code provisions	See note 2	See note 2
Confinement (cross tie) reinforcement	Current code provisions	Current code provisions	NZS 3101 provisions[3]
Splicing of vertical reinforcement in plastic hinge regions of the wall[1]	Lap splices permitted	Lap splices permitted	NZS 3101 provisions[3] or mechanical splices[4]
Development of horizontal reinforcement[5]	No requirement	Required at ends of walls and all wall intersections	Required at ends of walls and all wall intersections
Axial load ratio[6]	≤ 0.2	≤ 0.2	≤ 0.2
Shear design	No requirement	$\phi V_u \geq (1.6M_u/M^*)V^*$	$\phi V_u \geq (1.6M_u/M^*)V^*$
Slenderness ratio in plastic hinge regions of the wall1	Current code provisions	$\frac{h}{t_w} \leq 16$	$\frac{h}{t_w} \leq 16$
Aspect ratio[7]	No requirement	$\frac{H_w}{L_w} \geq 2$	$\frac{H_w}{L_w} \geq 2$
Precast construction	Permitted	Permitted	Permitted
Dowel bars in precast grout tube connections	No requirement	D500N bars only	D500N bars only
Dowel area in precast grout tube connections	No requirement	$A_{st,dowel} \geq A_{st,wall}$	$A_{st,dowel} \geq A_{st,wall}$

Remarks

1) The plastic hinge region of walls in first mode dominant structures is to be taken as the bottom two storeys of the building or twice the depth of the member, whichever is greater. Designers should consider higher mode effects and the development of secondary hinges up the height of the wall in slender walls.
2) The vertical reinforcement ratio is dependent on the grade of concrete specified. Menegon et al. (2017d) suggests reinforcement ratios of 0.007, 0.008, 0.009 and 0.010 for concrete grades N32, N40, N50 and S65 respectively. The vertical reinforcement ratio can be decreased at a rate of 15% per storey away from the plastic hinge regions.
3) The NZS 3101 provision for ductile RC walls should be adopted. The moderately ductile class, in the Australian context, corresponds to a level of performance between NZS 3101 classes 'structures of limited ductility' and 'ductile structures'. Therefore, the provisions of the higher, ductile structures classification should be adopted.
4) Mechanical splices to be bar break systems only, i.e. under tensile load the bar shall fracture either side of the mechanical splice, and be able to sustain inelastic strains across multiple cycles. The mechanical splices shall also be staggered vertically by a length equal to the standard lap length of that bar.
5) e.g. additional 'U' bars lapped with horizontal reinforcement at wall intersections and end regions of walls or cogging horizontal reinforcement into confined end regions of walls (refer Menegon et al. (2017c)).
6) Axial load ratio is equal to N^*/((f_c^' A_g)), where N^* is calculated using the load combination for earthquake actions given in AS/NZS 1170.0 and AS 1170.4.
7) Walls with an aspect ratio less than 2 should be designed as a non-ductile element using strut and tie methods.

6. Axial load ratio

Reducing the axial load ratio on an RC element can be the simplest and most effective method for increasing the maximum displacement capacity of the element. The axial load ratio is taken as the design load on the element (e.g. column or wall) divided by the product of the gross cross-sectional area of the element and the concrete strength. Using a recent study by Wilson et al. (2015) it can be shown that increasing the axial load ratio from 10 to 30 per cent can decrease the maximum drift capacity of an RC column by a factor greater than 2, as shown in Menegon et al. (2017d). The displacement capacity of RC columns is of particular importance in torsional eccentric buildings with external gravity frames. While the gravity frame may be assumed to take none of the lateral load, they may in fact be subject to large displacements due to the large deformations the core will have to undergo to develop the assumed level of ductility in the design. Designing gravity frames with high axial load ratios in these scenarios is not recommended.

The effect of high axial load ratios on RC walls has also been highlighted in a recent experimental study by Alarcon et al. (2014). This study included three identical specimens, which were tested under quasi-static cyclic in-plane lateral loading until failure with axial load ratios of 15, 25 and 35 per cent. The specimens failed at lateral drifts of 2.7, 1.8 and 1.5 per cent respectively, meaning the lateral drift at failure decreased by a factor of 1.8 when the axial load ratio was increased from 15 to 35 per cent.

7. Conclusions

This chapter has presented a summary of the current activities being performed as part of a long-term research project by the authors, aimed at reducing the seismic risk and rationalising seismic design procedures in Australia. This component of the project is studying the seismic performance of RC wall buildings in Australia and other regions low seismicity. The work included the experimental testing of 17 boundary element prism specimens and 5 large scale RC walls. The wall testing has shown that different plastic hinge mechanisms are developed in 'limited ductile' walls, typical of regions of low seismicity, due to lap splicing of the vertical reinforcement at the base of the wall. It has also shown that limited ductile walls in these regions, despite not being detailed to sustain large amounts of displacement, can sustain relatively large in-plane lateral drifts, prior to axial load failure of the wall, due to the low axial load ratios that are generally present.

This chapter discusses a number of poor detailing practices observed in RC wall construction in Australia that will result in the overall structural system of the building having limited or no displacement ductility capacity. These detailing practices include the use of centrally reinforced walls, walls with minimum percentages of vertical reinforcement and walls detailed using low ductility reinforcement. When any of these practices are adopted, it is recommended that a new ductility classification to be known as 'non-ductile', with a displacement ductility factor of 1.0 and overstrength factor of 1.3, be adopted when calculating earthquake design actions for the building. A summary table of detailing requirements for different ductility classifications for designing RC walls in low seismic regions has been provided within to assist designers.

Acknowledgements

The authors would like to thank the Brown family for their generous donation in establishing the Dr William Piper Brown AM Scholarship, of which the lead author is the recipient. Financial support from the Australian Research Council (ARC) Discovery Project DP140103350 entitled Collapse Assessment of Reinforced Concrete Buildings in Regions of Low Seismicity is gratefully acknowledged.

References

Alarcon, C., Hube, M.A. and Liera, J.C.D.L (2014) "Effect of axial loads in the seismic behaviour of reinforced concrete walls with unconfined wall boundaries", Engineering Structures, Vol. 73, pp. 13-23.

Dashti, F., R. P. Dhakal, and S. Pampanin (2017) "An Experimental Study on Out-of-plane Deformations of Rectangular Structural Walls Subject to In-plane Loading." Proceedings of the 16th World Conference on Earthquake Engineering, Santiago, Chile, January 9–13.

Griffith, M.C., Lam, N.T.K., Wilson, J.L. and Doherty, K. (2004) "Experimental investigation of unreinforced brick masonry walls in flexure", Journal of Structural Engineering, Vol. 130(3), pp. 423-432.

Griffith, M.C., Lam, N. and Wilson, J., (2006) "Displacement-Based Assessment of the Seismic Capacity of Unreinforced Masonry Walls in Bending", Australian Journal of Structural Engineering, Vol. 6(2), pp. 119-131.

Hashemi, M.J., Al-Mahaidi, R., Kalfat, R. and Burnett, G. (2015) "Development and validation of multi-axis substructure testing system for full-scale experiments", Australian Journal of Structural Engineering, Vol. 16(4), pp. 302-315.

Lam, N., Wilson, J., Chandler, A. and Hutchinson, G. (2000a) "Response spectral relationships for rock sites derived from the component attenuation model", Earthquake Engineering and Structural Dynamics, Vol. 29, pp. 1457-1489.

Lam, N., Wilson, J., Chandler, A. and Hutchinson, G. (2000b) "Response spectrum modelling for rock sites in low and moderate seismicity regions combining velocity, displacement and acceleration predictions", Earthquake Engineering and Structural Dynamics, Vol. 29, pp. 1491-1525.

Lumantarna, E., Lam, N. and Wilson, J., (2013), "Displacement-Controlled Behaviour of Asymmetrical Single-Story Building Models", Journal of Earthquake Engineering, Vol. 17(6), pp. 902-917.

Menegon, S.J., Wilson, J.L. and Lam, N.T.K. (2015a) "Local strain of reinforcement and tension stiffening in reinforced concrete walls", Proceedings of the Tenth Pacific Conference on Earthquake Engineering, Building an Earthquake-Resilient Pacific, 6-8 November 2015, Sydney, Australia.

Menegon, S.J., Wilson, J.L., Gad, E.F. and Lam, N.T.K. (2015b) "Out-of-plane buckling of limited ductile reinforced concrete walls under cyclic loads", Proceedings of the 2015 New Zealand Society of Earthquake Engineering Technical Conference, Rotorua, New Zealand.

Menegon, S.J., Wilson, J.L., Lam, N.T.K. and Gad, E.F. (2017a) "Experimental assessment of RC walls and building cores in regions of lower seismicity", Proceedings of the 16th World Conference on Earthquake Engineering, Santiago, 9-13 January 2017, Chile.

Menegon, S.J., Wilson, J.L., Lam, N.T.K. and Gad, E.F. (2017b) "Experimental testing of reinforced concrete walls in regions of lower seismicity", Bulletin of the New Zealand Society for Earthquake Engineering (in press).

Menegon, S.J., Wilson, J.L., Lam, N.T.K. and Gad, E.F.n (2017c) "RC Walls in Australia: Reconnaissance Survery of Industry and Literature Review of Experimental Testing", Australian Journal of Structural Engineering, Vol. 18(1), pp. 24-40.

Menegon, S.J., Wilson, J.L., Lam, N.T.K. and Mcbean, P. (2017d) "RC Walls in Australia: Seismic Design and Detailing to AS 1170.4 and AS 3600", Australian Journal of Structural Engineering (in press).

Priestley, M. J. N. G. M. Calvi, and M. J. Kowalsky (2007) "Displacement-Based Seismic Design of Structures". Pavia: IUSS Press.

Rosso, A., J. P. Almeida, and K. Beyer (2016) "Stability of Thin Reinforced Concrete Walls under Cyclic Loads: Stateof- the-art and New Experimental Findings." Bulletin of Earthquake Engineering 14 (2): 455–484.

Standards Australia (2007) "AS 1170.4-2007 Structural design actions, Part 4: Earthquake actions in Australia", Standards Australia, Sydney.

Standards Australia (2009) "AS 3600-2009 Concrete structures", SAI Global Limited, Sydney.

Standards New Zealand (2004) NZS 1170.5:2004 Structural Design Actions Part 5: Earthquake actions - New Zealand, Standards New Zealand, Wellington.

Standards New Zealand (2006) "NZS 3101:Part 1:2006 Concrete Structures Standard Part 1 - The Design of Concrete Structures", Standards New Zealand, Wellington.

Wallace, J. W. (2012) "Performance of Structural Walls in Recent Earthquakes and Tests and Implications for US Building Codes." Proceedings of the 15th World Conference on Earthquake Engineering, Lisboa.

Wibowo, A., Wilson, J.L., Gad, E.F., Lam, N.T.K. and Collier, P. (2011) "Drift capacity of a precast soft-storey building in Melbourne", Australian Journal of Structural Engineering, Vol. 11(3), pp. 177-193.

Wibowo, A., Wilson, J., Lam, N. and Gad, E. (2014) "Drift capacity of lightly reinforced concrete columns", Australian Journal of Structural Engineering, Vol. 15(2), pp. 131-150.

Wilson, J. and Lam, N. (2003) "A recommended earthquake response spectrum model for Australia", Australian Journal of Structural Engineering, Vol. 5(1), pp. 17-27.

Wilson, J.L., Wibowo, A., Lam, N.T.K. and Gad, E.F. (2015) "Drift Behaviour of Lightly Reinforced Concrete Columns and Structural Walls for Seismic Performance Assessment", Australian Journal of Structural Engineering, Vol. 16(1), pp. 62-74.

Design and Performance of Steel Buildings in Regions of Low to Moderate Seismicity

Luís Macedo[a], José M. Castro[a], Tak-Ming Chan[b] and Goman W. M. Ho[c]

[a] Department of Civil Engineering, Faculty of Engineering
University of Porto, Portugal

[b] Department of Civil and Environmental Engineering
The Hong Kong Polytechnic University, Hong Kong

[c] ARUP Group, Hong Kong

In recent decades, a new generation of seismic design codes has been developed with the aim of providing practitioners with better control of the seismic performance of structures. This control is mainly based on several defined performance levels, seeking to ensure that structures exhibit adequate performance at different seismic intensity levels. Currently, this is achieved through the adoption of codified seismic force modification factors (or behaviour factors) combined with the application of capacity design procedures. Behaviour factors, which allow for nonlinear structural behaviour to be taken into account in the design process, play a major role in determining the seismic performance of a structure.

During the last few years, a new seismic design code has been under development for Hong Kong, with the aim of introducing the most recent developments in the seismic design of structures. Hong Kong, like Portugal, is a region of low to moderate seismicity. It is nevertheless necessary to understand the implications of adopting seismic design criteria that are appropriate for structural systems subjected to high seismic demands. In fact, in modern seismic design codes there are few references to seismic design procedures which are appropriate for regions of low to moderate seismicity.

A set of 30 archetypal steel moment resisting-framed (MRF) buildings, designed according to Eurocode 8 (CEN, 2005a), for regions of low to moderate seismicity have been assessed with the following objectives: 1) to evaluate the consequences of choosing code recommended behaviour factors and 2) to assess the expected direct economic losses and corresponding disaggregation in terms of structural, non-structural and demolition losses, using the PEER-PBEE methodology (Cornell and Krawinkler, 2000), The designs relate to the seismic intensity levels considered in Part 3 of EC8 (CEN, 2005c), the European standard for the seismic assessment of existing buildings.

The research results described in this chapter enable a better understanding of the likely seismic behaviour of steel MRFs designed according to EC8 requirements for regions of low to moderate seismicity, whilst also demonstrating the critical influence that behaviour factor selection has on the seismic performance of the structures and the expected direct losses.

Keywords: seismic design, building design, building configuration, numerical modelling, seismic loss

1. Introduction

During recent decades the new seismic design philosophy of "Performance-Based Seismic Design" (PBEE) has emerged, aiming at better control of structural performance as affected by seismic loads. In PBEE design, the structure is designed to meet pre-defined levels of damage (acceptable performance) for pre-defined earthquake design intensities. The defined levels of damage are based on building occupancy and the expected consequences of failure.

Although the PBEE concept and application procedures are well defined nowadays, their application by practitioners is proving difficult, because of the complexity of the modelling techniques, analysis procedures, hazard analysis and ground motion records selection procedures. The PBEE design philosophy has been steadily introduced in modern seismic design codes, including Eurocode 8 (EC8-1), in terms of the two limit states i) no-local collapse, termed the Ultimate Limit State (ULS), which aims to protect human life in cases of rare earthquake occurrences by avoiding the collapse of any structural member, and ii) damage limitation, termed the Serviceability Limit State (SLS), which aims at damage limitation to non-structural elements for structures subjected to more frequent, but less severe, seismic events. The design process involved in the verification of these limit states is straightforward and follows well-established force-based design approaches. For the SLS, the designer demonstrates that building deformations (ie. inter-storey drift ratios), for reduced seismic intensity levels, comply with code-prescribed limits, given as functions of the ductility of the non-structural elements concerned. As for the ULS, the first design procedure step, concerns definition of the level of ductility expected from the structure, followed by the selection of a behaviour factor value (q). The selection/definition of the behaviour factor plays a key role in the design process since it can be interpreted, in its essence, as the design performance evaluator. This factor parameter provides designers with an understanding of the seismic response of the structure and its ability to dissipate energy through inelastic behaviour. In addition, the selection of the behaviour factor is a crucial step in the design process since the ductility demands and the detailing specifications of energy dissipating members are governed by that choice. Additionally, assessment of the building's sensitivity to second-order effects, according to EC8, is a function of the adopted behaviour factor in evaluating inelastic displacements (Peres and Castro, 2010).

Recently, the Federal Emergency Management Agency (FEMA) proposed the FEMA P695 framework for the calibration of building seismic performance factors such as behaviour and over strength factors. Without questioning the great usefulness of the proposed framework, the behaviour factors validation procedure ensures only that structures exhibit adequate margins against collapse, but without any reference to the economic losses associated with selection/definition of specific behaviour factors. Furthermore, application of the FEMA P695 framework is not straightforward, involving complex modelling techniques and advanced analysis procedures. In addition, for sites outside the United States, careful ground motion record selection may be needed because the FEMA framework assumes ground motions directly relevant only to seismicity levels experienced on US territory.

Hong Kong is a region of low to moderate seismicity. After giving due consideration to seismicity, safety as well as economical and social impact, Hong Kong now requires a seismic resistant provision for all new buildings/structures. A new seismic code is in preparation and should be ready by 2019, after which work to enhance compatibility

between this code and other Hong Kong structural codes now enforced will commence. As the seismicity level of Hong Kong is not high, compatibility of the new seismic code and existing codes is the main concern. A 475 years return period is to be adopted as the hazard level for the ultimate limit state. The need to design for wind effects now statutorily required in Hong Kong implies that ductility in buildings at performance level is rather limited. Therefore, it is expected that the new Hong Kong seismic code will be close to ductility classes medium (DCM) and high (DCH) of EC8.

The research reported in this chapter is part of a more extensive study conducted by Macedo (2017) which aims at evaluating the expected direct economic losses of steel moment-resisting frame structures located in low to moderate seismic regions, if designed according to Eurocode 8 using the recommended behaviour factors prescribed by the European standard. To this end, the PEER-PBEE methodology has been used to evaluate the expected economic losses.

2. Description of the buildings studied

Despite the significant number of buildings that have been evaluated by Macedo (2017), in this chapter, only buildings of 5 and 8 storeys designed with code recommended behaviour factors are presented. Fig. 1 shows the elevation and plan views of one of the building configurations, in which the analysed frame is also identified. Seismic resistance was considered to be provided by the MRFs in the longitudinal (*x*) direction and by a bracing system in the transversal (*y*) direction. In this study, only the internal longitudinal frames were examined. The buildings are located in Lisbon for which, according to the Portuguese National Annex of EC8, the peak ground acceleration associated with a 475 years return period, is equal to 0.15g. Soil type of class B, as defined in EC8, has been assumed.

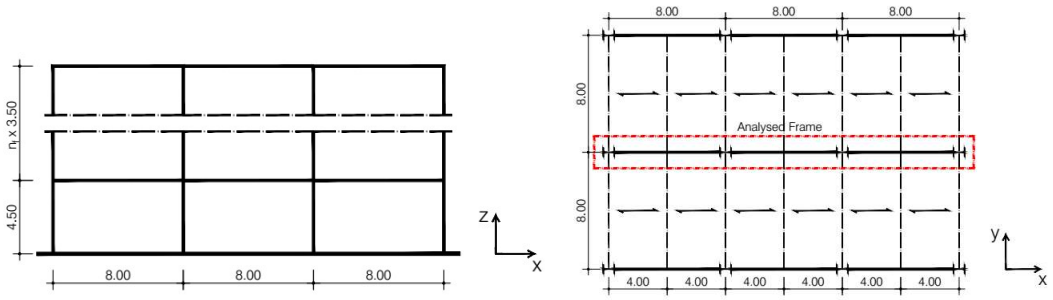


Figure 1. Building configuration a) Elevation; b) Plan view. (Macedo, 2017)

The steel moment-resisting frames were initially designed to resist gravity loads in accordance with the provisions of Part 1-1 of Eurocode 3 (EC3-1-1) (CEN, 2005b) for sectional resistance, stability checks and deflection limits. European steel open sections with H (HE) or I (IPE) shape were adopted for the beams and columns, respectively. The steel grade considered for all members was S275. Seismic design was then performed in accordance with the provisions of Part 1 of Eurocode 8 (EC8-1) (CEN 2005b), designing to meet the two upper limits for the behaviour factors recommended by the standard, q=6.5 and q=4, corresponding to ductility classes high (DCH) and medium (DCM),

respectively. The serviceability inter-storey drift ratio (IDR) was limited to 1% and the inter-storey drift sensitivity coefficient, θ, as defined in EC8-1, was limited to 0.2. Capacity design of the non-dissipative members was conducted according to the requirements of EC8-1, with the modifications proposed by Elghazouli (2009). Steel buildings designed using the EC8-1 recommended behaviour factors for medium and high ductility class are mostly controlled by lateral stiffness requirements associated with the control of P-Delta effects.

The vertical loads assumed in the structural design are listed in Table 1, where g_k and q_k are the permanent and the imposed loads, respectively. The transmission of vertical loads to the central frame were assumed as point loads in accordance with the positioning of the secondary beams. Additionally, and in order to calculate the storey masses for seismic design purposes, a load combination defined as gk+0.3qk was assumed for the intermediate storeys and g_k+0.0q_k for the roof storey, in accordance with EC8 design requirements. For the floors, a composite slab (HAIRCOL 59S) solution consisting of a profile steel sheeting, 59 mm deep, with a total slab depth of 160 mm was adopted. The slabs are considered to act as rigid diaphragms, thus, the mass of each storey was assumed equally distributed between the frames in the x-z plane.

Table 1. Vertical loads

Floor level	Load type	Load [kN/m^2]
Roof	g_k	4.75
	q_k	1.00
Other floors	g_k	5.75
	q_k	2.00

The member sizes, the dynamic characteristics and the design details of the 5 and 8-storey buildings are listed in Tables 2 and 3.

Table 2. Properties of the 5-storey buildings

Floor	Beams	External Columns	Internal Columns	SLS ISD	θ	T_1 (s)	q
1	IPE 600	HEB 500	HEM 600	0.166	0.137		
2	IPE 550	HEB 500	HEM 600	0.266	0.193		
3	IPE 450	HEB 450	HEM 500	0.332	0.197	0.92	6.5
4	IPE 450	HEM 450	HEM 500	0.325	0.171		
5	IPE 400	HEM 340	HEM 400	0.262	0.133		
1	IPE 500	HEB 400	HEB 500	0.213	0.147		
2	IPE 450	HEB 400	HEB 500	0.334	0.199		
3	IPE 450	HEB 360	HEB 400	0.335	0.172	1.13	4
4	IPE 450	HEB 360	HEB 400	0.26	0.121		
5	IPE 400	HEB 320	HEB 360	0.192	0.086		

Table 3. Properties of the 8-storey buildings

Floor	Beams	External Columns	Internal Columns	SLS ISD	θ	T_1 (s)	q
1	HEA 600	HEM 500	HEM 650	0.169	0.143	1.16	6.5
2	HEA 600	HEM 500	HEM 650	0.247	0.194		
3	HEA 600	HEM 500	HEM 650	0.254	0.175		
4	IPE 600	HEM 450	HEM 600	0.293	0.18		
5	IPE 500	HEM 450	HEM 600	0.356	0.196		
6	IPE 500	HEM 450	HEM 600	0.382	0.191		
7	IPE 400	HEB 450	HEB 600	0.379	0.169		
8	IPE 360	HEB 450	HEB 600	0.355	0.167		
1	IPE 600	HEB 400	HEB 600	0.195	0.152	1.5	4
2	IPE 600	HEB 400	HEB 600	0.272	0.191		
3	IPE 550	HEB 400	HEB 600	0.297	0.186		
4	IPE 500	HEB 360	HEB 550	0.349	0.197		
5	IPE 500	HEB 360	HEB 550	0.359	0.185		
6	IPE 400	HEB 360	HEB 550	0.366	0.173		
7	IPE 400	HEB 340	HEB 500	0.337	0.147		
8	IPE 360	HEB 340	HEB 500	0.267	0.115		

As shown by the tables, the buildings designed with the larger behaviour factor (q=6.5) resulted in stiffer/stronger members. This observation may seem contradictory, but the use of a high behaviour factor may lead to savings in element sizes (and therefore material quantities), as the seismic forces are directly reduced by this parameter. However, this is justified by the fact that the criterion currently established in EC8 for the treatment of P-Delta effects, namely the inter-storey drift sensitivity coefficient, θ, is dependent on the value adopted for the behaviour factor (Peres and Castro, 2010). A closer look at the code prescribed criterion shows that a condition of minimum elastic lateral stiffness is "indirectly" imposed by the code and that the minimum lateral stiffness is directly proportional to the behaviour factor adopted (Eq(1)). Consequently, the use of large behaviour factors will implicitly lead to higher lateral stiffness requirements and consequently to a heavier lateral loading structural system.

$$\theta = \frac{P_{tot} \times d_r}{V_{tot} \times h} \leq 0.2 \Leftrightarrow \frac{P_{tot} \times \frac{d_{el}}{q} q_d}{\frac{V_{tot,el}}{q} \times h} \leq 0.2 \Leftrightarrow \frac{P_{tot} \times d_{el}}{V_{tot,el} \times h} \times q \leq 0.2 \Leftrightarrow K_e \geq \frac{P_{tot} \times q}{0.2 \times h} \quad (1)$$

3. Numerical modelling and nonlinear analysis

Assessment of the structures was carried out through nonlinear response-history analyses using the nonlinear finite element analysis program OpenSEES (PEER, 2006). The material nonlinear behaviour was taken into account via a concentrated plasticity approach allowing for strength, stiffness, and deterioration effects (Lignos and Krawinkler, 2011, Araújo et al., 2017). The influence of axial load on the flexural capacity of the columns was taken into account in an approximate manner reducing the bending resistance according to the interaction equations proposed in EC3-1-1. No modification of the stiffness and deterioration parameters was considered (Zareian et al., 2010). The behaviour of panel zones was represented by a beam-column joint element taking account of the tri-linear moment-distortion model proposed by Krawinkler (1978). The panel zones were designed assuming a "balanced" design methodology (Castro et al., 2007), with no strength degradation. Fig. 2 illustrates the adopted strategy for modelling the panel zones.

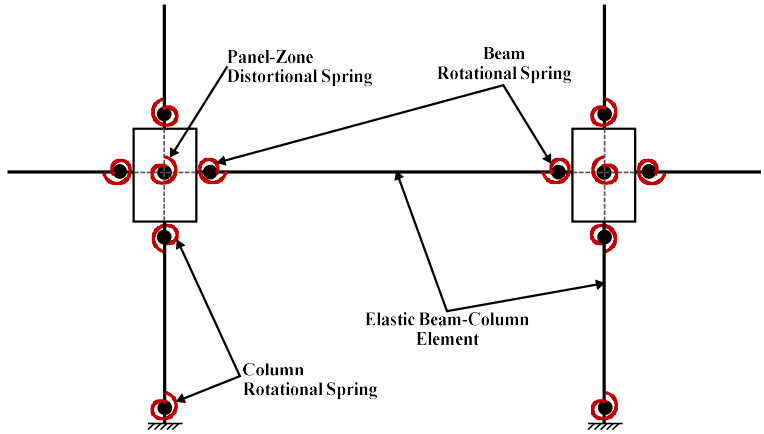


Figure 2. Numerical modelling overview of the beams/columns elements and panel zones (Macedo, 2017)

Ground motion record selection was based on distance and magnitude parameters from Lisbon disaggregation results and the average shear wave velocity for the first 30 metres of soil. A suite of 40 ground motion records were selected and scaled to obtain an appropriate matching between the median spectra of the suite and the EC8 elastic spectrum, for the range of periods of interest. A similar technique was applied in FEMA P695 (FEMA, 2009). The ground motion record selection used the SelEQ tool (Macedo and Castro, 2017), an advanced ground motion record selection and scaling framework. Fig. 3 shows the response spectra for the selected ground motion records for the site location under study and the corresponding mean and median. The recommendations proposed by Araújo et. al (2016) were followed by imposing an additional spectral mismatch control for each individual record (dotted lines Fig. 3).

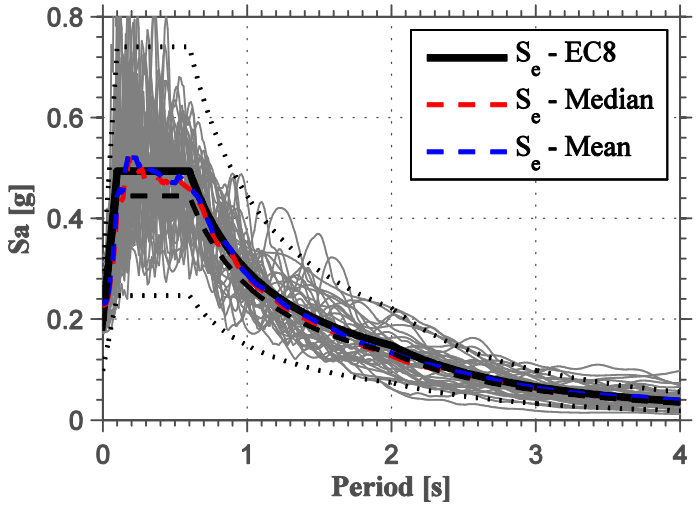


Figure 3. Response spectra of selected ground motion records and EC8 spectrum for Lisbon

The seismic performance of the buildings was assessed through incremental dynamic analysis (IDA) (Vamvatsikos and Cornell, 2002). The 5% damped first mode spectral acceleration, $S_a(T_1)$, was taken as the seismic intensity measure, IM, and the three engineering demand parameters, EDP, were considered, ie. the maximum inter-storey drift ratio (IDR), the peak floor acceleration (PFA) and the maximum residual inter-storey drift ratio (RIDR). Figs. 4 and 5 show the maximum values of the three EDPs along buildings height, for several seismic intensity levels.

The figures show that the selection of the behaviour factor has an influence on the seismic response of the buildings. Nevertheless, it is worth noting that all the designs resulted in structures with relatively uniform distributions of deformation and acceleration demands along the height of the buildings.

When evaluating the collapse fragility curve for each building, both aleatory and epistemic uncertainties, were taken into account. The total uncertainty was computed assuming that both uncertainties were lognormally distributed and independent. The value of total system uncertainty was taken as 0.53 (Macedo, 2017). The median collapse capacity was adjusted to account for the spectral shape effect, in accordance with Method 2 proposed by Haselton et al. (2011). Figs. 6 and 7 show the IDA curves and the corresponding collapse fragility curves for the 5 and 8-storey buildings.

A careful inspection of Figs. 6 and 7 reveals that the collapse capacity of the buildings designed with the lower behaviour factor (q=4) is actually lower than that observed for the buildings designed for higher ductility. This results from the strict requirements associated with P-Delta effects in the seismic design process. As discussed in Section 2, the adoption of high behaviour factor values results in stiffer and hence stronger solutions, particularly for low to moderate seismic regions where lateral force demands do not typically govern the sizing of structural members.

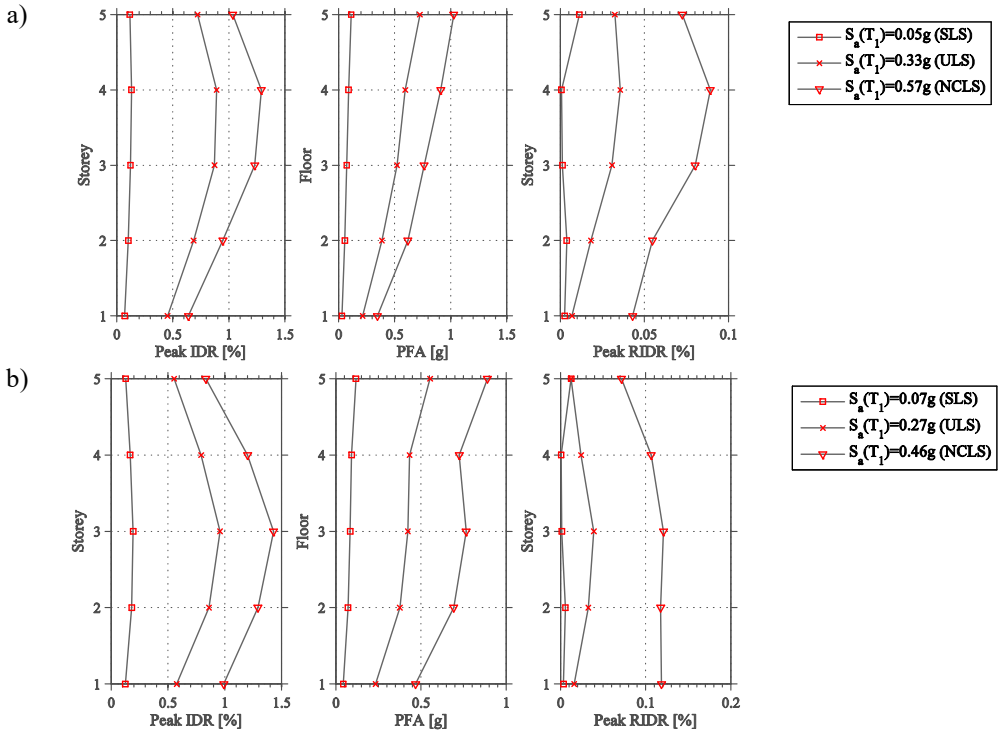


Figure 4. Maximum IDR, PFA and RIDR along building height for the 5-storey buildings designed with a) q=6.5 and b) q=4.0.

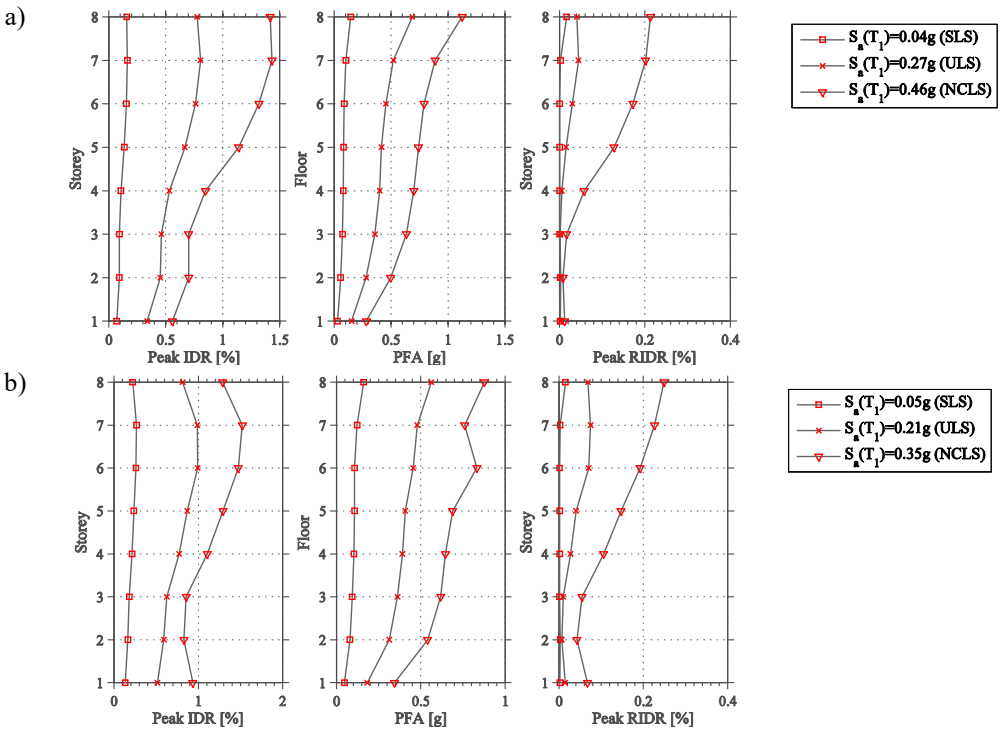


Figure 5. Maximum IDR, PFA and RIDR along building height for the 8-storey buildings designed with a) q=6.5 and b) q=4.0

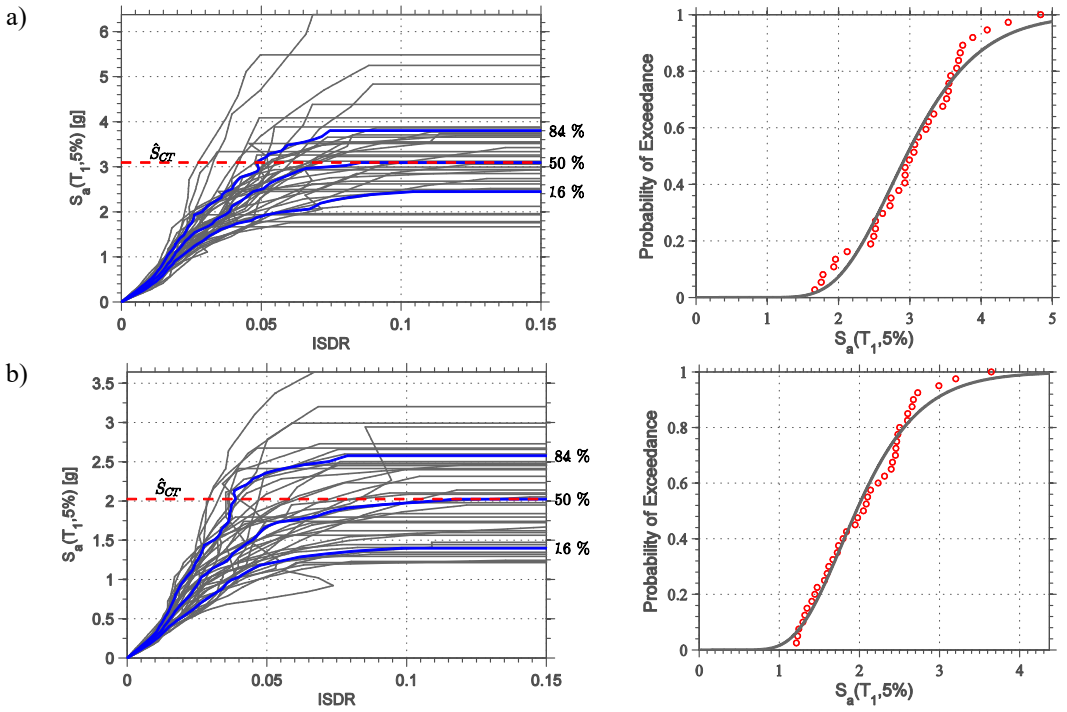


Figure 6. IDA and Collapse fragility curve for the 5-storey buildings designed with a) q=6.5 and b) q=4.0

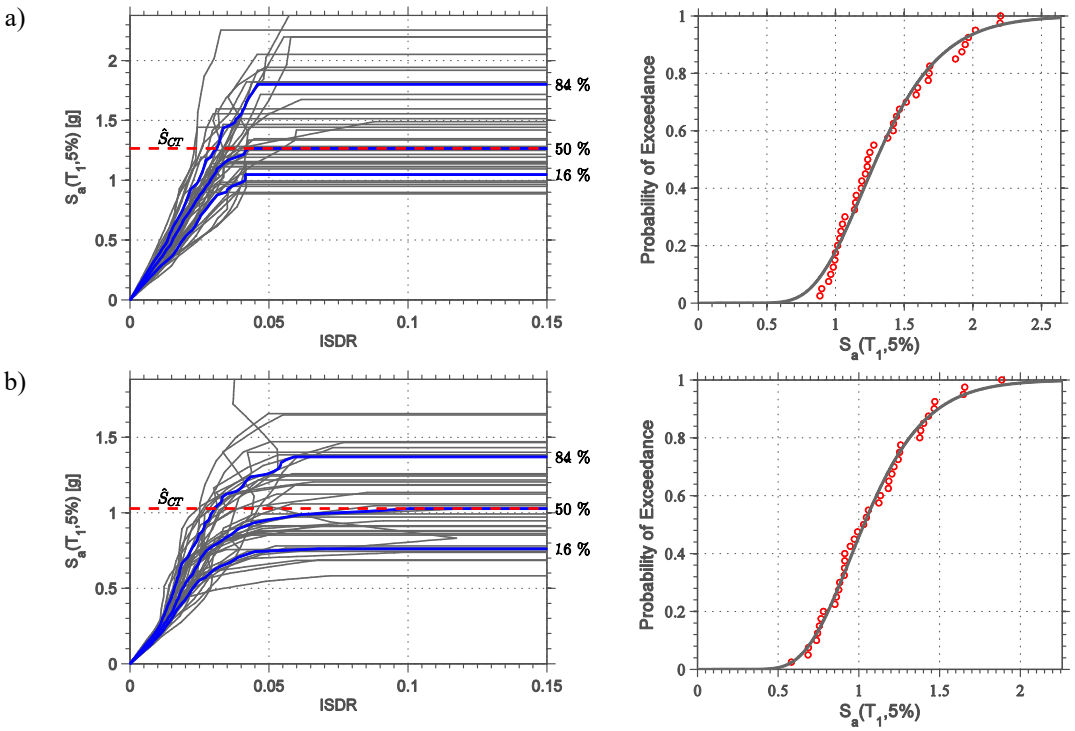


Figure 7. IDA and Collapse fragility curve for the 8-storey buildings designed with a) q=6.5 and b) q=4.0

4. Economic seismic losses and results

Economic seismic losses were computed using the PBEE methodology developed by the Pacific Earthquake Engineering Research (PEER) Center (Cornell and Krawinkler, 2000; Porter, 2003). A detailed description of the economic loss calculation procedure can be found in Macedo (2017).

The expected total economic losses in buildings can be due to three mutually exclusive events: i) the building does not collapse and can be repaired; ii) the building does not collapse but needs to be demolished and rebuilt; iii) the building collapses and needs to be rebuilt (Ramirez and Miranda, 2012). The expected value of total economic losses in a building, therefore, can be computed as shown in Eq. (2):

$$L_T = L_{NC \cap R} + L_{NC \cap D} + L_C \tag{2}$$

where L_T is the expected total loss , $L_{NC \cap R}$ is the expected loss given that collapse does not occur and the structure is repaired, $L_{NC \cap D}$ is the expected loss when there is no collapse but the building is demolished and L_C is the expected loss when collapse occurs. According to Ramirez and Miranda (2012) and Hwang et al. (2015), the expected economic losses for a given ground motion intensity can be estimated by Eq. (3):

$$E[L_T \mid IM] = \left\{ \begin{array}{c} E[L_T \mid NC \cap R, IM] \cdot \{1 - P(D \mid NC, IM)\} \cdot \{1 - P(C \mid IM)\} \\ + \\ E[L_T \mid NC \cap D, IM] \cdot P(D \mid NC, IM) \cdot \{1 - P(C \mid IM)\} \\ + \\ E[L_T \mid C, IM] \cdot P(C \mid IM) \end{array} \right\} \tag{3}$$

where $E[L_T \mid NC \cap R, IM]$, $E[L_T \mid NC \cap D, IM]$ and $E[L_T \mid C, IM]$ are, respectively, the expected losses for IM=im given that collapse does not occur and the building is repaired, the expected losses for IM=im when there is no collapse but the building is demolished and the expected losses for IM=im when collapse does occur. $P(D \mid NC, IM)$ and $P(C \mid IM)$ are the probabilities that the building will not collapse, but will be demolished due to large residual deformations and the probability that the building will collapse given that the ground motion intensity is IM=im.

The expected losses given that collapse does not occur and the building is repaired was calculated using the storey-based building-specific loss estimation method proposed by Ramirez and Miranda (2009). Storey components were grouped into the three categories linked to the corresponding EDP (drift-sensitive structural components (LS|IDR), drift-sensitive non-structural components (LNS|IDR) and acceleration-sensitive components (LNS|PFA)). According to current construction price ratios in Europe, weights of 25%, 55% and 20% were adopted for each category respectively.

The probability that the building will not collapse but will be demolished due to large residual deformations, given that the ground motion intensity is IM=im, can be computed as shown in Eq. (4):

$$P(D \mid NC, IM) = \int_0^\infty P(D \mid RIDR)\, dP(RIDR \mid NC, IM) \tag{4}$$

where, $P(D \mid NC, IM)$ is the probability of having to demolish the structure depending on

the maximum residual inter-storey drift ratio (*RIDR*) among all storeys in the building and *P*(*RIDR*|*NC*,*IM*) is the probability of experiencing a certain level of *RIDR* in the building given that it has not collapsed and that it has been subjected to an earthquake with a given ground motion intensity *IM*=im. According to Jayaram et al. (2012), the probability of demolition depends on the *RIDR,* which follows a lognormal distribution with a median of 0.0185 and coefficient of variation (COV) of 0.3.

Figs. 8 and 9 depicts the vulnerability curves for the 5 and 8-storey buildings designed with the code recommend behaviour factors and the corresponding losses for four different seismic intensities. In this study the four following intensity levels were examined: 1) SLS-1, defined in EC8-1 for damage limitation checks, 2) SLS-3, defined in EC8-3 for damage limitation checks, 3) ULS, defined in EC8-3 for significant damage assessment (coincides with the design intensity level) and 4) CLS, defined in EC8-3 for the evaluation of near collapse.

In general, it may be observed that for the damage limitation limit states (SLS-1 and SLS-3), as expected, most of the losses result from non-structural repairs with a slight contribution from structural repairs. Expected losses of 12 to 18%, respectively, of building initial cost, can be seen. A similar performance was observed for the design level intensity case (ULS), with most expected losses resulting from non-structural repairs Finally, for the near collapse intensity level, CLS, minor demolition losses still appear but there are no collapse related losses.

It is worth noting that similar expected losses were obtained for the DCM building (q=4.0) and DCH building (q=6.5).

Another interesting consideration is the evaluation of losses normalized to return periods. Figs 10 and 11 show the hazard curves for Lisbon corresponding to the 5 and 8-storey buildings designed with q=6.5 and q=4, respectively. A detailed description of the derivation of the hazard curves can be found in Macedo (2017).

Site specific hazard analysis allows more realistic evaluation of the expected losses associated with building performance and site hazard. Fig. 12 shows the vulnerability curves as functions of the return period for the 5 and 8-storey buildings designed with code recommend behaviour factors. The plots also include vulnerability curves corresponding to other 5 and 8-storey buildings with different geometrical configurations. Further information is available in Macedo (2017).

It can be concluded from the figures, that similar values of expected losses are achieved independently of the behaviour factor value and the structural configuration. Comparing these results with those of Figs. 8 and 9, a reduction in expected losses can be observed from the site specific hazard analyses, with losses at ULS (TR=475 years) below 10% of building initial cost. This is justified by the differences between the hazard model used to derive the EC8 spectra and the SHARE (Woessner et al., 2015) model, recently proposed for Europe and utilized in the derivation of the site-specific hazard curves.

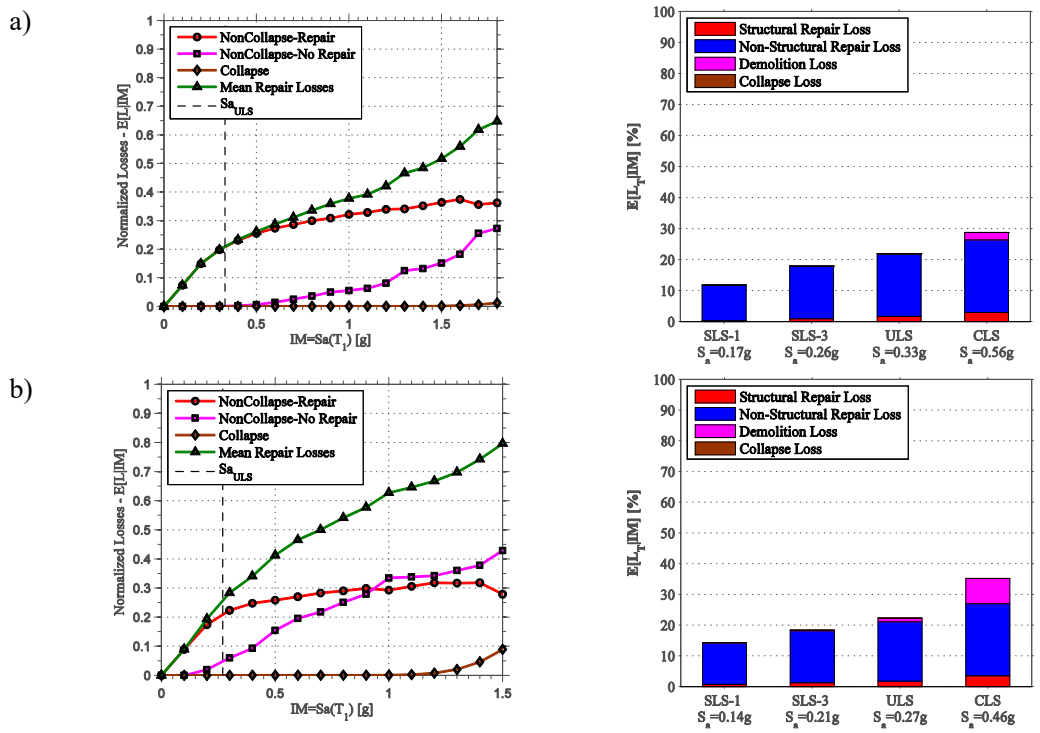


Figure 8. Vulnerability curves and normalized expected losses at several seismic intensity levels for the 5-storey buildings designed with a) q=6.5; b) q=4

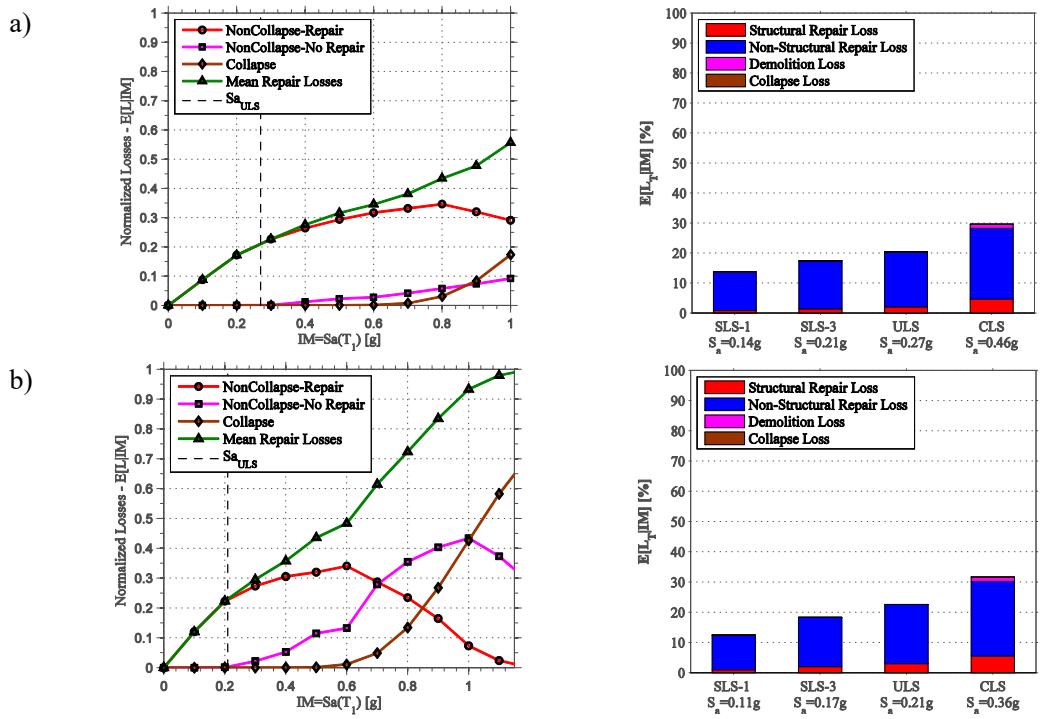


Figure 9. Vulnerability curves and normalized expected losses at several seismic intensity levels for the 8-storey buildings designed with a) q=6.5; b) q=4

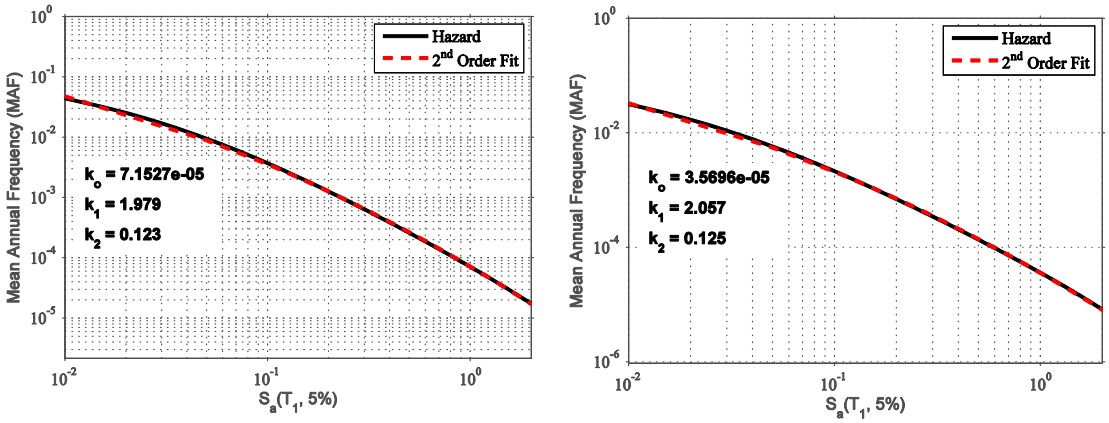


Figure 10. Hazard curves corresponding associated for the 5-storey buildings designed with a) q=6.5; b) q=4

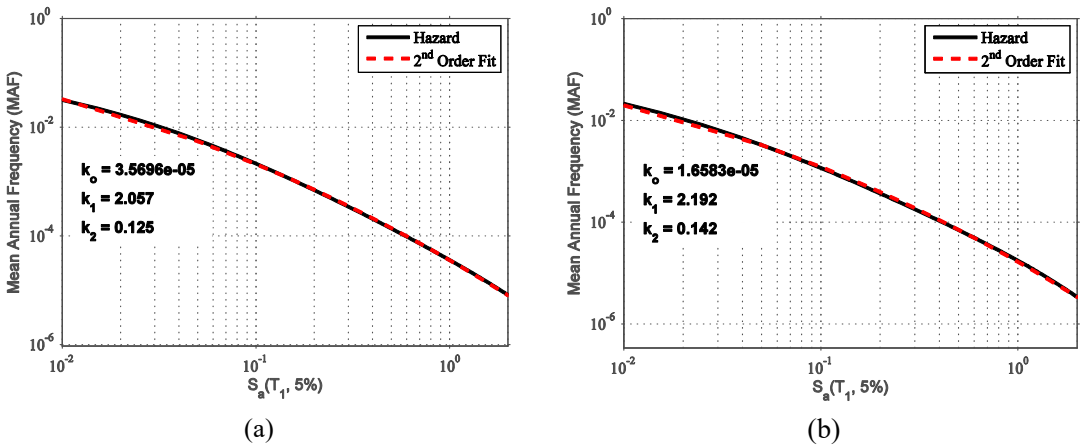


Figure 11. Hazard curves corresponding associated for the 8-storey buildings designed with a) q=6.5; b) q=4

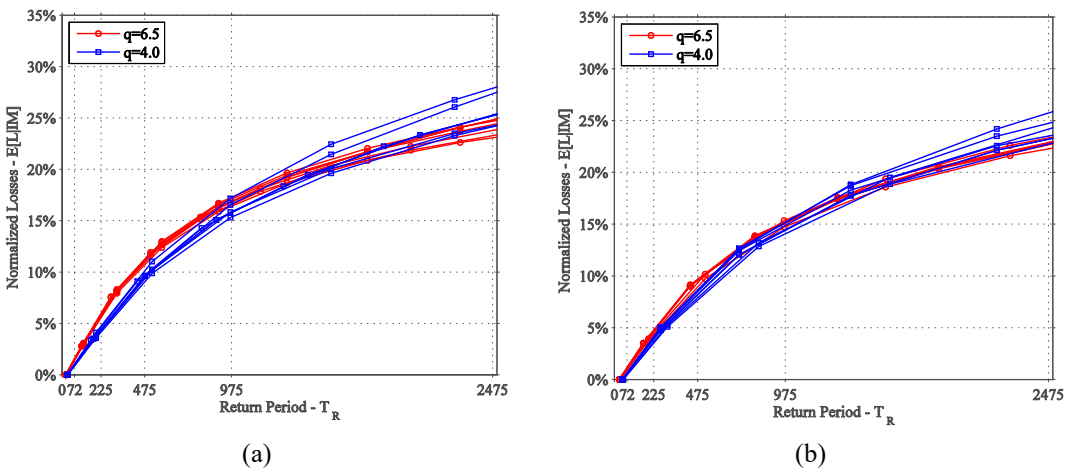


Figure 12. Vulnerability curves for a) 5-storey buildings and b) 8-storey buildings

5. Conclusions

The study evaluated the consequences of choosing EC8 recommended behaviour factors, in the design of steel moment-resisting frames according to Eurocode 8 for low to moderate seismic intensity regions. Expected economic losses in such regions have been estimated for various earthquake induced levels of damage. The PEER-PBEE methodology procedure with the improvements proposed by Ramirez and Miranda (2012), using a storey-based building-specific loss approach, was adopted for cost computations.

Firstly, it should be mentioned that the steel MRF archetypes designed in accordance with the requirements of EC8-1 comply with the no-collapse requirement defined in the code for the design intensity level since no collapses have been observed for earthquakes at this intensity level. Reduced demolition losses due to excessive inter-storey residual drifts were also obtained. Comparing the buildings designed to different code recommended behaviour factors, it can be concluded that seismic induced economic expected losses are similar. Nevertheless, the buildings designed for q = 4 are associated with lower steel quantities than the buildings designed for the higher ductility class, q=6.5. This observation highlights the critical importance of the choice of behaviour factor in the design process, particularly in regions of low to moderate seismicity, such as Portugal and Hong Kong.

Finally, it is worth noting that a reduction of the expected seismic losses was observed when site-specific hazard was considered. The differences resulted from the inconsistency between the seismic action defined in EC8 for Portugal and the hazard determined with the most recent model proposed for the European territory.

References

Araújo, M., Macedo, L., Marques, M. and Castro, J.M. (2016) "Code-based record selection methods for seismic performance assessment of buildings". Earthquake Engineering & Structural Dynamics, 45-1, 129-148.

Araújo, M., Macedo, L. and Castro, J.M. (2017) "Evaluation of the rotation capacity limits of steel members defined in EC8-3". Journal of Constructional Steel Research, 135, 11-29.

Castro, J.M., Elghazouli, A.Y. and Izzuddin, B.A. (2005) "Modelling of the panel zone in steel and composite moment frames", Engineering Structures, 27-1, 129-144.

CEN (2005a) "EN 1998–1 Eurocode 8: design of structures for earthquake resistance, Part 1, General Rules, Seismic Actions and Rules for Buildings" European Committee for Standardization (CEN), Brussels, Belgium.

CEN (2005b) "EN 1993-1-1 Eurocode 3: Design of steel structures. Part 1-1, General rules and rules for buildings" European Committee for Standardization (CEN), Brussels, Belgium.

CEN (2005c) "EN 1998–3 Eurocode 8: Design of Structures for Earthquake Resistance, Part 3, Assessment and Retrofitting of Buildings" European Committee for Standardization (CEN), Brussels, Belgium.

Cornell, A.C., Krawinkler, H. (2000) "Progress and challenges in seismic performance assessment" in PEER Center News, Berkeley, CA 3, 1–4.

Elghazouli, A.Y. and Castro, J.M. (2009) "Design of Steel Structures, in Seismic Design of Buildings to Eurocode 8". Elghazouli AY, ed. Spon Press.

FEMA (1999) "HAZUS Earthquake Loss Estimation Methodology" Department of

Homeland Security - Federal Emergency Management Agency (FEMA), Washington, DC, USA.

Haselton, C.B., Baker, J.W., Liel, A.B. and Deierlein, G.G. (2011) "Accounting for Ground Motion Spectral Shape Characteristics in Structural Collapse Assessment Through an Adjustment for Epsilon", Journal of Structural Engineering 137(3), 332–344.

Hwang, S.H., Elkady, A., AlBardaweel, S. and Lignos, D.G (2015) "Earthquake loss assessment of steel frame buildings designed in highly seismic regions" Proceedings of the 5th ECCOMAS Thematic Conference on Computational Methods in Structural Dynamics and Earthquake Engineering, Crete, Greece.

Jayaram, N., Shome, N. and Rahnama, M. (2012) "Development of earthquake vulnerability functions for tall buildings", Earthquake Engineering and Structural Dynamics 41, 1495–1514.

Krawinkler, H. (1978) "Shear in beam-column joints in seismic design of frames", Engineering Journal 15(3), 82–91.

Lignos, D.G. and Krawinkler, H. (2011) "Deterioration modeling of steel components in support of collapse prediction of steel moment frames under earthquake loading" Journal of Structural Engineering 137(11), 1291–1302.

Macedo, L. (2017) "Performance-Based Seismic Design and Assessment of Steel Moment Frame Buildings" PhD Thesis, Faculty of Engineering of the University of Porto, Portugal.

Macedo, L. and Castro, J.M. (2017) "SelEQ: An advanced ground motion record selection and scaling framework", Advances in Engineering Software.

PEER (2006) "OpenSees: Open system for earthquake engineering simulation", Pacific Earthquake Engineering Research Center, University of California, Berkeley, CA, USA.

Peres, R. and Castro, J. M. (2010). Comparison of European and American approaches for consideration of P-Delta effects in seismic design. Proceedings of the 14th European Conference on Earthquake Engineering. Ohrid, Republic of Macedonia.

Porter, K. (2003) "An overview of PEER's performance-based earthquake engineering methodology" Proceedings of Ninth International Conference on Applications of Statistics and Probability in Civil Engineering. San Francisco, CA, USA.

Ramirez, C.M. and Miranda, E. (2009) "Building-Specific Loss Estimation Methods & Tools for Simplified Performance-Based Earthquake Engineering" Technical Report No. 171, John A. Blume Earthquake Engineering Center, Stanford, CA, USA.

Ramirez, C.M. and Miranda E. (2012) "Significance of residual drifts in building earthquake loss estimation" Earthquake Engineering and Structural Dynamics 41(11), 1477-1493.

Vamvatsikos, D. and Cornell, C.A. (2002) "Incremental dynamic analysis", Earthquake Engineering and Structural Dynamics 31(3), 491–514.

Woessner, J., Laurentiu, D., Giardini, D., Crowley, H., Cotton, F., Grünthal, G., Valensise, G.,Arvidsson, R., Basili, R., Demircioglu, M. B. et al. (2015). "The 2013 European seismic hazard model: Key components and results" Bulletin of Earthquake Engineering 13(12), 3553-3596.

Zareian, F. and Krawinkler, H. (2009) "Simplified Performance Based Earthquake Engineering". Technical Report No. 169, John A. Blume Earthquake Engineering Center, Stanford, CA, USA.

Zareian, F., Lignos, D.G. and Krawinkler H. (2010) "Evaluation of seismic collapse performance of steel special moment resisting frames using FEMA P695 (ATC-63) methodology", Proceedings of the 2010 Structures Congress, Orlando, FL, USA.

A Case Study of Code Compliant Design of Buildings in Regions of Low to Moderate Seismicity

Daniel T. W. Looi[a,b], Ek P. Lim[b] and M. C. Hee[b]

[a] Department of Civil Engineering
The University of Hong Kong, Hong Kong

[b] Working Group 1, Technical Committee on Earthquake
The Institution of Engineers Malaysia, Malaysia

This chapter presents a case study example of a reinforced concrete building, for the benefit of practicing structural engineers working in regions of low to moderate seismicity, who have not had to take earthquake actions into account in the past and have little experience in earthquake code compliant design. A worked example of a 9-storey medium rise building located in Malaysia is presented, starting with site period calculations based on borehole records and proceeding to a generalised force method of analysis as opposed to the conventional code lateral force method. This approach is to circumvent issues generated by the various uncertainties involved when deriving the natural period properties of a real building structure. The underlying concept is explained with a simple 2D example in the first part of the chapter, followed by how best to make use of a structural analysis computer package when faced with the real design 3D environment challenges.

Keywords: Eurocode 8, code compliant, RC building, low to moderate seismicity, lateral force method, generalised force method

1. Introduction

With the aim of achieving a more robust level of structural safety, seismic design codes have been recently introduced and enforced in regions of low to moderate seismicity where earthquake actions have not been taken into account in the past. For example, Eurocode 8 (EC8) National Annex (NA) has been enforced in Singapore (SS EN1998-1:2013) and a completed NA which went through public comments in 2017 in Malaysia (NA for MS EN1998-1:2015). It is noted however, that structural engineers in these regions have little experience in earthquake code compliant design. This chapter, as an example, elaborates the seismic design of a typical medium rise Reinforced Concrete (RC) building. Such a building type is most vulnerable because of its short natural period ($T < 1.25$s) which may well coincide with the low period range of an earthquake response spectrum. This example, in addition to the RC hospital building example (Looi et al., 2015) aims to enhance the confidence of engineers in using a checking method, as an alternative to the typical commercial software dynamic modal analysis method, when deriving a seismic code compliant design.

2. Site natural period

A calculation of the site period based on borehole records is demonstrated below, so as to estimate the seismic loading demand, using a proposed Response Spectrum (RS)

model expressed as a function of site period (Tsang et al., 2016).

2.1 Borehole records

The project site, not identified here, has an area of approximately 12 acres (48562 m^2) and is intended for the construction of one block of residential staff quarters, a main hospital block and a multi-storey car park in Peninsular Malaysia (see Figure 1). A general rule of thumb specifies that two boreholes for a low-rise building block are sufficient, and that the spacing of boreholes for multi-storey buildings should be between 15 m and 45 m. More boreholes are necessary for problematic and erratic soil formations (Sowers, 1979). For this site example, a total of 11 borehole records were selected, spread as evenly as possible over the whole site area.

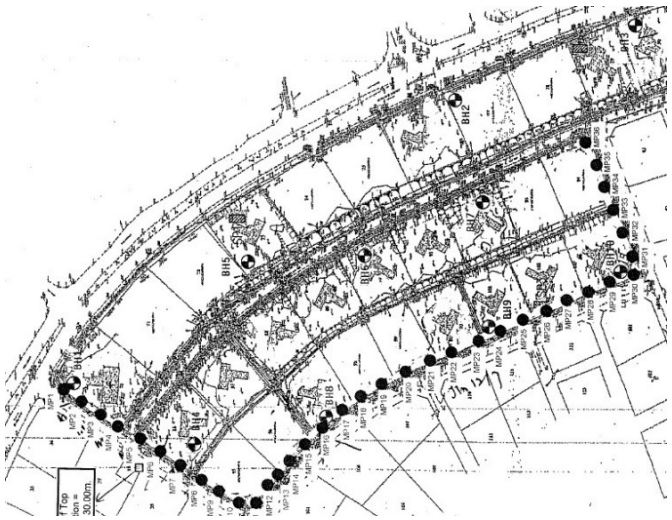


Figure 1. A site in Peninsular Malaysia with borehole layout

2.2 Computation of site natural period

The site natural period (T_S) is estimated by correlating Standard Penetration Test (SPT-N) values with shear wave velocity (SWV). Wair et al. (2012) summarised empirical formulae applicable to all types of soil. In this example, the Imai and Tonouchi (1982) SPT-N to SWV equation of SWV = $97N^{0.31}$ was adopted. For SPT-N ≥ 50, the equivalent SPT-N is derived by proportioning the SPT-N to a 300 mm penetration, e.g. if an SPT-N = 50 for a 270 mm penetration, the equivalent SPT-N is 50×300/270 = 55.6.

The individual soil layer thicknesses (di) divided by the respective initial SWV ($V_{s,i}$) ratio were calculated to obtain the weighted average SWV (VS) using Eq. (1).

$$V_s = \sum_{i=1}^{n} d_i \Big/ \sum_{i=1}^{n} \frac{d_i}{V_{s,i}} \tag{1}$$

where $V_{s,i}$ = the SWV in m/s; d_i = the thickness of any layer.

$$T_S = \sum_{i=1}^{n} \frac{d_i}{V_{s,i}} \times 4 = \frac{4H_S}{V_S} \tag{2}$$

An example of site natural period computation for borehole number 1 is shown in Table 1.

Table 1. Computation of site natural period based on borehole number 1

Depth	d_i	SPT-N	$V_{s,i}$ (Imai and Tonouchi, 1982)	$d_i / V_{s,i}$	Depth	d_i	SPT-N	$V_{s,i}$ (Imai and Tonouchi, 1982)	$d_i / V_{s,i}$
0	0	0	0.0	0	22.5	1.5	29	279.2	0.005
1.5	1.5	6	170.3	0.009	24	1.5	24	263.1	0.006
3	1.5	7	178.7	0.008	25.5	1.5	29	279.2	0.005
4.5	1.5	10	199.9	0.008	27	1.5	31	285.1	0.005
6	1.5	10	199.9	0.008	28.5	1.5	34	293.5	0.005
7.5	1.5	16	231.7	0.006	30	1.5	31	285.1	0.005
9	1.5	17	236.1	0.006	31.5	1.5	33	290.8	0.005
10.5	1.5	17	236.1	0.006	33	1.5	55.6	342.6	0.004
12	1.5	21	252.3	0.006	34.5	1.5	60	350.8	0.004
13.5	1.5	19	244.5	0.006	36	1.5	88.2	396.0	0.004
15	1.5	21	252.3	0.006	37.5	1.5	107	420.7	0.004
16.5	1.5	24	263.1	0.006	39	1.5	100	411.9	0.004
18	1.5	27	273.0	0.005	40.5	1.5	150	467.8	0.003
19.5	1.5	25	266.5	0.006	42	1.5	214	523.0	0.003
21	1.5	27	273.0	0.005	Sum:	42	-	-	0.155

Hence, from Eq. (1), $V_s = \sum_{i=1}^{n} d_i \Big/ \sum_{i=1}^{n} \frac{d_i}{V_{s,i}} = 42/0.155 = 272$ m/s

From Eq. (2), $T_S = \sum_{i=1}^{n} \frac{d_i}{V_{s,i}} \times 4 = \frac{4H_S}{V_S} = \frac{4(42)}{272} = 0.62$ s

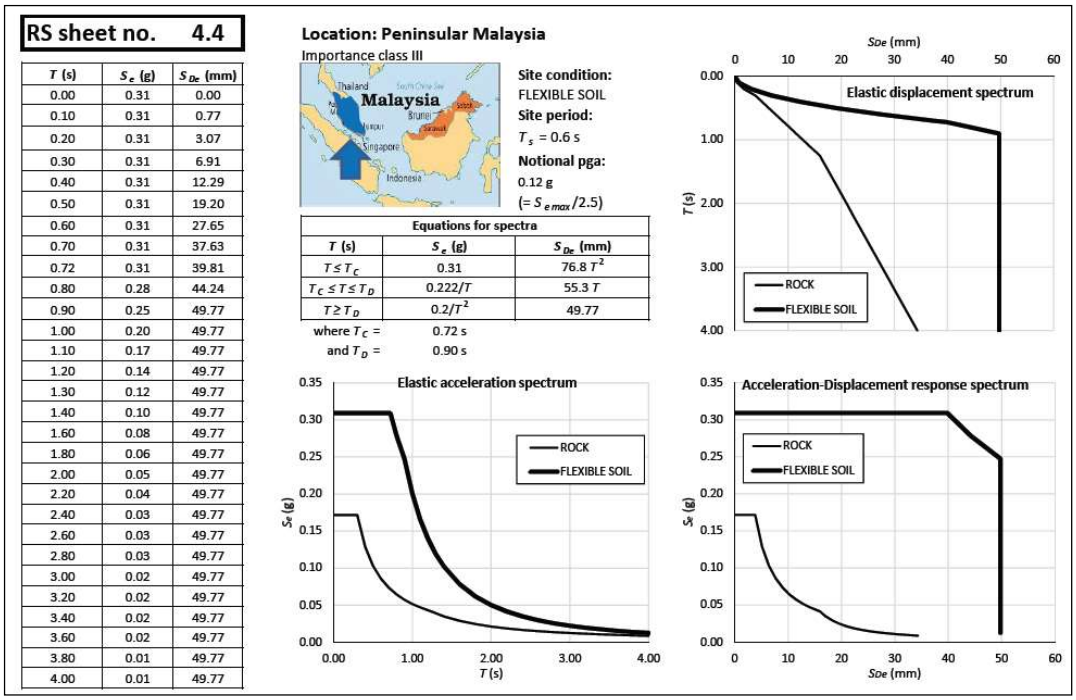
It is suggested that the arithmetic mean of the site natural periods (T_S) derived from all the boreholes should be adopted for site classification purposes. In this example, the mean value of T_S is computed as 0.60 s (see Table 2).

Table 2. Arithmetic mean of the site natural periods

Borehole no.	T_S (s)	Borehole no.	T_S (s)
1	0.62	7	0.65
2	0.55	8	0.75
3	0.45	9	0.50
4	0.51	10	0.65
5	0.64	11	0.61
6	0.71	Mean	0.60

2.3 The corresponding elastic RS

The soil RS model in this section is based on the draft Malaysia NA (MS EN1998-1:2015). In Table 2, T_s = 0.6 s falls within the Flexible Soil (FS) classification range where 0.5 s ≤ T_s ≤ 1.0 s. For the region in Peninsular Malaysia, the elastic RS (S_e) is shown in different formats in Figure 2 (Looi et al., 2015).



T (s)	S_e (g)	S_{De} (mm)
0.00	0.31	0.00
0.10	0.31	0.77
0.20	0.31	3.07
0.30	0.31	6.91
0.40	0.31	12.29
0.50	0.31	19.20
0.60	0.31	27.65
0.70	0.31	37.63
0.72	0.31	39.81
0.80	0.28	44.24
0.90	0.25	49.77
1.00	0.20	49.77
1.10	0.17	49.77
1.20	0.14	49.77
1.30	0.12	49.77
1.40	0.10	49.77
1.60	0.08	49.77
1.80	0.06	49.77
2.00	0.05	49.77
2.20	0.04	49.77
2.40	0.03	49.77
2.60	0.03	49.77
2.80	0.03	49.77
3.00	0.02	49.77
3.20	0.02	49.77
3.40	0.02	49.77
3.60	0.02	49.77
3.80	0.01	49.77
4.00	0.01	49.77

Figure 2. Elastic RS in different formats (Peninsular Malaysia, T_S = 0.6 s, Class III Importance)

3. RC building description

3.1 Briefs of the 9-storey RC building

One block of the residential staff quarters on the unidentified project site is presented. Figure 3 shows the architectural perspectives of the 9-storey RC building.

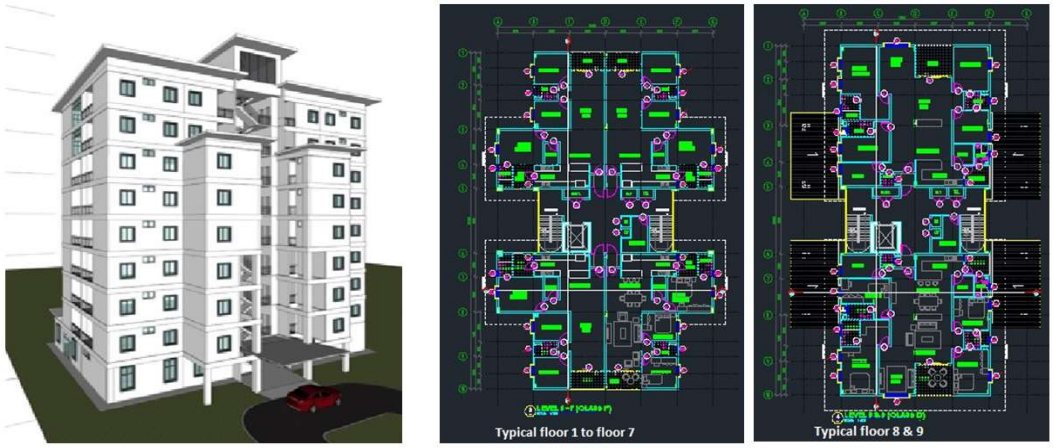


Figure 3. A 9-storey residential RC building – architectural perspective & plan

The RC building corresponds to the Class III importance level, i.e. buildings with large numbers of occupants (condominiums, shopping centres, schools and public buildings) according to Table B1 in the draft Malaysia NA (MS EN1998-1:2015), possessing an importance factor of 1.2, are assumed to experience a notional peak ground acceleration (PGA) of 0.08g. The building measures 34.2 m × 21.6 m on plan for the lower 7 floors, 34.2 m × 14.4 m on plan for the upper 2 floors and is 27 m high, above ground. The lateral force resisting system is by wall-frame interaction. The typical storey height is 3 m, typical beam size is 300 mm × 600 mm and slabs are 150 mm thick. The main columns are sized at 300 mm × 1000 mm (lower 7 floors except wings) and 300 × 750 mm (wings of lower 7 floors and all columns at upper 2 floors). The core wall thickness is 300 mm and the shear walls, 200 mm. The concrete grade is C30/37 according to Eurocode 2 (MS EN1992-1:2010). Figure 4 shows the computer model using ETABS (CSI, 2003) and its typical structural key plans. Frames are modelled as line elements, shear walls as membrane elements and typical floor slabs as shell elements. Rigid diaphragm behaviour is assumed for all floors. The supports are modelled as fixed.

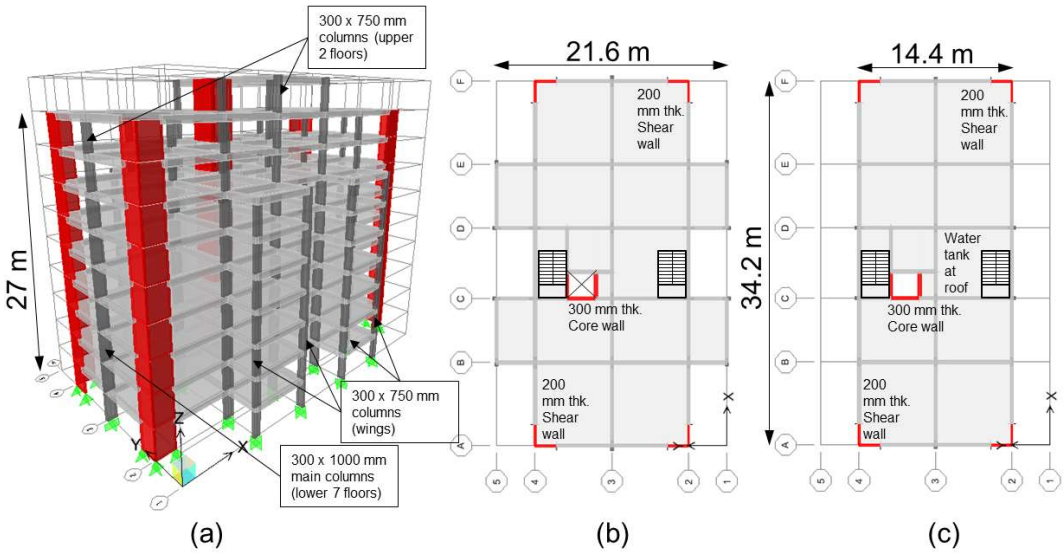


Figure 4. A 9-storey residential RC building (a) computer structural model (b) Typical structural key plan lower 7 floors (c) Typical structural key plan upper 2 floors 9-storey residential RC building – architectural perspective & plan

3.2 Actions for the building

For gravity load, the average building density, including selfweight of 4 kN/m^3, was estimated, arriving at a typical floor permanent action of 10.5 kPa (0.875 × 4 kN/m^3 × 3 m) plus a variable action of 1.5 kPa (0.125 × 4 kN/m^3 × 3 m). At roof level, 6 kPa and 0.25 kPa were applied as permanent and variable actions respectively. The water tank permanent action was 25 kPa and variable action was 5 kPa, situated at the slab panel at grid C2-D3 at roof level. For lateral loading, wind action was calculated in accordance with the generic Eurocode 1, where the building is situated in terrain category 4 (city area), with local basic wind speed 20 m/s and wind eccentricity of 15% perpendicular to wind direction. A unique imperfection load requirement of EC2 (MS EN1992-1:2010 and simplified in Table 3.1 of IStructE Manual 2006), was applied for stability robustness

purposes, by taking a maximum inclination 1/400, amounting to 0.25% of the ultimate permanent and variable actions. ie. 0.25% (1.35 × 6007 kN + 1.5 × 858 kN) = 24 kN.

For computation of the storey mass of the building, Eq. (3) in accordance with EN 1998-1 Cl 3.2.4(2)P,

$$m = \sum G_{k,i} + \sum \psi_{E,I} \quad Q_{k,i} \tag{3}$$

where $G_{k,i}$, and $Q_{k,i}$ = characteristic permanent and variable mass respectively

$\psi_{E,I} = \phi\psi_{2i}$ (EN 1998-1 Cl 4.2.4(2)P)

ϕ = 0.8 (Category A in EN 1991-1 Cl 6.3.1.1)

ψ_{2i} = 0.3, quasi-permanent value of the variable action Q_i.

Hence, it is assumed that 100% of permanent action and 24% (being 0.8 × 0.3) of variable action will 'translate' into the mass of the building during an earthquake.

In view of the minimum requirement for EC8 Ductility Class Low (DCL) and in line with the limited ductile construction detailing practice in Malaysia, the elastic spectrum is reduced using the behaviour factor (q) 1.5 into a design spectrum. Figure 5 shows the design RS acceleration (S_d).

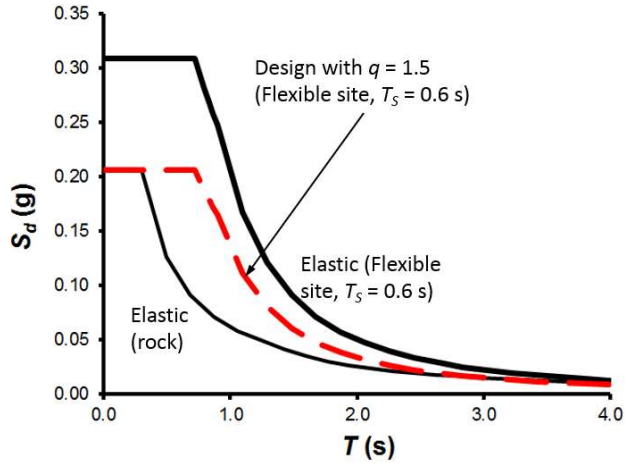


Figure 5. The design acceleration spectrum

4. Generalised force method (GFM)

The approximate fundamental period of a building is uncertain and is regionally dependent as to its structural configuration, construction materials and local construction practice (Jacobs, 2008), which explains the inconsistencies among the empirical formulae in different design codes. A GFM of analysis, as opposed to the conventional code lateral force method, is used to circumvent issues generated by the uncertainties in the natural period of real building structures.

4.1 The code lateral force method

The lateral force method of analysis as stipulated in EC8, entails the determination of the natural period of vibration, T1, using Eq. (4a) and the determination of the design base shear, F_b, using Eq. (4b).

$T_1 = 0.05H^{0.75}$, where H is building height. (4a)

$$F_b = S_d(T_1)\,\lambda m \tag{4b}$$

where $S_d(T_1)$ is the design RS acceleration at period T_1, and λ_m is the effective mass of the building where the correction factor, λ, can be taken as 85% of the total mass for the first mode (EC8 Cl. 4.3.3.2.2(1)P).

Figure 6 shows the 2D plane frame of the 9-storey RC building in the X and Y directions along with the standard lateral force method calculation steps according to EC8.

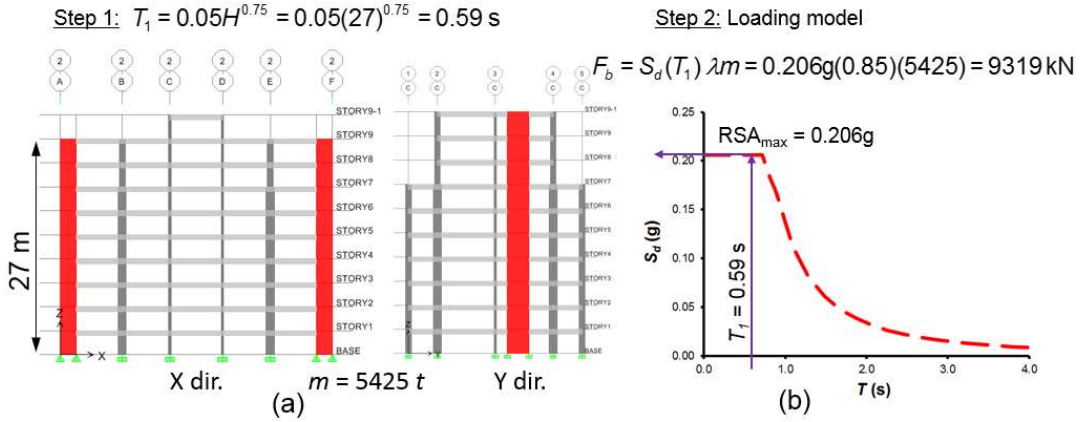


Figure 6. Code lateral force method, as EC8. (a) Step 1, estimating the fundamental period (b) Step 2 computing the base shear demand

The lateral forces, F_j, are applied to individual floor levels in the building using Eq. (4c), assuming the fundamental mode shape is approximated by a lateral displacement increasing with z (see Table 3).

$$F_j = F_b \frac{m_j z_j}{\sum_j m_j z_j} \tag{4c}$$

where z_j is the height at floor level j of the building when subject to the lateral force and m_j is the floor mass.

Table 3. Base shear distribution according to code lateral force method

Floor	mj (ton)	zj (m)	mj zj	Fj (kN)
R	54.6	30	1637	194
9F	397.7	27	10739	1275
8F	537.9	24	12910	1532
7F	633.6	21	13305	1579
6F	633.6	18	11405	1354
5F	633.6	15	9504	1128
4F	633.6	12	7603	903
3F	633.6	9	5702	677
2F	633.6	6	3802	451
1F	633.6	3	1901	226
BASE		0	0	0.00
	5425.3		78506.6	9319

The static load should be applied to two orthogonal directions on plan (see Figure 7).

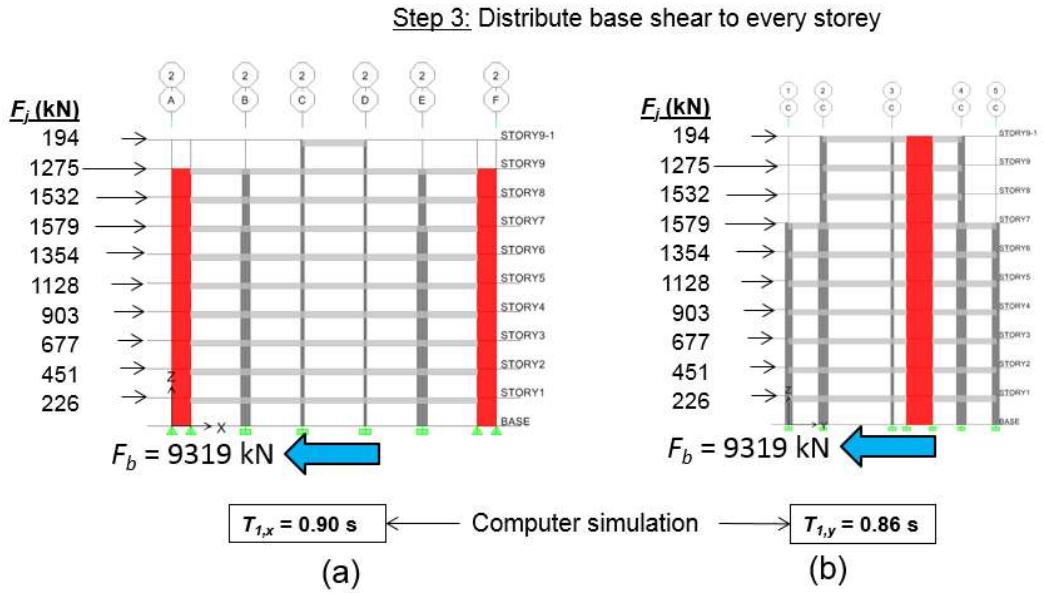


Figure 7. Step 3 of code lateral force method to distribute base shear for (a) X-direction (b) Y-direction

The code lateral force method as required by EC8 is completed at this point. It can be seen that the force distribution in the code lateral force method is identical in both X and Y directions, unrelated to changes of fundamental period obtained from computer modelling. The uncertainties stemming from the inconsistencies in the natural period value calculated by Eq. (4a) (where T_1 = 0.59 s) and that reported by the computer structural model (where $T_{1,x}$ = 0.90 s and $T_{1,y}$ = 0.86 s) can be circumvented by continuing with the GFM method to obtain improved estimates.

4.2 Operating the GFM

The force obtained at each storey using the code lateral force method is loaded into a computer structural analysis system to obtain the lateral displacement (δ_j). Table 4 shows the computation of GFM in the X direction, where simple spreadsheet computation enables $m_j\delta_j^2$ and $m_j\delta_j$, to be obtained. This is Step 4.

Table 4. Step 4 – Deflection obtained from code lateral force method and further computation of GFM in the X direction

Floor	m_j (ton)	F_j (kN)	δ_j (mm)	$m_j\,\delta_j^2$	$m_j\,\delta_j$
R	54.6	194	71.8	281372.5	3918.1
9F	397.7	1275	66.4	1753497.1	26409.3
8F	537.9	1532	59.7	1918741.1	32126.3
7F	633.6	1579	52.5	1749176.4	33290.4
6F	633.6	1354	44.6	1262447.5	28281.9
5F	633.6	1128	35.9	818662.7	22774.8
4F	633.6	903	26.8	453809.4	16956.6
3F	633.6	677	17.6	196593.5	11160.6
2F	633.6	451	9.3	54610.2	5882.2
1F	633.6	226	2.9	5237	1821.6
BASE		0.00	0.0	0.0	0.0
	5425.3	9319		8494147.4	182621.6

The objective of the GFM is to obtain the "correct" natural period estimate as a function of mass and stiffness. The effective displacement (δ_{eff}) is required, therefore, to evaluate the equivalent effective stiffness (k_{eff}) together with the effective mass (m_{eff}) using simple structural dynamic relationships.

The effective displacement is calculated using Eq. (5).

Step 5:

$$\delta_{eff} = \frac{\sum m_j\delta_j^2}{\sum m_j\delta_j} = \frac{8{,}494{,}147.4}{182{,}621.6} \approx 46.5 \text{ mm} \tag{5}$$

The equivalent effective stiffness is calculated using Eq. (6).

Step 6:

$$k_{eff} = \frac{F_b}{\delta_{eff}} = \frac{9319}{46.5/1000} = 200{,}356 \text{ kN/m} \tag{6}$$

The effective mass is calculated using Eq. (7).

Step 7:

$$m_{eff} = \frac{\left(\sum m_j \delta_j\right)^2}{\sum m_j \delta_j^2} = \frac{(182{,}621{,}6)^2}{8{,}494{,}147.4} \approx 3926 \text{ tons} \quad (7)$$

Step 8:

$$T_{eff} = 2\pi\sqrt{\frac{m_{eff}}{k_{eff}}} = 2\pi\sqrt{\frac{3926}{200356}} = 0.88 \text{ s} \quad (8)$$

Step 9:

Reading the loading demand from Figure 5 at 0.88 s, results in S_d = 0.168g, hence F_b = 0.168g (0.85) 5425.3 = 7600 kN.

Table 5. Step 9 - Base shear distribution of GFM in the X direction

Floor	m_j (ton)	z_j (m)	$m_j z_j$	F_j (kN) *revised as per GFM	δ_j (mm) *revised as per GFM
R	54.6	30	1637	158	58.5
9F	397.7	27	10739	1040	54
8F	537.9	24	12910	1250	48.7
7F	633.6	21	13305	1288	42.8
6F	633.6	18	11405	1104	36.4
5F	633.6	15	9504	920	29.3
4F	633.6	12	7603	736	21.8
3F	633.6	9	5702	552	14.3
2F	633.6	6	3802	368	7.6
1F	633.6	3	1901	184	2.3
BASE		0	0		0.0
	5425.3		78506.6	7600	

The revised lateral forces and the corresponding deflections obtained using the GFM Eqs. (5 – 8) can be notably lower than those estimated using the conventional code lateral force method in Eqs. (4a – 4c) (see Table 5, Figures 8 and 9). It should be noted that the newly estimated natural period is 0.88 s, which is closer to the results obtained using a computer analysis package (0.90 s in the X direction).

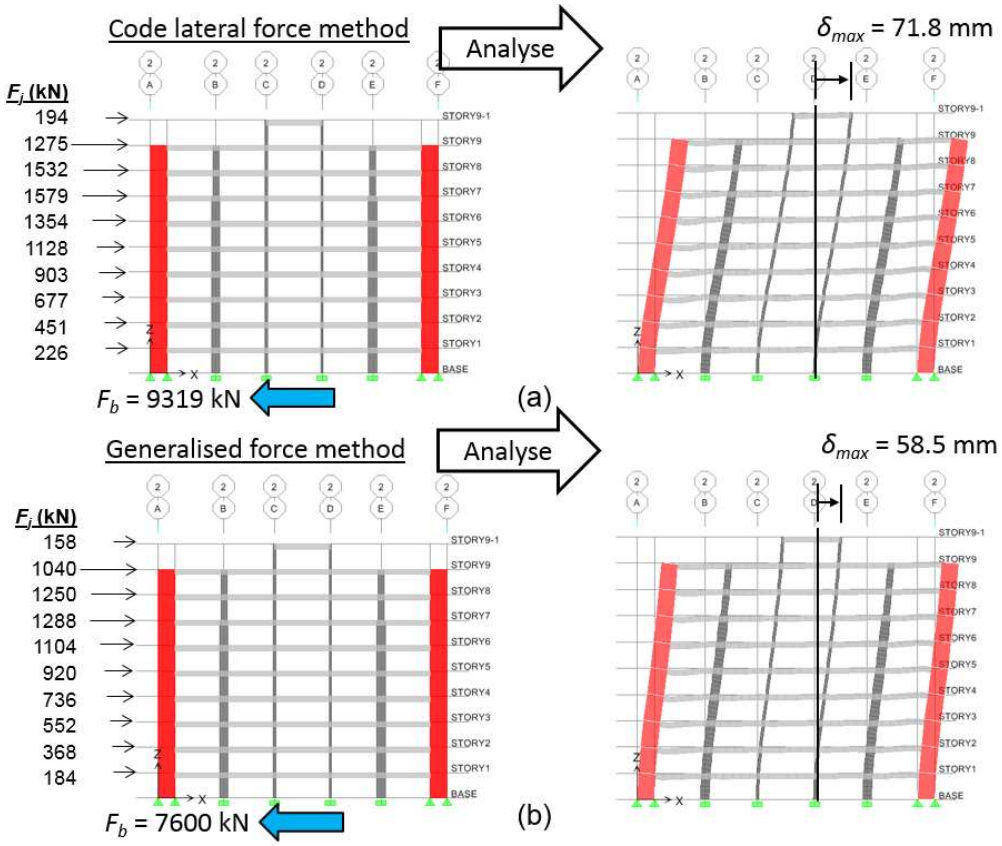


Figure 8. Comparison of base shear and deflection in the X direction (a) Code lateral force method; (b) Revised lateral force as per GFM

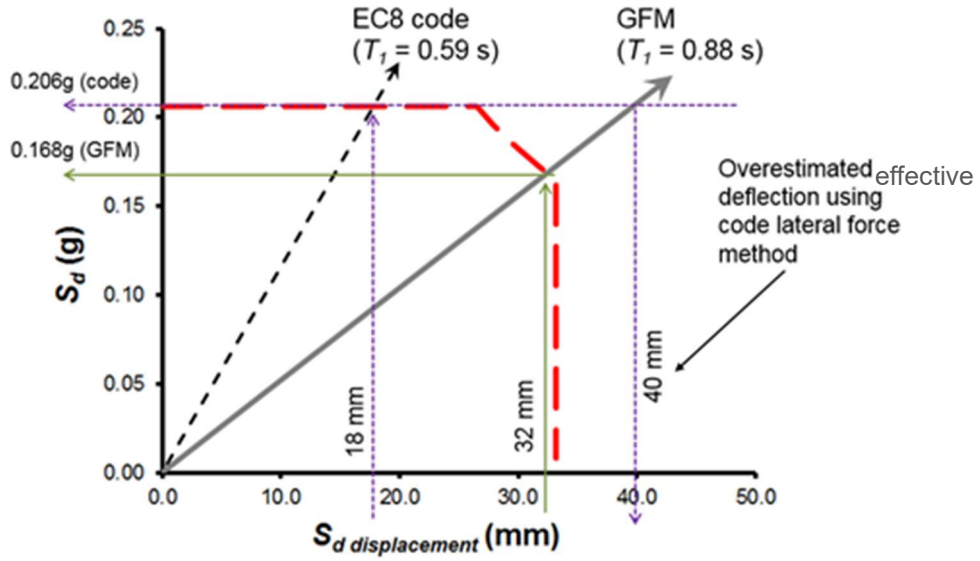


Figure 9. The comparison of results in RS formats for the different methods.

5. Dynamic modal analysis

A typical dynamic modal analysis using the response spectrum of Figure 5 was carried out, to compare with the code lateral force method and the GFM in the X direction. Table 6 shows the results of the modal analysis.

Table 6. Results of modal participation mass ratio (%) using commercial structural analysis package

Mode	Period	UX	UY	UZ	RX	RY	RZ
1	0.90	65.80	2.95	0.00	65.80	2.95	0.00
2	0.86	5.05	59.43	0.00	70.86	62.38	0.00
3	0.72	1.19	9.31	0.00	72.05	71.69	0.00
4	0.26	11.82	1.34	0.00	83.87	73.03	0.00
5	0.24	1.82	12.23	0.03	85.69	85.26	0.04
6	0.20	0.35	1.86	0.01	86.05	87.13	0.04
7	0.15	0.01	0.00	16.91	86.06	87.13	16.95
8	0.14	0.00	0.00	10.64	86.06	87.13	27.59
9	0.13	0.15	0.00	4.69	86.21	87.13	32.27
10	0.12	1.65	2.41	1.04	87.86	89.54	33.32
11	0.12	3.17	0.83	2.05	91.03	90.37	35.36
12	0.12	0.76	1.44	7.69	91.78	91.81	43.06

Since most structures have some form of irregularity, in order to fulfil architectural and functional requirements, the criterion, as stipulated in Cl. 4.2.3 in EC8, is very stringen, because it probably precludes the majority of building structures from being designed based on static analysis only. The vertical regularity prerequisite in EC8 should be relaxed in view of recent findings (in the literature) that buildings with $T_1 < 1.5$ s (which is fulfilled by most buildings with heights up to 50 m, or 16 storeys) are unlikely to experience any significant higher mode effects in their dynamic response to earthquake ground shaking. Reported analyses support this proposition including buildings possessing mass and stiffness irregularity in the building elevation (Su et al. 2011, Fardipour et al. 2011, Zhu et al. 2007). In Australia (AS 1170.4 2007, AEES 2009), dynamic analysis is only required for buildings exceeding 50 m (16 storeys) which are founded on rock, or stiff soil. In Singapore (NA to SS EC8 2013, BC3 2013) only one of the two prerequisites allowing the lateral force method listed in EC8 needs to be fulfilled. In view of the findings reported from the literature and prerequisites imposed by codes of practice in other areas of low to moderate seismicity, it is recommended that buildings up to 25 m high may be analysed using the lateral force analysis method irrespective of its degree of regularity in elevation. Table 7 summarises the various provisions applying to dynamic modal analysis and the GFM and EC8 code lateral force method, in the X direction.

Table 7. Summary of dynamic modal analysis, GFM and code lateral force method in the X direction

Approach	T_1 (s)	*Fb* (kN)	*Remarks*
Dynamic modal analysis	0.90	6338 (CQC combination)	This method is particularly encouraged in EC8 and is regarded as the 'reference method' in view of availability of commercial software possessing dynamic analysis capability. However, it is not easy to comprehend by the average structural engineer with limited experience in dynamic analysis.
GFM	0.88	7600	Buildings of up to 25 m in height may be subject to GFM irrespective of its regularity conditions in elevation. Results are comparable with dynamic modal analysis. This method is easy to comprehend and able to serve as a quick check against 3D structural dynamic analysis results
EC8 lateral force method	0.59	9319	Applicable when a) Fundamental period $T_1 \leq 4T_c$ and $T_1 \leq 2$ s. b) Building regular in elevation (EC 8 Cl.4.2.3.3.)

Subsequent rigorous design check based on acceptance criteria of ultimate strength and serviceability drift in accordance to design codes should be carried out.

6. Conclusions

One of the major drawbacks of the code lateral force method is that it prescribes building period estimation using empirical formula. This chapter discusses the generalised force method as a way of improving code lateral force method results. Calculations relating to a 9-storey RC building case study are presented above, as a demonstration for those practicing structural engineers, working in regions of low to moderate seismicity, who have not taken earthquake actions into account in the past. In the authors' opinion, since GFM involves only static analysis, it is easily adopted by those average structural engineers who possess limited experience of dynamic analysis. Through GFM, ballpark figures can be obtained to serve as a quick check against 3D structural dynamic analysis results. It is noted, that since torsional behaviour is not captured, readers are advised to refer to Lam et al. (2016), if necessary, for the enhanced version of GFM which is suitable for torsionally unbalanced buildings.

Acknowledgements

The continuous support by IEM in the facilitation of numerous workshops and meetings over the years culminating in the drafting of the NA is acknowledged. Valuable intellectual input by Mr. A.Z. Zaeem and other active participants from EC8 TC are also gratefully acknowledged.

References

AS 1170.4 (2007) Structural Design Actions – Part 4 Earthquake Actions. Standards Australia.

AEES (2009) AS 1170.4 Commentary: Structural Design Actions – Part 4 Earthquake Actions. Victoria: Australian Earthquake Engineering Society.

BC3 (2013) Guidebook for Design of Buildings in Singapore to Design Requirements in SSEN-1998-1. Singapore: Building and Construction Authority.

CSI (2003) ETABS Integrated Building Design Software Introductory User's Guide. Computers and Structures, Inc. Berkeley, California, USA.

Eurocode 1 - Actions on structures. UK: British Standards Institution.

Eurocode 8 - Design of structures for earthquake resistance. EN 1998-1 Part 1: General rules, seismic actions and rules for buildings. UK: British Standards Institution.

Fardipour M., Lumantarna E., Lam N., Wilson J. and Gad, E. (2011) "Drift Demand Predictions in Low to Moderate Seismicity Regions", Australian Journal of Structural Engineering 11(3). 195-206.

Imai, T, and Tonouchi, K. (1982) "Correlation of N value with S-wave velocity and shear modulus", Proc., 2nd European Symp. on Penetration Testing, Amsterdam, 67–72.

IStructE Manual. (2006) Manual for the design of concrete building structures to Eurocode 2. The Institution of Structural Engineers, London, UK.

Jacobs, W. P. (2008) "Building periods: Moving forward (and backward)", updates and discussions related to codes and standards, STRUCTURE magazine.

Lam, N. T. K., Wilson, J. L. and Lumantarna, E. (2016) "Simplified elastic design checks for torsionally balanced and unbalanced low-medium rise buildings in lower seismicity regions", Earthquakes and Structures, Vol. 11, No. 5, 741-777.

Looi, D. T. W., Lam, N. T. K., Tsang, H. H. and Hee, M. C. (2015). "Seismic analysis in the low to moderate seismicity region of Malaysia based on the draft handbook", Proceedings of the 10th Pacific Conference on Earthquake Engineering, 6 - 8 November 2015, Sydney, Australia.

MS EN1992-1:2010 (2010) Eurocode 2: Design of concrete structures – part 1-1: General rules and rules for Buildings.

MS EN1998-1:2015 (2015) Eurocode 8: Design of structures for earthquake resistance – part 1: General Rules, Seismic Actions and Rules for Buildings. (National Annex undergone public comments)

Sower, G. F. (1979) Introductory soil mechanics and foundations, 4th ed., Macmillan Publishing: New York.

SS EN1998-1:2013 (2013) Singapore Standards Eurocode 8: Design of structures for earthquake resistance – part 1: General Rules, Seismic Actions and Rules for Buildings. SPRING, Singapore.

Su R. K. L, Tsang H. H. and Lam N. T. K. (2011) Seismic Design of Buildings in Hong Kong, Department of Civil Engineering, The University of Hong Kong.

Tsang, H. H., Wilson, J. L., Lam, N. T. K. and Su, R. K. L. (2017) "A design spectrum model for flexible soil sites in regions of low-to-moderate seismicity", Soil Dynamics and Earthquake Engineering, Vol. 92, 36-45.

Wair, B. R., DeJong, J. T. and Shantz, T. (2012) Guidelines for Estimation of Shear Wave Velocity Profiles, PEER Report 2012/08.

Zhu Y., Su R. K. L. and Zhou F. L. (2007) "Cursory Seismic Drift Assessment for Buildings in Moderate Seismicity Regions", Earthquake Engineering and Engineering Vibration 6(1), 85-97.

Simplified Design Checks for Buildings with a Transfer Structure in Regions of Low Seismicity

Mehair Yacoubian, Nelson T. K. Lam and Elisa Lumantarna

Department of Infrastructure Engineering
The University of Melbourne, Australia

Buildings featuring a transfer structure are commonly found in metropolitan cities situated in regions of low seismicity. A transfer structure can be a rigid plate or an array of deep girders positioned at the podium level of the building to support the tower structure above. The sharp increase in the shear force demand on the tower walls above the podium is a major cause for concern. Design guidance on how to quantify these adverse effects is not available. In this chapter a simplified method for quantifying the increase in shear force demand on the tower walls is presented. In view of the very limited ductile nature of this type of construction the analysis is based on linear elastic behaviour.

Keywords: displacement-controlled behaviour, transfer structures, transfer plate, transfer girder, tower walls

1. Introduction

Buildings incorporating a transfer plate, or transfer girders, as a structural feature at the podium level of the building are commonly found in cities in regions of low seismicity. A transfer structure redistributes gravitational loads, where there is a discontinuity in the load paths, to accommodate changes in the architectural layout of floor spaces in the building. It can be regarded as a major vertical irregularity feature, which compromises the ductility of the building in projected seismic conditions (ASCE, 2010; CEN, 2005). Even so, many such buildings have been built in regions of low seismicity.

Research studies have investigated the potential seismic performance of buildings featuring a transfer structure at the podium level, using shaking table testing of scaled down models (Li et al., 2006, Lee and Hwang, 2015). Analytical investigations have also revealed a significant increase in the ductility demand of the building as a result of this type of vertical irregularity (Mwafy and Khalifa, 2017). Studies have also gained insights into the potential adverse effects of the high flexural stiffness of the transfer structure on the seismic behaviour of the building, both locally (close to the transfer structure itself) and globally on the building as a whole (Su et al. 2002, 2008 & 2009; Zhitao, 2000; Qian & Wang, 2006). A significant increase in shear force in the tower walls just above the transfer floor level (TFL) has been confirmed experimentally as reported in Li et al. (2005 & 2008) and Kuang and Zhang (2003).

Su et al. (2011) investigated the appropriateness of use of displacement-controlled behaviour for quantifying the seismic demands on a flexible structure (e.g. a tall building). As such, the deformation demands imposed on the building are proportional to the maximum ordinate of the displacement response spectrum of the ground motion (i.e. RSD_{max}).

An analysis methodology which compares the displacement demand behaviour of the building with its displacement capacity (Priestley et al., 2007, Priestley, 1997, Tsang et al., 2009) provides robust predictions of the seismic performance behaviour of buildings incorporating a transfer structure.

The next section, below, gives examples of the large increase in shearing force in tower walls supported by a transfer structure. The shear force increase is particularly pronounced just above the podium level, where the transfer structure is positioned. Below, a simplified method is developed which quantifies the adverse effects. In the final section of the chapter this prediction method is illustrated with a worked example.

2. High shear force concentrations in tower walls above the TFL

Earlier investigations on transfer plate buildings highlighted the high shear concentration phenomenon in the tower walls just above the transfer floor level (TFL) when the building is subjected to lateral loads (Su et al., 2002, Tang and Su, 2014). These concentrations result mainly from out-of-plane bending of the transfer structure supporting the tower walls. Differential rotations of the transfer structure along its length results in displacement incompatibilities between adjacent tower walls. The incompatibilities induce high in-plane forces in the link beams and slabs connecting the tower walls, resulting in significant increases in shear forces above the TFL. Similar significant increases have been reported for tower walls featuring setbacks (Yacoubian et al., 2017a).

A 2D model of an example building (Figure 1) was employed to illustrate such shear force increases. Details of the tower walls, the connecting slabs and the loading protocol for the example buildings can be found in Yacoubian et al., (2017b). There are three tower walls, numbered (1 – 3). Walls 1 and 3 are the exterior walls, Wall 2, is the middle (interior) wall. The displacement ratio (Δ_r) is the ratio of the lateral displacement of wall no. 1 (δ_1), or wall no. 3 (δ_3), divided by the displacement (δ_o) of a control model where the transfer plate was modelled as infinitely rigid to bending out-of-plane. In the control model all three walls have identical deflection profiles. The increase in shear force demand on wall no. 3 (which is paralleled by a reduction in the shear force demand on wall no. 1) is the result of incompatible displacements between the tower walls ($\Delta_r \neq 1$) at the level immediately above the TFL (refer to Figure 2a). Strutting forces developed in the elements connecting adjacent tower walls are shown in Figure 2c. Interestingly, the increase in shear force demand diminishes rapidly with height and is negligible at only two-to-three storeys above the TFL (compare Figures 2a & 2d). Designers are cautioned that these shear increases will not have been identified in FE analyses where the usual "rigid diaphragm" assumption has been made. Thus, actual shear demands on the tower walls have probably been underestimated in certain building FE analyses.

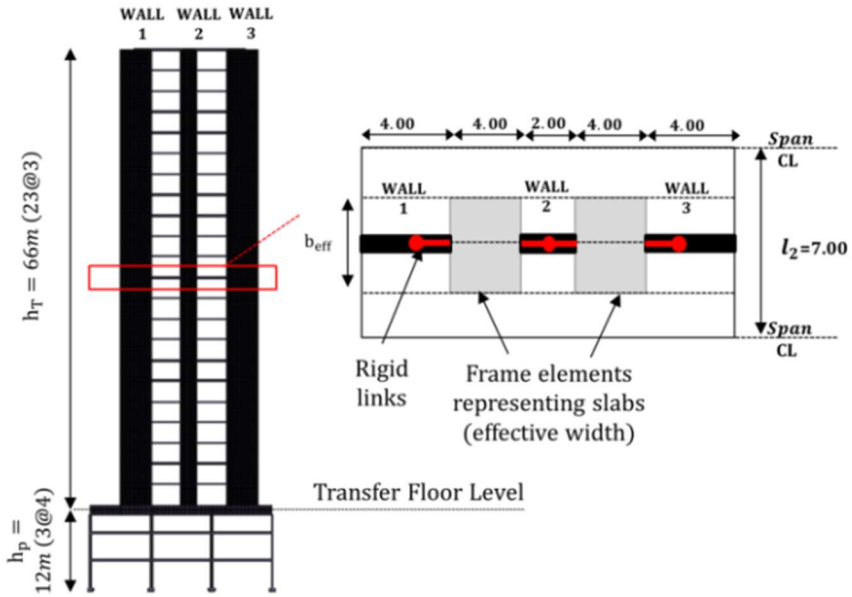
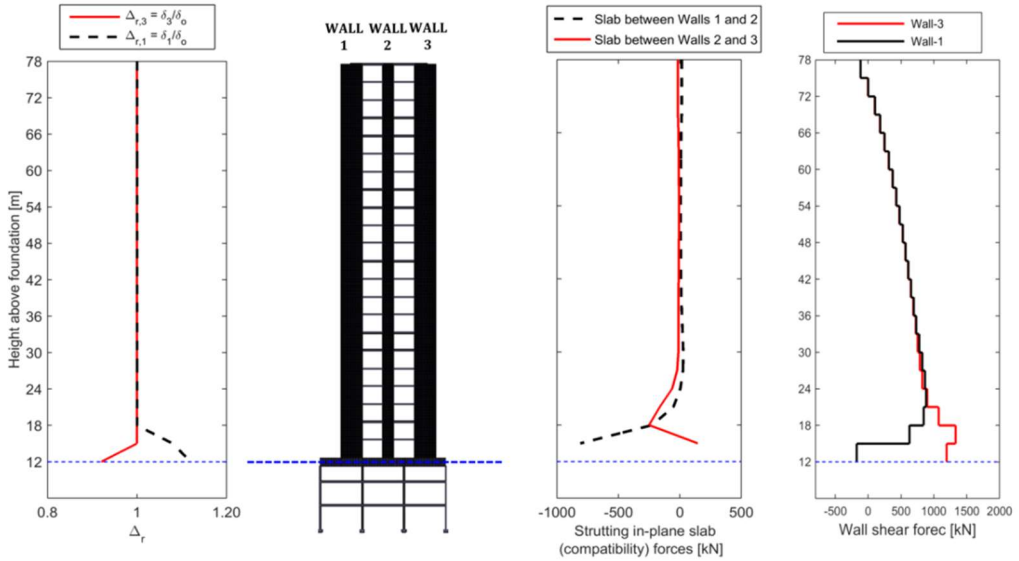


Figure 1. 2D model of the building featuring a transfer plate



(a) Displacement ratio

(b) 2D planar model of the building

(c) Strutting force distribution in the connecting slabs

(d) Shear force distribution in the tower walls

Figure 2. Displacement incompatibility between connected walls and the resulting strutting (compatibility) slab force and wall shear force distributions

3. In-plane strains between tower walls above TFL

Strutting forces between adjacent tower walls can result from differential wall deflections together with in-plane compatibility restoring actions exerted by the connecting slabs (Figure 3). The magnitude of the strutting force developed in a connecting member (e.g. link beam and slab) is the product of the in-plane strains arising from the differential deflections of adjacent tower walls and the axial stiffness of the member. Equation (1) gives that strutting force (F_{STRUT})

$$F_{STRUT} = \varepsilon_{STRUT} \times E_c A_{eff} \tag{1}$$

where ε_{STRUT} is the in-plane strain in between two adjacent tower walls above the TFL and the effective slab area (A_{eff}) is the product of the width of the column-strip and the gross thickness of the slab.

The amount of in-plane strain (ε_{STRUT}) is, in turn, dependent on differences in the angles of rotation of two adjacent tower walls, at their bases. Parameter $\Delta_{\theta TP}$ (which is θ_{TP1} - θ_{TP2} or θ_{TP2} - θ_{TP3}) characterises the differential wall rotation (see Figure 4). If walls 1 and 3 have identical dimensions then the values of θ_{TP1} - θ_{TP2} and θ_{TP2} - θ_{TP3} are dependent on the positioning of the wall along the supporting span. Direct correlation between ε_{STRUT} and $\Delta\theta_{TP}$ as modelling parameters is confirmed by comparing the ε_{STRUT} profiles for various values of $\Delta\theta_{TP}$ (Figure 5). Close correlation between the strutting forces F_{STRUT} (hence ε_{strut}) and $\Delta\theta_{TP}$ is demonstrated further by plotting their time-histories on the same graph (Figure 6). Clearly the two quantities are directly correlated.

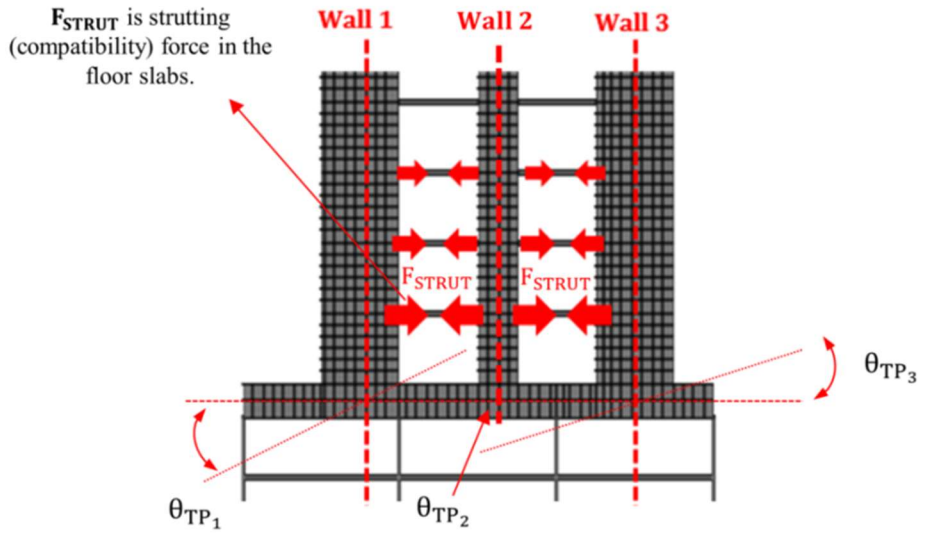
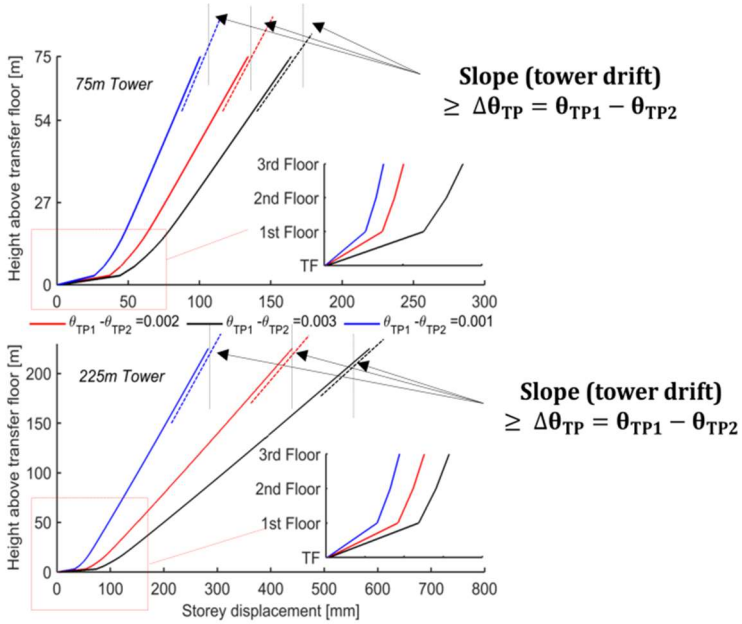
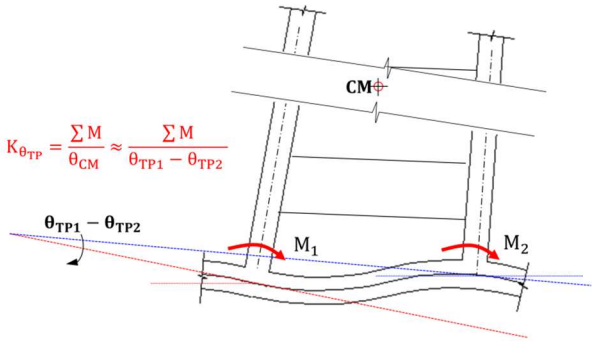


Figure 3. Introducing F_{STRUT}, ε_{STRUT} and $\Delta\theta_{TP}$



(a) Tower displacement profile



(b) Angle of rotation at base of tower walls

Figure 4. Deflection of individual tower wall

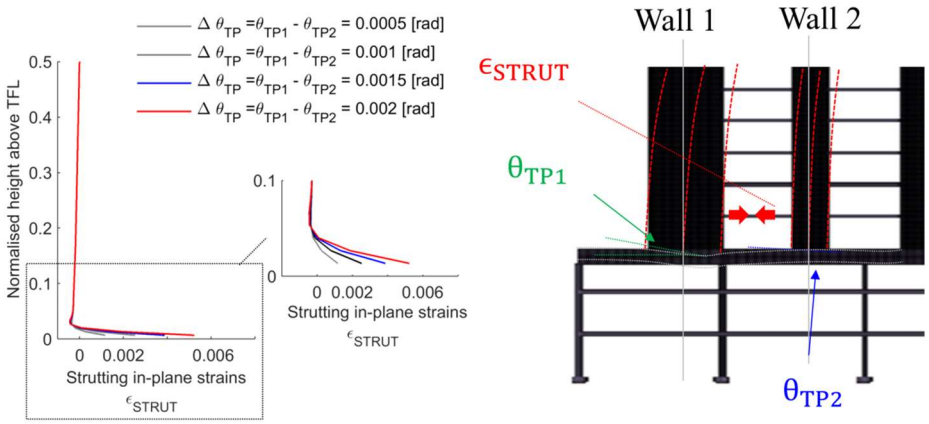


Figure 5. In-plane strains between walls and differential angle of rotation at their base $\Delta\theta_{TP} = \theta_{TP1} - \theta_{TP2}$

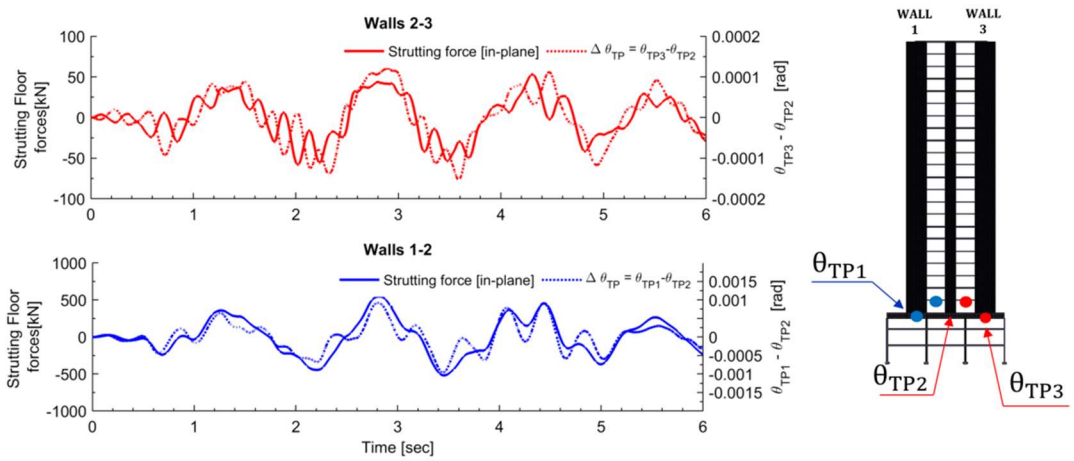


Figure 6. Time histories of in-plane strutting forces between walls and differential angle of rotation at their base $\Delta\theta_{TP} = \theta_{TP1} - \theta_{TP2}$

4. Analytical modelling of the Flexibility Index

In section 3, the strutting force in a link element connecting two adjacent tower walls is shown to be correlated with $\Delta\theta_{TP}$. The correlation is consistently linear as shown in Figures (7a) - (7f). If the slope of the correlation is defined as the Flexibility Index (FI), the in-plane strain (ε_{STRUT}) is expressed as the product of FI and $\Delta\theta_{TP}$, as shown by equation (2). Importantly, FI, the slope of this correlation, is shown to be dependent on the relative flexural stiffness of the transfer structure $(E_cI)_{TP}$ and tower wall $(E_cI)_{wall}$. Relative stiffness is expressed in terms of parameter α_r which is defined by equation (3).

$$\varepsilon_{STRUT} = FI \times \Delta\theta_{TP} \tag{2}$$

$$\alpha_r = \sqrt{\frac{(E_cI)_{TP}}{(E_cI)_{Wall}}} \tag{3}$$

The combined effects of $\Delta\theta_{TP}$ and α_r on the magnitude of the strutting forces F_{STRUT} are well demonstrated in Figure 7. Sensitivity analyses by the authors revealed that in-plane strains and stresses in struts (and ties) connecting individual tower walls, caused by flexing of the transfer plate, were not sensitive to wall spacing.

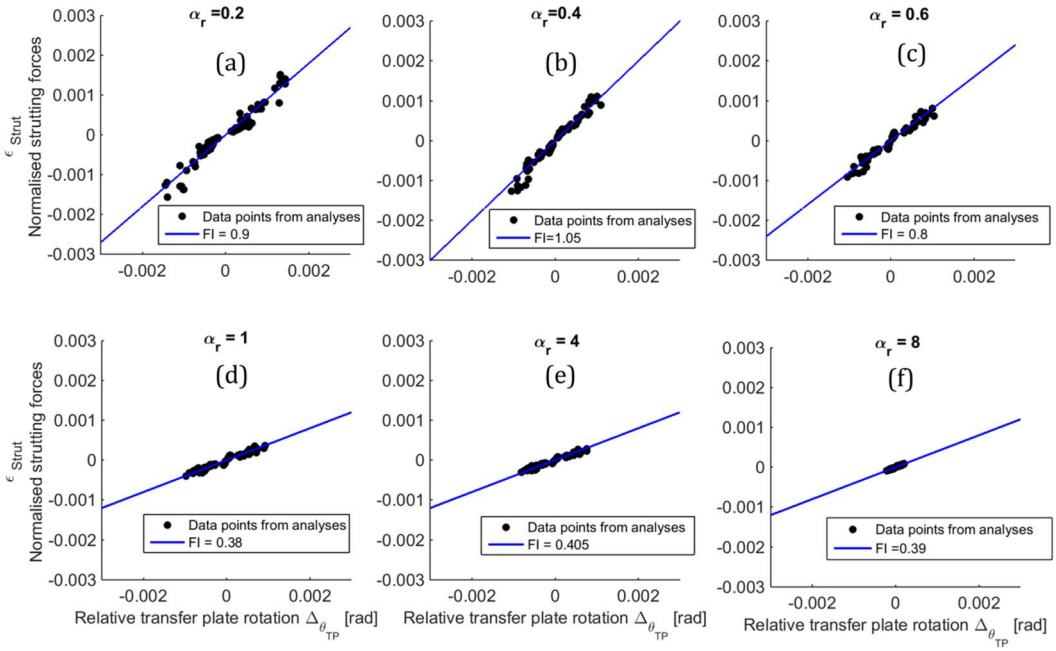


Figure 7. Effects of α_r on strutting forces in between tower walls

It is shown further in Figure 8 that higher values of *FI* (meaning higher strutting forces) can be developed between very stiff tower walls, in which case the value of α_r is less than 0.4. On the other hand, the strutting forces can be reduced by as much as 60%, with relatively flexible tower walls, in which case, $\alpha_r > 1$. In cases of multiple tower walls above the TFL α_r is based on the sectional properties of the most flexible wall in the assembly (maximum of three walls for interior bays and two walls for the exterior bays). Where a stiff continuous core shaft is present, α_r is based on the properties of the transferred tower wall connected to the core (verifications are presented in Section 7).

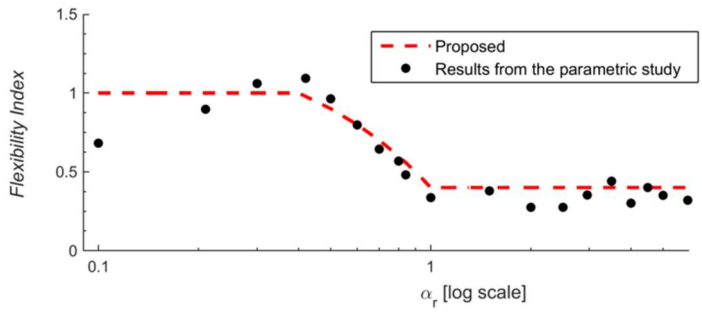


Figure 8. Correlation of Flexibility Index with α_r

In summary, the value of F_{STRUT} can be estimated using equation (4) which was derived by combining equations (1) and (2).

$$F_{STRUT} = FI \times \Delta\theta_{TP} \times E_c A_{eff} \tag{4}$$

5. Analytical modelling of peak rotational demand of building

It is demonstrated in sections 3 & 4 that strutting forces between tower walls depend on $\Delta\theta_{TP}$ which characterises the differential tower wall deflections. The calculation of the $\Delta\theta_{TP}$ parameter can be computationally intensive, so other displacement related parameters have been explored to obtain approximate estimates for this parameter. From the designer's perspective it is convenient to note that $\Delta\theta_{TP}$ can be approximated by the angle of drift of the building tower at mid-height level (i.e. at the level of the centre of mass of the tower block). Good consistencies between the two angles of rotation mean that the in-plane stresses and strains developed between two adjacent tower walls can be predicted conveniently by referring to the global displacement (and rotational) demand of the tower block as a whole. The degree of consistency has been tested in a parametric study. A vertical line showing the angle of differential rotation between two adjacent tower walls at their bases was superimposed onto a graph showing the changing angle of drift at the centre line of the building up its height; the comparison was repeated for a range of parameters demonstrating good consistency in the trend (Figure 9).

Equation (4), for estimating F_{STRUT} may, therefore, be written as follows:

$$F_{STRUT} = FI \times \theta_{CM} \times E_c A_{eff} \tag{5}$$

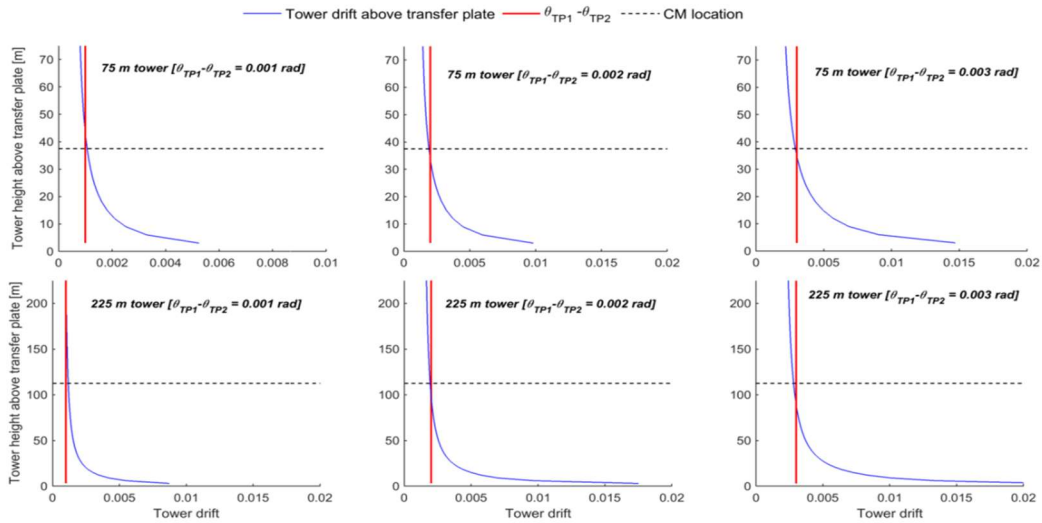


Figure 9. Angle of drift at position of CM in comparison with differential angle of rotation at base of wall $\Delta\theta_{TP} = \theta_{TP1} - \theta_{TP2}$

The viability of linking in-plane strains between adjacent tower walls to the (global) angle of drift of the tower wall as a whole (e.g. θ_{CM}) motivated the development of a simplified hand calculation procedure which enables strutting forces in the link elements to be predicted, provided that the structural configuration and gross dimensions of the tower walls and the podium are known, and the stiffness properties of the transfer plate and the tower walls are also known. Estimates of the strutting forces can therefore be made without the need to execute memory intensive finite element analysis of a complete model of the tower - podium assemblage.

The simplified calculation model, below, is based on simplifying the tower walls collectively as a rectangular "rigid-body" supported on the podium structure (Figure 10). The elastic stiffness of the translational spring positioned at the base of the rigid body is to model the influences of the elastic behaviour of the podium structure (Figure 11a) and that caused by tower block sway (Figure 11b). The elastic stiffness of the rotational spring (also positioned at the base of the rectangular rigid body) is to model the effects of the shortening-lengthening (push-pull) actions of the columns which support the podium and the building as a whole (Figure 11c). The rotational spring also incorporates the effects of transfer girder flexibility on the rotations at the centre of mass (θ_{CM}) of the rigid block (Figure 10). Sway deflection of the tower, as above, is actually not compatible with the rigid-body assumption of the simplified model which, strictly speaking, does not represent real behaviour. Thus, results derived using the simplified calculation method (assuming rigid-body behaviour of the tower block of Figure 10) must be verified to demonstrate that idealisation errors are within acceptable limits in the practical context (as demonstrated, below, in this section and in section 7).

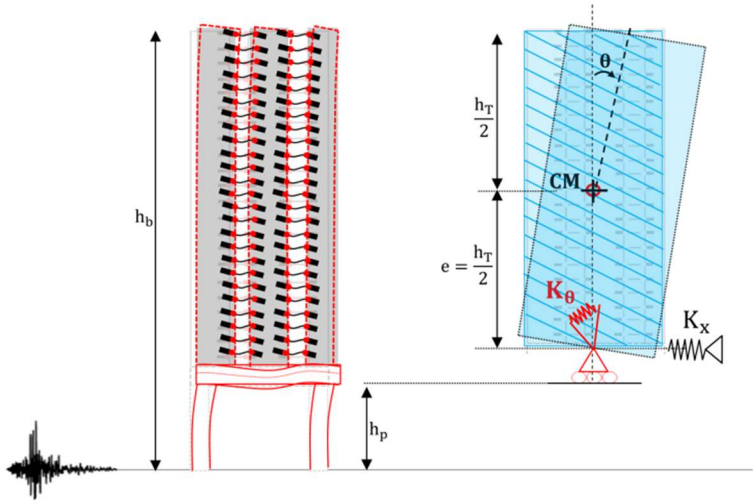


Figure 10. Schematic representation of the rigid body rotation model

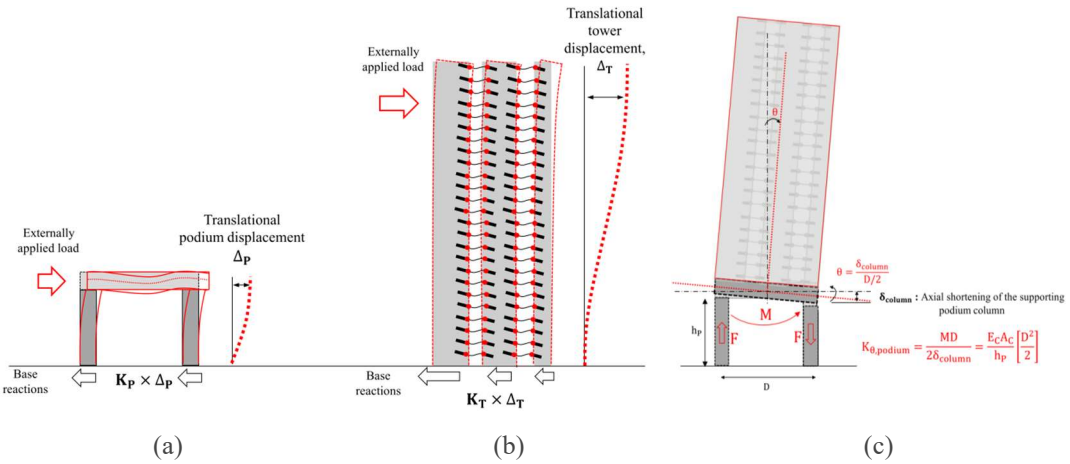


Figure 11. Translational and rotational stiffness

The value of the elastic stiffness of the translational, and rotational, spring of the rigid-body model (of Figure 10) is defined by equations (6) and (7) respectively.

$$K_X = \left(\frac{1}{K_T} + \frac{1}{K_P} \right)^{-1} \tag{6}$$

where K_T and K_P are lateral stiffness values for tower and podium structure respectively

$$K_\theta = \frac{1}{\left(\frac{1}{K_{\theta_{TP}}} + \frac{1}{K_{\theta,podium}} \right)} \tag{7}$$

where the meaning of $K_{\theta,podium}$ is as indicated schematically in Figure 11c; $K_{\theta_{TP}}$ is the rotational stiffness parameter, defined as the aggregated bending moment at the base of all the walls (ΣM) divided by the rotation at the CM of the tower structure θ_{CM} (Figure 4b).

The value of $K_{\theta_{TP}}$ can be estimated using equation (8).

$$K_{\theta_{TP}} = E_c t_{TP}^2 W \sqrt{\left(\frac{D}{h_T} \right)^3} \tag{8}$$

where D is gross dimension of the building tower (as a whole) in the direction of loading, t_{TP} and W are the thickness and width of the transfer plate, respectively and E_c is the modulus of elasticity of the transfer plate concrete.

The $K_{\theta_{TP}}$ parameter does not just represent the flexural stiffness of the transfer plate on its own as it also includes the restraint on the rotation of the building tower at the centre of mass. Thus, the aspect ratio of the building tower: D/h_T, is a parameter in equation (8) for estimating the value of $K_{\theta_{TP}}$.

In summary, the spring-connected rigid-body ("rocking") model of the building as depicted in Figure 10 is complete when the value of K_x and K_θ have been determined using equations (6) – (8) and the distribution of mass up the height of the tower block is also known. The original computer model of the building may have thousands of degrees-of-freedom (DOFs). The rocking model reduces the number of DOFs to just two, one translational and one rotational. The problem is essentially one of dynamic rotational coupling. A similar approach to modelling has been adopted for analysing the dynamic coupling of torsionally unbalanced buildings featuring plan irregularities. The building models employed in those studies have also been reduced to 2 DOFs (Lam et al., 2016; Lumantarna et al., 2013).

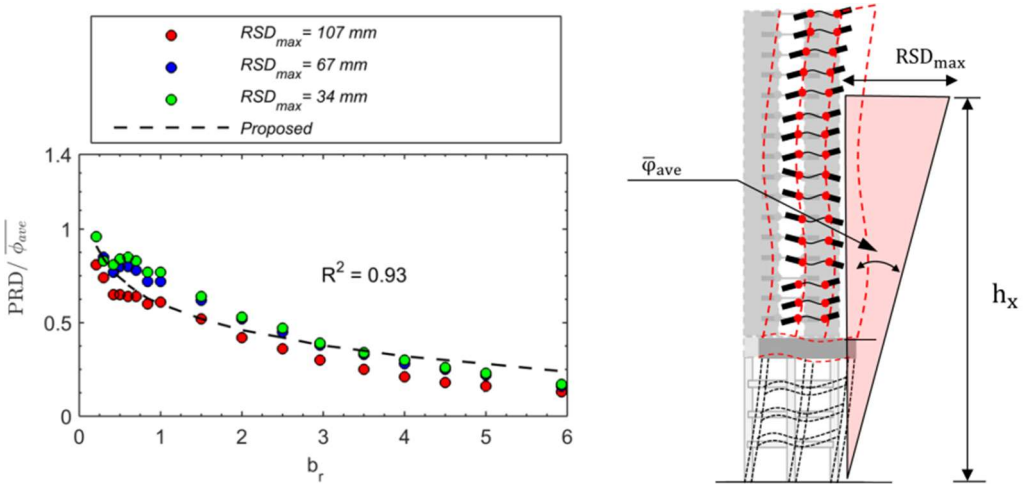
The dynamic rotational coupling analysis of the rigid-body model of the building towers (of Figure 10) provides predictions of the *Peak Rotational Demand (PRD)*. Analytical details of the rotational coupling problem are presented in Section 6. Solutions for PRD so derived are presented in the remainder of this section, below, in both graphical (Figures 12 – 14) and algebraic formats (equations 9a & 9b).

$$\frac{PRD}{\varphi_{ave}} = -0.2 \times \ln\left(b_r\right) + 0.6 \tag{9a}$$

where b_r is a dimensionless parameter representing the stiffness properties of the rotational spring which restrains the rigid-body from rotation. Refer to Section 6, and Figure 22, for the algebraic definition of the parameter and the associated details.

$$\overline{\varphi_{ave}} = \frac{RSD_{\max}}{h_x}$$ (refer Figure 12b for the diagrammatic illustration) (9b)

where h_x is the effective height of the building, which may be taken as 0.7 times the total height of the building; and RSD_{max} is the highest response spectral displacement value.



(a) Normalised PRD values obtained from the study

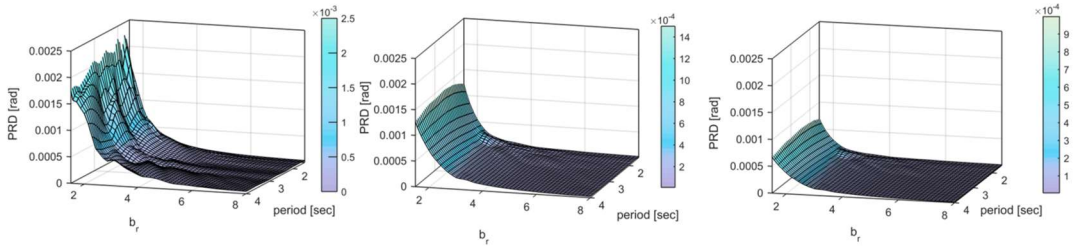
(b) Schematic description of the parameter $\overline{\varphi_{ave}}$

Figure 12. Analytical model for the estimation of PRD on a building

Essentially, PRD is the parameter approximating $\Delta\theta_{TP}$ and θ_{CM} so that equations (4) & (5) can be replaced by equation (10) as shown below.

$$F_{STRUT} = FI \times PRD \times E_c A_{eff}$$ (10)

The simple expression for estimating F_{STRUT} using equation (10) provides a conservative estimate of the additional shear forces in the tower walls transferred from the connecting slabs $|\Delta V_{Slab}|$.



(a) Record No. 3-9 (RSD_{max} = 107mm)

(b) Record No. 10-16 (RSD_{max} = 67mm)

(c) Record No. 17-23 (RSD_{max} = 38mm)

Figure 13. Effects of (b_r) and (RSD_{max}) on the Peak Rotational Demand (PRD)

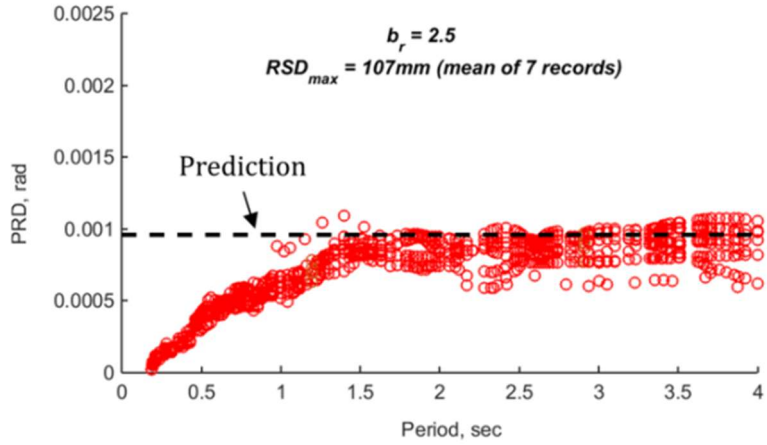


Figure 14. Results of Parametric studies on Peak Rotational Demand (b_r=2.5) based on use of records nos. 3 - 9 (refer Table A1 of Appendix A)

It is demonstrated further in Figures 15 & 16 that PRD, as an output parameter from the dynamic rotational coupling analysis (of the simplified rigid-body model of the building), can be used to constrain the values of differential wall rotation ($\Delta\theta_{TP}$) and the in-plane strain (ε_{STRUT}) developed between adjacent tower walls.

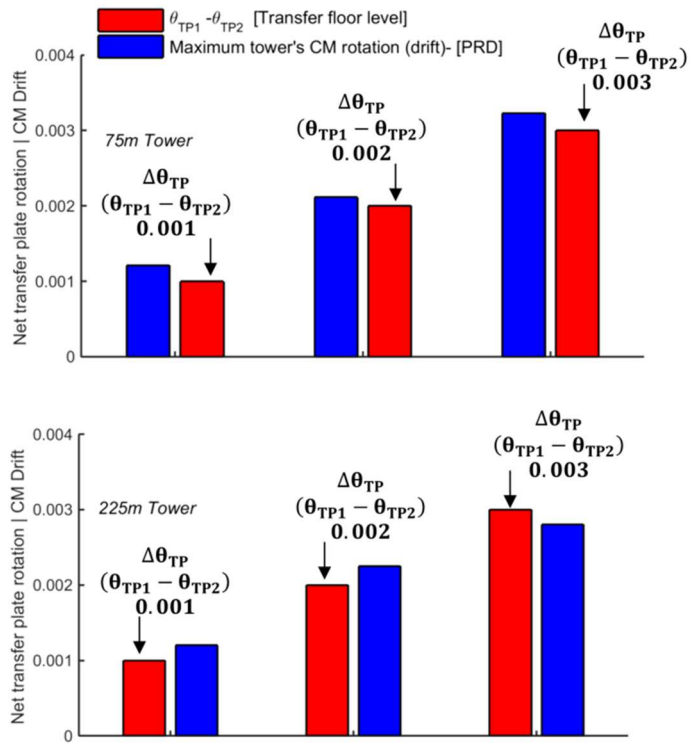
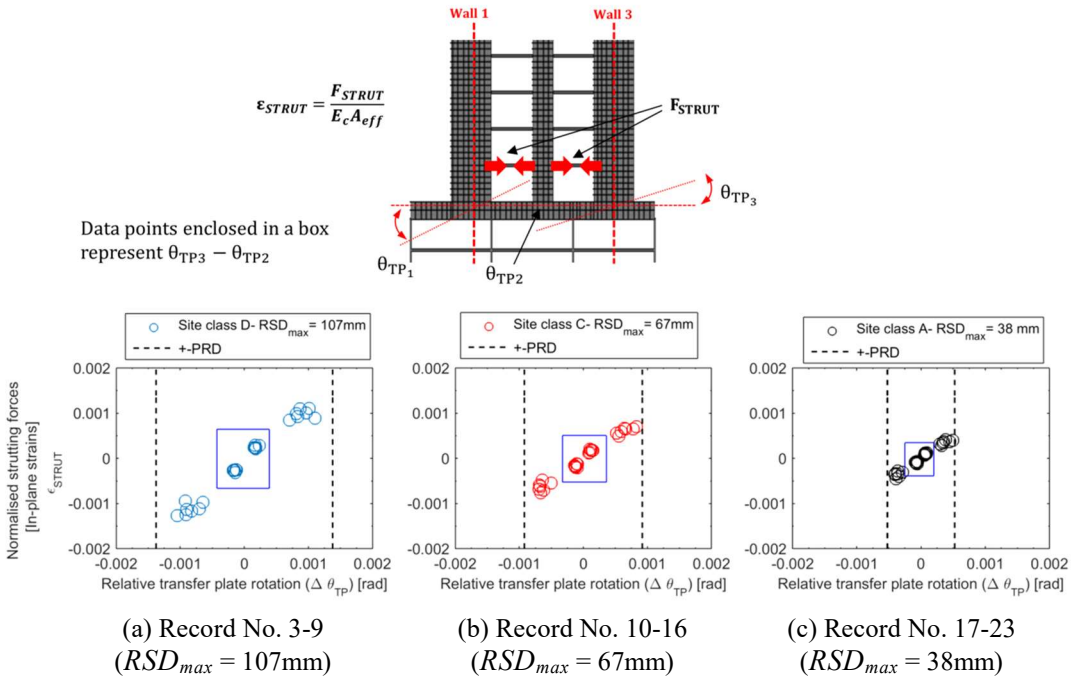


Figure 15. Peak Rotational Demand as a parameter to approximate peak differential wall base rotations



(a) Record No. 3-9 (RSD_{max} = 107mm)

(b) Record No. 10-16 (RSD_{max} = 67mm)

(c) Record No. 17-23 (RSD_{max} = 38mm)

Figure 16. Peak Rotational Demand as a parameter to constrain in-plane strutting forces

6. Analysis of dynamic rotational coupling of the rigid body model of the building

This section details the solution process in the analysis of the dynamic rotational coupling behaviour of the rigid body model. Readers primarily interested in the application of the simplified analytical model and not its derivation may skip this section.

The dynamic equilibrium equations (equations 11 - 12) are employed to solve for the coupled dynamic properties of the building and the displacement/rotation response behaviour of the tower when subjected to earthquake ground accelerations.

$$m\ddot{x} + K_x\left(x + e\theta\right) = 0 \tag{11}$$

$$J\ddot{\theta} + K_x\left(x + e\theta\right) + K_\theta\theta = 0 \tag{12}$$

where m in equation 11 represents the translational mass of the building, J (in equation 12), the mass moment of inertia of the tower; K_θ is the total rotational stiffness of the tower structure above the TFL (defined in equation 7) and K_X is the equivalent translational stiffness of the building (equation 6).

Equations 11 & 12 are next normalised with respect to mr and mr^2 respectively. The parameter r is the radius of gyration of the tower block undergoing rigid body rotation $\left(\mathrm{r} = \sqrt{\frac{\mathrm{h_T^2}+\mathrm{D^2}}{12}}\right)$ and b^2 is the ratio of the total rotational and translational stiffnesses $\left(\mathrm{b^2} = \frac{\mathrm{K_\theta}}{\mathrm{K_x}}\right)$.

The normalised dynamic equilibrium equations are presented in matrix format by equation 13. The eccentricity, *e,* defining the rigid body rotation of the tower block is evaluated as the distance between the TFL and the CM of the tower (at mid-height).

$$\begin{bmatrix} 1 & 0 \\ 0 & 1 \end{bmatrix} \begin{pmatrix} \ddot{x}_r \\ \ddot{\theta} \end{pmatrix} + \omega_x^2 \begin{bmatrix} 1 & e_r \\ e_r & \left(b_r^2 + e_r^2\right) \end{bmatrix} \begin{pmatrix} x_r \\ \theta \end{pmatrix} = \begin{pmatrix} 0 \\ 0 \end{pmatrix} \tag{13}$$

where $\mathrm{x_r} = \frac{\mathrm{x}}{\mathrm{r}}; \mathrm{e_r} = \frac{\mathrm{e}}{\mathrm{r}}$ $\ddot{\mathrm{x}}_\mathrm{r} = \frac{\ddot{\mathrm{x}}}{\mathrm{r}}$, $\omega_\mathrm{x}^2 = \frac{\mathrm{K_x}}{\mathrm{m}}$ and

$$b_r^2 = \frac{K_\theta}{K_x}\left(\frac{12}{h_T^2 + D^2}\right) \tag{14}$$

The coupled Eigen solution for conditions of free vibration is computed to determine the coupled dynamic properties of the building. The parameters Ω_i and λ_i represent the coupled angular velocity and the angular frequency ratio for the i-th mode of vibration respectively (as shown by equation 15).

$$\Omega_i = \lambda_i \omega_x \tag{15}$$

where ω_x is the angular velocity of a torsionally balanced model of the building. Full details of the derivations are presented elsewhere (Lumantarna et al., 2013, Lam et al, 2016). The two coupled angular frequency ratios λ_i are obtained by solving the 2x2 matrix expressed in equation 16.

$$\lambda_i^2 = \left(\frac{1 + \left(b_r^2 + e_r^2\right)}{2} \mp \sqrt{\left[\frac{1 - \left(b_r^2 + e_r^2\right)}{2}\right]^2 + e_r^2} \right) \tag{16}$$

The analytical model prompts a framework for estimating the CM rotations of the tower ($\theta_{CM}(t)$) which are primarily imposed by the transfer plate distortions as shown by equation 17.

$$\theta_{CM}(t) = \sum_{j=1}^{j=2} \left(\frac{\theta_j}{1 + \theta_j^2} \right) \frac{u_{\Omega_i,\zeta}(t)}{r} \tag{17}$$

where

$$\theta_j = \frac{\lambda_i^2 - 1}{e_r} \tag{18}$$

$\mathrm{u}_{\Omega_\mathrm{i},\zeta}(\mathrm{t})$ in equation 17 is the damped single-degree of freedom displacement response of an equivalent system with an angular velocity of Ω_i.

The peak rotation demand (*PRD*) is defined as the maximum value of θ_{CM} obtained from the dynamic analysis (as shown by equation 19).

$$PRD = \max\left(\theta_{CM}(t)\right) \geq \max(\Delta\theta_{TP}) \tag{19}$$

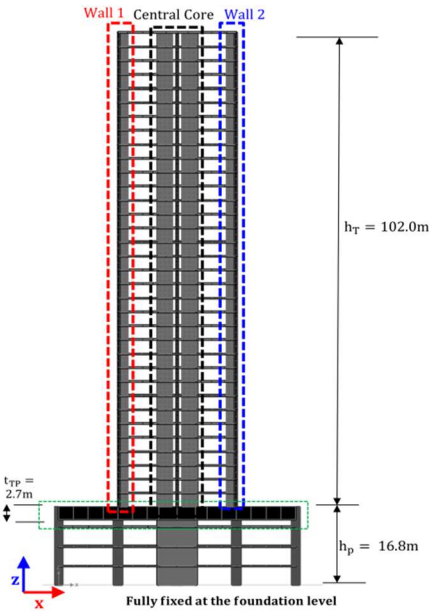
Building models similar to that of Fig. 1 were employed in a parametric study to investigate the *PRD* trends for varying intensities of ground shaking. The building models

were proportioned to achieve a range of b_r values varying from 0.1 to 8. For all models the value of K_θ was approximately equal to the value of $K_{\theta_{TP}}$, because the deformation due to flexing of the transfer plate was much greater than that of the (much more rigid) podium structure below. The computed value of b_r depends on the flexural rigidity (hence thickness) of the transfer plate.

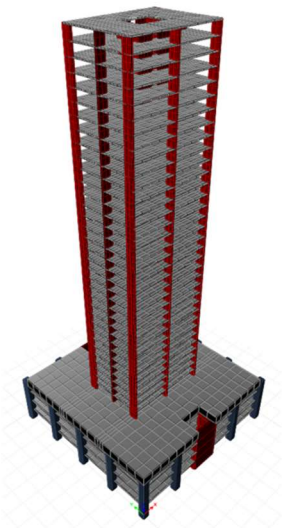
The building models were analysed using three suites of synthetic ground accelerations matching the Australian Standard code spectrum (AS1170.4, 2007). Details of the accelerograms used in this study are summarised in Table A-1 of Appendix A. Results of the analyses for buildings of increasing fundamental periods of vibration (T_X) and b_r values are given above (see Figure 13).

7. Case study of the 3D analysis of a building to illustrate the use of the simplified procedure and to verify its accuracy

A 3D model of a building featuring a transfer structure, as shown in Figure 17, was used to illustrate the simplified analytical procedure introduced in this chapter and to verify its accuracy in quantifying the strutting forces developed between adjacent tower walls and the significant increase in shear force demand for tower walls above the TFL. The 120m reinforced concrete building features a four-storey podium and a 2.7m thick transfer plate. The 102m tower comprises structural walls and a central core coupled with 200mm thick reinforced concrete flat slabs. The building model accords with design guidelines stipulated in the Australian Standard (AS 3600, 2009). The lateral load resisting system is designed for wind loads, taking no account of potential seismic loading. Floor loads were uniformly applied following Australian Standard recommendations (AS 1170.0, 2002) as summarised in Table A-3.



(a) Elevation view of the case study building showing the analysed walls



(b) 3D render of the FE model of the case study building

Figure 17. Case study building

The numerical (FE) model of the building was developed using program ETABS (Habibullah, 1997). The seismic response behaviour of the building was analysed using a suite of accelerogram records, the details of which are summarised in Table A-1 (in Appendix A). The *Hilber-Hughes-Taylor* direct linear integration scheme was adopted to solve for the response behaviour of the building using a time step of 0.005 seconds. The magnitudes of the strutting forces in the floor slabs (modelled as thin shell elements) were obtained by integrating in-plane slab stresses at different locations along the slab for each time step.

As explained above, in Sections 5 & 6, the dynamic rotational coupling behaviour of the building tower can be approximated by the use of the 2DOF model the schematic diagram of which is shown in Figure 10 (further details can be found in Yacoubian et al., 2017b). This coupling analysis provides predictions of the Peak Rotational Demand (*PRD*) which are central to the simplified analytical methodology introduced in this chapter. Verification of the accuracy of the dynamic coupling analysis is therefore important so as to verify the simplified analytical methodology as a whole. A summary of the input parameters and their use in the calculation procedures is given in Table A-2 (Appendix A).

In Figure 18, the roof displacement time histories derived from program ETABS are compared with those from the 2DOF model to demonstrate the consistencies. It is shown further in Figure 18, that the 2DOF model is capable of accurately estimating the displacement response behaviour. Proportionality between the two parameters: (a) relative transfer plate rotation $\Delta\theta_{TP,}$ which equals $(\theta_{TP1} - \theta_{core}, \theta_{TP2} - \theta_{core})$ and (b) strutting forces F_{STRUT} developed in the slabs connecting adjacent tower walls (walls 1 and 2) have been well demonstrated in Figures 19a & 19b, where the time-histories of both parameters are superimposed on the same graph.

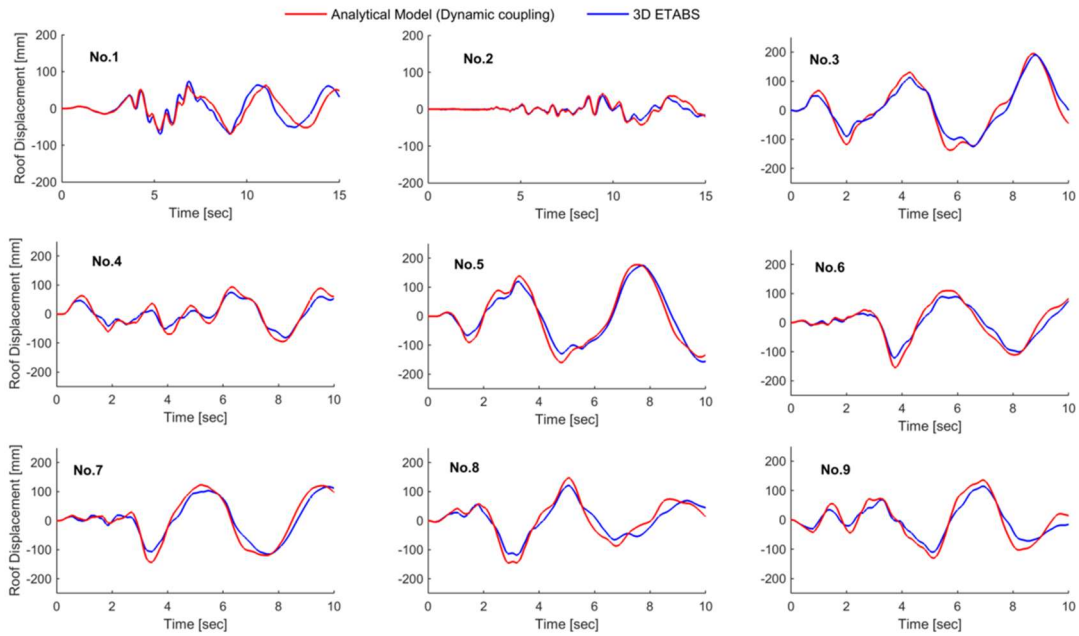
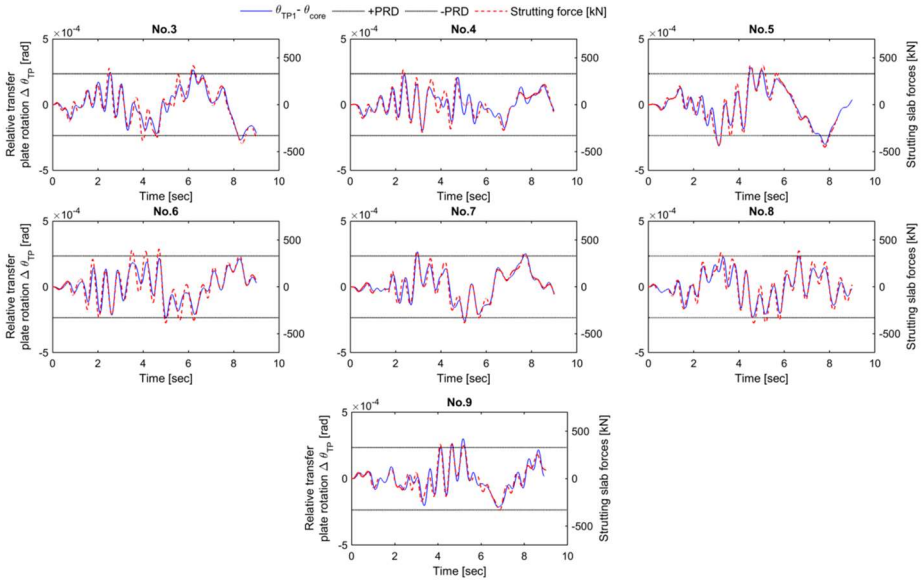
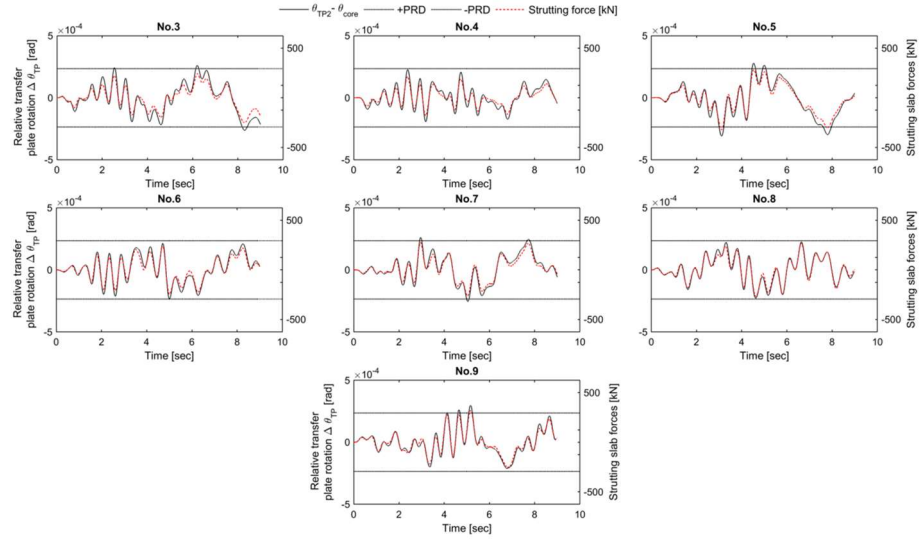


Figure 18. Comparison of roof displacement time-histories as obtained from the 2DOF model (of Figure 10) and from the FE Model in ETABS

The flexibility index (*FI*) for the wall/plate assembly took the value of 0.4 as per recommendations of Figure 8 (see also Table A-2, which lists all design parameters). This value of *FI* which defines the linear correlation slope between $\Delta\theta_{TP}$ and ε_{STRUT} is consistent with FE analysis results produced by ETABS for a 3D model of the building (noting that Figure 20 also shows slope of 0.4 in the linear correlation of data retrieved from the FE analysis). Good consistencies between the value of $\Delta\theta_{TP}$ at the base of wall nos. 1 and 2 as derived from FE analyses by program ETABs and the value of PRD (as defined by equations 9a & 9b) have also been demonstrated in Figure A-2 in the form of bar charts (in Appendix A). Verification of the *FI* and PRD parameters are essential as the value of F_{STRUT} is controlled by the two parameters in equation 10.



(a) Wall 1



(b) Wall 2

Figure 19. Slab strutting (in-plane) force and relative base rotation trends for the walls

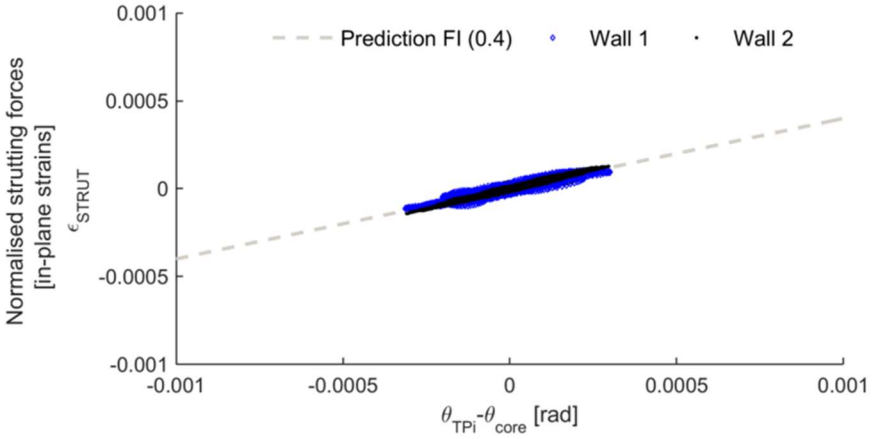


Figure 20. $\Delta\theta_{TP}$ versus ε_{STRUT} (for records nos. 3- 9)

The force transfer by the floor slabs connected to the tower walls (which has been shown to be the primary contributor to the sharp shear force increases in the tower walls) is examined next. Figure 21 presents that sharp increase in shear force on tower walls 1 and 2 at the storey just above TFL (the design details of the tower walls 1 and 2 are summarised in Table 1).

It is shown that the sharp increase in shear force on the tower walls above TFL was not detected by ETABs when "rigid-diaphragm" assumptions were specified. When "semi-rigid diaphragm" constraints were applied the additional shear force was found to be of the order of 500 kN (as shown in Figure 21 which reports the median results from analyses based on records 3 - 9). This ETABS prediction is in good agreement with the prediction of 557 kN made by the simplified method introduced in this chapter (as listed in Table A-2).

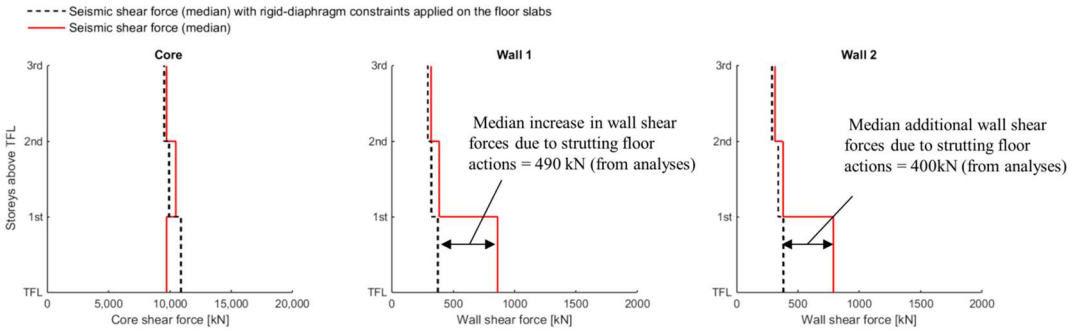
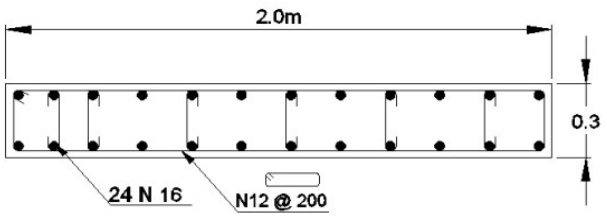


Figure 21. Shear force distribution above TFL from ETABs (record nos. 3 - 9)

Table 1. Design details of Wall nos. 1 & 2

Design parameter	Value	Section detail
l_w, mm	2000	
t_w, mm	300	
$f_c^{'}, MPa$	40.0	
$\rho_v, \%$	0.8	
$\rho_t, \%$	0.38	
Shear capacity $\emptyset V_n$ (AS 3600, 2009), kN		862

8. Conclusions

This chapter is primarily aimed at addressing the adverse effects of the flexing of the transfer structure on the shear force demand on the tower walls above the TFL The shear force increases are the result of the significant strutting forces (F_{STRUT}) developed in the slabs (and beams) connecting adjacent tower walls.

The strutting force (and the in-plane strain: ε_{STRUT}) has been shown to be linearly correlated with the differential rotation of the adjacent tower walls about their bases ($\Delta\theta_{TP}$). The slope of the correlation line, the Flexibility Index (FI), is a function of the stiffness of the transfer structure relative to the tower walls stiffness. The differential wall rotation, in turn, correlates with the angle of drift of the building at mid-height. A 2DOF model of the building tower provided predictions of Peak Rotational Demand (PRD) which can be taken as a conservative estimate of $\Delta\theta_{TP}$. The value of F_{STRUT} may then be expressed as the product of FI, PRD, E_cA_{eff} which is the axial stiffness of the connecting elements, as shown by equation 10.

Equation 10 is central to the simplified calculation procedure introduced in this chapter, for predicting F_{STRUT} which is responsible for the increase in shear force above the TFL. The design flow-chart of Figure 22 summarises the procedure. Its application is illustrated with a worked example, which provides further evidence of the simplified procedure's accuracy by comparison with ETABS FE analyses results. Numerical details of the case study are given in the appendices.

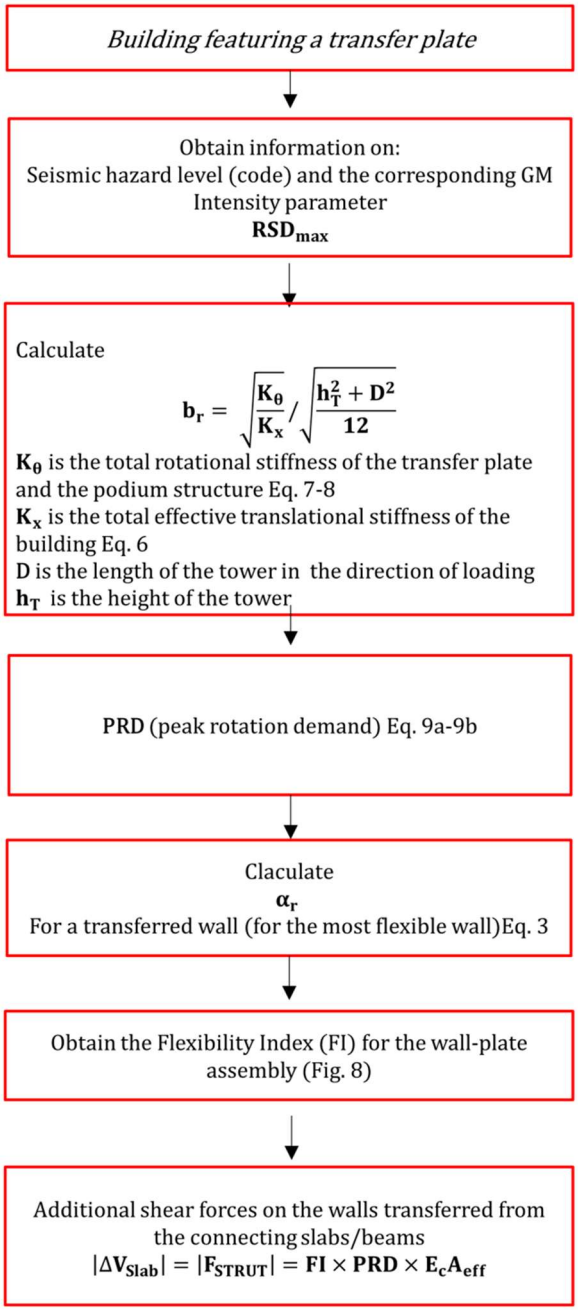


Figure 22. Design flow chart for calculation of the additional shear force demands on the tower walls above TFL

References

AS 1170.0:2002, Structural design actions - Part 0: General principals Sydney, NSW 2001, Australia: SAI Global Limited under licence from Standards Australia Limited

AS 1170.4. 2007. Structural design actions - Part 4: Earthquake actions in Australia. Sydney, NSW 2001, Australia.

AS 3600. (2009) Concrete Structures. Sydney, NSW 2001, Australia: SAI Global Limited.

ASCE 7-10. (2010) Minimum Design Loads for Buildings and Other Structures. American Society of Civil Engineers.

Chopra, A. K. (1995) Dynamics of structures, Prentice Hall New Jersey.

European Committee for Standardization (CEN) (2005) Eurocode 8: Design of Structures for Earthquake Resistance- Part 1: General rules, Seismic action and rules for buildings, CEN, Brussels, Belgium.

Habibullah, A. (1997) ETABS-Three Dimensional Analysis of Building Systems, Users Manual. Computers and Structures Inc., Berkeley, California.

TBI. (2010) Guidelines for performance-based seismic design of tall buildings. Pacific Earthquake Engineering Research Center.

Kuang, J. and Zhang, Z. (2003) "Analysis and behaviour of transfer plate–shear wall systems in tall buildings", The Structural Design of Tall and Special Buildings, 12, 409-421.

Lam, N., Lumantarna, E. and Wilson, J. (2016) Simplified elastic design checks for torsionally balanced and unbalanced low-medium rise buildings in low seismicity regions. Earthquake and Structures, 741-777.

Lee, H. S. and Hwang, K. R. (2015) Torsion design implications from shake-table responses of an RC low-rise building model having irregularities at the ground story. Earthquake Engineering & Structural Dynamics, 44, 907-927.

Li, C., Lam, S., Zhang, M. and Wong, Y. (2006) Shaking table test of a 1: 20 scale high-rise building with a transfer plate system. Journal of structural engineering, 132, 1732-1744.

Lumantarna, E., Lam, N. and Wilson, J. (2013) Displacement-controlled behavior of asymmetrical single-story building models. Journal of Earthquake Engineering, 17, 902-917.

Lumantarna, E., Lam, N., Wilson, J. and Griffith, M. (2010) Inelastic displacement demand of strength-degraded structures. Journal of Earthquake Engineering, 14, 487-511.

Mwafy, A. and Khalifa, S. (2017) Effect of vertical structural irregularity on seismic design of tall buildings. The Structural Design of Tall and Special Buildings.

PEER. (2015) PEER strong motion data base [Online]. Pacific Earthquake Engineering Research Center. Available: http://peer.berkeley.edu/smcat/index.htm [Accessed].

PEER/ATC (2010) Modeling and acceptance criteria for seismic design and analysis of tall buildings. Redwood City, CA: Applied Technology Council in cooperation with the Pacific Earthquake Engineering Research Center.

Priestley, J. N., Calvi, G. M. and Kowalsky, M. J. (2007) Displacement-based Seismic Design of Structures, IUSS Press.

Priestley, M. (1997) Displacement-based seismic assessment of reinforced concrete buildings. Journal of earthquake engineering, 1, 157-192.

Qian, C. G. and Wang, W. (2006) Effect of the thickness of transfer slab on seismic behavior of tall building structure. Optimization of Capital Construction, 27, 98-100.

Seismosoft. SeismoArtif (2014) Version 5.1.2 Build:1, June 2014. Retrieved from www.seismosoft.com.

Su, R. K. L, Tsang, H. and Lam, N. (2011) Seismic design of buildings for Hong Kong conditions. Hong Kong Institution of Engineers.

Su, R. K. L (2008) Seismic behaviour of buildings with transfer structures in low-to-moderate

seismicity regions. Department of Civil Engineering, The University of Hong Kong, Hong Kong, China.

Su, R. K. L and Cheng, M. (2009) Earthquake-induced shear concentration in shear walls above transfer structures. The Structural Design of Tall and Special Buildings, 18, 657-671.

Su, R. K. L., Chandler, A. M., Li, J. H. and Lam, N. (2002) Seismic assessment of transfer plate high rise buildings. Structural Engineering and Mechanics, 14, 287.

TBI. (2017) Guidelines for Performance-based seismic design of tall buildings. Report 2017/06, Pacific Earthquake Engineering Research Center, University of California, Berkeley, CA.

Tang, T. O. and Su, R.K.L. (2014) Gravity-induced shear force in reinforced concrete walls above transfer structures.

Tsang, H. H., Su, R. K.L, Lam, N. and Lo, S. (2009) Rapid assessment of seismic demand in existing building structures. The structural design of tall and special buildings, 18, 427-439.

Yacoubian, M., Lam, N., Lumantarna, E. and Wilson, J. L. (2017a) Effects of podium interference on shear force distributions in tower walls supporting tall buildings. Engineering Structures, 148, 639-659.

Yacoubian, M., Lam, N., Lumantarna, E. and Wilson, J. L. (2017b) Simplified design checks for buildings featuring transfer structures in regions of lower seismicity The 2017 World Congress on Advances in Structural Engineering and Mechanics (ASEM17). Ilsan (Seoul), Korea.

Zhitao, Z. J. W. G. L. (2000) Dynamic Properties and Response of the Thick Slab of Transfer Plate Models with Dual Rectangular Shape in Tall Building [J]. Building Structure, 6, 010.

Appendix A

Table A-1. Description of the accelerograms used in the study

Record Reference	Earthquake name	M_w	distance [km]	PGA [g′s]	PGV [mm/s]	Source
No. 1	Friuli (1976)	6.5	23	0.36	-	PEER(PEER, 2015)
No. 2	Northridge (1994)	6.69	27	0.25	211	PEER(PEER, 2015)
No.3-No.9	D-x	-	-	-	-	Code-Compliant Suite of records based on the response spectrum of the Australian Standard 1170.4 for site class D (2% in 50 years)- SeismoArtif (SeismoSoft)
No.10-No.16	C-x	-	-	-	-	Code-Compliant Suite of records based on the response spectrum of the Australian Standard 1170.4 for site class C (2% in 50 years)- SeismoArtif (SeismoSoft)
No.17-No.23	A-x	-	-	-	-	Code-Compliant Suite of records based on the response spectrum of the Australian Standard 1170.4 for site class A (2% in 50 years)- SeismoArtif (SeismoSoft)

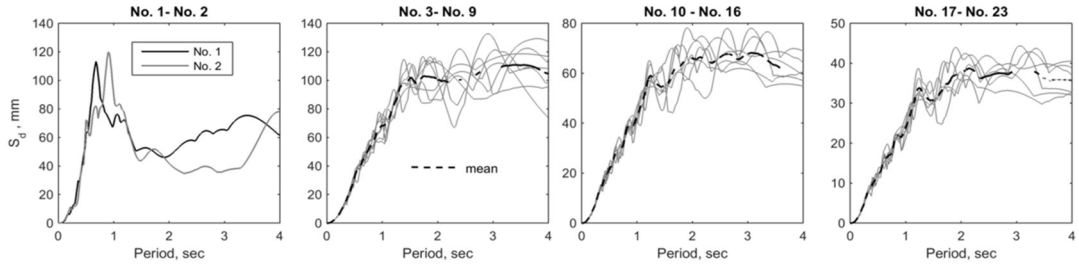


Figure A-1. Spectral displacements for the records used in the study

Table A-2. Detailed calculation summary for the case study building

Parameter	Calculation		Value
$\mathbf{K_T}$, kN/m	The procedure is summarised in the Appendix B (Table B-2)		17841
$\mathbf{K_P}$, kN/m	The procedure is summarised in the Appendix B (Table B-1)		3369410
$\mathbf{K_x}$, kN/m	$\left(\frac{1}{17841}+\frac{1}{3369410}\right)^{-1}$		17747
$\mathbf{r}$, m	$\sqrt{\frac{102^2+28^2}{12}}$		30.53
$\mathbf{K_{\theta_{TP}}}$ kNm/rad (Eq. 8)	$31.62 \times 10^6 \times 2.7^2 \times 22.35 \times \left(\frac{28}{102}\right)^{1.5}$		7.41×10^8
$\mathbf{K_\theta}$, kNm/rad (Eq. 7)	For infinitely stiff podium columns and fixed at the base $\mathbf{K_\theta} = \mathbf{K_{\theta_{TP}}}$		7.41×10^8
$\mathbf{b_r}$ $\sqrt{K_\theta/K_x}/r$	$\left[\sqrt{\frac{7.41 \times 10^8}{17747}}\right] / 30.53$		6.69
PRD (Eq. 9a-9b)	Records No: 3-9 $RSD_{max} = 107mm$	$\left(\frac{107}{99346}\right)[-0.2\ln(6.69)+0.6]$ *	0.00024
	Records No: 10-16 $RSD_{max} = 67mm$	$\left(\frac{67}{99346}\right)[-0.2\ln(6.69)+0.6]$ *	0.00015
	Records No: 17-23 $RSD_{max} = 38$ mm	$\left(\frac{38}{99346}\right)[-0.2\ln(6.69)+0.6]$ *	8.41×10^{-5}
$\boldsymbol{\alpha_r}$ (Eq. 3)	$\sqrt{\frac{\left(\frac{1}{12}\times 2.7^3 \times 5.02\right)}{\left(\frac{1}{12}\times 2.0^3 \times 0.3\right)}}$		6.42
FI	From Fig. 8		0.40
$\mathbf{F_{STRUT}}, kN$ (Eq. 10)	Records No: 3-9 $RSD_{max} = 107mm$	$0.4 \times 0.00024 \times 5.88 \times 10^6$ †	557
	Records No: 10-16 $RSD_{max} = 67mm$	$0.4 \times 0.00015 \times 5.88 \times 10^6$ †	349
	Records No: 17-23 $RSD_{max} = 38$ mm	$0.4 \times 8.41 \times 10^{-5} \times 5.88 \times 10^6$ †	198

* The value of h_x used in the calculation of PRD has been obtained directly from the FE analysis using ETABS program package. In the absence of a detailed numerical model, the recommended value of $h_x = 0.7\ h_b$ (Section 5) may be used for preliminary (conservative) estimate of the value of PRD (Eq. 9a-9b).

† The value of $E_C A_{eff}$ is calculated based on the in-plane sectional properties of the connecting slab with concrete grade (characteristic compressive strength) of $f_c' = 24MPa$: $\left(5000 \times \sqrt{24} \times (2.4 \times 0.2) \times 0.5 \times 10^3\right)$. The term (2.4 x 0.2) is the product of the width of the column strip as obtained from the FE analysis (using the program package ETABS) and the gross thickness of the slab. The factor (0.5) is recommended by TBI (2017) guidelines for computing the in-plane stiffness of reinforced concrete slabs subjected to transfer forces (Table 4-3 of TBI 2017).

Table A-3. Floor load assignment

Tower	
Additional dead loads $\boldsymbol{kN/m^2}$	1
Live loads $\boldsymbol{kN/m^2}$	2
Podium	
Additional dead loads $\boldsymbol{kN/m^2}$	1.2
Live loads $\boldsymbol{kN/m^2}$	5

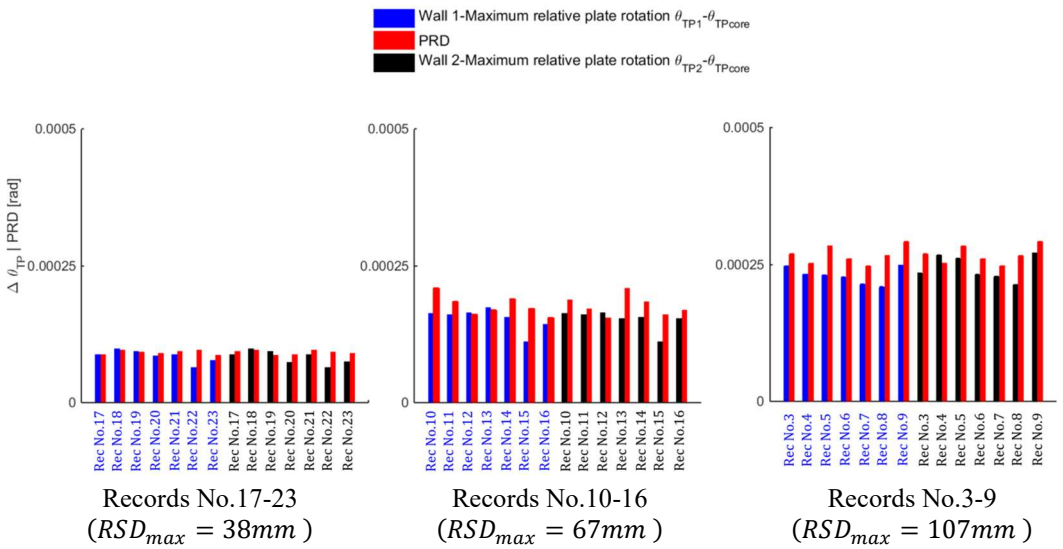


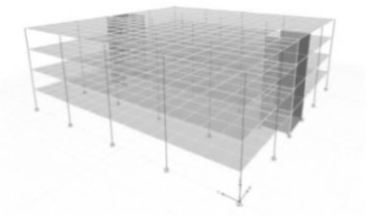
Figure A-2. Comparison between the maximum relative transfer plate rotations (for Walls 1 and 2) with the PRD computed for individual record

Appendix B

A summary of the procedure for calculating the translation stiffness of the tower (K_T) and the podium (K_P) structures is described. The translational stiffness parameters K_T and K_P for the case study building are computed by evaluating the effective displacement and base shear of the building when subject to lateral loads. The storey masses (m_i) and the applied lateral loads (F_i) have been computed and distributed following recommendations by the Australian Standard (AS 1170.4).

Table B-1. Effective translational stiffness of the podium $\mathbf{K_P}$

Level	m_i[kg]	z_i[m]	δ_i[mm]	F_i[kN]	$m_i\delta_i$	$m_i\delta_i^2$
4	7083894	16.8	8.696	19218.90	97839256	867149330.3
3	2019757	12.6	7.03	4109.76	14035291	97531237.0
2	2019757	8.4	4.054	2739.84	8371893	34701494.5
1	2019757	4.2	1.487	1369.92	3037714	4568722.5
GF		0	0	0	0	0
			$\sum$	27438.42	1.23E+08	1003950784



$\delta_{eff} = \sum m_i\delta_i^2 / \sum m_i\delta_i$ [mm]	8.14
Base shear V_b[kN]	27438
K_P[kN/m] $= BS/\delta_{eff}$	3369410

Table B-2 Effective translational stiffness of the Tower $\mathbf{K_T}$ (Fixed at TFL)

Level	m_i[kg]	z_i[m]	δ_i[mm]	F_i[kN]	$m_i\delta_i$	$m_i\delta_i^2$
34	371514	102	242.92	200.23	90248341	21923139862
33	439004	99	236.65	224.30	1.04E+08	24586030012
32	439003	96	230.49	212.52	1.01E+08	23321953215
31	439003	93	224.14	201.02	98396251	22054095449
30	439003	90	217.56	189.79	95510829	20779609165
29	439003	87	210.75	178.84	92520570	19498838487
28	439003	84	203.69	168.17	89422047	18214672236
27	439003	81	196.39	157.78	86215261	16931695198
26	439003	78	188.85	147.68	82903638	15655946317
25	439003	75	181.07	137.87	79491289	14393659465
24	439003	72	173.09	128.35	75986436	13152378561
23	439003	69	164.91	119.12	72397303	11939246548
22	439003	66	156.57	110.19	68733482	10761401400
21	439003	63	148.07	101.56	65005250	9625626715
20	439003	60	139.46	93.24	61222887	8538071010
19	439003	57	130.75	85.22	57398727	7504757495
18	439003	54	121.97	77.51	53544417	6530711977
17	439004	51	113.15	70.12	49671695	5620168457
16	439003	48	104.31	63.05	45792629	4776648592
15	439003	45	95.49	56.31	41921187	4003126420
14	439003	42	86.73	49.89	38073044	3301926224
13	439003	39	78.05	43.81	34263958	2674282137
12	439003	36	69.50	38.08	30509004	2120255588
11	439003	33	61.11	32.69	26828738	1639580080
10	439003	30	52.94	27.66	23241660	1230456996
9	439003	27	45.04	23.00	19771068	890414892
8	439003	24	37.45	18.71	16441629	615774739
7	439003	21	30.26	14.80	13284179	401977348
6	439003	18	23.54	11.30	10332291	243178650
5	439003	15	17.37	8.21	7627080	132510022

Table B-2. Effective translational stiffness of the Tower $\mathbf{K_T}$ (Fixed at TFL) (cont.)

Level	m_i[kg]	z_i[m]	δ_i[mm]	F_i[kN]	$m_i\delta_i$	$m_i\delta_i^2$
4	439003	12	11.89	5.55	5217879	62018345
3	439003	9	7.21	3.35	3164988	22817932
2	439003	6	3.51	1.65	1541039	5409527
1	439003	3	1.00	0.49	439905	440809
GF	67488.9	0	0.00	0.00	0	0
				$\sum$ 3002	1.74E+09	2.93E+11
				$\delta_{eff} = \sum m_i\delta_i^2 / \sum m_i\delta_i$ [mm]	168.27	
				Base shear V_b[kN]	3002.04	
				K_P[kN/m] $= BS/\delta_{eff}$	17841	



Recommended Earthquake Loading Model for Performance-Based Design of Building Structures in Hong Kong

Hing-Ho Tsang[a] and Nelson T. K. Lam[b]

[a] Department of Civil and Construction Engineering
Swinburne University of Technology, Australia

[b] Department of Infrastructure Engineering
The University of Melbourne, Australia

This chapter provides recommendations for determining a loading model applicable to the seismic design of building structures in Hong Kong. Fundamental issues concerning the required level of structural safety are first addressed to explain the rationale behind the seismic performance requirements of a building. The choice of design return period for the corresponding performance criteria is discussed. The development of the seismic hazard model for Hong Kong is then reviewed. The determination of the design response spectrum and the choice of design parameters for structures of different classes of importance are also presented. A site-specific seismic action model which takes subsoil conditions into account is a topic of great significance in the Hong Kong context given the amount of reclaimed land founded on unconsolidated marine deposits.

Keywords: seismic hazard, response spectrum, performance criteria, return period, site classification

1. Introduction

Seismic design provisions for bridges in Hong Kong have been in use for a long time, but Hong Kong has no official regulatory document which defines the minimum design requirements for building structures in relation to seismic hazard. Although Hong Kong is located some 600 km away from the nearest tectonic plate boundary, the level of seismicity is actually higher than for many parts of Australia where seismic design provisions have been mandated for over two decades. The first seismic design code for building structures in Hong Kong, however, is now under development.

Research into the seismic hazard of Hong Kong commenced in the early 1990's. Probabilistic seismic hazard analysis (PSHA) led by ARUP and The University of Hong Kong, respectively, in recent years culminated in the development of Uniform Hazard Spectrum models that can be simplified and codified for the structural design of buildings and other types of structure.

Capitalising on this achievement, is the key motivation behind the writing of this chapter, aimed at providing recommendations on the key decisions that need to be made when drafting the first edition of the seismic design standard for Hong Kong. This chapter contains recommendations for some improvements on the conventional codification practices applied in regions of low to moderate seismicity. Justifications for these recommendations derive from on-going research over two decades.

General performance objectives and decisions over the choice of the design return

period for seismic actions is discussed first. This is followed by a review of the literature relating to the development of the seismic hazard model for a region. The design peak ground acceleration (PGA) values and the corresponding design response spectrum models for the respective return period levels are then provided.

Eurocode 8 (CEN 2004) must be a key reference, guiding the drafting of the future earthquake loading standard for Hong Kong. The adoption of Eurocode 8 is justified by the fact that other parts of Eurocode have already been adopted in Hong Kong, for the design of concrete, steel and composite structures for certain types of construction. In addition, Eurocode 8 has already been implemented in Singapore (BC3, 2003; NA to SS EN199801, 2013) and will soon be implemented in Malaysia.

2. Performance criteria and design return periods

2.1 Performance criteria

According to Eurocode 8 – Part 1 (CEN 2004), building structures shall be designed and constructed in such a way that the requirements of (i) No Collapse (NC) and (ii) Damage Limitations (DL) must be met. The state of "No Collapse" (NC) is essentially in alignment with design according to the Ultimate Limit State (ULS) which entails the protection of life in a rare earthquake event by ensuring that no part of the structure collapses and that adequate residual lateral resistant capacity remains in the structure, after the event, to withstand strong aftershocks should they occur. The safety of occupants of the building can be assured but the built facility might be uninhabitable and the damage too costly to repair. The "No Collapse", or "No Local Collapse", design criterion as described is comparable to the "Life Safety" performance criterion as defined in SEAOC Vision 2000 document (SEAOC 1995) in the United States and the "Significant Damage" (SD) performance criterion stipulated in Eurocode 8 – Part 3 which contains provisions for the seismic assessment and retrofitting of existing buildings. The "No Collapse" performance criterion is not to be confused with the "Near Collapse" performance criterion of SEAOC Vision 2000, nor with the "Collapse Prevention" (CP) level as defined in FEMA Publication 273 (ATC 1997), which is to ensure that the building is able to retain sufficient vertical load carrying capacity during a very rare earthquake event when the structure is on the verge of wholesale collapse with little, or no, residual lateral resistance, and falling hazards may be present (Fardis 2009).

The "Damage Limitation" (DL) performance criterion which corresponds to the Serviceability Limit State (SLS) criterion (in the conventional limit state design approach) has also been written into both Part 1 and Part 3 of Eurocode 8 and is intended to address the damage potential of frequent, or occasional, earthquake events in the design of ordinary buildings. The DL performance criterion is comparable to the "Immediate Occupancy", or "Operational", performance criterion as defined in SEAOC Vision 2000 which is to ensure no permanent drift and no loss of lateral strength, and stiffness, of the building structure. The built facility is then fit for continuous occupation in the recovery period. The functionality of the building must also not be interrupted significantly by repair activities. In regions of low to moderate seismicity that are remote from tectonic plate boundaries. Only rare, or very rare, earthquake events are of concern. Thus, the DL performance criterion need not be checked in such an environment except for those more important built facilities forming part of lifeline facilities in the aftermath of an earthquake disaster, or buildings containing hazardous materials. See Table 1 for a summary of the performance criteria for building structures as defined by the two parts

of Eurocode 8 and the SEAOC Vision 2000 document.

In the past decade, attempts have been made to incorporate the extent of risk and loss as quantifiable measures for defining performance objectives for adoption in seismic structural design. The first risk-based seismic provision was stipulated in the 2010 edition of the structural design standard ASCE/SEI 7-10 and the 2012 edition of the International Building Code (IBC, 2012) which is adopted principally in the United States. It is required that the collapse risk of ordinary building be limited to 1% in 50 years (i.e. an annual probability of exceedance of $2 \times 10\text{-}4$). However, Porter (2014) pointed out that the rationale behind such a risk limit is not well justified, except that it would not result in too significant changes to the design seismic hazard levels already in use across the whole of the United States.

There has been similar development in Europe and other parts of the world (Douglas et al. 2013; Tsang et al. 2018a; 2018b). A decision model containing important parameters for risk-based seismic design of buildings, which could be used to guide the future revision of Eurocode 8, was proposed by Dolšek et al. (2017), in which, a slightly more stringent collapse risk limit of 10-4 is adopted as it would then be consistent with the recommendation by Tsang and Wenzel (2016). Stipulating this risk limit would be sufficient to limit the individual annual fatality risk of 10-6, which is a tolerable level recommended by various organizations and well supported by historical mortality data associated with natural hazard events.

2.2 Design return periods

In this section, recommendations over the choice of design return period for seismic actions and design PGA values for buildings of different classes of importance and the 'behaviour factor' are discussed. The return period of design seismic actions that are aligned with the No Collapse (NC) performance criterion is to be decided on a country-by-country basis, given that factors governing the decision involve social, economic and political considerations. Thus, the design return period for the NC performance criterion is to be specified in the respective National Annex of each country. The recommendations provided below are considered reasonable for the well-developed parts of the world.

It is stated in the footnote attached to Clause 2.1 in Eurocode 8 – Part 1 that ground motion intensity in a rare earthquake event consistent with a 10% chance of exceedance for a design life of 50 years (i.e. Return Period of 475 years) is recommended as the design seismic action. It is noted that this recommendation was drafted in the late 1990's at a time when it was still the norm not to consider return periods exceeding 500 years in the design of structures supporting ordinary buildings. Implicit in the NC performance criterion is that the building is expected to have sufficient additional reserve capacity to sustain a very rare, and extreme, earthquake event without experiencing wholesale collapse (Fardis 2009).

Seismic design provisions around the world have been evolving over many decades, during which time experience gained through field observations from places such as California have been taken into account in numerous code revisions. In such an environment which is dominated by active faults the intensity of ground shaking is increased by a factor which is slightly greater than 1.5 as the return period is increased from 500 to 2500 years (Tsang 2014). Code compliant construction designed to fulfil NC performance criteria is expected to have sufficient additional reserve capacity to also fulfil collapse prevention critera when subject to seismic actions that are already 1.5 times the design level. Despite this margin of safety from collapse, implicit in contemporary

practice, the major earthquake disasters occurring in recent years, including the 1995 Kobe earthquake in Japan, the 2008 Wenchuan earthquake in China and the 2011 Christchurch earthquake in New Zealand prompted a critical review of the adequacy of this long established convention of designing for a return period of 500 years (Tsang 2011).

In regions of low to moderate seismicity (where earthquakes occur infrequently and active faults are difficult to identify), the ground shaking intensity ratio associated with an increase of return period from 500 to 2500 years can escalate to values much greater than 1.5. A factor varying between 2.4 and 5 is predicted for earthquakes in an intra-plate environment (Lam et al. 2016; Tsang 2014; Geoscience Australia 2012). Given these predictions, building structures that have been designed for a return period of 500 years, to fulfil NC performance criteria in an intra-plate environment, would not automatically possess adequate additional reserve capacity to prevent collapse in a very rare event.

The trend of moving away from the conventional practice of designing for a return period of 500 years was initiated by the influential FEMA450 document (BSSC 2003), aimed at guiding the design of new buildings in the United States. The design seismic action was recommended based on a maximum considered earthquake (MCE) of 2500 years scaled down by a factor of 2/3 (reciprocal of 1.5). This scaling factor can be interpreted as the margin between the states of NC and CP of the structure, in order that code compliant buildings can always be assured of their capacity to avoid collapse in a very rare earthquake event. However, it was shown in a recent study that this level of design action might still result in intolerable levels of annualized individual fatality risk (Tsang et al. 2017c) based on the collapse probability estimated by Haselton and Deierlein (2007), Liel and Deierlein (2008), Tsang et al. (2016) and Hashemi et al. (2017).

Table 1. Performance Criteria of Building Structures

Eurocode 8 Part 1	Eurocode 8 Part 3	SEAOC Vision 2000	Descriptions
		Fully Operational	Components that are sensitive to drift and/or acceleration remains fully functional in a frequent event.
Damage Limitation (DL)	Damage Limitation (DL)	Operational or Immediate Occupancy	No permanent drift and no loss of lateral strength or stiffness of the building. The built facility remains to be fit for continuous occupation in an occasional event.
No Collapse (NC)	Significant Damage	Life Safety	No part of a structure collapses and adequate residual lateral resistant capacity remains in the structure after a rare event to withstand strong aftershocks in order that safety of the occupants can be secured but building may be inhabitable and repair too costly.
	Near Collapse	Collapse Prevention or Near Collapse	Structure is able to sustain sufficient vertical load carrying capacity in a very rare earthquake event when the structure is at the edge of wholesale collapse. Residual lateral resistant capacity of the building might be lost.

The 2005 edition of the *National Building Code of Canada* (NRCC 2005) has increased the design return period from 500 to 2500 years without applying a scaled down factor of 2/3 (Mitchell et al. 2010) but a generous 2.5% drift limit, which is consistent with the CP performance criterion, has been specified. In perspective, a design return period of 2500 years is actually not overly conservative given that the individual annual fatality risk

of an occupant in a building which has been designed for a return period of 2500 years can possibly be reduced to a tolerable level of the order of one in a million (i.e.10^{-6}). Nevertheless, it is considered pragmatic to adopt the "two-thirds" scaled down approach as in IBC, and particularly so for the first time that seismic design provisions are being enforced in Hong Kong.

According to the current Code of Practice on Wind Effects in Hong Kong (BD, 2004), structures are designed for a 50-year return period wind load, together with a load factor of 1.4. At first glance, the huge difference between the "design return period" for earthquake and wind actions, should be queried. A much more stringent performance requirement seems to be proposed for countering earthquake hazard. In fact, the reality is the opposite because the level of life risk in an extreme typhoon scenario is actually substantially higher. Detailed discussion can be found in Tsang (2014; 2018).

3. Seismic action models and design parameters

3.1 Design response spectrum model for rock sites

Research into the seismic hazard affecting Hong Kong, dates back to the early 1990's (e.g. Pun and Ambraseys 1992; Lee et al. 1998). In those early investigations, the ground motion prediction equations (also known as attenuation models) employed in seismic hazard modelling were mainly based on relationships developed from the empirical database of records collected in the high seismicity region of North America (e.g. California) and Europe (e.g. Greece). Little evidence was available to support the argument that those relationships could be taken as representative of conditions in the South China region. Ground motion properties were represented simply by the PGA values. Response spectral parameters were not calculated in those early studies, partly because suitable equations predicting spectral parameters were not available.

More recent investigations including that by Free et al. (2004) took into account the distinct ground motion features and response spectral attenuation properties in the more stable regions of low to moderate seismicity such as Central and Eastern North America (CENA) and many parts of China including South China. A technique known as stochastic simulation of the seismological model, originally developed in CENA for modelling earthquake ground motions, enables reliable predictions to be made based on regional information related to wave generation at the earthquake source and the wave transmission properties of the earth's crust (refer to Lam et al. 2000 for a review of the methodology for engineering applications). Central to the modelling methodology is the generation of artificial accelerograms for rock sites by computer program (e.g. GENQKE of Lam 1999) to circumvent the lack of locally recorded strong motion data. This technique was adapted for modelling ground motions in South China, including areas surrounding Hong Kong in particular (Lam et al. 2002; Chandler and Lam 2002; Tsang 2006; Chandler et al. 2005; 2006a; 2006b). Similar modelling techniques were adapted to develop attenuation relationships in other parts of China (Tsang et al. 2010) and many other parts of the world including Australia, Iran, Singapore, Malaysia and India (e.g. Lam et al. 2003, 2006 and 2009; Yaghmaei-Sabegh and Lam 2010; Chandler and Lam 2004). Importantly, intensity attenuation relationships developed from site reconnaissance data collected from historical earthquake events in these regions have been reconciled with predictions by the respective seismological models.

The anelastic attenuation model of Mak et al. (2004) was specifically developed to

model conditions in the wider Hong Kong region based on analyses of data from seismological monitoring conducted locally. Artificial accelerograms generated in accordance with this locally developed seismological model using the program GENQKE enabled ground motion prediction equations to be developed, as though there were an abundance of locally recorded accelerograms (Pappin et al. 2008). This ground motion prediction equation has been reported in the literature (Pappin et al. 2015a) as the "ARUP – HKU attenuation relationship (2006)" acknowledging joint efforts between ARUP and The University of Hong Kong in collaboration with The University of Melbourne where GENQKE was written.

Since the 1990's, the concept of a Uniform Hazard Spectrum (UHS) has become common practice for constructing a design response spectrum. A UHS incorporates hazards from all potential seismic sources surrounding the site. Normally, short-period spectral values of a UHS are attributed to near-source moderate earthquakes, whereas long-period spectral values are attributed to distant (large magnitude) earthquake hazard (Tsang 2015). UHS provides response spectral ordinates for a range of oscillator periods based on PSHA. The advantage of adopting a UHS is that it has a uniform (or constant) probability of exceedance at all structural periods, and hence reflects the site-specific frequency content more accurately.

The development of UHS models for Hong Kong has been dominated by the work of two research groups. The first is The University of Hong Kong. Its Uniform Hazard Spectrum (HKU UHS) model was first published in Tsang (2006), and presented in Tsang et al. (2009) and Tsang and Lam (2010), based on the location of the Hong Kong Observatory at Tsim Sha Tsui. The Direct Amplitude-Based (DAB) methodology of Tsang and Chandler (2006) was employed to model seismic activities in the development of the HKU UHS model. Implementing the DAB approach does not require detailed characterization of the seismic sources, thereby avoiding the uncertainties associated with assumptions made in the modelling of the seismic sources (Tsang et al. 2011).

The second research group, ARUP, was consultant to the Buildings Department (BD) in 2002, and the Geotechnical Engineering Office (GEO) in 2011. The recommended UHS model reported in ARUP (2002) is denoted herein as the ARUP-BD UHS model whereas those recommendations reported in ARUP (2011) relate to the ARUP-GEO UHS model. In the 2011 study, ARUP and GEO collaborated with the Earthquake Administration of Guangdong Province in China to make seismic hazard recommendations for the Northwest New Territories of Hong Kong. Seismic hazard modelling for other parts of Hong Kong was also undertaken during this period. Results are presented in the form of seismic hazard contour maps in ARUP (2011), which were subsequently published in Pappin et al. (2015a,b). The conventional PSHA methodology, pioneered by Cornell (1968), coded into a FORTRAN program by McGuire (1976), and subsequently completed with a deaggregation approach by McGuire (1995), has been adopted in studies undertaken by ARUP.

Good consistency between the independently developed HKU UHS and the ARUP-GEO UHS models in the intermediate, and high, natural period ranges can be seen in Fig. 1. Both studies made use of the ARUP – HKU (2006) attenuation relationship which was underpinned by stochastic simulations of the seismological model (implemented using GENQKE). In the 2011 study by ARUP, the ARUP – HKU (2006) attenuation relationship was assigned a 50% weighting factor whereas much lower weighting factors have been assigned to relationships developed elsewhere in North America and China. Different assumptions associated with seismic source modelling in PSHA by the two

groups resulted in only minor differences between the two sets of recommendations.

As the hazard levels predicted by the ARUP-GEO UHS model vary by 20 – 30% across Hong Kong (given the different distances from the potential earthquake sources), a Design Response Spectrum (HKU DRS) model was derived to take into account spatial seismic hazard variations within Hong Kong (Su et al. 2011; 2015). The HKU DRS model is essentially an envelope, incorporating the findings of both the HKU and the ARUP-GEO UHS models. The HKU DRS model as shown by the dark bold line in Fig. 1 is recommended for codification for Hong Kong. Given a maximum response spectral acceleration (i.e. the highest ordinate of the spectrum in Fig. 1) of 5.5 m/s2, or 0.56g, at a return period of 2500 years, the corresponding PGA value is 0.225g.

The recommended DRS model for reference (rock) sites in Hong Kong as expressed in Eq. (1) is presented in the form of a response spectral displacement (*RSD*) versus the natural period of the structure (*T*), and is based on a return period of 2500 years. This HKU DRS model mimics the shape of the actual UHS very well.

$$\begin{aligned} T \le 0.23 \quad &: \quad RSD_T(mm) = 0.56 \times \left(\frac{T}{2\pi}\right)^2 \times 9810 \\ 0.23 \le T \le 1.0 \quad &: \quad RSD_T(mm) = 32 \times T \\ 1.0 \le T \le 5.0 \quad &: \quad RSA_T(mm) = 32 + 14 \times (T - 1) \end{aligned} \tag{1}$$

The compatible acceleration *DRS* model can be obtained conveniently by direct transformation of the displacement *DRS* model using Eq. (2).

$$RSD_T(mm) = RSA_T(g) \times \left(\frac{T}{2\pi}\right)^2 \times 9810 \tag{2}$$

Alternatively, a form consistent with the default model in Eurocode 8 is preferred in some cases. Eq. (3) defines the response spectrum in the acceleration form.

$$\begin{aligned} T \le 0.1 \quad &: \quad RSA_T(g) = \frac{0.56}{2.5} \times (1 + 15 \times T) \\ 0.1 \le T \le 0.25 \quad &: \quad RSA_T(g) = 0.56 \\ 0.25 \le T \le 2.0 \quad &: \quad RSA_T(g) = 0.56 \left(\frac{0.25}{T}\right) \\ 2.0 \le T \le 5.0 \quad &: \quad RSA_T(g) = 0.56 \left(\frac{0.5}{T^2}\right) \end{aligned} \tag{3}$$

It is noted that the alternative *DRS* model as defined by Eq. (3), features a constant spectral displacement region in the long period range (i.e. *T* higher than 2.0s). The spectral demand is slightly overestimated for *T* in the range 1.0s - 3.5s, and underestimated when *T* exceeds 3.5s, in comparison with the actual *UHS* or the original *DRS* model of Eq. (1). The second corner period (i.e. the lower period limit of the constant displacement region) can be increased to avoid understating seismic actions on high period structures.

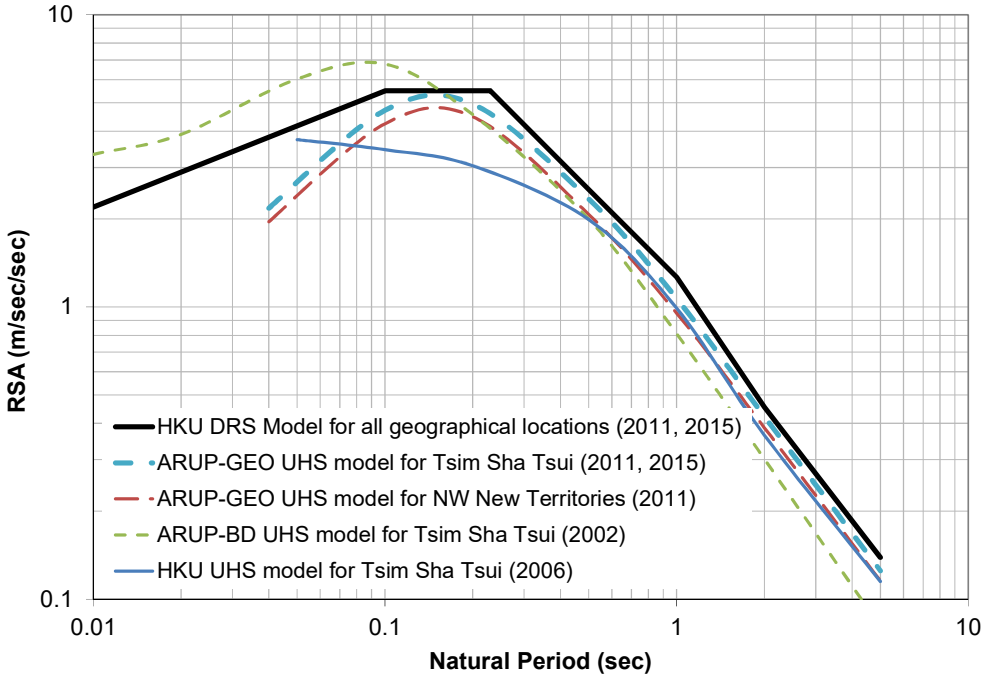


Figure 1. Uniform Hazard Spectrum (UHS) models and the recommended Design Response Spectrum (DRS) model for rock sites in Hong Kong (in the acceleration format) (Tsang 2018)

Literature references for every item on the legend in Fig. 1 are as follows:

HKU DRS model for all geographical locations (2011; 2015)

– Su et al. (2011 & 2015)

ARUP–GEO UHS model for Tsim Sha Tsui (2011; 2015)

– Report by ARUP (2011) and Pappin et al. (2015a; 2015b)

ARUP–GEO UHS model for NW New Territories (2011)

– Report by ARUP (2011)

ARUP–BD UHS model for Tsim Sha Tsui (2002)

– Report by ARUP (2002)

HKU UHS model for Tsim Sha Tsui (2006)

– Tsang (2006), Tsang & Chandler (2006), Tsang et al. (2009) & Tsang and Lam (2010)

3.2 Design response spectrum model for soil sites

The recommended response spectra for soil sites are based on a site factor model which takes into account effects pertaining to resonance behaviour on flexible soil deposits. The model is based on the theoretical model published in Tsang et al. (2006a; 2006b; 2012) and is in accordance with the response spectral shape as proposed in an earlier investigation reported in Lam et al. (2001). The purpose of introducing this new

site response model is to circumvent the need for design engineers to conduct dynamic analysis of the site subsoil model, a very labour intensive exercise in the normal design office setting.

The proposed site classification scheme adopts the site natural period (T_S) as the key parameter. The same approach as in Pitilakis et al. (2012; 2013) which will be used to guide the revision of Eurocode 8 in the coming years. In the proposed model, the value of the scaling parameter S which characterises amplification in the velocity controlled region of the response spectrum is recommended to be 1.5 for stiff soil sites (Tsang et al. 2017a) and 3.6 for flexible soil sites (Tsang et al. 2017b). The initial site natural period (T_S) at low amplitude of oscillation is either measured by geophones or by analysis of information reported in a standard borelog. Sedimentary layers with SPT-N values > 100 can be omitted in the computations of site natural period and weighted average *SWV*. If thickness (d_i) and initial *SWV* (V_i) of the individual soil layers are known, these can be computed with the use of Eq. (4), based on four times the shear-wave travel-time through the material between the surface and the underlying stiff sediments or bedrock.

$$T_S = \sum_{i=1}^{n} \frac{d_i}{V_i} \times 4 = \frac{4H_S}{V_S} \tag{4}$$

Alternatively, the site natural period can be expressed in terms of the total thickness of the soil layers (H_S) and the weighted average initial *SWV* (V_S) based on the use of Eq. (4). The proposed response spectral parameters, for various ground types, which are to be used in conjunction with Eq. (5) are summarised in Table 2.

$$\begin{aligned}
&0 \le T \le T_B && : \; RSA_T(g) = \frac{RSA_{\max}}{2.5} \times S \times \left(1 + 15 \times T\right) \\
&T_B \le T \le T_C && : \; RSA_T(g) = RSA_{\max} \times S \\
&T_C \le T \le T_D && : \; RSA_T(g) = RSA_{\max} \times S \times \left(\frac{T_C}{T}\right) \\
&T_D \le T \le 5.0 && : \; RSA_T(g) = RSA_{\max} \times S \times \left(\frac{T_C T_D}{T}\right)
\end{aligned} \tag{5}$$

A soil column with T_S > 1.2 s is considered extremely flexible. Thus, there could be significant higher mode effects in site response behaviour. For such Special Soil (Class E) sites, the envelope of DRS models for all other site classes (i.e. A to D) shall be taken. Alternatively, site-specific dynamic site response analyses may be undertaken to justify a lower level of seismic demand.

Table 2. Proposed site classification scheme and response spectral parameters

Ground Type	Description	T_S (s)	S	T_B (s)	T_C (s)	T_D (s)
A	Rock	$T_S < 0.15$	1.0	0.1	0.25	2.0
B	Stiff Soil	$0.15 \leq T_S < 0.5$	1.5	0.1	0.25	1.5
C	Flexible Soil	$0.5 \leq T_S < 0.8$	1.8	0.1	0.5	1.2
D	Very Flexible Soil	$0.8 \leq T_S \leq 1.2$	1.2	0.1	0.75	1.8
E	Special Soil	$T_S > 1.2$ *	1.8	0.1	0.5	1.8

* $T_S > 1.2$ s OR deposits consisting of at least 10 m thick of clays/silts with a high plasticity index (PI > 50), V_S less than 150 m/s, SPT-N values less than 6, or undrained shear-strength less than 12.5 kPa.

Generally, two boreholes for a block of low-rise building is sufficient to determine the natural period of the site. The spacing of boreholes for multi-storey buildings should be 15 m to 45 m. More boreholes are required should there be problematic, and erratic, soil formation. The arithmetic mean of the site natural period T_S may be adopted for site classification purposes.

3.3 Parameters for design seismic actions

Performance requirements vary with the type of structure. Structures are typically categorised into four classes in codes of practice, based on the nature of occupancy which defines the intended use of the structure and the anticipated occupant load. Higher reliability should be provided, either because of the consequences of damage or because the structure needs to remain operational during, and after, an earthquake event.

The classification schemes in major codes of practice are broadly consistent. In view of the facts above, design seismic actions, in terms of design PGA values on rock sites are recommended herein for various importance classes of building as summarised in Table 3. It is shown that all built facilities of importance class IV, including hospitals, emergency services and other lifeline facilities are to be designed for a return period of 2500 years to fulfil NC performance criterion so that lifeline facilities can be safely occupied in the aftermath of a very rare event and continue in service after more frequent events. The design seismic actions for ordinary buildings of importance class II are accordingly based on a PGA value of 0.15g (0.225g/1.5) which will provides adequate protection for these buildings from collapse in a very rare earthquake event. By interpolation, a design PGA of 0.18g is stipulated for buildings of intermediate class III such as condominiums, schools and public buildings which contain large numbers of occupants at times. This latter class of building represents the bulk of the building stock in Hong Kong.

The response spectrum to be used for design purposes for any building class is to be derived from the benchmark model (*HKU DRS 2011, 2015)* based on a return period of 2500 years as presented in Fig. 1 and then scaled down in accordance with the respective design PGA value as listed in Table 3. 1.5% is the allowed inter-storey drift limit to fulfil NC, or the life safety, performance criterion.

Table 3. Design PGA on rock sites for Hong Kong

Importance Class	Importance Factor	Descriptions	Design PGA (g's)
I	0.8	Minor constructions	0.12 (0.8 x 0.225/1.5)
II	1.0	Ordinary buildings (individual dwellings or shops in low rise buildings)	0.15 (0.225/1.5)
III	1.2	Buildings of large occupancies (condominiums, shopping centres, schools and public buildings)	0.18 (1.2 x 0.225/1.5)
IV	1.5	Lifeline built facilities (hospitals, emergency services, power plants and communication facilities)	0.225 (consistent with RP of 2500 years)

Finally, a behaviour factor (q) can be stipulated to take into account the capacity of the structure, at individual member level, to withstand seismic actions beyond its notional capacity limits. Design actions (such as bending moments and shear forces) are to be scaled down by the factor $1/q$, but no scaling factor is to be applied in the calculation of drifts, or deformation, in the structure.

In the Australian Standard (AS1170.4 2007), the additional capacity to withstand seismic actions is resolved into the performance factor (S_p) which takes into account contributions from the over-strength of materials and the structural system as a whole in sustaining earthquake generated lateral forces and the ductility ratio (μ) which takes into account the ability of the structure to deform in a ductile manner (AEES 2009). The value of S_p is taken by default as 0.77 and μ is taken as 2.0 by default for limited ductile reinforced concrete, structural steel or composite structures made of concrete and steel. The composite factor of 2.6 (being μ/S_p or 2/0.77), used as the default design value in Australia can be compared to the slightly lower, more conservative, q value of 2.0 recommended in the *National Building Code of Canada*, since its 2005 edition (NRCC 2005). The default q value stipulated in the National Annex for Singapore is 1.5 which is consistent with recommendations by Eurocode 8. The default q values stipulated in regulatory documents in various countries of low to moderate seismicity for limited ductile structures, are listed in Table 4, to facilitate decision making in Hong Kong.

Table 4. Default values of behaviour factor for limited ductile structures

Region/Country	Standards/Codes	Over-strength factor	Ductility factor	Behaviour factor
Europe Singapore	Eurocode 8 NA to SS	-	-	1.5
Canada	NBCC	1.3	1.5	2.0
Australia	AS1170.4	1.3	2.0	2.6

4. Conclusions

Fundamental and influential issues associated with the performance requirements and loading models for use in the seismic design of buildings in Hong Kong have been discussed in this chapter.

A return period (RP) of around 2,500 years, i.e. a 2% probability of exceedance (PE) in a design life of 50 years is recommended as the Collapse Prevention (CP) limit for the performance assessment of ordinary structures.

Lifeline facilities, including hospitals and infrastructure, in support of emergency services are to be designed to fulfil the "No Collapse" (NC) (Life Safety) performance criterion for a return period of 2500 years. Lower design seismic actions are recommended for buildings of other classes of importance.

Various response spectrum models developed for rock sites in Hong Kong by The University of Hong Kong and ARUP have been reviewed.

Response spectrum models to be used for design purposes are scaled in accordance with the design peak ground acceleration (PGA) values on rock sites, which vary between 0.12g and 0.225g. Exact values, as presented in tables, depend on the importance classification of the building concerned.

A suite of response spectrum models applying to various soil classes (ground types) are proposed. The site natural period, TS, shall be adopted as the key site classification parameter. Response spectral parameters in terms of amplification (S) factor and corner periods are also given.

Design actions at the member level, such as bending moments and shear forces, are to be scaled down by 1/q where q is the behaviour factor. Values ranging between 1.5 and 2.6 have been suggested.

References

AEES (2009) AS 1170.4 Commentary: Structural Design Actions – Part 4 Earthquake Actions. Victoria: Australian Earthquake Engineering Society.

Arup (2002) "Final Report on Evaluation of Seismic Response of Buildings. Consultancy to Study the Seismic Effects on Buildings in Hong Kong", Agreement No. CAO K49, Building Department, The Government of the HKSAR.

Arup (2011) "Final Report on Overall Seismic Hazard Assessment. Pilot Seismic Microzonation Study in North-west New Territories for the Study of Potential Effect of Earthquake on Natural Terrain Investigation", Agreement No. CE49/2008(GE), Landslip Prevention and Mitigation Programme, Geotechnical Engineering Office, Civil Engineering and Development Department, The Government of the HKSAR.

AS 1170.4 (2007) Structural Design Actions – Part 4 Earthquake Actions. Standards Australia.

ASCE/SEI 7-10 (2011) Minimum Design Loads for Buildings and Other Structures. Structural Engineering Institute (SEI), the American Society of Civil Engineers (ASCE), U.S.

ATC (1997) NEHRP Guidelines for the Seismic Rehabilitation of Buildings (FEMA Publication 273). Prepared by Applied Technology Council (ATC) for the Building Seismic Safety Council (BSSC), Washington, D.C., U.S.

BC3 (2013) Guidebook for Design of Buildings in Singapore to Design Requirements in SSEN-1998-1. Singapore: Building and Construction Authority.

BD (2004). Code of Practice on Wind Effects in Hong Kong 2004. Buildings Department (BD), The Government of the HKSAR, Hong Kong, China.

BSSC (2003) "NEHRP Recommended Provisions for Seismic Regulations for New Buildings and Other Structures (FEMA 450)", Building Seismic Safety Council for the Federal Emergency Management Agency, National Institute of Building Sciences, Washington, D.C., U.S..

CEN (2004) EN 1998 1. 2004. Eurocode 8: Design of Structures for Earthquake Resistance – Part 1: General Rules, Seismic Actions and Rules for Buildings. European Committee for Standardisation, Brussells.

Chandler A. M. and Lam N. T. K. (2002) "Intensity Attenuation Relationship for the South China Region and Comparison with the Component Attenuation Model", Journal of Asian Earth Sciences 2, 775-790.

Chandler A. M. and Lam N. T. K. (2004) "An attenuation model for distant earthquakes", Earthquake Engineering and Structural Dynamics 33:2, 183-210.

Chandler A. M., Lam N. T. K., Tsang H. H. (2005) "Shear Wave Velocity Modelling in Crustal Rock for Seismic Hazard Analysis", Soil Dynamics and Earthquake Engineering, 25(2):167-185.

Chandler A. M., Lam N. T. K., Tsang H. H. (2006a) "Near-surface Attenuation Modelling based on Rock Shear-Wave Velocity Profile", Soil Dynamics and Earthquake Engineering, 26(11):1004-1014.

Chandler A. M., Lam N. T. K. and Tsang, H. H. (2006b) "Regional and Local Factors in Attenuation Modellin", Journal of Asian Earth Sciences 27, 892 - 906.

Cornell C. A.(1968) "Engineering seismic risk analysis", Bull.Seismological Soc. of Am. 58, 1583- 1606.

Dolšek M., Sinković N.L. and Žižmond J. (2017) "IM-based and EDP-based decision models for the verification of the seismic collapse safety of buildings", Earthquake Engineering and Structural Dynamics 46(15):2665-2682.

Douglas J., Ulrich T., Negulescu C. (2013) "Risk-targeted seismic design maps for mainland France", Natural Hazards, 65(3): 1999-2013.

Fardis M. N. (2009) Seismic Design Assessment and Retrofitting of Concrete Buildings based on EN – Eurocode 8, Springer.

Free M., Pappin J. and Koo R. C. H. (2004) "Seismic hazard assessment in a moderate seismicity region, Hong Kong", In: Proceedings of 13th World Conf. on Earthquake Engr, Vancouver, Canada, Paper no. 1659, 10.

Geoscience Australia (2012) The 2012 Australian Earthquake Hazard Map. D. R. Burbridge ed. Canberra: Geoscience Australia publication, GeoCat 74811.

Haselton, C. B., Deierlein, G. G. (2007) "Assessing Seismic Collapse Safety of Modern Reinforced Concrete Moment Frame Buildings", Report No. 156, The John A. Blume Earthquake Engineering Center, Department of Civil and Environmental Engineering, Stanford University, U.S., 281 pp.

Hashemi, M. J., Tsang, H. H., Al-Ogaidi, Y., Wilson, J. L., Al-Mahaidi, R. (2017) "Collapse Assessment of Reinforced Concrete Building Columns through Multi-Axis Hybrid Simulation", ACI Structural Journal, 114(2):437-449.

International Building Code (IBC), (2012). International Code Council (ICC), Country Club Hill, Illinois, U.S.

Lam N. T. K. (1999). Program 'GENQKE' user's Guide. Department of Civil and Environmental Engineering, The University of Melbourne, Australia.

Lam, N. T. K., Tsang, H. H., Lumantarna, E. & Wilson, J. L. (2016). "Minimum loading requirements for areas of low seismicity", Earthquakes and Structures, 11:4, 539-561.

Lam N. T. K., Asten M., Roberts J., Srikanth V., Wilson J., Chandler A.M. and Tsang H.H. (2006) "Generic Approach for Modelling Earthquake Hazard", Invited paper. Journal of Advances

in Structural Engineering. 9:1, 67-82.
Lam N. T. K., Balendra T., Wilson J.L. and Srikanth V. (2009) "Seismic Load Estimates of Distant Subduction Earthquakes Affecting Singapore", Engineering Structures, 31:5, 1230-1240.
Lam N. T. K., Sinadinovski C., Koo R.C.H. and Wilson J.L. (2003) "Peak Ground Velocity Modelling for Australian Intraplate Earthquakes", International Journal of Seismology and Earthquake Engineering. 5:2, 11-22.
Lam N. T. K., Wilson J. L. and Chandler A. M. (2001) "Seismic Displacement Response Spectrum Estimated from the Frame Analogy Soil Amplification Model", Journal of Engineering Structures, 23 1437-1452.
Lam N. T. K., Wilson J. L. and Chandler A. M. and Hutchinson G.L. (2002) "Response Spectrum Predictions for Potential Near-Field and Far-Field Earthquakes Affecting Hong Kong: Rock Sites", Soil Dynamics and Earthquake Engineering. 22, 47-72
Lam N. T. K., Wilson J. L. and Hutchinson G. L. (2000) "Generation of Synthetic Earthquake Accelerograms Using Seismological Modelling", A Review, Journal of Earthquake Engineering , 4:3, 321-354.
Lee C. F., Ding Y. Z., Huang, R. H., Yu, Y. B., Guo, G. A., Chen, P. L. and Huang, X.H. (1998) "Seismic Hazard Analysis of the Hong Kong Region. (GEO Report No. 65)", Geotechnical Engineering Office, Civil Engineering Department, Government of the Hong Kong SAR, 145 p.
Liel, A. B., Deierlein, G. G., (2008) "Assessing the Collapse Risk of California's Existing Reinforced Concrete Frame Structures: Metrics for Seismic Safety Decisions", Report No. 166, The John A. Blume Earthquake Engineering Center, Department of Civil and Environmental Engineering, Stanford University, U.S., 293 pp.
Mak S., Chan L. S., Chandler A. M. and Koo, R. C. H. (2004) "Coda Q estimates in the Hong Kong region", Journal of Asian Earth Sciences 24,127-136.
McGuire R. K. (1976) "FORTRAN Computer program for seismic risk analysis", U.S. Geol. Surv. Open-File Rept. 76-67.
McGuire R. K., (1995) "Probabilistic seismic hazard analysis and design earthquakes: Closing the loop", Bull. Seismological Soc. of Am., 85:5, 1275-1284.
Mitchell D., Paultre P., Tinawi R., Saatcioglu M., Tremblay R., Elwood K., Adams J. and DeVall, R. (2010). "Evolution of seismic design provisions in the National building code of Canada", Canadian Journal of Civil Engineering 37, 1157-1170.
NA to SS EN 1998 1. (2013). Singapore National Annex to Eurocode 8: Design of Structures for Earthquake Resistance – Part 1: General Rules, Seismic Actions and Rules for Buildings. Singapore: SPRING Singapore
NRCC (2005) National Building Code of Canada, Associate Committee on the National Building Code, National Research Coun-cil of Canada, Ottawa, ON.
Pappin J. W., Jiang H., Koo R. C. H., Yu Y. B., Kwan J. S. H., So M. M. L., Shiu Y. K., Ho K. K. S. and Pun W. K. (2015a). "An Updated Seismic Hazard Analysis of the Hong Kong Region. Hong Kong", Institution of Engineers Transactions. 22(3): 153-178.
Pappin J. W., Koo R. C. H., Jiang H., Kwan J. S. H., Yu Y. B., So M. M. L., Shiu Y. K., Ho K. K. S. and Pun W. K. (2015b). "A Rigorous Probabilistic Seismic Hazard Model for Southeast China: A Case Study of Hong Kong", Bulletin of Earthquake Engineering. 13(12): 3597-3623.
Pappin J. W., Koo R. C. H., Free M. W. and Tsang H. H. (2008) "Seismic hazard of Hong Kong", Electronic Journal of Structural Engineering, Special Issue, 42-56.
Pitilakis K., Riga E., Anastasiadis A. (2012) "Design spectra and amplification factors for Eurocode 8", Bulletin of Earthquake Engineering. 10(5). 1377-1400.

Pitilakis K., Riga E., Anastasiadis A. (2013) "New code site classification, amplification factors and normalized response spectra based on a worldwide ground-motion database", Bulletin of Earthquake Engineering. 11(4). 925-966.

Porter K. A. (2014) "Safe enough? How building codes protect our lives but not our cities", Proceedings of the 10th U.S. National Conference on Earthquake Engineering, Earthquake Engineering Research Institute, Anchorage, Alaska, US, July 21–25, 2014.

Pun W.K. and Ambraseys N.N. (1992) "Earthquake Data Review and Seismic Hazard Analysis for the Hong Kong Region", Earthquake Engineering and Structural Dynamics 21, 433-443.

SEAOC (1995) "Vision 2000: Performance-Based Seismic Engineering of Buildings", Structural Engineers Association of California Sacramento, California, U.S.

Su R.K.L, Tsang H.H. and Lam N.T.K. (2011) "Seismic Design of Buildings in Hong Kong", Department of Civil Engineering, The University of Hong Kong.

Su, R.K.L., Lee, C.L., He, C.H., Tsang, H.H. & Law, C.W. (2015) "Rare earthquake response spectra for typical site conditions in Hong Kong", The Hong Kong Institution of Engineers Transactions 22(3), 179-191.

Tsang H.H. (2006). "Probabilistic Seismic Hazard Assessment: Direct Amplitude-Based Approach", PhD Thesis, Department of Civil Engineering, The University of Hong Kong, p. 246

Tsang H.H. (2011) "Should we design buildings for lower-probability earthquake motion?" Natural Hazards 58, 853-857.

Tsang H.H. (2014) "Seismic Performance Requirements and Collapse Risk of Structures" Proceedings of the Annual Seminar entitled "Advances in Seismic Engineering" HKIE/IStructE Joint Structural Division. 58-75.

Tsang H.H. (2015) "Evaluation of Codified Elastic Design Spectrum Models for Regions of Low-to-Moderate Seismicity", Soil Dynamics and Earthquake Engineering, 70:148-152.

Tsang, H.H. (2018) "Recommended Seismic Performance Requirements for Building Structures in Hong Kong", Earthquakes and Structures, accepted.

Tsang H.H., Chandler A.M. and Lam N.T.K. (2006a) "Estimating non-linear site response by single period approximation", Journal of Earthquake Engineering and Structural Dynamics 35:9, 1053-1076.

Tsang, H.H., Chandler, A.M. and Lam, N.T.K. (2006b) "Simple Models for Estimating Period-Shift and Damping in Soil", Earthquake Engineering and Structural Dynamics, 35(15):1925-1947.

Tsang, H.H., Chandler, A.M. (2006) "Site-Specific Probabilistic Seismic-Hazard Assessment: Direct Amplitude-Based Approach", Bulletin of the Seismological Society of America, 96(2):392-403.

Tsang, H.H., Su, R.K.L., Lam, N.T.K., Lo, S.H. (2009) "Rapid Assessment of Seismic Demand in Existing Building Structures", The Structural Design of Tall and Special Buildings, 18(4):427-439.

Tsang, H.H., Lam, N.T.K. (2010) "Seismic Hazard Assessment in Regions of Low-to-Moderate Seismicity", LAP Lambert Academic Publishing, Koln, Germany.

Tsang H.H., Sheikh N. and Lam N.T.K. (2010) "Regional Differences in Attenuation Modelling for Eastern China", Journal of Asian Earth Sciences, 39:5, 451- 459.

Tsang H.H., Yaghmaei-Sabegh S., Anbazhagan P., Sheikh M.N. (2011). "A Checking Method for Probabilistic Seismic-Hazard Assessment: Case Studies on Three Cities", Natural Hazards, 58(1):67-84.

Tsang, H.H., Sheikh, M.N., Lam, N.T.K. (2012) "Modeling Shear Rigidity of Stratified Bedrock in Site Response Analysis", Soil Dynamics and Earthquake Engineering, 34(1):89-98.

Tsang, H.H., Wenzel, F. (2016) "Setting Structural Safety Requirement for Controlling

Earthquake Mortality Risk", Safety Science, 86: 174-183.
Tsang, H.H., Lumantarna, E., Lam, N.T.K., Wilson, J.L., Gad, E.F. (2016) "Annualised Collapse Risk of Soft-Storey Building with Precast RC Columns in Australia", In: Proceedings of the 24th Australasian Conference on the Mechanics of Structures and Materials, December 6-9, 2016.
Tsang, H. H., Wilson, J. L., Lam. N. T. K. (2017a) "A Refined Design Spectrum Model for Regions of Lower Seismicity", Australia Journal of Structural Engineering, 18:3-10.
Tsang, H. H., Wilson, J. L., Lam. N. T. K., Su, R. K. L. (2017b) "A Design Spectrum Model for Flexible Soil Sites in Regions of Low-to-Moderate Seismicity", Soil Dynamics and Earthquake Engineering, 92:36-45.
Tsang, H.H., Wenzel, F. and Daniell, J.E. (2017c) "Residual fatality risk estimates for setting earthquake safety requirement", In: Proceedings of the 16th World Conference on Earthquake Engineering, Santiago, Chile, January 9-13, 2017.
Tsang, H.H., Daniell, J.E., Wenzel, F., Werner, A.C. (2018a) A Semi-Probabilistic Procedure for Developing Societal Risk Function. Natural Hazards, DOI: 10.1007/s11069-018-3233-z.
Tsang, H.H., Daniell, J.E. and Wenzel, F. (2018b) "Earthquake safety requirements based on individual and societal fatality risk", In: Proceedings of the 16th European Conference on Earthquake Engineering, Thessaloniki, Greece, June 18-21, 2018.
Yaghmaei-Sabegh, S and Lam N.T.K. (2010) "Ground motion modelling in Tehran based on the stochastic method", Soil Dynamics and Earthquake Engineering. 30, 525-535.

Should We Use the Chinese Seismic Code for Hong Kong?

Goman W. M. Ho

ARUP Group, Hong Kong

Hong Kong is located in a low to moderate seismicity zone. In the last couple of years, much discussion has taken place on the necessity for seismic provisions when designing buildings. Following public consultations by the Buildings Department, completed in early 2014, it was decided that seismic provision should be included in the design of new buildings and structures in Hong Kong. The next stage is to decide what seismic provisions should be implemented and what design philosophy and code approach should be adopted.

Across the Hong Kong boundary line and within an order of 50km radius, Shenzhen follows the Chinese seismic code GB50011, while Macau (by 65km from Hong Kong), also uses the Chinese code as its basis for design. Whether Hong Kong should do the same is now much discussed among local engineers, developers and architects. This chapter briefly lists the differences between the Chinese seismic code and other international codes, promoting a better understanding of the various philosophies as an aid to the decision.

Keywords: seismic design, Chinese seismic code, seismicity of Hong Kong, moderate seismicity, ductility demand

1. Introduction

Hong Kong has been an international transit port since 1898 because of its deep and wide harbour. With the development of aviation and the cargo industry, Hong Kong has now evolved into an important world financial centre and international city. The population of Hong Kong has increased rapidly since World War II. Most buildings in Hong Kong are now high-rise, averaging 30 to 40 storeys and of the order of 120m~150m in height. Because of population density with limited lands, developments usually comprise retail at lower levels and either residential or commercial premises at upper levels. As a result, transfer structures are usually adopted, intermediate between the two types of structure needed.

Since codes of practice were first introduced in Hong Kong in the 1950's (Ma, 2007), British codes were adopted as the standards for building design in Hong Kong. Wind code CP3: Chapter 5 therefore becomes the standard for Hong Kong. At that time, there was no British seismic code. Although new local codes of practice were introduced in Hong Kong in late 1990's, seismic considerations are yet to be included in the design of building structures in Hong Kong.

Geographically, Hong Kong is located on the Southeast China coast and west of the Philippines Tectonic Plate. The historical record demonstrates that earthquakes do happen in Hong Kong (CEDD, 2012). Much study has been made (Pun and Ambraseys, 1992; Pappin et al., 2012) which concluded that the seismicity level of Hong Kong is low to moderate. The Buildings Department of Hong Kong carried out several public consultations (BD, 2012) to collect global feedback from the industry and the public in 2012 and 2013. A summary of the consultation results with stakeholders can be found in

Legislative Council Panel for Development (2013). The feedback from the consultation is very positive on introducing seismic provision to buildings in Hong Kong to reduce both casualty and economic lost in case earthquake occurs in Hong Kong.

Hong Kong has already developed its own Loading Code (BD, 2011a), Wind Code (BD, 2004), Concrete Code (BD, 2013) and Steel Code (BD, 2011b), which are independent of Chinese Codes. There were a number of engineers who considered that HK could easily adopt the Chinese seismic code as if taken from a shelf. Unfortunately, whether "easy" equates to "appropriate" is not that simple. Compatibility with existing design codes and local practice are key issues. With the limited space available, this chapter briefly questions whether some major aspects of the Chinese seismic code are entirely appropriate for Hong Kong. If the solutions to these questions can be found, Hong Kong may then be in a position to decide whether to adopt the Chinese Seismic Code for Hong Kong.

2. Background on Chinese seismic code development

The Chinese seismic code was first written in 1974 based on the Russian Code but was quickly updated to TJ11-78 (中国建筑工业出版社出版, 1978) in 1978 after the Tangshan Earthquake in 1976. The next update was in 1989 and the code was renamed as GBJ11-89 (中国建筑工业出版社出版, 1989). Starting from TJ11-78, the earthquake design level was based on a 475 years return period with force reduction factors for different structural systems. The design philosophy is similar to that of the New Zealand code at that time.

A major update resulted in the 2001 "Code for Seismic Design of Buildings – GB50011" (中国建筑工业出版社出版, 2001) introducing the performance based concept for three levels of earthquake, defined as Level 1 (Minor/frequent) with a return period of 50 years (the probability of exceedance, Pe ,= 63% in 50 years), Level 2 (Moderate) with a return period of 475 years (Pe = 10% in 50 years) and Level 3 (Major/Severe) with return period of 1641 years (Pe = 3% in 50 years) to 2475 years (Pe = 2% in 50 years). It contains the performance based concept with a design target of no damage in a Level 1 Earthquake (EQ), repairable damage for Level 2 EQ and no collapse in a Level 3 EQ. Although most of the clauses within the code are similar to the American UBC97 (ICBO 1997), the design philosophy, in some ways, combine the Japanese seismic code.

Design is divided into the two stages:

Stage 1 - elastic design based on a Level 1 EQ and

Stage 2 - an elasto-plastic check on a Level 3 EQ

Should the engineer follow the code, the building is supposed to achieve the target performance at three levels of earthquake. The first version of GB50011 was published in 2001, with a partial update in 2008 shortly after the Sichuan EQ. The latest version was published in 2016. The code was first developed for low to medium rise structures with an extensive chapter on reinforced concrete (RC) and masonry structures. The steel structures content focused on steel connections and bracing systems only. This is probably because nearly 95% of buildings in China in the late 90's were RC and masonry structures. Steel structures by that time were mainly industrial buildings.

Hong Kong is located in a low to moderate area of seismicity but with strong winds. Most buildings in Hong Kong are high-rise possessing the high stiffness to resist those

winds. The demand for ductility is low. The following sections address the implications for Hong Kong of adopting the Chinese Code.

3. Seismic Hazard

Generally, an earthquake is caused when two blocks of the earth suddenly slip past one another, releasing the strain energy built up in the blocks. Earthquakes are classified into 'Inter-plate' (occurs at a plate boundary), 'Intra-plate' (occurs in the interior of a tectonic plate) and 'Inter-slab' (occurs at either a shallow or a deep level in a subduction plate). Such classifications are illustrated by Gioncu & Mazzolani (2011) as in Figure 1. As for most of the world, where low to moderate seismicity levels exist, the main characteristics of earthquakes striking Hong Kong will be of the intra-plate type.

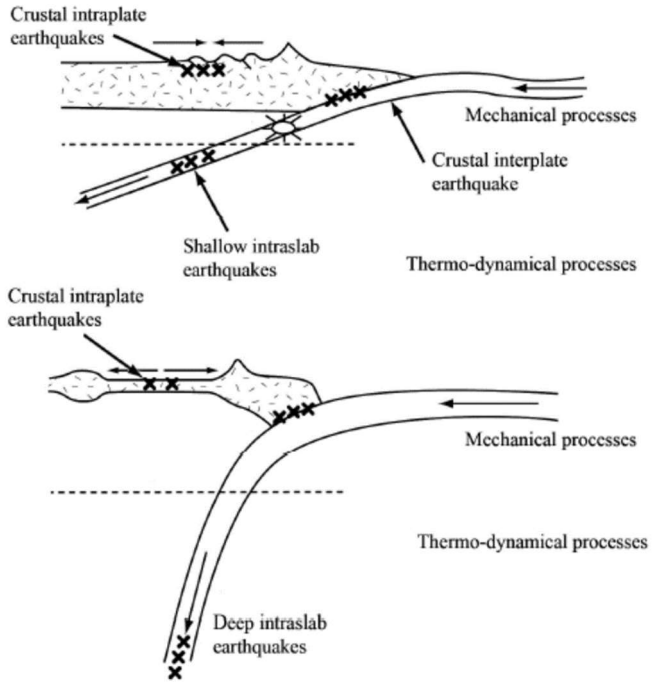


Figure 1. Classification of Earthquakes (Extracted from Earthquake Engineering for Structural Design, Spon Press 2011)

The first EQ level of the Chinese Code, with a return period of 50 years (i.e Pe = 63% in 50 years) is based on an extensive study by 高小旺, 鮑蔼斌 (1985) of 45 cities in Northeast, Northwest and Southwest China. These cities are close to active faults. Based on statistical analysis, the relationship between the Design Seismic Intensity at Level 1 EQ (i.e. I_1) and Seismic Fortification Intensity (I_2) is

$I_1 = I_2 - 1.55$

Hence, the differences in force levels between the three levels of EQ are in the ratio approximately of 1: 3: 6. This means that the forces for a Level 3 EQ design should be approximately six times those for a Level 1. Under the Chinese Code, Hong Kong is located in a zone of moderate seismicity with design intensity $I_2 = 7.0$ and peak ground

acceleration, PGA=0.15g for a return period of 475 years as shown in Figure 2.



Figure 2. PGA Value for Hong Kong as in Chinese Seismic Code (extract from GB 18306—2015)

As the statistical results did not include cities in Southeast China such as Hong Kong, where only intra-plate earthquakes are likely, an independent study should be carried out.

Extensive study was made of the seismic hazard in Southeast China and Hong Kong by Arup (2012) and Pappin et al. (2015). The calculated PGA for various periods for rock sites have been expressed as contours across the Hong Kong region. The contours give the ground motions with a 2% and a 10% probability of being exceeded in the next 50 years. The PGA contours are generally consistent with the PGA contours presented in GEO Report (GEO, 2012) as shown in Figures 3a and 3b.

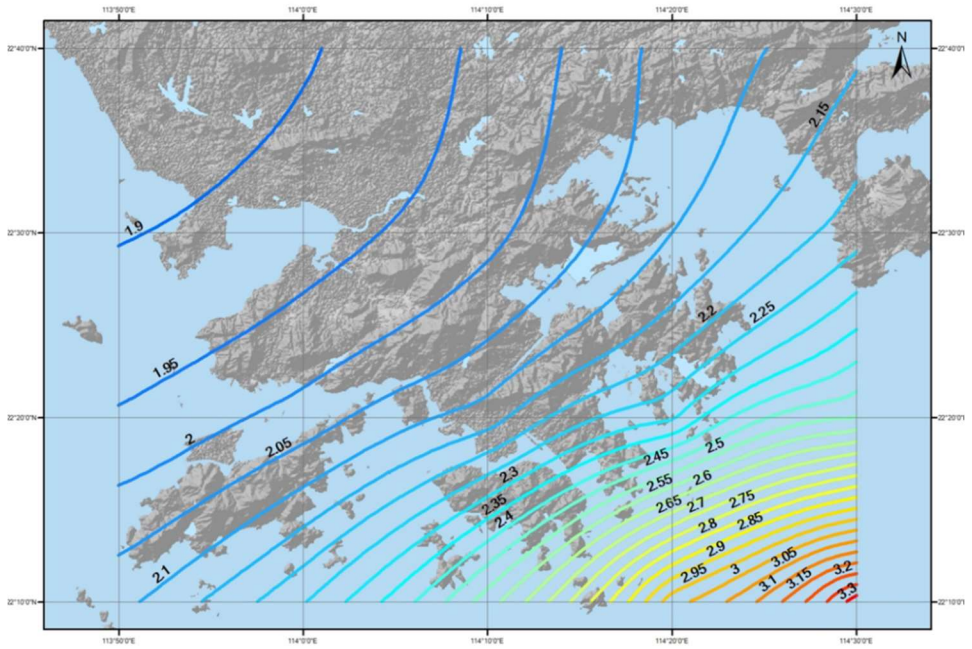


Figure 3a. Contour plot for PGA (m/s2) for a 2% probability of being exceeded in the next 50 years (Arup 2012)

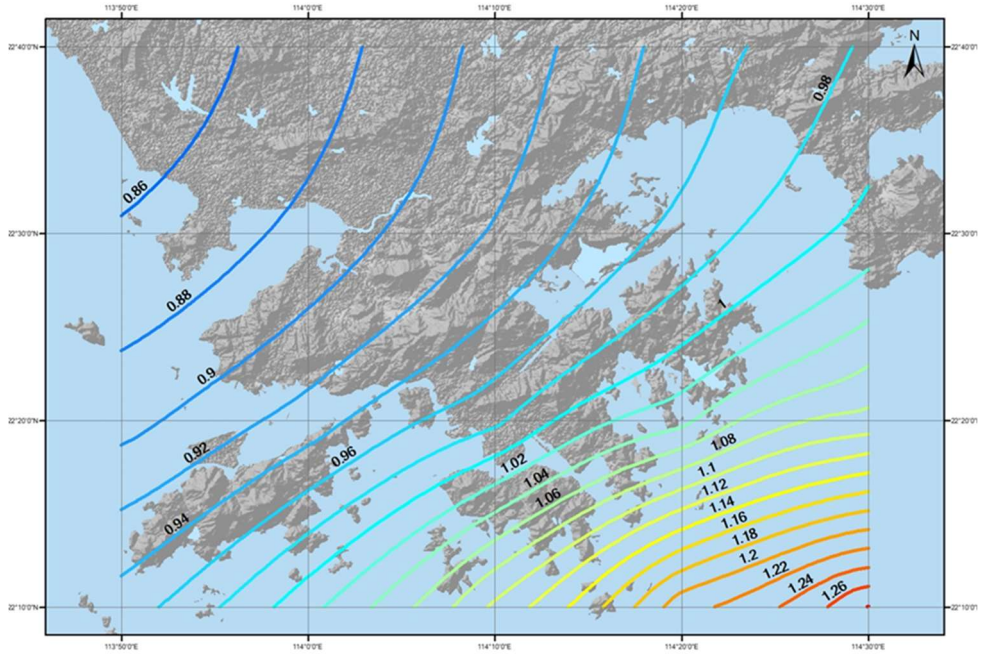


Figure 3b. Contour plot for PGA (m/s²) for a 10% probability of being exceeded in the next 50 years (Arup 2012)

From the contours, a PGA value which covers 99% of the Hong Kong area is of the order of 1.12m/s² or 0.114g, which is less than, but close to the 0.15g specified by GB18306 (中国标准出版社出版, 2015) for 10% in 50 years or a 475 years return period earthquake.

4. Importance Factors

In nearly all national seismic codes, buildings are classified into different occupancy categories. An importance factor, IE, is used to reflect the consequences for the building of an earthquake. Essential facilities, including hospitals, fire stations, emergency centers and government buildings are classified as important according to government and local government ordinances. These buildings are designed capable of maintaining functionality during and after an earthquake event. Importance factors are applied to amplify the seismic force. (An alternative approach is to change the earthquake return period). The importance factor is represented by the following equation:

$$I_E = \frac{S_a\left(T, design\ P_e\right)}{S_a\left(T, reference\ P_e\right)} \tag{1}$$

where S_a = Spectral Acceleration

P_e = Probability of Exceedance

The corresponding values for IE for Hong Kong, based on various return periods are listed in Table 1 and Figure 4.

In the Chinese code, the importance of buildings is defined by the degree of ductility which needs to be provided for that building. A hospital, for example, in most national codes, is defined to be not less that category B, including the Chinese code. In other national seismic codes, hospitals are designed to resists seismic forces 1.4 times those of ordinary buildings (i.e. 1000 years return period). In the Chinese code, however, amplification factors are applied to the design of elements and special detailing enhances ductility. This causes category B building (such as hospitals) in Chinese code to deform more than buildings designed to other national codes. Nowadays, many hospitals are equipped with expensive equipment with very stringent drift/vibration limits. Although a hospital designed using the Chinese code would be structurally sound and not collapse after an earthquake, extensive checking of the equipment would be required before it could resume operation.

Table 1. Return Period – Importance Factor relationship

P_e in 50yrs	Return period (yrs)	Importance factor (I_E)
1%	4975	2.8
2%	2475	2.2
3%	1640	1.7
5%	975	1.4
10%	475	1.0

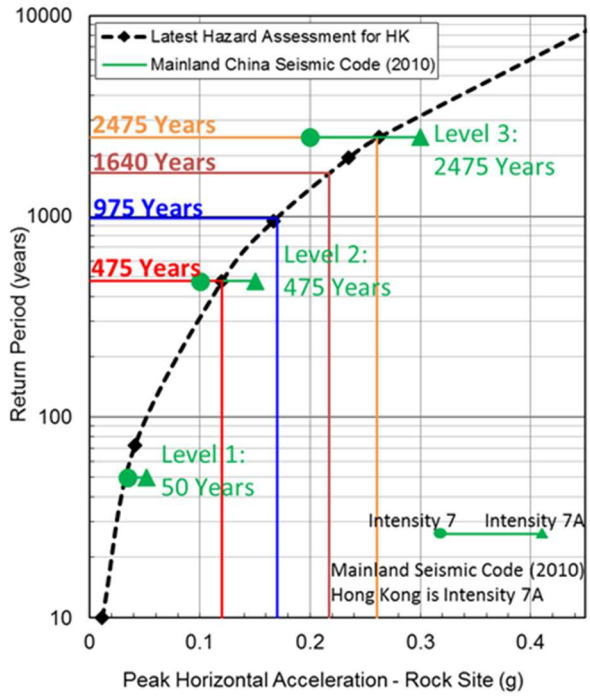


Figure 4. Return Period – PGA plot

In Hong Kong, there are a very limited number of hospitals. All of which must remain in full operation immediately after a disaster event. To be collapse proof is not the only objective and a full performance based seismic code, implemented locally looks to be worthy of consideration. In the meantime, to increase design loading is a good alternative for buildings with high importance.

5. Design of Buildings

In the Chinese code, many factors need to be checked and sometime it is very difficult or nearly impossible to meet all desirable limit states. Such factors include stiffness/building weight ratio; storey shear/building weight/ minimum base shear ratio etc. A study by Ho and Ching (2013) demonstrated that these Chinese code requirements will result in very heavily braced structural systems for buildings over 300m tall.

The Chinese code limits transfer structures to certain locations and the transfer plate system is not allowed. In Hong Kong, most buildings have a transfer structure, fundamentally due to the limited supply of land, causing most buildings to be multi-functional. Taking into account the fact of the strong winds and the only moderate level of seismicity, a complete prohibition on transfer plate structures seems unrealistic in Hong Kong. Su et al. (2000) carried out studies for several buildings based on the local situation and a further study by Li and Law (2002) indicated that buildings with a transfer plate are possible. The new seismic code for Hong Kong, therefore, should allow a practical gateway for the continued construction of transfer structures, especially for tall buildings.

The Chinese code is also very restrictive/rigid in respect of building height. RC buildings higher than 80m require non-linear analysis and those more than 100m tall require time-history analysis. In Hong Kong the design work load would increase considerably as most buildings are higher than 100m.

6. Load Combination and Factors

The damping ratio related to design against wind for tall buildings should be in the range of 1~1.5% for serviceability and 2% for strength. In seismic case, nearly all national codes use 5%. The Chinese code uses 2% damping for steel structures and 5% for RC structures. Composite structures are in the range of 3~4.5% depending on whether the structure behaves like a steel structure or an RC structure. The Chinese code requires a combination of wind load and seismic load to be assumed at the same time, creating a fundamental conflict, seemingly missed by many engineers. Wind design aims at un-cracked structures with lower damping ratios. Seismic design assumes cracked structures and higher damping ratios. It is not structurally logical to combine the two load cases. In other national codes, seismic loads are imposed alone, not combined with wind and temperature loads etc.

As discussed above in section 3. the Chinese code design seismic intensity, I1, is I2 - 1.55. According to Chinese code, the load factor for design combination is 1.3. It means that 1.3xI1 is supposed to be equal to I2 (i.e 1.3I1=I2). In reality, this 1.3 load factor is insufficient to increase the seismic forces to I2, a lot of design parameters and coefficients are therefore introduced in Chinese code to ensure the reliability.

7. Ductility Demand

Because of limited space, this section covers only reinforced concrete (RC) structures. Under GB50011-2016, RC elements are classified into different Earthquake-resistant Grades (ductility classifications, the 4th to the 1st grade) are assigned on the basis of seismic intensity, structural type, building height and fortification category, and element earthquake resistant designs must comply with the required corresponding calculated requirements and detailing measures (ductility detailing). Table 2 lists the requirement for stirrups for various Earthquake-resistant Grades.

Table 2. Maximum spacing and minimum diameter of stirrups at core

Earthquake-resistant Grade	Maximum spacing of stirrups (mm)	Minimum diameter of stirrup (mm)
1st	Smaller of 6 times diameter of longitudinal tensile reinforcement and 100	10
2nd	Smaller of 8 times diameter of longitudinal tensile reinforcement and 100	8
3rd	Smaller of 8 times diameter of longitudinal tensile reinforcement and 150 (100 at column root)	8
4th	Smaller of 8 times diameter of longitudinal tensile reinforcement and 150 (100 at column root)	6 (8 at column root)

For the core zone in a nodal point of frame with Earthquake-resistant Grades 1 to 3, the characteristic strength factor for stirrup provision cannot be less than 0.12, 0.10 and 0.08 respectively, and the volumetric ratio of reinforcement for stirrups cannot be less than 0.6 %, 0.5 %, 0.4 % respectively.

In accordance with the Earthquake-resistant Grades, the load capacity design of a structure must take account of the seismic failure characteristics of individual structural member and prevent non-ductile failure modes such as shear failure and sudden collapse. That can be controlled with appropriate section design, load capacity coefficient adjustments and construction measures. Capacity design is appropriate for structure controlled by seismic loading. Should member size be controlled by stiffness, member would be oversize. In Chinese code, load combination includes both wind and seismic to be considered at the same time. To adopt capacity design approach for these oversize members would be inappropriate and sometimes unrealistic.

Furthermore, it is interesting to realize that the design seismic force according to GB 50011 is independent of the structural system. This means that even for a structure whose whole system and its individual member elements provide a very high level of ductility, the design seismic force could not be reduced.

8. Conclusions

The integrity of the Chinese seismic code cannot be questioned as it has been validated in the past by real earthquakes. As above, however, there is a compatibility issue, if Hong Kong uses the Chinese code, "in combination with" the existing Hong Kong RC and steel codes. To use Chinese codes as a whole package in design is easy but to use the Chinese seismic code for the design of buildings in Hong Kong is not straight forward.

A brief review of the Chinese seismic code discussed some areas of concern on its effect has been conducted. The "limit state" defined in the Chinese seismic code is 50 years return period multiply by a load factor of 1.3 while the international practice is based on 475 years. From the author's view, this load factor is not sufficient to increase the level 1 EQ to level 2 EQ. A lot of factors has to be used in member design codes to ensure the structural reliability.

Hong Kong is located in an area with strong winds and tall buildings higher than 15 storeys are the norm. Buildings with such height in Hong Kong will mainly be controlled by wind load and stiffness. Therefore, high rise buildings in Hong Kong must contain reserve strength to resist lateral load. Buildings designed only to low to medium ductility levels should be able to resist wind forces and be able to provide adequate protection against the 2475 years return period earthquake. Chinese code emphasis on providing high ductility for all kinds of buildings discards in terms of function and height while most buildings in Hong Kong is controlled under wind load and the ductility demand for these buildings is generally low.

Should we adopt the Chinese seismic code for Hong Kong? A new set of design parameters needs to be redeveloped in order to make it compatible with other local Hong Kong codes. The effort for that is believed to be not less than developing a new code with local practice and requirement.

References

Arup (2012) Final Report on Overall Seismic Hazard Assessment. Pilot Seismic Microzonation Study in North-west New Territories for the Study of Potential Effect of Earthquake on Natural Terrain – Investigation.

BD (Buildings Department). (2004) Code of Practice on Wind Effects in Hong Kong 2004, HKSAR.

BD (Buildings Department). (2011a) Code of Practice for Dead and Imposed Loads 2011, HKSAR.

BD (Buildings Department). (2011b) Code of Practice for the Structural Use of Steel 2011, HKSAR.

BD (Buildings Department). (2012) Consultation Paper for Introducing Seismic-resistant Building Design Standards in Hong Kong, HKSAR.

BD (Buildings Department) (2013) Code of Practice for Structural Use of Concrete 2013, HKSAR

CEDD (Civil Engineering and Development Department). 2012. Seismicity of Hong Kong, HKSAR, February 2012.

ICBO (International Conference of Building Officials). (1997) Uniform Building Code 1997.

GEO (Geotechnical Engineering Office). (2012) "Review of Earthquake Data for the Hong Kong Region". GEO Publication No. 1/2012, HKSAR.

Gioncu, V. and Mazzolani, F. M. (2011) "Earthquake Engineering for Structural Design", Spon Press.

Ho, G. and Ching, R. (2013) "A Comparison Study for the design of a 500m tall building structures by US and China Codes", Proceeding of the 10th Sino-Japan Structural Engineering Conference, July 2013, Nanjin.

Legislative Council Panel for Development. (2013) "Consultation on Introduction of Seismic-resistant Building Design Standards in Hong Kong", CB(1)1110/13-14(01).

Li, C. S. and Law S. S. (2002) "Response of a reinforced concrete high-rise building with transfer plate system under seismic actions", Proceeding of Structural Engineering World Congress

(SEWC 2002), Yokohama, Japan, 9-12 October 2002

Ma, K. Y. (2007) "The Development of Hong Kong Structural Engineering Standards after the Second World War and before 1997", MA Thesis, The University of Hong Kong, 2007

Pappin, J., Jiang, H., Koo, R. C. H., Yu, Y. B., Kwan, J. S. H., So, M. M. L., Shiu, Y. K., Ho, K. K. S. and Pun W. K. (2012) "An updated seismic hazard analysis of the Hong Kong Region", HKIE Transaction, Vol 22, No 3, 2015, Taylor & Francis.

Pappin, J., Koo, R. C. H., Free, M. W. and Tsang, H. H. (2008) "Seismic Hazard of Hong Kong", EJSE Special Issue: International Earthquake Engineering in the low and moderate seismic regions of Southeast Asia and Australia.

Pun W. K. and Ambraseys, N. N. (1992) "Earthquake data review and seismic hazard analysis for the Hong Kong region", Journal of Earthquake Engineering Structural Dynamics, Vol 21, Issue 5.

Su R. K. L., Lam, N. T. K., Chandler A. M. and Li J. H. (2000) "The Seismic Assessment of Transfer Building Structures in Hong Kong". Joint University of Hong Kong/ University of Melbourne Internal Research Report, May 2000.

高小旺 鲍蕴斌. (1985) "地震作用的概率模型及其统计参数" ，地震工程与工程振动, 1985 年第 1 期 5.

中国标准出版社出版. (2015)《中国地震动参数区划图 GB 18306－2015》.

中国建筑工业出版社出版. (1978)《工业与民用建筑抗震设计规范》 TJ11-78 》

中国建筑工业出版社出版. (1989)《建筑抗震设计规范 GBJ11—89》

中国建筑工业出版社出版. (2001, 2008, 2016)《建筑抗震设计规范 GBJ50011》

Seismic Design and Engineering Practice in China

Aaron J. Wang

Project Design and Development Management
Capitaland China Corporate, China

China went through a construction and building boom in the past two decades and the demand for high-rise buildings has been ever increasing, including demands for more integrated building functions, open and tailor-made outlooks, better connection to municipal infrastructure and higher grades of building importance. The seismic design of such modern high-rise buildings poses engineering challenges in hazard mitigation with respect to extreme actions, requiring integrated structural frameworks and building skins, complex connections and overall building and constructional efficiency. This chapter introduces current trends and innovations in seismic design and engineering practice in China. The topic is elaborated through case studies of several major and iconic projects. The application of energy dissipation devices is discussed and the benefits explored in enhancing overall structural performance without over detraction from the architectural function. The re-engineering of composite joints is also introduced, which play an important role in safeguarding overall building rigidity and ductility. A new type of hybrid outrigger system was investigated and piloted, involving the application of low-yield steel dampers leading to a higher level of engineering and construction performance.

Keywords: seismic design, project design and construction, performance-based design, sustainability

1. Introduction

1.1 Engineering practice and industry trends

China has its own major set of structural design codes. The latest codes and design practices are system driven, incorporating many features of international codes such as IBC, FEMA, Eurocode and New Zealand standards. The determination, however, of basic seismic intensity (BI) and earthquake zoning still relies on local region monitoring and historical records of earthquakes. The definition of BI, therefore, relates to the territory concerned and design earthquakes with different levels of probabilities of exceedance are shown in Table 1. BI can be determined either according to the code of practice GB 18306 (MHURD 2015) or through a site seismic hazard assessment. In GB50223 (MHURD 2008), different buildings are classified by building function and building occupant numbers.

Buildings are engineered to withstand ordinary to severe/extreme level design earthquakes for various predicted structural responses. The design and construction of high-rise buildings in China requires a rigorous consideration of the impact of wind and earthquakes. The current national seismic design codes (MHURD, 2010 and 2011), introduce performance-based design approaches, which require a structurally complex building to meet the corresponding stringent requirements when subject to different strength earthquakes with exceedance rates of 63%, 10% and 2-3% over a design life of 100 years for low, moderate and severe design earthquakes respectively. 'Dual system'

requirements also need to be met for high-rise buildings in many circumstances. Wind is another concern for many coastal cities, where typhoons commonly strike.

Under the performance-based structural design philosophy, various levels of structural response and damage are designed for, in relation to different levels of design earthquake, as set out in Table 2. Normally, all structural members need to remain elastic under an ordinary earthquake. Under a severe/extreme design earthquake, all critical structural elements must still remain 'non-yielded' to ensure overall structural integrity. Thus, the building structures are able to maintain stability even when subject to extreme seismic action. Figure 1 gives an indicative visual illustration of the different levels of structural damage sustained by a typical structural member over a load history.

Energy dissipation devices such as dampers and isolating bearings are becoming popular in high-rise buildings in China, in order to enhance overall structural performance under destructive loading, as an alternative to additional steel and concrete, the latter making the overall structure chunky and costly. China has established codes of practice relating to the seismic energy dissipation design of building structures, JGJ 297 (MHURD 2013). The manufacture and verification testing of energy dissipation devices must satisfy both GB 50011 (MHURD 2010) and JG/T 209 (MHURD 2012).

The construction and building boom in China has increasingly called for high-rise mega-scale buildings during the last two decades. The main features of such mega-scale buildings include:

- Higher grades of building importance and hazard resistance performance;
- Application of energy dissipation devices for engineering and architectural efficiency;
- High performance composite joints allowing for both high structural rigidity and ductility; and
- Adoption of outrigger systems to maintain the structural stability of slender buildings.

This chapter introduces these current trends and innovations in seismic design and engineering practice in China. The above topics are elaborated through case studies on several major and iconic projects.

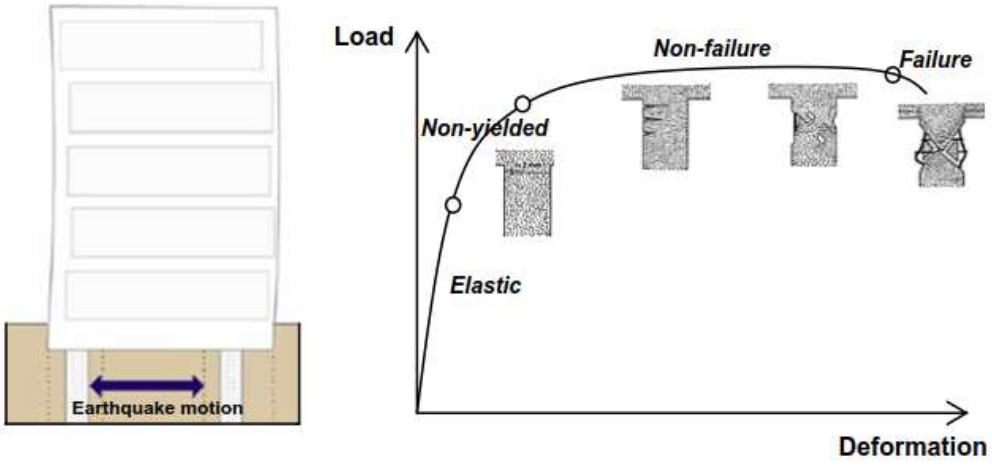


Figure 1. Structural response under earthquake

Table 1. Seismic Design Intensity

Design Earthquake	**Ordinary**	**Moderate**	**Severe/Extreme**
Probability of exceeding	63%	10%	2-3%
Design Intensity	*BI* – 1.55	*BI*	*BI* + 1

Notes:

1) *BI* denotes 'basic intensity' and can be either referred from Appendix A of GB 50011 (2010) or determined through a site seismic hazard assessment;

2) The design period is normally 50 years for an ordinary building, and 100 years for an especially important and complex building.

Table 2. Structural Performance Requirement

Earthquake Level	**Ordinary**	**Moderate**	**Severe/Extreme**
Column	Elastic	Elastic	Elastic to Non-yielded
Shear wall	Elastic	Elastic	Elastic to Non-yielded
Lintel beam	Elastic	Elastic	Non-yielded to Non-failure
Floor beam	Elastic	Elastic	Non-yielded to Non-failure
Retrofitting	None	None to Minor	Moderate to Major

Notes:

The above table is generic, and details refer to Appendix M of GB 50011 (2010).

1.2 Projects Covered in Case Studies

This chapter introduces the design and construction of three high-rise developments situated in different major cities of China, including:

- **Capital Square Shanghai (CSS)**

CSS is in the downtown area of Shanghai. The project includes one 180 m tall office tower, 2 composite office towers 120 m tall, a 7 storey commercial podium and a 4 storey basement. The overall gross floor area (GFA) is 360,000 m^2. Existing MTR tunnels run underneath the project site and significant provision was made out to minimize the construction and building impact on the existing MTR facilities.

- **Raffles City Chongqing (RCCQ)**

RCCQ includes a total of 6 mega-scale high-rise towers 250 to 370 m tall for offices, hotels, residential apartments, a sky conservatory, a 4-storey high shopping mall and a 4-storey basement for car parking. The overall gross floor area (GFA) is over 1 million square meters. The engineering design of the sky conservatory allows for semi-continuous connections between the conservatory decking structures and four of the tower structures below.

- **Raffles City Hangzhou (RCH)**

RCH, located in the central business district of Hangzhou, is composed of two 60-storey, 250m tall super high-rise twisting towers, a commercial podium and a 3-storey basement car park. The gross floor area (GFA) is 390,000 m^2.

2. Seismic energy dissipation systems

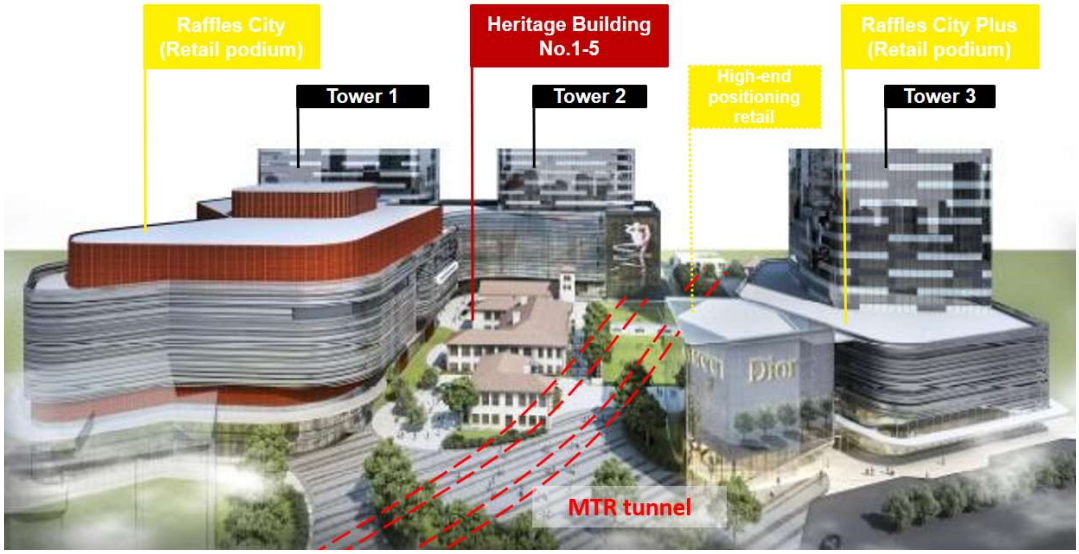
Seismic energy dissipation devices, such as dampers and isolating bearings, are becoming more and more popular in high-rise buildings because they can enhance overall structural performance under disaster-causing loads, as an alternative to additional steel and concrete. The latter approach leads to 'chunkier" and more costly structures. The proper adoption of seismic energy dissipation devices leads to higher engineering and architectural efficiencies.

2.1 The Low-yield Steel Damper

One of the characteristics of Capital Square Shanghai (CSS) is that existing MTR tunnels run directly underneath the project site, and divide the basement and super-structure of the project into western and eastern blocks as shown in Figure 2. Much effort was spent to eliminate any direct impact on the settlement and daily operation of the existing MTR tunnels from basement excavation and the building's self-weight. Rigorous numerical simulation was carried out to assess any possible settlement effects on the MTR tunnel due to the excavation work and additional loads caused by the weights of the new adjacent tower buildings.

A detailed study of the distribution of building weight for the tower structures 120 and 180m high showed that the concrete cores account for more than 65% of the structural self-weight, implying that the overall tower self-weight can be well controlled simply by controlling the thickness of the core walls. Low-yield steel dampers were installed in the core wall, as shown in Figure 3. These act as sacrificial members, dissipating some of the seismic energy impacting the main structure of the tower. Very usefully, these low-yield steel dampers are small and can be directly embedded into shear

walls with minimum impact on the architectural layout. The seismic energy dissipation mechanism is mobilized as the result of inter-floor drifting. This approach allows thinner core walls and a better controlled building self-weight.



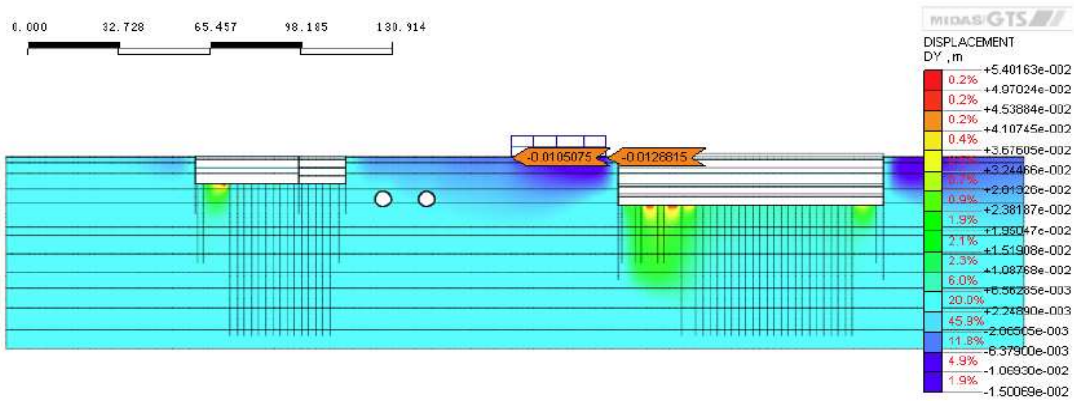


Figure 2. Raffles City Changning with MTR tunnel underneath

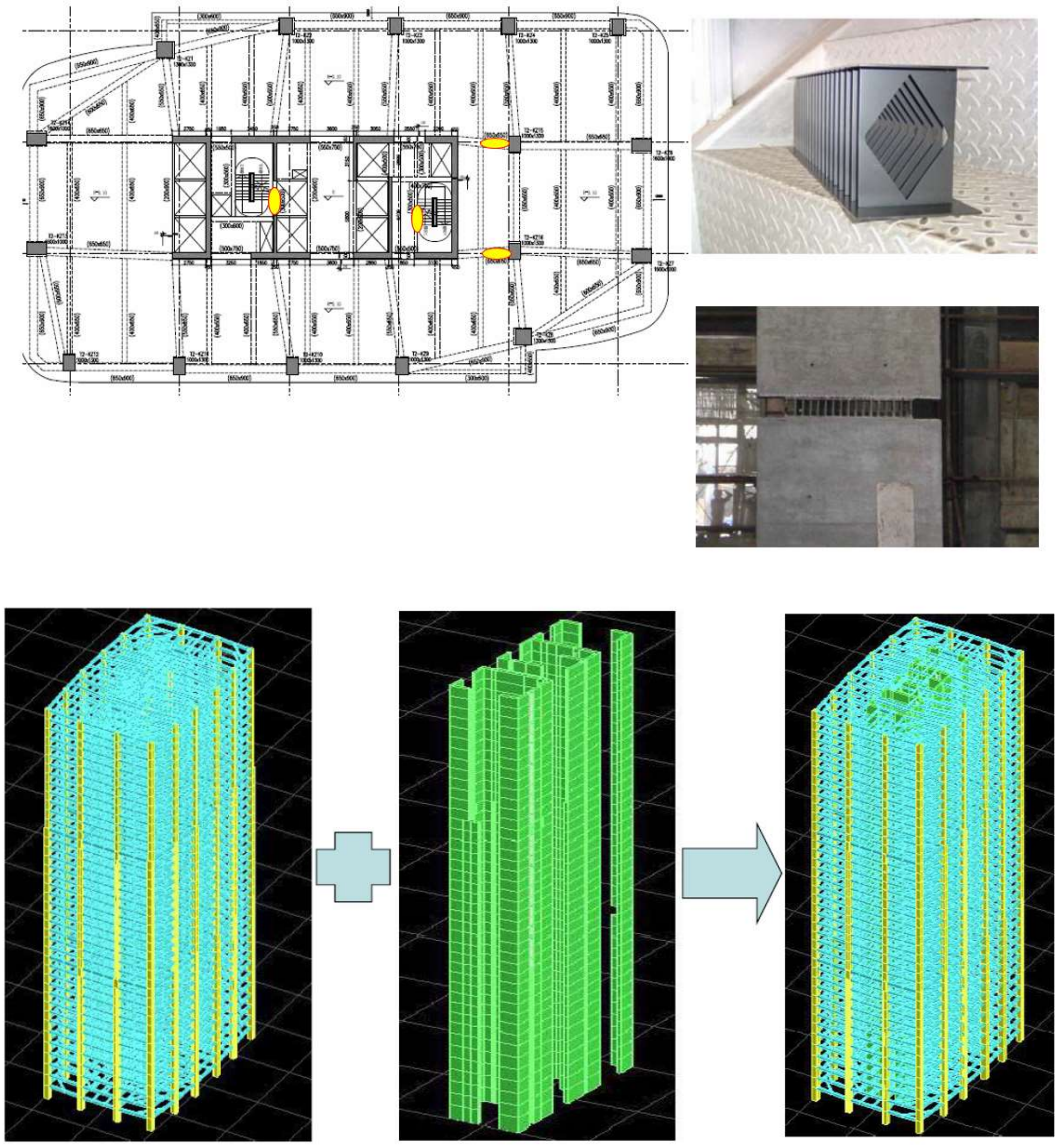
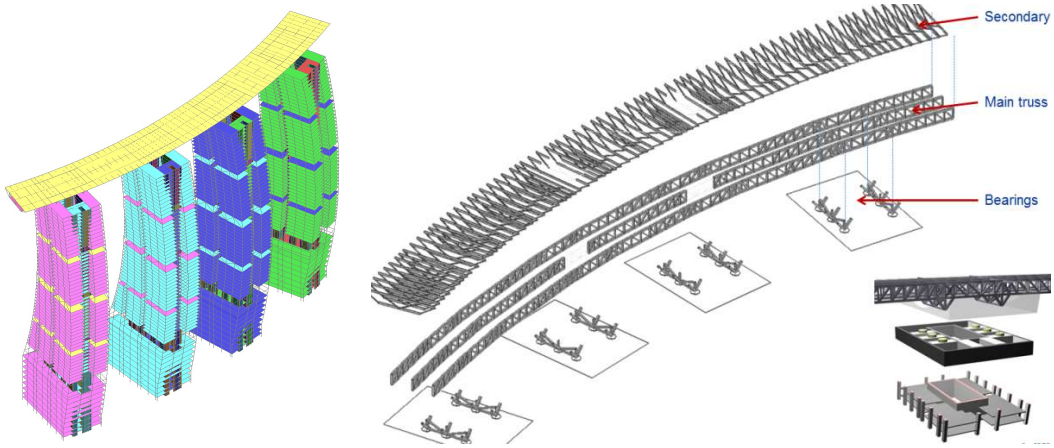


Figure 3. Application of low-yield steel damper

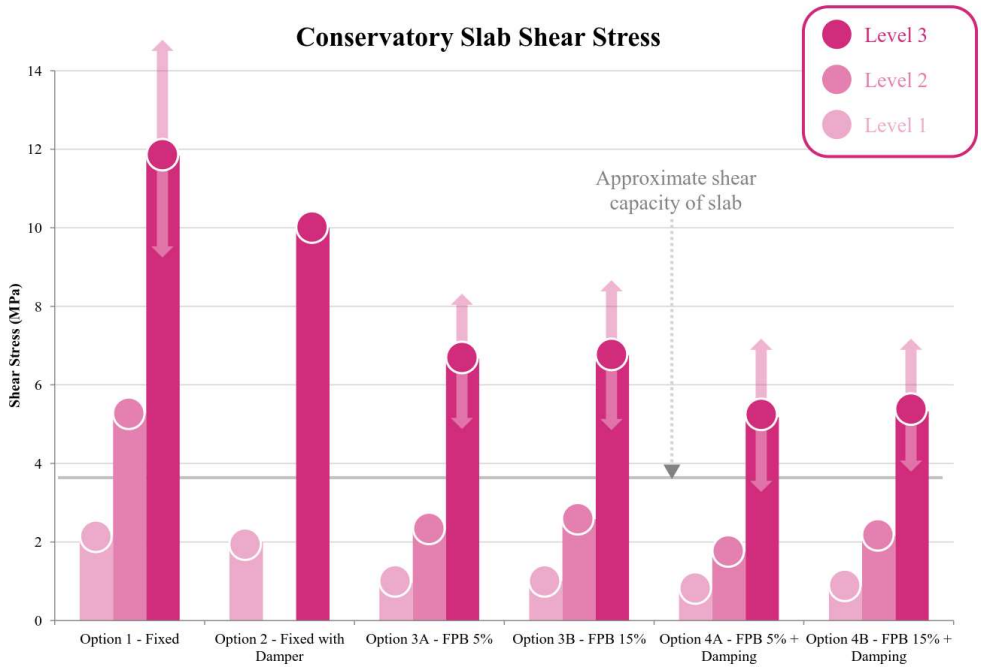
2.2 Intrinsic Mass Damping Design

The engineering design of RCCQ's conservatory allows for semi-continuous connection between the conservatory decking structures and four of the tower structures below. Figure 4a shows the overall structural configuration. Friction pendulum bearings (FPBs) were installed between deck structures and supporting towers A. A friction coefficient of 5% was chosen after detailed consultation with the FPB suppliers. FPBs work on the viscous damper principle by dispersing seismic energy during earthquakes, allowing relative movement between towers and conservatory. The overall engineering design also innovatively utilizes the mass of the conservatory itself, as a 'mass damper' to

both absorb seismic energy and control the lateral deflection of the tower structures. Figure 4b shows the overall effectiveness of the 'mass damping' effect on tower base shear for various levels of earthquake. Generally, a 35 to 40% base shear reduction is achieved by this innovative installation. This lead to significant materials savings in columns and core walls. A steel reinforced concrete (SRC) structural moment frame together with the core wall system was adopted for all of the 250m towers in RCCQ. The structural design of the project had to deal with multiple structural irregularities. The site is located in an Intensity 6.5 seismic zone of Chongqing.



a) Intrinsically engineered observatory and mass damper

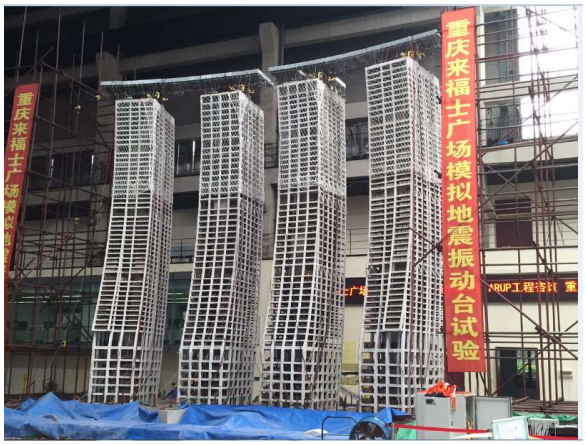


b) Effectiveness of mass damping

Figure 4. Intrinsically engineered mass damping

2.3 Shaking Table Tests

Shaking table tests on the linked towers verified the effectiveness of the 'mass damping' mechanism and the structural adequacy of the buildings, under moderate to extreme earthquakes. Figure 5 shows the test configuration for various levels of earthquake and Figure 5b shows the bearing details in a physical model at scale 1:25. The purpose of the earthquake simulation shaking table tests was to verify the rationality of the design calculations and structural provisions, and at the same time, provide guidance on the further strengthening at any particular weak portions revealed. The total self-weight of the model, shaking deck and counterweight was 252 tons. Taking account of the load capacities of the shakers, the four towers were placed on two shakers generating simultaneous earthquakes from various directions and at multiple magnitudes. Materials of suitable elastic moduli and strengths were chosen for the manufacture of the physical model. Concrete was modelled with mortar of corresponding strength. Steel wire simulated steel reinforcement. Encased steel sections were simulated with welded steel angles. The tests were conducted for a severe earthquake with an Intensity 6.5 as required by the China Seismic Code (MHURD, 2010). Generally, the structural design of the tower proved to be sound for the various levels of earthquake.



a) Table setup



b) Details of bearings

Figure 5. Shaking table tests on linked tower in RCCQ

3. Re-engineering the Composite Joint

The design and engineering of composite high-rise buildings demands high rigidity and ductile composite joints. The detailed requirements and design guidance are given in prevailing design codes (BSI, 2005; AISC, 2005; SCI & BCSA, 2002; MHURD, 2011). In RCH, structural design of the composite connection between concrete filled tubular (CFT) columns and steel reinforced concrete (SRC) beams needs to safeguard overall structural stability through fully rigid connections. The conventional ring beam type composite connection was regarded as too bulky and not suitable because of interference with façade erection and interior decoration. An innovative and high-performance corbel type of composite joint was accordingly proposed, which intrudes only minimally into the interior space and achieves the fully rigid connection (Lou & Wang 2015; Wang 2015). These proposed corbel type composite joints have the following key features as shown in Figure 6:

- **Corbel and ring stiffener are butt welded to the CFT column**

To ensure a full strength rigid connection, the I-section corbel is enlarged and stiffened by welding a ring stiffener inside the steel tube, such that the overall rigidity and load carrying capacity of the connection is not less than that of the typical SRC full beam section.

- **Tapered section from corbel to steel beam**

To ensure smooth loading and stress transfer from the corbel to the ordinary SRC beam in the joint region, a tapered steel section is proposed with a slope of 1:6.

- **Steel section within the SRC beam**

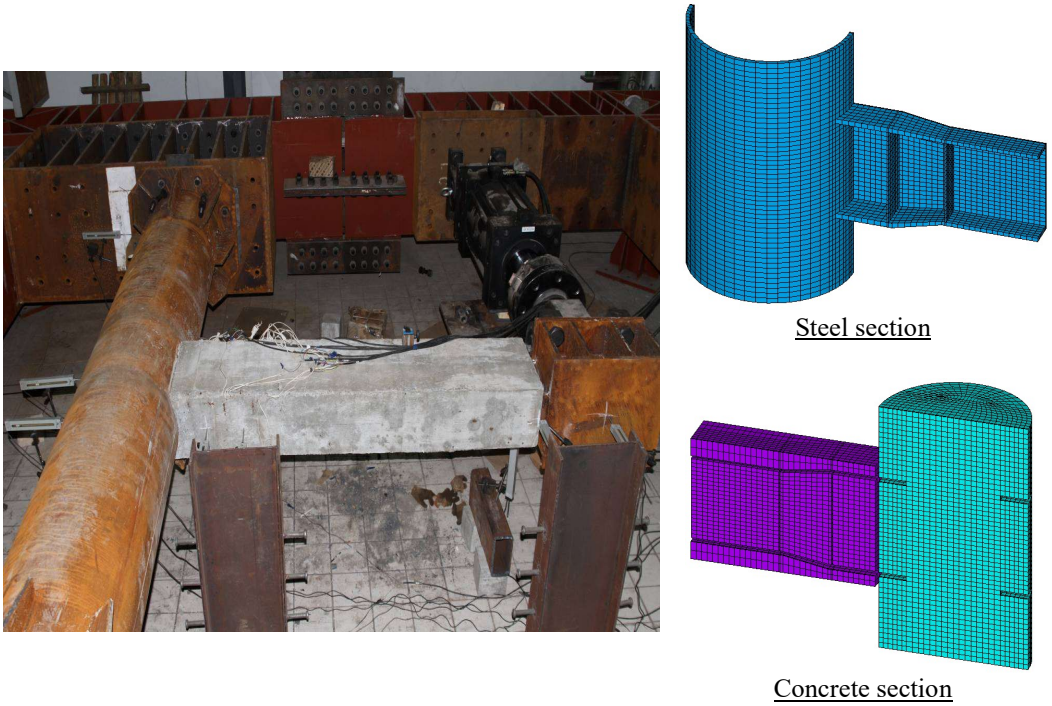
An ordinary I-steel section in the composite SRC beam is fully connected to the outer edge of the corbel through fully bolted joints on both flanges and webs.

- **Lapped reinforcement bars**

All the longitudinal reinforcement bars are lapped along the flanges of the steel corbel, so that both loads and stresses can be fully transferred from the longitudinal main reinforcement bars onto the corbel in the connection region.

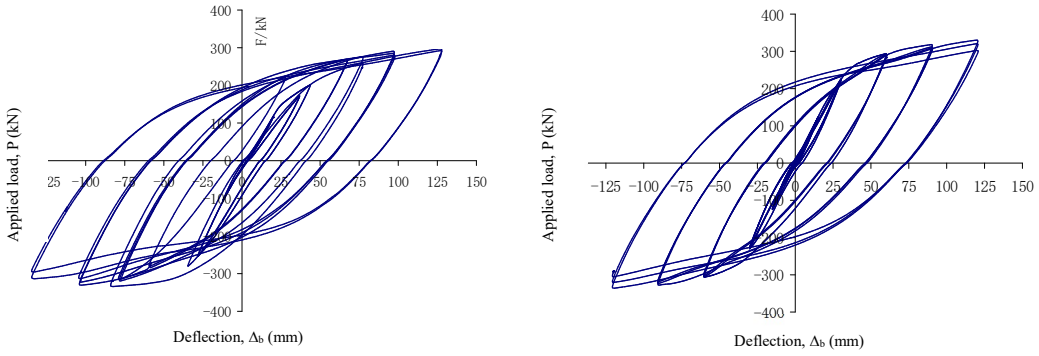
Physical tests, under both static and cyclic loads, were conducted to investigate the load carrying capacities and deformation characteristics of this new type of composite connection in compliance with both ASTM (2011) and CABR (1997). Figure 6a shows the overall testing arrangement. A variety of structural responses were examined in detail, including load-deformation characteristics, the development of sectional direct and shear strains, and the history of cumulative plastic deformation and energy dissipation. A three-dimensional finite solid-element model was also proposed and carefully calibrated to take account of the materiasl, boundaries and geometrical non-linearities as shown in Figure 6b. Both experimental and numerical studies demonstrate the high rigidity, strength and rotation capacities of the corbel type composite connections, providing the detailed structural understanding necessary to underpin the practical engineering design and practice. Quasi-static cyclic loading tests were conducted on specimens SP3 and SP4. Figure 7 presents the load-deflection curves. The cumulative plastic deformations of specimens SP3 and SP4 measured 0.3 and 0.24 radians respectively, which respectively correspond to 88 and 80 times the first yield rotation of the composite connections. These results convincingly demonstrate the high ductility and energy absorbing capacity of corbel type composite joints.

A nonlinear three-dimensional finite element model was established using the finite element package ANSYS 12.1 (2011). The mesh structure of the model is shown in Figure 6b. To simplify the problem and save computation time, only half of the specimen was modelled. The simulation gives a quite close prediction of the load-deformation characteristics in the connection regions, on comparing with the load-deformation curves at the end of the connection corbel (Lou & Wang, 2015; Wang 2015). Figure 8 illustrates typical failure models for the corbel type composite joints, as observed in the physical tests and derived by numerical simulation. The corbel type composite joint, therefore, has been verified as one of high strength, rigidity and ductility and suitable for high rise buildings in seismic sensitive regions.



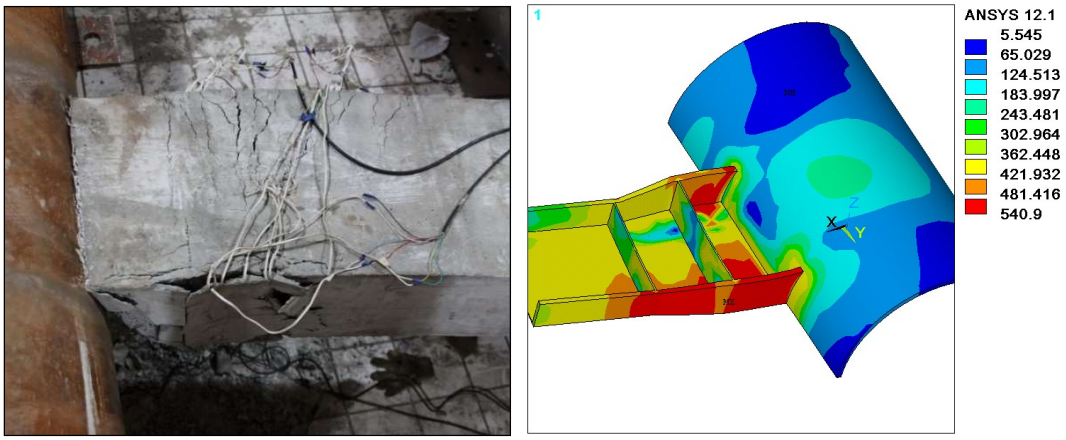
a) Test setup b) Finite Element Model

Figure 6. Connection test and numerical simulation



a) Specimen SP3 b) Specimen SP4

Figure 7. Load-deflection curves



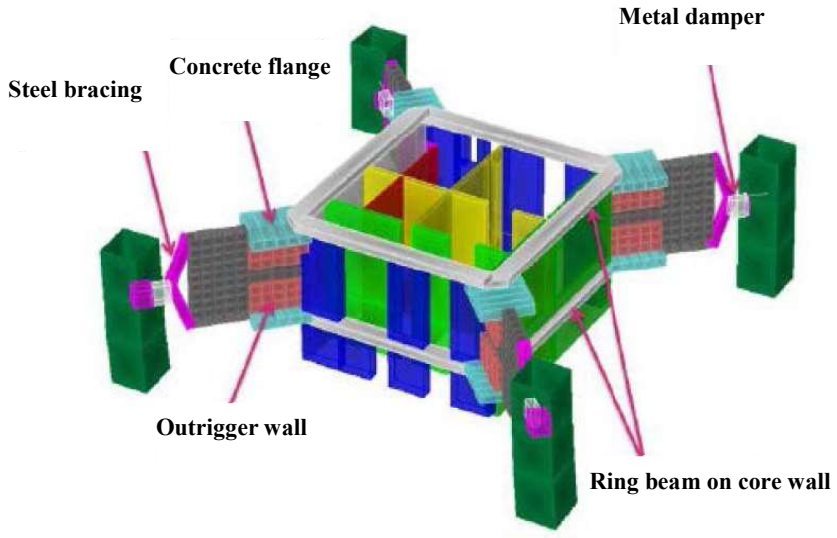
a) Test b) FEM

Figure 8. Typical failure mode

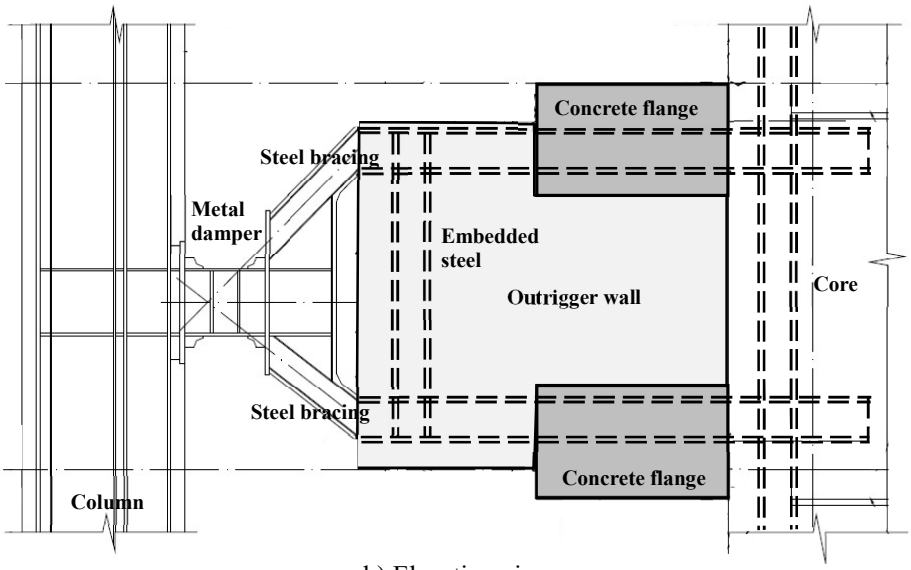
4. Hybrid Outrigger System with Dampers

A new type of steel-concrete hybrid outrigger system was developed for the two mega high-rise towers, 370 m tall, in Raffles City Chongqing (Wang 2015), where steel bracing is embedded into reinforced concrete outrigger walls as shown in Figures 9a and 9b. The steel bracing and concrete outrigger wall work compositely to enhance the overall structural performance of the tower structures under extreme loads. In addition, metal dampers of a low-yield steel material are used as a "fuse" device connecting the hybrid outrigger and the mega column. The dampers are engineered to be "sacrificed" and to yield first under moderate to severe earthquakes so as to protect the structural integrity of the important structural components of the hybrid outrigger system. Thus, brittle failure is not likely to occur, as a result of severe concrete cracking, implying a higher level of structural integrity and energy dissipation performance. In addition, the design may enable the contractor to "shoot" the core, by leaving in place the construction joints between core and outrigger walls, thereby shortening the overall period of construction, because the tedious welding of the steel outrigger truss on the refugee floors can be removed from the critical path.

Both experimental and numerical investigations were conducted into a new type of steel-concrete hybrid outrigger system for high-rise building structures. Finite-element models were proposed incorporating geometrical and material non-linearities. Key component and overall system tests were conducted, which revealed the detailed structural response under various levels of monotonic and quasi-static cyclic loads. The low-yield steel dampers were verified to be able to work effectively during earthquakes and so enhance overall structural performance. In addition, the hybrid outrigger system exhibited sufficient ductility under seismic action being effectively protected by the low-yield steel dampers as "fuse' devices.



a) 3-dimentsional view



b) Elevation view

Figure 9. Steel-concrete hybrid outrigger system

4.1 Component test on the Hybrid Outrigger Arm

Two specimens of hybrid outrigger arms were tested under monotonic and quasi-static cyclic loads as shown in Figure 10, which comprises steel bracing, embedded steel section and a concrete outrigger wall. Various key structural responses, including the load-deformation characteristics, the development of stress in steel members and the growth of cracks in concrete, were observed and studied, providing valuable insights into the load deformation characteristics and damage mechanism undergone by the hybrid outrigger arm under monotonic and quasi-static cyclic loads. No low-yield steel damper was included in this group of mechanical tests.

- **System Study of the Hybrid Outrigger System with Steel Dampers**

This group of tests was to study the performance of the overall hybrid outrigger system including the low-yield steel damper and hybrid outrigger arm, both connected to the column and core wall. The load-deformation characteristics due to monotonic and quasi-static cyclic loads were examined in detail. The damage and failure modes for various key components of the hybrid outrigger system were also examined.

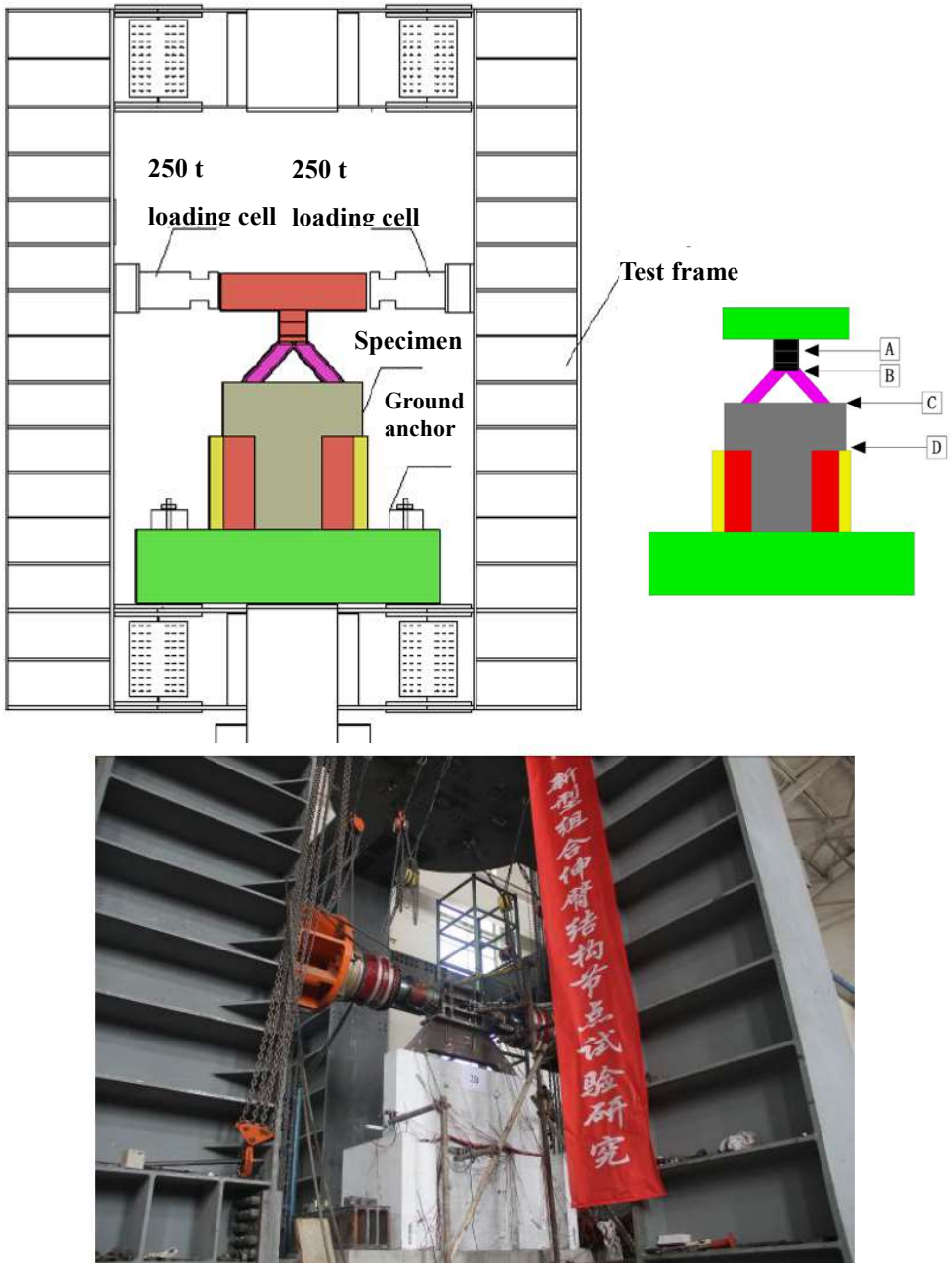
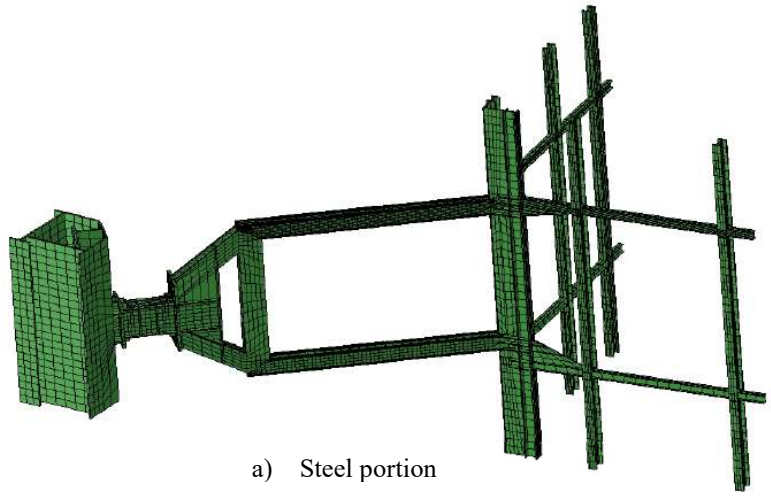


Figure 10. Test setup on hybrid outrigger system

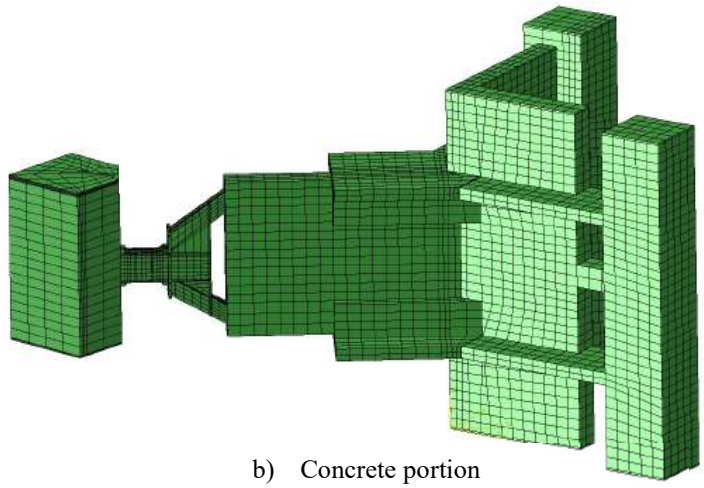
4.2 Numerical Modelling

Three-dimensional finite element models were studied with the geometrical and material non-linearities under monotonic loads as shown in Figure 11. Thus, the load-deformation characteristics of the outrigger system at both elastic and large-deformation plastic stages could be properly captured. The structural performance under various loading conditions was studied and calibrated specifically the load-carrying capacities, load-deformation curves, stress distribution, stress concentration, etc. Figure 4c illustrates a numerical simulation of the hybrid outrigger system under earthquake loading.

Figure 12 shows the overall test configuration and the load deflection curves due to cyclic actions. The hybrid outrigger system exhibited sufficient ductility under seismic actions, also effectively protected by the low yield steel metal damper 'fuse' devices. This showed the metal dampers worked effectively under Level 2 and Level 3 earthquakes and enhanced overall structural performance. Finite element modelling and physical component tests, both verified the effectiveness of the hybrid outrigger system.



a) Steel portion



b) Concrete portion

Figure 11. Finite element modelling on hybrid outrigger system

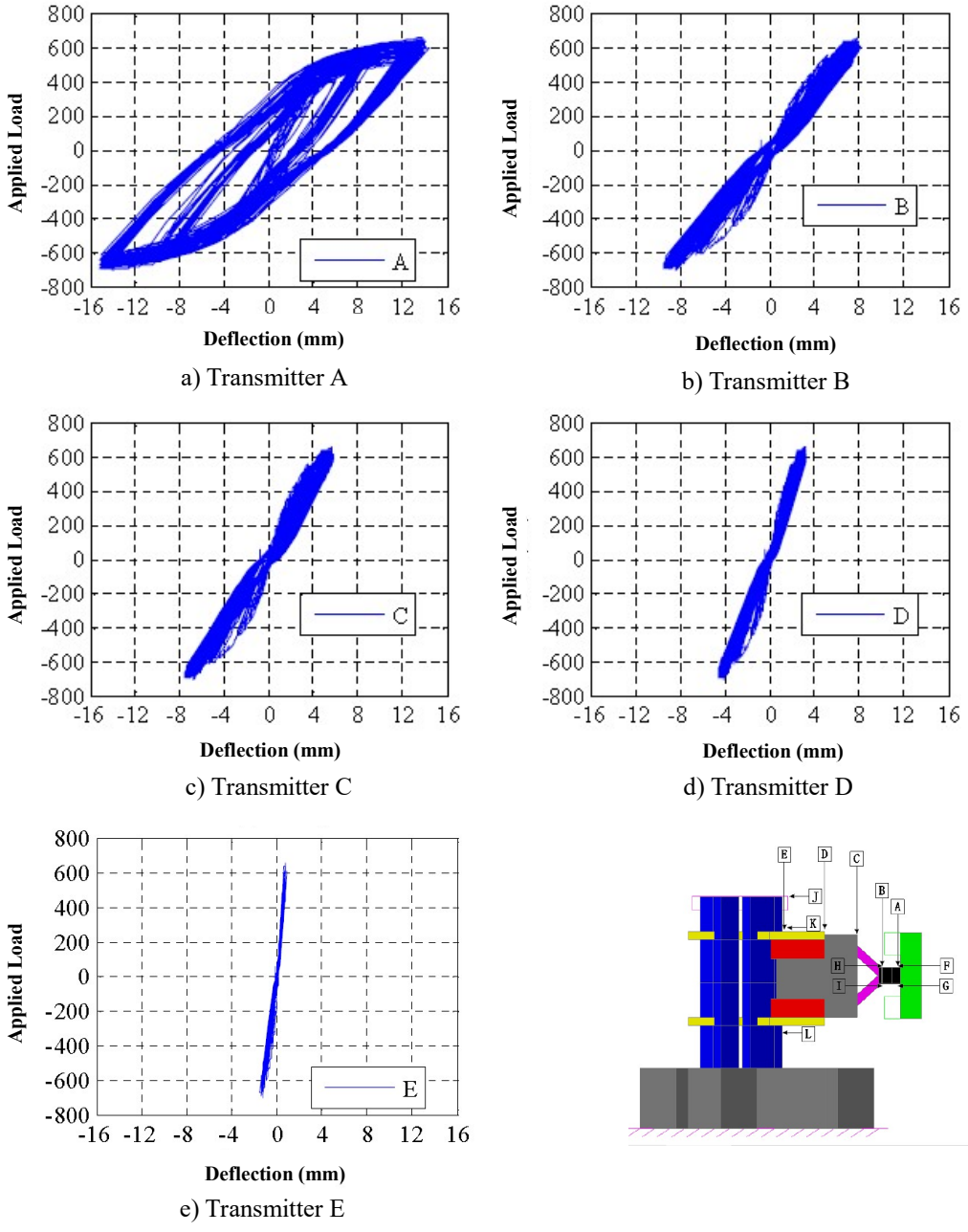


Figure 12. Performance of hybrid outrigger system under quasi-static cyclic loads

5. Conclusions

This chapter introduces current trends and innovations in seismic design and engineering practice in China, elaborated through case studies on several major and iconic projects. The following conclusions are reached.

- Seismic energy dissipation devices, such as dampers and isolating bearings, are becoming popular in high-rise buildings because they can enhance overall structural performance under disaster causing loads, as an alternative to additional steel and concrete. The proper adoption of seismic energy dissipation devices leads to higher engineering and architectural efficiency.
- The design and engineering of composite joints in high-rise buildings demands both high rigidity and ductility. Careful detailing is necessary to safeguard the overall structural stability, ductility and building functions.
- The proposed new type of hybrid outrigger system exhibited sufficient ductility under seismic actions, also effectively protected by the low yield steel metal damper 'fuse' devices. Both finite element modelling and physical component tests verified the effectiveness of the hybrid outrigger system. This showed that the metal dampers worked effectively under Level 2 and Level 3 earthquakes and enhanced overall structural performance and resilience.

References

AISC (American Institute of Steel Construction) (2005) ANSI/AISC 360-05: Specification for Structural Steel Buildings, AISC.

ANSYS (2011). User's Manual Version 12.1, ANSYS.

ASTM (2011) E2126-11: Standard Test Methods for Cyclic (Reversed) Load Test for Shear Resistance of Vertical Elements of the Lateral Force Resisting Systems for Buildings, ASTM.

Brockenbrough R. L. and Merritt F. S. (2006). Structural Steel Designer's Handbook, American Institute of Steel Construction.

BSI (British Standards Institution) (2005) Eurocode 3: Design of Steel Structures, Part 1.8: Design of Joints, European Committee for Standardization.

CABR (China Academy of Building Research) (1997) Specification of Test Methods for Earthquake Resistant Building, CABR.

Lou, G. B. and Wang, A. J. (2015) "Studies into a high performance composite connection for high-rise buildings." Steel and Composite Structures, 19(4), pp.789-809.

MHURD (The Ministry of Housing and Urban-Rural Development) (2008) Standard for Classification of Seismic Protection of Buildings: GB50223-2008.

MHURD (The Ministry of Housing and Urban-Rural Development) (2010) Code for Seismic Design of Buildings: GB50011-2010.

MHURD (The Ministry of Housing and Urban-Rural Development) (2015) Seismic Ground Motion Parameter Zoning Map of China: GB18306-2015.

MHURD (The Ministry of Housing and Urban-Rural Development) (2011) Technical Specification for Concrete Structures of Tall Buildings: JGJ3-2010.

MHURD (The Ministry of Housing and Urban-Rural Development) (2013) Technical Specification for Seismic Energy Dissipation of Buildings: JGJ297-2013.

MHURD (The Ministry of Housing and Urban-Rural Development) (2012) Dampers for Vibration Energy Dissipation of Buildings: JG/T209-2012.

SCI (The Steel Construction Institute) and BCSA (the British Constructional Steelwork Association Limited) (2002) Joints in Steel Construction, the Steel Construction Institute.

Wang, A. J. (2015) "Re-engineering composite connections for a higher construction and cost Effectiveness." Proceedings of 11th International Conference on Advances in Steel and Concrete Composite Structures, pp. 538-543, Tsinghua University, Beijing, China.

A Probabilistic Seismic Hazard Map of India

S.T.G. Raghukanth, J. Dhanya and P. Muthuganeisan

Department of Civil Engineering
IIT – Madras, India

Engineers require hazard estimates for the retrofitting of existing structures and for the safe design of proposed structures. In India, the looming seismic risk to our cities can be perceived in the backdrop of active faults in the Himalayas and the Indo-Gangetic plain. Even in the less active peninsular region, strong earthquakes can cause considerable damage. The prognosis of seismic hazard plays a key role in planning and protecting buildings, life line facilities, industries and other safety sensitive structures. This necessitates estimation and quantification of future ground vibration. This chapter highlights how seismic hazard can be estimated at hard rock sites (A-type) in India. The chapter also discusses the application of the hazard contours developed in ascertaining the design values for a site. All known data about past earthquakes and mapped faults have been taken into account in characterizing the seismic activity levels of the thirty-two source zones in the country. Geologically, India is divided into seven homogeneous regions. Ground motion prediction equations (GMPE) are derived for all seven regions using a finite source seismological model. State-of-the-art probabilistic hazard analysis is carried out covering the whole country on a grid size of $0.2^\circ \times 0.2^\circ$. Contours of peak ground acceleration (PGA) for short period and long period spectral accelerations, for 2500yrs return periods, are obtained for India.

Keywords: PSHA, seismic hazard maps

1. Introduction

India faces threats from a variety of natural hazards such as floods, droughts, landslips, cyclones, earthquakes and tsunamis. The spate of earthquakes in the recent past, causing extensive damage has heightened the sensitivity of administrators, engineers and the general public to the looming hazard of future earthquakes occurring near densely populated Indian cities. Strong earthquakes are rare events, rarer than cyclones, windstorms and tidal waves. Nevertheless, India has seen quite a few earthquakes in the recent past. Earthquakes have occurred from pre-historic times, more or less in the same regions, as they are presently experienced. The present heightened awareness towards earthquake disaster mitigation in the country is attributable to the large loss of life and property suffered during the Khillari (30th September 1993), Jabalpur (22nd May 1997), Chamoli (29th March 1999), Bhuj (26th January 2001) and Nepal (25th April 2015) earthquakes. The level of seismic hazard predicted at any given site cannot be altered by the occurrence of an earthquake event, but the risk faced by human habitat due to earthquakes can be reduced by making man made systems and structures less vulnerable and more robust to withstand ground motions. Seismic risk has the characteristic of increasing with time if continuous mitigating actions are not taken. This fact may be appreciated by recognizing that increasing population puts greater demands on the housing, energy, water and transport needs of society. In turn, these needs have to be met by increased construction activity, of buildings, dams, reservoirs, bridges, power plants

etc. Thus, even in areas of low seismic activity, the loss due to unexpected earthquakes may be high due to heavy infrastructure development, unless the new structures are engineered and maintained to withstand future earthquakes.

It is not just new construction that has to be made earthquake resistant. Engineers are called upon to protect existing cities, monuments and other structures built at a time when knowledge about earthquakes was limited. Moreover all types of construction may not be equally important, particularly so, when available financial resources are limited. Damaging earthquakes are rare, with recurrence periods being of the order of several decades or centuries. But once they occur, due to the ground vibration the resultant catastrophe can be huge if proper precautionary measures are not implemented. Hence, engineers usually characterize seismic hazard in terms of the ground motion that can be experienced at the construction site. This way the dynamic response of structures can be studied to foresee where they may fail and for what level of seismic forces. This in turn helps in site selection, design and retrofitting strategies. The point to be noted here is that the quantification of hazard is needed for unpredictable future events. The nature and amplitude of ground motion at a site can be described in a probabilistic sense by combining past information with engineering methods of risk estimation.

This chapter focuses on estimating the hazard posed by earthquakes in India. For this the seismic characteristics of the region need to be studied and implemented in the hazard model to ascertain hazard in terms of peak ground acceleration and short and long period spectral accelerations for the hard rock (A) type site condition. Further, an illustration of the hazard deaggregation procedure, to identify the controlling fault and the magnitude at a site is performed. In addition, it is known that the design of a structure should account for the local site condition. The procedure proposed in IBC (2009) to obtain site specific design response spectra from short (T=0.2s) and long period (T=1s) spectral acceleration values is discussed in Appendix A.

2. Seismicity and tectonic setting of India

The Indian sub-continent has experienced several moderate to large earthquakes owing to the under thrusting of the Indian plate against the slow-moving Eurasian plate. This collision phenomenon has resulted in several major tectonic faults in the Indian sub-continental region. Since these faults are fractured zones, they have a higher rupture potential to generate seismic events at a rate depending on the amount of stress build up. The identification of these potential rupture areas is crucial for assessing the probable seismic hazard of a study region. The Seismotectonic Atlas of India GSI (2000) has delineated the faults identified in India and its adjoining region which have been used to construct the fault map of India shown in Fig. 1. By overlapping the seismicity of India over the fault map (Fig. 2), it becomes apparent that the regions coinciding with the boundary of the Indian tectonic plate exhibit higher levels of seismic activity. These regions are the Hindukush-Pamir region in the North West, the Himalayan arc in the North and the Burmese-Andaman arc in the East. The Himalayan arc borders the entire northern part of the Indian sub-continent and its formation can be attributed to the northerly dipping continental collision. Some of the major fault systems identified along the Himalayan range are the Indus Suture Thrust, the Main Frontal Thrust (MFT), the Main Central Thrust (MCT) and the Main Boundary Thrust (MBT). These fault systems of the Himalayan range have caused several devastating earthquakes such as the Kangra earthquake (M7.8, 1905), the Bihar-Nepal earthquake (M8, 1934), the Uttarkashi

earthquake (M6.8, 1991), the Chamoli earthquake (M6.8, 1999), the Sikkim earthquake (M6.9, 2011) and the Nepal earthquake (M7.8, 2015), etc. High seismicity is also observed at both the ends (syntaxis) of the Himalayan range. The western syntaxis is marked by several prominent faults, namely, the Main Karakoram Thrust (MKT), the Main Mantle Thrust (MMT), etc. Further to the west, the Hindukush-Pamir region is seismically very active, experiencing several major earthquakes of magnitudes above seven, e.g. the Kashmir earthquake (M7.6, 2005). To the south of the Hindukush region, the Chaman fault marks the western plate boundary. The eastern end of the Himalayan arc is also a region of very high seismicity and has produced several major earthquakes, namely, the Assam earthquake (M8.1, 1897), the Assam-Tibet earthquake (M8.6, 1950), etc. The N-S trending Burmese-Andaman arc marks the eastern plate boundary and runs southward from the Assam syntaxis (located at the North-Eastern edge of the Himalaya) to the Andaman-Nicobar archipelago. The Sagaing fault and the Eastern Boundary Thrust Zone, etc. are some of the major fault systems. Several subduction events have been recorded in this region, notably, the tsunamogenic Andaman-Sumatra earthquake (M9.3, 2005).

Apart from the above regions, the stable continental region has also experienced numerous large magnitude intra-plate events such as the Kutch earthquake (M7.7, 2001), the Koyna earthquake (M6.5, 1967), the Killari earthquake (M6.2, 1993), the Jabalpur earthquake (M6, 1997), etc. The Himalayan region and peninsular India are separated by the sediment plains of the Indo-Gangetic foredeep with its very low seismicity. However, extensive damage witnessed during the Bihar-Nepal earthquake (M8, 1934) indicates that these sediment plains can cause significant amplification of the ground motion when major events occur in the lower Himalayas.

Thus, from the exhibited seismicity characteristics it can be observed that certain regions are more active than others. This activity is correlated to the past events and the location of faults and lineaments. But, all past events need not be uniquely identified with a particular fault. This postulates the diffusion of aerial sources in some places to be the cause of seismic activity. However, only line sources are considered in this study and all the known activity is associated to the mapped faults. Depending on the pattern of epicentres and fault alignments, 32 seimogenic zones have been identified for the Indian subcontinent as shown in Fig. 2. Here, in addition to the faults considered in NDMA (2011), the Teesta lineament, due to its proximity to the epicentre of the Sikkim earthquake (M6.9, 2011) has been added to the fault model. The resulting fault based source model consists of 936 fault segments and 32 seismogenic zones (SZ). Among these 32 zones, the active zones are SZ: 1 to 4 (Himalayan range), SZ: 5 and 8 (North-eastern India region), SZ: 30 (Hindukush-Pamir), SZ: 21 to 26 (Chaman fault), SZ: 10 to 15 (Andaman region) and SZ: 27 (Kutch). The seismic characterizations of these source zones, as well as faults, require complete information of their past seismic activity. The following section briefly discusses the process of collecting and compiling a database of the sizes and occurrence times of past earthquakes.

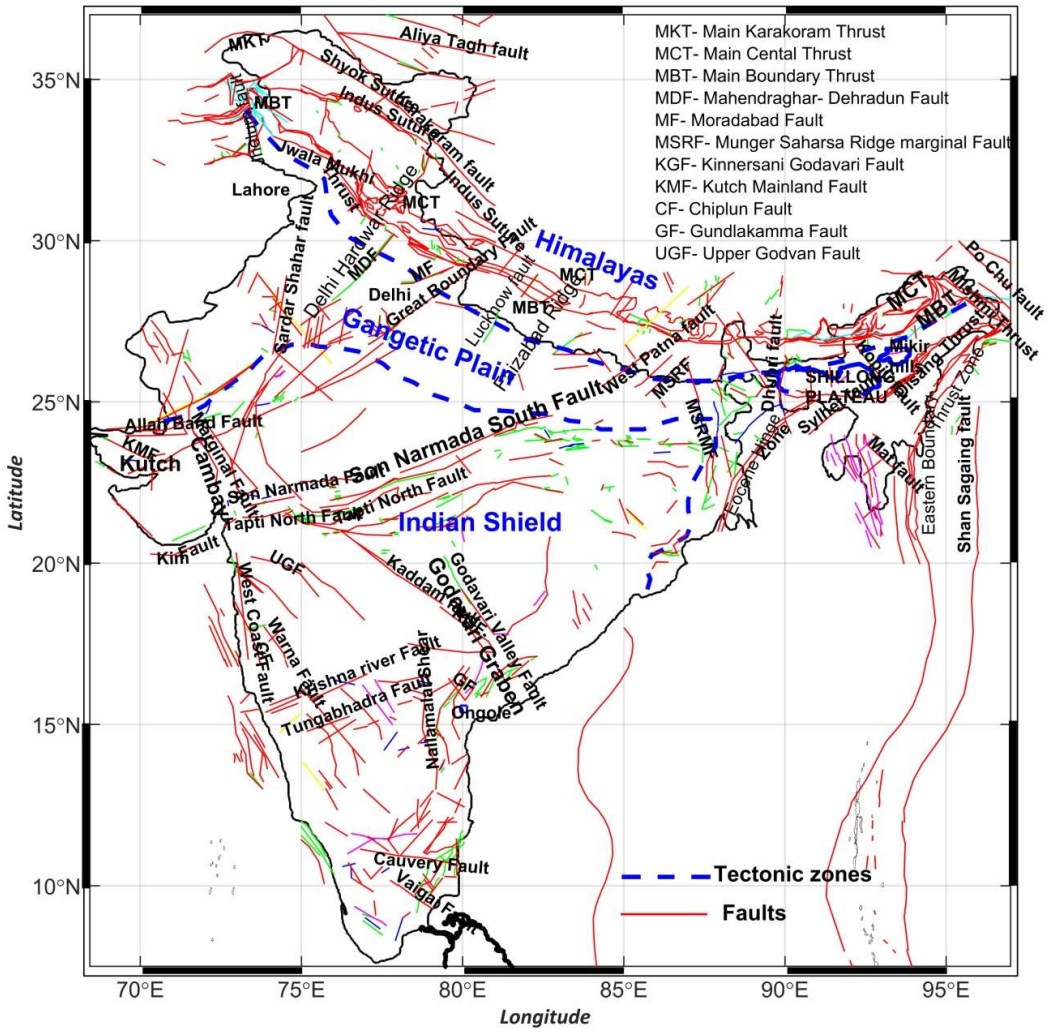


Figure 1. Fault map of India (Geological Survey of India (GSI), 2000; Balakrishnan et al., 2009; NDMA, 2011).

3. Earthquake catalogue and recurrences

3.1 All India Catalogue

The next stage of seismic hazard analysis is the characterization of the seismicity of the potential sources identified in the section above. This requires the assembling of a comprehensive database of past seismic records, referred to as an earthquake catalogue, which contains information on the magnitudes, spatial, and temporal occurrences of the events. A robust earthquake catalogue is a prerequisite for assessing the seismicity of each of the identified probable sources. These data were sourced from available records (instrumented or by examining historic transcriptions) or by paleoseismic studies. The most reliable records are those deriving from instrumental data, which is available for the study region from the seismic instrumentation network of the Indian Meteorological Department (IMD), the International Seismological Centre (ISC), the U.S. Geological

survey (USGS), and the Pakistan Meteorological Department (PMD). Some of the earlier historical events in these regions have been reported by Oldham (1883); Milne (1911) for the period between 1664 and 1899 AD. Quittmeyer and Jacob (1979) have reported the events during 1914 to 1965 AD. The data from paleoseismic investigations based on the available geomorphologic evidence helps to identify large magnitude events that have recurrence periods of several 100 years. The seismic catalogue of India was recently assembled by NDMA (2011) for the period up to 2008 AD. The data in this catalogue is a composite derived from the three sources, instrumental data, historical data retrieved from government archives and data gathered from paleoseismic investigations. The earliest data in this catalogue is approximately estimated to have occurred in 2475 BC with a M7.3 magnitude at Dholavira in Gujarat (NDMA 2011).

In this report, the above catalogue developed by (NDMA 2011) has been updated by including the events of magnitude M>4 recorded during the period 2009-2016 AD. These additional events were obtained from instrumented data available at the earthquake databases of the International Seismological Centre (ISC) and the US Geological Survey (USGS) (url: http://earthquake.usgs.gov/earthquakes). With the addition of 7449 events recorded between 2009 and 2016, the catalogue for the study region (which is bounded by latitudes: 2° N - 40°N and longitudes: 61° E-100° E) contains a total of 46310 events. The reported magnitudes in other magnitude scales, such as body wave magnitudes have been converted to the moment magnitude based on the conversion relationships of Scordilis (2006). This updated homogeneous catalogue has to be de-clustered and forms the basis for estimating the seismicity parameters of the considered seismic sources shown in Fig. 2. De-clustering is essential as the estimation of recurrence parameters assumes the sample data series to be temporally statistically independent. Aftershocks and foreshocks are admittedly dependent on the main shock and hence such events get clustered in a general catalogue. Here the widely used de-clustering approach introduced by Gardner-Knopoff-Uhrhammer (Gardner and knopoff 1974; Uhrhammer 1986), is used to remove time-dependent events from the earthquake catalogue. The de-clustered catalogue contains a total of 24365 independent events of magnitude M≥4. This includes 4,820 independent events recorded between 2009 and 2016.

The all India catalogue developed in this study is a combination of instrumental, historic and pre-historic data. As such, the completeness of magnitudes in time has to be established before proceeding further. Here the widely used visual approach by Stepp (1972) was applied to determine the complete part of the catalogue in specific magnitude ranges. The earthquake data is grouped into seven magnitude classes; 4≤Mw<5, 5≤Mw<6, 6≤Mw<7, 7≤Mw<8 and 8≤Mw. With a time interval of 10 years, the average number of events per year in each magnitude range is determined. If x1, x2, ...xn are the number of events per year in a magnitude range, then the mean rate for this sample is :

$$\chi = \frac{1}{n}\sum_{i=1}^{n} x_i \tag{1}$$

where n is the number of unit time intervals. The variance is given by

$$\sigma_x^2 = \frac{\chi}{T} \tag{2}$$

where T is the duration of the sample. If χ were to be constant, $\sigma\chi$ would vary as $1/\sqrt{T}$. Following Stepp (1972) the standard deviation of the mean rate as a function of sample length

is plotted along with nearly tangent lines with slope $1/\sqrt{T}$. The deviation of the standard deviation of the estimate of the mean from the tangent line, indicates the length up to which a particular magnitude range may be taken to be complete. The standard deviation shows stability in shorter windows for smaller earthquakes and in longer time windows for large magnitude earthquakes.

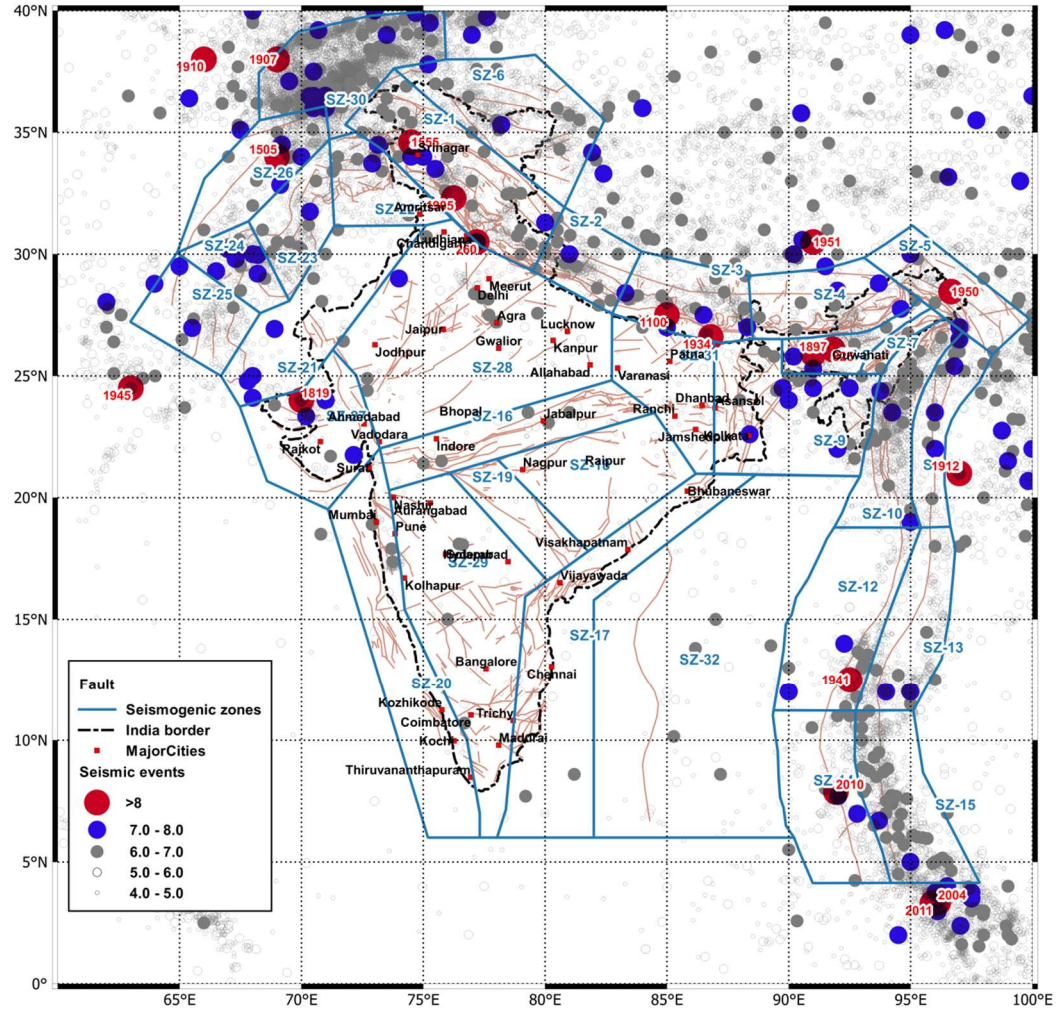


Figure 2. Seismicity and seismogenic zones of India

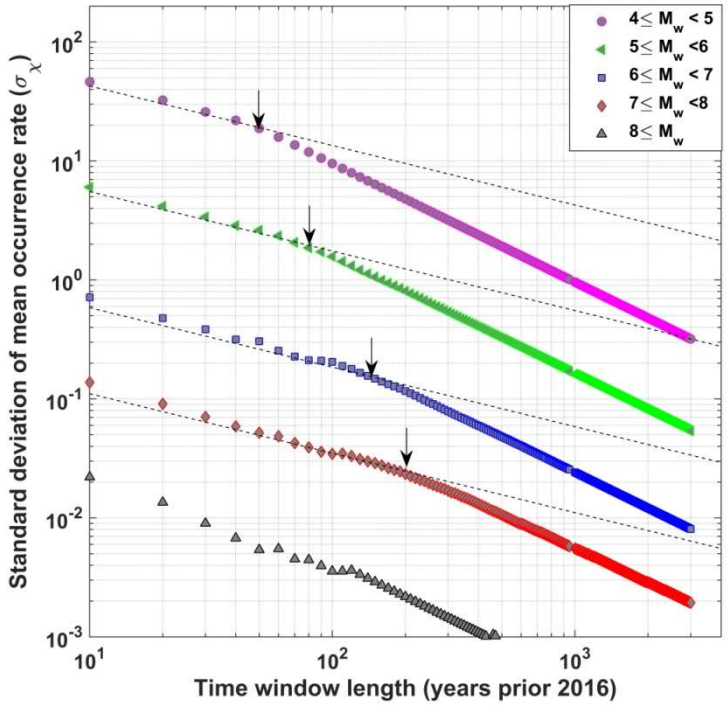


Figure 3. Completeness test of Indian earthquake data. Dotted lines have constant slope: $1/\sqrt{T}$

The standard deviation of the mean of the annual number of events as a function of sample length for the all India data is shown in Fig. 3. This provides an easy criterion for testing the completeness of the data. Accordingly, the completeness intervals for the all India catalogue are estimated to be 50 years (1966-2016) for magnitudes 4≤M<5; 80 years (1936-2016) for magnitudes 5≤M<6; 140 years (1876-2016) for magnitudes 6≤M<7; 200 years (1816-2016) for magnitudes 7≤ M<8. The complete period for magnitudes M≥ 8 is taken to be the entire available range. The completeness period of the catalogue is clearly demarcated in Figure 4.

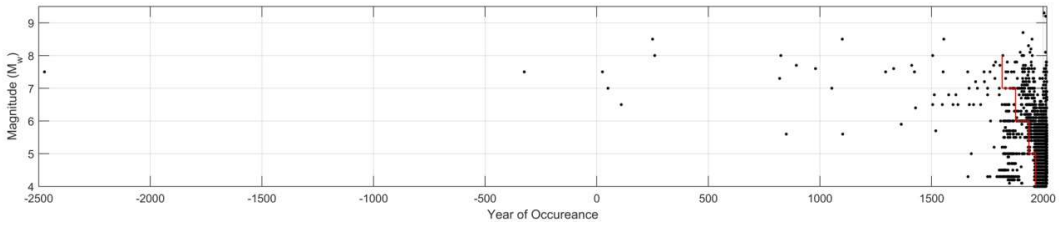
3.2 Recurrence

The seismic activity of a source zone is characterized by the Gutenberg-Richter (G-R) recurrence relation

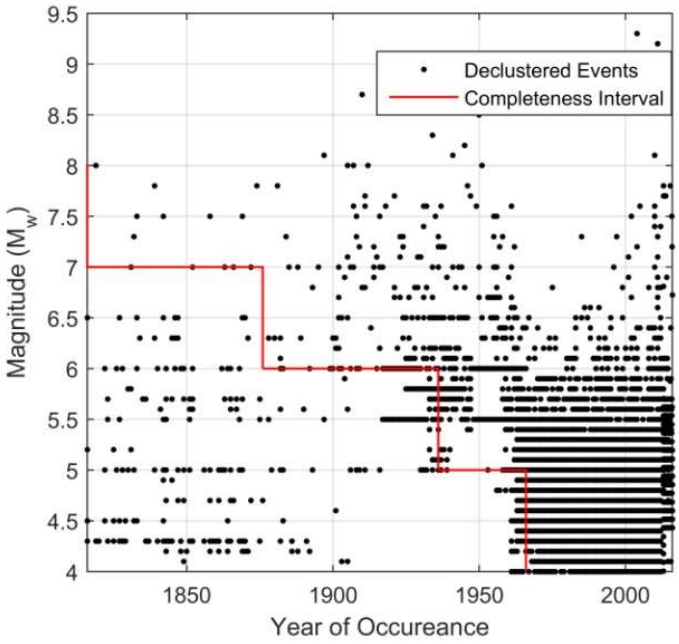
$$\log_{10} N(m) = a - bm \tag{3}$$

Here, N(m) is the number of earthquakes greater than or equal to magnitude m. The (a, b) values characterize the seismicity of the region. A lower b value means that out of the total number of earthquakes, a larger fraction occurs at the higher magnitudes, whereas a higher b value implies a larger fraction of low magnitude events in the catalogue. Although the value of b varies from region to region, it lies typically in the range 0.6 < b < 1.5. The general level of earthquake activity in a given area during the study period is represented by the parameter a. The value of a directly indicates the number of (Mw > 4) earthquakes per year. The seismic hazard at any site is controlled by the parameters (a, b). Knopoff and Kagan (1977) demonstrated that an upper bound magnitude (Mmax) has

to be introduced if the G-R relation is to be applied further in a realistic fashion. The catalogue developed for India is a combination of instrumental, historic and pre-historic data of differing quality. Large uncertainties in the magnitude values and locations have to be accounted for by probabilistic hazard analysis. These issues can be addressed using the procedure of Kijko and Graham (1998) and Kijko (2002). This method assumes a Poisson distribution for earthquake occurrences with activity rate N(m) and a truncated G–R relationship for magnitude values. The uncertainty in the estimation of magnitudes and time of occurrence of earthquakes can be incorporated in deriving the parameters. Further computation of the parameters (a, b) by the maximum likelihood method of Kijko and Graham (1998) requires the earthquake catalogue to be partitioned into two parts called extreme and complete. The extreme part refers to the time interval where information on large historical events only, is available. The complete part represents the time period in which information on both large as well as small magnitude earthquakes is available. This partitioning of the catalogue is carried out systematically using the method of Stepp (1972) as discussed above.



(a) Complete catalogue



(b) Zoomed to 1816-2016

Figure 4. Time distribution of earthquakes

The seismic parameters, namely (a, b) and the potential maximum magnitude (Mmax) are estimated for the thirty-two tectonic sesimogenic zones. Since earthquakes with magnitudes less than 4 do not cause structural damage, the threshold magnitude (m0) is taken as 4 Based on the completeness test of magnitude class $4 \leq M_w < 5$, the data set is divided into a *complete part* (1966-2016) and an *extreme part* (-1965) for all 32 regions. The starting points of the extreme part of the catalogue for each region are different and taken as the year of first occurrence of an earthquake in that particular region. Once the catalogue was divided in time, the standard computer program developed by Kijko and Graham (1998) was used for determining the earthquake recurrence relationship. The uncertainty in the reported magnitudes was taken as 0.5 in the extreme part. For the complete part, the magnitude uncertainty was assumed to be 0.3 (Giardini et al 2004). The three seismic parameters [N(4), b and M_{max}] for all the thirty-two zones are reported in Table 1. Since earthquakes occur frequently in the Himalayas, ANI and NEI, catalogues in these zones are fairly complete for both small and large earthquakes. Hence uncertainty in the estimated parameters is low in these regions. In the Indo-Gangetic Plain, Gujarat, Central India and Peninsular India, the catalogues contain fewer samples and hence the errors in the estimates are higher. The recurrence relationship for all the 32 regions is shown in Table 1. It can be seen that most zones have a maximum magnitude potential of $M_w > 7$. Also, eleven have $N(4) > 5$ which means that they produce at least 5 events of $M_w > 4$ every year. It can be observed that the seismogenic zones SZ: 1, SZ: 3, SZ: 5 and SZ: 30 have the highest maximum magnitude potential. While the Hindukush-Pamir and the Andaman regions have the highest annual occurrence of earthquakes with magnitude $Mw \geq 4$. The bounded G-R distribution for recurrence relationships are shown in Fig. 5 for all 32 zones. It can be clearly seen that the Hindukush region (SZ: 30) has the highest seismic potential followed by the Andaman region (SZ: 15).

Since the faults within the same zone exhibit varying levels of seismicity, it may be even more appropriate to consider the fault level recurrences. However, the gaps in the existing catalogue and a lack of information on the slip characteristics of the faults make it difficult to achieve a clear consensus on the rupture potential of all the identified faults. In order to circumvent this issue, a heuristic approach to disaggregate the zonal parameters obtained earlier was adopted here. In this approach, the zonal parameter 'N(4)' is disaggregated to individual faults while conserving the regional seismicity. Thus, the fault specific N(4) values are estimated by taking into consideration the potential of a fault to rupture and known activity. The background seismicity within a source zone is also taken into consideration by associating these events with the nearest faults in the zone. The disaggregation factor for an individual fault is obtained as the average of fault length ratio and fault activity ratio. The fault length ratio is defined as the ratio of individual fault length (l_i) to the sum of the length of all the faults in the zone (L_z). Similarly, the fault activity ratio is defined as the ratio of the number of fault-level events (s_i) to total zonal events (S_z). Thus, N(4) of ith fault is determined as:

$$N_i(4) = 0.5\left(\frac{s_i}{S_z} + \frac{l_i}{L_z}\right) N_z(4) \tag{4}$$

where $N_z(4)$ is the zonal value of N(4).

Table 1. Seismicity parameters for 32 seismogenic zones of the study region

ID	Zones	b	N(4)	M_{max}	No. of Events
1	Western Himalaya	0.90±0.02	5.61±0.60	8.8	179
2	Central Himalaya-I	0.77±0.03	3.44±0.53	7.8	377
3	Central Himalaya-II	0.80±0.03	2.39±0.31	8.8	403
4	Eastern Himalaya	0.74±0.03	2.87±0.54	8.0	243
5	Mishmi Block	0.68±0.02	3.81±0.77	8.8	263
6	Altya Tegh and Karakoram	0.95±0.02	8.46±1.39	7.3	873
7	Naga Thrust	0.69±0.07	0.29±0.07	7.1	38
8	Shillong plateau & Assam	0.76±0.03	2.00±0.34	8.4	200
9	Bengal Basin	0.75±0.03	2.00±0.22	8.1	330
10	Indo-Burmese Arc	0.82±0.02	12.04±1.74	7.8	1126
11	Shan-Sagaing fault	0.68±0.03	5.64±1.11	8.1	319
12	West Andaman-I	0.73±0.02	4.38±0.81	8.4	334
13	East Andaman-I	0.66±0.02	6.14±1.15	7.5	398
14	West Andaman-II	0.74±0.02	5.35±1.15	8.4	333
15	East Andaman-II	0.63±0.01	15.74±2.29	7.6	1119
16	SONATA	0.63±0.07	0.47±0.12	6.8	33
17	Eastern Passive margin	0.80±0.07	0.36±0.07	6.3	42
18	Mahanandi Graben & Eastern Craton	0.79±0.09	0.30±0.10	5.8	27
19	Godavari Graben	0.85±0.09	0.10±0.06	5.6	20
20	Western Passive Margin	0.87±0.06	0.33±0.05	6.8	76
21	Sindh-Punjab	0.80±0.05	0.73±0.13	8.0	103
22	Upper Punjab	1.06±0.04	1.91±0.30	7.8	258
23	Koh-e-Sulaiman	0.88±0.03	5.69±1.01	7.3	433
24	Quetta-Sibi	0.76±0.03	6.27±1.23	7.8	328
25	Southern Baluchistan	0.77±0.04	3.25±0.62	8.1	240
26	Eastern Afganistan	0.95±0.03	5.89±0.9	8.3	627
27	Gujarat region	0.98±0.05	0.80±0.14	8.3	105
28	Gangetic region	0.87±0.05	1.41±0.25	7.4	128
29	Southern Craton	1.14±0.07	0.63±0.13	6.8	45
30	Hindukush and Pamirs	0.97±0.01	100.23±8.3	8.3	8108
31	Gangetic region	0.89±0.08	0.33±0.08	6.3	31
32	Bay of Bengal	0.63±0.06	1.07±0.26	6.8	75

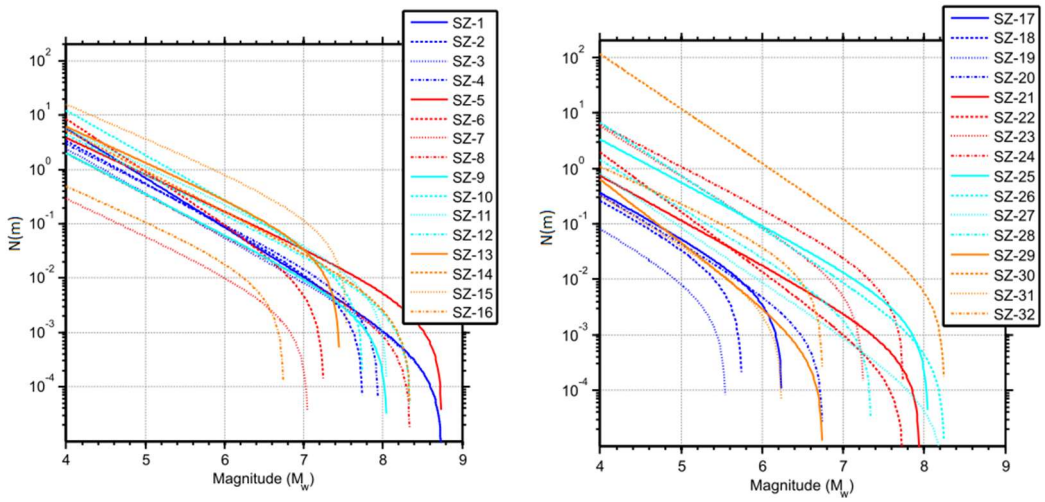


Figure 5. Recurrence relationship for 32 Seismogenic Zones

Using this approach, the recurrence parameters of the source zones have been disaggregated to fault level recurrence parameters. The fault level seismicity si was estimated by associating the earthquakes with the closest fault. Since it is difficult to ascertain the magnitude versus rupture potential of individual faults due to the uncertainties in the fault activity, the b-value of all the faults within a zone was assumed the same as the zonal b-value. The Mmax value for all the faults in each zone were taken as the maximum magnitude of past events associated with the fault and an additional 0.5 units to account for uncertainty in the data. For faults lacking past event records, the Wells and Coppersmith (1994) relationship has been used to evaluate Mmax based on rupture length. Furthermore, the Mmax values for individual faults are constrained by the zonal Mmax values. These fault level recurrence parameters were estimated for all the 936 faults identified in the 32 seismogenic zones considered in this study.

4. Ground motion prediction equation

After determining the recurrence relationship for each of the faults, an attenuation relationship valid for the region under consideration had to be derived. The attenuation equation is a key component in PSHA. This equation describes the average or other moments of the hazard parameter in terms of magnitude and distance. The instrumental database for India is sparse and hence not useful for deriving instrument based attenuation relationships. Here the attenuation relationships for different regions of India were developed based on the synthetic ground motions generated according to the regional characteristics. The seismological model developed by Boore (2009) was used to generate this synthetics ground motion. For the various inputs required for the model, the effects specific to Indian geological regions appear in the quality factor Q(f), stress drop value ($\Delta\sigma$), focal depth and the site amplification function F(f). In the past, several seismologists have analysed instrumental data to arrive at estimates of the frequency dependent quality factor, which is similar to the damping coefficient in elastic materials. On similar lines, the value of stress drop that can occur in different regions for a given magnitude of earthquake is available. The other important regional parameter is the focal depth which can vary from as low as 5 km to as deep as 100 km or more. The variation

in focal depth is fairly well known for the different regions in India (Shukla et al. 2007; Kayal 2008) Thus, the geological parameters reported for different regions in India are shown in Fig. 6. Here spectral acceleration values have been simulated for moment magnitudes (Mw) ranging from 4 to 8.5 in increments of 0.5 units, at 20 values of hypocentral distances ranging from 1 to 500 km. To capture finiteness of the source the ground motions were also simulated for eight azimuths ranging from 0° to 315° in increments of 45°. Thus a total number of 160 distance samples were considered for each magnitude. In all, there are 1600 pairs of magnitudes and distances. Thus, a database of 80,000 PGA and Sa samples corresponding to 1600 simulated earthquake events were generated. This synthetic database was developed separately for each of the seven regions above using their respective quality factors. The variation of quality factor at certain sub regions in India was accounted for by generating separate sets of data and combining them with a specific weightage as discussed in NDMA (2011).

The generated data, needed fitting, using a GMPE with a physically significant functional form. After reviewing the various available forms of equations, it was decided to develop the attenuation relationship for all seven regions in the form

$$\ln\left(\frac{S_a}{g}\right) = c_1 + c_2 M + c_3 M^2 + c_4\, r + c_5 \ln\left(r + c_6 e^{c_7 M}\right) + c_8 \log(r)\mathrm{f}_0 + \ln(\varepsilon)$$
$$\mathrm{f}_0 = \max(\ln(r/100), 0) \tag{5}$$

where, S_a is the spectral acceleration, M is the moment magnitude, r is the hypocentral distance in kilometres. This form of the attenuation accounts for geometrical spreading, anelastic attenuation and magnitude saturation similar to the finite source seismological model discussed above. The coefficients of the above equation were obtained from the simulated database of 80,000 samples by a two-step stratified regression, following Joyner and Boore (1981). For brevity, the coefficients and the standard error obtained for different periods, for the Himalayan region alone are shown in Table 2. In similar fashion the coefficient of the GMPE was determined for the other six geological provinces of India. One can refer to NDMA (2011) for the corresponding values. The resultant response spectra for the different regions for Mw 5.5 and 7.5 at varying distances are shown in Fig. 7. These results can be used to construct the mean and (mean+sigma) response spectrum on A-type rock for any part of India.

5. Probabilistic seismic hazard

Probabilistic seismic hazard analysis estimates the probability of exceedance of various ground motion levels at a site given all possible earthquakes. The basic formulation for PSHA has been derived by Cornell (1968) assuming a point source earthquake model. Later PSHA was improved to include a finite source and its uncertainty by Kiureghian and Ang (1977). Nowadays, PSHA has become a standard tool for estimating ground motion. The procedure required for PSHA has been discussed in great detail in the literature (Kramer 1996). The same methodology has been followed in this study also. The basic steps are briefly mentioned here. The uncertainty in the magnitude of a future event is represented as an exponential random variable as shown by Eq. (6).

$$p_M(m) = \frac{\beta e^{-\beta(m-m_0)}}{1-\beta e^{-\beta(m_u-m_0)}}; \quad (m_0 \le m \le m_u),\ \beta = 2.303\,b \tag{6}$$

where m_o and m_u are the lower and upper limits of the earthquake magnitudes considered in the analysis.

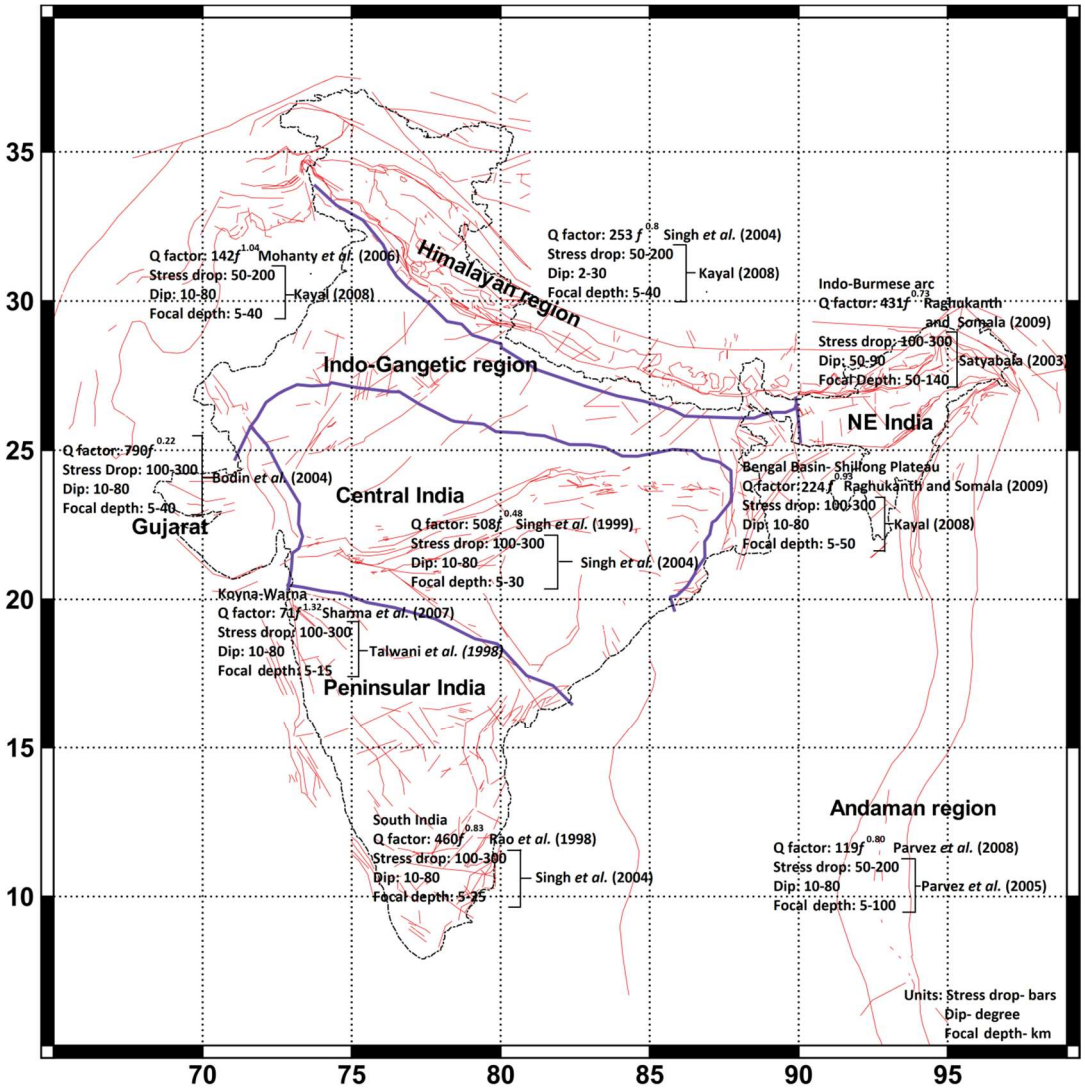


Figure 6. Seven geological province of India

Table 2. The coefficients in the attenuation relation for Himalayan Region

Period	C1	C2	C3	C4	C5	C6	C7	C8	σ(ε)
0	-3.7438	1.0892	0.0098	-0.0046	-1.4817	0.0124	0.995	0.1249	0.4094
0.01	-3.7486	1.0877	0.0099	-0.0046	-1.4804	0.0123	0.9955	0.1247	0.4083
0.015	-2.7616	0.955	0.0188	-0.0049	-1.4649	0.0111	1.0051	0.1234	0.4678
0.02	-2.7051	0.9588	0.0179	-0.0049	-1.4387	0.0092	1.0246	0.1223	0.4445
0.03	-2.7582	0.9755	0.0162	-0.0048	-1.4121	0.0081	1.0372	0.1179	0.4137
0.04	-2.9321	1.0173	0.0126	-0.0047	-1.4014	0.0087	1.0248	0.1165	0.4001
0.05	-3.0839	1.0461	0.0106	-0.0046	-1.3992	0.0089	1.0217	0.1124	0.3941
0.06	-3.3069	1.0905	0.0075	-0.0046	-1.3958	0.0095	1.0129	0.115	0.391
0.075	-3.6744	1.1532	0.0024	-0.0046	-1.3738	0.0086	1.0202	0.1145	0.3885
0.09	-4.1011	1.2448	-0.0045	-0.0046	-1.3582	0.0086	1.0173	0.1146	0.3873
0.1	-4.4163	1.3088	-0.0092	-0.0045	-1.348	0.0089	1.0131	0.1095	0.3873
0.15	-5.8898	1.6365	-0.0331	-0.0043	-1.3168	0.0101	0.9903	0.1011	0.3882
0.2	-7.3244	1.9682	-0.0572	-0.0043	-1.2859	0.0096	0.9891	0.0987	0.3929
0.3	-9.96	2.6152	-0.1031	-0.004	-1.2659	0.0134	0.9404	0.0926	0.401
0.4	-12.1052	3.1363	-0.1391	-0.004	-1.2445	0.0166	0.9136	0.0878	0.406
0.5	-13.8894	3.5767	-0.1691	-0.0039	-1.2403	0.0188	0.894	0.0906	0.4069
0.6	-15.6887	3.9957	-0.1974	-0.0038	-1.2192	0.0181	0.893	0.0876	0.4085
0.7	-16.8075	4.2512	-0.2137	-0.0038	-1.2118	0.0187	0.8939	0.0863	0.4078
0.75	-17.3641	4.3748	-0.2219	-0.0038	-1.2038	0.0183	0.8934	0.0842	0.4096
0.8	-17.9297	4.5173	-0.2306	-0.0037	-1.2175	0.0221	0.8745	0.0847	0.407
0.9	-19.0065	4.7521	-0.2452	-0.0037	-1.2109	0.0231	0.867	0.0861	0.4072
1	-19.5191	4.8564	-0.2515	-0.0037	-1.2044	0.0224	0.8699	0.0854	0.4081
1.2	-20.8567	5.1139	-0.2652	-0.0036	-1.2027	0.0236	0.872	0.0868	0.4007
1.5	-22.0907	5.3398	-0.2751	-0.0035	-1.2231	0.0254	0.8731	0.0871	0.3958
2	-23.4263	5.5337	-0.2796	-0.0034	-1.2496	0.0283	0.8733	0.0946	0.3898
2.5	-24.1315	5.5606	-0.2742	-0.0033	-1.2525	0.0245	0.8965	0.0971	0.3924
3	-24.6217	5.5327	-0.2635	-0.0032	-1.2779	0.0238	0.9092	0.1009	0.3951
4	-24.866	5.3573	-0.2394	-0.0031	-1.3022	0.0224	0.928	0.1076	0.4023

The other unknown factor is the distance R of the site from the future hypocentre. The conditional probability distribution function of R, given that magnitude M = m for a rupture segment uniformly distributed along a fault can be numerically computed following the method of Der Kiureghian and Ang (1977).

Referring to Fig 8. we have:

$$
\begin{aligned}
&P(R<r\mid M=m)=0 \quad for\ R<\left(D^2+L_o^2\right)^{1/2}\\
&P(R<r\mid M=m)=\frac{\left(r^2-D^2\right)^{1/2}-L_o}{L-X(m)}\\
&\qquad for\ \left(D^2+L_o^2\right)^{1/2}\le R<\left\{D^2+\left[L+L_o-X(m)\right]^2\right\}^{1/2}\\
&P(R<r\mid M=m)=1 \quad for\ R>\left\{D^2+\left[L+L_o-X(m)\right]^2\right\}^{1/2}
\end{aligned}
\tag{7}
$$

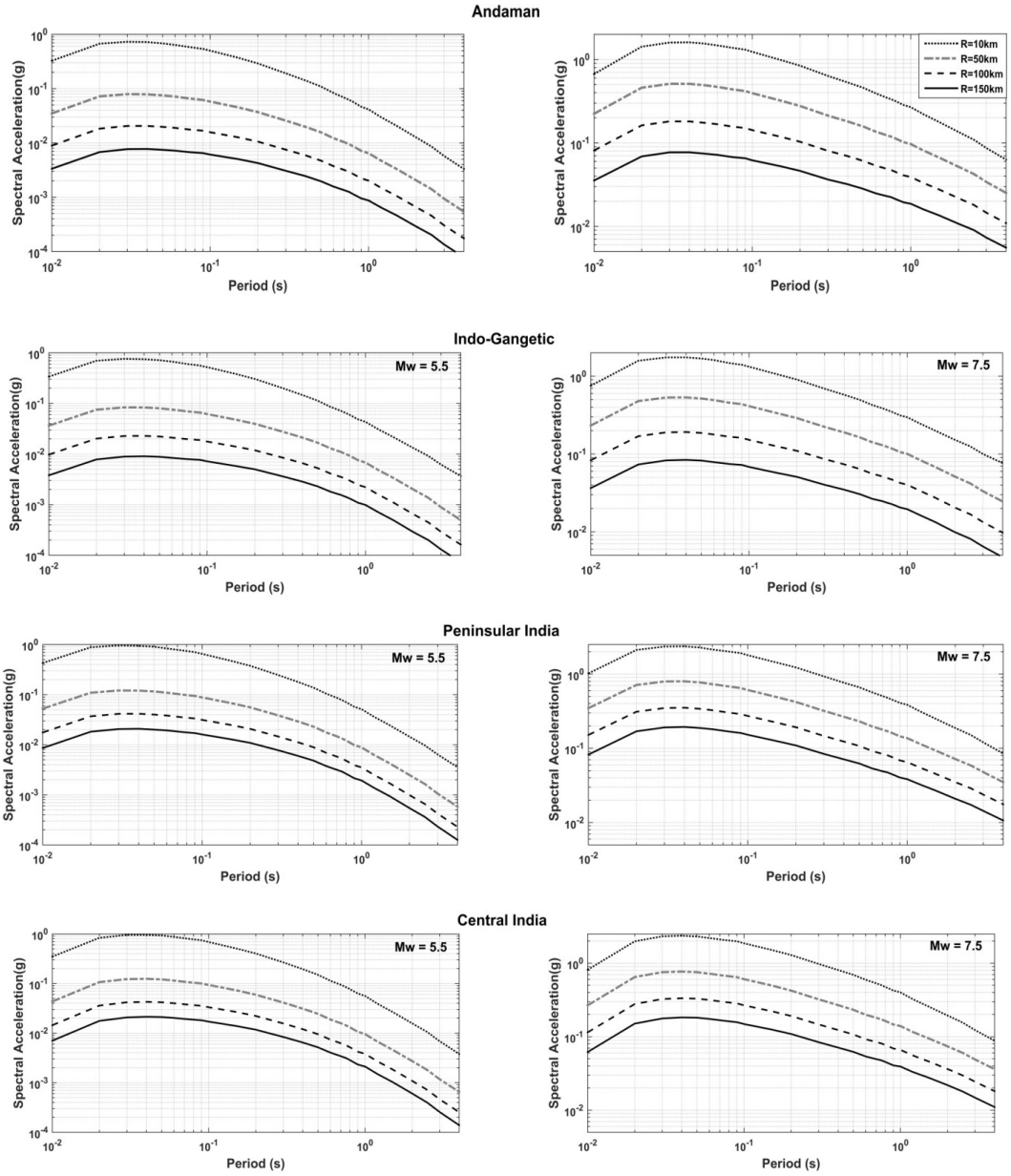


Figure 7. Ground motion prediction variation with magnitude and distance for the seven geological province of India

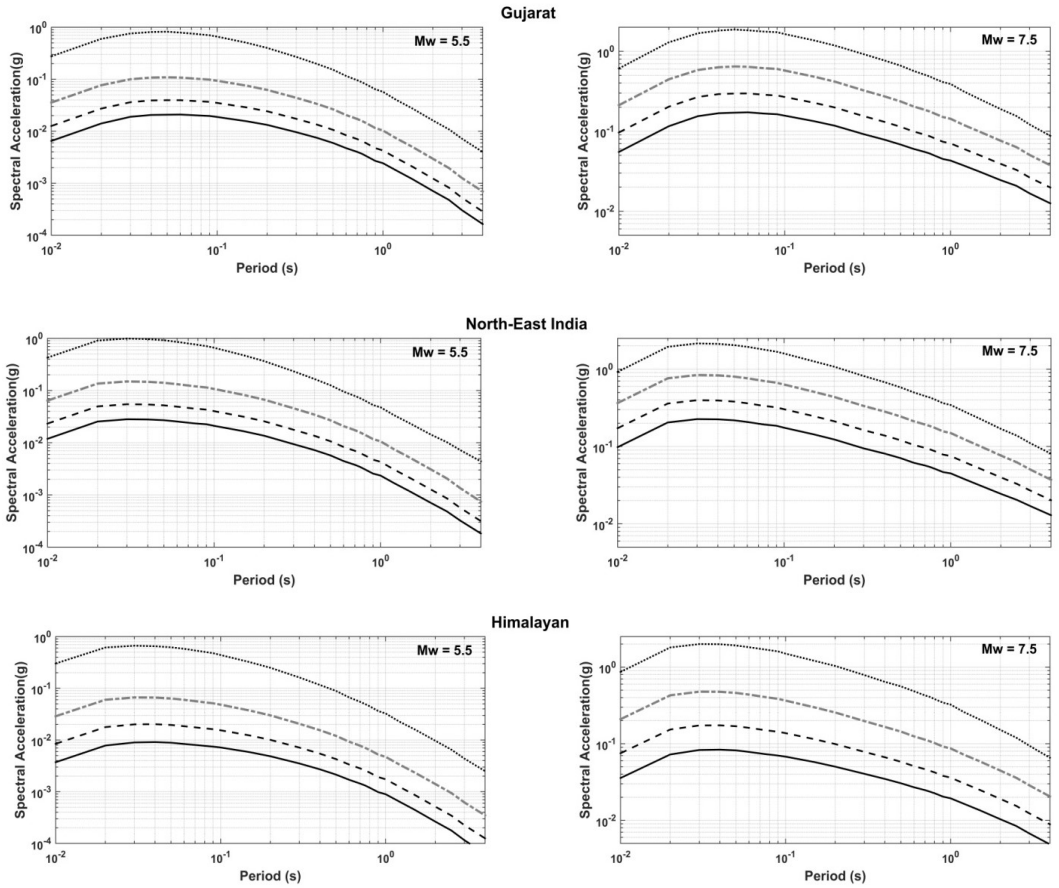


Figure 7. Ground motion prediction variation with magnitude and distance for the seven geological province of India (continued)

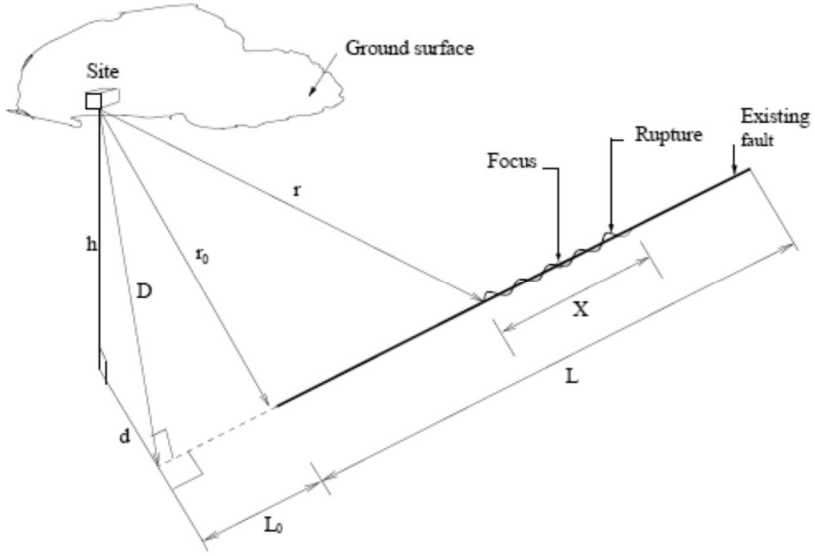


Figure 8. Source, Site and Path for PSHA

In Figure 8, L is the length of the fault, X is the rupture length for a particular magnitude of earthquake, h is the focal depth, r is the minimum distance from site to the region of rupture, ro is the minimum distance of the site from the fault, D is the perpendicular distance from site to the projection of the fault line, Lo is the projected length of the fault line from the end of the fault as far as the perpendicular from the site(Source: Der Kiureghian and Ang (1977)

The rupture length, X(m), for an event of magnitude m, is given by

$$X(m) = \min\left[10^{(-2.44+0.59m)}, \textit{fault length}\right] \tag{8}$$

Probabilistic seismic hazard analysis estimates the probability of exceedance of spectral acceleration Sa at a site due to all possible future earthquakes as visualized by the previous hazard scenario. Assuming that the number of earthquakes occurring on a fault follows a stationary Poisson process, the probability that the control variable Y exceeds level y*, in a time window of T years is given by

$$P(Y > y^* \textit{ in } T \textit{ years}) = 1 - exp(-\mu_{y^*} T) \tag{9}$$

The rate of exceedance, μ_{y^*} is computed from the expression

$$\mu_{y^*} = \sum_{i=1}^{K} N_i(m_0) \int_m \int_r P(Y > y^* \mid m, r) p_{R|M}(r \mid m) p_M(m) \; dr dm \tag{10}$$

Here, K is the total number of faults in the zone, *pM(m)* and *pR|M (r | m)* are the probability density functions of magnitude and hypocentral distance respectively. *P(Y >y* |m, r)* is the conditional probability of exceedance of the ground motion parameter *Y*. This is found as a lognormal random variable with mean value given by the attenuation equation conditioned on particular m and r values. The reciprocal of the annual probability of exceedance gives the return period for the corresponding ground motion value. The mean annual rate of exceedance of *y** is obtained by summing over the individual probabilities due to all faults. This is repeated for various ground motion values *y** to obtain the seismic hazard curves. These curves are first obtained individually for all the faults located in the thirty-two tectonic zones and combined to estimate the aggregate hazard at the region of interest.

6. Hazard estimates for India

6.1 Hazard Curve and Uniform Hazard Response Spectra

The hazard curves for a site, are plots of ground motion parameter versus the mean annual rate of exceedance of the parameter obtained by summing the probabilities due to all faults around the site. Here, the hazard curves for PGA are obtained for Delhi and Kolkata, both cities located in the IGP region, as illustrated in Fig. 9. It is clear that Kolkata exhibits higher values for all return periods. It can also be noticed that the attenuation of the expected PGA value for Delhi is high at larger return periods than is

the case for Kolkata. Further, uniform hazard response spectra (UHRS) which are spectra having the same mean recurrence intervals at all frequencies are calculated. Here, UHRS was obtained for return periods of 2500 yrs, which corresponds to 2% probability in 50 years or the Maximum Considered Earthquake (MCE). The corresponding value at A Type soil condition for Delhi and Kolkata are shown in Figure 10. It is clear from the figure that Kolkata has higher hazard values than Delhi.

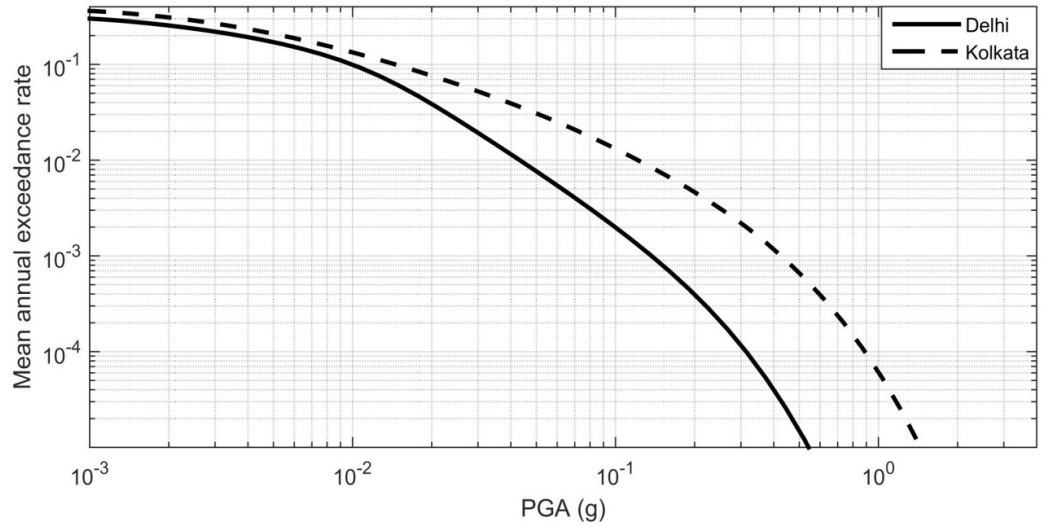


Figure 9. PGA hazard curve for Delhi and Kolkata on A type site.

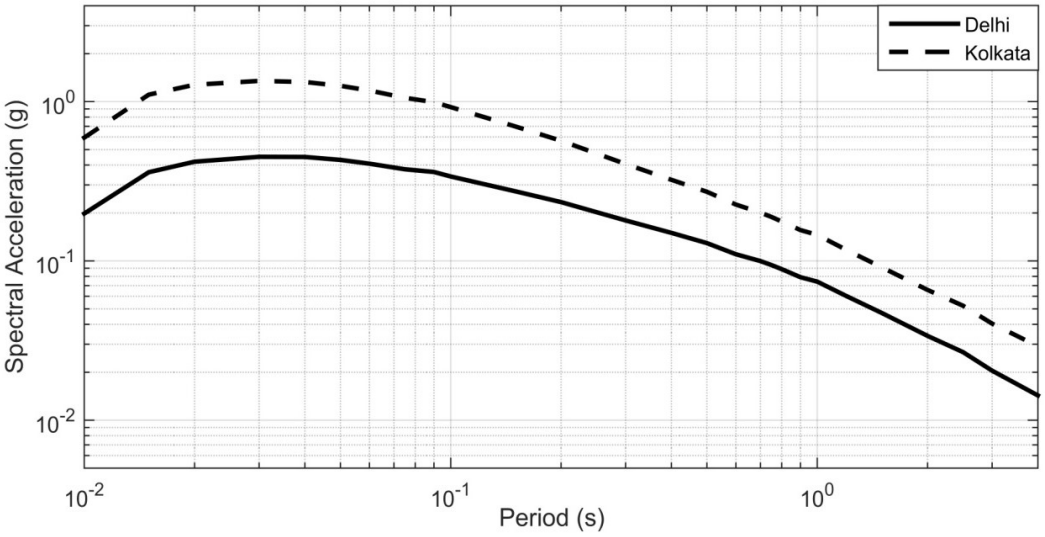


Figure 10. Uniform Hazard Response Spectra for 2500 years return period on A type site.

6.2 Hazard Contour

This section presents the probable seismic hazard of India in terms of PGA and spectral accelerations at 0.2 s and 1 s, obtained by implementing the PSHA methodology outlined in the section above. The probable hazard maps were prepared by contouring

the hazard values estimated at a 0.2° × 0.2°grid level. These seismic hazard maps give an insight into the expected levels of ground intensity and are crucial for the safety assessment of vital infrastructure. These maps are presented for 2% probability of exceedance in 50 years, which correspond to return periods of nearly 2500 years. These hazard values are presented for hard rock conditions only. The results are presented as hazard contours in Figs. 11, 12 and 13 respectively for PGA, spectral accelerations at 0.2 s and 1 s, for a return period of 2500 years. Further the PGA corresponding to a 2500 years return period for the important cities are presented in Table 3. It is observed from the figures that the region near Guwahati is expected to have a high PGA of 0.75g. In the continental regions, the Son-Narmada region, South-Western Rajasthan and the Koyna region display high PGA values and spectral values. In addition, following IBC (2009) the spectral acceleration values of 0.2 s and 1 s at 2500 years return period can be used to construct design response spectra for any site in India.

7. Hazard deaggregation

It is common practice to replace the integrals of PSHA by discrete magnitude and distance segments (Kramer 1996) for numerical simplicity. Hence, instead of summing up the exceedance rates from these discrete intervals to arrive at the total mean exceedance rate at a site, the hazard deaggregation procedure (McGuire 1995, Bazzurro and Cornell 1999) involves identifying the contribution of each of these discrete M - R bins to the total seismic hazard at the site. The controlling ground motion can then be determined by identifying the discrete M - R bin that makes the maximum contribution to the seismic hazard. The USNRC (2007) suggests the following disaggregation framework for identifying the controlling earthquake at the short period and long period levels from the disaggregated median probability level of ground motion exceedance obtained from PSHA.

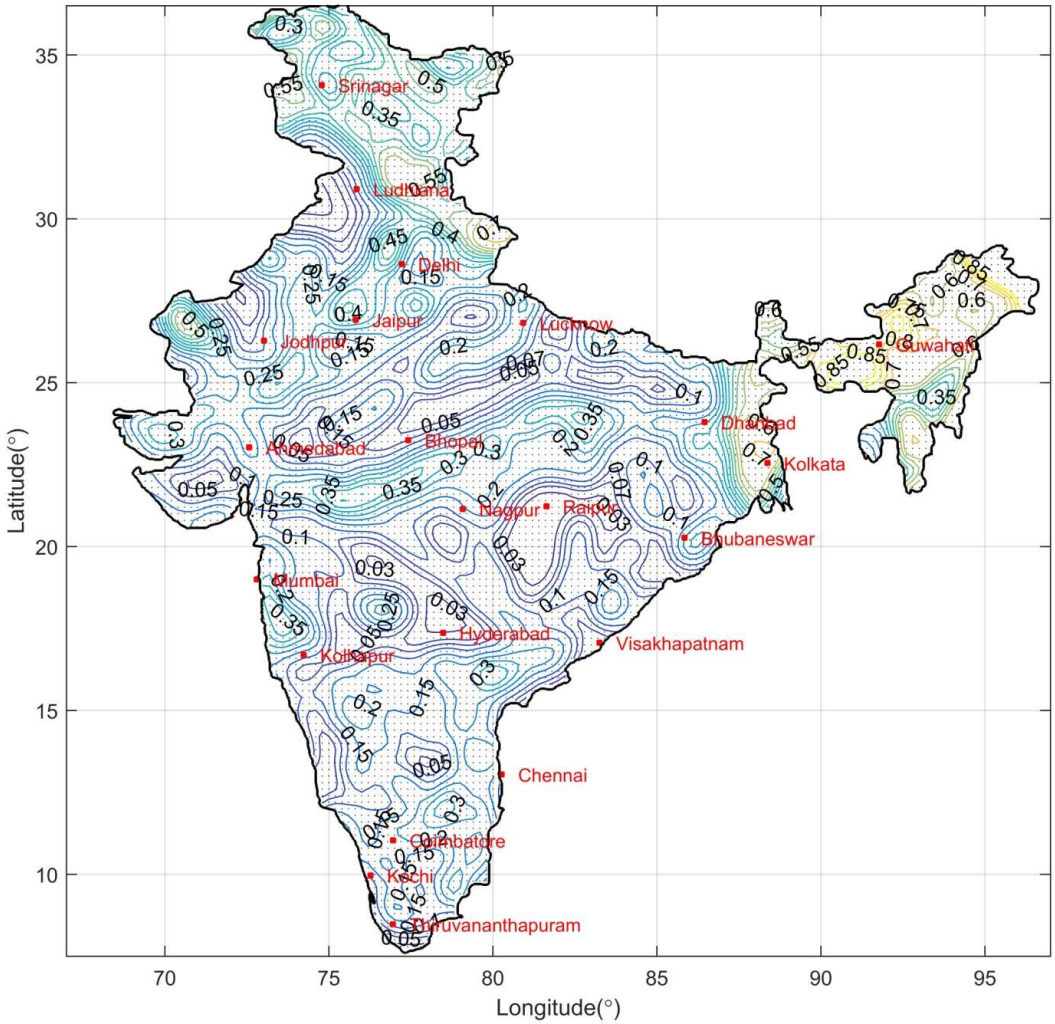


Figure 11. PGA(g) Contours with 2% probability of exceedence in 50 years (Return Period~2500 Years) on Type A site

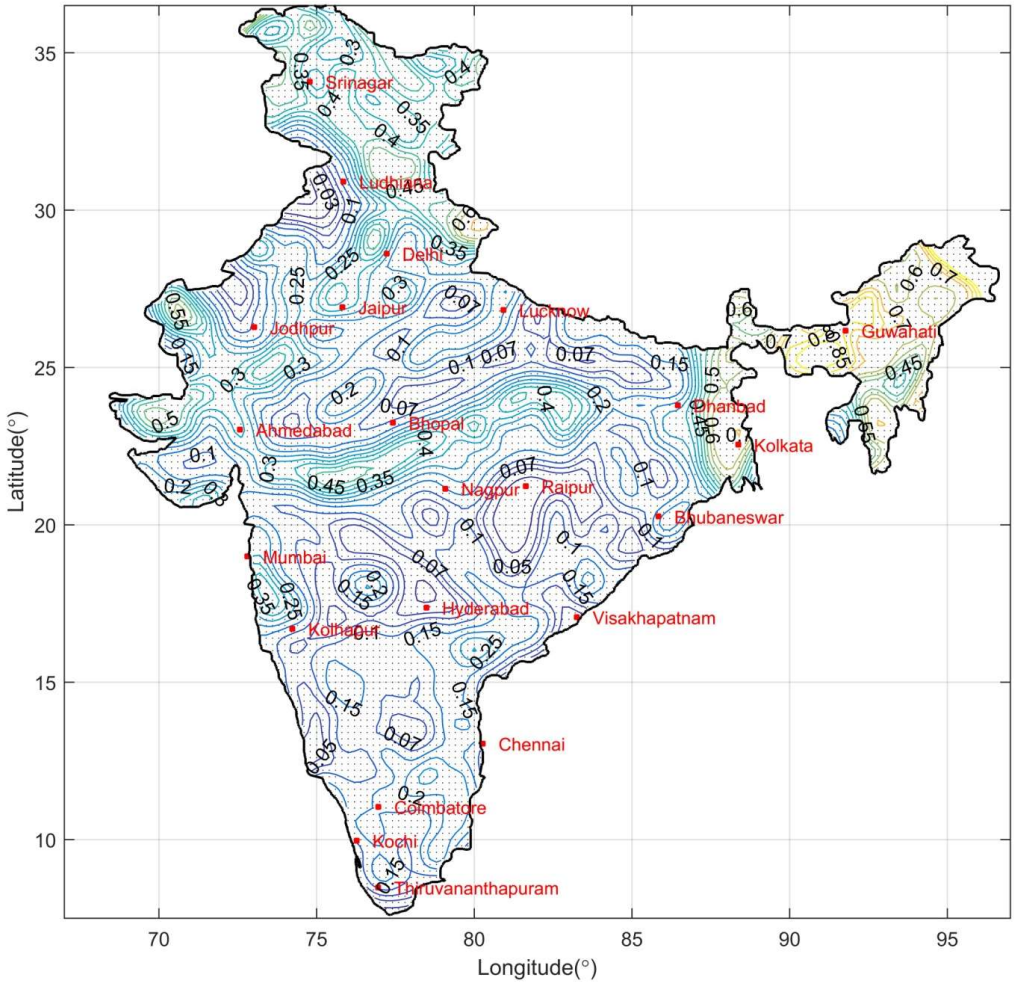


Figure 12. Short Period Spectral Acceleration at T = 0.2 s, with 2% probability of exceedence in 50 years (Return Period ~ 2500 Years) on Type A site (5% damping)

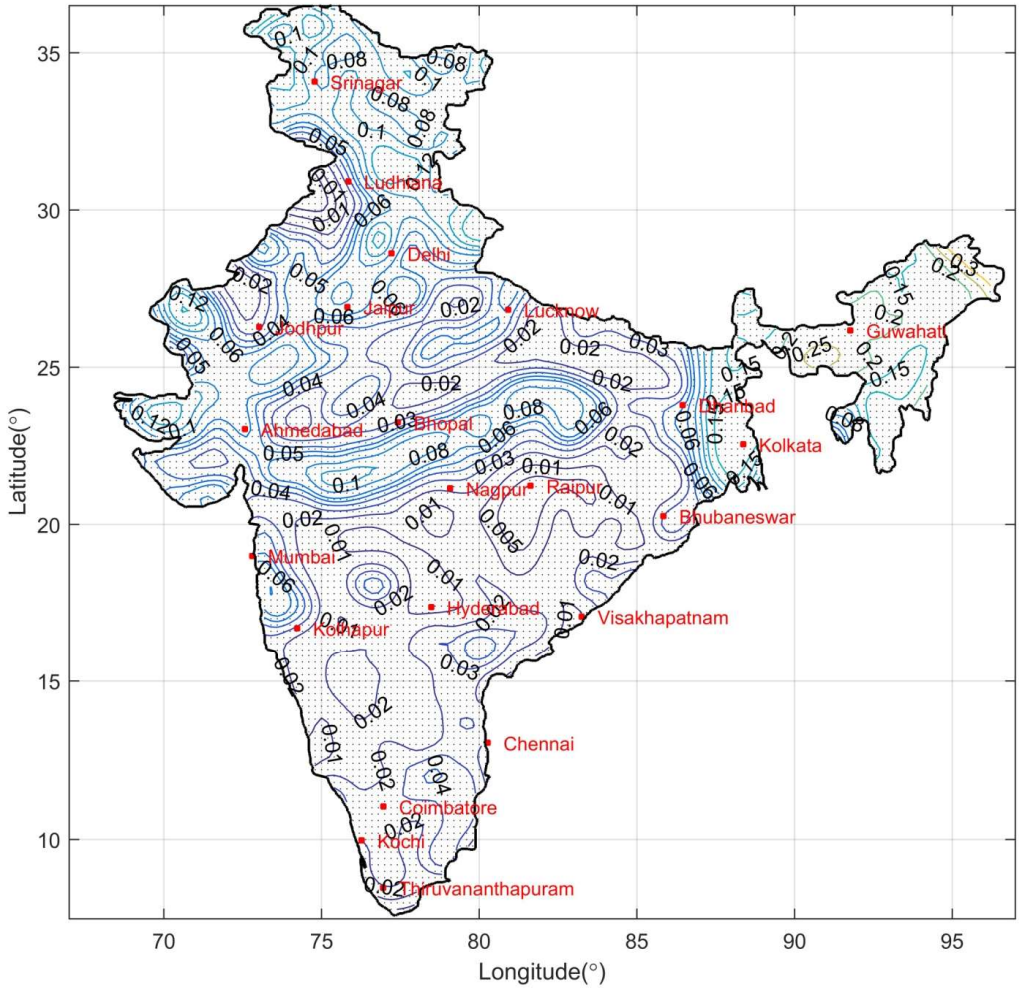


Figure 13. Long Period Spectral Acceleration at T = 1 s, with 2% probability of exceedence in 50 years (Return Period ~ 2500 Years) on Type A site (5% damping)

Table 3. Relative Seismic Hazard for Indian Cities on Type A sites in PGA

Cities	Longitude	Latitude	PGA (g), at 2500Yrs return Period
Guwahati	91.770	26.170	0.793
Kolkata	88.370	22.550	0.638
Asansol	86.980	23.680	0.383
Chandigarh	76.780	30.750	0.382
Srinagar	74.780	34.080	0.339
Jaipur	75.820	26.920	0.318

Jabalpur	79.930	23.150	0.276
Delhi	77.220	28.620	0.265
Jamshedpur	86.180	22.800	0.249
Dhanbad	86.450	23.800	0.248
Agra	78.020	27.180	0.245
Vijayawada	80.610	16.510	0.229
Mumbai	72.800	19.000	0.220
Meerut	77.700	28.990	0.201
Trichy	78.690	10.810	0.197
Pune	73.850	18.520	0.195
Kanpur	80.330	26.460	0.194
Lucknow	80.920	26.830	0.190
Ahmedabad	72.570	23.030	0.190
Coimbatore	76.960	11.040	0.180
Vadodara	73.200	22.300	0.178
Ranchi	85.330	23.350	0.172
Bhubaneswar	85.840	20.270	0.171
Kozhikode	75.770	11.250	0.170
Patna	85.120	25.600	0.156
Surat	72.780	21.230	0.144
Nashir	73.780	20.000	0.143
Indore	75.540	22.420	0.142
Madurai	78.100	9.800	0.141
Kolhapur	74.230	16.700	0.137
Nagpur	79.080	21.150	0.137
Gwalior	78.100	26.140	0.128
Bangalore	77.580	12.970	0.118
Ludhiana	75.850	30.910	0.115
Chennai	80.270	13.050	0.113
Jodhpur	73.020	26.280	0.112
Allahabad	81.850	25.450	0.093
Solapur	75.920	17.680	0.093
Thiruvananthapuram	76.950	8.480	0.092

Bhopal	77.420	23.250	0.090
Aurangabad	75.290	19.780	0.089
Rajkot	70.780	22.300	0.085
Varanasi	82.980	25.320	0.069
Kochi	76.270	9.970	0.068
Amritsar	74.860	31.640	0.045
Visakhapatnam	83.250	17.070	0.044
Hyderabad	78.480	17.370	0.041
Raipur	81.630	21.230	0.020

Thus, the $P(m,r)_l$ and $P(m,r)_s$ representing the mean fractional contribution of each of the M-R bins towards the total hazard at long (1 and 2.5 Hz) and short (5 and 10 Hz) periods respectively can be calculated as follows,

$$P(m,r)_s = \frac{\sum_{f=5,10Hz} \frac{H_{mr}(f)}{2}}{\sum_m \sum_r \sum_{f=5,10Hz} \frac{H_{mr}(f)}{2}} \tag{11}$$

$$P(m,r)_l = \frac{\sum_{f=1,2.5Hz} \frac{H_{mr}(f)}{2}}{\sum_m \sum_r \sum_{f=1,2.5Hz} \frac{H_{mr}(f)}{2}} \tag{11}$$

where, $Hmr(f)$ is the estimated hazard value for a M→m and R→r combination at frequency f, the spectral frequency f takes the value of (1,2.5 Hz) and (5,10 Hz) for long and short periods respectively. Since the contributions from near and far sources vary with time and return periods, it becomes necessary to consider them while identifying the controlling parameters.

Here, the deaggregation of hazard is demonstrated for the capital city, Delhi (77.22°E, 28.62°N), for a return period of 2500 years. Table 4 shows the percentage contribution, after the deaggregation of hazard estimates for a median spectral acceleration corresponding to a 2500 years return period at Delhi. Using the USNRC (2007) recommendation, the short period spectral acceleration (Sas) is obtained by averaging the median spectral acceleration estimated at 5 and 10 Hz. Similarly, the long period spectral acceleration (Sal) is obtained by averaging the median spectral acceleration estimated at 1 and 2.5 Hz. It is clear that for short period spectral accelerations the critical fault distance is in the range 44 -67 km and magnitude 6.8 - 7.3, whereas for long period spectral acceleration the corresponding values are 22-44 km with the same magnitude range. The fault that lies within this distance range for Delhi City is the Mahendraghar-Dehradun Fault.

Further deaggregation of hazard was obtained separately for PGA, Sa (0.2 s) and Sa (1 s) at a return period of 2500 years as shown in Fig. 14. It is clear that though the plot shows a dominant peak at a distance of 45 km and magnitude 6.5, there are also contributions from faults at larger distances for Delhi city. The corresponding faults are the Moradabad fault and the Great Boundary Fault. Hence it is clear that through disaggregation a proper insight into the controlling faults and magnitude for a site can be ascertained.

Table 4. Deaggregation of median spectral acceleration values (%) at 2500 years return Period for Delhi

	M				Distance Bin (km)				
	0-22	22-44	44-67	67-89	89-111	111-133	133-156	156-178	178-222
For short period averaged between 5 and 10 Hz									
4-4.56	0.00	0.00	0.00	0.00	0.00	0.00	0.00	0.00	0.00
4.56-5.11	0.00	0.00	0.00	0.00	0.00	0.00	0.00	0.00	0.00
5.11-5.67	0.00	0.01	0.00	0.00	0.00	0.00	0.00	0.00	0.00
5.67-6.22	0.00	1.54	0.19	0.00	0.00	0.00	0.00	0.00	0.00
6.22-6.78	0.00	17.88	8.53	0.26	0.01	0.00	0.00	0.00	0.00
6.78-7.33	0.00	17.52	20.36	3.28	0.46	0.03	0.00	0.00	0.00
7.33-7.89	0.00	5.16	10.96	5.69	1.63	0.26	0.06	0.01	0.00
7.86-844	0.00	0.14	2.50	2.02	0.76	0.43	0.13	0.03	0.00
8.44-9.00	0.00	0.00	0.04	0.04	0.01	0.01	0.01	0.01	0.01
For long period averaged between 1 and 2.5 Hz									
4-4.56	0.00	0.00	0.00	0.00	0.00	0.00	0.00	0.00	0.00
4.56-5.11	0.00	0.00	0.00	0.00	0.00	0.00	0.00	0.00	0.00
5.11-5.67	0.00	0.15	0.01	0.00	0.00	0.00	0.00	0.00	0.00
5.67-6.22	0.00	4.29	0.51	0.00	0.00	0.00	0.00	0.00	0.00
6.22-6.78	0.00	21.67	9.18	0.17	0.00	0.00	0.00	0.00	0.00
6.78-7.33	0.00	17.16	18.11	1.98	0.18	0.01	0.00	0.00	0.00
7.33-7.89	0.00	5.05	10.55	4.21	0.91	0.11	0.01	0.00	0.00
7.86-844	0.00	0.14	2.45	1.94	0.63	0.34	0.08	0.01	0.00
8.44-9.00	0.00	0.00	0.04	0.03	0.01	0.02	0.02	0.01	0.01

8. Conclusions

This chapter focuses on outlining the development of a backbone seismic hazard model for India for the purpose of estimating the probable peak ground acceleration and spectral acceleration at 0.2 s and 1 s for a return period earthquake of 2500 years, which correspond to a 5 % probability of exceedence in 50 years, for the A type soil class. The regional ground motion prediction equations developed for each of the seven geological provinces have been implemented in the regional seismic hazard models. The Cornell-McGuire PSHA method was adopted using an entirely linear fault source model consisting of 936 linear fault sources. The compiled earthquake catalogue comprises historic and instrumented seismicity records for events recorded up to December 2016. The fault level recurrence parameters have been derived using a disaggregation procedure. The choice of linear fault source model alone is useful for identifying the critical near-field regions. The seismic hazard was carried out at 0.2° grid intervals and the hazard contours maps have been produced for PGA and Sa at T=0.2 s and 1 s, for hard rock conditions only (Vs30 >1500 m/s).

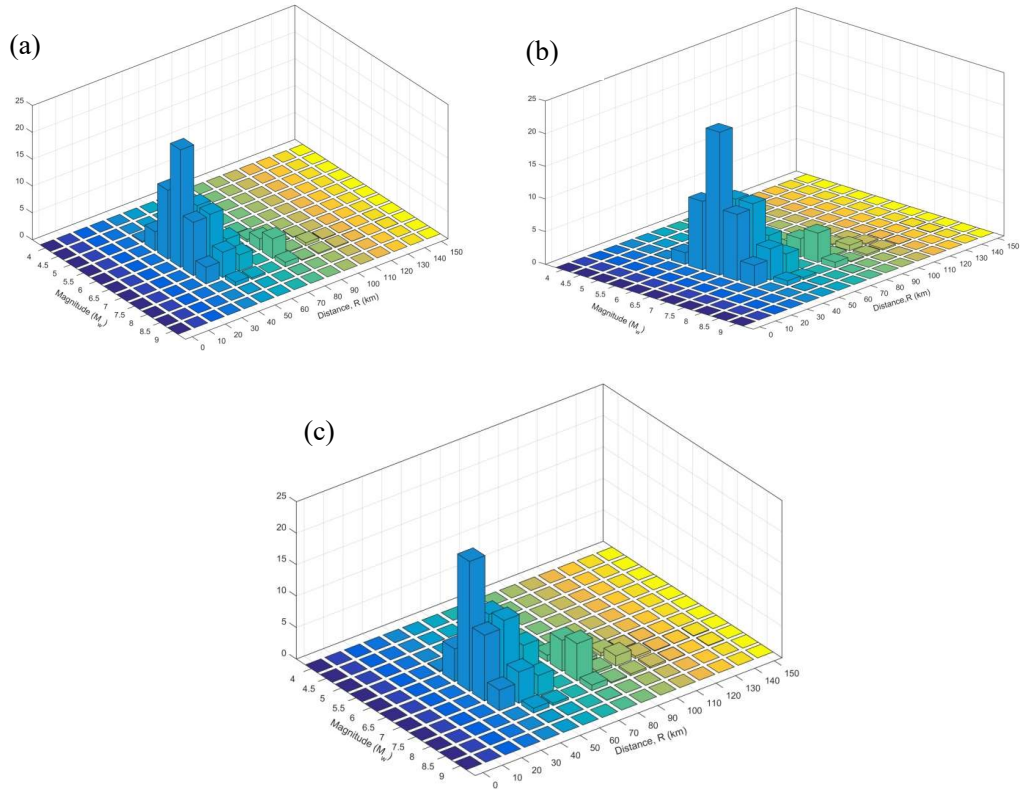


Figure 14. Deaggregation at 2500 years return period for Delhi. (a) PGA (b) Sa (0.2 s) and (c) Sa (1 s)

Results indicate that the active regions, especially the NW Himalayas and North-eastern India exhibit high PGA and spectral acceleration values. In the continental regions, the Son-Narmada region, South-Western Rajasthan and Koyna region display high values. The procedure for estimating the critical fault and magnitude range is discussed by illustrating its application to Delhi. In addition, the procedure described in IBC (2009) to obtain site specific design spectra from the hazard contours reported in Fig. 12 and 13 is discussed in Appendix A.

It should be noted that the present hazard contour is applicable only for Type A soil conditions. It is seen that there are sites in India especially in the IGP region which belongs to D or E type soil classes. Although IBC describes the procedure to obtain site specific spectra, it does not replicate the actual site features of all geological regions in India. Hence the present work needs to be extended to embrace other soil conditions. As a first step, a ground motion prediction equation needs to be developed for other soil conditions consistent with the characteristics of the seven geological provinces of India. Further, a technique to provide hazard constant acceleration time histories would be of great interest to engineers. In addition, as displacement based design procedures are gaining importance in seismically active regions, it would be interesting if the hazard could be quantified for earthquake velocity and displacement characteristics.

Acknowledgements

The work presented here has been supported by Department of Science and Technology under Grant No. SR/S3/MERC-0085/2011.

References

Balakrishnan, T. S., Unnikrishnan, P., and Murthy, A.V.S. (2009), "The tectonic map of India and contiguous areas", J. Geol. Soc. India, 74, 158-170.

Bazzurro, P. and C. A. Cornell (1999), "Disaggregation of seismic hazard", Bull.Seismol. Soc. Am., 89(2), 501–520.

Bodin, P. et al. (2004), "Ground motion scaling in the Kachchh basin, India, deduced from aftershocks of the 2001 Mw 7.6 Bhuj earthquake", Bull. Seism. Soc. Am., 94(5),1658-1669.

Boore, D.M. (2009), "Comparing stochastic point-source and finite-source ground motion simulations: SMSIM and EXSIM", Bull. Seism. Soc. Am., 99(6), 3202-3216.

Cornell, C.A. (1968), "Engineering seismic risk analysis", Bull. Seism. Soc. Am., 58, 1583-1606.

Gardner, J.K. and Knopoff, L. (1974), "Is the sequence of earthquakes in Southern California, with aftershocks removed, Poissonian?", Bull. Seism. Soc. Am., 64, 1363–1367.

Giardini, G., Wiemer, S., Fäh, D. and Deichmann, N. (2004), "Seismic Hazard Assessment of Switzerland, Publication Series of the Swiss Seismological Service", ETH Zürich, 91 p.

GSI (2000), "Seismotectonic Atlas of India and its Environs", Geological Survey of India.

IBC. (2009). International Building Code. International Code Council.

Joyner, W.B. and Boore, D.M. (1981), "Peak horizontal acceleration and velocity from strong-motion records including records from the 1979 Imperial Valley, California, Earthquake", Bull. Seism. Soc. Am., 71, 2011–2038.

Kayal J.R. (2008), "Microearthquake Seismology and Seismotectonics of South Asia." Capital Publishing Company, New Delhi.

Kiureghian, A. D. and Ang, A. H.-S. (1977), "A fault rupture model for seismic risk analysis", Bull. Seismol. Soc. Am., 67, 1173–1194.

Kijko, A. (2002), "Statistical estimation of maximum regional magnitude mmax", Proceedings of the 12th European Conference on Earthquake Engineering, London, Sept. 9-13, Elsvier Science, paper Reference FW:022.

Kijko, A. and Graham, G. (1998), "Parametric-historic procedure for probabilistic seismic hazard analysis: Part I - estimation of maximum regional magnitude mmax", Pure Appl. Geophys., 152, 413-442.

Knopoff, L. and Kagan, Y. (1977), "Analysis of the theory of extremes as applied to earthquake problems", J. Geophys. Res., 82, 5647-5657.

Kramer S L (1996), Geotechnical Earthquake Engineering, Prentice-Hall, Inc.

Milne, J. (1911), "A catalogue of destructive earthquakes: A.D. 7 to A.D. 1899", British Association for the Advancement of Science London, 92 p.

McGuire, R. (1995), "Probabilistic seismic hazard analysis and design earthquakes: Closing the loop", Bull. Seismol. Soc. Am., 85(5), 1275–1284.

NDMA (2011), Development of probabilistic seismic hazard map of India, Technical report of the working comittee of experts National Disaster Management Authority (NDMA), Govt. of India, New Delhi

Oldham, T. (1883), "A catalogue of Indian earthquakes from the earliest times to the end of 1869 A.D.", Mem. Geol. Surv. India., XIX, Part. 3.

Parvez, I.A, Sutar, A.K, Mridula, M., Mishra, S.K. and Rai, S.S. (2008), "Coda Q estimates in the Andaman Islands using local earthquakes", Pure Appl. Geophys, 165, 1861–1878.

Quittmeyer, R.C. and Jacob, K.H.(1979), "Historical and modern seismicity of Pakistan, Afghanistan, north-western India and south-eastern Iran", Bull. Seism. Soc. Am., 69, 773-823.

Raghukanth S.T.G. and Somala S N, (2009), Modeling of strong motion data in Northeastern India: Q, stress drop and site amplification, Bull. Seism. Soc. Am., 99(2A), 705-725.

Rao, R., Seshamma, C.V. and Mandal, P. (1998). "Estimation of Coda Qc and spectral characteristics of some moderate earthquakes of southern Indian peninsula" Unpublished Report.

Satyabala, S. P., (2003), "Oblique plate convengence in the Indo-burma-myanmar subduction region, Pure Appl. Geophys., 160, 1611-1650.

Sharma, B., Teotia, S.S. and Dinesh Kumar (2007), Attenuation of P, S, and coda waves in Koyna region, India, J. Seismol., 11, 327–344.

Singh, S.K., Bansal, B.K., Bhattacharya, S.N., Pacheco, J.F., Dattratrayam, R.S., Ordaz, M., Suresh, G., Kamal and Hough, S.E. (2004), "Estimation of ground motion for Bhuj (26th January 2001. Mw = 7.6) and for future earthquakes in India", Bull. Seismol. Soc. Am., 93(1), 353–370.

Singh, S.K., Dattatrayam, R.S., Shapiro, N.M., Mandal, P., Pacheco J.F., and Midha, R.K. (1999), "Crustal and upper mantle structure of peninsular India and source parameters of the 21 May 1997 Jabalpur earthquake (Mw = 5.8): Results from a new regional broadband network", Bull. Seismol. Soc. Am., 89, 1631–1641.

Singh, S.K., Garc, D., Pacheco, J.F., Valenzuela, R., Bansal, B.K. and Dattatrayam, R.S. (2004), "Q of the Indian Shield", Bull. Seismol. Soc. Am., 94(4), 1564-1570.

Stepp, J.C. (1972), "Analysis of completeness of the earthquake sample in the Puget sound area and its effect on statistical estimates of earthquake hazard", International Conference on Microzonation, II, 897–909.

Scordilis, E. M. (2006), "Empirical global relations converting Ms and mb to moment magnitude", J. Seismol. , 10, 225-236.

Shukla, A. K., Prakash, R., Singh, R. K., Mishra, P.S. and Bhatnagar, A. K. (2007), "Seismotectonic implications of Delhi region through fault plane solutions of some recent earthquakes", Current Science, 93(12), 1848-1853.

Talwani, P., (1997) "Seismotectonics of the Koyna-Warna Area, India." Seismicity Associated with Mines, Reservoirs and Fluid Injections. Birkhäuser, Basel, 511-550.

Uhrhammer, R. (1986), "Characteristics of northern and southern California seismicity", Earthq. Notes, 57, 21.

USNRC (2007), Regulatory guide 1.208 - "A Performance-based Approach to Define Site-specific Earthquake Ground Motion".

Wells, D.L. and Coppersmith, K.J. (1994), "Empirical relationships among magnitude, rupture length, rupture width, rupture area and surface displacements", Bull. Seismol. Soc. Am., 84(4), 974-1002.

Appendix A

SITE SPECIFIC DESIGN RESPONSE SPECTRA

Traditionally, PGA has been used to characterize ground motions. However, in recent times, the preferred parameter has been the spectral acceleration (Sa). It may be pointed out that the old practice of scaling a response spectral shape to the design PGA level leads to different probabilities of exceedance normalized over the frequency range of civil engineering structures. The present approach in engineering practice is to use design response spectra, with equal probabilities of exceedance over the entire frequency range of interest. The international code IBC(2009) prescribes design forces based on Sa corresponding to a 2% exceedance probability in 50 years. This corresponds to a 2475 year return period. IBC (2009) defines response spectra through short period (Fa) and long period (Fv) coefficients as shown in Table A-1. These coefficients have to be estimated for a given site condition. Classification of sites based on the average shear wave velocity of the top 30 meters of subsoil is popular among engineers as a quick way of understanding how ground motions during an earthquake differ between rock sites and soil sites. Standard documents such as IBC (2009), can be referenced for classifying sites based on borehole data or velocity profiling. The standard site classification definitions are shown in Table A-2. Once spectral accelerations at 0.2 sec and 1 sec corresponding to 2475 years return period are known, the design response spectrum can be constructed as below.

Step 1: Determine, maximum considered earthquake spectral response acceleration at 0.2s period and 1 s period as

$$S_{MS} = F_a S_s$$
$$S_{M1} = F_v S_1 \tag{A-1}$$

S_S and S_1 are mapped spectral accelerations for short period and 1 s period

Step 2: Determine design basis earthquake spectral response acceleration at 0.2s period and 1s period using the equations

$$S_{DS} = (2/3) S_{MS}$$
$$S_{M1} = (2/3) S_{M1} \tag{A-2}$$

Step 3: Calculate characteristic time periods To and Ts

$$T_0 = 0.2 S_{D1} / S_{DS}$$
$$T_S = S_{D1} / S_{DS} \tag{A-3}$$

Step 4: Elastic response spectra construction:

Let T is the fundamental time period of the structure

a) For periods less than or equal to T_0, design spectral response acceleration, S_a is given by

$$S_a = 0.6\left(S_{DS} / T_0\right) + 0.4S_{DS} \quad \text{(A-4)}$$

b) For periods greater than or equal to T_0 and less than or equal to T_s,

$$S_a = S_{DS} \quad \text{(A-5)}$$

c) For periods greater than or equal to Ts

$$S_a = S_{D1}/T \quad \text{(A-6)}$$

Table A-1. Site coefficients for other site conditions (IBC 2009)

Site Class	Mapped spectral response acceleration at short periods (F_a)				
	$S_s \leq 0.25$	$S_s = 0.50$	$S_s = 0.75$	$S_s = 1.0$	$S_s \geq 1.25$
A	0.8	0.8	0.8	0.8	0.8
B	1.0	1.0	1.0	1.0	1.0
C	1.2	1.2	1.1	1.0	1.0
D	1.6	1.4	1.2	1.1	1.0
E	2.5	1.7	1.2	0.9	0.9
F	Site -specific analysis shall be performed				
Site Class	Mapped spectral response acceleration at 1 sec period (F_v)				
	$S_1 \leq 0.1$	$S_1 = 0.50$	$S_1 = 0.75$	$S_1 = 1.0$	$S_1 \geq 1.25$
A	0.8	0.8	0.8	0.8	0.8
B	1.0	1.0	1.0	1.0	1.0
C	1.7	1.6	1.5	1.4	1.3
D	2.4	2.0	1.8	1.6	1.5
E	3.5	3.2	2.8	2.4	2.4
F	Site -specific analysis shall be performed				

Table A-2. Site class definition (IBC 2009)

Site Class	Average shear wave velocity	Average Standard penetration resistance	Average undrained shear strength in the case of cohesive soils
A: Hard Rock	>1500 m/s	N. A.	N. A.
B: Rock	760 to 1500 m/s	N. A.	N. A.
C: Very dense soil or soft rock	370 to 760 m/s	>50	>100 kPa
D: Stiff soil	180 to 370 m/s	15 to 50	50 to 100 kPa
E: Soft soil	<180 m/s	<15	<50 kPa
	Any profile with more than 3 m of soil having Plasticity Index PI>20 Moisture content ω≥40% Average undrained shear strength <24 kPa		
F: Soils requiring site-specific evaluation	Soil vulnerable to potential failure or collapse (liquefiable, quick- or highly sensitive clays, collapsible weakly cemented soils) More than 3m of peat and/or highly organic clays More than 7.5m of very high plasticity clays (PI>75) More than 37m of soft to medium clays		

Illustrative Example for a Hypothetical D- Type Site at Delhi:

The latitude and longitude of the site considered are 28.62° and 77.22°, respectively. Based on interpolation of PSHA results available at 0.2°×0.2° square grid point encompassing the site the value of S_s and S_1 for A-type rock level are summarized in Table A-3:

Return Period Yrs	S_s(g)	S_1(g)
2500	0.2115	0.0671

Here we are assuming the site possesses a D Type soil condition. Since the IBC procedure requires the maximum considered earthquake spectra response acceleration at 0.2 s and 1 s period as belonging to the B type soil class, a correction factor of 1.25 has to be applied. The maximum considered earthquake spectral response acceleration at 0.2s period and 1s period for Type B rock are obtained as

$S_s(g) = 0.2115 \times 1.25 = 0.2644$

$S_1(g) = 0.0671 \times 1.25 = 0.0839$

The site coefficients F_a and F_v for D-Type site are obtained as 1.6 and 2.4 from Table A-1. The short and long period MCE spectral response acceleration are obtained as:

$$S_{MS} = F_a S_s = 1.6 \times 0.2644 = 0.4230$$

$$S_{M1} = F_v S_1 = 2.4 \times 0.0839 = 0.2013$$

The design basis spectral accelerations are:

$$S_{DS} = (2/3)\, S_{MS} = (2/3) \times 0.4230 = 0.2820$$

$$S_{D1} = (2/3)\, S_{M1} = (2/3) \times 0.2013 = 0.1342$$

The characteristic periods are

$$T_0 = 0.2\, S_{D1} / S_{DS} = 0.2 \times 0.1342 / 0.2820 = 0.0952$$

$$T_S = S_{D1} / S_{DS} = 0.1342 / 0.2820 = 0.4759$$

The design spectrum for the chosen is constructed as shown below:

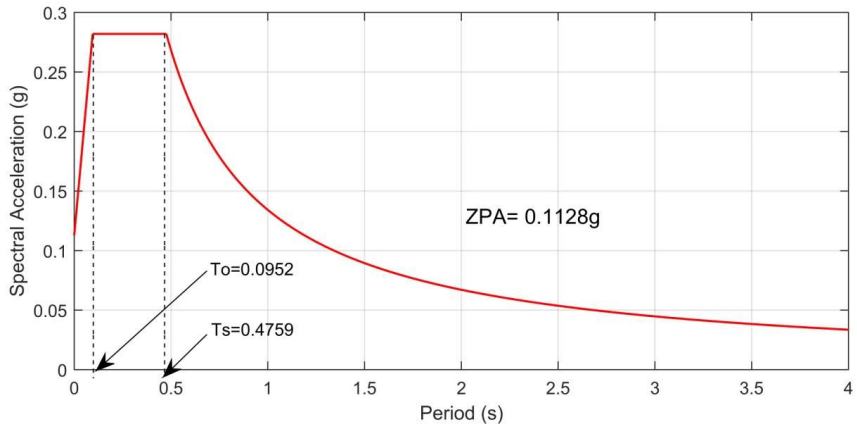


Figure A-1. Design spectra for Type D site in Delhi City (5% Damping)

Following the procedure illustrated above the design response spectra obtained for four major cities in India namely Delhi, Mumbai, Chennai, Kolkata are shown in Fig. A-2, corresponding to the A-type soil condition. It can be observed that the design values for Kolkata are higher than for the other three cities.

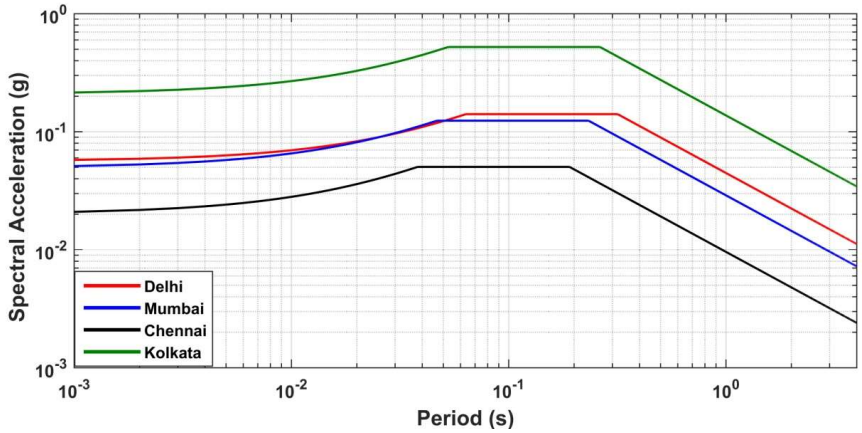


Figure A-2. Design response spectra at major cities in India (Type A - Soil Condition).

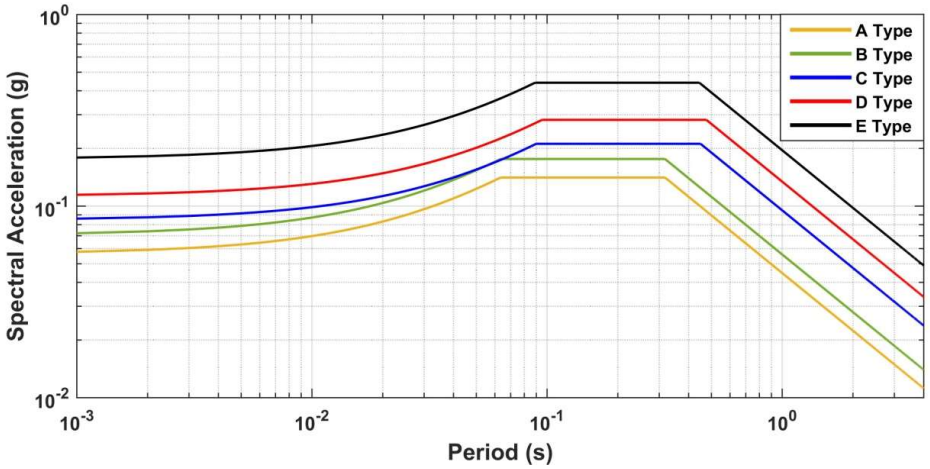


Figure A-3. Design response spectra corresponding to different soil type at Delhi.

For the design of structures, it is desirable to have site specific spectra. With the known values of S_a at 0.2 s and 1 s, the site specific spectra can be constructed using suitable coefficients as given in Table A-1. The design response spectra using IBC (2009) are constructed for five different hypothetical soil types in Delhi city as shown in Fig. A-3. It is clear that seismic demand increases as the soil condition translates from hard rock to soft soil. Thus, the hazard contours reported in this article in conjunction with IBC procedure can be employed to obtain design response spectra for any site in India.

Seismic Hazard Assessment of the City of Chennai, India

S. Banerjee and A. Boominathan

Department of Civil Engineering
IIT – Madras, India

In general, peninsular India has been considered a stable continental region for years. The city of Chennai, however, experienced moderate tremors during recent earthquakes and aftershocks. In fact, the site conditions in Chennai vary considerably in terms of the thickness of subsurface layers, strength and type of soil, and depth of the bedrock. All these factors may lead to significant differences in ground motion parameters at different parts of the city. This chapter discusses a comprehensive study assessing the seismic hazard of Chennai taking account of the seismo-tectonics of the region and local site conditions. The seismicity and seismo-tectonics of the region were first studied to establish a faults map and the recurrence rates of earthquakes were established. Secondly, deterministic and probabilistic seismic hazard analyses were carried out to obtain the ground motion characteristics at bedrock level. Next site specific response analyses were undertaken for representative sites in Chennai. Detailed cyclic characterization of the Chennai marine clay was established, based on cyclic triaxial tests and resonant column tests, to augment the ground response analysis. Finally seismic hazard contours for Chennai city, in terms of peak ground accelerations (PGA), predominant natural periods and spectral acceleration ratios were developed.

Keywords: PSHA, Stepp model, spatial uncertainty, temporal uncertainty, hazard curves

1. Introduction

In general, peninsular India has been considered a stable continental region for years. The city of Chennai, however, experienced moderate tremors during the aftershocks of the Bhuj earthquake (2001; Mw 7.6), Pondicherry earthquake (2001; Mw 5.5) and Sumatra Earthquake (2004; Mw 9.1). Intra-plate earthquakes, however, are rare compared to plate boundary events but usually tend to be more harmful. (Johnston and Kanter, 1990). It was reported that a number of multi-storey buildings in selected regions of the city suffered large oscillations during the above earthquakes. After the Bhuj earthquake, the Indian Standard on Criteria for Earthquake Resistant Design of Structures (IS: 1893–2002) was revised and Chennai has been upgraded from Seismic Zone II to Zone III leading to a substantial increase in the design ground motion parameters. Moreover, the site conditions in Chennai vary considerably in terms of the thickness of subsurface layers, the strength and type of soil, and depth of the bedrock. All these may lead to significant differences in the ground motion parameters at different parts of the city. Past experience with several major earthquakes including the 1985 Mexico, 1989 Loma Prieta, 1995 Kobe and the 1999 Turkey earthquakes suggest that structures located even as far as 200 to 300 km from the epicentre can experience overwhelming damage when there are thick soil deposits (Kramer 1996; Hasancebi and Ulusav 2006). Probabilistic hazard analyses have been carried out for selected regions in India such as New Delhi (Iyengar and Ghosh, 2004), North East India (Das et al., 2006) and Bangalore (Sitharam and Anbazhagan, 2007). But there has been no such study for Chennai city. The occurrences of earthquakes

are treated probabilistically. Cornell (1968) suggested that seismicity may be randomized in both time and space. This is achieved by modelling the seismicity in zones having a uniform spatial and temporal probability of earthquakes occurrence. These so-called 'source zones' are chosen on the basis of structural geological and neo-tectonic data and the seismicities registered and historically observed.

This chapter, therefore, describes a comprehensive study aimed at assessing the seismic hazard of Chennai city taking into account the seismo-tectonics of the region and local site conditions. First, the seismicity and seismotectonics of the region were studied to establish fault maps and recurrence rates of earthquakes. Secondly, deterministic and probabilistic seismic hazard analyses were carried out to obtain the ground motion characteristics at bedrock level. Next, site specific response analyses are presented for representative sites in Chennai city. To augment the ground response analysis a detailed cyclic characterization based on cyclic triaxial tests and resonant column tests of Chennai marine clay was carried out. Finally, seismic hazard contours for Chennai city in terms of peak ground accelerations (PGA), predominant periods and spectral acceleration ratios were developed.

2. Seismicity and seismo-tectonics of the region

The seismicity of Peninsular India has been previously presented by Chandra (1977), Rao and Rao (1984) and Khattri (1992). Seismological information and seismo-tectonics features of the region were garnered from the latest Seismo-tectonics Atlas of India (2000). General practice is to consider seismic and seismo-tectonics information at around a 300 km radial distance from the site, as giving the best representation of the seismic status of the region. Many new faults identified by the Oil and Natural Gas Commission (ONGC) were also recognised in the study. A total of 36 faults, including the two principal deep-seated faults (fault 26 and fault 17) were identified around the city as shown in Figure 1. Due to the lack of sufficient information on the seismic activity details of these faults, all faults were assumed to be active and given equal weightings in the analysis.

The distribution of sizes of earthquake in a given period of time can be characterized using the Gutenberg and Richter recurrence relationship (1954), expressed as follows:

$$\log \lambda_m = a - bM \tag{1}$$

where λm is the mean annual rate of exceedance of magnitude M, 10a is the mean yearly number of earthquakes of magnitude greater than and b describes the relative likelihood of large and small earthquakes. The a and b parameters can be obtained by regression analysis on the seismic database. The straight line fit of equation (1) between log10 N and M, gives the a and b parameters as 1.53 and 0.65 respectively. The value of 0.65 may be due to the un-truncated Gutenberg-Richter recurrence law followed by Stepp's method. It can be observed from Figure 1 that fault 24 and the Palar fault are the longest faults within this 300 km radial distance. At present, the fault activity levels are not properly known.

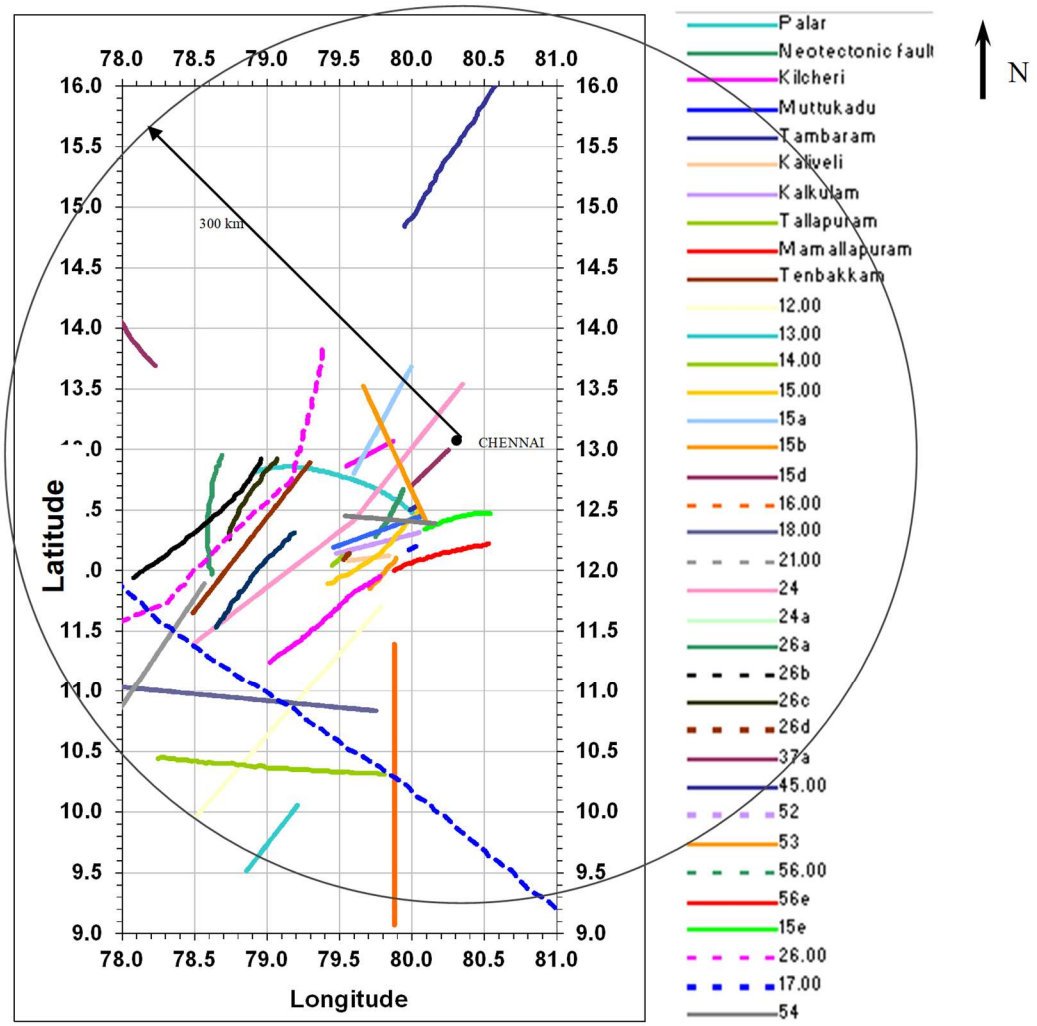


Figure 1. Fault map

A key input parameter for seismic hazard analysis is an estimate of the size of the largest earthquake possible for the fault segment or seismic zone under consideration. The maximum earthquake magnitude that a seismic source is capable of generating defines the upper bound to the earthquake recurrence relationship. There are two basic approaches to assessing maximum magnitudes for fault sources: Constraints are reprovided by historical seismicity and estimates of the maximum rupture dimensions. In the absence of source parameter details, the largest historical earthquake is commonly enhanced by a magnitude unit between of 0.25 and 1.0. In this study, the properties and rupture characteristics of the faults are not well established and hence, for each seismic source, the largest observed past magnitude was increased by 0.5 units to arrive at an assumed maximum possible magnitude (Kijko and Graham, 1998; Sokolov et al., 2001). Table 1 gives details of the faults located within 300 km of the city along with their lengths and maximum possible potential earthquake magnitudes.

Table 1. Fault details

S.No.	Name of the fault	Fault length (km)	Magnitude (Mw)
1	Palar Fault	85	4.0
2	Neotectonic Fault	105	3.8
3	Kilcheri Fault	26	4.0
4	Muttukadu Fault	11	3.5
5	Tambaram Fault	10	4.4
6	Kaliveli Fault	16	3.7
7	Kalkulam Fault	36	3.6
8	Mahapalipuram Fault	5	4.0
9	Tallapuram Fault	15	3.6
10	Tenbakkam Fault	14	3.6
11	Fault 12	60	4.0
12	Fault 13	110	4.0
13	Fault 14	180	4.7
14	Fault 15	96	3.7
15	Fault 15a	105	4.5
16	Fault 15b	34	3.5
17	Fault 15d	40	4.0
18	Fault 15e	50	4.5
19	Fault 16	258	4.0
20	Fault 17	700	3.5
21	Fault 18	211	3.5
22	Fault 21	208	3.5
23	Fault 24	365	4.4
24	Fault 24a	106	3.5
25	Fault 26	1000	4.5
26	Fault 26a	110	4.5
27	Fault 26b	150	4.1
28	Fault 26c	80	4.9
29	Fault 26d	160	4.5
30	Fault 37a	260	5.0
31	Fault 45	220	6.3
32	Fault 52	115	3.6
33	Fault 53	137	4.1
34	Fault 54	129	3.8
35	Fault 56	100	3.5
36	Fault 56e	100	4.5

3. Regional seismicity

The Seismo-tectonic Atlas of India (2000), provides useful information on the seismicity environment. Post AD 1800 historical earthquake information, within a 300 km radius of Chennai, was obtained from the US National Earthquake Information Center (NEIC). Data for a total of 65 earthquakes was obtained from this catalogue. A summary of the earthquake events is given in Table 2.

Table 2. Summary of earthquake events

S. No.	Magnitude Range **M_L - M_H	Global data		*GBA Data	
		No. of events	No. of events with M>M_L	No. of events	No. of events with M>M_L
1	2.0 – 2.5	1	39	109	417
2	2.5 – 3.0	3	38	110	308
3	3.0 – 3.5	1	35	103	198
4	3.5 – 4.0	7	34	54	95
5	4.0 – 4.5	19	27	35	41
6	4.5 – 5.0	1	8	4	6
7	5.0 – 5.5	6	7	2	2
8	5.5 – 6.0	0	1	0	0
9	6.0 – 6.5	1	1	0	0

*GBA is acronym for Gauribidanur Seismic Array

** M_L and M_H are the low and high magnitude limits respectively

The historical earthquake data prior to 1968 and recent seismicity data about the region for 1991 to 2001 obtained from the NEIC, USA catalogue, was added to the data compiled by Ghosh (1994). Repeated events were removed and finally a new catalogue of data on 638 earthquakes was prepared. Earthquake events with magnitudes greater than 2, only, were taken into account in this study. It can be seen that the number of low magnitude earthquakes is much greater than the number of high magnitude earthquakes. Earthquake events of magnitude greater than 5 are minimal in number and only seen at places far from the city.

4. PSHA Procedure

The probabilistic seismic hazard analysis model assumes that the magnitudes, distances, and resulting ground motions of earthquakes potentially affecting the site in question are random variables, thereby reflecting the fact that the exact size, location and times of occurrence of future earthquakes cannot be predicted. Figure 2 shows the four steps involved in the probabilistic seismic hazard analysis (Reiter, 1990).

a) Identification and characterization of all earthquake sources capable of producing significant ground motions at the site.

b) Next, the seismicity, or temporal distribution of earthquake recurrences must be characterized.

c) The ground motion produced at the site by earthquakes of all possible sizes occurring at any possible point in each source zone must be determined with the use of predictive relationships.

d) Finally, the uncertainties in earthquake location, earthquake size, and ground motion parameter prediction are combined, in order to obtain the probability that the ground motion parameter will be exceeded during a particular time period.

The four steps procedure outlined, is known as probabilistic seismic hazard analysis (Reiter, 1990; Finn et al., 2004).

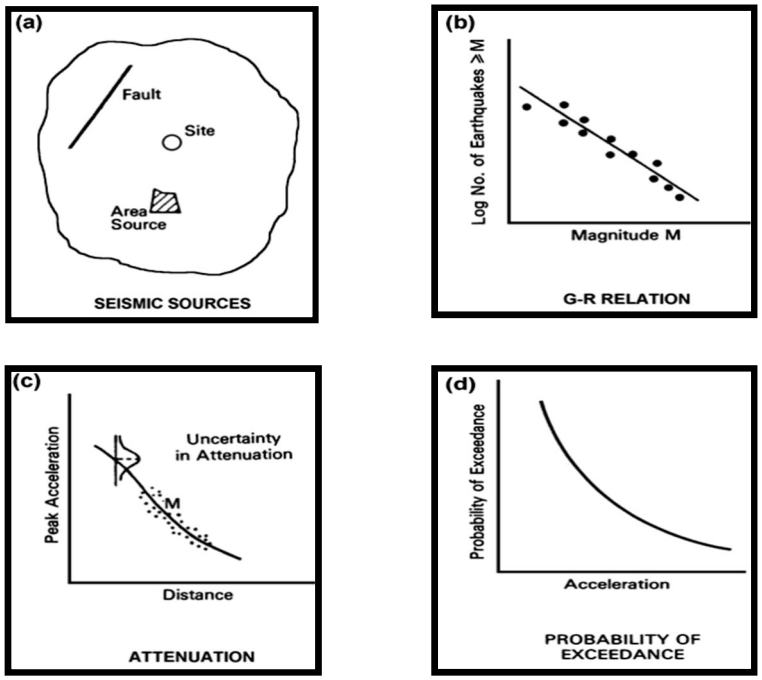


Figure 2. Four steps of probabilistic seismic hazard analysis (Finn et al., 2004)

5. Completeness Analysis

There are a number of uncertainties, which affect historic earthquake catalogues. The quality of a good earthquake catalogue depends on its completeness and uniformity. The level of completeness varies as a function of space, time and earthquake size. The degree oof incompleteness reflects the settlement history of the continent. Generally, earthquake catalogues are biased against small earthquakes and this makes them incomplete. An analysis of completeness of the catalogue has to be performed before carrying out seismic hazard analysis. A statistical analysis of the data has been accordingly conducted in order to identify which time periods provided complete data. Time periods represent the time span over which earthquakes of given magnitude ranges are completely recorded. The reliable average rate of earthquake occurrence for each magnitude range, for each source zone, was then estimated from the corresponding complete data. The common method adopted for treating this incompleteness is to apply the Stepp model (Shanker and Sharma, 1997). This method uses a moving time window. The entire catalogue is grouped into several magnitude classes and modelled as a point process in time. A statistical treatment

is carried out for each of the magnitude classes. Tangent lines of slope, where T is the duration of the sample, have been drawn through the stable values of the standard deviation for various magnitude ranges. It is observed that for the 3-4, 4-6 and 5-6 magnitude groups the data is complete for 30, 60 and 100 years respectively. Table 3 shows the earthquake distribution data by time and magnitude. A time interval of 10 years has been taken for the period 1792 to 2001. Rates of occurrence for the three different magnitude ranges have been established for the different time intervals using the above procedure. The time periods for which the data is complete for different magnitude groups are also shown in the table.

Table 4 shows the time period and magnitude above which the data is complete for the magnitudes 3-4, 4-6 and 5-6. It can be seen from Table 4 that the number of earthquake events per year reduces with an increase in magnitude which leads to an increase in the completeness period.

6. Earthquake source characterisation

A seismic source represents a portion of the earth's crust with the potential to generate earthquakes. Within a seismic source, the probability of earthquake occurrence and the size of the maximum magnitude are generally considered to be invariant. The seismic source characteristics that must be assessed for probabilistic seismic hazard analysis are discussed in the following section.

The three principal components of a seismic source characterization are source location and geometry, maximum earthquake magnitude, and earthquake recurrence. In identifying and characterizing seismic sources, the scale of the features to be considered and the level of investigation vary with distance from the site. As ground motion attenuates with distance to the site, an earthquake size must increase with distance to the site to produce significant ground motion at the site. The size of earthquake that a feature can generate is related to its physical dimensions. Thus, the further the distance from the site, the larger a fault must be for a significant ground motion potential to exist at the site. Within these sources, earthquakes are assumed to occur randomly, in terms of their epicentral locations, as well as in terms of their occurrence times.

7. Spatial uncertainty

The entire Chennai city and its surroundings have been divided into a 1 km x 1 km grid, and the hazard level assessed for each node of this grid. The uncertainty in the source to site distance (R) can be described by a probability density function. The probability density functions of R for each source were then determined. The source zones were divided in to a large number of segments of equal length and a histogram was constructed by tabulating the values of R that correspond to the centre of each element. The ordinates of the normalized histogram represent the relative frequency, which can be approximated as the probability (Figure 3).

Table 3. Earthquake distributions by time and magnitude

Time Period	Time Interval	Rate of occurrence for magnitude		
		3-4	4-5	5-6
1992-2001	10	0.0000	0.0000	0.1000
1982-2001	20	0.2958	0.1118	0.0500
1972-2001	30	0.3480	0.1106	0.0333
1962-2001	40	0.3082	0.1392	0.0433
1952-2001	50	0.2466	0.1149	0.0346
1942-2001	60	0.2055	0.0957	0.0289
1932-2001	70	0.1761	0.0821	0.0247
1922-2001	80	0.1541	0.0718	0.0217
1912-2001	90	0.1370	0.0648	0.0192
1902-2001	100	0.1233	0.0583	0.0173
1892-2001	110	0.1121	0.0530	0.0157
1882-2001	120	0.1031	0.0486	0.0144
1872-2001	130	0.0951	0.0449	0.0133
1862-2001	140	0.0886	0.0429	0.0143
1852-2001	150	0.0843	0.0416	0.0133
1842-2001	160	0.0791	0.0390	0.0125
1832-2001	170	0.0744	0.0367	0.0118
1822-2001	180	0.0703	0.0356	0.0111
1812-2001	190	0.0668	0.0349	0.0105
1802-2001	200	0.0634	0.0335	0.0100
1792-2001	210	0.0604	0.0323	0.0095

Table 4. Activity rate and completeness interval

Magnitude, m	No. of events per year ≥ m	Completeness period (years)
3	0.34801	30
4	0.0957	60
5	0.0173	100

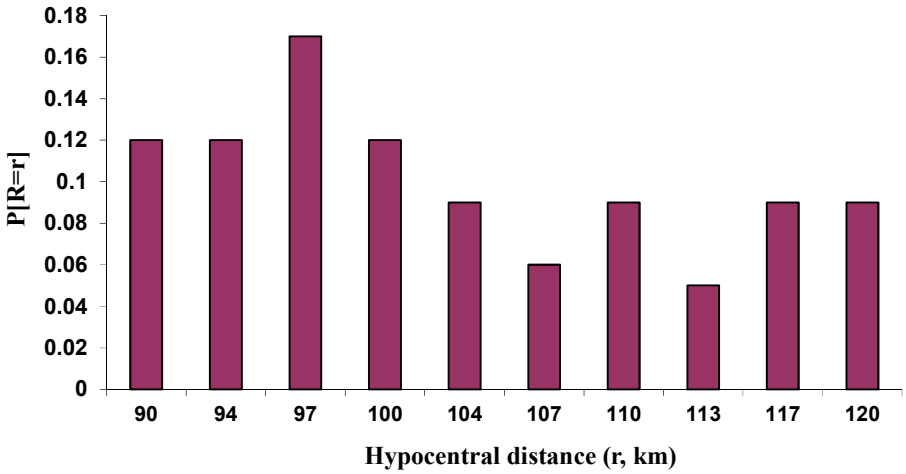


Figure 3. Probability density function of hypocentral distance

8. Size uncertainty

The probability density function of the magnitude was found in a similar manner. A lower level magnitude, M_L of 3 was assumed. The maximum possible magnitude, M_u on a particular seismic source was found using the commonly adopted approach of increasing the largest, observed past magnitude by 0.5. The maximum observed magnitudes plus 0.5 for each fault source are also given in Table 1. Then the magnitude range was divided into several intervals. For each source zone, the probability that the magnitude (m) will be within an interval between a lower bound m_l and an upper bound m_u is given by,

$$P\left[m_1 < m_2 < m_u\right] = \int_{M=m_1}^{M=m_u} f_M\left(m\right) dm \approx f_M\left(\frac{m_1 + m_2}{2}\right)\left(m_u - m_1\right) \tag{2}$$

The probability density function, $f_M\left(m\right)$ is given by:

$$f_M\left(m\right) = \frac{\beta \exp\left[-\beta\left(m - m_o\right)\right]}{1 - \exp\left[-\beta\left(m_{\max} - m_o\right)\right]} \tag{3}$$

where β= 2.303 b, m_o = Lower magnitude, m_{max} = maximum magnitude

A coarse histogram, which represents the magnitude probability distributions, is shown in Figure 4. The ordinates of which approximate to the probability of various magnitudes for each source zone.

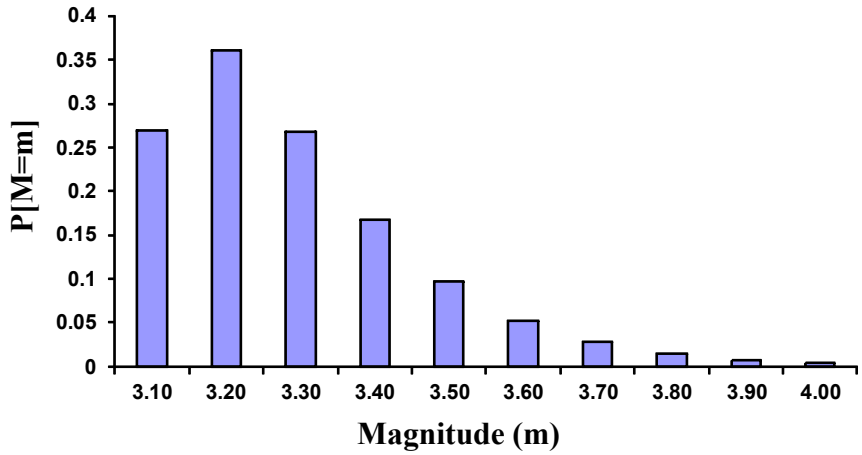


Figure 4. Probability density function of magnitude

9. Probability computations

For each combination of hypo-central distance and magnitude, the peak ground acceleration was computed using the appropriate strong ground motion attenuation equation . The scarcity of strong motion accelerograph (SMA) data in *Peninsular India* (PI) and its heterogeneity with respect to the seismogenic properties makes unreliable any empirical equation obtained using the available incomplete SMA data. Moreover such sparse data causes over estimation in some locations and under estimation in few locations. This difficulty can be overcome by adopting a stochastic seismological model as demonstrated by Boore (1983, 2003). With this approach, regional quality factor differences within *PI*, uncertainties in stress-drop, radiation coefficient, cut-off frequency and focal depth can be included. With the help of a large synthetic database a frequency dependent attenuation relation can be obtained corresponding to bed rock conditions (Iyengar and Raghukanth 2004).

The attenuation relationship, as proposed, particularly for Peninsular India, is based on a statistically simulated seismological model. The equation developed for estimating the peak ground acceleration (*g*), under bed rock condition, is of the form,

$$\ln\left(PGA \text{ in g's}\right) = C_1 + C_2\left(M-6\right) + C_3\left(M-6\right)^2 + \ln\left(R\right) + \ln\left(\varepsilon\right) \tag{5}$$

where C_1 = 1.7816; C_2 = 0.9205; C_3 = -0.0673; C_4 = 0.0035 and σ *(Ln* ε*)* = 0.3136.

M refers to moment magnitude and *R* is the hypo-central distance from the point of focus to the closest distance to the fault. Since the peninsular shields in general are more susceptible to shallow focus earthquakes (Rao and Rao, 1984), a focal depth of 10 km is assumed and the hypo-central distance is calculated for all fault sources.

The probabilities that various target peak acceleration levels y* t will be exceeded were calculated using,

$$P\left[Y > y^* \mid m, r\right] = 1 - F_Y\left(y^*\right) \tag{5}$$

where $F_Y(y)$ is the value of the cumulative distribution function of Y at m and r.

10. Hazard curves

Seismic hazard curves can be obtained by computing the mean annual rate of exceedance , λ_{y*}, for different specified ground motion value, y^*. The annual rate of exceedance, λ_{y*} of each peak acceleration level for each magnitude and distance interval for a particular source zone can be computed using,

$$\lambda_{y*} = v_i P\left[Y > y^* \mid M = m, R = r\right] P\left[M = m\right] P\left[R = r\right] \tag{6}$$

where $v_i = \exp(\alpha - \beta m)$, $\alpha = 2.303\ a$; $\beta = 2.303b$

These curves are first obtained individually for all thirty-six faults and then combined to estimate the aggregate hazard at the site. The process is repeated for other possible combinations of magnitude and distance for a particular source and the probabilities of each are summed. By repeating this process for different target accelerations, the seismic hazard curves are obtained. The seismic hazard curve in terms of bedrock PGA is obtained by the above procedure for all grid points. Typical hazard curves obtained by this procedure are shown in Figure 5. Consequently, the probability that a particular target acceleration will be exceeded by an earthquake of magnitude of $M > m_o$ at any of these sources are obtained from the cumulative seismic hazard curve. The reciprocal of the annual probability of exceedance gives the return period for the corresponding PGA value.

11. Temporal uncertainty

Temporally, earthquakes are assumed to follow a simple Poisson process. The Poisson model is the most tractable that can be applied to this type of analysis, and has been employed as the "standard" model for hazard analysis for many years. The Poisson model is widely used and is a reasonable assumption for regions where data are sufficient only to provide an estimate of average recurrence rates (Cornell, 1968). The most important assumption is that earthquakes associated with a given source have no "memory" of past earthquakes. Large earthquakes have been shown to occur in a time-dependent manner: i.e., the probability of a large shock in fact depends upon the time elapsed since the last large shock on a given fault, or in a given source area.

The seismic hazard curve combined with the Poisson model to estimate the probabilities of exceedance of a particular value y^* in finite time period, T can be expressed as

$$P\left[Y_T > y^*\right] = 1 - e^{\lambda_{y*}T} \tag{7}$$

It should be noted that the assumption of a Poisson process for the number of events is not critical. This is because the mean number of events in time T, $\lambda_{y*}T$, can be shown to be a close upper bound on the probability, $P[Y_T > y^*]$ for the small probabilities (less

than 0.10) that are generally of interest for engineering applications.

By rearranging the terms, we get,

$$\lambda_{y^*} = \frac{\ln\left(1 - P\left[Y_T > y^*\right]\right)}{T} \tag{8}$$

The procedure is repeated for all grid points to obtain PGA at bed rock level. A MATLAB code was written to carry out the PSHA analysis following the above procedure to arrive at the seismic hazard contours. Figure 6 shows the PGA contours at rock level for a 2% probability of exceedance in 50 years, which corresponds to a return period of 2500 years.

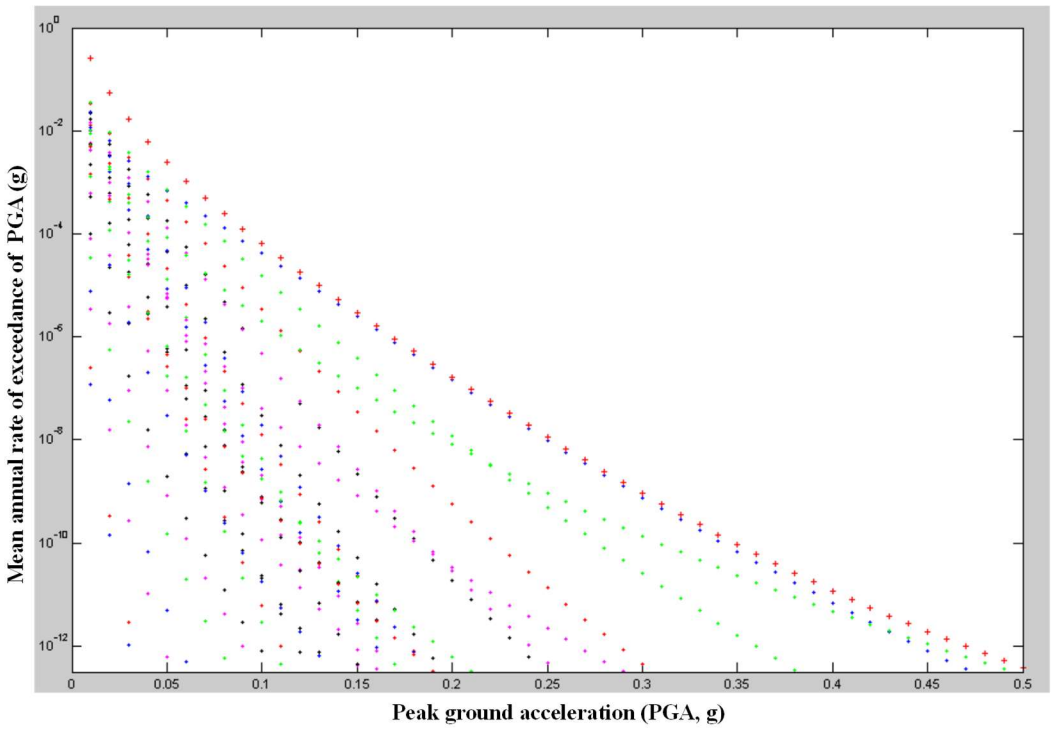


Figure 5. Typical Seismic Hazard Curves (Coordinates: 13.04, 80.17)

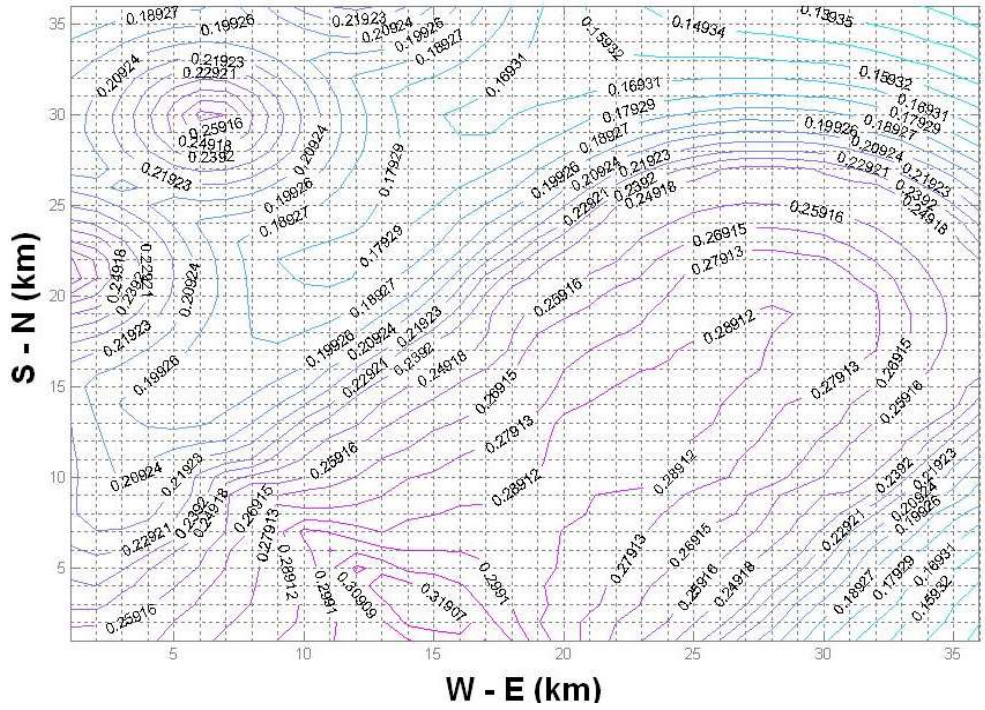


Figure 6. Contours of rock level PGA (in g's) with 2% probability of exceedance in 50 years

In this case, the bedrock level PGA varies from 0.139g to 0.319g. By comparing the PGA hazard contours shown in Figure 6 with the fault map shown in Figure 1, it can be easily seen that the hazard pattern basically follows the fault pattern. The orientation of the contours is observed to follow the orientation of the faults. The distribution of high PGA values along the north-western, central and southern parts of the city is primarily due to the presence of faults 24, 15d and 53 respectively. The increase in hazard towards the southern parts is due to the closeness of the cluster of faults to those regions. However, the north-eastern parts show comparatively minimal hazard reflecting the lower seismic source potential in that region. Similarly, rock level PGA contours have been plotted for a 10% probability of exceedance in 50 years (Figure 7). This corresponds to a return period of 500 years.

The rock level PGA, in this case, varies from 0.106g to 0.248g. The site classification study has been carried out for 38 representative sites in Chennai city based on the NEHRP classification. The $V_{s\text{-}30}$ procedure (Kramer and Stewart 2004), which takes into account the weighted average shear wave velocity in the upper 30 m, is used in this study. In general, the $V_{s\text{-}30}$ method is based on the principle that the first 30 m of the soil layer participates in the amplification phenomenon of the bed rock motion. The geographical PGA distribution for a 2% probability of exceedance in 50 years for the 38 representative areas in Chennai is given in Table 5. The estimated $V_{s\text{-}30}$ values and their corresponding site classifications for each area are also given, in Table 6. It can be seen from Table 5 that all areas fall under a B, C or D classification. However, most areas in the city are categorized under site classification C. It can be seen that the site class B is found predominantly in southern parts of the city and site class D is found predominantly in western parts of the city. The majority site class, C, is found in the Northern, Eastern and Central parts of the city.

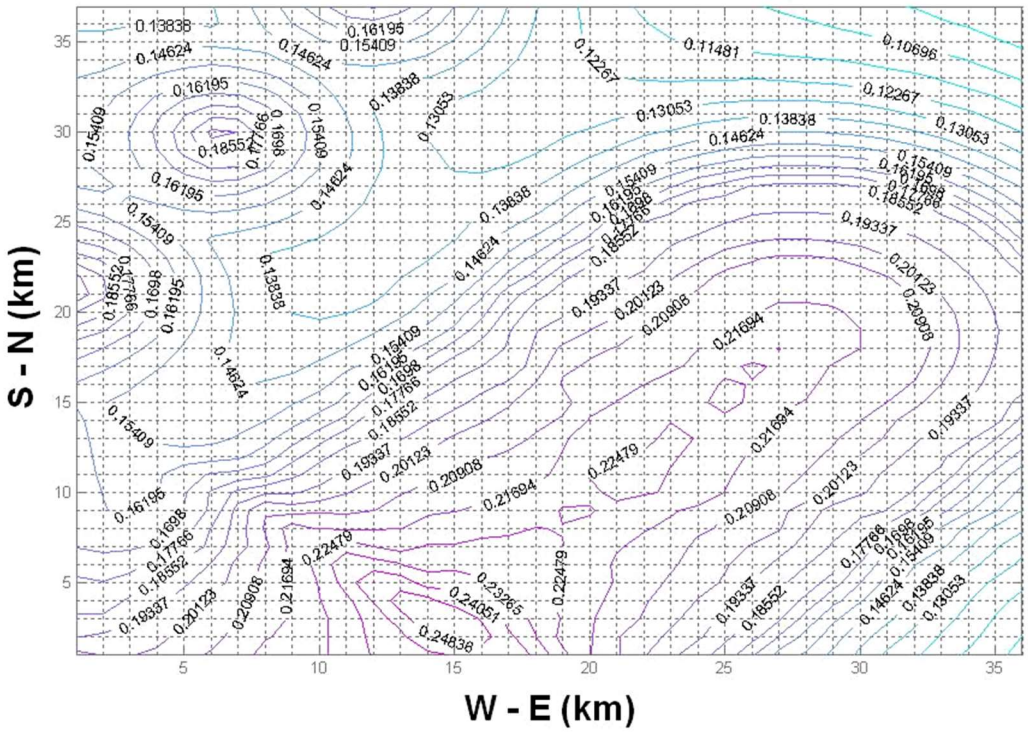


Figure 7. Contours of rock level PGA (in g's) with 10% probability of exceedance in 50 years

12. Conclusions

A comprehensive study has assessed the seismic hazard of Chennai city using a probabilistic approach. A detailed study of the seismicity and seismo-tectonics of the region was carried out and a fault map developed covering a 300 km radial distance from the city. The Probabilistic Seismic Hazard Analysis was carried out with MATLAB code for the 36 seismic sources within a 300 km radius of the city. The entire city and its surroundings were divided into 1 km x 1 km grid , and the hazard level assessed at each node of the grid. The hazard level towards southern parts of the city mainly result from the nearness of the cluster of faults in those regions. The minimal hazard in the north-eastern parts indicates the lower seismic source potential in that region. Similarly, rock level PGA contours have been plotted for a 10 % probability of exceedance in 50 years. The rock level PGA varies from 0.106g to 0.248g. Site classification was also carried out using the V_{s-30} method and site class "C" was found to be the majority site class within the city.

Table 5. Details of representative sites and the geographical distribution of PGA

S.No	Area	Latitude (º)	Longitude (º)	Thickness of overburden, (m)	V_{s-30}, (m/s)	Site Classif-ication	PGA (g) for 2500 years RP
1	Abiramapuram	80.2591	13.0292	30	251	D	0.219
2	Adyar	80.2564	13.0073	25	345	D	0.199
3	Alwarpet	80.2483	13.0354	24	430	C	0.219
4	Ambattur	80.1570	13.0989	20	515	C	0.279
5	Anna Nagar	80.2149	13.0888	28	260	D	0.259
6	Ashok nagar	80.2181	13.0315	21	431	C	0.249
7	Avadi	80.1060	13.1123	12	776	B	0.289
8	Aynavaram	80.2273	13.0956	28	346	D	0.259
9	Balaji Nagar	80.2666	13.0707	12	731	C	0.229
10	Cpr Road	80.2602	13.0357	34	271	D	0.189
11	Guindy	80.2364	13.0263	9	788	B	0.239
12	Kolathur	80.2207	13.1177	12	769	B	0.249
13	Korattur	80.1835	13.1018	20	484	C	0.269
14	Koyambedu	80.2030	13.0712	26	391	C	0.279
15	Madavaram	80.2389	13.1461	28	241	D	0.189
16	Manali	80.2613	13.1664	22	438	C	0.179
17	Mandaveli	80.2677	13.0236	21	491	C	0.199
18	Nandambakkam	80.1987	13.0149	5	918	B	0.259
19	Nandanam	80.2390	13.0237	19	496	C	0.239
20	Nesapakkam	80.1855	13.0358	17	579	C	0.269
21	Nungambakkam	80.2436	13.0582	18	530	C	0.249
22	Palavakkam	80.2531	12.9603	12	723	C	0.169
23	Perambur	80.2591	13.1103	17	637	C	0.209
24	Perungudi	80.2373	12.9561	10	747	C	0.179
25	Poes	80.2509	13.0403	20	485	B	0.219
26	Ramapuram	80.1817	13.0313	12	728	C	0.269
27	RA Puram	80.2609	13.0201	20	474	C	0.199
28	Royapuram	80.2985	13.1016	12	756	C	0.149
29	Saidapet	80.2114	13.0229	8	809	B	0.259
30	Santhome	80.2808	13.0324	25	345	D	0.169
31	Tambaram	80.1423	12.9252	5	915	B	0.209
32	Thoapakkam	80.2358	12.9511	14	680	C	0.179
33	Tiruvottiyur	80.3054	13.1644	22	398	C	0.139
34	T. Nagar	80.2136	13.0582	25	399	C	0.259
35	Vadapalani	80.2174	13.0542	19	538	C	0.259
36	Velachery	80.2263	12.9795	10	768	B	0.189
37	Vepery	80.2684	13.0845	17	557	C	0.209
38	Vyasarpadi	80.2574	13.1342	18	594	C	0.199

References

Boore, D. M. (1983), "Stochastic simulation of high-frequency ground motions based on seismological models of the radiated spectra," Bulletin of the Seismological Society of America, 73(6A), 1865-1894.

Boore, D. M. (2003), "Simulation of ground motion using the stochastic method," Pure and Applied Geophysics, 160, 635-675.

Chandra, U. (1977), "Earthquakes of Peninsular India – A Seismotectonic Study," Bulletin of the Seismological Society of America, 67(5), 1387-1413.

Cornell, C. A. (1968), "Engineering Seismic Risk Analysis," Bulletin of the Seismological Society of America, 58 (1), 583–1,606.

Das, S., Gupta, I.D. and Gupta, V.K. (2006), "A Probabilistic Seismic Hazard Analysis of Northeast India," Earthquake Spectra, 22(1), 1-27.

Finn W. D. L., Onur, T. and Ventura, C. E. (2004), "Microzonation: Developments and Applications," In Recent Advances in Earthquake Geotechnical Engineering and Microzonation, Kluwer Academic Publishers, Dordrecht.

Ghosh, A. K. (1994), "Design basis ground motion parameters for PFBR site," Internal report, BARC, Mumbai.

Gutenberg, B. and Richter, C. F. (1944), "Frequency of earthquakes in California," Bulletin of the Seismological Society of America, 34(4), 1985-1988.

Hasancebi, N. and Ulusay, R. (2006), "Evaluation of site amplification and site period using different methods for an earthquake-prone settlement in Western Turkey," Engineering Geology, 87, 85–104.

IS 1893 (Part 1): 2002 Indian Standard Criteria for Earthquake Resistant Design of Structures Part 1 General Provisions and Buildings (Fifth Revision).

Iyengar, R. N. and Raghukanth, S. T. G. (2004), "Attenuation of Strong Ground Motion in Peninsular India," Seismological Research Letters, 75, 530-540.

Iyengar, R. N. and Ghosh, S. (2004), "Microzonation of earthquake hazard in Greater Delhi area," Current Science, 87(9), 1193-1202.

Johnston, A. C. and Kanter, L. R. (1990), "Earthquakes in stable continental crust," Scientific American, 262(3), 68–75.

Kijko, A. and Graham, G. (1998), "Parametric-historic Procedure for Probabilistic Seismic Hazard Analysis, Part I: Estimation of Maximum Regional Magnitude M_{max}," Pure and Applied Geophysics, 152, 413–442.

Khattri, K.N. (1992), "Seismic hazard in Indian region," Current Science, 62(1&2), 109 116.

Kramer, S. L (1996), "Geotechnical Earthquake Engineering," Prentice-Hall, Inc. Upper Saddle River, New Jersey.

Kramer, S. L. and Stewart, J. P. (2004), "Geotechnical Aspects of Seismic Hazards in Earthquake Engineering: From Engineering Seismology to Performance-Based Engineering," CRC Press.

Rao, B. R. and Rao, P. S. (1984), "Historical seismicity of Peninsular India," Bulletin of the Seismological Society of America, 74(6), 2519-2533.

Reiter, L. (1990), "Earthquake Hazard Analysis: Issues and Insights," Columbia Univ. Press, New York.

Seismotectonic Atlas of India (2000). Geological Survey of India, New Delhi.

Shanker, D. and Sharma, M. L. (1997), "Statistical analysis of completeness of seismicity data of the Himalayas and its effect on earthquake hazard determination," Bulletin of the Indian Society of Eaethquake Technology, 34(3), 159-170.

Sitharam, T. G. and Anbazhagan, P. (2007), "Seismic Hazard Analysis for the Bangalore Region," Natural Hazards, 40, 261–278.

Sokolov, Y. V., Loh, C. H. and Wen, K. L. (2001), "Empirical Models for Site- and Region-Dependent Ground Motion Parameters in the Taipei Area: A Unified Approach," Earthquake Spectra, 17(2), 313-332.

New Site Classification Scheme and Design Response Spectra for Korea

Dong-Soo Kim[a], Satish Manandhar[b] and Hyung-Ik Cho[c]

[a] Department of Civil and Environmental Engineering
Korea Advanced Institute of Science and Technology, Korea

[b] Renewable Energy Group
KEPCO Research Institute, Daejeon, Korea

[c] Earthquake Research Centre
Korea Institute of Geoscience and Mineral Resources, Korea

A new site classification scheme and design response spectra (DRS), based on local site conditions have been developed and implemented as some part of new minimum general seismic design requirements in Korea, enabling more reliable estimates of earthquake ground motions. The new site classification scheme relates to bedrock depth (*H*) and average V_S of soil above the bedrock ($V_{S,Soil}$) as parameters for site classification, because these are the two factors which mainly affect site amplification, especially for regions of shallow bedrock such as in Korea. The 20 m depth to bedrock was selected as the initial parameter for site classification purposes based on the trends observed during site-specific response analyses. Sites where $H < 20$ m were sub-divided into two site classes, using 260 m/s for $V_{S,Soil}$, whereas sites where $H > 20$ m were sub-divided into two site classes with $V_{S,Soil}$ equal to 180 m/s. The site classification scheme and the DRS were verified using dynamic centrifuge tests to simulate representative Korean site conditions, such as the shallow depth to bedrock and short-period amplification characteristics. The simulated results have been incorporated within the new DRS. The new site classification scheme and DRS reasonably represent the site amplification characteristics of shallow bedrock conditions in Korea. Thus, it is possible to conclude that the newly implemented seismic provisions are more reliable and superior to those defined in the previous seismic code.

Keywords: site classification scheme, design response spectra, shallow bedrock region, Korea

1. Introduction

The effect of local soil conditions on earthquake motions is a key issue in geotechnical earthquake engineering practice. Local soil either amplifies or attenuates the seismic energy reaching the ground surface, thereby directly affecting the response of structures during an earthquake event. The 1985 Mexico City earthquake and the 1989 Loma Prieta earthquake provide abundant evidence of local site amplification (Seed et al. 1988; Borcherdt and Glassmoyer 1992). To quantify local site effects, the response spectrum method is widely used around the world. This method shows clearly, and conveniently, how a given structure will respond to complex earthquake ground motions.

The previous Korean seismic code (Ministry of Construction and Transportation, MOCT 1997), which has been in use for the last 20 years, uses a site classification scheme and corresponding site coefficients that are similar to the 1994 and 1997 NEHRP provisions, which were revised based on data recorded during the Loma Prieta (1989) and Northridge (1994) earthquakes in the western United States (BSSC 1997). However, site

coefficients derived from earthquakes recorded under considerably different site and seismicity conditions cannot represent the actual motions of ground and structures in other regions. Recent studies performed in Korea (Sun et al. 2005; Kim and Yoon 2006; Lee et al. 2012) have shown that the site coefficients obtained from site response analyses for inland areas of the Korean Peninsula were significantly different from those given in the previous Korean seismic code. Naturally, the spectral accelerations obtained from the site response analyses also contrasted with the design response spectra (DRS) in the previous Korean seismic code. Therefore, appropriate site coefficients based on local site conditions in the Korean Peninsula are required, if reliable estimates of earthquake ground motions are to be made.

In general, 30 m is the typical depth for ground composition test borings and detailed site characterization in a number of regions, including the western US. Therefore, many countries have adopted the soil parameter $V_{S,30}$, which indicates the mean shear wave velocity for the top 30 m of soil, as a criterion for site classification (BSSC 1997; MOCT 1997; CEN 2004; ICC 2012). This kind of site classification scheme is acceptable for regions with relatively deep bedrock and sites with a gradual transition from soil to hard rock, both of which are common geological conditions in the western US. However, the scheme may not be acceptable for regions with bedrock located at depths less than 30 m below ground level and with abrupt transitions from soil to much stiffer rock, both of which are common in Korea. In regions of shallow bedrock, site investigations are often made down to the bedrock, so the depth to bedrock is clearly defined, and VS values can generally be reliably determined for the soil layers and bedrock for site response analysis purposes.

In this study, the development of a new Korean site classification scheme and DRS, which was implemented as a part of new minimum requirements for general seismic design in July 2017 (Ministry of Public Safety and Security, MPSS 2017), are described based on site-specific response analyses for more than 300 Korean soil sites. The database of input parameters used for the site-specific response analyses are briefly explained. Next, reasons for selecting bedrock depth (H) and average V_S of soil above the bedrock ($V_{S,Soil}$) as parameters for site classification and detailed criteria for sub-dividing the sites, are discussed, based on the results of site-specific response analyses. Finally, the new DRS, which were developed based on the new classification parameters, are verified by dynamic centrifuge tests. The development of site classification scheme and DRS as described in this paper is based on a recent study by Manandhar et al. (2017).

2. Database for site response analysis

For the site-specific response analyses, a total 300 subsurface geologic profiles were collected from all over the Korean Peninsula. Of the 300 sites, 100 sites were classified under each of the site classes S_C, S_D, and S_E based on $V_{S,30}$, according to the previous code. The bedrock depth, $V_{S,30}$, $V_{S,Soil}$ and site period (T_G) of 300 sites are summarized in Table 1.

Site response analysis was performed using the SHAKE 91 program (Idriss and Sun 1992) for estimating ground motions at the 300 sites. Design rock outcrop accelerations were 0.110 g, 0.154 g, 0.220 g and 0.286 g corresponding to earthquake return periods of 500 years, 1000 years, 2400 years and 4800 years, respectively, according to the Korean seismic hazard map. As strong ground motions records are lacking in Korea, eight accelerograms recorded at various types of site were used as input motions for site

response analyses, such that the average input motion is compatible with the DRS of the reference site class S_B. Figure 1 shows the response spectra for different input motions along with the DRS for the S_B site class. The soil non-linear deformation characteristics, expressed in terms of normalized modulus reduction curves (G/G_{max} – log γ) and damping ratio curves (D - log γ) were used for representative soil types in Korea (Kim and Choo 2001; Sun et al. 2005).

Table 1. Information on bedrock depth (H), $V_{S,30}$, $V_{S,Soil}$ and T_G of 300 sites

	S_C site class			S_D site class			S_E site class		
	Min.	Max.	Ave.	Min.	Max.	Ave.	Min.	Max.	Ave.
H (m)	1.0	22.5	11.3	9.0	30.0	18.6	14.0	30.0	26.9
$V_{S,30}$ (m/s)	364.5	744.5	480.1	182.0	358.2	312.2	65.6	179.8	141.0
$V_{S,Soil}$ (m/s)	134.9	633.2	295.2	138.7	346.9	223.2	65.6	179.5	127.1
T_G (s)	0.16	0.33	0.26	0.33	0.66	0.39	0.67	1.83	0.92

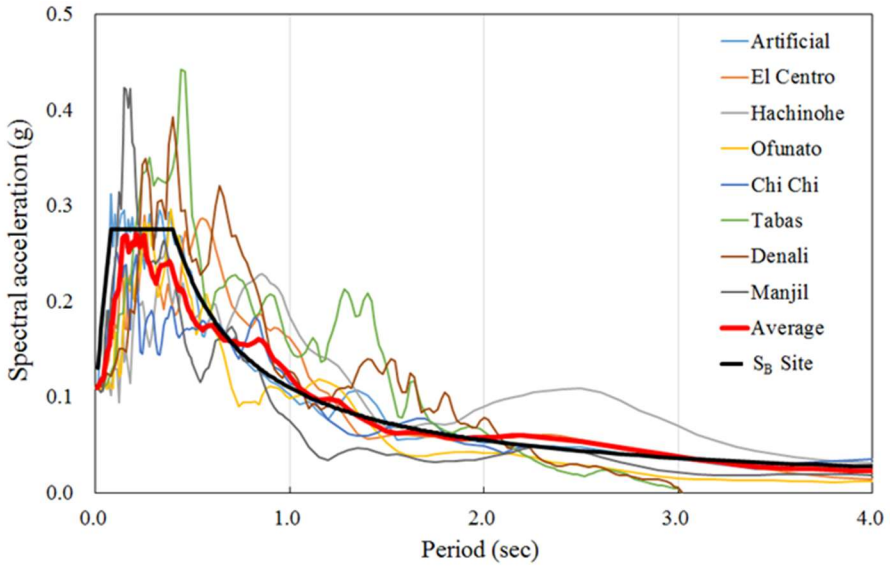


Figure 1. Response spectra of input motions compared with the design response spectrum of reference site class S_B (all motions scaled to 0.154 *g*)

3. New site classification scheme and design response spectra

The most important factors affecting site amplification are H and V_S for the soil (Rodriquez-Marek et al. 2001). The transfer function (|F1(ω)|), which describes soil amplification in parametric form as in equation 1, shows that H and $V_{S,Soil}$ are fundamental variables that affect soil amplification, and hence are ideal parameters for the classification of shallow bedrock sites. In this section, a new site classification scheme is described based on H and $V_{S,Soil}$, , developed after analyzing trends and the dispersion of site amplification coefficients obtained from site response analyses.

$$\left|F_1(\omega)\right| = 1 / \left|\cos\left(\frac{\omega H}{V_S}\right)\right| \quad (1)$$

where ω is the angular velocity of the seismic wave components.

Site coefficients were calculated for each output from program SHAKE (Idriss & Sun, 1992) from a total of 9600 SHAKE runs (300 sites, 4 rock outcrop accelerations, and 8 input motions) and were divided into short-period site coefficients (F_a) and long-period site coefficients (F_v). These coefficients were calculated from the ratio of soil surface and corresponding rock surface response spectra (RRS), (Borcherdt 1996; Dobry et al. 1999). The F_a and F_v values were determined using the average RRS curve obtained by averaging the RRS curves of eight input earthquake motions at a particular intensity.

In order to develop a new site classification scheme, the trends and dispersion of the site coefficients were examined to group those sites with similar amplification characteristics. Initially, the bedrock depth (H) was used to divide the site into two groups. Based on the trend in variation of F_a and F_v with site period, H = 20 m was determined to be a reasonable boundary at which to divide the sites into two categories ($H \leq 20$ m and $H > 20$ m). The first site class mostly contains shallow and stiff soils, whereas most sites in the second site class are relatively deep and soft. The site classes were next subdivided using $V_{S,Soil}$. Based on the dispersion of F_a and F_v values with respect to $V_{S,Soil}$, the boundaries corresponding to 260 m/s and 180 m/s were deemed appropriate for sub-dividing the sites. These boundaries were decided according to the average $V_{S,Soil}$ of the first and second site classes. Consequently, four new classes (S_2, S_3, S_4 and S_5) were formed for soil sites, while a rock site is specified as S_1 site class.

Table 2. New Korean seismic site classification scheme (MPSS 2017)

Site class	Site description	Parameters for classification	
		Bedrock* depth, H (m)	$V_{S,Soil}$ (m/s)
S_1	Rock	$H < 1$	-
S_2	Shallow and stiff soil	$1 \leq H \leq 20$	≥ 260 m/s
S_3	Shallow and soft soil		< 260 m/s **
S_4	Deep and stiff soil	$H > 20$	≥ 180 m/s
S_5	Deep and soft soil		< 180 m/s **
S_6	Special soil requiring site-specific evaluation		

* Stratum showing a shear wave velocity higher than 760 m/s

** stratum with shear wave velocity lower than 120 m/s is considered as site class S_5

The site classification scheme is presented in Table 2. In this scheme, for all sites in class S_6 a site-specific evaluation of seismic response should be made. Additionally, soil sites with $V_{S,Soil} \leq 120$ m/s are included in the S_5 class regardless of bedrock depth, as these sites are too soft for inclusion in class S_3 . Likewise, very deep sites ($H > 50$ m) are included in the S_6 site class as these sites are rare in Korea (Lee et al. 2012; Sun et al. 2012).

$$F_{a\ or\ v} = \frac{1}{\beta - \alpha}\int_{\alpha}^{\beta} \frac{RS_{soil}(T)}{RS_{rock}(T)}dT \tag{2}$$

The F_a values for the four soil site classes listed in Table 3 were calculated using equation (2) from mean RRS curves with an integration interval of 0.1 - 0.5 s, whereas the F_v values were calculated using equation (2) from the mean+1σ RRS curves (where σ is standard deviation) with an integration interval of 0.4 - 1.5 s. The adjustment of the integration interval for F_v values was needed to improve the DRS at long-period ranges for Korean site conditions (Kim and Yoon 2006; Lee et al. 2012). As the database of 300 sites had bedrock depths limited to 30 m, additional analyses of sites with bedrock depths between 30 m and 50 m were performed in this study. The coefficients listed in Table 3 represent the modified coefficients after taking deep bedrock sites into account (H = 30 ~ 50 m). In addition, the F_a values for S_3 and S_4 site classes were modified by excluding extremely high short-period amplification according to the criterion suggested in Eurocode 8. The site coefficients at different rock outcrop acceleration levels are included to account for the effects of soil non-linearity on site coefficients. The F_a and F_v values are then used to construct the DRS.

Table 3. Site coefficients* with respect to site class and rock outcrop acceleration levels

Site class	Short-period site coefficient, F_a			Long-period site coefficient, F_v		
	S** ≤ 0.1	S = 0.2	S = 0.3	S ≤ 0.1	S = 0.2	S = 0.3
S_2	1.4	1.4	1.3	1.5	1.4	1.3
S_3	1.7	1.5	1.3	1.7	1.6	1.5
S_4	1.6	1.4	1.2	2.2	2.0	1.8
S_5	1.8	1.3	1.3	3.0	2.7	2.4

* Use straight-line interpolation for intermediate values of S
** Effective peak acceleration (rock shaking intensity)

4. Verification by dynamic centrifuge tests

Performing dynamic free-field centrifuge tests is a novel way to circumvent the problem of a lack of strong ground motion records, for direct evaluation of seismic response during scenario earthquake events. In this section, dynamic free-field seismic centrifuge tests are described aimed at the study of amplification due to various types of soil. The free-field seismic response of a centrifuge model was compared with the DRS developed in this study for similar soil conditions.

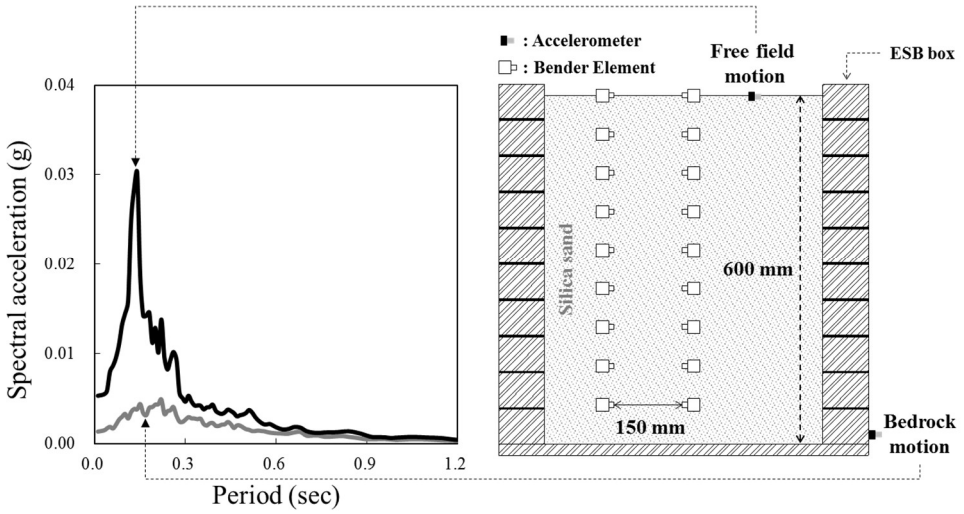


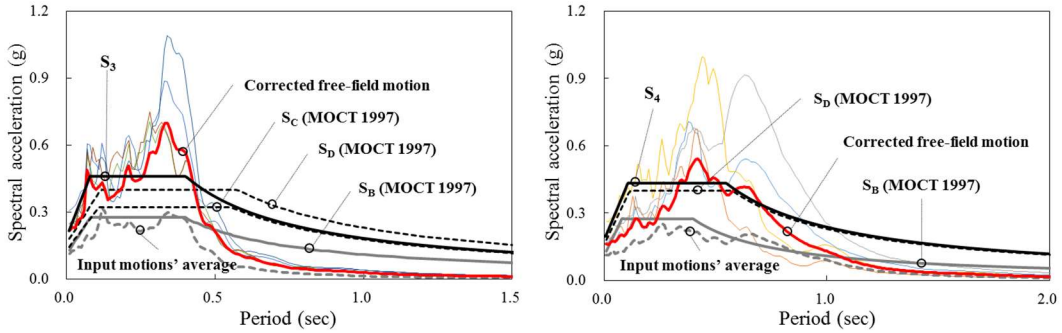
Figure 2. Evaluation of seismic response of centrifuge model ground

The typical Korean shallow bedrock condition was simulated in dynamic centrifuge tests. Figure 2 shows the centrifuge configuration for a uniform sand model with sensors embedded at various depths. The scale height of the model was 60 cm and centrifugal accelerations of 20 g and 40 g were applied. The depths simulated were 12 m and 24 m at 20 g and 40 g, respectively. Tests also related to different relative densities of 44 % and 81 %. The models were prepared using dry silica sand by the air pluviation method. Four inputs, the Morgan hill, Kobe, San Francisco and Northridge earthquakes were used to evaluate the seismic response at each centrifugal acceleration level.

Table 4 shows the test information at soil depth (H), and values of $V_{S,30}$, $V_{S,Soil}$, and T_G. V_S was determined using bender element arrays during the centrifuge tests, as shown in Figure 2. For the determination of $V_{S,30}$, a bedrock stiffness of 2000 m/s was assumed based on the stiffness of aluminum, the material of the model container. Based on the information tabulated in Table 4, the soil models were classified according to both the previous seismic code (MOCT 1997) site classification system and the new site classification system (MPSS 2017).

Table 4. Information of dynamic centrifuge models

#	Model thickness (cm)	Relative density (%)	Target G-level (g)	Simulated(prototype) site conditions				
				Height (m)	$V_{S,Soil}$ (m/s)	$V_{S,30}$ (m/s)	Site class	
							MOCT 1997	MPSS 2017
1	60	81	20	12	194	423	S_C	S_3
			40	24	234	284	S_D	S_4
2		44	20	12	157	352	S_D	S_3
			40	24	204	249	S_D	S_4



(a) 20g level (b) 40g level

Figure 3. Comparison of response spectra from centrifuge tests with DRS (0.110 g)

The response spectra obtained from the centrifuge tests are compared with the DRS in Figure 3. The free-field response spectrum of the earthquake motions at an input acceleration of 0.110 g (500 year earthquake return period) at prototype scale was used for comparisons. Because both uniform sand models with different relative densities were classified into the S3 site class at 20 g and S4 at 40 g the response spectra derived from each test were combined for each site class modeled. The average response spectra at the surface and at bedrock (base motion) for all input earthquake motions were calculated and compared with the design response spectra. The average base motions were also compared with those of reference site class SB as defined in the current Korean seismic code. Except for the average base motion above the 0.5 s period range for the sand model at 20 g level, the average base motions match well with the DRS of the SB site class.

In order to take account of the unavoidable effect of the high impedance contrast at the soil-container interface on the free-field response, the average free-field response spectra obtained from centrifuge tests were reduced using one-dimensional numerical simulation of soil profiles similar to those used in the centrifuge tests. The so-modified free-field response spectra are well represented by the DRS proposed in this study, but fail to cover the peak spectral response at the short-period range. Meanwhile, the current code underestimates the level of spectral acceleration and is limited in covering the spectral accelerations at short-periods when compared with the DRS proposed in this study. Hence, the DRS results derived in the study are better than those produced by the current seismic code, based on the shallow bedrock model centrifuge tests.

5. Conclusions

The development and verification of the newly implemented Korean site classification scheme and DRS, as a part of new minimum requirements for general seismic design, are described, based on the response analyses of more than 300 Korean specific soil sites and dynamic centrifuge tests. The new site classification system, which includes four typical soil site classes, adopts H and the time-averaged VS,Soil as site classification parameters. Verification, using dynamic centrifuge tests showed that the new site classification system and DRS reasonably well represents the site amplification characteristics of the shallow bedrock condition usual in Korea. Thus, it is possible to conclude that the newly proposed seismic provisions are more reliable and more appropriate than those defined in the current seismic code.

References

Borcherdt, R. D. and Glassmoyer, G. (1992) "On the characteristics of local geology and their influence on ground motions generated by the Loma Prieta earthquake in the San Francisco Bay region. California", Bulletin of the Seismological Society of America 82(2): 603-641.

Borcherdt, R. (1996) "Preliminary amplification estimates inferred from strong ground-motion recordings of the Northridge earthquake of January 17, 1994", Proceedings of International Workshop on Site Response Subjected to Strong Earthquake Motions 1: 21-46.

Building Seismic Safety Council (1997) NEHRP recommended seismic provisions for new buildings and other structures, FEMA 302, Part 1 (Provisions). Washington, D.C.

Dobry, R., Ramos, R. and Power, M. (1999) Site factors and site categories in seismic codes. Technical Multidisplinary Center for Earthquake Engineering Research, Report No. MCEER-99-0010, Buffalo, NY.

European Committee for Standardization (2004) Eurocode 8: Design of structures for earthquake resistance, Part 1: General rules, seismic actions and rules for buildings. EN 1998-1:2004, Brussels, Belgium.

Idriss, I. and Sun, J. I. (1992) User's Manual for SHAKE91, Center for Geotechnical Modeling, Department of Civil Engineering, University of California, Davis, CA.

International Code Council (2012) International Building Code, Washington D.C.

Kim, D. S. and Choo, Y. W. (2001) "Deformation characteristics of hydraulic-filled cohesionless soils in Korea", Proceedings of the 4th International Conference on Recent Advances in Geotechnical Earthquake Engineering and Soil Dynamics, San Diego, CA.

Kim, D. S. and Yoon, J. K. (2006) "Development of new site classification system for the regions of shallow bedrock in Korea." Journal of Earthquake Engineering 10(3): 331-358.

Lee, S. H., Sun, C. G., Yoon, J. K. and Kim, D. S. (2012) "Development and verification of a new site classification system and site coefficients for regions of shallow bedrock in Korea", Journal of Earthquake Engineering 16(6): 795-819.

Manandhar, S., Cho, H. I. and Kim, D. S. (2017) "Site Classification System and Site Coefficients for Shallow Bedrock Sites in Korea", Journal of Earthquake Engineering, DOI: 10.1080/13632469.2016.1277570

Ministry of Construction and Transportation (1997) Korean Seismic Design Standard. Seoul, Korea (in Korean).

Ministry of Public Safety and Security (2017) Minimum requirements for seismic design. Sejong, Korea (in Korean).

Rodriguez-Marek, A., Bray, J. D. and Abrahamson, N. A. (2001) "An empirical geotechnical seismic site response procedure," Earthquake Spectra 17(1): 65-87.

Seed, H. B., Romo, M. P., Sun, J. I., Jaime, A. and Lysmer, J. (1988) "The Mexico earthquake of September 19, 1985 - Relationships between soil conditions and earthquake ground motions", Earthquake spectra 4(4): 687-729.

Sun, C. G., Han, J. T. and Cho, W. (2012) "Representative shear wave velocity of geotechnical layers by synthesizing in-situ seismic test data in Korea", The Journal of Engineering Geology 22(3): 293-307.

Sun, C.G., Kim, D.S. and Chung, C.K. 2005. "Geologic site conditions and site coefficients for estimating earthquake ground motions in the inland areas of Korea", Engineering Geology, 81(4): 446-469

Seismic Hazard Modelling for Peninsular Malaysia and Singapore

Daniel T. W. Looi[a,c], Hing-Ho Tsang[b] and M. C. Hee[c]

[a] Department of Civil Engineering
The University of Hong Kong, Hong Kong

[b] Department of Civil and Construction Engineering
Swinburne University of Technology, Australia

[c] Working Group 1, Technical Committee on Earthquake
The Institution of Engineers, Malaysia

Malaysia and Singapore are two examples of countries outside Europe which have adopted Eurocode 8 (EC8) for the earthquake resistant design of building structures. The authors are active researchers studying seismic hazard modelling of the region surrounding Malaysia and Singapore and have been key contributors to the drafting of the Malaysia EC8 National Annex (NA to MS EN1998-1:2015). The purpose of this chapter is to explain the principles underlying the derivation of the seismic zoning, modelling of earthquake recurrences, ground motion modelling and the elastic response spectrum model for Peninsular Malaysia. The current EC8 NA for Singapore is primarily intended to address the distant hazards arising in Sumatra and is not intended to provide coverage for potential local intra-plate hazards. Hence, recommended in this chapter is a reconciled elastic response spectrum for Singapore, which should be similar to that of Peninsular Malaysia, aiming to achieve a more robust level of safety.

Keywords: Eurocode 8, National Annex, seismic hazard, distant earthquakes, local earthquakes

1. Introduction

In this chapter the approach used for the seismic hazard modelling of Peninsular Malaysia (enhanced and updated from Lam et al. 2016b) and its neighbouring country, Singapore is elaborated. Both are characterised by the need to cater for different types of seismicity conditions (see Figure 1). The approach to seismic zoning, earthquake recurrence modelling, ground motion attenuation modelling and probabilistic seismic hazard analysis (PSHA) of local intra-plate and distant earthquakes, to arrive at a hybrid elastic response spectrum model is explained with justifications. The outcome of the recommended modelling approach for low to moderate seismicity region has been incorporated into the draft National Annex (NA) to Eurocode 8 (EC8) for Malaysia (MS EN1998-1:2015), namely "Design of structures for earthquake resistance – Part 1: General rules, seismic actions and rules for buildings". The Malaysia EC8 NA went through the public comment process in 2016 and 2017. The current NA for Singapore to EC8 (SS EN1998-1:2013), which became mandatory in 2015, intends primarily to address distant hazards, hundreds of kilometres away, arising in Sumatra and is not intended to provide coverage for potential local intra-plate hazards (Lam et al. 2015a). Importantly, this latter type of hazard does have safety implications for low-rise structures including many among the aged building stock. This chapter provides coverage for Peninsular Malaysia and Singapore only. Details relating to East Malaysia comprising Sarawak and Sabah are covered in Looi et al. (in press).

Peninsular Malaysia and the adjoining country Singapore are subject to a combination of earthquake hazards generated from the two main distant sources of the Sumatran strike-slip fault zone and the Sunda Arc subduction fault. Most, if not all, seismic hazard modelling research available in the literature has focused on the ground motions generated by distant earthquakes (e.g., Balendra et al. 2002, Lam et al. 2009, Megawati & Pan 2010, Megawati et al. 2005, Pan & Megawati 2002, Pan et al. 2007, Petersen et al. 2004, Pappin et al. 2011). Historical records of local seismic activity in low to moderate regions wholly a long distance from tectonic plate boundaries (including Peninsular Malaysia and Singapore) are very limited. Nevertheless, the consequences of potential local seismic hazard events can be significant in the case of buildings which are non-seismically engineered. Thus, a hybrid response spectrum model is proposed for Peninsular Malaysia and Singapore. The hybrid model captures innovative PSHA results for local earthquakes based on a broad source zone model (Lam et al., 2016a) and distant earthquakes based on conventional PSHA procedures applied to those source zones identified from historical earthquake records.

Table 1 shows the seismic activities characterising the local and distant hazards for Peninsular Malaysia and Singapore. The boundary between the low and high period ranges at 1.25 s is representative of the corner period at the beginning of the constant displacement region of magnitude (M) 6.5 earthquake (Lam et al. 2000, Lumantarna et al. 2012).

Table 1. Types of seismic activities characterising the hazards for Peninsular Malaysia and Singapore

Period range of building	Type of activity dominating seismic design
Low period ($T \leq 1.25$ s)	dominated by local seismicity
High period ($T > 1.25$ s)	dominated by distant (offshore) seismicity

2. Zonation and recurrence modelling of local seismic activities

This section discusses the zonation and recurrence modelling of local earthquakes generated within the low seismicity areas of Peninsular Malaysia and Singapore (Zone 1, see Figure 1). The local seismic activities should not be confused with distant hazards generated in Sumatra. The seismic hazard modelling for Zone 2 and Zone 3 is covered elsewhere (Looi et al., in press).

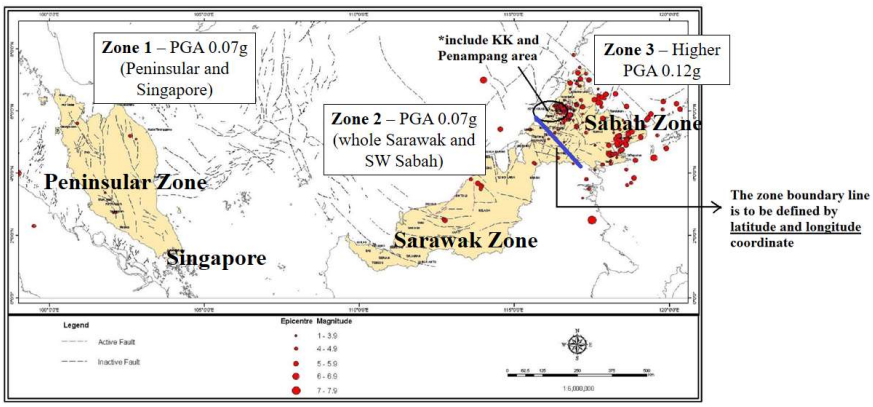


Figure 1. Seismic hazard zonation across Malaysia and Singapore (proposed by the authors after receiving feedbacks of public comments in Tongkul, 2016)

In Malaysia, there are merely 39 years (1979 onwards) of complete instrumented records (Che Abas 2001, MOSTI 2009). The authors' literature review revealed that no existing Malaysian seismic hazard maps (summarised in MOSTI 2009) were able to predict the series of earthquake tremors (maximum M3.7) which occurred in the Bukit Tinggi area, in the centre part of the Peninsula and the M4.1 earthquake which occurred in 2013 inr the area surrounding Perak, in the northern part of the Peninsula. This is one of many examples indicating that local intra-plate earthquakes can occur in areas where there are no recognisable earthquake activity precedents.

Hence, in the study for Zone 1, a broad source zone modelling approach (Lam et al., 2016a) was adopted to circumvent the challenges of limited recorded intra-plate earthquake data. The broad source zone model predicts directly by counting the number of M > 5 events for recurrence modelling. Earthquakes exceeding magnitude 5 are used in the counting process since the records are more complete and because intra-plate hazards are mainly contributed by events in the range M5 – M6. For the same reason, the event count was based on a 50 year observation period. In view of the generally very low rates of occurrence of intra-plate earthquakes, the number of events counted was normalised to a standard land area of 1,000,000 square kilometres (sq. km), which is consistent with conventions adopted by Bird et al. (2010) and by Bergman and Solomon (1980). Lam et al. (2016a) suggested that the global average must be within the range of five to ten M > 5 events occurring over an area of 1,000,000 sq. km, for a better prediction of the global average suitable for a 50-year period. Hence, the parameter KD was introduced to represent the rate of recurrence of intra-plate events. A value of KD = 1 refers to five events and KD = 2 to ten events. A minimum KD value of 2 was recommended to account for uncertainties and to err on the safe side, provided that the local earthquake occurrence data does not infer a value higher than ten.

The rate of local seismic activity is defined using the Gutenberg-Richter magnitude recurrence relationships shown in Eq. (1a) and Eq. (1b):

$$\log_{10} N(M) = a - bM \tag{1a}$$

$$\text{or} \quad , \log_{10} N(M) = a_5 - b\left(M - 5\right) \tag{1b}$$

where $N(M)$ is the number of earthquakes ≥ M occurring within an area of 1,000,000 km^2 over a 50-year period. The seismic constants a, a_5 and b are defined according to KD. For example, for KD = 1, a_5 = 0.7 or a = 5.2 (being 0.7 + 0.9 x 5) assuming b = 0.9. Similarly, for KD = 2, a = 5.5.

3. Ground motion modelling of local earthquakes in Peninsular Malaysia and Singapore

The big majority of empirical ground motion prediction equations (GMPEs) are based on strong motion data collected from regions of high seismicity. Hence, adopting those GMPEs for the use in PSHA analysis of local intra-plate earthquakes in low to moderate seismicity countries, such as Malaysia and Singapore, must consider: (a) the wave generation behaviour at the source of the earthquake and (b) wave modification behaviour of the crustal rocks (in the upper 3 to 4 km in particular, and should not be confused with the modification behaviour of near-surface sediments). The discussions below in

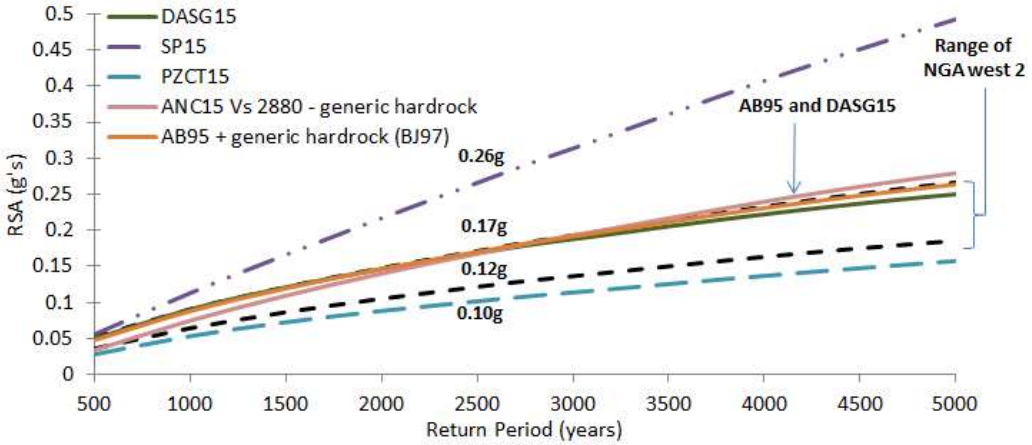
Section 3 mainly relate to the previous work in Lam et al. (2016a).

In this relatively stable region of Peninsular Malaysia and Singapore, the ground motion models intended for use in stable (intra-plate) regions such as eastern North America should be adopted. The Next Generation Attenuation of the eastern North American (NGA-East) database comprises 29000 records from 81 earthquake events recorded at 1379 stations (PEER 2015/04). Ground Motion Models (GMMs) based on this database have the merit of deriving from the most elaborate existing database of intra-plate events, hence can be taken to be representative of seismic wave generation behaviour in any intra-plate tectonic setting. A literature review of the seismological studies of ground motion models for Eastern North America (ENA) identified some 40 models developed in the period 1983-2014. Six representative models were filtered out, selected based on the quality and age of the data. Table 3 summarises the six selected published ground motion models with acronyms: (i) AB95, (ii) SGD02, (iii) A04*, (iv) BCA10d, (v) BS11 and (vi) AB14*. Models labelled with an asterisk feature a geometrical attenuation factor of $R^{-1.3}$ within about 50 km site-source distance as opposed to the conventional factor of R^{-1}.

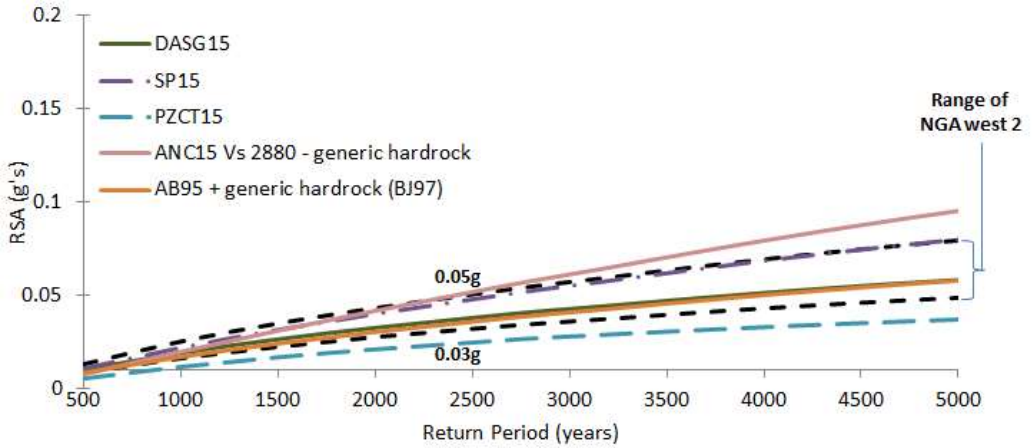
Table 3. A selection of ground motion models for tectonically stable regions

Literature	Acronyms of GMMs	Remarks
Atkinson and Boore (1995)	AB95	BSSA article
Pezeshk, Zandieh, Campbell and Tavakoli (in PEER, 2015)	PZCT15*	PEER report 2015/04
Darragh *et al*. (in PEER, 2015)	DASG15	PEER report 2015/04
Shahjouei and Pezeskh (in PEER, 2015)	SP15*	PEER report 2015/04
Al Noman and Cramer (in PEER, 2015)	ANC15	PEER report 2015/04
Silva, Gregor and Darragh (2002)	SGD02	PEA report 2002
Atkinson (2004)	A04*	BSSA article
Boore, Campbell and Atkinson (2010)	BCA10d	BSSA article
Boatwright and Seekins (2011)	BS11	BSSA article
Atkinson and Boore (2014)	AB14*	BSSA article

Figures 2a and 2b show the PSHA results of response spectral acceleration (RSA) values at 0.3 s and 1.0 s based on the selection of GMMs of NGA-East and superimposed with the range of predictions based on the GMMs of NGA-West2. GMMs of AB95 (with generic hard rock in cratonic continental crust) and DASG15 show robust and better inter-model consistencies than SP15* and PZCT15*, with only marginally higher predictions at 0.3 s. Similar findings were supported by Ogweno and Cramer (2014), where AB95 was ranked favourably for ENA in view of the consistencies of the model predictions and field recordings.



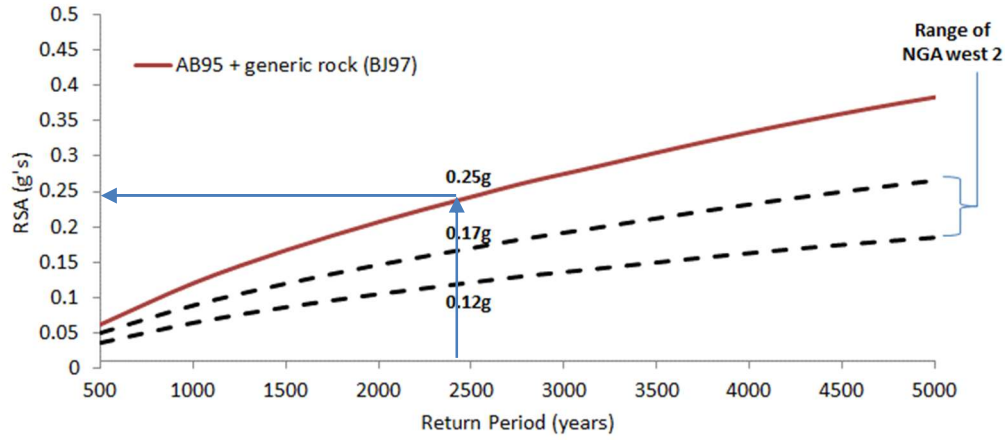
(a) 0.3 s period



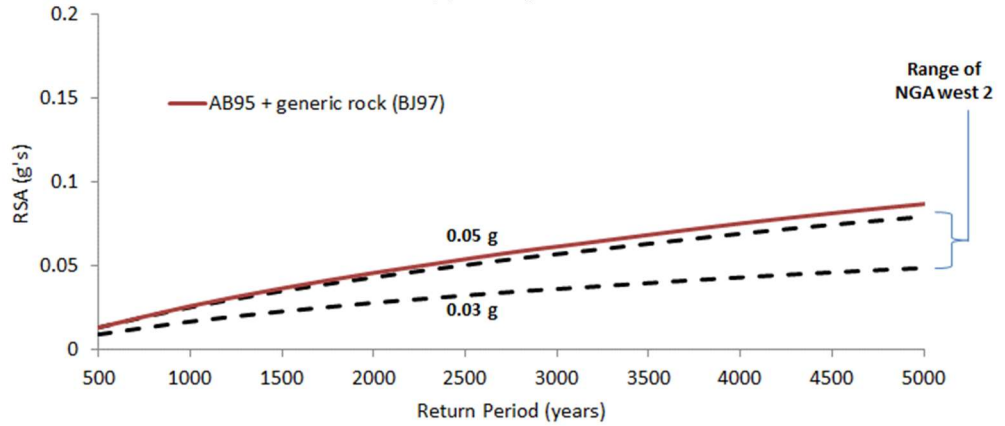
(b) 1.0 s period

Figure 2. Selected ENA (cratonic) models overlaid on NGA-West2 models for $\log_{10} N = 5.5 - 0.9\,M$

The authors had the experience of combining the source model of AB95 with the (non-cratonic) crustal model of generic rock (Boore and Joyner 1997, which is abbreviated herein as BJ97) for predicting ground motions generated by intra-plate earthquakes. It is found that the predictions by the (non-cratonic) model can be significantly higher than the upper limit of predictions by the NGA-West2 models (see Figures 3a and 3b). This modified AB95 with generic rock model, which is suitable for Peninsular Malaysia and Singapore, located in a non-cratonic continental crust, is to be adopted. In Figure 3a, the RSA value at 0.3 s is about 0.25g for a return period of 2475 years. The 0.25g translates to an effective peak ground acceleration (PGA) of 0.1g or 0.07g (being rounded up from 0.1g/1.5) for a notional return period of 475 years.



(a) 0.3 s period



(b) 1.0 s period

Figure 3. ENA (non-cratonic) model (AB95 + BJ97) overlaid on NGA-West2 models for $\log_{10} N = 5.5 - 0.9\,M$

4. Modelling of distant earthquakes in Peninsular Malaysia and Singapore

Figure 4 illustrates the distant earthquake hazards affecting Peninsular Malaysia and Singapore, which are from two major sources of Sumatra, Indonesia: (1) the Sunda Arc subduction fault source off-shore of Sumatra formed by convergence of the Indian-Australian plate with the Eurasian plate (some 530 km – 730 km away from Peninsular Malaysia and Singapore); and (2) the 1500 km long Sumatran strike-slip fault source within the Sumatran island (some 300 – 400 km from Peninsular Malaysia and Singapore). The megathrust earthquakes, e.g. Aceh 2004 (*M*9.3) and Nias 2005 (*M*8.7) events were generated by the subduction source. The greatest magnitudes of recorded historical earthquakes generated at the strike-slip fault source are limited to around *M*7.8.

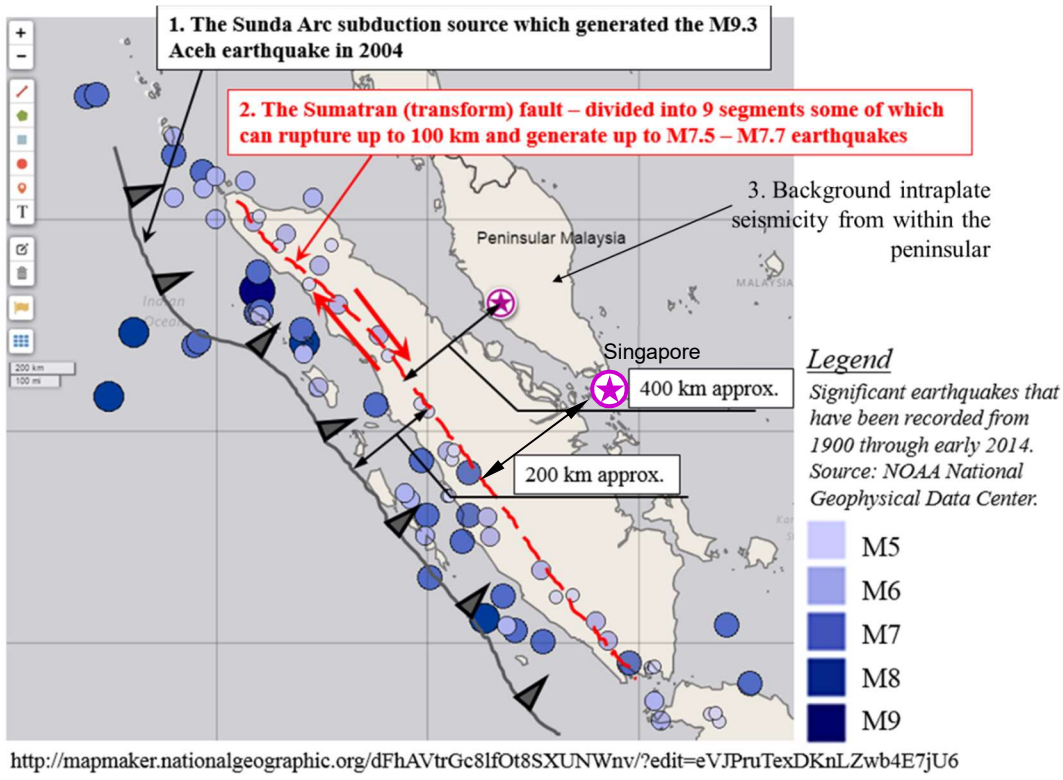


Figure 4. Offshore earthquake generating sources affecting Peninsular Malaysia and Singapore

Numerous research groups have contributed to the assessment of the above distant seismic hazards as they affect Peninsular Malaysia and Singapore. Numerous representative GMPEs for the prediction of ground motion levels as functions of magnitude and distance have been developed in these studies. A literature review undertaken by the authors provides coverage of some twenty research articles spanning the period 2002 – 2011 (see a listing of the literature in the review of Looi et al. 2011). This database features a combination of probabilistic and deterministic (scenario-based) hazard analysis (PSHA and DSHA) studies. In view of the inconsistencies in predicted ground motions between different GMPEs, verification analyses have been undertaken to identify those models which give results that match well with instrumented data collected in the field (Chandler & Lam, 2004). Two GMPEs reported in the literature have been validated based on benchmarking against ground motion data instrumentally recorded from a long distance. These two models are: (1) the Component Attenuation Model (CAM) and (2) the Megawati attenuation relationship.

CAM was first developed and coded into the program GENQKE which generates synthetic earthquake accelerograms based on stochastic simulations of the seismological model of Atkinson & Boore (1995) along with the generic crustal model of Boore & Joyner (1997). See Lam et al. (2000) for more details. Whilst CAM was initially developed to predict ground motions generated by local earthquakes, the modelling framework was found to be capable of predicting ground motions generated by large magnitude earthquakes from the far-field (Chandler and Lam 2004). CAM has been successfully demonstrated as capable of modelling distant mega-magnitude earthquake events generated at the Sunda-Arc subduction source, offshore of Sumatra, affecting Singapore

and Peninsular Malaysia (Lam et al. 2009, Balendra et al. 2002 and Balendra & Li 2008). The CAM simulation model could have been used to quantify the reduction of hazard across Peninsular Malaysia (from west to east) but it is considered prudent not to do so, given that the model has been validated for a site-source distance of up to 600 km. The modelled attenuation rate is so gradual at a long distance from the source, that the change in hazard level across the width of the Peninsula is small. In perspective, buildings that are vulnerable to collapse and severe damage in an earthquake are low-rise and medium-rise as opposed to high rise buildings which respond to long distance earthquakes. In other words, the part of the response spectrum in the low period range (and the level of PGA) is governed by local hazard sources anyway. Thus, the long distance earthquake hazard affecting Peninsular Malaysia and Singapore is to be based on the one response spectral model for all areas.

The Megawati's attenuation relationship when modelling ground motions generated at the Sumatran fault source (Megawati et al. 2003) and those from the Subduction fault source (Megawati et al. 2005) were reported in Pan et al. (2007) and revised in Megawati & Pan (2010). Synthetic seismograms derived from the analysis of a finite-fault kinematic model have been verified in a manner similar to that for the CAM. This attenuation relationship is based on hard rock conditions and site-source distances ranging between 200 and 1500 km. The use of the relationship developed, for predictions outside this distance range, should be treated with caution.

In addition to the deterministic studies described above, Pappin et al. (2011) conducted PSHA for Malaysia based on historical earthquake data recorded over the past 40 years since 1972, along with the use of the attenuation relationship in Pan et al. (2007). Based on the earthquake catalogue compiled from the USGS database, the seismic source zone was divided into four categories of seismogenic depth up to 500 km, and an earthquake database, from which small events ($M < 5$) and aftershocks have been removed. The maximum earthquake magnitude was assigned to different areas and depths in Pappin et al. (2011).

The response spectrum produced from a PSHA is known as a Uniform Hazard Spectrum (UHS) in which contributions from multiple fault sources are taken into account (Pappin et al. 2011). The attenuation behaviour of the simulated ground motions in the development of the UHS was based on GMPEs developed by Pan et al. (2007). Different parts of the UHS can be associated with very different contributory earthquake scenarios. According to the latest PSHA (Pappin et al. 2011), seismic hazard levels vary across Peninsular Malaysia (due to the different distances from potential earthquake sources), with Penang possessing the highes level of hazard. A seismic zoning map could be prepared for the region, but it is considered unnecessary for two reasons: (1) the attenuation behaviour of very long period waves that are characteristic of earthquakes generated a very long distance away is very gradual and (2) the low level of contribution of distant earthquakes to the total hazard in the low to intermediate period range. Thus, the UHS for Penang has been selected as the basis of the recommended design spectrum model for Peninsular Malaysia aqs a whole. Singapore is located right next to the Peninsula, hence the design spectrum model for a distant earthquake is similar to that for Peninsular Malaysia.

The UHS model developed initially required modifications because of subsequent improvements made to the accuracies of region-specific attenuation relationships. The original attenuation relationship of Pan et al. (2007) has been updated to that of Megawati & Pan (2010). In parallel with improvements made by Megawati's model, CAM has also

been shown able to simulate ground motions which match the instrumented field recordings of major events including the Aceh earthquake of 2004 and the Nias earthquake of 2005 (Lam et al. 2009).

In this study, to achieve a more robust UHS, the attenuation model has been revised to incorporate both the updated model of Megawati & Pan (2010) and the latest development of CAM (Lam et al. 2009). A logic tree weighting factor of 0.5 has been allocated to both attenuation relationships in the aggregation analysis. The modified UHS presented in Figure 5 was obtained by an adjustment procedure comprising the following steps:

- The original UHS (for Penang) was firstly scaled down by a notional factor of 2.0 (Musson, 1999) in order to obtain the median UHS.
- Seven earthquake scenarios were selected by calibrating the response spectra based on the (original) attenuation model of Pan et al. (2007) with the median UHS at three reference natural periods of 1 s, 2 s and 5 s.
- The response spectra of the calibrated earthquake scenarios were then re-calculated using the updated attenuation model of Megawati & Pan (2010) along with CAM based on equal weightings. The differences in the spectral parameters were represented by the spectral ratio (SR) geometric means, at the three reference periods, from amongst the seven calibrated scenarios. The SR for other UHS periods were determined accordingly, by interpolating between the three reference periods.
- The modified UHS was then obtained by scaling the original UHS by the geometric mean SR.

The revised response spectral values in the long period range of 2 s – 5 s, based on probabilistic analysis, is approximately double the response spectral values based on deterministic (median) predictions as published in Lam et al. (2009).

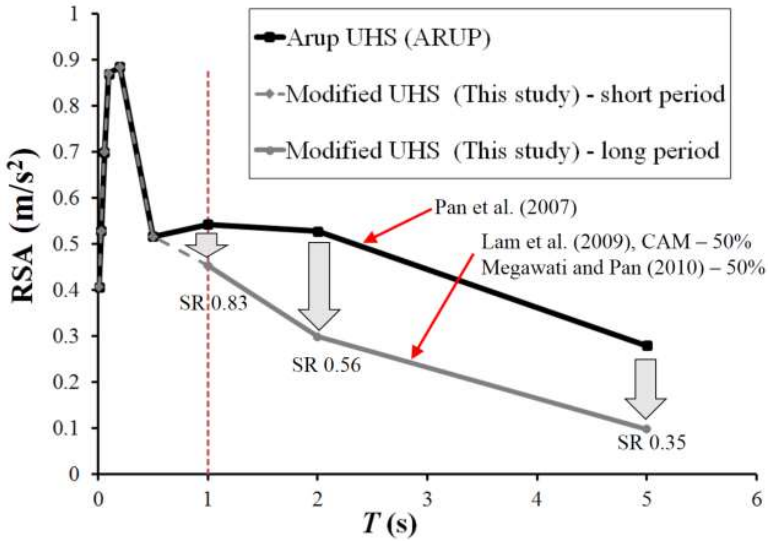
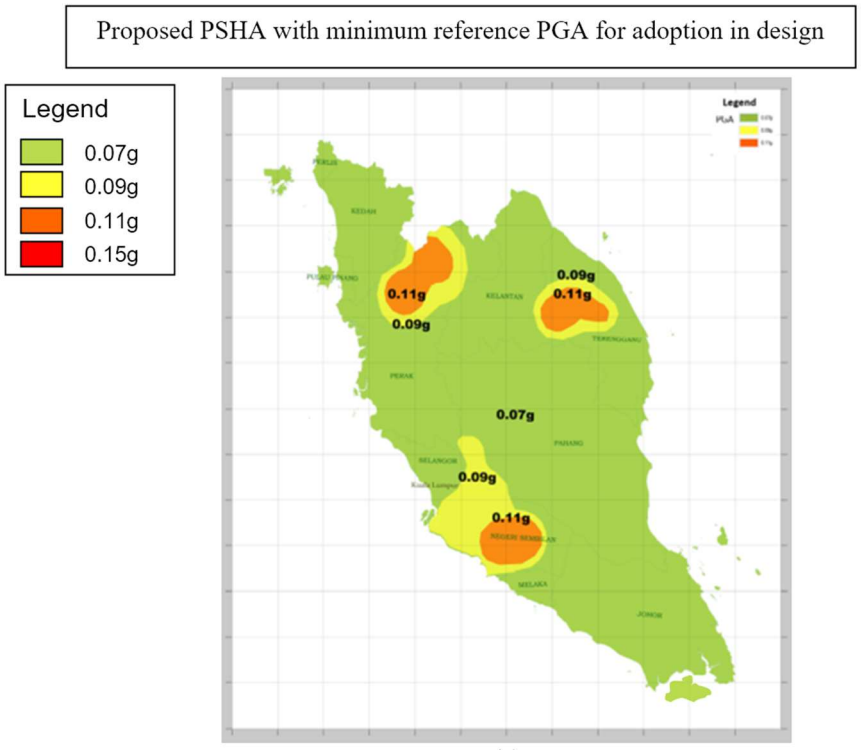


Figure 5. The original and adjusted uniform hazard response spectra on rock representing distant hazard affecting Peninsular Malaysia and Singapore

5. Proposed seismic hazard featuring minimum loading

Any country located in a low to moderate seismic region should impose, it is recommended, a minimum loading, to constrain the seismic hazard estimates, particularly if the land area is not sufficiently large to have captured a statistically meaningful database of records of destructive earthquakes from within the country. Nevertheless, the option exists of superimposing the modelled hazard (for the identified hot spots) on a map showing uniform hazard zones (that has been derived from the broad source zone model) in order that no area is stipulated with a level of hazard which is below a certain hazard threshold. For Peninsular Malaysia, hotspots can be identified (Adnan, 2017). For Singapore, being small in land area, no major event has occurred in history, consequently the level of local intra-plate earthquake hazard to be stipulated, can be based entirely on the results derived from the broad source zone model.

To address the modelling of uncertainties, a seismic zonation map with hot spots which features a minimum reference PGA value of 0.07g for Peninsular Malaysia and Singapore is shown in Figure 6. The seismic zonation maps for Sarawak and Sabah are discussed elsewhere (refer Looi et al., in press).



(a)

Figure 6. Proposed seismic hazard contours featuring a minimum reference PGA value for Peninsular Malaysia and Singapore

6. Elastic response spectra on rock for Peninsular Malaysia and Singapore

It is noted that the response spectrum models proposed for Malaysia (NA to MS EN1998-1) and Singapore (NA to SS EN1998-1:2013) do not follow EC8 which stipulates

Type 1 and Type 2 spectra in Cl. 3.2.2.2 (2)P, to allow for distant seismic hazard. This is evident in Figure 7, which compares the normalised spectrum shape of the proposed response spectrum model for soil sites in Peninsular Malaysia in the Malaysia NA with the generic EC8 models for Europe and that stipulated in the Singapore NA.

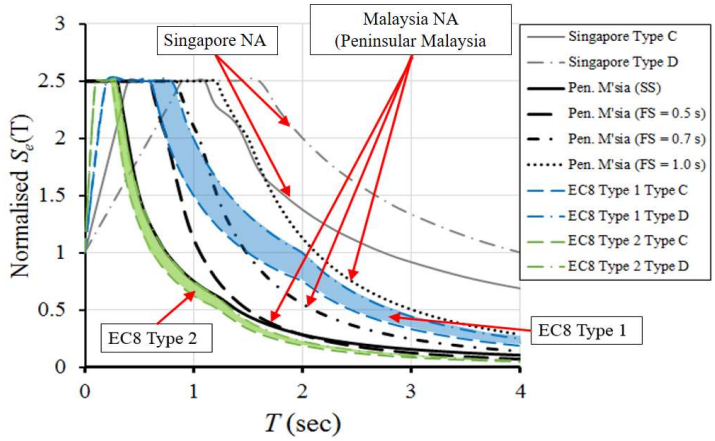


Figure 7. Normalised spectrum shape comparison of the proposed response spectrum model in the Malaysia NA (Peninsular Malaysia) with the generic EC8 for Europe and the Singapore NA. (*Note: Stiff Soil (SS) and Flexible Soil (FS) with site natural period)

The rock sites model proposed for Peninsular Malaysia (in Figures 8a and 8b) is a hybrid model which encapsulates results from the conventional PSHA of recorded distant earthquakes, as well as from the probabilistic predictions of local earthquakes based on broad source zone modelling as described above. This approach makes good use of the abundant distant events data, whilst obtaining robust estimates for locally generated hazards. Singapore is located at the south of the Peninsula, so the response spectrum model for Peninsular Malaysia should also be applicable to Singapore, given that no major event has occurred in the vicinity of Singapore in history. The PGA values for the notional 475-year RP and the benchmarked 2475-year RP are 0.07g and 0.1g respectively. It should be noted that the short corner period (known as T_B in EC8) is not defined for the spectrum in Figure 8(b) which has a flat plateau. The maximum RSA value (S_e) of 0.17g is not to be confused with the notional PGA of 0.07g (being 0.17g divide by 2.5).

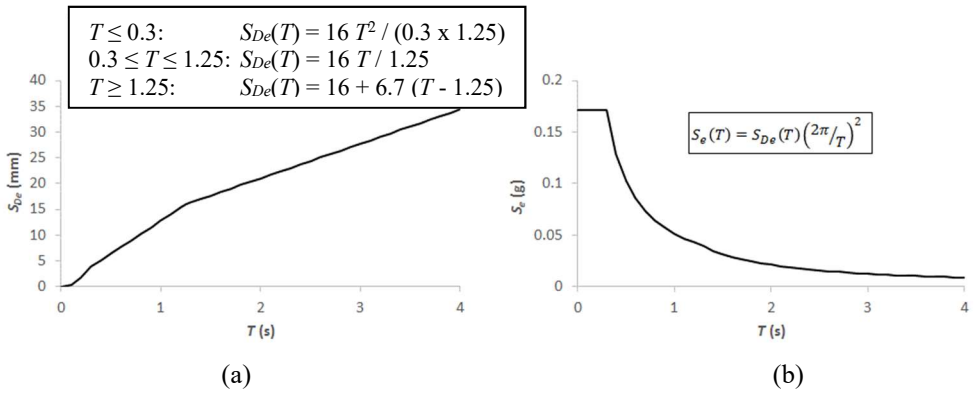


Figure 8. Elastic Response Spectrum on rock in the (a) displacement (S_{De}) and (b) acceleration (S_e) formats, for Peninsular Malaysia for Importance Class II ordinary buildings (similar for Singapore) (Design PGA = 0.17g/2.5 = 0.07g, notional RP = 475 years)

7. Conclusions

In this chapter an explanation has been given of the approach taken in the NA to EC8 drafted for Malaysia for quantifying the design seismic hazard for the low to moderate seismicity regions of Peninsular Malaysia and Singapore. The study first identified those seismic activities, which have occurred in the vicinity of, and locally within, the landmass, and categorised the types of seismic activities into low and high period response spectra ranges. The modelling of local intra-plate hazard is based on the broad source zone model according to Lam et al. (2016a). Conventional PSHAs on distant earthquakes and an updated UHS for Peninsular Malaysia and Singapore are presented. A hybrid design response spectrum for Peninsular Malaysia and Singapore encapsulating both distant (Sunda Arc subduction and Sumatran fault) earthquakes and local intra-plate earthquakes, based on probabilistic modelling approaches, is proposed. It is noted that the current NA to EC8 for Singapore, is primarily intended to address distant hazards arising in Sumatra. The hybrid model, therefore, provides a reconciled elastic response spectrum for Singapore, aiming to achieve a more robust level of structural safety. The minimum earthquake loading model (based on a broad source zone), applicable to low to moderate seismic risk geographical zones in conjunction with conventional PSHA results for hot spots are synchronised into one map to take account of the few, if any, earthquake records for relatively small areas. Finally, the elastic response spectra for rock sites have been derived for Peninsular Malaysia and Singapore.

Acknowledgements

The authors, from IEM, are grateful for the contributions made by the international advisor Prof. Nelson Lam from The University of Melbourne and the international panel member Prof. John Wilson from Swinburne University of Technology. The continuous support of IEM in facilitating numerous workshops and meetings over the years culminating in the drafting of the NA is acknowledged. Valuable intellectual inputs by other active participants from EC8 TC are also gratefully acknowledged.

References

Adnan, A. (2017) "Probabilistic Seismic Hazard Assessment of Malaysia for the Malaysia National Annex MS EN1998: Part 1", Proceedings of 2-day workshops on the Proposed Seismic Analysis Methods for Regions of Low to Moderate Seismicity, 10 – 11 April 2017, Armada Hotel Petaling Jaya, Malaysia.

Atkinson, G. M. (2004) "Empirical attenuation of ground motion spectral amplitudes in southeastern Canada and the northeastern United States", Bulletin of the Seismological Society of America 94(3), 1079-1095.

Atkinson, G. M. and Boore, D. M. (2014) "The attenuation of Fourier amplitudes for rock sites in eastern North America", Bulletin of the Seismological Society of America 104(1), 513-528.

Atkinson, G. M. & Boore, D. M. (1995) "Ground Motion Relations for Eastern North America", Bulletin of the Seismological Society of America 85, 17-30.

Balendra, T., Lam, N. T. K., Wilson, J. L. and Kong, K. H. (2002) "Analysis of long-distance tremors and base shear demand for buildings for Singapore", Engineering Structures 24: 99-108.

Balendra, T. and Li, Z. (2008) "Seismic Hazard of Singapore and Malaysia", EJSE Special Issue: Earthquake Engineering in the low and moderate seismic regions of SEA and Australia.

Bergman, E. A. and Solomon, S. C. (1980) "Oceanic intraplate earthquakes: implications for local and regional interpolate stress", Journal of Geophysical Research 85(BI0): 5389-5410.

Bird, P., Kreemer, C. and Holt, W. E. (2010) "A long-term forecast of shallow seismicity based on the global strain rate map", Seismological Research Letter 81(2), 184-194.

Boatwright, J. and Seekins, L. (2011) "Regional spectral analysis of three moderate earthquakes in northeastern North America", Bulletin of the Seismological Society of America 101, 1769-1782.

Boore, D. M. and Joyner, W. B. (1997) "Site amplifications for generic rock sites", Bulletin Seismological Soc of America 87, 327-341.

Boore, D. M., Campbell, K. W. and Atkinson, G. M. (2010) "Determination of stress parameters for eight well-recorded earthquakes in eastern North America", Bulletin Seismological Soc of America 100, 1632-1645.

Chandler, A. M. and Lam, N. T. K. (2004) "An attenuation model for distant earthquakes", Earthquake Engineering and Structural Dynamics 33, 183–210.

Che Abbas, M. R. (2001) "Earthquake monitoring in Malaysia", Proceedings of the Seismic Risk Seminar Malaysia, 25th September, Malaysia.

Eurocode 8 - Design of structures for earthquake resistance. EN 1998-1 Part 1: General rules, seismic actions and rules for buildings.

Lam, N. T. K., Balendra, T., Wilson, J. L. and Venkatesan, S. (2009) "Seismic load estimates of distant subduction earthquakes affecting Singapore", Engineering Structures 31, 1230-1240.

Lam, N. T. K., Wilson, J. L. and Hutchinson, G. (2000) "Generation Of Synthetic Earthquake Accelerograms Using Seismological Modelling: A Review", Journal of Earthquake Engineering 4(3), 321-354.

Lam, N. T. K., Tsang, H. H., Lumantarna, E. and Wilson, J. L. (2016a) "Minimum loading requirements for areas of low seismicity", Earthquake and Structures 11(4), 539-561.

Lam, N. T. K., Tsang, H. H., Looi, D. T. W., Lumantarna, E. and Wilson, J. L. (2016b.) "Seismic Hazard Modelling for Malaysia", Australian Earthquake Engineering Society 2016 Conference, Nov 25-27, Melbourne, Victoria, Australia.

Lam, N. T. K., Tsang, H. H., Lumantarna, E. and Wilson, J. L. (2015a) "Local intraplate earthquake considerations for Singapore", The IES Journal Part A: Civil & Structural Engineering 8(1), 62-70.

Lumantarna, E., Wilson, J. L. and Lam, N. T. K. (2012) "Bi-linear displacement response spectrum model for engineering applications in low and moderate seismicity regions", Soil Dynamics and Earthquake Engineering 43, 85-96.

Looi, D. T. W., Hee, M. C., Tsang, H. H. and Lam, N. T. K. (2011) "Probabilistic Approach for Determination of Design Spectrum Model for Peninsular Malaysia: Part One (Background & Methodology) and Part Two (Literature Review)", Proceedings of 1-day symposium and 1-day workshop on earthquake engineering in Malaysia and Asia Pacific Region, 6 – 7 December 2011, Armada Hotel Petaling Jaya, Malaysia.

Looi, D.T.W., Tsang, H.H., Hee, M.C. and Lam, N.T.K. (in press) "Seismic hazard and response spectrum modelling for Malaysia and Singapore", Earthquakes and Structures.

MOSTI. (2009) Final report on seismic and tsunami hazards and risks study in Malaysia, Academy of Sciences Malaysia.

MS EN1998-1:2015 (2015) Eurocode 8: Design of structures for earthquake resistance – Part 1: General Rules, Seismic Actions and Rules for Buildings.

Megawati, K. and Pan, T. C. (2010) "Ground-motion attenuation relationship for the Sumatran megathrust earthquakes", Earthquake Engineering and Structural Dynamics 39, 827-845.

Megawati, K., Pan, T. C. and Koketsu, K. (2003) "Response spectral attenuation relationships for Singapore and the Malay Peninsula due to distant Sumatran-fault earthquakes",

Earthquake Engineering and Structural Dynamics 32, 2241-2265.
Megawati, K., Pan, T. C. and Koketsu, K. (2005) "Response spectral attenuation relationships for Sumatran-subduction earthquakes and the seismic hazard implication to Singapore and Kuala Lumpur", Soil Dynamics and Earthquakes Engineering 25, 11-25.
Musson, R. M. W. (1999) "Determination Of Design Earthquakes In Seismic Hazard Analysis Through Monte Carlo Simulation", Journal of Earthquake Engineering 3(4), 463-474.
Ogweno, L. P. and Cramer, C. H. (2014) "Comparing the CENA GMPEs Using NGA-East Ground Motion Database", Seismological Research Letters 85(6), 1377-1393.
Pacific Earthquake Engineering Research Centre. (2015) NGA-East: Median Ground Motion Models for the Central and Eastern North America Region, PEER Report No. 2015/04 University of California, Berkeley PEER.
Pan, T. C. and Megawati, K. (2002) "Estimation of PGA of the Malay Peninsula due to Distant Sumatra Earthquakes", Bulletin of the Seismological Society of America 92:3, 1082-1094.
Pan, T. C., Megawati, K. and Lim, C. L. (2007) "Seismic shaking in Singapore due to past Sumatran earthquakes", Journal of Earthquake and Tsunami 1(1), 49-70.
Pappin, J. W., Yim, P. H. I. and Koo, C. H. R. (2011) "An approach for seismic design in Malaysia following the principles of Eurocode 8", IEM Jurutera Magazine, 22-28.
Petersen M. D., Dewey J., Hartzell S., Mueller C. et al. (2004) "Probabilistic seismic hazard analysis for Sumatra, Indonesia and across the Southern Malaysian Peninsula", Tectonophysics 390, 141-158.
Silva, W. J., Gregor, N. and Darragh, R. B. (2002) "Development of regional hard rock attenuation relations for central and eastern North America", Report to Pacific Engineering and Analysis, El Centro, C.A.
SS EN1998-1:2013 (2013) Singapore Standards Eurocode 8: Design of structures for earthquake resistance – Part 1: General Rules, Seismic Actions and Rules for Buildings. SPRING, Singapore.
Tongkul, F. (2016) Public comments to draft MS EC8 NA and meeting at IEM Kota Kinabalu Sabah branch on 9th June 2016.

Site Classification Scheme and Response Spectrum Models for Malaysia

Daniel T. W. Looi[a,d], Hing-Ho Tsang[b], Nelson T. K. Lam[c] and M. C. Hee[d]

[a] Department of Civil Engineering
The University of Hong Kong, Hong Kong

[b] Department of Civil and Construction Engineering
Swinburne University of Technology, Australia

[c] Department of Infrastructure Engineering
The University of Melbourne, Australia

[d] Working Group 1, Technical Committee on Earthquake
The Institution of Engineers Malaysia, Malaysia

The original site classification scheme written into the main body of Eurocode 8 is out of date and unsuitable for use in low to moderate seismicity regions such as Malaysia because of its failure to model the phenomenon of soil resonance. In addressing this shortcoming, the National Annex to Eurocode 8 for Malaysia stipulates that this conventional site classification model can only be applied to sites that are covered by soil sediments not exceeding 30 m. An alternative site classification scheme which involves calculation of the natural period of the site provides more accurate predictions of real behaviour and without restriction as to soil depth. Details of the two site classification schemes and comparisons of their associated response spectra are presented in this chapter with the aim of helping designers to interpret the National Annex correctly and to adopt the less conservative (more economical) site classification scheme and response spectrum model.

Keywords: Eurocode 8, National Annex, site classification, response spectrum, site period parameterisation

1. Introduction

The National Annex (NA) to Eurocode 8 (EC8) for Malaysia (NA-2017) stipulates two site classification schemes alongside their respective response spectrum models. These two schemes are represented by Models A and B (Figures 1 and 2). The common feature of the site classification scheme across the two models is that five ground types are defined, each with its own definition. Apart from ground type A, which refers to rock sites, all others refer to soil sites which are classified differently in the two models. This dual classification system, which is atypical of seismic codes of practice generally, easily causes confusion. For example, ground type D refers to very different types of site conditions in Models A and B. The writing of this chapter was motivated by the need for a site classification system and the associated response spectra, to be well explained, if there is to be no risk of misinterpretation by designers.

The response spectrum of Model A is not in accordance with that stipulated by the main body of EC8. It is understood to have been derived from analyses made by local investigators. Details of these analyses justifying their model, have not been published in

any international archival source. It is stated in the NA that Model A is only applicable if the total depth of the overlying rock soil sediments does not exceed 30 m. With deeper soil sediments Model B has to be adopted.

The inability of the current site factor model in EC8 to properly address deep site geology is a matter of concern, in view of the potential occurrence of resonance with non-ductile construction in deep soil sites in particular. This message came across very strongly in the speech by Professor Pitilakis in a forum of experts hosted by the *Institution of Engineers Malaysia* on 11-12 April 2017. Professor Pitilakis is the Vice President of the *European Association of Earthquake Engineering (EAEE)* and has been a leader in drafting EC8 in relation to geotechnical matters. The next edition of EC8 is to be revised to the form proposed in numerous publications by Pitilakis et al. (2012 & 2013) and by Riga et al. (2016). The proposal is consistent in form to the site factor model founded on displacement principles, and once incorporated into the draft NA to EC8 for Malaysia (NA-2016), the draft circulated for the first round of public comments in 2016. The displacement-based site factor model was subsequently modified to achieve consistencies in format with Model A (NA-2017). The basis and justification of the displacement-based site factor model, and its modified form (i.e. Model B) can be found in numerous prestigious international peer reviewed archival sources (e.g. Tsang et al., 2006 & 2017). This modified site factor model that takes into account the phenomenon of soil resonance is denoted herein as Model B.

In summary, Model B was introduced to address the concern that the site response behaviour of deep soil sediments (where the total thickness of the soil sedimentary layers overlying bedrock exceeds 30 m) cannot be modelled accurately by Model A. The key feature of Model B is the incorporation of the site natural period which takes into account depth of the soil sediment to bedrock as a modelling parameter. It should be noted that Model B, which is generic in nature and derived using sound theoretical principles, more consistently emulates real behaviour than Model A for all soil conditions (including both shallow and deep soil sites). Model A is out of date. The stipulation of the dual model approach was purely a pragmatic decision to address political issues in the regulatory process.

2. Site classification systems

In Model A, only ground types A, D and E are valid ground types and applicable to Malaysian conditions. This is because NA-2017 limits the application of this model to soil sites where the total depth of the soil sediments overlying bedrock does not exceed 30 m. Given that ground types B and C in EC8 were intended to represent deep sedimentary layers, for these two ground types Model A cannot be used, for reasons explained above. Ground types S1 and S2 of Model A are also irrelevant to Malaysia. In summary, Model A has provisions for ground type A which refers to rock or very shallow soil sites overlying bedrock; ground type D for soft shallow soil sites; and ground type E for stiff shallow soil sites. Refer to Figure 1 for the ground type descriptions based on Model A.

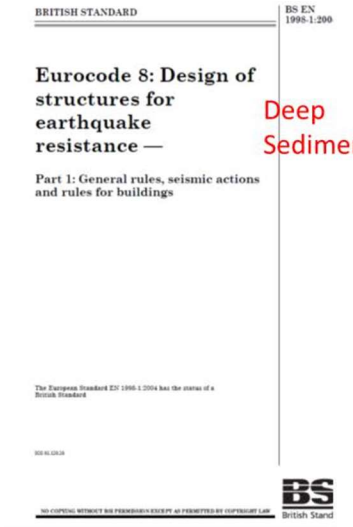


Table 3.1: Ground types

Ground type	Description of stratigraphic profile	Parameters		
		$v_{s,30}$ (m/s)	N_{SPT} (blows/30cm)	c_u (kPa)
A	Rock or other rock-like geological formation, including at most 5 m of weaker material at the surface.	> 800	–	–
B	Deposits of very dense sand, gravel, or very stiff clay, at least several tens of metres in thickness, characterised by a gradual increase of mechanical properties with depth.	360 – 800	> 50	> 250
C	Deep deposits of dense or medium-dense sand, gravel or stiff clay with thickness from several tens to many hundreds of metres.	180 – 360	15 - 50	70 - 250
D	Deposits of loose-to-medium cohesionless soil (with or without some soft cohesive layers), or of predominantly soft-to-firm cohesive soil.	< 180	< 15	< 70
E	A soil profile consisting of a surface alluvium layer with v_s values of type C or D and thickness varying between about 5 m and 20 m, underlain by stiffer material with v_s > 800 m/s.			
S_1	Deposits consisting, or containing a layer at least 10 m thick, of soft clays/silts with a high plasticity index (PI > 40) and high water content	< 100 (indicative)	–	10 - 20
S_2	Deposits of liquefiable soils, of sensitive clays, or any other soil profile not included in types A – E or S_1			

Figure 1. Site Classification System of Model A

In Model B, site classes are dictated by the site natural period parameter (T_S) which is proportional to the total depth of the soil sediment and is inversely proportional to the average value of the shear wave velocity of the soil material (V_S). Ground types A to E correspond to T_S values ranging from low to high, and with transitions at T_S = 0.15 s, 0.5 s, 0.7 s and 1.0 s as listed in Figure 2. The calculation of the value of T_S is illustrated with an example borehole record as shown in Figure 3. More detailed descriptions of the calculation can be found in Chapter 7 in this technical guidebook on a case study of code compliant design of buildings.

Table AA.1 Ground classifications scheme in accordance to site natural period

Ground Type	Description and Range of Site Natural Period, T_S (s)*
A	Rock site, OR a site with very thin sediments and T_S < 0.15 s
B	A site not classified as Ground Type A, C, D or E
C	A site with sediments of more than 30 m deep to bedrock AND T_S = 0.5 – 0.7 s
D	A site with sediments of more than 30 m deep to bedrock AND T_S = 0.7 – 1.0 s
E	A site with sediments of more than 30 m deep to bedrock AND T_S = > 1.0 s, OR deposits consisting of at least 10 m thick of clays/silts with a high plasticity index (PI > 50)

Figure 2. Site Classification System of Model B (taken from Table AA.1 in the NA-2017)

Type	*Thickness (m)*	*N*	V_i *(m/s)*	
Fill	5.2	13	217	
MD	2	11	206	
MD	2	11	206	
MD	2	6	170	
MD	2	7	179	
Alluvium	2.14	14	222	
Alluvium	1.86	13	217	
Alluvium	1.9	17	236	
	H_S = **19.1 m**		$V_{S,i}$ = **206 m/s**	T_i = **0.370 s**

$$T_S = \frac{4H}{V_S} = \frac{4 \times 19.1}{206} = 0.37s$$

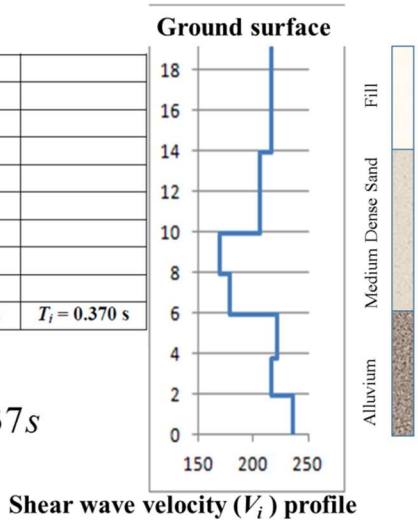


Figure 3. Example calculation of site natural period

3. Response spectrum models

The general construct of the ground type dependent response spectrum is shown in the schematic diagram of Figure 4 which is annotated with values for the various corner periods to characterise the shape of the spectrum. The value of each corner period and the site amplification factor S are listed in Figures 5a and 5b for Models A and B for Peninsular Malaysia respectively.

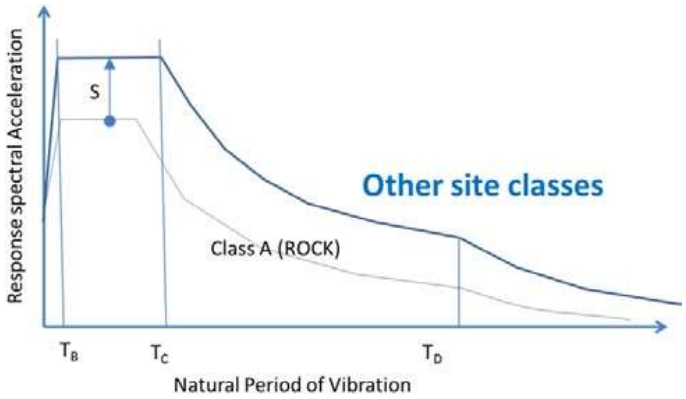


Figure 4. Basic construct of the response spectrum model

4. Guidance over selection of response spectrum model

The purpose of this section, in making comparisons between Models A and B, is purely to assist designers in selecting the lower of the values provided by the two models to achieve a more economical design. The response spectra presented in this section are based on a reference peak ground acceleration for rock sites (a_{gR}) of 0.07g which is the recommended minimum design PGA values across the whole of Malaysia (a higher value of 0.12g is recommended for Central and Eastern Sabah) for important Class II structures

in Peninsular Malaysia. Response spectra in areas within Peninsular Malaysia that have a different value of a_{gR} to 0.07g may be derived by scaling from the response spectra presented herein.

4.1 Rock sites or very shallow soil sites (T_S < 0.15s)

This site category refers to rock outcrops or sites in which the thin layer of soil overlying bedrock does not exceed 5 m. The dual response spectra of ground type A, given by Models A and B are shown on the same graph for comparison purposes, in Figure 6. The designer is free to choose between the two models shown.

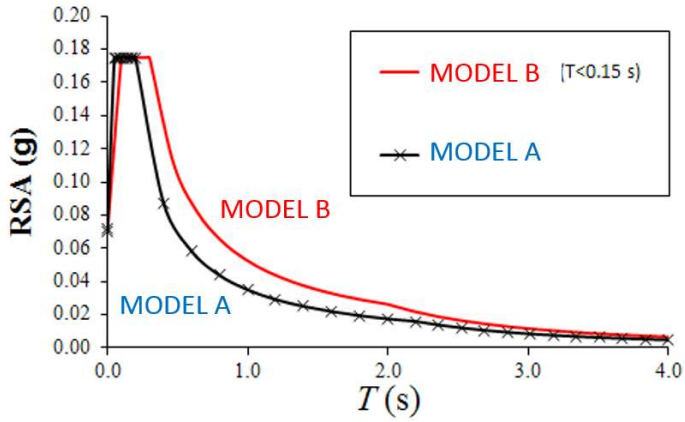


Figure 6. Model A (ground type A) versus Model B (ground type A)

4.2 Stiff soil sites (0.15 s < T_S < 0.5 s)

This site category refers to conditions where the soil material is stiff enough for the value of T_S to lie within the range 0.15 s - 0.5 s. If the total thickness of the soil is less than 30 m the designer is free to choose between the response spectrum of ground type E of Model A and ground type B of Model B which are plotted on the same graph for comparison in Figure 7. The response spectrum stipulated for ground type B of Model B is shown to be less conservative than that for ground type E of Model A in most cases. If the total thickness of the soil exceeds 30 m then ground type B of Model B has to be adopted.

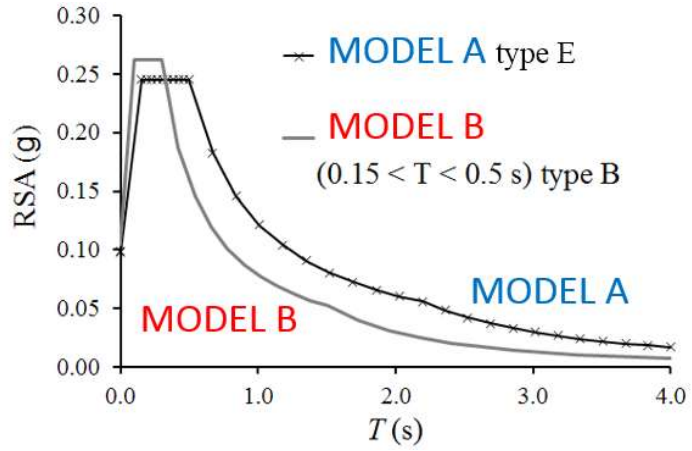


Figure 7. Model A (ground type E) versus Model B (ground type B)

4.3 Medium soft soil sites (0.5 s < T_S < 0.7 s)

This site category refers to conditions where the soil layer consists of soft materials and/or is of a thickness which results in the value of T_s to be in the range 0.5 s - 0.7 s. If the total thickness of the soil is less than 30 m the designer is free to choose between the response spectrum for ground type D of Model A and ground type C of Model B which are plotted on the same graph for comparison in Figure 8. The response spectrum stipulated for Ground type C of Model B is shown to be higher than the response spectra stipulated by ground type D of Model A in the low period range (T < 0.8 s approximately) to account for amplification associated with the resonance phenomenon. Response spectra stipulated by Model B are less conservative than those for Model A in the higher period range. If the total thickness of the soil exceeds 30 m then ground type C of Model B has to be adopted.

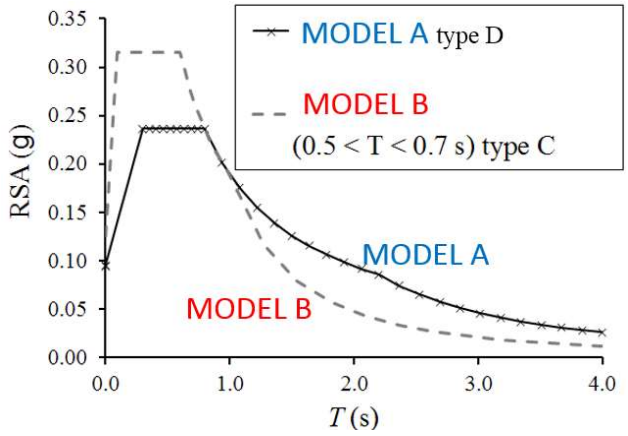


Figure 8. Model A (ground type D) versus Model B (ground type C)

4.4 Flexible soil sites (0.7 s < T_S < 1.0 s)

This site category refers to conditions where the soil layers are sufficiently deep and/or soft to result in values of T_S in the range 0.7 s - 1.0 s. The total depth of the soil layers should exceed 30 m in most cases and hence Model A would be irrelevant. Thus, designers do not have an option and have to adopt the response spectrum for ground type D of Model B as shown in Figure 9.

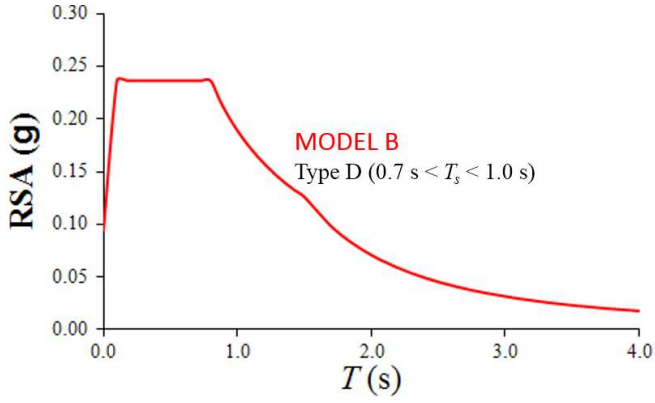


Figure 9. Model B (ground type D) for flexible soil site > 30 m (0.7 s < T_s < 1.0 s) (note: Model A is irrelevant in this case)

4.5 Very flexible soil sites (T_S > 1.0 s)

This site category refers to soil conditions where the soil layers are exceptionally deep and/or so soft that results in the value of T_S exceeding 1.0 s. The total depth of the soil must be well above 30 m. Thus, designers have to adopt the response spectrum for ground type E of Model B as shown in Figure 10.

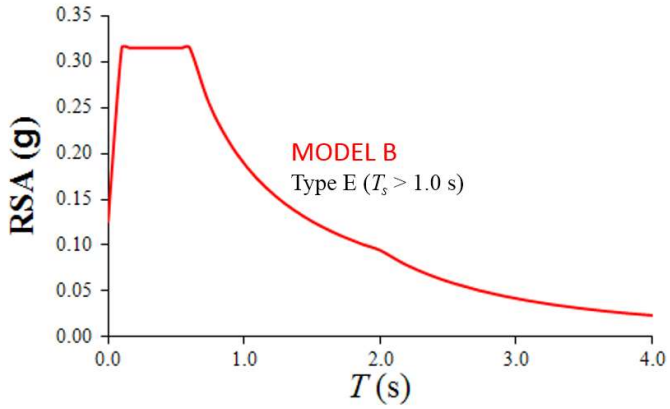


Figure 10. Model B (ground type E) for flexible soil site > 30 m (T_s > 1.0 s) (note: Model A is irrelevant in this case)

5. Conclusions

The site classification system of Model A is out of date as it fails to model the phenomenon of soil resonance. This is a significant shortcoming in regions of low to moderate seismicity where limited ductile construction is the norm. The alternative displacement-based site amplification model which had been developed to take into account the effects of soil resonance was circulated for the first round of public comment in 2016 (NA-2016).

The displacement-based model, which has a firm foundation as evidenced by publications in prestigious international archival sources has since been modified to conform to the format of Eurocode 8 and is referred to herein as Model B. Both Models A and B involve five ground types (A to E). Definitions of the ground types adopted by the two models are very different. Model A is restricted to rock or shallow soil sites which are less than 30 m deep. Model B, which does not have this restriction features the use of the site natural period as the criterion for classification. A key objective of this chapter is to assist engineers in deciding between Models A and B when identifying the response spectrum to be adopted in design. On the whole, Model B is preferred as it is less conservative (hence more economical) than Model A except for the following conditions: (1) rock sites or very shallow soil sites (ground type A) (2) the low period section (T < 0.8 s) of the response spectrum on a stiff soil site (ground type B of Model B).

Acknowledgements

The continuous support by IEM in the facilitation of numerous workshops and meetings over the years culminating in the drafting of the NA is acknowledged. Valuable intellectual input by other active participants from EC8 TC are also gratefully acknowledged.

References

Eurocode 8 - Design of structures for earthquake resistance. EN 1998-1 Part 1: General rules, seismic actions and rules for buildings. UK: British Standards Institution.

MS EN1998-1:2015 Eurocode 8: Design of structures for earthquake resistance – part 1: General Rules, Seismic Actions and Rules for Buildings. (National Annex undergone public comments in 2016).

NA-2016 to MS EN1998-1:2015 Eurocode 8: Design of structures for earthquake resistance – part 1: General Rules, Seismic Actions and Rules for Buildings. (National Annex undergone public comments in 2016).

NA-2017 to MS EN1998-1:2015 Eurocode 8: Design of structures for earthquake resistance – part 1: General Rules, Seismic Actions and Rules for Buildings. (National Annex undergoing public comments in 2017).

Pitilakis K., Riga E., Anastasiadis A. (2013) "New code site classifica1on, amplification factors and normalized response spectra based on a worldwide ground-motion database", Bulletin of Earthquake Engineering, 11, 4, 925-966.

Pitilakis K., Riga E., Anastasiadis A. (2012) "Design spectra and amplification factors for Eurocode 8", Bulletin of Earthquake Engineering, 10, 5, 1377-1400.

Riga E., Makra K., Pitilakis K. (2016) "Aggravation factors for seismic response of sedimentary basins: A code- oriented parametric study", Soil Dynamics and Earthquake Engineering, Special Issue of Invited Papers at the 6th International Conference on Earthquake Geotechnical Engineering (6ICEGE), Christchurch, New Zealand, 2-4 November 2015, vol. 91, pp. 116-132.

Tsang, H. H., Wilson, J. L., Lam, N. T. K. and Su, R. K. L. (2017) "A design spectrum model for flexible soil sites in regions of low-to-moderate seismicity", Soil Dynamics and Earthquake Engineering, Vol. 92, 36-45.

Tsang, H. H., Chandler, A. M. and Lam, N. T. K. (2006) "Estimating non-linear site response by single period approximation", Journal of Earthquake Engineering and Structural Dynamics. 35(9): 1053-1076.

Seismic Hazard Maps and Design Response Spectra for Sri Lanka – A Generic Approach

Srikanth Venkatesan, Janaka Gamage and Saman De Silva

School of Engineering
RMIT University, Australia

Seismic hazard maps and design acceleration response spectra for rock and soil sites in Sri Lanka are presented in this chapter. These were derived from a combination of the standard Probabilistic Seismic Hazard Approach (PSHA), the deterministic approach and site response analyses. Six seismic zones were identified in and around Sri Lanka (with Colombo considered as a separate zone). The de-clustered earthquake data showed Gutenberg-Richter 'b' values in the range 0.3 to 0.9. About 180 records of broadband ground motion data obtained from three recording stations in Sri Lanka were analysed to derive seismological parameters such as the wave transmission quality factor (Q_0), upper crustal amplification factor (κ) and stress drop (σ). Using these parameters, synthetic accelerograms [GENQKE (Lam, 1999)] were developed and compared with recorded ground motions. Based on the satisfactory comparisons, ground motion prediction equations (GMPE) were developed for the region. All these parametric combinations were utilized to produce seismic hazard maps for return periods of 500, 1000, 2500 and 10,000 year return periods. Furthermore, target ground motions of Peak Ground Accelerations (PGA) of 0.08 g and 0.05 g were generated for site response studies. Site amplification factors were derived using five borehole records that were consistent with the definitions of notional site classes C and D according to standard building codes. Results obtained from the above approaches were compared and benchmarked with international codes of practice. Based on these observations, design response spectra are presented in accordance with the Eurocode format for the benefit of practicing engineers. Simple manual calculations for site specific spectra are also presented. Our study shows that Sri Lanka should be considered as a low to moderate seismic region, similar to regions such as Australia.

Keywords: seismic hazard, Sri Lanka, response spectra, site factor, building codes of practice, seismic hazard maps

1. Introduction

Sri Lanka is situated far from major tectonic plate boundaries. However, the infamous Aceh earthquake of 2004 and the tsunami that affected the region, prompted considerable awareness of seismic risk in the country. It is noted that seismic hazard estimations generally require a significant knowledge of possible seismic sources, levels of seismicity attenuation including the behaviour of the regional and local soil conditions. Normally the availability of ground motion data pertinent to a region, facilitates the use of convenient analysis procedures (Lam & Wilson, 2004). For Sri Lanka, seismic hazard estimations prior to 2008, including those undertaken by Fernando and Kulasinghe (1986) and Abayakoon, (1996, 1998), were limited to historical information and limited data. Furthermore, Sri Lanka has no earthquake code of practice. Engineers, therefore, are forced to adopt site specific provisions used in other codes. Given this knowledge gap,

this chapter presents the initial results of a seismic hazard analysis for the benefit of practitioners, researchers and government authorities in Sri Lanka.

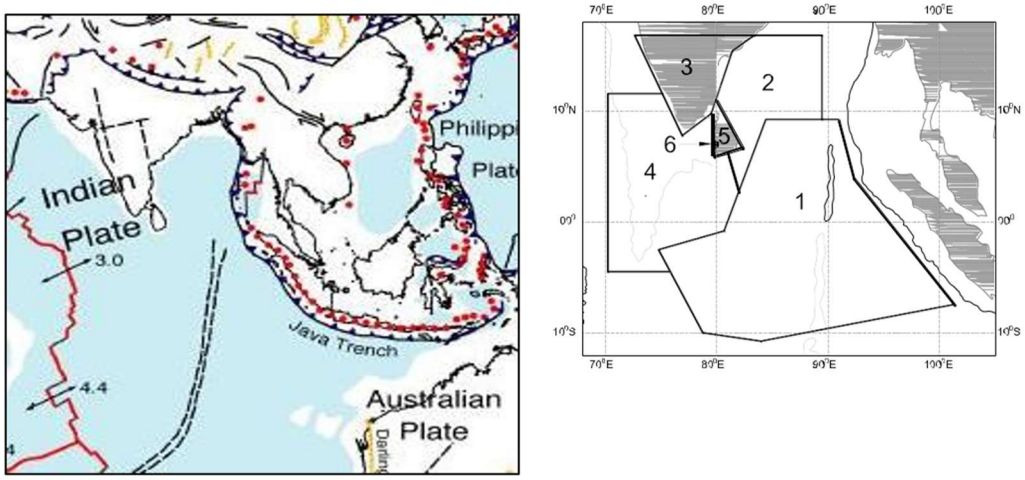
The authors collected ground motion data from three stations located within the country. With this database, Venkatesan and Gamage (2013) derived the wave transmission quality factor (Q_0) as 389 ± 2.5. Further analysis from 62 shallow crustal events resulted in the estimation of the upper crustal attenuation factor κ (pronounced as Kappa) as 0.041± 0.009. Attenuation models were also developed for the region and compared with the New Generation Attenuation (NGA) models (Venkatesan et al. 2015). Using these key inputs and the probabilistic seismic hazard analysis (PSHA) approach, the reference PGA was estimated as 0.04 g on average, confirming the low levels of seismic hazard in the country. However, a detailed analysis of the contributions from zones around Sri Lanka (Figure 1, next page) resulted in an estimated reference PGA value of around 0.11 g. It is noted that the above discussion relates to seismic hazard on rock sites only. As the presence of soil is known to amplify earthquake ground motions many fold, most codes of practice, such as the Eurocode 8 (EN 1998), Uniform Building Code (UBC, 1997) and the Australian Standards (AS 1170.4), specify a suite of site response factors for analysis and design purposes. Therefore, site response analyses using Shake 91(Idriss & Sun, 1992) have been conducted on local soil profiles to derive representative site response factors.

2. Seismic hazard maps development

2.1 Source characterisation

The island of Sri Lanka is bounded by the latitudes 5^0N to 10^0N and longitudes 79^0E to 82^0E (Figure 1, next page). Well-known and active seismogenic sources surrounding Sri Lanka are located at the boundaries of the Indo-Australian Plate, e.g., the Sunda Arc subduction zone and Great Sumatran fault towards the east (about 1100 km distance), northern transform faults of the Central Indian Ridge towards the west (about 1500 km) and the convergent Himalayan plate boundary to the north (more than 2000 km). The location of plate boundaries well away from the landmass may have led to the low levels of seismicity previously experienced in this region.

Although there is a fair distribution of M>5 events in the region outside Sri Lanka, the land mass is typically subjected to M<4 earthquakes (Figure 2a). Of importance to note is the evidence of a few historical earthquakes. Out of these, a magnitude 5 event that caused significant destruction around Colombo in the 1600's is well recognised (although the magnitude, distance and intensity are questioned by researchers).



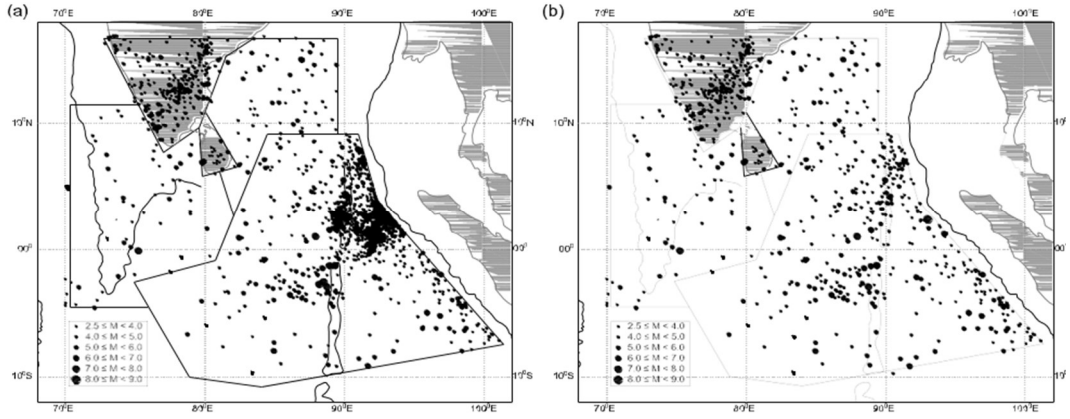
(a) Map of the Region (b) Seismic zonation

(Source: Regents of University of Michigan)

Figure 1. Location of Sri Lanka relative to major plate boundaries and earthquake occurrences

2.2 Catalogue data

Data were obtained from several sources; ISC (International Seismological Centre), ANSS (Advanced National Seismic System), NEIC (National Earthquake Information Centre) and GFZ-GEOFON (German Research Centre for Geosciences), GCMT (Global Centroid Moment Tensor catalog), and some previously published data (Abayakoon, 1996; Fernando and Kulasinghe 1986; Uduweriya et al. 2013) were also used. Events repeated in several data bases were carefully avoided with priority given to the ANSS database, because of the quality of information available. Records encompass a long period from 1507 until 2014.



(a) before declustering (2421 events) (b) after declustering (870 events)

Figure 2. Epicentral locations of earthquake catalog data in hazard computation in the study

The original catalogue of all source zones contained a total of 2421 events (including dependent events) for the selected period. Variations in the hypo-central depth of selected events was assumed to not have any relation with recurrence rates, and therefore, effects due to "depth" and any uncertainty in depth, were ignored for the study. Data were originally of various magnitude types such as M_L and M_S for most of the older events and M_w and M_b for newer events reported within the instrumented period where M_L is the local magnitude, M_s is surface wave magnitude, M_w is moment magnitude and M_b is body wave magnitude. These different magnitude types, other than M_w, have been converted to a unified scale M_w, using relationships developed for mid-plate and stable continental regions based on global data (Johnston 1996; Nuttli 1983). It is noted that Mw is widely used in ground motion attenuation models worldwide. Local events, available in the form of intensity values, were converted to Mw using relationships developed by Greenhalgh et al (1988). Epicentral locations of earthquake catalogue data in assigned source zones are shown in Fig. 2, where Figures 2a and 2b, respectively, show data before and after the removal of dependent events. It is evident that source zone 1 contains the highest number of dependent events out of all the zones for the selected time period.

2.3 De-clustering approach

In this study, dependent events were eliminated by applying the time and space windows of Gardner and Knopoff (1974). However, Gardner and Knopoff's (1974) spatial windows for dependent events of a large magnitude main event, appeared to be underestimating the actual areas likely to experience the aftershocks of some major earthquakes occurring in the region. Two such mega events are worthy of mention; M_w 8.6 on 11th April 2012 and M_w 9.3 on 26th December 2004. The former was an intra-plate event located within source zone 1 near Ninety East Ridge, while the latter was identified as an inter-plate event at the subduction zone outside source zone 1. Events dependent on the second event were identified based on rupture areas given in Ammon et al (2005) and US Geological Survey's earthquake summary maps (2005). Such analysis helped in the elimination of other major aftershocks generated in the aftermath of the M_w 9.3 earthquake in 2004. Similarly, the M_w 8.6 earthquake has so far generated hundreds of dependent events since April 2012, and probably represents the largest known aftershock sequence in the selected data set (see Fig. 2b). Many dependent shocks of this event were carefully removed through a manual process based on observations such as small time gaps from the main event and significant increases in the rate of activity in the area after the main event.

The final catalogue after the de-clustering included 870 events, about 36% of the original catalogue size. This is not a surprise, since many small and moderate magnitude events, particularly in source zone 1, were aftershocks of major earthquakes. The temporal distribution of the final "independent" earthquake data set for the whole region was compared with the Poisson distribution. Events with medium and higher sizes (Mw $\geq$ 4.0), generated only after 1965, were included in the comparison, choosing 1965 as the cut-off year, in parallel with the World Wide Standard Seismograph Network (WWSSN) program launched in 1964. It was found that the de-clustered catalogue sufficiently complied with the Poisson distribution. Although this compliance cannot be expected for all "independent events", a Poisson distribution was assumed because it provides a convenient basis for future hazard estimates and for comparisons with data in the literature.

2.4 Recurrence rates analysis

The Stepp method (1972) was adopted for estimating completeness periods in the study. The method assumes that an earthquake occurrence in a particular magnitude class, is a point process in time, following a Poisson event arrival. In the study, the emphasis was on completeness periods of "smaller magnitude events" that are still capable of producing sufficient ground shaking at the selected sites. This minimum magnitude varied from M_w 3.0 to 5.0 for identified source zones depending on the availability of smaller magnitude events in each source zone, and site-source distance which "calibrates" the size of magnitude needed for a lower bound shaking level. For instance, for source zone 1, M_w 5.0 was considered the minimum magnitude for the completeness check, because there was very little event data smaller than that ($M_w < 5.0$) in the zone and because of the large site-source distance. For source zones 5 and 6, however, a small magnitude M_w 3.0 was chosen, mainly because of the inadequacy, or sometimes the complete absence, of other moderate and strong events ($M_w > 4.0$) reported within the country (this situation is true in source zone 5). Recurrence of earthquakes in the region are presented in Figure 3; minimum and magnitude values for the zones and 'a' and 'b' values according to the Gutenberg-Richter law are presented in Table 1.

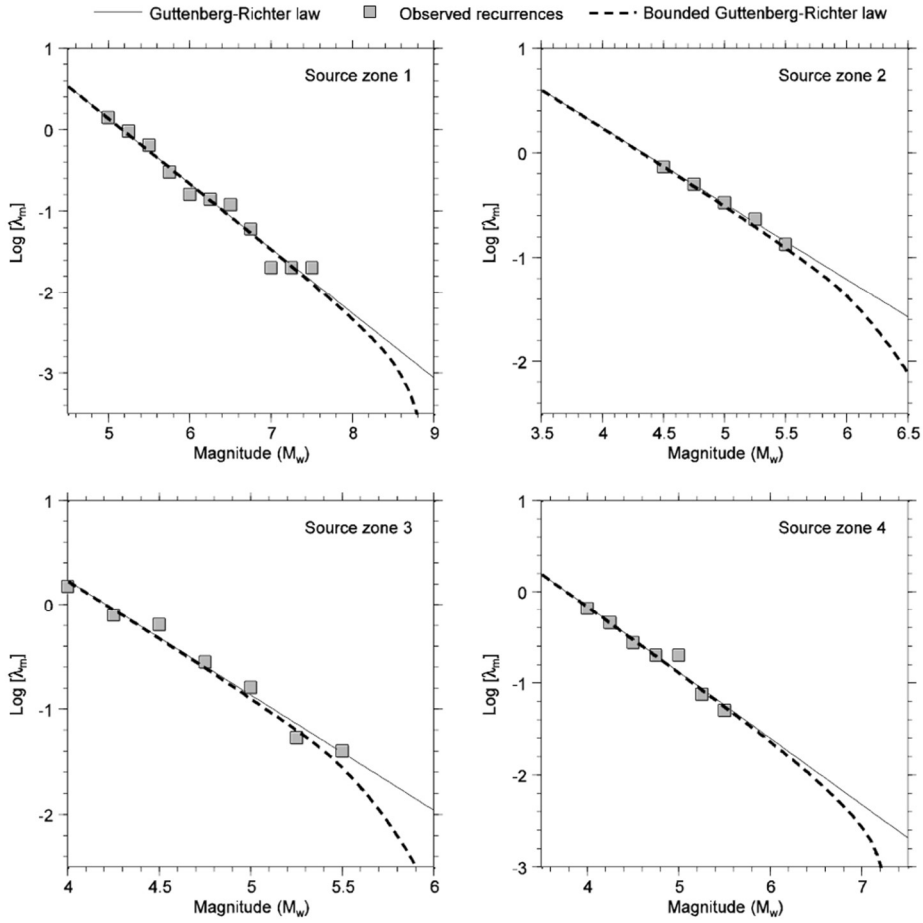


Figure 3. Earthquake recurrences for main source zones. (Note: values for region 5 and 6 are negligible and hence not shown; method of least squares used in the calculations)

From the above figures, it is clear that source zones 1-4 do not exhibit more than 2 earthquake occurrences. Source zones 5 and 6 are dominated by historical records, so the completeness of the dataset for zones 5 and 6 is unreliable.

Table 1. Seismicity parameters of defined source zones

Source zone	Stepp's test for the completeness		Input parameters for hazard computation				
	Min magn. considered for the test (M_w)	Completeness periods (yrs)	a*	b**	CV of b	m_o (M_w)	m_{max} (M_w)
1	5.0	50	2.22	0.59	0.018	4.5	9.0
2	4.5	30	1.98	0.51	0.004	3.5	6.7
3	4.0	75	2.36	0.93	0.017	4.0	6.0
4	4.0	40	1.83	0.51	0.017	3.5	7.5
5	3.0	Incomplete	1.60	0.49	0.026	3.0	6.0
6	3.0	Incomplete	0.97	0.33	0.000	3.0	6.5

a^* and b^{**} values in the Gutenberg-Richter magnitude recurrence relationship.

CV of b - Coefficient of variation of b

m_0 - Minimum threshold magnitude used in the hazard computation

m_{max} - Maximum expected magnitude for the source zone

2.5 Ground motion prediction equations

Gamage and Venkatesan (2014), and Gamage (2015) developed attenuation models for local (mainland Sri Lanka) and regional (outside landmasses) based on crustal classifications and seismic activities. The local attenuation model was employed in computing the seismic hazard for source zones 5 and 6. The regional attenuation model was applied for source zones 1, 2 and 4 consistent with Figure 1. For source zone 3 the Raghu Kanth and Iyengar (2007) model developed for southern India was adopted.

2.6 Ground motion prediction equations

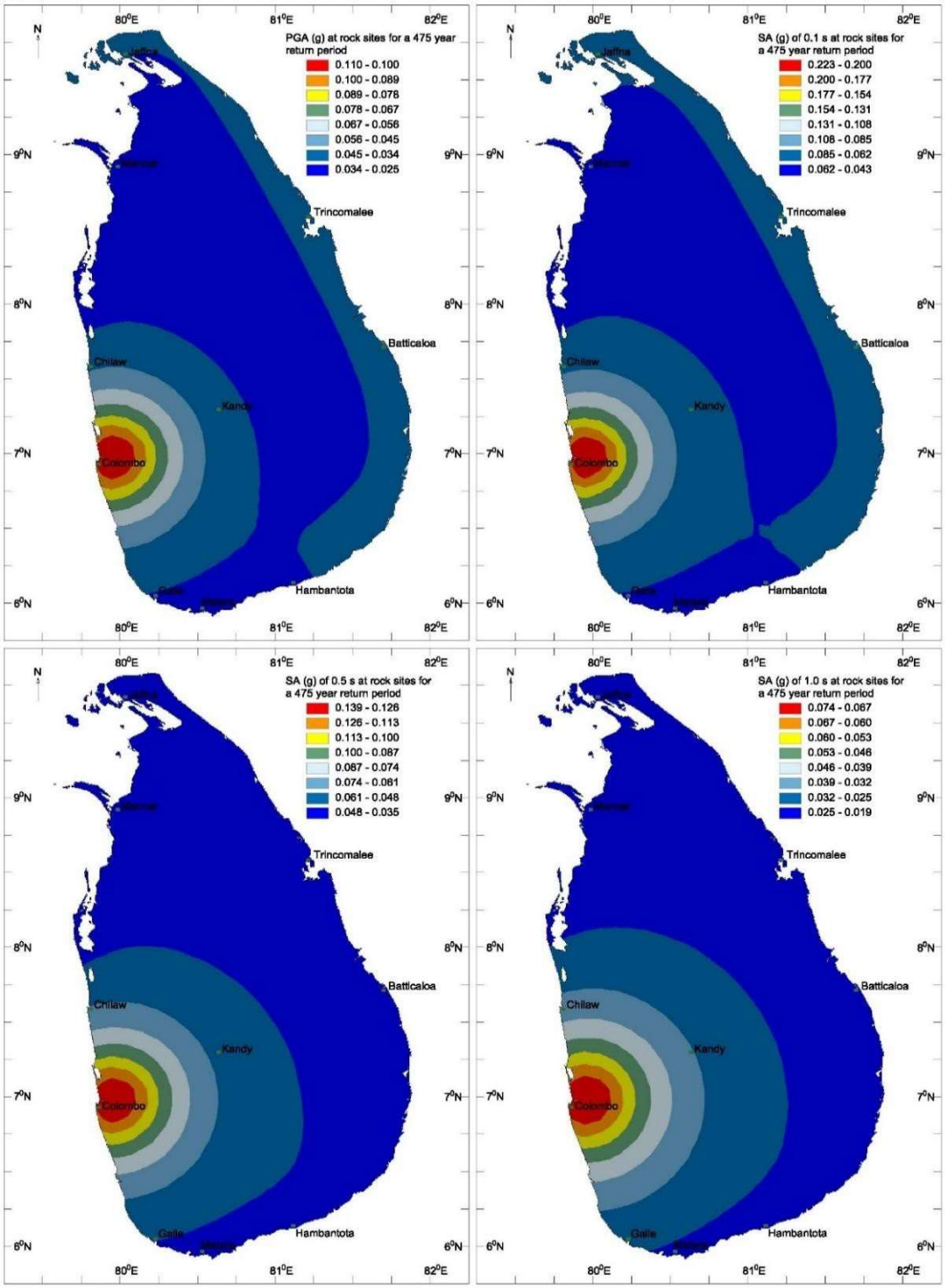
Hazard computation based on the probability of a selected ground motion parameter (Y) exceeding a certain value (y) due to a M magnitude event at an independent distance, R, from the target site can be computed according to Equation (1) as established in most studies.

$$P[Y > y] = \iint P[Y > y \mid M, R] \cdot f(M) \cdot f(R) \cdot dM \cdot dR \tag{1}$$

where f(M) and f(R) are probability density functions for the magnitude and distance parameters, respectively. The authors used the open-source package CRISIS2007 (Ordaz et al. 2007) to derive representative values.

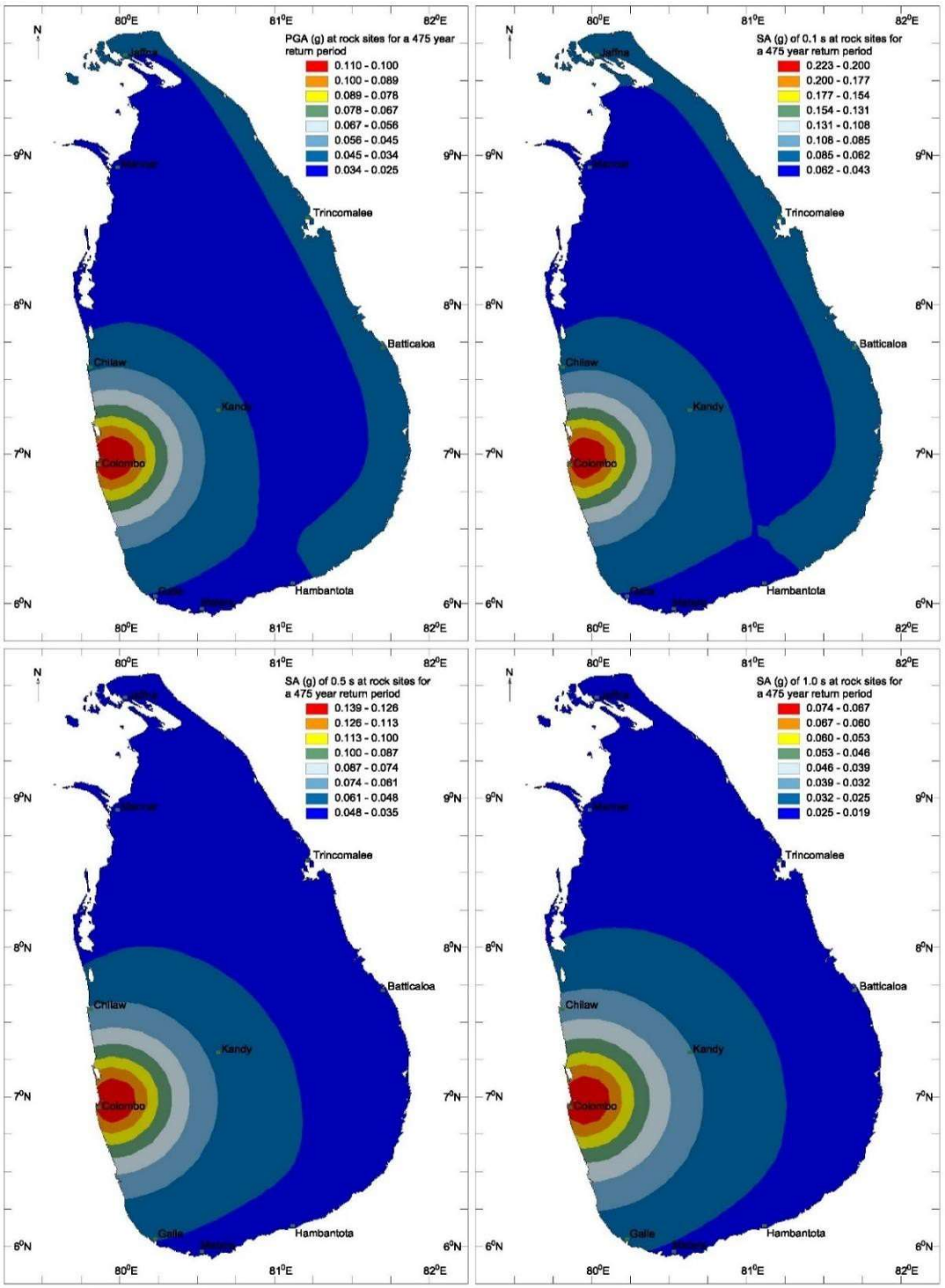
2.7 Seismic Hazard maps

Hazard computations in the form of expected ground motions (PGA and SAs at 0.1, 0.5 and 1.0 s natural periods) at rock sites in Sri Lanka having 10% (500 year return period), 5% (1000 year return period) 2% (2500 year return period) and 0.5% (10,000 year return period) probability of exceedance in 50 years were analysed (Figures 4a to 4d).



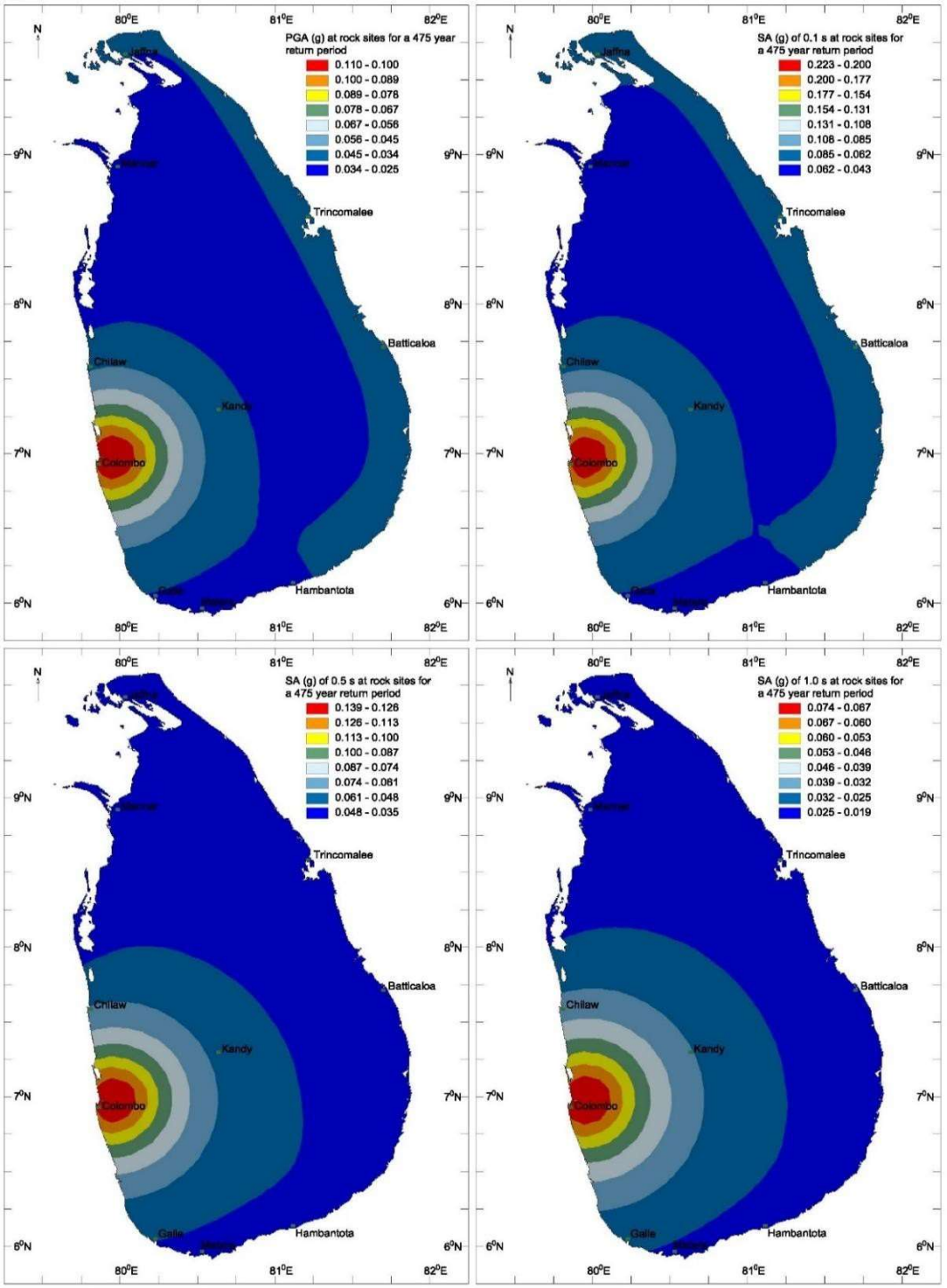
(a) Probability of exceedance – 10% in 50 years (500/475 year return period)

Figure 4. Seismic hazard expressed as PGA and spectral acceleration (SA) at 0.1, 0.5 and 1.0 s natural periods for rock sites



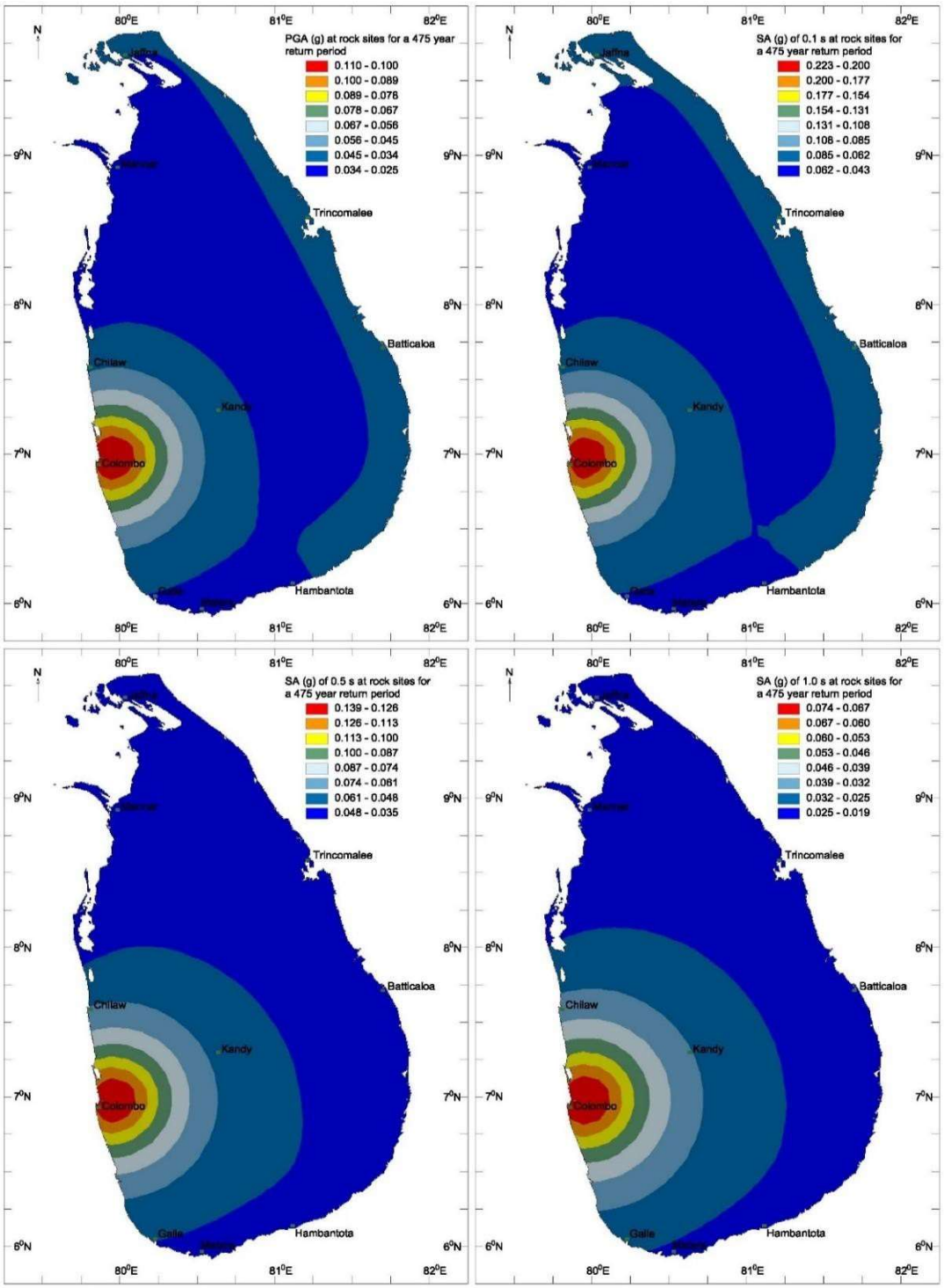
(b) Probability of exceedance – 5% in 50 years (1000 / 975 year return period)

Figure 4. Seismic hazard expressed as PGA and spectral acceleration (SA) at 0.1, 0.5 and 1.0 s natural periods for rock sites (cont.)



(c) Probability of exceedance – 2% in 50 years (2500 / 2475 year return period)

Figure 4. Seismic hazard expressed as PGA and spectral acceleration (SA) at 0.1, 0.5 and 1.0 s natural periods for rock sites (cont.)



(d) Probability of exceedance – 0.5% in 50 years (10000 / 9975 year return period)

Figure 4. Seismic hazard expressed as PGA and spectral acceleration (SA) at 0.1, 0.5 and 1.0 s natural periods for rock sites (cont.)

Results show that the area surrounding Colombo is by far the most vulnerable in the country with a value of about 0.045g (g is gravitational acceleration) PGA expected to be exceeded in a 500 (or 475) year return period. This increases to about 0.053g and 0.065g for 1000 and 2500 year return periods, respectively. The rest of the country faces relatively small PGA values. The minimum value of 0.045 g as observed from the above analysis is close to the international recommendations of 0.05g for regions of hard rock (cratonic) geology such as that of the pre-cambrian formation typifying Sri Lanka (Lam, 2017). Therefore, it is suggested that a minimum reference PGA value of 0.05g should be used in the design of normal structures anywhere in Sri Lanka. Note, in non-cratonic regions a minimum reference PGA value of 0.07g should be used instead.

3. Design Response Spectra Development

3.1 Definition of soil amplification factor

A very important consideration in site response analysis should be given to the definition of soil amplification factor. In most codes of practice, recommended site response factors are usually derived from the average of response spectral ratios over many sites and period ranges chosen for analysis. Lam et al (2004) suggest that this approach smears the actual amplification potential, indicative of resonance, and may not be suitable for regions where most construction is non-ductile. Furthermore, the soil amplification factor recommended is based on the ratios of Response Spectral Displacement (RSD) measured at the site's natural period. This definition, adopted in the chapter, is presented in Figure 5. Furthermore, it is also clear that most of the construction in Sri Lanka is indeed non-ductile. As can be seen from Figures 6a to 6d, de-amplification is observed in the short period range of the spectra which implies that amplification factors are less than unity. However, in Figures 6e to 6h, values greater than unity are observed in the short period range. Therefore, averaging based on the ratios of response spectra (RRS procedure) over the whole period does not seem reasonable.

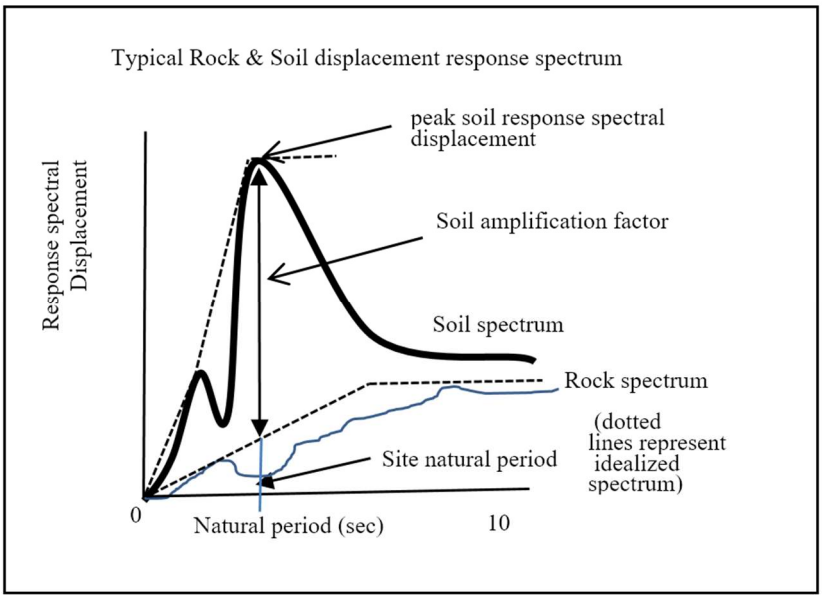


Figure 5. Definition of soil amplification factor

3.2 Estimation of initial site natural period & shear wave velocity from borehole records

The shear wave velocity profile of a site can be estimated from the Standard Penetration Test (SPT N) values. Although a number of equations are available in the literature, the Imai and Tonouchi (1982) equations for all soils were chosen for this study, as $V_s = 91\ N^{0.314}$. The Vs value thus obtained is averaged over the entire depth (not just the top 30 m). The initial site natural period (T_s) can be estimated from Equation 2 as shown below (see Wair et al., 2012 for further details):

$$T_s = \sum \left(d_i / V_{s,i} \right) \times 4 = 4 H_s / V_s \tag{2}$$

where d_i is the depth of each layer, V_s, i is the shear wave velocity of each layer and V_s is the weighted average shear wave velocity over the entire depth and Hs is the total thickness of the layer.

3.3 Soil response analyses

About 50 borehole records were collected from regions including Colombo, Batticola, Mannar, Trinconmalee, Galle and Kandy. As many of these sites were of thickness less than 10 m and the Standard Penetration Test (N) values were more than 50, only five borehole records, that were deeper than 15 m and N values ranging between 5 and 50 were analysed for this study. The shear wave velocity (SWV also noted as V_s) averaged over the whole depth is observed to be of the order of 220 m/s to 350 m/s (and natural periods ranging from 0.25 s to 0.6 s). These values suggest a site class B and C or C and D according to most codes of practice. Further, six ensemble input accelerograms were simulated for a notional Peak Ground Velocity (PGV) of 60 mm/s (approximately 0.08g) and another set of ensembles for a PGV of 40 mm/s (approximately 0.05 g) using GENQKE. Results from response spectrum analyses for a number of soil sites are presented in Figures 6a to 6g.

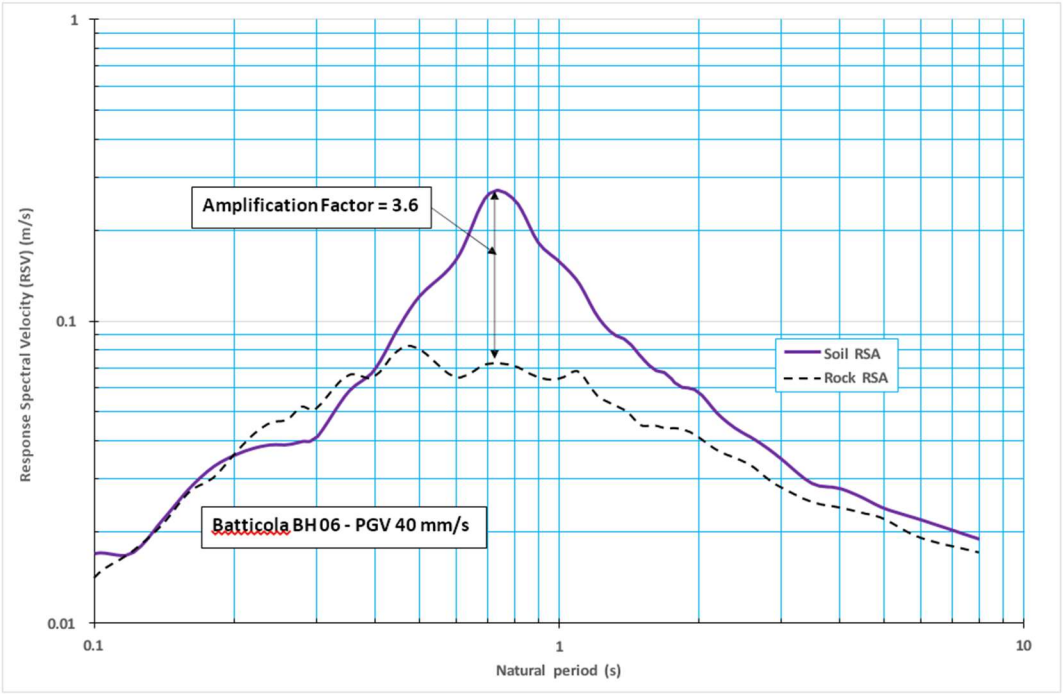


Figure 6a. Velocity response spectra for Batticola site BH 06 – PGV 40 mm/s (PGA 0.05 g)

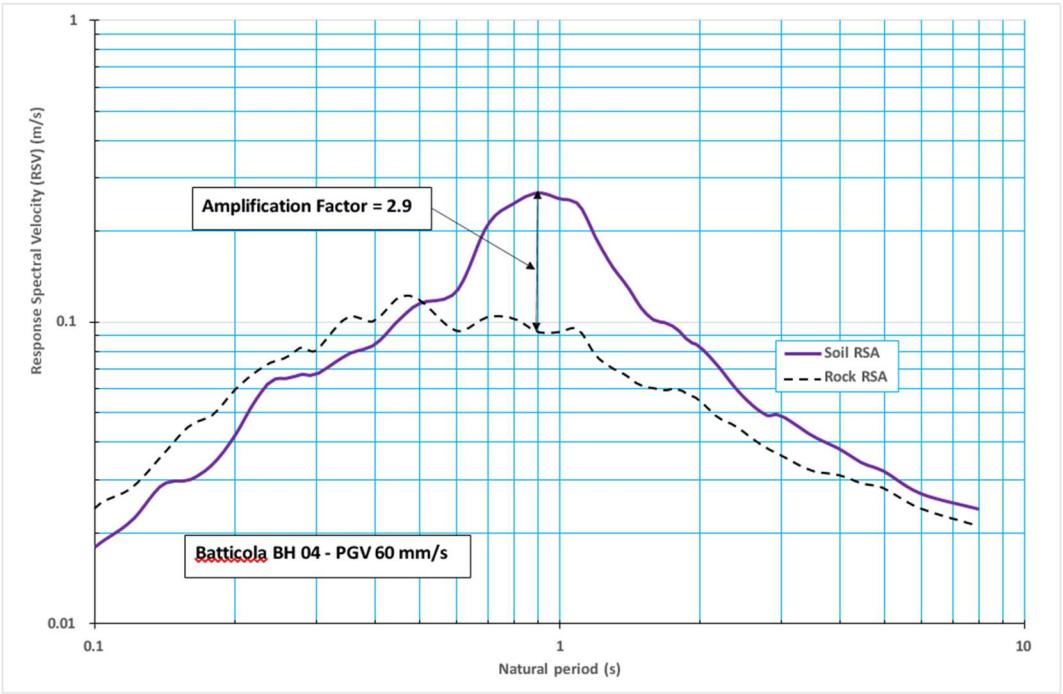


Figure 6b. Velocity response spectra for Batticola site BH 04 – PGV 60 mm/s (PGA 0.08 g)

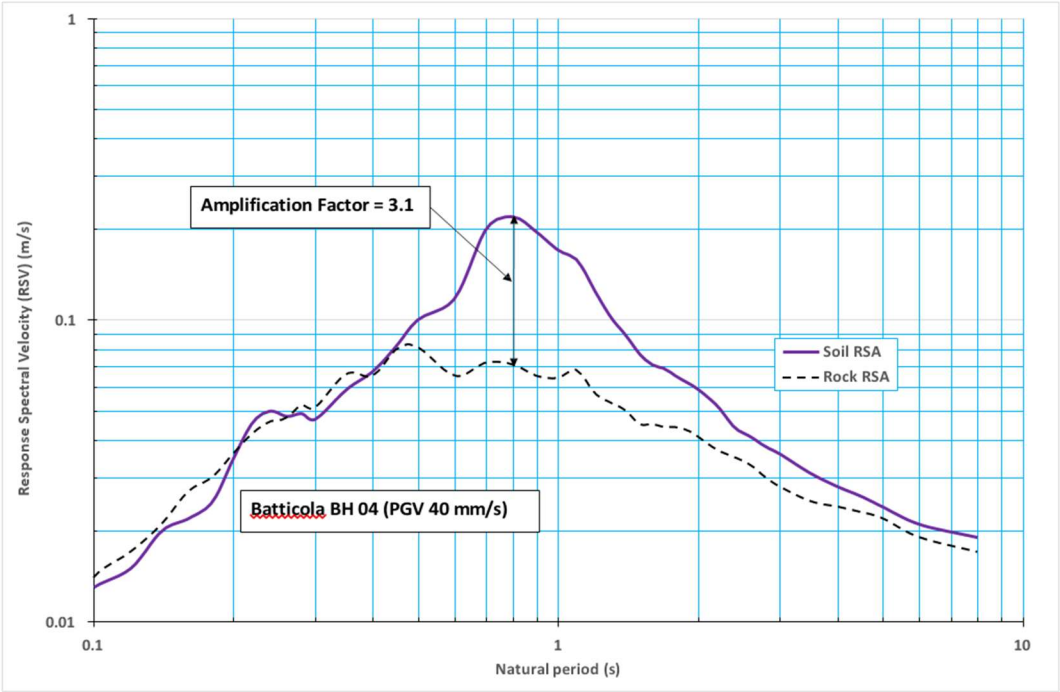


Figure 6c. Velocity response spectra for Batticola site BH 04 – PGV 40 mm/s (PGA 0.05 g)

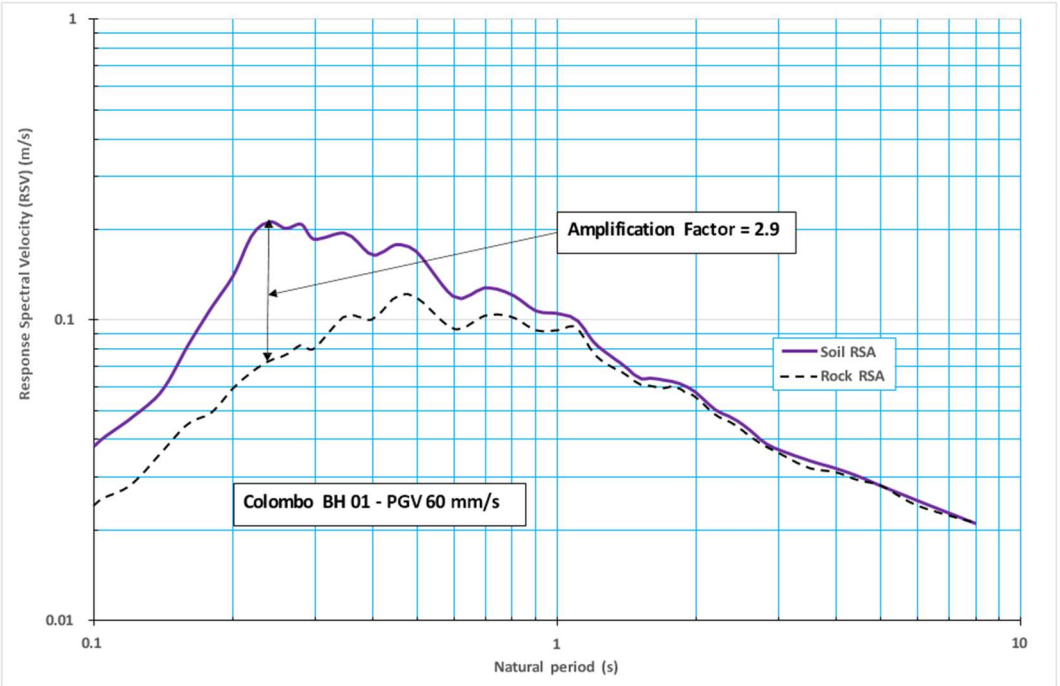


Figure 6d. Velocity response spectra for Colombo site BH 01– PGV 60 mm/s (PGA 0.08 g)

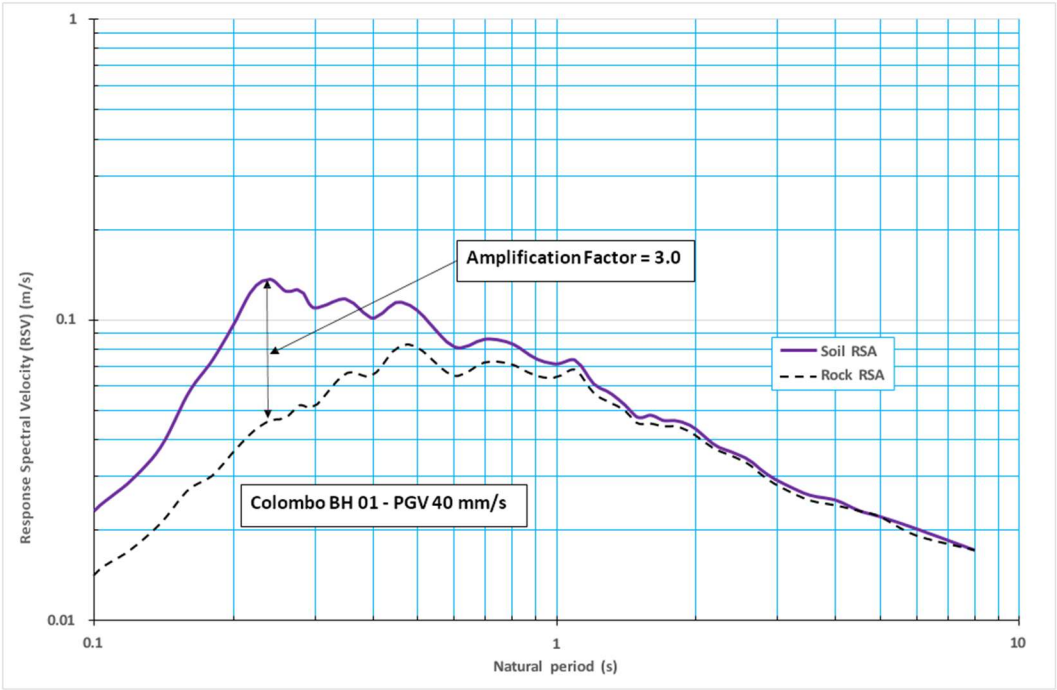


Figure 6e. Velocity response spectra for Colombo site BH 01– PGV 40 mm/s (PGA 0.05 g)

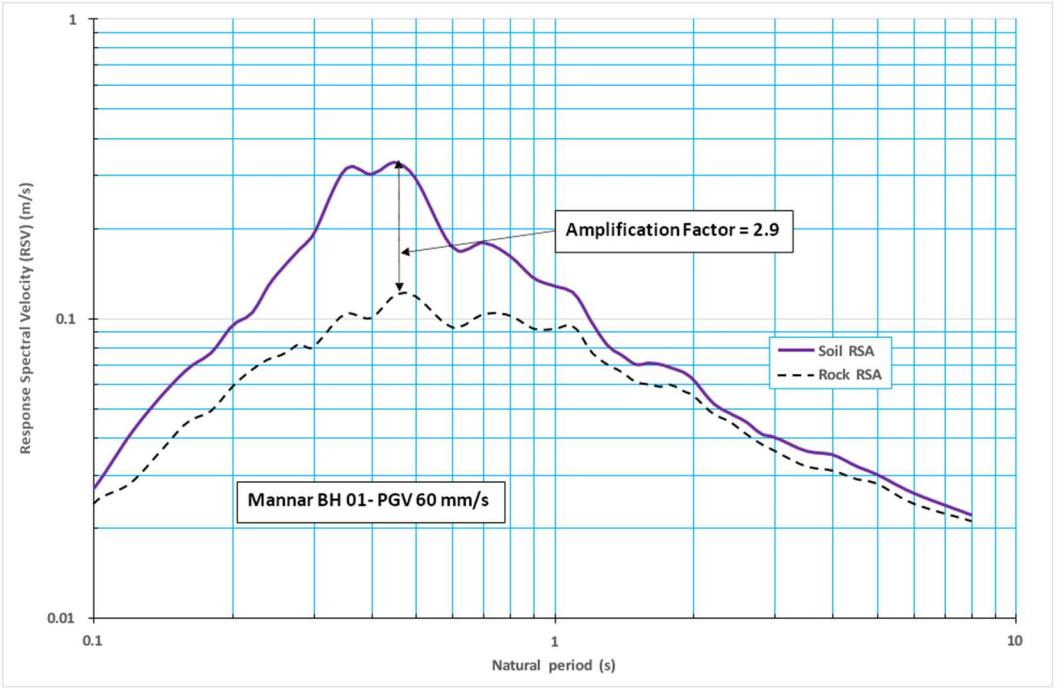


Figure 6f. Velocity response spectra for Mannar site BH 01– PGV 60 mm/s (PGA 0.08 g)

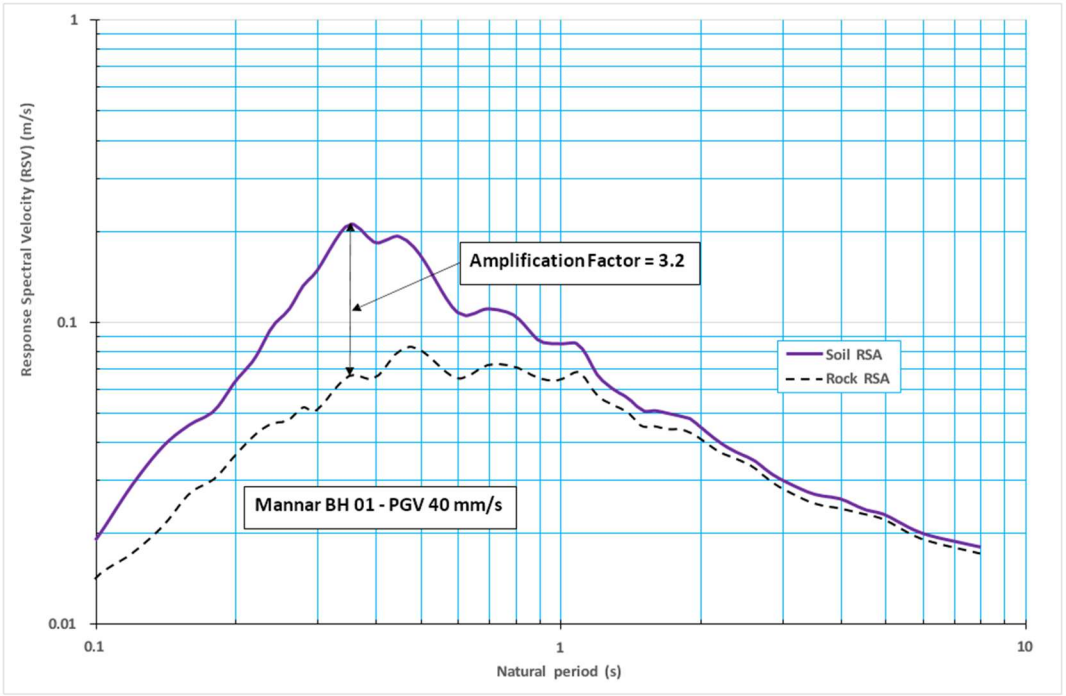


Figure 6g. Velocity response spectra for Mannar site BH 01– PGV 40 mm/s (PGA 0.05 g)

3.4 Design response spectra

Based on Figures 6a to 6g, amplification factors are in the range 2.9 to 3.6. The common notion that amplification factors are sensitive to ground motion intensity has not been observed in this instance. This insensitivity is intriguing although it might be attributed to local characteristics of the site (soil layering, type of material and vertical heterogeneity of the medium) or due to the high degree of non-linear behaviour evident from the period shift phenomenon. Nonetheless, these observations also facilitate a convenient average amplification factor of about 3.3 (on average) for all sites. Another interesting observation is that the corner period coincides with the constant acceleration part of the spectrum. A value close to 0.35s was observed as opposed to 0.3s suggested in the Australian Code AS 1170.4. Our analysis of some of the other borehole records (not presented in this chapter) exhibited rigid-body motion behaviour of the soil column. Given that the local geology of Sri Lanka is mostly Pre-Cambrian, it seems appropriate to consider a 0.35s duration for the constant acceleration part. However, the constant velocity part of the spectrum seems to hover around 1.2s, as opposed to 1.5s or 2s noted in some international codes. Further investigation may be necessary to confirm the second corner period. It must also be stated that the site response analysis presented herein does not include soil profiles of 1s period. Such sites may exhibit higher amplification factors close to 5 or 6. Based on the above discussions (pending further investigation), design response spectra for rock and soil sites according to the guidelines specified in Eurocode 8 are explained below:

3.5 Horizontal elastic response spectrum procedure recommended by Eurocode 8

For the horizontal components of the seismic action, the elastic response spectrum Se(T) is defined by the following expressions:

$$0 \le T \le T_B; \quad S_e(T) = a_g \cdot S\left[1+\left(T/T_B\right)\times\left(2.5-1\right)\right] \tag{3}$$

$$T_B \le T \le T_C; \quad S_e(T) = a_g \cdot S \cdot 2.5 \tag{4}$$

$$T_C \le T \le T_D; \quad S_e(T) = a_g \cdot S \cdot 2.5\left[T_C/T\right] \tag{5}$$

$$T_D \le T \le 4s; \quad S_e(T) = a_g \cdot S \cdot 2.5\left[T_C T_D/T^2\right] \tag{6}$$

where

$S_e(T)$ is the elastic response spectrum;

T is the vibration period of a linear single-degree-of-freedom system;

a_g is the design ground acceleration for type of ground concerned

T_B is the lower limit of the period of constant spectral acceleration branch;

T_C is the upper limit of the period of constant spectral acceleration branch;

T_D is the value defining the beginning of the constant displacement response range of the spectrum;

S is the soil factor;

(5% viscous damping is assumed in the above equations).

Using values of a_g = 0.1g, T_B = 0.1 s and T_C = 0.35 s, T_D = 1.2 s (as observed from the rock spectra) and S = 3.3 (as observed from the soil response analyses) the design rock and soil response spectrum are shown in Figure 7.

The response spectrum model shown in Figure 7 was originally derived from the Australian Standard for Seismic Actions: AS1170.4 (2007). In most Australian capital cities of the eastern seaboard a reference PGA value of 0.08g is stipulated. The response spectrum parameters are accordingly listed as follows for this PGA value: PGV = 60 mm/s; RSA_{max} = 0.25 g (for 0.1 s < T < 0.35 s); RSV_{max} = 120 mm/s (for 0.35 s < T < 1.2 s) and RSD_{max} = 23 mm (this RSD_{max} value is close to the 25 mm that would be calculated using AS1170.4 (2007) with T_2 = 1.5 s). In cases where the PGA value is different to 0.08g the listed parameter values are scaled accordingly. Similar values for soil conditions can be worked out. It is noted that RSD_{max} = 76 mm for soil. These soil condition values clearly highlight the seismic hazard potential in the region. In the absence of detailed calculations users can adopt the following formulae:

$$RSV_{\max} = RSA_{\max} \times T_C / 2\pi \tag{7}$$

$$RSD_{\max} = RSV_{\max} \times T_D / 2\pi \tag{8}$$

A further condensed version of the above spectra can be presented in the form of Acceleration-Displacement Response Spectra (ADRS) format as shown in Figure 8.

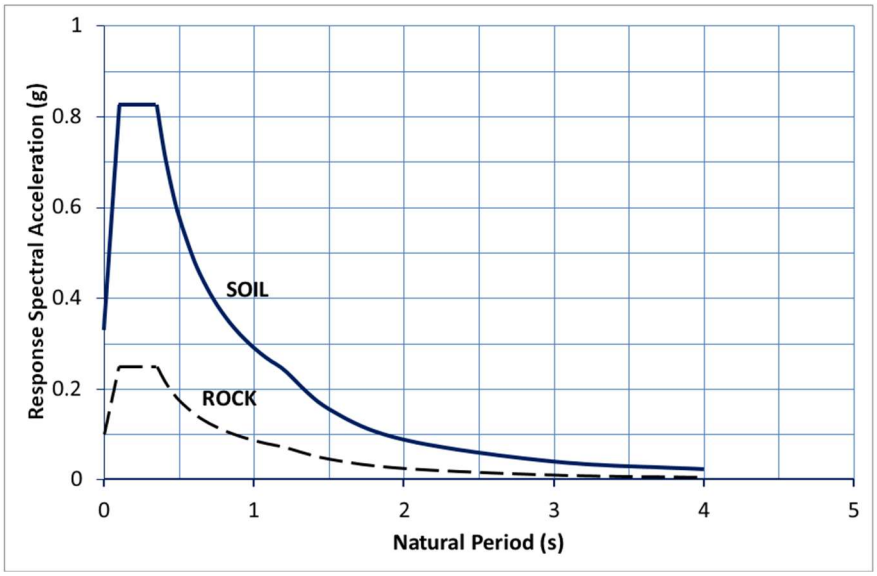


Figure 7. Recommended design response spectra for rock and soil (5% damping)

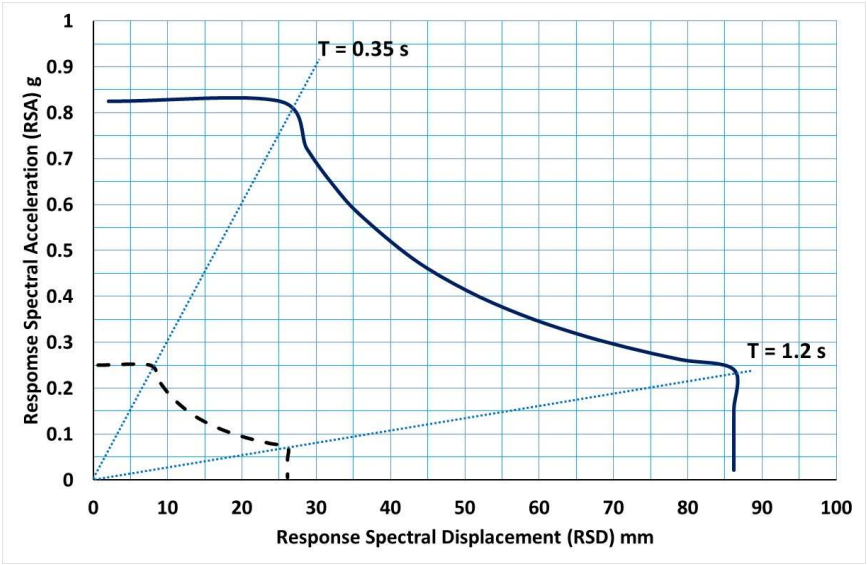


Figure 8. Response spectra in ADRS format

4. Conclusions

Seismic hazard maps for Sri Lanka and Design Response Spectra for rock and soil conditions have been systematically developed and are presented in formats useful to practicing engineers. Critical values have been compared with those of international codes and practice. Further work to include a range of magnitude-distance combinations and deep soil profiles pertaining to site classes D and E still needs to be carried out, in addition to consideration of different magnitude-distance combinations encompassing a range of PGV values. In addition, efforts are currently being made to develop a uniform hazard spectra for the entire country.

References

Abayakoon, S. B. S. 1996. “Seismic risk analysis of Sri Lanka”, Journal of the Geological Society of Sri Lanka, 6, 65-72.

Abaykoon S.B.S. 1998. “Seismic response of low lying areas in Colombo, Sri Lanka”, Engineer, Journal of Institution of Engineers, Sri Lanka, 28(2), 29-36.

AS 1170.4: Standards Australia 2007. “Structural design actions Part 4: Earthquake actions in Australia”, (AS 1170.4-2007), Retrieved from http://www.saiglobal.com

EN 1998-1:2004. "Design of structures for earthquake resistance, EN 1998-1 -Part 1: General rules, seismic actions and rules for buildings", CEN.

Fernando, M. J. & Kulasinghe, A. N. S. 1986. "Seismicity of Sri Lanka", Physics of the Earth and Planetary Interiors, 44(2), 99-106.

Gardener, J. K. & Knopoff, L.1974. "Is the sequence of earthquakes in Southern California, with aftershocks removed, Poissonian?", Bulletin of the Seismological Society of America, 64, 1363-1367.

Grennhalgh, S. A., Denham, D., McDougall, R. & Rynn, J. M. W. 1988. "Magnitude-intensity relations for Australian earthquakes", Bulletin of the Seismological Society of America, 78, 374-379.

Idriss, I. M. and Sun, J. I. 1992. "User's Manual for SHAKE91, A computer Program for Conducting Equivalent Linear Seismic Response Analyses of Horizontally Layered Soil Deposits Program Modified based on the Original SHAKE Program by Schnabel, Lysmer and Seed."

Johnston, A. C. 1996. "Seismic moment assessment of earthquakes in stable continental regions - Instrumental seismicity", Geophysical Journal International, 124, 381-414.

Nuttli, O. W.1983. "Average seismic source-parameter relations for mid-plate earthquakes", Bulletin of the Seismological Society of America, 73, 519-535.

Imai, T, and Tonouchi, K. 1982. “Correlation of N value with S-wave velocity and shear modulus”, Proc., 2nd European Symp. on Penetration Testing, Amsterdam, 67–72.

Lam, N. T. K. 1999. "Program "GENQKE" User's Guide-Program for generating synthetic earthquake accelerograms based on stochastic simulations of seismological models", Department of Civil and Environmental Engineering, The University of Melbourne, Australia.

Lam, N.T.K. and Wilson, J.L. 2004. "Displacement modelling of intraplate earthquakes, Special issue on Performance Based Seismic Design", (Ed. Nigel Priestley), ISET Journal of Earthquake Technology, Indian Institute of Technology, 41(1), 15-52.

Lam, N. Wilson, J.L. Balendra, T. Venkatesan, S. 2009, "Seismic load estimates of distant subduction earthquakes affecting Singapore", Engineering Structures, 31(5), 1230-124.

Lam N.T.K. (2017) personal communication with the authors

Ordaz, M., Aguilar, A., Arboleda, A. 2007. CRISIS2007: "A program for computing seismic hazard", https://sites.google.com/site/softwarecrisis/about

Peiris, N. 2007, “Seismic hazard assessment of Sri Lanka and seismic risk in Colombo”, Paper presented at the 8th Pacific Conference on Earthquake Engineering, Singapore.

Raghu Kanth, S. T. G. & Iyengar, R. N. 2007. "Estimation of seismic spectral acceleration in Peninsular India", Journal of Earth System Science, 116, 199-214.

Stepp, J. C.(1972). "Analysis of completeness of the earthquake sample in the Puget Sound area and its effect on statistical estimates of earthquake hazard", First microzonation Conference, 1972 Seattle, WA. 897-909.

Uduweriya, S. B. Wijesundara, K. K. & Dissanayake, P. B. R. 2013. "Seismic risk in Colombo – probabilistic approach" Paper presented at the SAITM Research Symposium on Engineering Advancements 2013, Colombo, Sri Lanka.

Uniform Building Code. 1997. "International Conference of Building Officials 1997", Uniform Building Code Volume 2, International Conference of Building Officials Publication Department, Whittier, CA.

Venkatesan, S. & Gamage, P. 2013. "Spectral analysis of seismic waves in the Northern Indian Ocean Region", Bulletin of the Seismological Society of America, 103(6), 3305-3320. doi: 10.1785/0120130079

Venkatesan, S., Gamage, P., Lumantarna, E., & Lam, N. (2015). "A hybrid probabilistic seismic hazard analysis of a low and moderate seismic region: Sri Lanka – a case study", Proceedings of the Pacific Earthquake Engineering Conference, Sydney, Australia.

Wair, B.R., DeJong, J.T. and Shantz, T. (2012). Guidelines for Estimation of Shear Wave Velocity Profiles, PEER Report 2012/08.

A Review of the Vietnamese Seismic Design Code

Tuan D. Ngo[a], Nam H. Nguyen[a], Minh D. Nguyen[b] and Hai H. Nguyen[b]

[a] Department of Infrastructure Engineering
The University of Melbourne, Australia

[b] Institute of Building Science and Technology, Vietnam

The Vietnamese seismic code has evolved via multiple stages, based on different foreign codes. The current code (TCVN 9386:2012) is based on Eurocode 8. A new version, however, based on the Russian seismic code (SP 14.13330.2014) is currently being drafted. The Russian code has been selected because most Vietnamese design codes follow their Russian counterparts. This chapter reviews seismic activities in Vietnam and the seismic design of building structures based on the current code and the proposed draft. Key differences include changes in design return periods, seismic hazard classification, and design criteria. Replacement is proposed for the current three zoning maps with exceedance probabilities of 10%, 5%, and 1% in 50 years, by only one map with a 10% probability of exceedance in 50 years. The seismic zoning maps are presented in MSK-64 scale instead of the peak ground accelerations of the current code. The draft code proposes analyses should be made at two earthquake levels, the design earthquake and the maximum considered earthquake.

Keywords: seismic design, building codes of practice, Vietnam, low to moderate seismicity

1. Introduction

Vietnam lies on the Eurasian Plate, close to the boundary of the Andaman-Sumatra-Myanmar plate. Active faults are mostly concentrated in the north. The most active fault is *LaiChau-DienBien-SongMa-SonLa* which was at the centre of an earthquake of magnitude 6.8 (a shaking intensity of VII to IX on the MSK scale) in 1983 (Nguyen, 1996). Several moderate earthquakes with magnitudes ranging from 5 to 7 were recorded in the north during the years 1980-1990. The earliest recorded historic seismic activity in Vietnam dates from 114 AD. Nowadays, seismic activities are monitored by the Institute of Geophysics (IGP), the Vietnam Academy of Science and Technologies (VAST).

Vietnam's seismic design code has evolved in multiple stages based on different foreign codes. Several foreign seismic codes from the US, Europe, and Russia have been adopted in the past. The current design code, TCVN 9386:2012, is based on Eurocode 8 (2004), but a new draft of the code is being proposed. Since the majority of Vietnam's design codes follow Russian counterparts, the new seismic design code draft will be based on the Russian, SP 14.13330.2014 (2014).

This chapter reviews seismic activities in Vietnam and the seismic design of building structures based on the current code and the proposed draft. Note that the key differences between the current and proposed codes include changes in design return periods, seismic intensity classification, and design criteria.

2. Site activities in Vietnam

Based on the data collected by IGP and historical records, from 114 AD to 2003, 1645 earthquakes have occurred with a magnitude (M) of 3 or greater on the Richter scale. Among these, 10 earthquakes with magnitudes of 6 and over occurred between from 1900 and 2003 (Ngo and Nguyen, 2008). Figure 1 presents past earthquake locations with magnitudes of 4 and above and fault lines in Vietnam and adjacent areas (Nguyen and Pham, 2015).

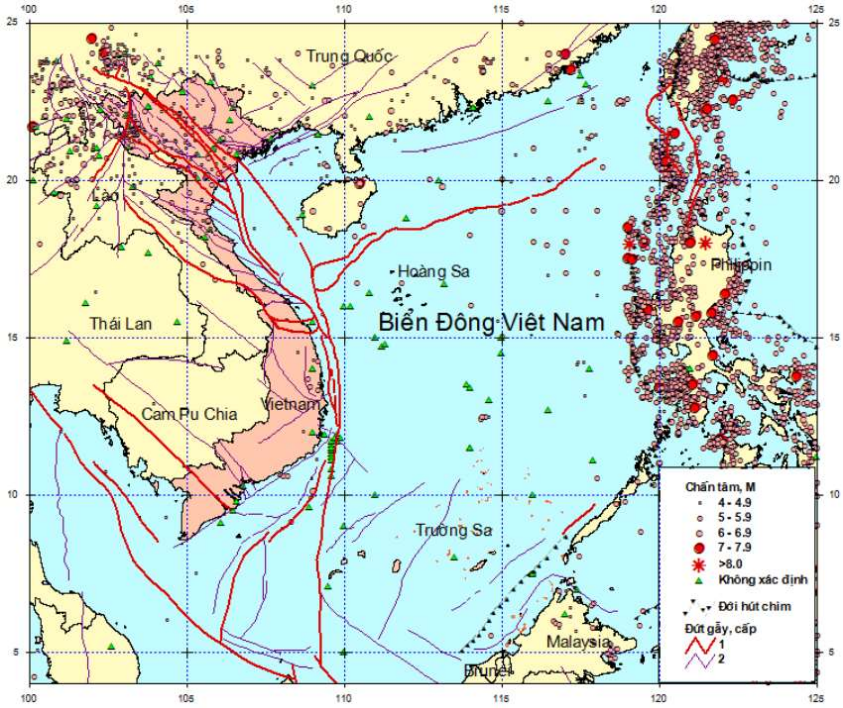


Figure 1. Seismotectonic map of Vietnam (Nguyen and Pham, 2015)

Key earthquakes in Vietnam, all of which occurred in the north of the country, are:

- The Dien Bien Phu earthquake on 1st November 1935, with an estimated magnitude of 6.8 (Richter scale) is considered the strongest earthquake of the past century. The damage to buildings and structures, as measured on the MSK-64 scale, gives a seismic intensity (I) between VII and IX
- Of magnitude 5.5 TheTuan Giao earthquake on 24th June 1983, in Lai Chau province, with a magnitude of 6.7 and a seismic intensity of VIII.
- The Dien Bien Phu earthquake on 19th February 2001, with a magnitude of 5.3 and a seismic intensity between VII and VIII. This earthquake was followed by hundreds of aftershocks with magnitudes up to 4.9.

Southern Vietnam is considered a region of low seismicity, not expected to have major tectonic activities. However, several earthquakes with magnitudes around 5 and above occurred in this region in 2005. On 5th August, an earthquake occurred offshore of Vung Tau city of M = 4.6 and I =V. On 8th November, an earthquake of magnitude 5.5 rocked Ho Chi Minh City which is possibly the strongest earthquake ever, in the south of Vietnam (IGP, 2005).

3. Seismic hazards

The first seismic hazard map of Vietnam was established in 1993 (Nguyen and Pham, 2015). The attenuation relationships employed in the early seismic hazard assessment work of Cornell (1968) were used in conjunction with 7 known seismic source zones. The hazard map was revised by the same author in 1997 and 2004, updated with 17 seismic source zones, including those in surrounding countries, the Indian and Pacific Oceans, using the geological conditions of Yunnan, Kunming, China.

The seismic hazard map for a 10% probability of exceedance in 50 years used in TCXDVN 375:2006 and TCVN 9386:2012, was established by Nguyen and Le (2008). The attenuation relationships of Campbell (1997) and Toro et al. (1997) were used at the time.

In 2010, hazard maps for the mainland and its continental shelf were updated using Campbell's (1997) attenuation relationships and were further extended in 2014 to include the mainland and adjacent areas. The attenuation relationships of Toro et al. (1997) were used, which had been established for the eastern USA where the geological conditions are similar to those of Vietnam (Nguyen and Pham, 2015).

The seismic hazard maps of Vietnam are presented in Figure 2. Figure 2 was established by Nguyen and Pham (2015) for 10%, 5%, 2%, and 0.5% probabilities of exceedance, corresponding to return periods of 475, 975, 2475, and 9975 years, respectively. Results are presented in terms of Peak Ground Acceleration (PGA) values.

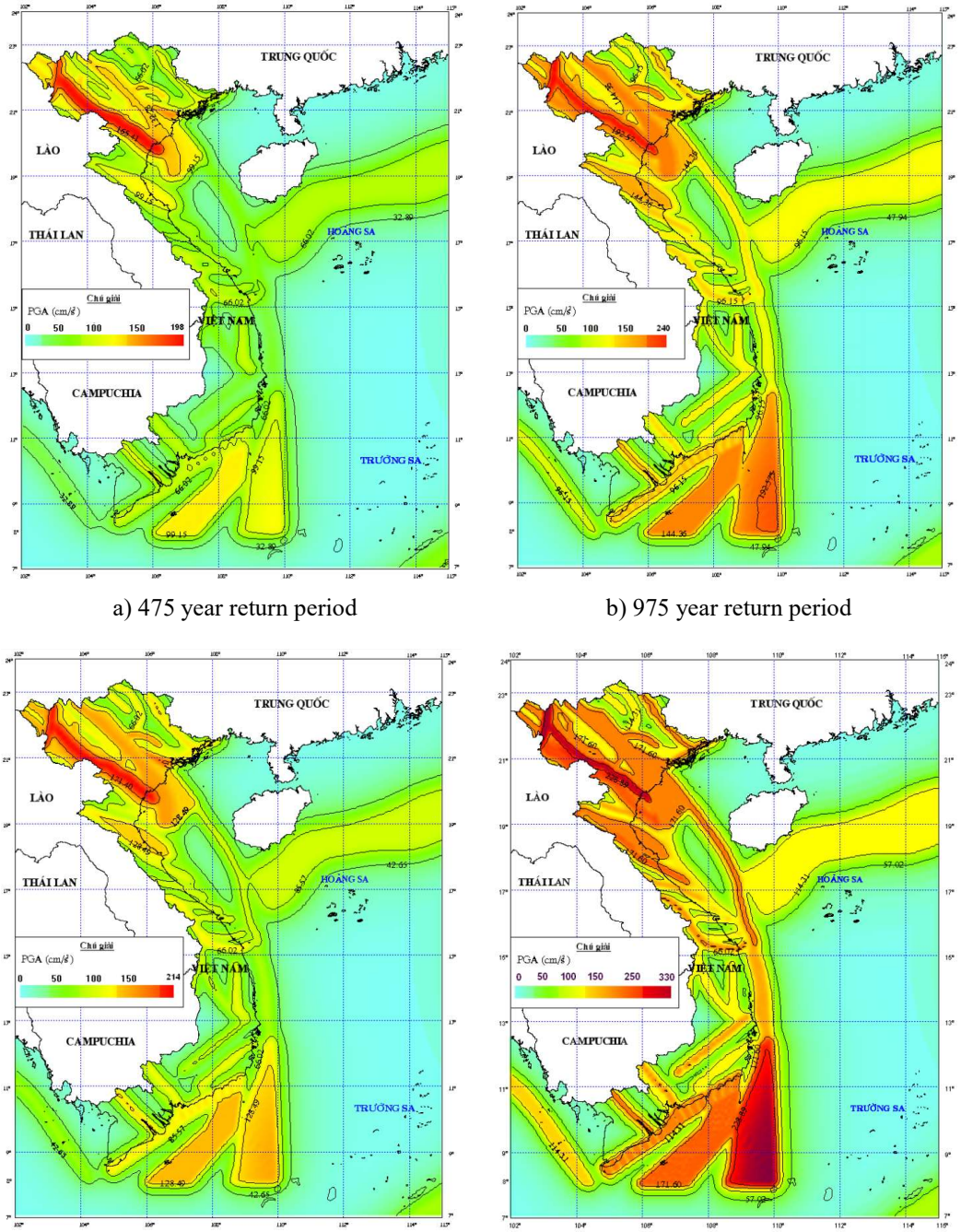
4. Seismic design practice

Seismic design practice in Vietnam has gone through many stages. Before 2012, Vietnam had no national seismic design code or seismically zoned maps. Foreign codes were used, including seismic codes from the the US, Europe, and Russia. The most commonly used were the Russian seismic code SNiP II-7-81 and its updated version SNiP II-7-81*. Design earthquake intensity was usually determined for each project on a case-by-case basis.

In 1997, the code of practice, TCXD 198:1997 (1997) - *Design of multi-storey monolithic reinforced concrete buildings*, was issued by the Ministry of Construction (MoC) providing guidelines for the design of tall concrete buildings against earthquakes. Seismic analysis under TCXD 198:1997 was based on SNiP II-7-81*. The design earthquake intensity, I, on the MSK- 64 scale was used.

In 2004, the seismic design code, TCXDVN 375:2006 (2006) – *Design of structures for earthquake resistance*, based on (Eurocode 8, 2004) - Design of structures for earthquake resistance, was issued by the MoC in 2006. In 2012, it became the national code, referred to as TCVN 9386:2012.

Since most of Vietnam's design codes, including those for concrete and steel structures, follow their Russian counterparts, incompatibilities occur when using a seismic code based on Eurocode 8. To avoid these incompatibilities, a new version of the seismic code, (TCVN, 2017), has been proposed, based on the revised Russian seismic code, SP 14.13330.2014 (2014).



a) 475 year return period

b) 975 year return period

c) 2475 year return period

d) 9975 year return period

Figure 2. Seismic hazard maps of Vietnam (Nguyen and Pham, 2015)

5. Vietnam seismic design code

The Vietnamese seismic design code, TCVN 9386:2012, is based on Eurocode 8, as above, but it includes several minor adjustments. For example, the values of the importance factor are slightly different from those of Eurocode 8. The seismic map adopted in the standard established for Vietnam is based on studies made by IGP.

The fundamental requirements of TCVN 9386:2012 are those of 'no-collapse' and 'damage limitation'. In relation to the 'limit state' concept, these two requirements correspond to the Ultimate Limit State (ULS) and the Serviceability Limit State (SLS). For no-collapse, the structure should be designed to withstand the design seismic action with no local or global collapse. To satisfy this requirement, the structure should retain its structural integrity and a residual load bearing capacity after a seismic event. The design seismic action is expressed in terms of: a) the reference seismic action associated with a probability of exceedance of 10% in 50 years, ie. a return period of 475 years, b) the importance factor γ_I to take into account the reliability required of different types of building.

To satisfy the damage limitation requirement, the structure should be designed to withstand a seismic action that has a higher probability of occurrence than the design seismic action, with no damage that would limit the use of the structure. This seismic action has a probability of exceedance of 10% in 10 years, or a return period of 95 years.

To satisfy the fundamental requirements of TCVN 9386:2012, the two limit states should be checked against earthquake loading during structural analysis. For buildings with heights less than 40 m, the seismic base shear force Fb for each horizontal direction of the building should be determined by the following equation:

$$F_b = S_d(T_1) \cdot m \cdot \lambda \tag{1}$$

where

$S_d(T_1)$ is the design spectrum for elastic analysis (see Eq. (2) to (5)) at the period T_1;

T_1 is the fundamental period of natural vibration of the building for lateral motion in the direction considered;

m is the total mass of the building above the foundation or above the top of a rigid basement;

λ = 0.85 (if $T_1 \leq 2\ T_C$ for buildings with more than two storeys) or λ = 1.0 (for other cases). The value of T_C can be found in Table 1, according to ground type.

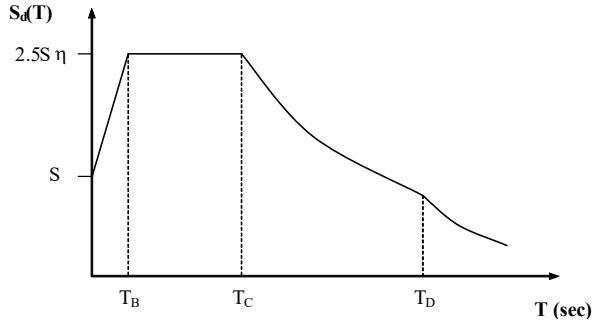


Figure 3. Design response spectrum (TCVN 9386:2012)

The design spectrum Sd(T) for the natural period T of the buildings (Fig. 3) can be determined by the following formula:

$$0 \le T \le T_B : S_d(T) = a_g.S.\left[\frac{2}{3} + \frac{T}{T_B}\left(\frac{2,5}{q} - \frac{2}{3}\right)\right] \quad (2)$$

$$T_B \le T \le T_C : S_d(T) = a_g.S.\frac{2,5}{q} \quad (3)$$

$$T_C \le T \le T_D : S_d(T)\begin{cases} = a_g.S \cdot \dfrac{2,5}{q} \cdot \dfrac{T_C}{T} \\ \ge \beta.a_g \end{cases} \quad (4)$$

$$T_D \le T : S_d(T)\begin{cases} = a_g.S \cdot \dfrac{2,5}{q} \cdot \dfrac{T_C.T_D}{T^2} \\ \ge \beta.a_g \end{cases} \quad (5)$$

in which:

β = 0.2 (is the lower bound factor for the horizontal design spectrum);

q is the behaviour factor that allows for the non-linear response of the material of the structure, the structural system and the design procedures;

a_g is the design peak ground acceleration on type A ground, in which

For the ultimate limit states, ag is calculated by

$$a_g = a_{gR}\gamma_I \quad (1)$$

where a_{gR} is determined from the Vietnam Seismic map attached to the code (see Fig. 4)

γ_I is the importance factor equal to 1.25, 1.0, 0.75 and 0.0 for buildings of class I, II, III and IV according to TCVN 9386:2012. For very important structures that are not allowed to suffer damage during an earthquake, the maximum possible ground acceleration at the site should be taken as the value of ag. Class IV buildings present low risk to human life should the building fail, such as sheds and barns, whereas class I buildings are considered as essential post-disaster recovery facilities, or are hazardous facilities themselves.

For the damage limitation states, the value of ag is taken as 0.585agR.

S, T_B, T_C and T_D are determined from Table 1 below:

Table 1. Values of *S*, T_B, T_C and T_D

Ground types	*S*	T_B (s)	T_C (s)	T_D (s)
A	1.00	0.15	0.4	2.0
B	1.20	0.15	0.5	2.0
C	1.15	0.20	0.6	2.0
D	1.35	0.20	0.8	2.0
E	1.40	0.15	0.5	2.0

Note: Ground types A, B, C, D & E, refer to Eurocode 8 or TCVN 9386:2012.

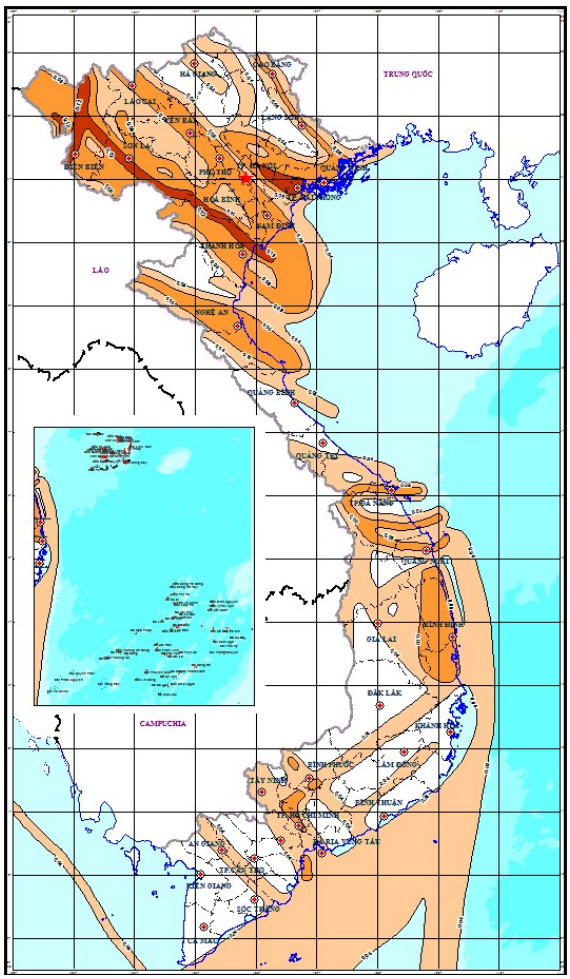


Figure 4. Seismic zonation map of Vietnam (TCVN 9386:2012)

The importance factor assigned to different building classes in Eurocode 8, is included

in the calculation of the design peak ground acceleration to account for higher or lower earthquake hazards (different return periods than the reference return period of 475 years).

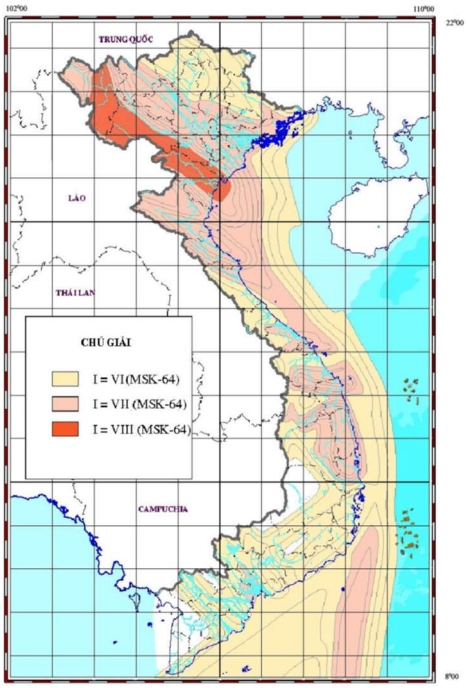
Because of the lack of data enabling the establishment of spectral curves and the unavailability of a formulation to determine the design spectrum Sd(T), in TCVN 9386:2012 the elastic spectral curve type 1 in Eurocode 8 (Fig. 3) has been adopted, as most earthquake regions in Vietnam experience magnitudes greater than 5.5 (Richter scale).

In TCVN 9386:2012, seismic hazard assessments are based on the reference peak ground acceleration agR for ground type A. This value can be determined from the seismically zoned map attached to the code (Fig. 4) or are provided by authorised government bodies. The seismically zoned map in TCVN 9386:2012 is the result of the long-term research project conducted by IGP. This map has been approved by the government authority at ministerial level. Ground type A (according to the Eurocode 8 ground classification) is a rock, or other rock-like geological formation, including at most 5 m of weaker material at the surface, with an average shear wave velocity vs,30 that exceeds 800 (m/s).

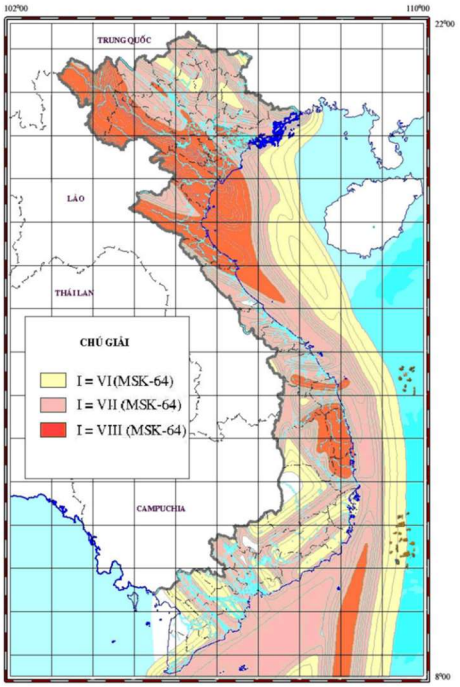
The new draft of the seismic code (TCVN, 2017), based on SP 14.13330.2014 (2014), has major differences with the current code. The proposed draft uses the seismic intensity MSK-64 scale, instead of peak ground acceleration, PGA. The conversion of some seismic intensity levels to PGA ranges is provided in Table 2. Structures must be designed for two levels of earthquake: (a) the Design Earthquake (DE), and (b) the Maximum Considered Earthquake (MCE). At the DE level, linear analysis of the structure is performed under a seismic intensity loading with a probability of exceedance of 10% in 50 years whereas at the MCE level, non-linear analysis is used with seismic intensities corresponding to 5% and 1% probabilities of exceedance in 50 years. Figures 5a to 5c present three proposed zoning maps (A, B, and C) at SMK-64 scale for 10%, 5%, and 1% probabilities of exceedance in 50 years, respectively. Assuming a Poisson model for the occurrence of earthquakes, the three maps (A, B, and C) correspond to return periods of 475, 975, and 4975 years, respectively.

Table 2. MSK-64 and PGA conversion

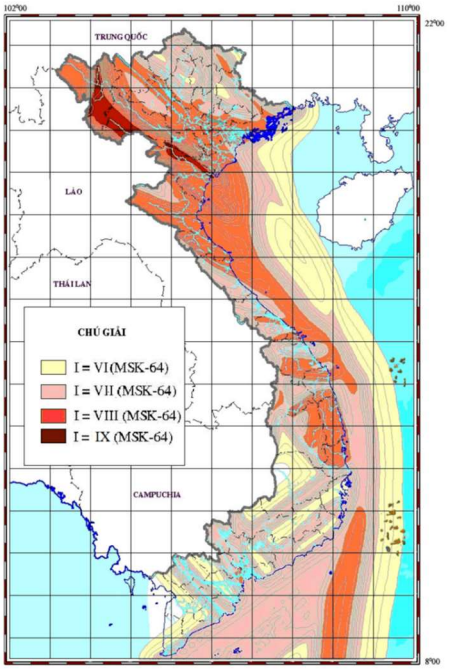
Seismic intensity	**PGA, cm/s^2**
V	12 - 25
VI	25 - 50
VII	50 - 100
VIII	100 - 200
IX	200 - 400
X	400 - 800



a) 475 year return period



b) 975 year return period



c) 4975 year return period

Figure 5. Proposed seismic zonation maps of Vietnam (TCVN, 2017)

The design seismic action (force or moment) at node k in natural vibration mode i of a structure in the direction j is denoted by (translational direction, j=1 to 3, or rotational direction around an axis, j=4 to 6), is given in Eq. 7.

$$S_{ik}^{j} = K_0 K_1 S_{0ik}^{j} \tag{7}$$

where K_0 is the importance factor. For building classes I, II, III, and IV, this is equal to 2, 1.5, 1.0, and 0.0 for MCE, and 1.2, 1.1, 1.0, and 0.8 for DE, respectively;

K_1 is a factor that accounts for allowable damage to the structure, depending on the energy dissipation capacity of the structure. K_1 varies from 0.12 to 1.0. For example, K_1 is equal to 1 for structures with no damage permitted (no plastic deformations), and to 0.2 for steel moment frames. K_1 is similar to the behavior factor q in TCVN 9386:2012 and Eurocode 8.

S_{0ik}^{j} is the seismic action for the vibration mode i:

$$S_{0ik}^{j} = m_k^j A \beta_i K_\psi \eta_{ik}^{j} \tag{8}$$

where m_k^j is the mass of the structure associated with node k.

A is the ground acceleration, taken as 1.0; 2.0; 4.0 m/s², corresponding to a seismic intensity I of VII, VIII, and IX.

β_i is the coefficient for mode i, based on two spectrum curves, 1 and 2 (as shown in Figure), for four ground types. The four ground types (I, II, III, and IV) are defined by the shear wave velocity, $v_{s,30}$ in the upper 30 m of the soil sediment. Ground type I is rock or other rock-like geological formation with an average shear wave velocity, $v_{s,30}$ that exceeds 700 (m/s) whereas those for ground types II, III, and IV have $v_{s,30}$ values in the range 250 - 700 (m/s), 150 - 250 (m/s), and 60 - 150 (m/s), respectively. The coefficient is defined by Eqs. 9 and 10, and plotted in Figure.

For ground types I and II (spectrum curve 1):

$$\begin{aligned} &T_i \le 0{,}1s && \beta_i = 1 + 15T_i \\ &0{,}1s < T_i < 0{,}4s && \beta_i = 2{,}5 \\ &T_i \ge 0{,}4s && \beta_i = 2{,}5\left(\frac{0{,}4}{T_i}\right)^{0{,}5} \end{aligned} \tag{9}$$

For ground types III and IV (spectrum curve 2):

$$\begin{aligned} T_i \le 0{,}1s \qquad & \beta_i = 1+15T_i \\ 0{,}4s < T_i < 0{,}8s \qquad & \beta_i = 2{,}5 \\ T_i \ge 0{,}8s \qquad & \beta_i = 2{,}5\left(\frac{0{,}8}{T_i}\right)^{0{,}5} \end{aligned} \tag{10}$$

The value of β_i must not be less than 0.8.

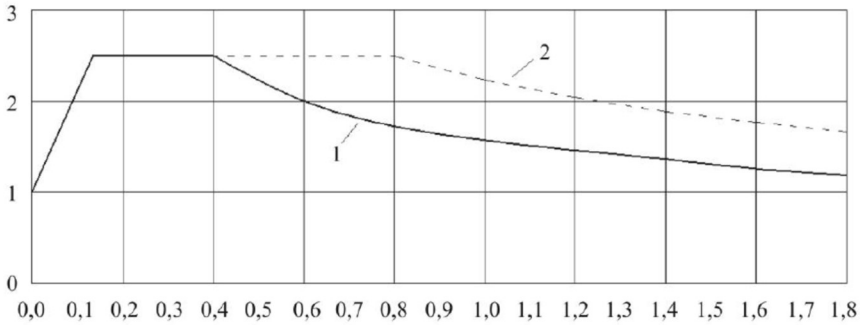


Figure 6. Coefficient β_i

K_ψ is a factor accounting for the shape of the building's structural frame, taken as 1.5, 1.3, and 1.0 for three types of structure. The three structural types consist of: 1) structures that are tall and narrow in plan, 2) unbraced frame structures, and 3) structures not of types 1 or 2 above. Most structures are of type 3, for which the value of 1 is used, except for those that are tall and narrow in plan (e.g. towers).

η_{ik}^{j} is the modal shape coefficient for mode *i*, at node *k*, determined by Eq. 11.

$$\eta_{ik}^{j} = \frac{U_{ik}^{j}\sum_{p=1}^{n}\sum_{l=1}^{3} m_p^l U_{ip}^l r_l}{\sum_{p=1}^{n}\sum_{j=1}^{6} m_p^j \left(U_{ip}^j\right)^2} \tag{11}$$

where *l* (from 1 to 3) is one of the three axes.

j is the action direction (1 to 3 for axial, 4 to 5 for moment about an axis).

p is the node number, from 1 to *n*, with n being the total number of nodes in the structure.

m is the mass (or mass inertial moment) at node *p*.

r is the cosine of the angle between the action direction and the axis *l*.

U is the modal displacement (or rotation)

For structures where the response can be found using a cantilever-type model, η_{ik}^{j}

can be simplified as in Eq. 12, in which one translational direction of action is considered, and the rotational components are neglected.

$$\eta_{ik} = \frac{X_i(x_k)\sum_{p=1}^{n} m_p X_i(x_p)}{\sum_{p=1}^{n} m_p X_i^2(x_p)}, \tag{12}$$

where X is the modal displacment of node number p (height level x_p) in mode i.

With the proposed draft, determining coefficient β can be complex, especially for structures that cannot be modelled as cantilever types. There is a need to develop spatial models to account for multi-directional displacements as in Eq. 11.

As the ground acceleration, A, is taken as the maximum value, within the range of peak ground accelerations corresponding to a specific seismic intensity level, the proposed draft design seismic action for a structure may be larger than the current code design action, leading to greater design and construction costs. A cost-benefit analysis study should be performed, in relation to earthquake resistant construction, comparing the proposed draft and the current code.

6. Conclusions

This chapter reviews seismic activities in Vietnam and its seismic design code for building structures, including the recently proposed draft code. Key earthquakes have occurred in the north of Vietnam whereas the south, which is considered a region of low seismicity, has recently experienced several earthquakes with magnitudes of about 5 and above. Seismic design practice in Vietnam has evolved alongside better understanding of its seismological and geological conditions. The current seismic code, TCVN 9386:2012, is based on Eurocode 8, whereas the proposed new code is based on the Russian seismic code SP 14.13330.2014. Analyses for the two earthquake levels, DE and MCE, are required. Hazard maps, showing seismic intensities on the MSK-64 scale, with probabilities of exceedance equal to 10%, 5%, and 1% in 50 years, are proposed.

References

Campbell, K. W. (1997) "Empirical near-source attenuation relationships for horizontal and vertical components of Peak Ground Acceleration, Peak Ground Velocity, and pseudo-absolute acceleration response spectra." Seismological Research Letters, 68: 154-179.

Cornell, C. A. (1968) "Engineering seismic risk analysis", Bulletin of the Seismological Society of America, 58(5): 1583-1606.

Eurocode 8 (2004) Design of structures for earthquake resistance. Part 1: General rules, seismic actions and rules for buildings.

IGP (2005) Recent eathquakes in the North, Middle, and South parts of Vietnam (Media release). Hanoi, Vietnam.

Ngo, T. D. and Nguyen, M. D. (2008) "A review of the current Vietnamese earthquake design code", Electronic Journal of Structural Engineering, 8(2): 32-41.

Nguyen, D. X. (1996) "Database for mitigation measures of earthquake hazard in Vietnam (in Vietnamese)", Institute of Geophysics (IGP), Vietnam Academy of Science and Technology,

Hanoi, Vietnam.
Nguyen, D. X. and Le, T. S. (2008) "Seismic zonation maps of Vietnam in TCXDVN 375-2006", 30(4): 503-513.
Nguyen, H. P. and Pham, T. T. (2015) "Probabilitistic seismic hazard maps of Vietnam and the east Vietanm sea", Journal of marine science and techonology, Institute of Geophysics - VAST, 15(1): 77-90.
SP 14.13330.2014 (2014) "Construction in seismic areas SNiPII-7-81 (in Russian)", Moscow.
TCVN (2017) "Draft of seismic design code" Hanoi, Vietnam.
TCXD 198:1997 (1997) "Design of multi-story monolythic reinforced concrete buildings (in Vietnamese)", Hanoi, Vietnam.
TCXDVN 375:2006 (2006) "Vietnam seismic design standard (in Vietnamese)", Hanoi, Vietnam.
Toro, G. R., Abrahamson, N. A. and Schneider, J. F. (1997) "Model of Strong Ground Motions from Earthquakes in Central and Eastern North America: Best Estimates and Uncertainties", Seismological Research Letters, 68(1): 41-57.